A high-resolution wide-angle seismic study of the crust beneath the Northumberland trough

West, Tracey Elizabeth

A HIGH-RESOLUTION WIDE-ANGLE SEISMIC STUDY OF THE CRUST BENEATH THE NORTHUMBERLAND TROUGH

by

TRACEY ELIZABETH WEST

A thesis submitted for the degree of

Doctor of Philosophy at the University of Durham

Department of Geological Sciences January 1992

"Ever since God created the world, his invisible qualities, both his eternal power and his divine nature, have been clearly seen; they are perceived in the things that God has made"

Romans 1: 20

ABSTRACT

In June 1987, during the BIRPS MOBIL normal-incidence seismic profiling programme, off the East coast of England, the University of Durham recorded simultaneously at several land based seismic stations in Northern England. The resulting wide-angle data, particularly from Line 1, have excellent resolution in both space and time due to the airgun source and 50 m shot spacing.

The interpretation of the Line 1 wide-angle data at Durham used **BEAM87**, Cerveny's Gaussian beam modelling package. The main arrivals interpreted include the upper crustal refraction (**Pg**), the Moho wide-angle reflection (**PmP**), the upper mantle refraction (**Pn**), and a very high amplitude arrival (**D**) which merges into PmP. Modelling gave a crust about 30 km thick with a change in velocity gradient and a slight velocity contrast at about 20 km depth. There are several wide-angle reflections from interfaces at mid-crustal depths, between 10 and 20 km depth, and the bottom 2 km of the crust has a high velocity of about 7 kms^{-1}.

Two interesting results are that a lateral velocity change about 40 km offshore is required to fit the Pg travel times; also that arrival **D** is modelled best as the remnant of a step on the Moho at the same location. These appear to be borne out by the normal incidence data for line 1, which show a lateral decrease in the mid-crustal reflectivity above a set of strong, westerly-dipping reflections at Moho depths.

These results suggest the presence of a major crustal fault about 40 km offshore. It is suggested that this fault may be the northward continuation of the Dowsing Fault Zone.

ACKNOWLEDGEMENTS

Where do I begin? So many people have played a part in this study that it is not possible to include everyone, but I'll try! First of all, I owe many thanks to my supervisor, Dr. Roger Long, for all his advice and enthusiasm throughout the whole project. Most of the staff of Durham's Department of Geological Sciences have been a great encouragement to me, particularly Prof. Martin Bott and Christine Roberts; Dave Stevenson has been infinitely patient with my many computer problems!

I have been financially supported by the University of Durham Geophysics Studentship Fund. However, none of the work could have taken place if Mobil North Sea Ltd. had not generously provided the shiptime for the MOBIL survey; Prof. Derek Blundell co-ordinated the project excellently, and I have greatly appreciated the help and interest of Richard Hobbs and Simon Klemperer at BIRPS. I am very grateful to Prof. Vlastislav Cerveny for letting me have a copy of BEAM87 before he was fully satisfied with it, also to Friedmann Wenzel and Karl-Josef Sandmeier for giving me a copy of the CYBER version of SYNSEI and teaching me how to use it. I have appreciated many interesting and encouraging discussions about my dataset with people whom I have met at conferences and workshops.

I have thoroughly enjoyed working alongside Tricia, Gordon, Joao, Samsudin and Stuart. Encouragment has been crucial throughout the whole period of study and I am very fortunate to have many supportive friends, especially Sandy, Ellie, Ray and many friends at St. Nicholas' Church, Durham, but above all, I am indebted to my parents and Jo-anne, Vicky and Peter for their love and support.

For Nana

CONTENTS

LIST OF FIGURES

TABLES

ENCLOSURES

(i) Transparency of station 54 wide-angle data section, plotted at 1 km shot spacing. For comparison with synthetic seismogram sections throughout Chapter 6.

(ii) Transparency of station 57 wide-angle data plotted at 1 km shot spacing. For comparison with Fig. 6.25.

(iii) Transparency of station 47 wide-angle data plotted at 1 km shot spacing. For comparison with Fig. 6.29.

(iv) Transparency of station 40 wide-angle data plotted at 1 km shot spacing. For comparison with Fig. 6.30.

(v) Transparency of station 54 wide-angle data plotted at 1 km shot spacing. For comparison with Fig. 6.33

(vi) Transparency of station 54 wide-angle data plotted at 1 km shot spacing. For comparison with Fig. 6.43.

CHAPTER 1: INTRODUCTION

1.1 Introduction

One of the most important tools for the investigation of the structure of the Earth's lithosphere today is the use of controlled source seismology. Over the last two decades, the normal-incidence seismic reflection method in particular has attained a very high level of sophistication in terms of acquisition and processing. Since 1981, the British Institutions Reflection Profiling Syndicate (BIRPS) has collected 12500 km of deep crustal normal-incidence profiles on the continental shelf around the UK. This huge amount of data has generated a comprehensive map of this portion of the continental crust, giving rise to the concept of a "typical BIRP" **(Matthews 1986)** which represents the main features of the crust of this region as seen by normal-incidence data: transparent upper crust apart from surface sedimentary basins and some low-angle faults, reflective lower crust, a variably continuous Moho reflection and (usually) a transparent upper mantle.

However, it is well known that the normal-incidence technique alone does not produce a complete picture of the crust; wide-angle reflection data is a far more accurate method of determining seismic velocity structure although the spatial resolution of wide-angle surveys has until recently been poor by comparison with normal-incidence surveys on the same scale. An understanding of the physical properties of crustal structures imaged by normal-incidence data may only be obtained by the use of coincident wide-angle reflection seismic data.

Mooney and Brocher(1987) have reviewed 46 coincident normal-incidence and wide-angle datasets obtained worldwide over continental crust up to 1986, comparing results and concluding that "reflection profiles allow us to refine our simplistic refraction models, and the refraction models allow us to better constrain the geometric interpretations of reflection models". Since 1986, several datasets have been recorded exactly coincidentally, obtaining wide-angle data of almost equal resolution to the normal-incidence by using a common source and the same shot or receiver spacing, usually with a large airgun array as the source. These include GLIMPCE, shot in the Great Lakes in 1986 (GLIMPCE

Seismic Refraction Working Group,1989) and MOBIL, the dataset upon which this study is based.

The BIRPS MOBIL programme (Measurements Over Basins to Image the Lithosphere) was the first successful attempt to record on land the shots from BIRPS profiles. The programme was shot in 1987, due to the gift from Mobil North Sea Ltd of two weeks ship time on the RV Mobil Search, and collected nearly 1500 km of normal-incidence data in eight profiles off the East Coast of England, as shown in **Fig. 1.1 (Blundell et al. 1990)**. Wide-angle recording was carried out by Durham University in Northumberland and in North Humberside, and by the Universities of Leeds and East Anglia at stations in Hull and Norfolk.

This study has mainly concentrated on the wide-angle recordings obtained from line 1 in the Northumberland area. This region had previously been studied as part of the Caledonian Suture Seismic Project (CSSP) of 1982 **(Bott et al 1985)**, a "traditional" wide-angle survey described later in this chapter. MOBIL line 1 was shot along exactly the same line as the explosive marine shots used in the CSSP, facilitating the selection of sites for recording stations and enabling a comparison between the CSSP sea-bottom explosive shots and the large airgun array used by the RV Mobil Search.

The interpretation of MOBIL line 1, which employed one of the most recently developed synthetic seismogram packages, BEAM87, reveals considerable lateral variation in the crust compared to the CSSP model of **Lewis (1986)** and has brought to light interesting details of the geology of this region. This chapter presents a broad picture of the background to this experiment, starting with the geological history of the area. The other seismic work carried out in the region up to now, including the CSSP, is then discussed, and finally, similar experiments using closely-spaced airgun shots or closely spaced stations are described, as an introduction to the MOBIL experiment.

1.2 Regional geological structure and history

Fig. 1.2 shows the location of the MOBIL normal-incidence profiles (solid black lines) and Durham's land recording stations (black dots) against the background of the geological structure of the region. The geology of the whole of the area still reflects the ENE-WSW grain of the early Palaeozoic Caledonian orogen, which set the pattern for the ensuing crustal development of Northern England. The

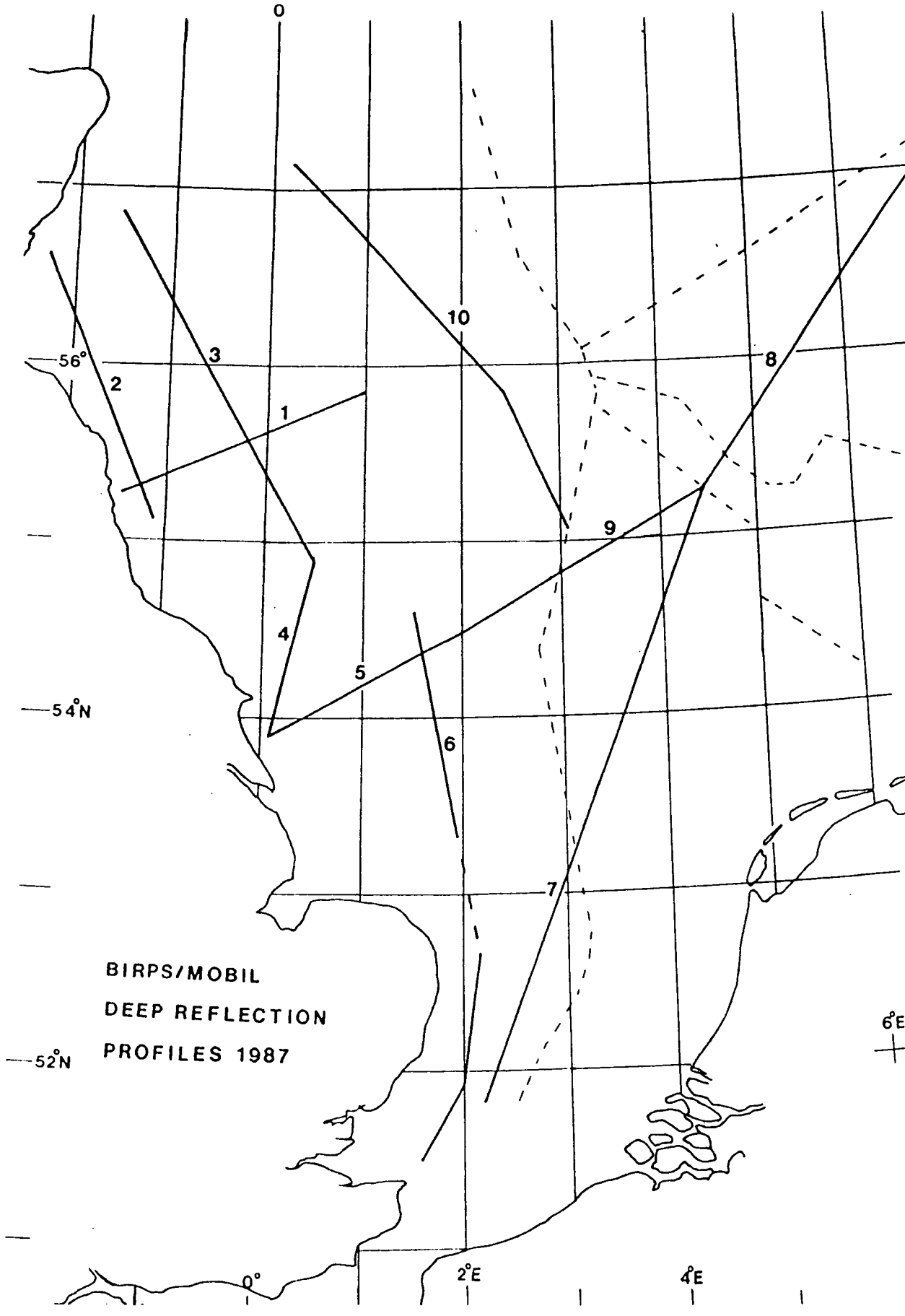

Fig. 1.1 Map of BIRPS MOBIL deep normal-incidence profiles.

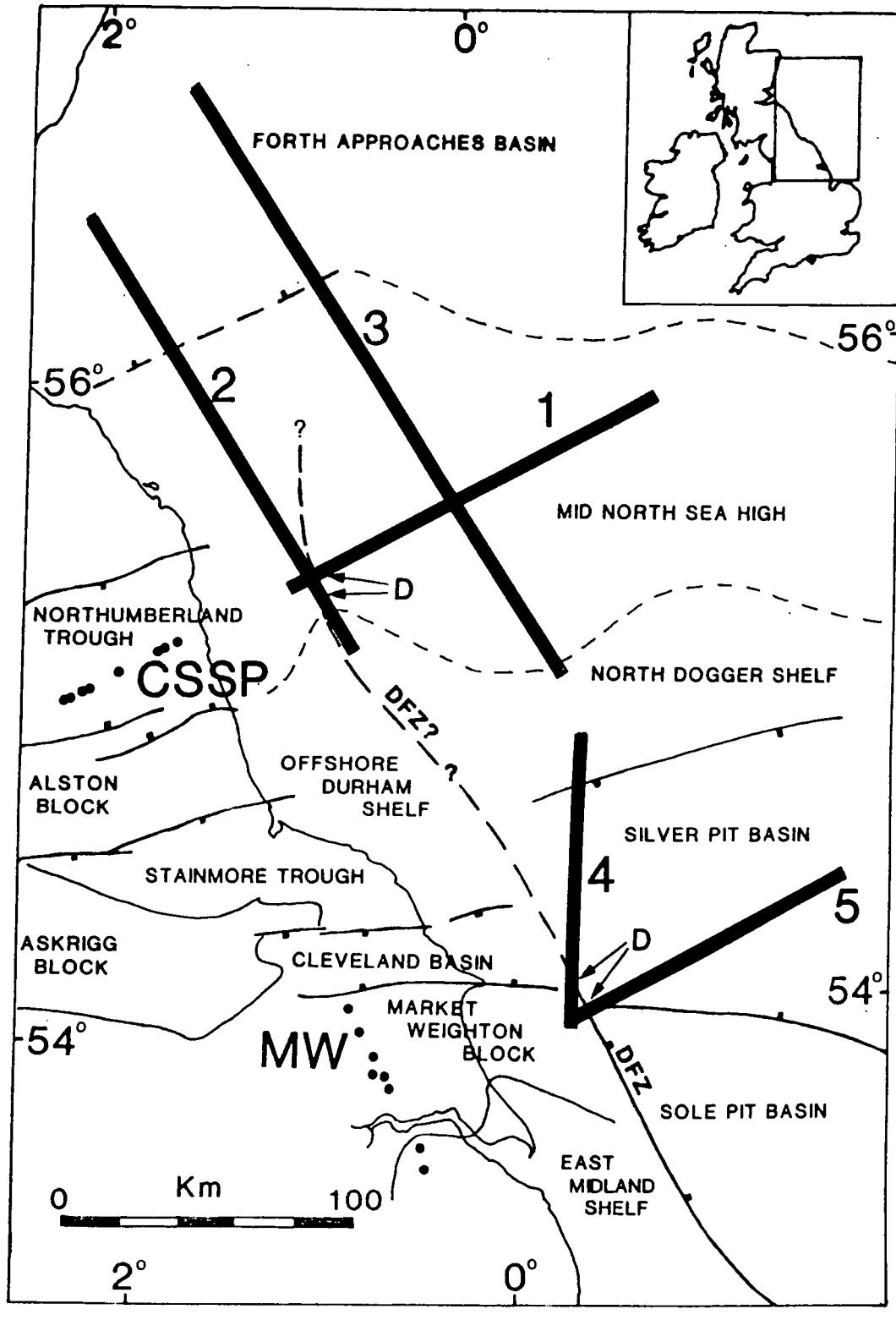

Fig. 1.2 Map of the major geological features of North-East England and the adjacent region of the North Sea, showing the BIRPS MOBIL normal-incidence profiles and the wide-angle reflection recording stations. DFZ: Dowsing Fault Zone. Onshore geology from Fraser and Gawthorpe (1990); Offshore geology (except the DFZ extension) from Glennie (1986).

onshore geology is therefore dominated by roughly east-west trending sedimentary basins and structural highs which developed during the Carboniferous. The area sampled by the MOBIL profiles 1, 2 and 3 falls within the Northumberland Trough onshore and the Mid-North Sea High offshore. The High also trends roughly east-west and has been a structural high since the late Palaeozoic (**Donato et al., 1983**).

The marine area south of this, sampled by the MOBIL lines 4 and 5 off the coast of East Yorkshire and North Humberside, has been more visibly affected by the Mesozoic and Tertiary tectonic events in Europe, including the opening of the North Sea and the Alpine orogeny. These events have caused extension, inversion and some strike-slip activity along the major faults in this region. This complexity is reflected in the quality of both normal-incidence and wide-angle records from the area.

Green(1984), has described the surface geology of the area in which the CSSP was carried out, and **Lewis(1986)** gave a detailed account of the Caledonian orogen and the terranes visible today. The following account does not attempt to repeat these; it is merely an attempt to provide the geological context for the MOBIL programme.

1.2.1 Caledonian geology

Broadly speaking, the Caledonian orogeny involved continental rifting and separation during the late Precambrian, eventual closure of the Tornquist Sea in the late Ordovician, and closure of the Iapetus Ocean during the Late Silurian/ Early Devonian (**Cocks and Fortey, 1982**). This brought together the continents Laurentia, Baltica and Gondwanaland, during the formation of the supercontinent Pangaea. The Grampian orogen is believed to have been caused by the collision of a microcontinent (now the Midland Valley) with the Northern continent, Laurasia (Laurentia and Baltica) before the closure of Iapetus (**Watson 1984**). An approximate time-plan for the orogen and its associated igneous and metamorphic events is shown in **Fig. 1.3.**

Large-scale strike slip movements have played an important role in the development of the present-day Caledonides(**Soper and Hutton 1984**). Large movements along the Great Glen Fault are believed to have taken place during the Devonian, shortly after the closure of Iapetus further south and **Hutton (1987)** interprets many of the different geological provinces of the Caledonides of Great Britain

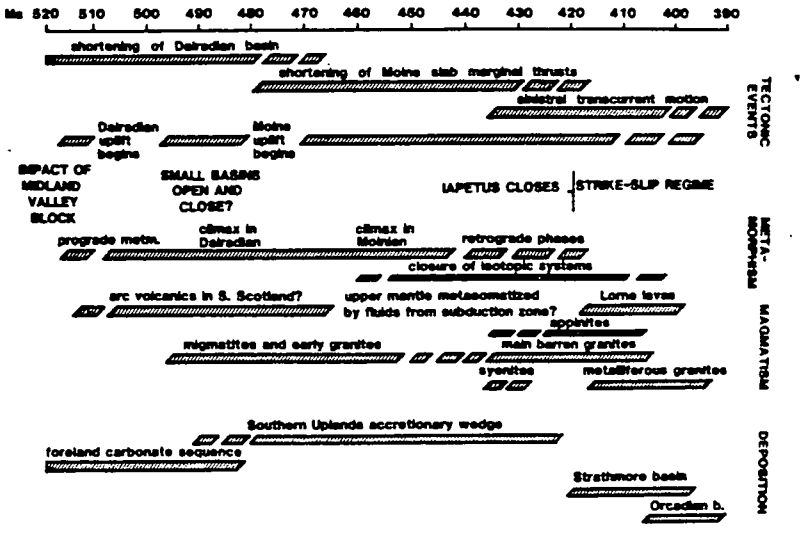

Fig. 1.3 Chart summarising the chronology of the late Caledonian events. From Watson (1984).

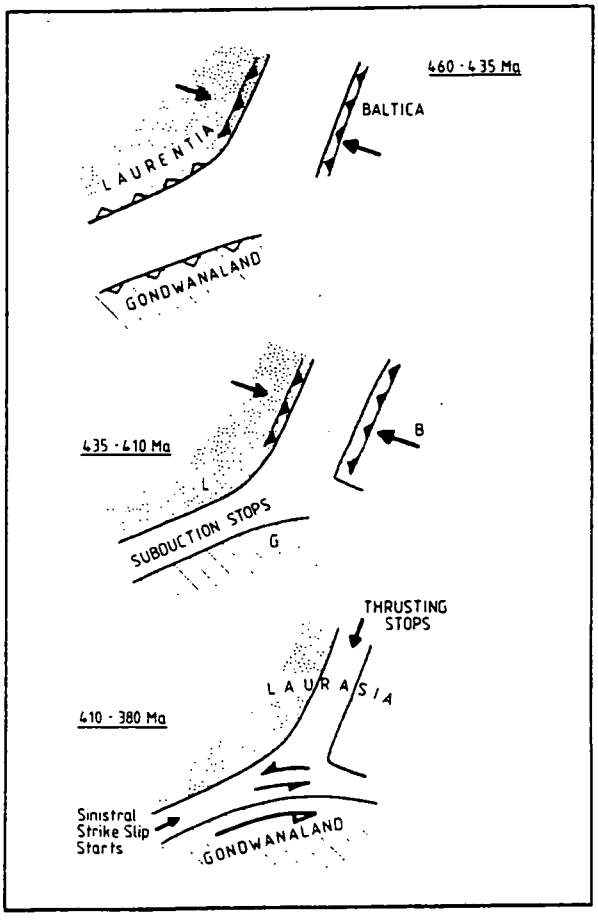

Fig. 1.4 (a) 3-plate scheme for the Caledonides from Hutton (1987)

and Ireland as the result of strike slip movements which docked the different terranes against each other after continental collision (**Fig 1.4**).

The wide-angle recording of MOBIL line 1 was located close and probably parallel to the "Iapetus Suture", the location of subduction of the Iapetus Ocean beneath the northern Laurasian continent and the junction between the Laurasian and Gondwanan continents. The Southern Uplands accretionary complex north of the Suture is interpreted as the product of this ancient subduction zone and the Suture itself is believed to be buried beneath the approximately ENE-WSW trending Northumberland Trough.

1.2.2 The Northumberland Trough

The Northumberland recording stations, annotated as CSSP on the map, were located along the Northumberland Trough, an approximately east-west structure which comprises the Northumberland Basin in the east and the Solway Basin to the west. The whole Trough was initiated during the early Carboniferous and strong differential subsidence took place during the Dinantian, when some 2000 m sediments were deposited in the Northumberland basin compared to the 550 m thick sequence on the Cheviot block and 700 m over the Alston block (**Johnson,1984**). To the south, the Stublick-Ninety Fathom fault system acted as a hinge belt against the Alston block; to the north, the basin is not fault bounded but subsided relative to the stable Southern Uplands and the Cheviot block.

The rapid differential subsidence of the Dinantian slowed down throughout the Namurian and by the Westphalian, uniform epeirogenic sinking of blocks and troughs was taking place, bringing the total thickness of Carboniferous sediments in the Northumberland basin to at least 3 km. At the end of the Carboniferous, either inversion and uplift caused by the Variscan orogeny (**Fraser and Gawthorpe, 1990**) or a eustatic fall in sea-level (**Johnson 1984**) caused the emergence of the region and led to the weathering and erosion of the land surface.

Swinburn (1975) has proved a maximum depth of 3 to 4 km for the Northumberland Basin by inversion of time terms from quarry blast refraction seismic data. The depth to basement, which is the depth of the Carboniferous determined from this work is shown in **Fig. 1.5**.

The mechanism of formation of the Northumberland Trough, especially the differential

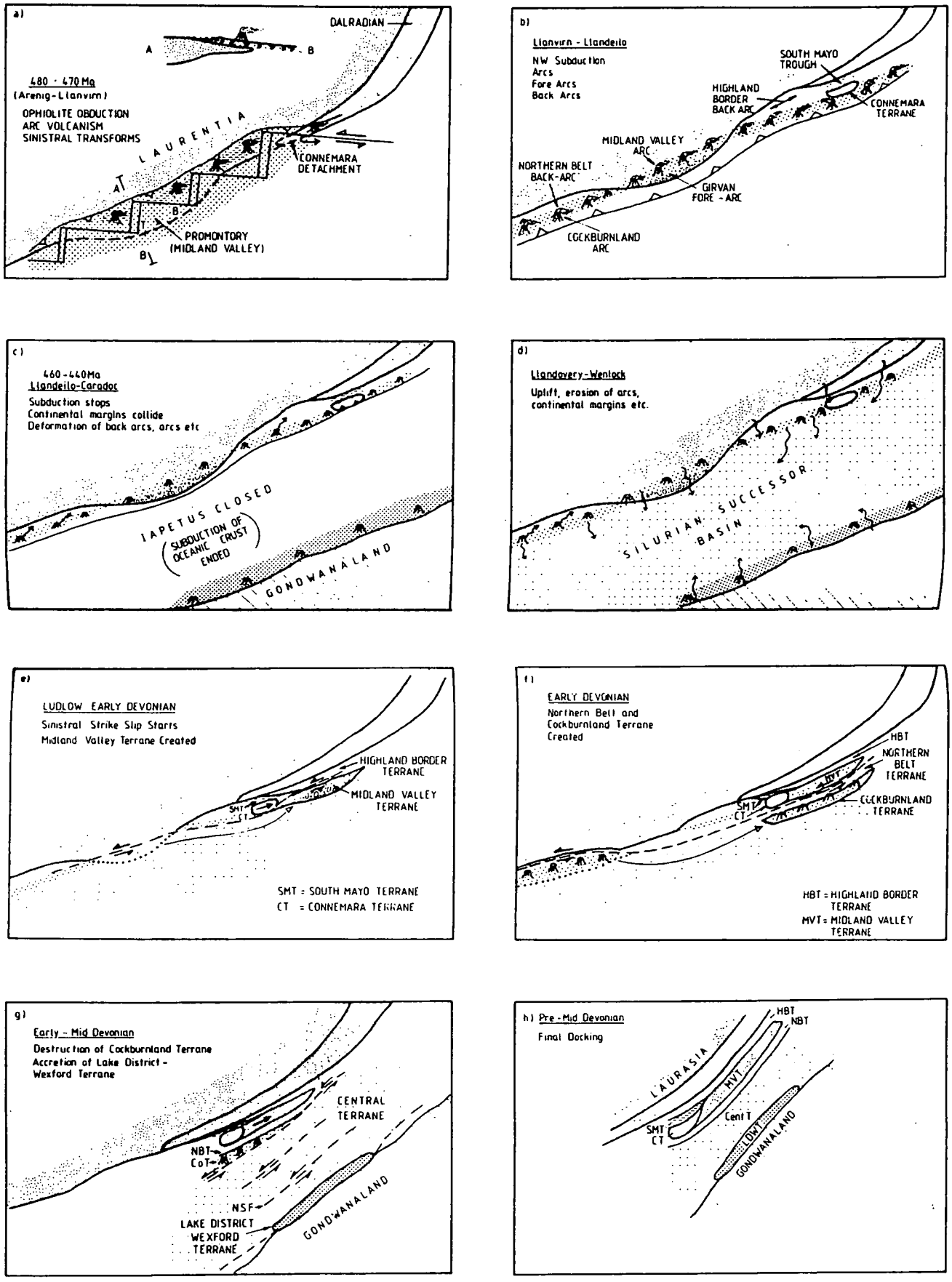

Fig. 1.4 (b) Highly stylised model for the evolution of Iapetus in the British Isles sector in the Arenig to mid-Devonian interval. From Hutton (1987).

subsidence, has been debated by **Leeder(1982)** and **Bott et al.(1984)** and summarised by **Johnson(1984)**. The structural trends which defined the blocks and basins of Northern England at this time were inherited from the Caledonian orogeny and the faults reactivated as a result of the north-south tension which prevailed, particularly during the Dinantian. This gave rise to the pattern of east-west basins which subsided between granite supported blocks and which is still reflected in the present-day geology (see **fig. 1.2**).

Leeder suggested that the strong differential subsidence during the Dinantian was due to an initial stretching event, along the lines of the **MacKenzie(1978)** model, and attributed the later regional subsidence to the thermal subsidence effect which would be expected to follow such stretching. However, Bott et al. argue that thermal subsidence alone cannot explain the subsidence rates indicated for the Namurian and Westphalian in the central Pennines, also that the subsidence rate increased into the Westphalian instead of showing exponential decay, which would be expected of thermal subsidence.

The cause of the early Carboniferous crustal tension has been attributed to the "slabpull" force (or trench suction) which arose from the subduction taking place to the south as the Hercynian marginal sea (Rheic Ocean) was closing. Bott et al. believe that the crust was stretched differentially, the lower, more ductile crust being stretched more and subducted faster than the brittle upper crust. The upper crustal response to this was to form blocks and troughs by normal faulting. The later regional subsidence would be the isostatic response to the thinning of the lower crust and to some extent, thermal subsidence as the lithosphere cooled and contracted.

As the Carboniferous came to an end, the tensional regime evolved into a compressional regime due to continental collision (the Variscan orogen) to the south. This caused mild inversion of the Carboniferous basins, with some gentle folding and uplift of the area (**Fraser and Gawthorpe, 1990**).

1.2.3 The Mid-North Sea High

The Mid-North Sea High is a major structural high, trending roughly east-west from the Northumberland coast, which is known to have formed a barrier between the Northern and Southern North Sea basins from the early Permian to the Early Cretaceous (**Ziegler,1982**). It was a relatively

continuous feature across the North Sea until the opening of the Central Graben, which now splits it into the Mid-North Sea High and the Rynkobing-Fyn High.

The High spent some time from the end of the Carboniferous as an emergent feature, so the thickness of sediments from then until the Middle Jurassic were considerably reduced compared to the neighbouring Northern and Southern North Sea basins. **Donato et al. (1983)** have proposed the presence of granite bodies within the Lower Palaeozoic basement of the High, to explain the gravity anomalies. These granites would have contributed to the faulting and stability of the High over the period in which it had greatest effect.

However, the High was not a complete barrier between the North and South sedimentary basins. **Jenyon et al.(1984)** identified one or more passages across the central part of the High, (off the eastern end of MOBIL line 1) which formed a connection between the Northern and Southern Zechstein basins. More significant for this study is the suggestion from sedimentological and geophysical evidence of a Permian "North-west Passage" across the Mid-North Sea High which ran close to the present coastline **(Smith and Taylor, 1989)**. The inferred Permian outline of the High is shown in **Fig. 1.6.** The passage is believed to have been filled by later Zechstein deposits so that its effect on later sedimentation was minimal. Smith and Taylor suggest that the channel was bounded to the east by a roughly N-S fault, shown in **Fig. 1.7.**

Although relatively little is known so far about the detailed structural history of the Mid-North Sea High, it has obviously played an important role in the development of the offshore sedimentary basins since at least the Early Permian. Its emergence may be connected to the effect of the Variscan orogeny and the resulting uplift which also inverted the Northumberland basin **(Fraser and Gawthorpe, 1990)**. The Northumberland basin and the Mid-North Sea High now seem to be part of the same structural unit, although the Upper Carboniferous sediments are known to thin out to the east onto the High.

The fault proposed by Smith and Taylor **(Fig. 1.7)** may therefore define the boundary between the thicker Upper Carboniferous sediments of the basin against the Middle Devonian to Lower Carboniferous sequence which is present on the High. This fault occurs directly beneath the western end of MOBIL line

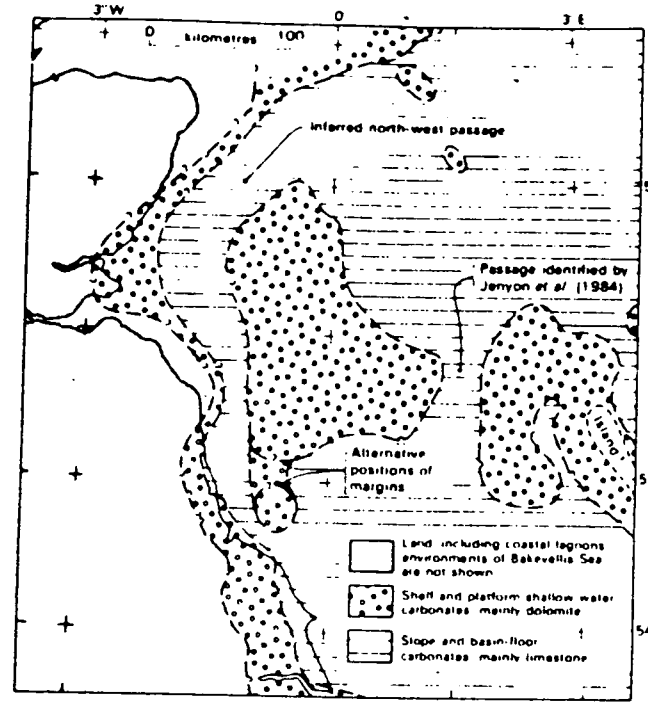

Fig. 1.6 Tentative palaeogeographical reconstruction of the Mid North Sea High during carbonate sedimentation of English Zechstein cycle 2, showing position of inferred passage or channels. From Smith & Taylor (1990).

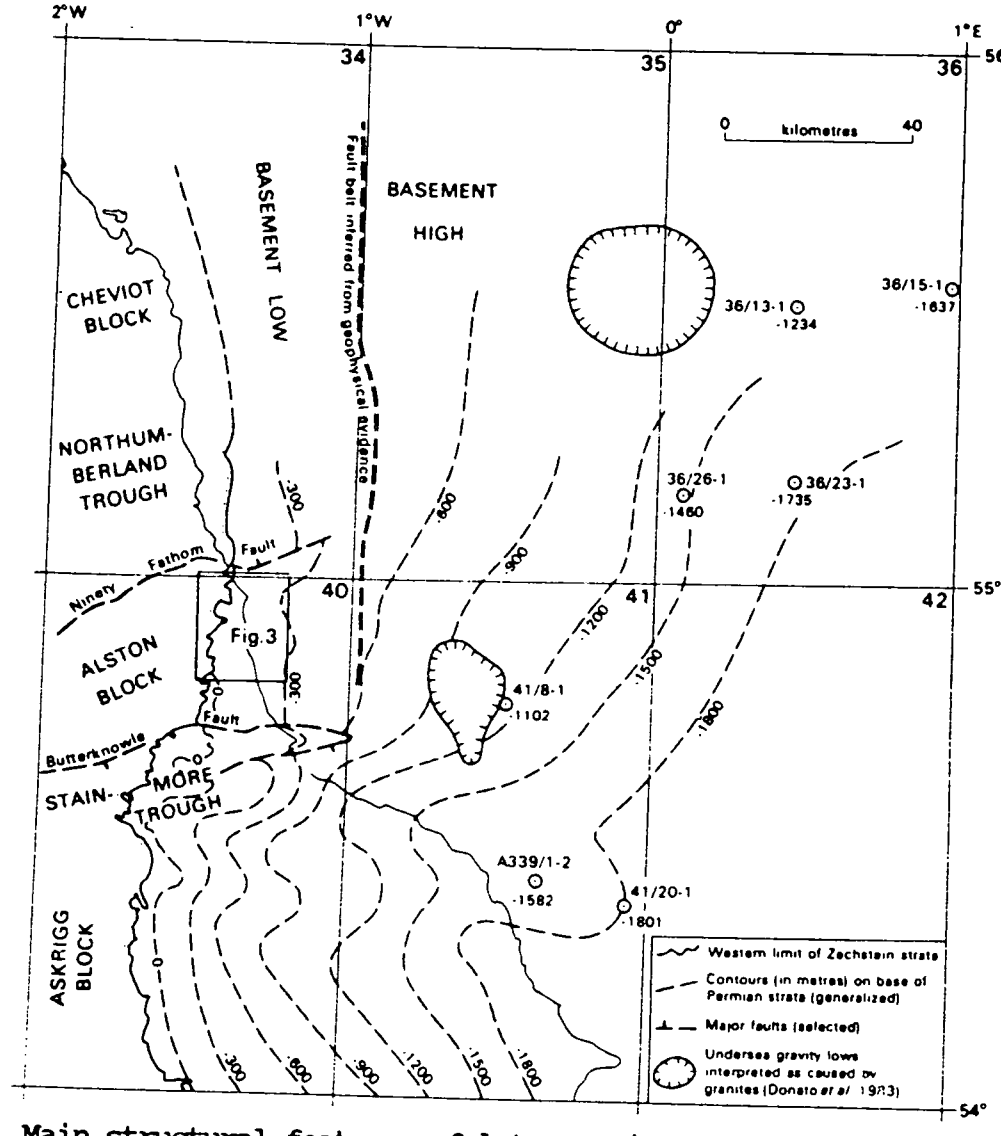

Fig. 1.7 Main structural features of late Permian and other rocks of the north-east coastal area of England. Note the proposed fault. From Smith & Taylor (1989).

1 shots, and so it may be detected by both the normal-incidence and wide-angle seismic data of this experiment. This had important implications for the interpretation and modelling of the datasets, as will be seen from later chapters of this thesis.

1.2.4 The geology of the Southern North Sea

MOBIL line 5 runs approximately ENE from the North Humberside coast onto a complicated system of highs, basins and inverted basins, as can be seen from **Fig. 1.2.** A rough sketch of the history of this region derived mostly from **Glennie (1986)** follows, and is summarised in **Fig. 1.8.**

Following the Caledonian orogeny of the Lower Palaeozoic, the Variscan orogeny completed the building of the supercontinent Pangaea. It was within this supercontinent that the subsidence of the Northern and Southern North Sea basins (separated by the Mid-North Sea High) took place during the Permian. The initiation of the Viking and Central Grabens took place in the late Permian/Triassic, when most of North-west Europe was undergoing extension and graben formation; maximum graben development was reached in the late Jurassic/early Cretaceous, coinciding with the opening and development of the Central Atlantic spreading centre and the sea-floor spreading which parted Laurasia from Africa, producing the Tethys Ocean.

This graben development ceased when initial sea-floor spreading in the North Atlantic parted Laurasia into North America and Europe. By the Tertiary, sea-floor spreading in the North Atlantic was taking place along the present Mid-Atlantic Ridge and the whole of the North Sea was undergoing regional subsidence. Also at this time, the closure of the Tethys Ocean between Africa and Eurasia was causing the Alpine orogeny.

The part of the southern North Sea basin which is sampled by MOBIL lines 4 and 5 has been affected by the above tectonic events far more than the stable Mid-North Sea High which is crossed by lines 1 to 3. The southern region now consists of a relatively stable basin margin (the North Dogger, Offshore Durham and East Midland shelf areas), two inverted basins (the Sole Pit Trough and the Cleveland Hills), and the Silver Pit basin.

Most of the faults which have shaped the present day geology are again inherited Caledonian

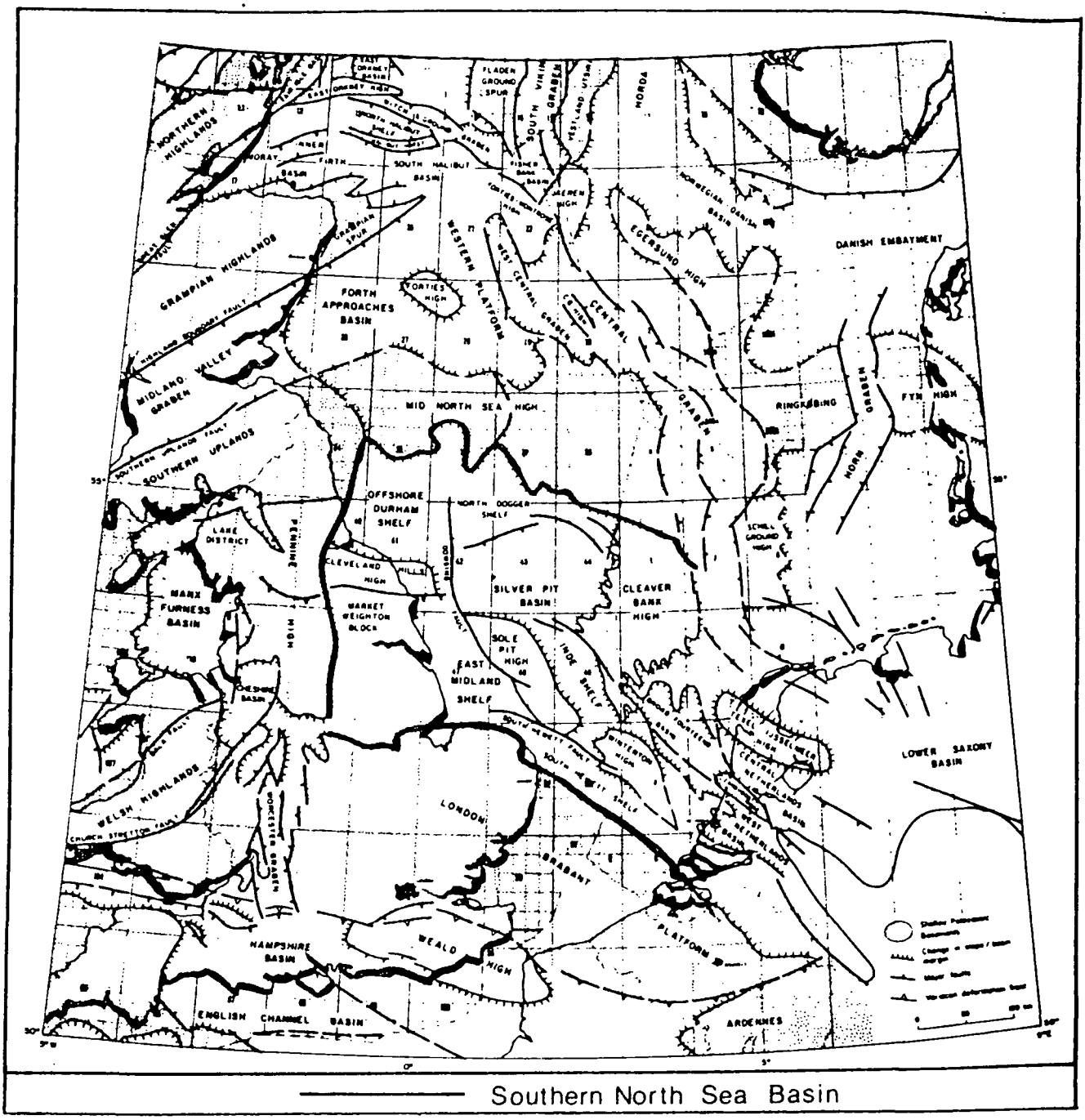

Fig. 1.8 Structural map of the Southern North Sea. From Glennie (1986)

NE-SW and NW-SE trends which have been reactivated in different roles during their history. The one of most interest to this study is the Dowsing Fault Zone which is crossed by both lines 4 and 5 (see **Fig. 1.2**). This seems to have played an important role in first the formation of the Sole Pit Trough (and possibly the Cleveland Hills Basin) and then later the two phases of inversion during the Late Cretaceous and the Mid-Tertiary. The recognition of flower structures (**Glennie 1986**) and the vertical nature of the fault support the idea that considerable strike-slip displacement has taken place. **Van Hoorn (1987)** relates the Permian to mid-Jurassic subsidence of the Sole Pit Trough to late Hercynian pull-apart movements and the periods of inversion to reactivation of the existing faults in a transpressional sense.

The continuation of the Dowsing Fault Zone north of line 5 is variously mapped as continuing northwards (**Glennie,1986**) or running onto land into the Flamborough Head fault system (**Kent, 1975**). In fact, it is poorly known. The location of the Fault zone in **Fig. 1.2** is that postulated as a result of this study and will be discussed further in chapter 7.

1.2.5 The Market Weighton block

The Market Weighton block has been a relatively stable area since at least the Jurassic, causing reduced sedimentation from the early Jurassic to early Cretaceous period. **Bott et al.(1978)** have interpreted the cause of this stability as a granite in the underlying pre-Carboniferous basement rocks. This interpretation is reinforced by the regional gravity and magnetic data, although **Aveschough (1986)** has argued that the observed gravity anomaly would be consistent with the presence of a Carboniferous sedimentary basin instead.

The Market Weighton seismic network was installed to resolve this question from teleseismic data, and the existence of the network provided the opportunity to record wide-angle reflection data from the MOBIL lines 4 and 5 during the MOBIL survey. In fact, **Lewis (1988)** found that the delay times from the teleseismic data and the wide-angle data seem to support the hypothesis of an underlying granite.

The wide-angle recording at this location yielded high-quality records containing a great deal of information about the crustal structure (**Lewis 1988, Bassom 1988, Matthews 1989**) and has also shed

extra light on the interpretation of features visible on the line 1 wide-angle data.

1.3 The Caledonian Suture Seismic Project

The Caledonian Suture Seismic Project **(Bott et al, 1985)** was designed to obtain a picture of the velocity structure of the crust relatively uncomplicated by major lateral structural features. For this reason, it was located across Northern England approximately parallel to Caledonian strike, just south of the proposed Iapetus Suture. The map in **Fig. 1.9** shows the layout of the experiment, which used over 60 land recording stations located across the country at 2 km spacing and explosive, sea-bottom shots fired at 4 km spacing: 27 in the Irish Sea and 30 in the North Sea. Two shots were also detonated on land, around the middle of the profile.

The fieldwork was co-ordinated and the preliminary interpretation of the data carried out by **Green(1984)**, who concentrated on the shallow structure to be extracted from the data. His interpretation of the shallow structure beneath the North Sea is shown in **Fig. 1.10**. The deep crustal interpretation and synthetic seismogram modelling was carried out by **Lewis(1986)**, whose model is shown in **Fig. 1.11.** The positions of the stations re-occuppied during the MOBIL programme are marked, with the location of the airgun profile. This model, and the near-surface interpretation of Green were used as a starting model for the MOBIL line 1 data. This will be described further in chapter 6.

The CSSP P-wave data were of excellent quality for an experiment of such shot and station spacing; the signal to noise ratio of the recordings is very good (see section in **Fig. 4.10**). However, the data has been completely superseded by the high resolution of the MOBIL dataset. Most of the phases picked from CSSP were picked very differently on the MOBIL records.

Nevertheless, the S-wave data recorded from some CSSP stations were excellent, and since the MOBIL airgun shots did not generate S-waves, it is the only S-wave information available from the area. Although some preliminary interpretations were made from the S-wave records before the acquisition of MOBIL (described further in chapter 7), full use has not yet been made of them. Using the P-wave model established from the MOBIL data, a further interpretation of CSSP S-wave records would be a very worthwhile exercise.

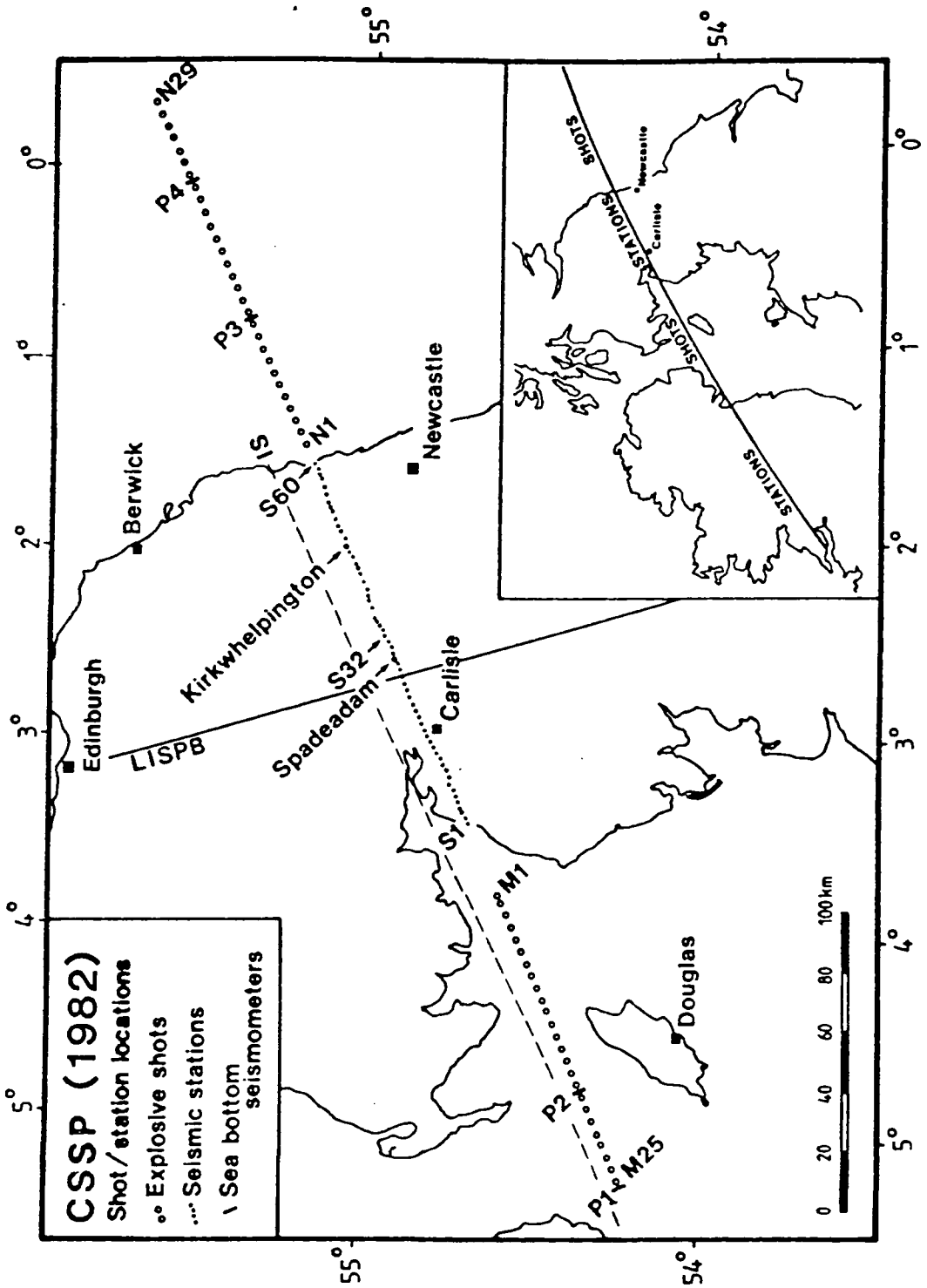

Fig. 1.9 Location of the Caledonian Suture Seismic Project of 1982. From Green (1984).

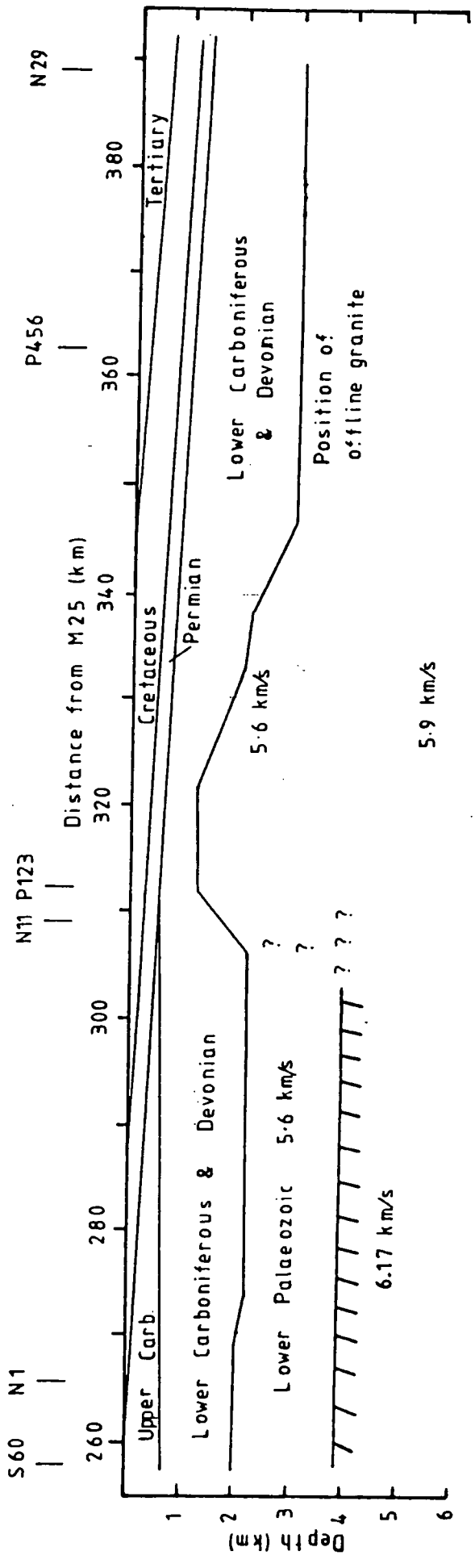

Fig. 1.10 Interpretation of the upper crustal structure beneath the North Sea from the CSSP. From Green (1984).

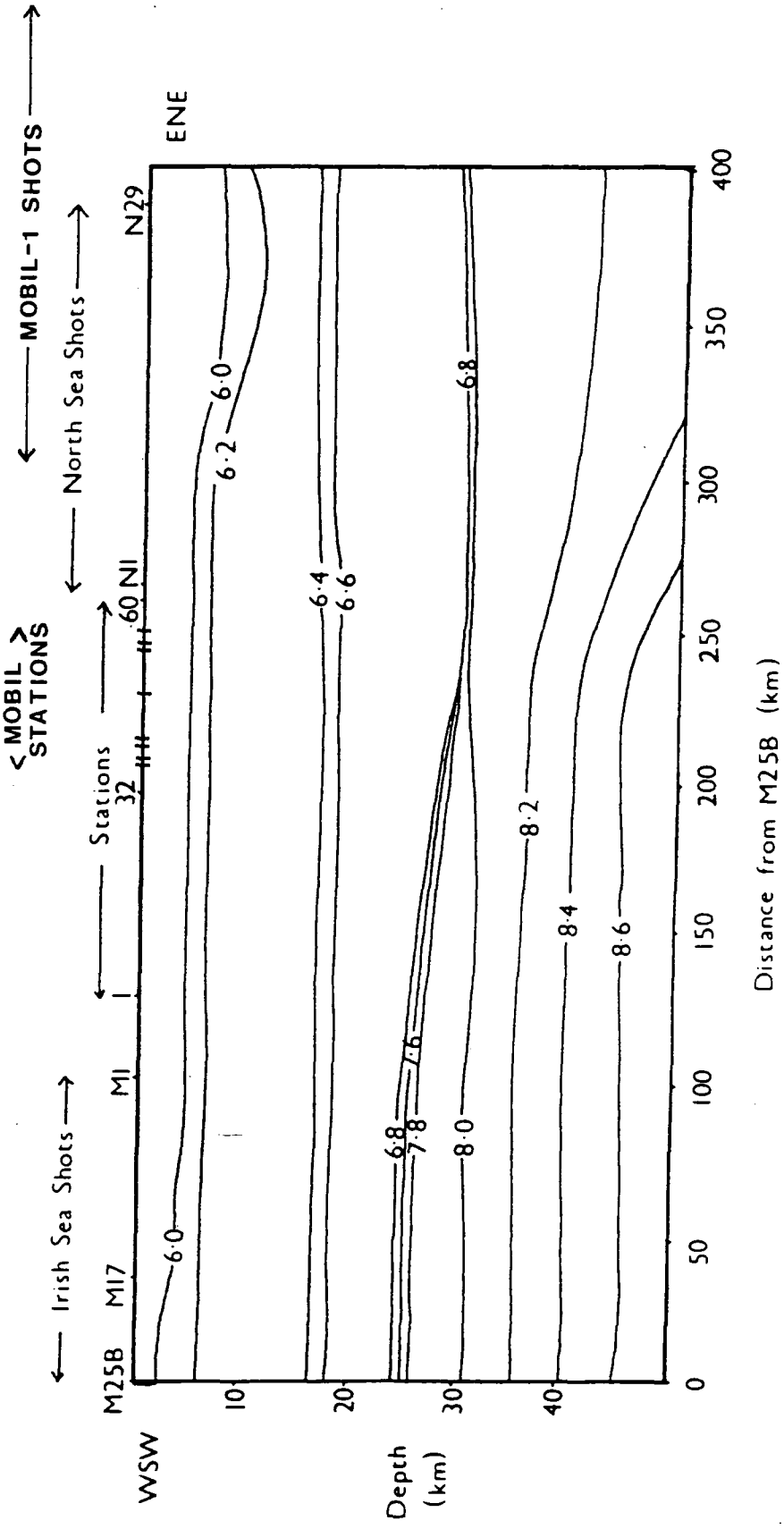

Fig. 1.11 Final laterally varying model obtained from the CSSP by Lewis (1986).

1.4 Other regional seismic surveys

Previous refraction/wide-angle reflection surveys in this area and their interpretations are described by **Lewis(1986)**, and include LISPB, shot approximately north-south to cross Caledonian strike, and NERL, which was recorded from the explosive shots of LISPB. **Fig. 1.12** shows the locations of these experiments relative to MOBIL-CSSP. These interpretations were incorporated, where possible, into Lewis' model for the CSSP data. **Collette et al (1970)** shot several refraction profiles in the region of lines 4 and 5, providing a starting model for **Matthews'(1989)** interpretation of line 5.

The most important development since the CSSP was carried out is the accumulation of so much deep normal-incidence seismic reflection data around the UK by BIRPS. Normal-incidence profiles of particular interest to this study include WINCH, which was shot in the Irish Sea across the line of Irish Sea explosive shots used for CSSP, and NEC, the North East Coast profile shot almost parallel to the Northumberland coast, approximately 20 km offshore.

Both these profiles show the usual transparent upper crust beneath surface sedimentary basins, reflective lower crust and fairly clearly defined Moho. However, they also image a northward-dipping lower crustal reflector in both the Irish and North Sea, just north of the location of CSSP and now MOBIL line 1. This is especially distinct on NEC and has been interpreted by **Klemperer and Matthews(1987)** as the buried trace of the Iapetus Suture. **Freeman et al.(1988)** recognise four different lower crustal terrane types along the length of NEC (from Hartlepool to Montrose), shown in **Fig.1.13.** The dipping reflector, or Iapetus Suture, forms the boundary between two terrane types: the Southern Uplands subduction complex, which would have constituted the continental margin of Laurasia, and the "Lake District" crust, which would have been the southern continent, Gondwanaland.

The MOBIL programme was shot to investigate further these different types of lower crust, particularly the suture zone. Line 2, shot parallel to and only 10 km away from NEC, was recorded to 24 s TWTT in order to see if the "suture" reflector penetrated the upper mantle on a migrated record section. Line 3 was shot 70 km from NEC, and again parallel in order to give further along strike information about the "suture". This dataset brings the total number of BIRPS profiles which cross the Iapetus suture

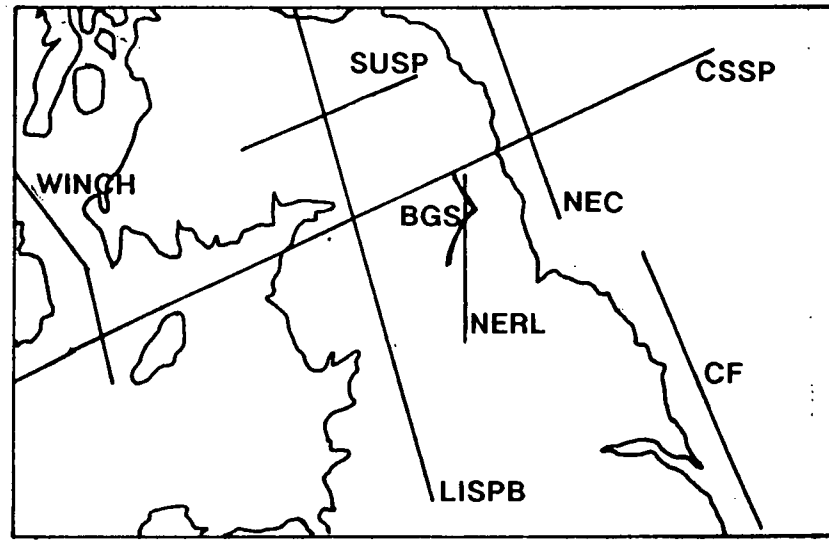

Fig. 1.12 Previous crustal seismic surveys carried out in Northern England in addition to the CSSP. SUSP: Hall et al. (1983); NERL: Swinburn (1975); LISPB: Bamford et al. (1978); CF: Collette et al. (1970); WINCH: Brewer et al. (1983); NEC: Freeman et al. (1988); BGS: Chadwick et al. (1989).

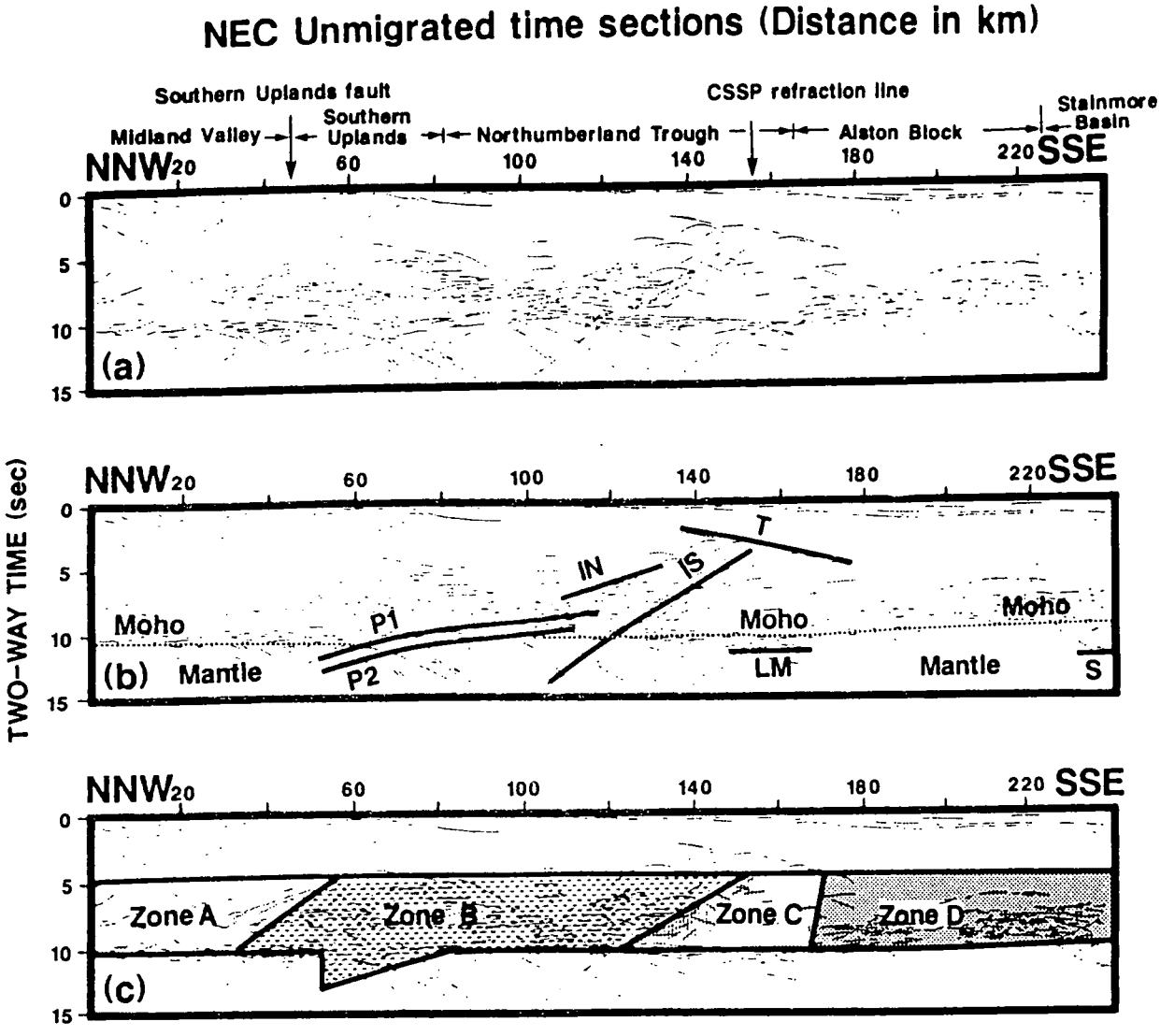

Fig. 1.13 NEC unmigrated time section and interpretation by Freeman et al. (1988).

in the UK to six (**Fig.1.14**): the others include NSDP, WINCH and WIRE (**Klemperer et al.,1990**).

MOBIL line 1 essentially provides a "strike" section over the Caledonian crust, with which to tie in the other "dip" sections over the suture. The wide angle recording of these profiles, to very high resolution, enables the derivation of the velocity structure to tie into the reflection interpretation.

1.5 High-resolution wide-angle reflection data

Although MOBIL was the first fully coincident seismic experiment of its kind in the UK, there has been an increasing trend in other countries to decrease either shot or receiver spacing in wide-angle reflection experiments. "Piggy-back" experiments during deep normal-incidence seismic reflection profiles, particularly those shot across land, have also become increasingly popular. Some of the most imaginative piggy-back experiments have been carried out by groups working with DEKORP in West Germany (**Bittner et al.,1987**) generating large wide-angle datasets to which various new inversion and processing methods have been applied.

One of the first experiments to use airguns for recording wide-angle data was EUGENO-S, shot in Sweden in 1984 (**Lund et al., 1987**) with great success. The increased resolution of the data, both spatially and temporally, means that many relatively low-amplitude crustal arrivals are correlated on record sections. Airgun shots were also used for wide-angle experiments in Maine, U.S.A. (**Hutchinson and Klitgord, 1986**) and during the GLIMPCE programme shot in the Great Lakes in 1986 (**GLIMPCE Seismic refraction working group, 1989**).

The ease with which the coincident wide-angle and normal-incidence recording of marine seismic profiles may be carried out and the relative inexpensiveness of the operation (compared to the cost of the normal-incidence acquisition) has led to a number of further similar experiments being planned. Since the acquisition of MOBIL, similar experiments have been shot off the coast of Alaska, TACT MCS and EDGE MCS (**Moses et al. 1989, Brocher et al. 1989**), and central California; in 1989, BIRPS shot a large coincident experiment in the Gulf of Bothnia and the Baltic (BABEL) which also appears to have been very successful.

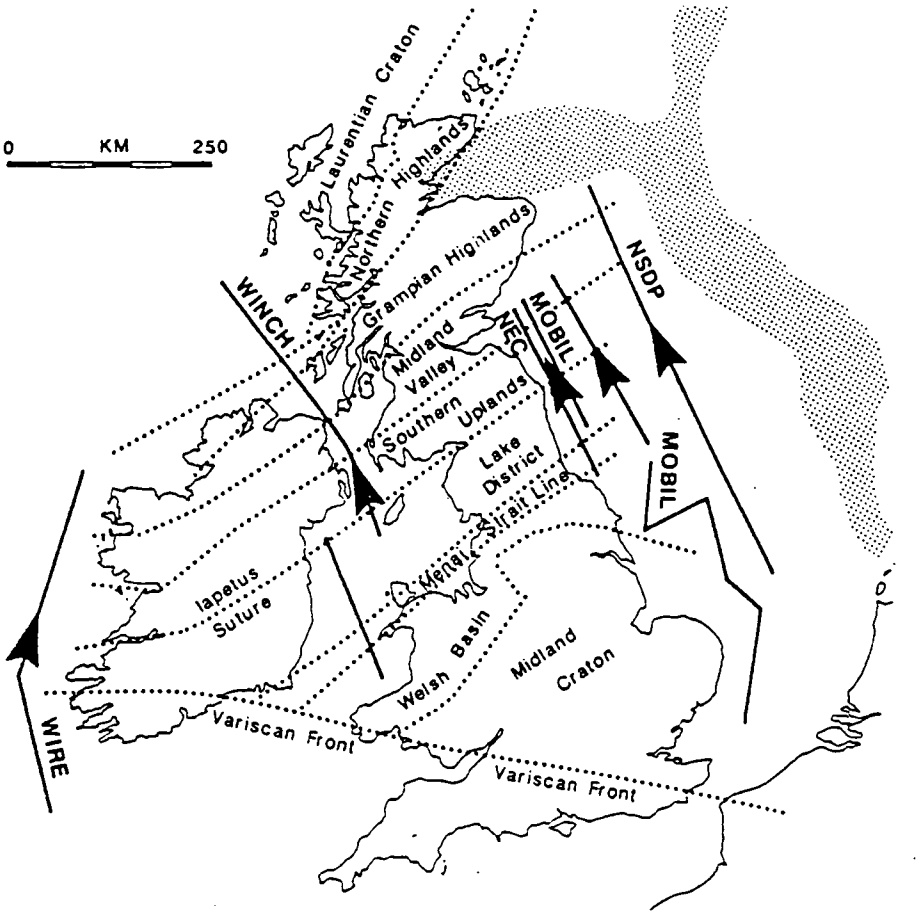

Fig. 1.14 Location of BIRPS profiles around the British Isles which cross the "Iapetus Suture", from Klemperer et al.(1990). Arrows represent the intersection of the suture and reflect its dip.

CHAPTER 2 : DATA ACQUISITION

2.1 Introduction

The fieldwork for this study was carried out in June 1987, when Durham was given two weeks notice of BIRPS' intention to carry out deep reflection profiling in the south eastern North Sea, made possible by Mobil's gift of two weeks' shiptime on the research vessel M/V Mobil Search. Hence the programme was named Measurements Over Basins to Image the Lithosphere (MOBIL).

As mentioned in chapter 1, line 1 was shot along the exact location of the explosive shots of the Caledonian Suture Seismic Project and so this was an ideal opportunity to re-install some of the CSSP seismic stations to record simultaneous wide-angle and normal-incidence reflection seismic data. The land recording network in Northumberland has been called MOBIL-CSSP, and provided a linear wide-angle reflection profile as far as line 1 was concerned and fan profiles with respect to lines 2 and 3. The installation of seismic stations was helped considerably by the careful notes of the CSSP sites which were produced by A.S.P.Green in 1982. These saved the large amount of time usually required to research favourable geology, land ownership and noise conditions.

Immediately prior to notification of the MOBIL programme, a wide-aperture seismic network had just been installed across the Market Weighton area by Dr. R.E. Long, J.F.B.D. Fonseca and the author, initially designed to study the deep structure of the area using teleseismic data. As it turned out, the network was suitably positioned to record wide-angle data from the MOBIL profiles 4 and 5, shot off the coast of Humberside and North Yorkshire. This network was therefore called MOBIL-MW and its installation proved to be good practice for the hurried installation of the more important Northumberland seismic stations in only one week between the completion of the Market Weighton exercise and the commencement of the MOBIL shots.

Shooting commenced on June 6th 1987 with line 1. Profiles 1 to 5 were recorded by both networks (**Fig. 2.1**) and the eastern (Morpeth) group of Northumberland stations was left running in the

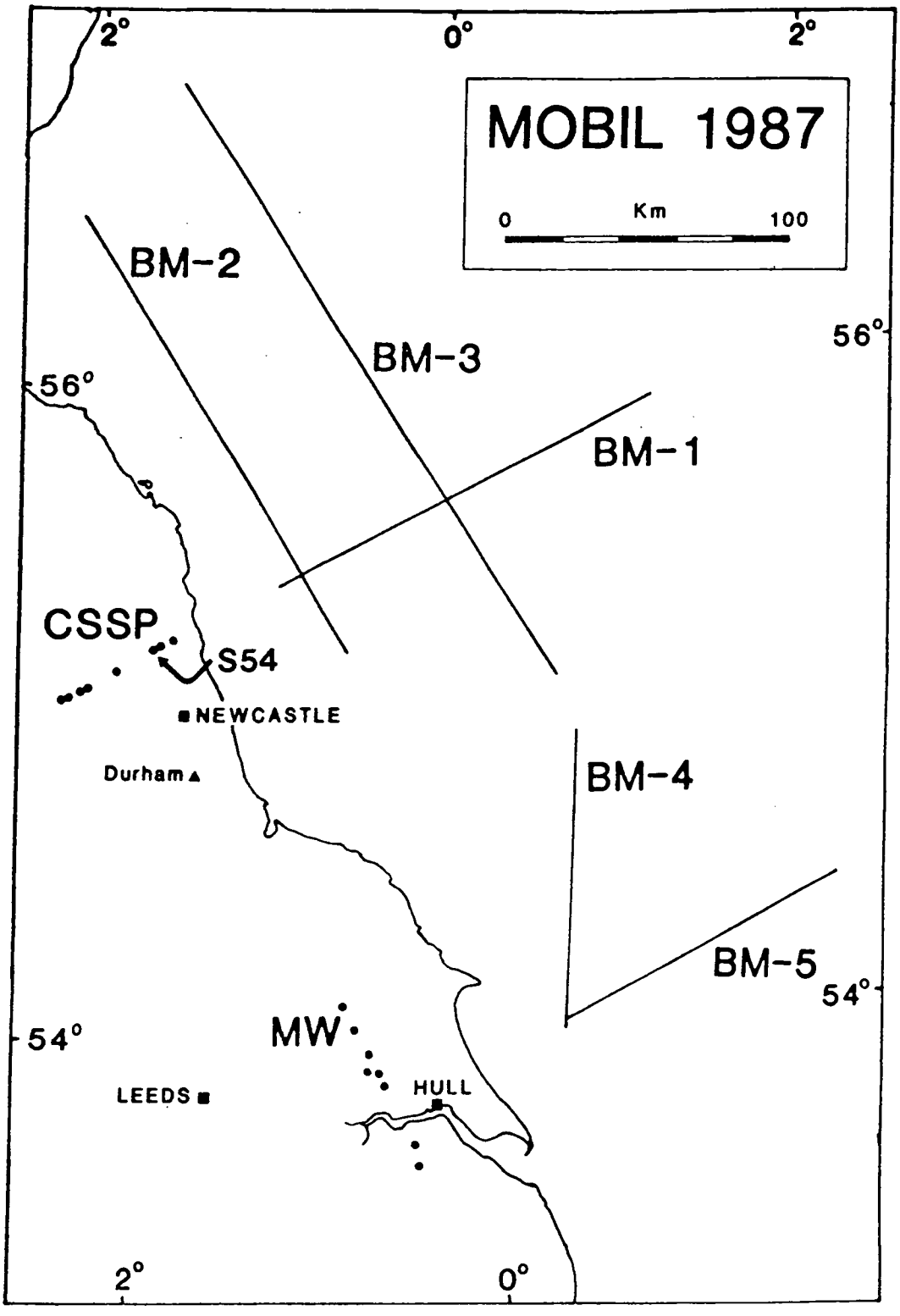

Fig. 2.1 Map of Northern England showing locations of Durham's wide-angle recording seismic stations relative to the BIRPS MOBIL normal-incidence profiles. CSSP: re-occupied CSSP station locations; MW: temporary Market Weighton seismic network.

hope that some records might be visible from the planned line 10, further out into the centre of the North Sea, although in the end this line was not shot.

2.2 Seismic recording stations

In Northumberland, eight of the original CSSP sites were chosen for re-installation, using the CSSP records to select those which were least noisy and in the optimum distance range for crustal arrivals. The stations were located in two groups: one close to Morpeth, not far from the coast (stations 54,55 and 57), the other near Bellingham in the Northern Pennines (stations 36, 37,39 and 40). In-line horizontal seismometers were installed at stations 55 and 40 to provide two-component coverage in case good shear waves were observed. An extra station, 47, was installed at the last minute between the two groups to to improve coverage. As it turned out, the records from this station played a very important part in the interpretation of the dataset, providing coverage where there might otherwise have been a 30 km gap in information. The width of the whole network was approximately 45 km. These station locations are shown in detail on the map in **Fig 2.2.**

The original purpose of the Market Weighton teleseismic network was to attempt to establish whether the low density body giving rise to the gravity anomaly is a buried granite or a sedimentary basin (**Bott et al. 1978, Lewis 1988**). The network was therefore installed in a roughly north-south linear profile centred on the gravity minimum but extending beyond its limits.It stretched approximately 80km from Acklam (near Malton) in North Yorkshire to Brigg in Lincolnshire. One off-line station was located at Holme-on-Spalding-Moor, in the Royal Observer Corps observation bunker which was also used as the base station for the network. Approximate station locations are shown in **Fig. 2.1.**

All the Northumberland sites were located in rather isolated areas, although relatively easily accessed by road, and hence suffered little cultural interference. Station 36 was the noisiest locality since it was located on Forestry Commission property with a generator nearby which produced continuous 22 Hz noise. Site 54 was located at Beacon Hill in a field containing a herd of Highland Cattle and several sheep, but in spite of this, the records from this station were the best of all at the crucial periods. Station

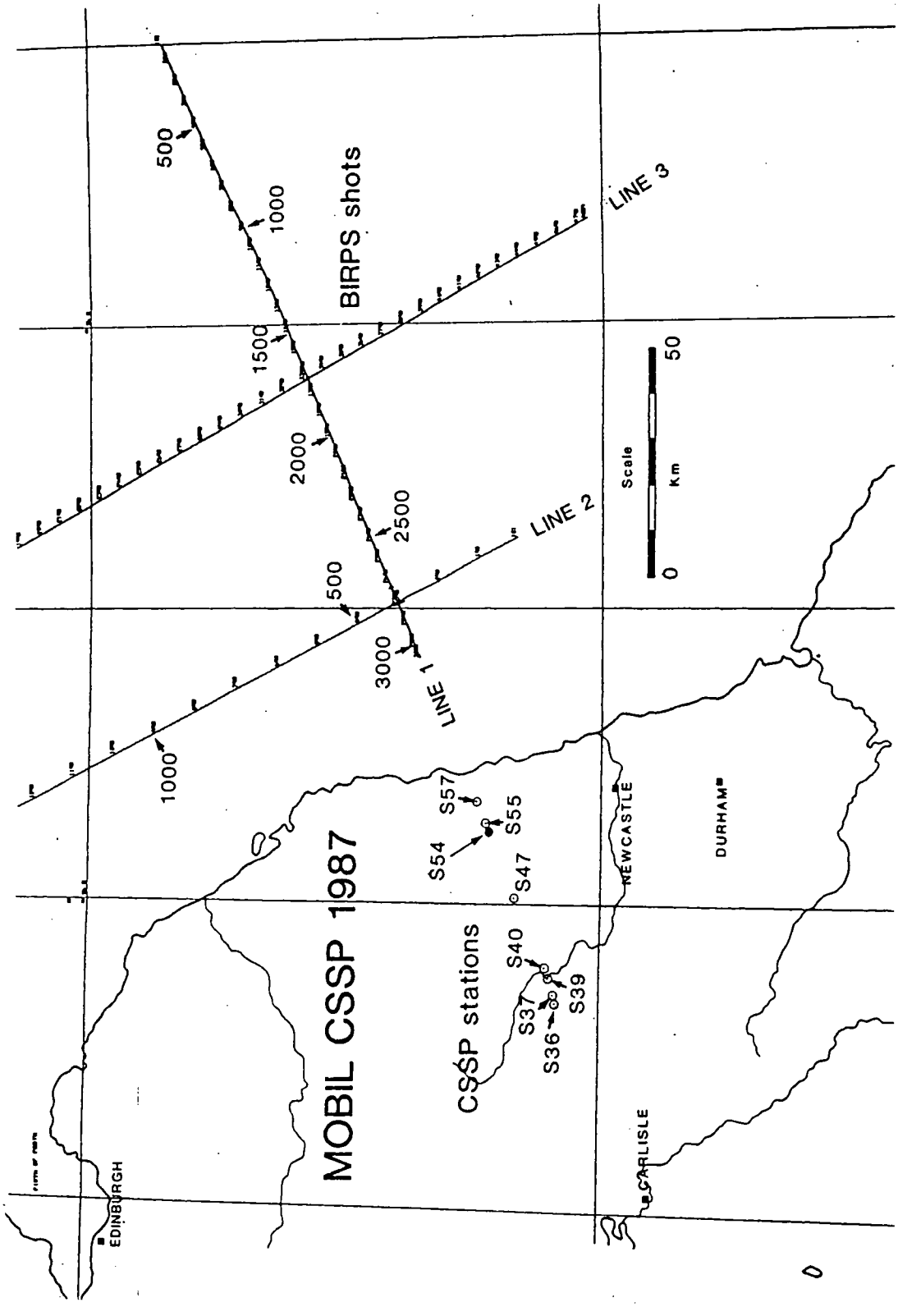

Fig. 2.2 Map of MOBIL-CSSP station locations across Northumberland.

47, the only CSSP station without a cemented base, also produced very good records, so the benefits of a cemented base are debatable. Station 55 was the noisiest of all, since the base of the seismometer pit was clay - bedrock was more deeply buried at this location. At all other sites, bedrock was encountered at a convenient depth of between 1 and 3 feet.

The Market Weighton sites were generally noisier than the CSSP sites. This was mainly due to the local geology which was Upper Cretaceous chalk, a notoriously bad horizon for seismic coupling and propagation of cultural noise. Also, since the region is much more densely populated and more industrial than Northumberland the sites could not be so isolated as those in CSSP.

2.3 Seismic Equipment

Both networks used Geostore equipment, with the network of outstations radiolinked to a central FM Geostore recorder. The equipment used in the CSSP part was loaned by the NERC seismic equipment pool, although this was only possible because of a delay in the RESTE project in Portugal (Fonseca 1989), for which the equipment had initially been loaned. The equipment used at Market Weighton is jointly owned by the Universities of Durham and Liverpool.

Each outstation used a Willmore Mk III seismometer, an amplifier modulator, a radio transmitter, an aerial and a 12-volt battery as power supply. Two Geostore recorders were used in Northumberland, one based at Hebron Hill Farm, near Morpeth, the other at High Carry House near Wark. Both locations provided good shelter for the equipment : the base of a water tank at Hebron Hill and a barn at High Carry House. Each base station consisted of the Geostore recorder itself, an MSF radio, aerials and receivers to receive the incoming signals from outstations and two 12 volt batteries for power.

Each seismic station was installed by digging a pit down to bedrock (between one and three feet deep), lining this with 12-inch PVC piping and (with the exception of the Market Weighton network and station 47 in Northumberland) cementing the base of the pit to maximise coupling. An aerial was erected nearby with a transmitter strapped to it, connected to the seismometer and amplifier modulator within the pit and to a battery buried in a plastic bag. The pit would be covered with a board wrapped in polythene

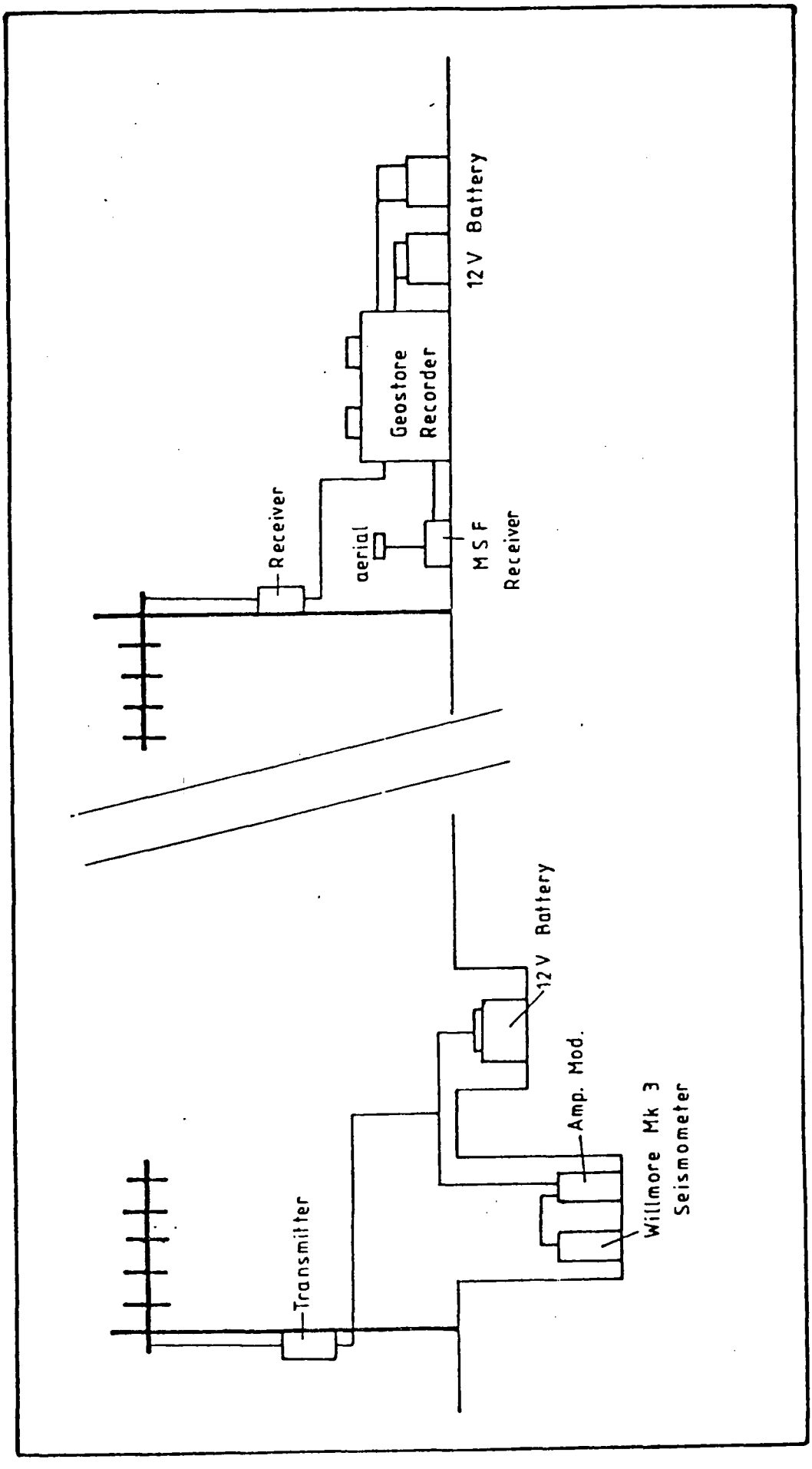

Fig. 2.3 Diagram of Geostore recording apparatus, from Green(1984).

and turf placed over this for protection. The arrangement of this apparatus is depicted in Fig. 2.3.

The Geostore recorder is a 14-channel F.M. recorder with two flutter tracks, one channel recording VELA time code generated internally and eleven data channels. One of the data channels was employed to record the MSF radio time signal, by which to calibrate the recordings to Universal Time. The analog data was recorded on 0.5 inch magnetic tape at 15/160 inches per second, which was considered adequate for this experiment since that provided a bandwidth of 0-32 Hz and a recording time of 2 to 3 days per tape. The suitability of this bandwidth is discussed in the next chapter. The recorder accepts F.M. data with a carrier frequency of 676 Hz and a maximum deviation of 40%. The recorders were left running continuously throughout the experiment except for the short breaks required for tape changes.

It was possible to check the signals on the geostore tape heads by means of an inbuilt test box. This made it possible to listen to each channel individually and to detect noise problems and equipment failures such as short-circuiting on aerials, breakdown of a transmitter or receiver, battery failure or damage at the outstation from man, beast or the elements. There was a failure of the Hebron Hill geostore for about 30 minutes towards the end of the recording of line 1, which caused the loss of 5 km data, but apart from that there were only minor equipment failures at this base station which were easily fixed. Unfortunately the Geostore recorder used at Wark had a faulty internal VELA clock, which meant that although recording was not affected, replay and digitisation of the tapes (as described in the following chapter) proved problematic. There were few problems at the CSSP outstations.

In the Market Weighton network, all equipment worked satisfactorily until the day before the shooting of line 4, when the Geostore itself broke down. Since by this time all the profiles off the Northumberland coast had been shot, the recorder from Wark was rushed down overnight to the Market Weighton base and installed in time to record lines 4 and 5. The only problem with this development was that the clock problem on that geostore was also transported. This meant that the replay and digitisation of the Market Weighton dataset was also problematic. One of the outstations, Station 5, was regularly disrupted by the harvesting and ploughing of the field in which it was located, but fortunately only after the MOBIL programme had finished.

The amplifier modulators amplify and frequency modulate the seismometer signal to give the full 40% deviation of the carrier frequency in the range 250mV to 0.25mV (1-10 on the instrument). During the MOBIL-CSSP experiment, most gains were set to 7, suitable for quiet sites, with only stations 55 (horizontal) and 54 requiring lower gains due to noisier conditions. All MOBIL-MW sites were set to gain 6.

The frequency of the UHF radio links was between 458 and 459 MHz with 25 kHz band separation. All the MOBIL CSSP sites except that at station 40 were linked in this way to a base. The Hebron Hill base received the signal from stations 47, 54, 55 (horizontal and vertical) and 57; the Wark base was actually located at station 40 and was therefore directly connected to the horizontal and vertical seismometers installed there, but also received from stations 36,37 and 39. Most links had line of sight between receiver and transmitter. Station 40, used as a base station in the original CSSP experiment, was known to satisfy this condition but Hebron Hill was newly chosen as a location with both shelter for the recorder and line of sight to stations 54, 55 and 57. The fact that it probably also had line of sight to station 47 was a happy coincidence which decided the installation of station 47.

A table of recorded tapes, base station and outstation information from the MOBIL-CSSP experiment is to be found in Appendix A.

2.4 Marine shots

As previously mentioned, the airgun shots recorded by Durham were fired by M/V Mobil Search for the BIRPS deep normal incidence profiles. The source consisted of 60 airguns in four sub-arrays 58.8 m long,11 m apart with a total capacity of 9100 cu.in. It was actually operated at 8500 cu.in capacity, 1800 psi air pressure and 7.5 m depth during the MOBIL programme. The shot interval was 20 s, corresponding to 50 m spacing, for all the lines recorded at wide-angle except line 2 which was shot at 100 m (40 s) spacing.

The shotpoint times, according to the shipboard atomic clock, were recorded separately to the normal incidence data onto floppy disk. The West German radio time signal DCF-77, which transmits

Universal Time (UTC), was recorded on an auxiliary channel, alongside the normal-incidence data. This allowed synchronisation between land and sea recordings and proved crucial during playout of the wide-angle records, when it transpired that the ship's clock, by which the detailed shot times had been logged, had a tendency to jump almost whole seconds for no recorded reason. Hence all the shot times for line 1, listed in Appendix B, are 0.961 s early. This error was not discovered until comparison of the MOBIL CSSP wide-angle records with the original CSSP records was carried out. Initially the mistake was thought to be in the wide-angle recording or processing, which used the Geostore recording of MSF radio time code to calibrate to Universal Time (UTC). Since the playout of line 2 wide-angle recordings showed a difference of almost 1 s when correlated with line 1, it became evident that it was not a recording fault. Upon studying the BIRPS playout of DCF-77 triggered at the shot times, it was possible to determine that the clock jump was 0.961 s, and to correct the travel time picks from the wide-angle data by this amount. This is constant for the whole of line 1. Since line 2 is correctly timed, the clock must have been reset between the shooting of the two lines.

The shot times for line 3 are still unavailable due to the accidental deletion of the shipboard floppy disk on which they were recorded and only one paper listing of the line details exists. Lines 4 and 5, as described by **Lewis (1988)** and **Bassom (1988)** require correction of the shot times by 0.965 s.

Navigation and position location at sea was based on satellite TRANSIT/PADS and sonar DOPPLER/SPEEDLOG systems. It should be noted that the shot positions printed onto the floppy disc for seismic processing have not been reprocessed to allow for navigational drift. This means that at a few places on the record sections, there is a gap due to an update in the navigation system. The largest gap produced by this problem is 500 m, which affects the reduced travel time by 0.5/6.0 s, that is, 0.083 s. Since this is the maximum error produced by this effect, and is **of the same order of magnitude** as the picking error (see section 4.3.3), it does not cause great problems.

CHAPTER 3 : WIDE-ANGLE DATA PROCESSING

3.1 Introduction

As described in Chapter 2, the wide-angle seismic data from MOBIL were acquired in analogue form on magnetic tape, so the first step involved in processing the data was to convert it to digital form in order to transfer information to Durham's main frame computer. This was carried out in the Seismic Refraction Processing Laboratory, using the PDP-11 system to convert the data and write to digital tape.

These tapes were then transferred to the mainframe computer, an AMDAHL 470 (updated during 1988 to the more powerful AMDAHL 5860), which uses the Michigan Terminal System (MTS) operating system. On this system the data was demultiplexed, separated into individual shot records, sorted into common station gathers, corrected in various ways (for different gain settings, shot times and locations and station locations), filtered and then plotted.

Line 1 consisted of 3000 shots and line 2 of 1800, so compared to the traditional CSSP-style refraction survey, the quantity of data for processing was huge, and the existing Seismic Processing System (SPS) software written at Durham by D.L.Stevenson had to be adapted. Fortunately, this was not too time-consuming since the software was written very flexibly. The actual use of the programmes was very lengthy, however, due to the volume of the data. The MTS multi-user operating system is not the ideal system to use for this since by day it tends to be heavily used and therefore slow, and the nature of the work is not suited to batch jobs.

It took approximately 3 months to digitise, process and plot roughly the data recorded on the Hebron Hill Geostore from Line 1; Line 2 recordings at this base have also been fully processed, the final tidying up and plotting of the data being completed by E.P. Jarvis, who also carried out preliminary modelling of the profile (**Jarvis, 1988**). Full records are therefore available of lines 1 and 2 from stations 47, 54, 55 and 57. However, due to the problem with the internal clock of the Wark Geostore, only half of Line 1 as recorded at Wark has been completely processed and plotted, which alone was very time

consuming. This data includes the stations 36, 37, 39 and 40, the more distant group, and in view of the time-consuming nature of the work it was considered unnecessary to digitise further, since judging from the quality of the preliminary sections from the Hebron Hill stations at this offset, it did not seem likely that good records would be obtained beyond 150 km offset. However, on examination of the final record sections, the data quality does appear good enough to justify digitising the other half of the recordings in the future. The Wark recordings of Line 2 have not been processed at all to date, since the lesser quality of the line 2 data at the Morpeth stations compared to those of Line 1 does not give much hope of the records from Wark being worth the effort required to process them.

The Market Weighton recordings of profiles 4 and 5 were digitised, processed and plotted by S.A. Lewis and C. H. Bassom, who also made preliminary interpretations. Further modelling has since been undertaken by P.A. Matthews (**Lewis,1988, Bassom, 1988, Matthews, 1989**).

3.2 Digitisation of the data

3.2.1 Seismic Processing Laboratory Digitising Software

The wide-angle MOBIL recordings were digitised and copied to multiplexed computer tape in Durham's Seismic Refraction Processing Lab, using the PDP-11 system and software written for this purpose by D.L. Stevenson. The equipment consisted of a Honeywell FM tape deck, a jet pen recorder, a VT100 terminal, a Tektronics 619 graphics screen with bit pad and the PDP-11 which incorporates three disc drives and two digital tape drives. The three discs include a system disc (DL0), control disc (DL1) and the user disc (DL2) to which digitised data is written.

The programme used for the MOBIL data was **DIG2**, since this is able to digitise large blocks of data at once. The main limitation was the space on the user disc, which restricted the block sizes to approximately 40 minutes recording (equivalent to about 120 shots) time and eight channels, sampled at 100 Hz. The channels digitised were the 5 seismic data channels, the VELA and MSF channels for time code and the flutter track, also for time information from the carrier.

The digitising sequence is illustrated by the flow chart in **Fig. 3.1**. The analog field tapes were mounted on the Honeywell tape deck which is controlled by the system. DIG2 initially decodes the

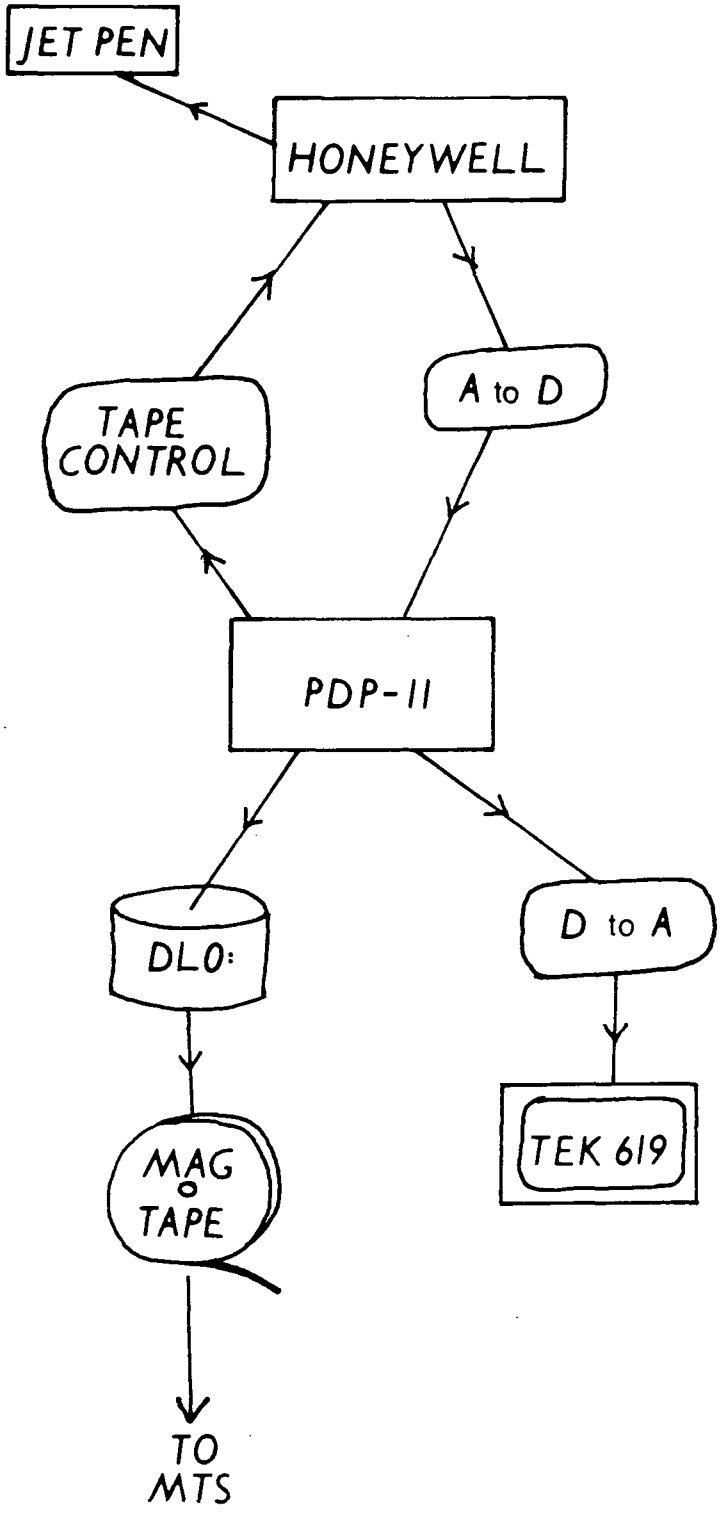

Fig. 3.1 Flow chart of digitisation procedure using the PDP-11 system.

VELA time from the analog tape, positions it at the start time specified by the user and proceeds to replay the tape at ten times the recording speed, in this case 15/16 inches per second, for the the specified duration. The data is converted from analog to digital form en route to the PDP -11, then written to disc and/or digital tape in multiplexed format. During the analog tape positioning and replay, the flutter track is used to estimate the tape time, not VELA. Two control files are required by the programme DIG2 to specify the analog tape parameters and the clock correction to be applied to the the VELA decoded time. The clock correction was obtained by playing out MSF (Universal Time, UTC) against VELA on the analog jet pen recorder.

Once digitised, the first 20 seconds of data in each block could be viewed using the programme **CHECK**, which would convert the data back to analog form to display all the digitised channels as raster lines on the Tektronics 619 graphics screen.

3.2.2 Digitisation of the Wark Geostore recordings

The analog tapes from the Hebron Hill Geostore, once the above technique was established and reasonably streamlined, were digitised without problems. However, as mentioned in Chapter 2, the Geostore used at Wark and also at Market Weighton had a faulty internal clock which meant that the VELA tape time could not be determined by the digitising software. The code did consist of a regular pulse, however, and `decoded' to read the same time everywhere on the tape, so it was possible to digitise by positioning the tape manually - using the jet pen and decoding MSF by hand - and specifying the start time for DIG2 as the erroneous time generated by VELA. Thus the system was manipulated into digitising the tape, since after the initial decode, the programme uses the flutter track for timing. This process was slightly more time-consuming than the digitisation of the Hebron Hill data due to the extra manual effort involved but could still be relatively streamlined. More problems were encountered with this data at the demultiplexing and editing stage, since the multiplexed files contained the wrong times. The way this was dealt with is described later in section 3.3.1.

3.2.3 Frequency response of the system

As mentioned in chapter 2, the bandwidth of the geostore recorder at the recording speed was 32 Hz. The anti-alias filter has a cutoff frequency of about 25 Hz, which narrows the window a little further. Whether this window is adequate for this type of data or not was checked by carrying out spectral analysis of some of the arrivals seen on the data.

Fig. 3.2 shows an analysis of the trace recorded at station 54 from shot 2633 of line 1. The arrival in this window is PmP, the wide-angle reflection from the Moho. From the amplitude-frequency plot, it may be seen that the dominant frequency is about 15 Hz. This therefore falls well within the window of the recording system. The smoothed version of this plot is sketched in **Fig. 3.3.**

However, there is considerable energy at above 25 Hz, which is beyond the -3dB point of the playback equipment and therefore being suppressed. A quick calculation of the original amplitude-frequency response for some of these suppressed frequencies produces the dotted curve on **Fig. 3.3.** From this it may be seen that the spectrum of the data has a gentle slope and a considerable amount of higher-frequency information has been eliminated by the recording system and the playback system used.

3.3 Main frame processing

3.3.1 Processing sequence

The flow chart in **Fig. 3.4** shows the sequence of processing carried out on the digitised tapes of the wide-angle data. The names in boxes correspond to the programmes used during the sequence - most being SPS programmes written by D.L. Stevenson. The SPS system was developed to enable convenient handling of seismic data, using a standard disc file format for the time series data known as **Trace Data** (TD) format, which is similar to SEG-Y format. The data may thus be handled on a trace-by-trace basis by each programme using routines stored in subroutine libraries. The system presents a user interface independent of the operating system since all system dependent routines are located in a system dependent library.

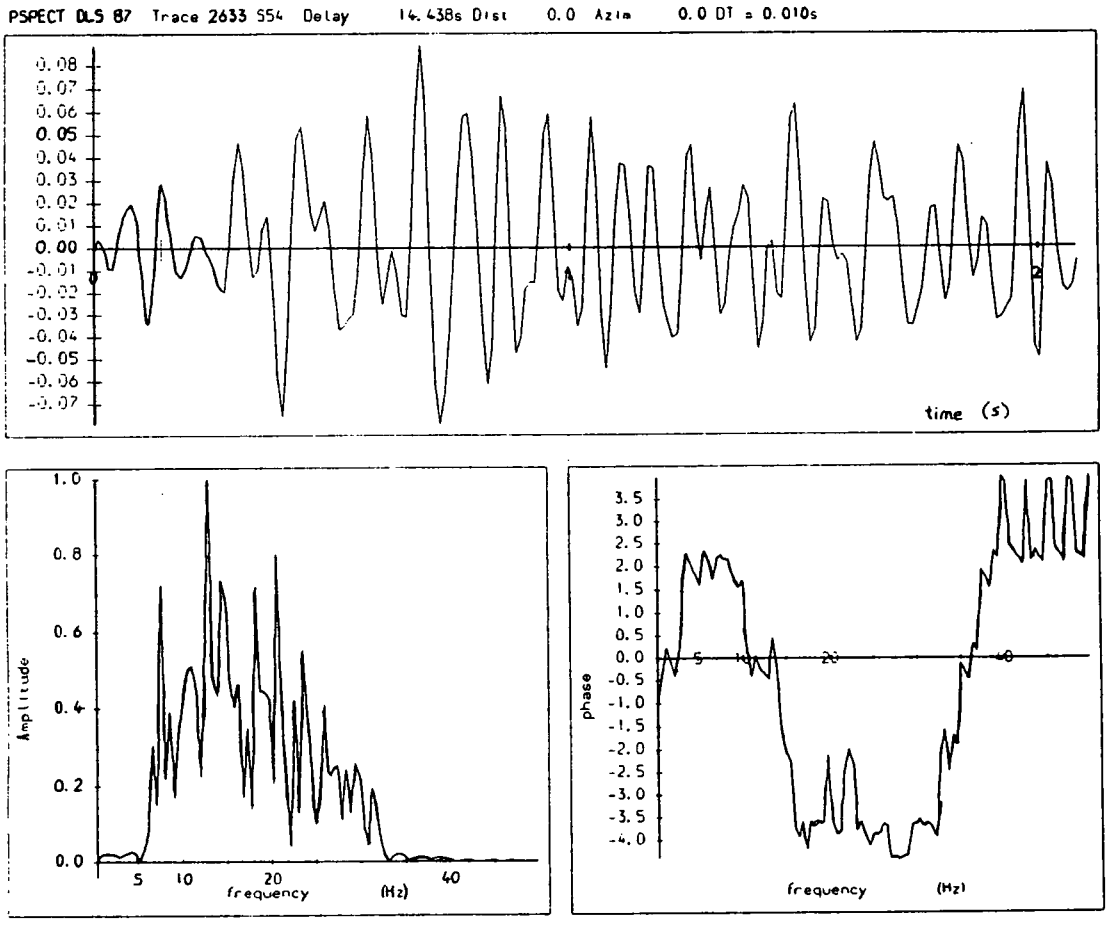

Fig. 3.2 Spectral analysis of PmP phase seen at station 54 from shot 2633.

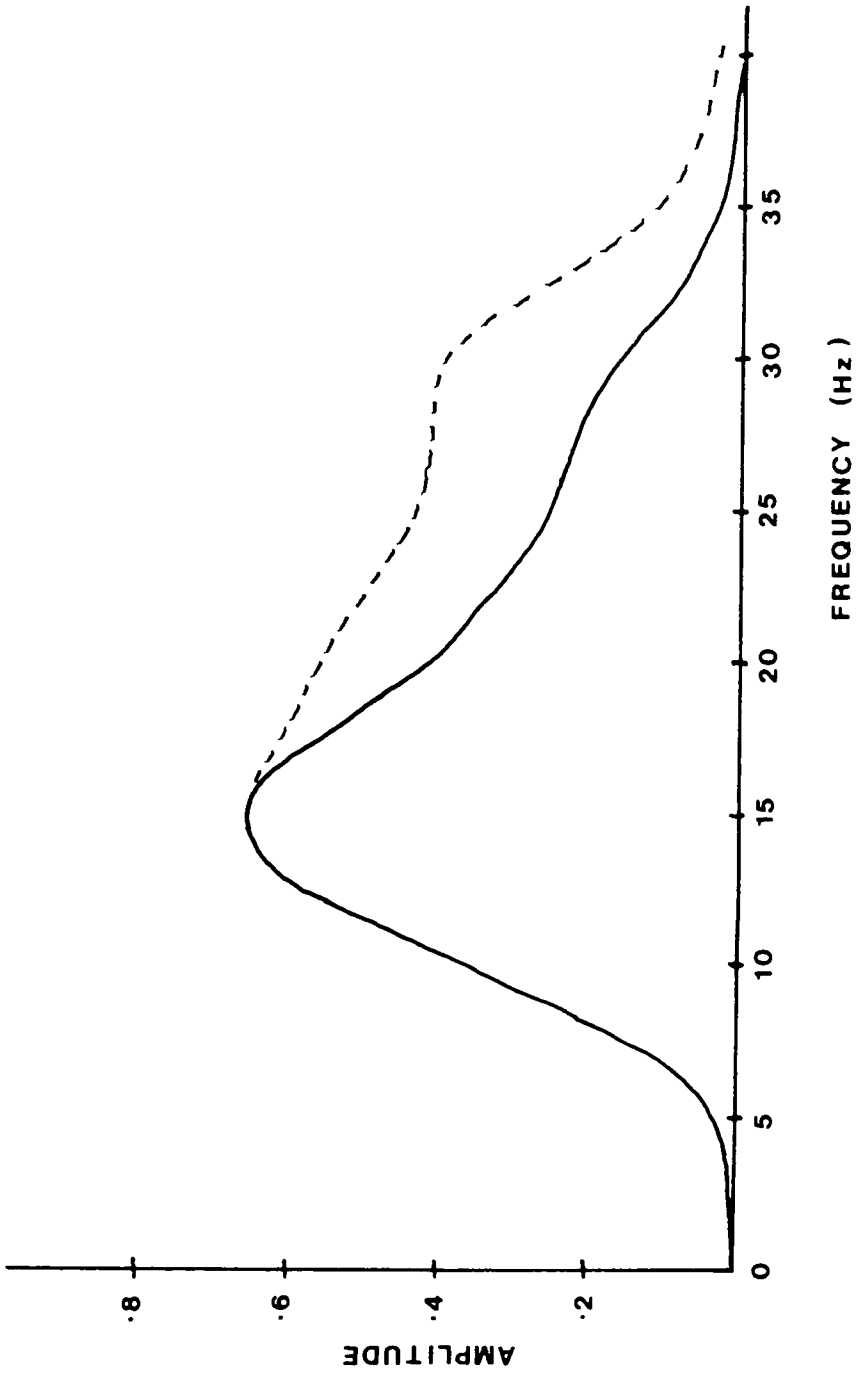

Fig. 3.3 Smoothed frequency spectrum for PmP arrivals (solid line) with correction for recording bandwidth (dotted line).

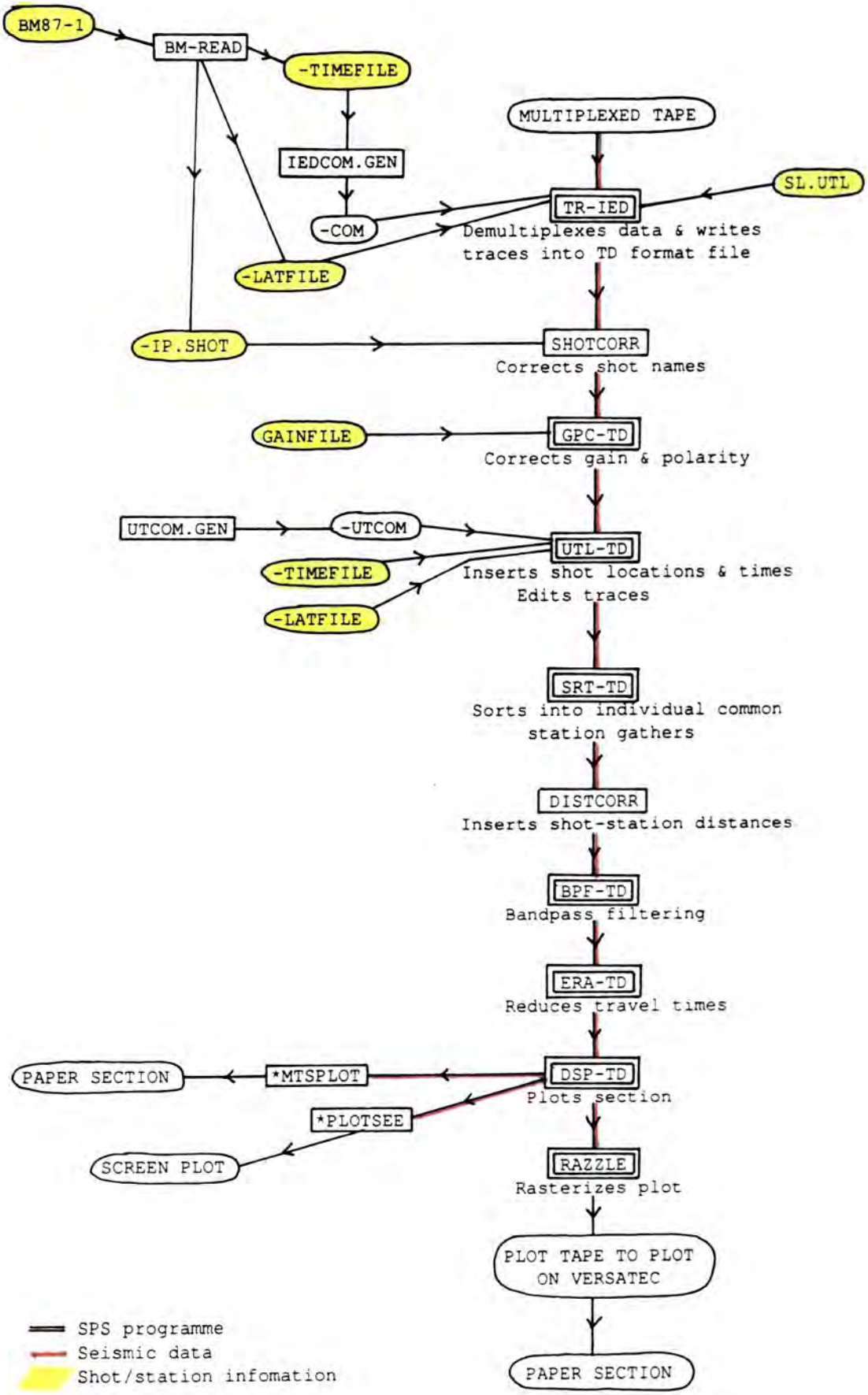

Fig. 3.4 Flow chart of processing procedure on main frame computer.

Up to 9999 traces may be stored in a TD file. The file structure is made up of a **FILE HEADER**, 4 lines of information describing the file contents, followed by the trace entries, which each consist of a **TRACE HEADER** (one line of information about the trace: shot and station location, shot time, gain setting and other relevant information) and the **TRACE BINARY DATA** stored as 2 byte binary integers. The file header, trace headers and each trace binary data line are read and written using specific routines from the SPS library.

The first step in the processing chain is therefore to convert the multiplexed digital data on tape to TD format. This requires the programme **TR-IED** (Tape Read- Interactive Edit & Demultiplex) which reads the appropriate file from tape, demultiplexes it and extracts the seismic data from requested shots and channels, writing them into a TD format datafile. The method used to run this for the MOBIL programme was to generate a command file, given the times of shots known to be included in the multiplexed file, which would then supply all the necessary information to the computer as the programme ran. This saved the need to type in by hand the time for every shot (about 120 per block). Eight traces were extracted per shot (one per recording channel), starting at the shot detonation time and lasting for 60 seconds. When all shots were extracted from the multiplexed file in this way, the programme would write the file header before closing the file.

The shot information required for the processing was obtained from a **BM87** matrix file for the profile being processed. These matrices were recorded on floppy discs on board M/V Mobil Search while the profiles were actually being shot. They contain all the information about the shot times, latitudes, longitudes and gyro details. Appendix B contains a listing of BM87-1. A routine, **BM-READ** was written to read these matrices and to generate the input files required by SPS routines, containing shot numbers, shot locations and shot times. Another routine, **IEDCOM.GEN**, uses the file of shot times to generate the command file to run TR-IED.

One of the problems caused by digitising en bloc was that the same shot name would be attributed to all the shots extracted from a multiplexed file. The next stage was therefore to correct these throughout the TD file, using the routine **SHOTCORR** and the file of shot names generated by BM-READ.

The gain setting of the amplifier modulator at each station was then required to be specified within the trace headers throughout the TD files. This was carried out by the programme **GPC-TD** (Gain & Polarity Correction) using a control file which contained details of the gain setting and polarity of each station.

Next, the individual shot times and locations need to be corrected, using the SPS Utility programme **UTL-TD** and the shot location and shot time files generated by BM-READ.

After this, the large data file would be sorted into separate files, each containing a common station gather, to enable easier handling. This was carried out using the programme **SRT-TD**. Before or after this process, the shot-station distance for each trace could be written into each trace header by the routine **DISTCORR**. The data had at this stage reached a usable form, ready to have any filtering carried out upon it, using **BPF-TD** (Band Pass Filtering routine), or any other enhancement techniques before plotting.

Minimal processing was carried out on the data, merely bandpassing between 3 and 30 Hz to eliminate low-frequency noise and reducing the travel times by 6.0 kms^{-1} for plotting in order to align horizontally the crustal arrivals of approximately 6 kms^{-1} apparent velocity. Time did not permit further experiments with processing.

The actual plotting of the data was carried out using the programme **DSP-TD**. This will be further described in section 3.4.

The most time-consuming and expensive operation in the sequence was the running of TR-IED, due to the length of time and large amount of virtual memory required to read in the large multiplexed files from tape. The rest of the execution of the programme was streamlined as far as possible by the use of the command file and by not viewing graphically the traces being edited.

UTL-TD and BPF-TD were the only other programmes in the chain which involved manipulation or editing of the trace binary data, hence these were also quite expensive routines to run. The whole sequence of processing, from TR-IED to `wiggly line' plot, took about one day per two blocks of 120 traces each, subject to the availability of disc space.

3.3.2 Demultiplexing and editing Wark recordings

As described in section 3.2.2, the digitisation of the data recorded at the Wark base produced multiplexed files with the wrong time information due to the faulty VELA clock code on the Geostore. This meant that during the running of TR-IED the time information had to be inserted manually in order to write the traces into TD files.

This operation employed the program's **TIME** option, which displays requested channels of the data, enabling the user to pick and specify a start time, pick an end point and specify the duration of the picked interval. This time definition is extrapolated over 240 seconds. This was carried out using the MSF channel for specifying the time, since the code was good enough to decode by eye from the display screen. The most accurate method of carrying out the operation was to pick the start time by decoding MSF, move the display forward and decode again, in order to make the picked interval 240 seconds long.

This method was obviously slow, since every 4 minutes of a 40- minute datafile had to be calibrated in this way. It was possible to use a command file to run the programme again, but a pre-run of TR-IED was necessary in order to determine the time specifications to be inserted in the command file, and the picking was a manual operation, using the bit pad attached to the Tektronics 619 graphics screen. The demultiplexing and editing therefore took twice the amount of time required for the Hebron Hill recordings, even when practice had made the operation relatively streamlined. This also applied to the data recorded at Market Weighton, which was digitised and processed by S.A. Lewis and C.H. Bassom. Once this was carried out, the rest of the processing was identical to that applied to the Hebron Hill data.

3.4 Plotting

3.4.1 `Wiggly line' record sections

Initially the processed data was plotted as the `wiggly line' record sections traditionally used for CSSP-type refraction/wide-angle reflection surveys, with one block of shots (120) per record. These sections were bandpass filtered between 3 and 30 Hz to remove low frequency seismic noise, then plotted directly with no enhancement techniques applied, since the quality of the data was best displayed this

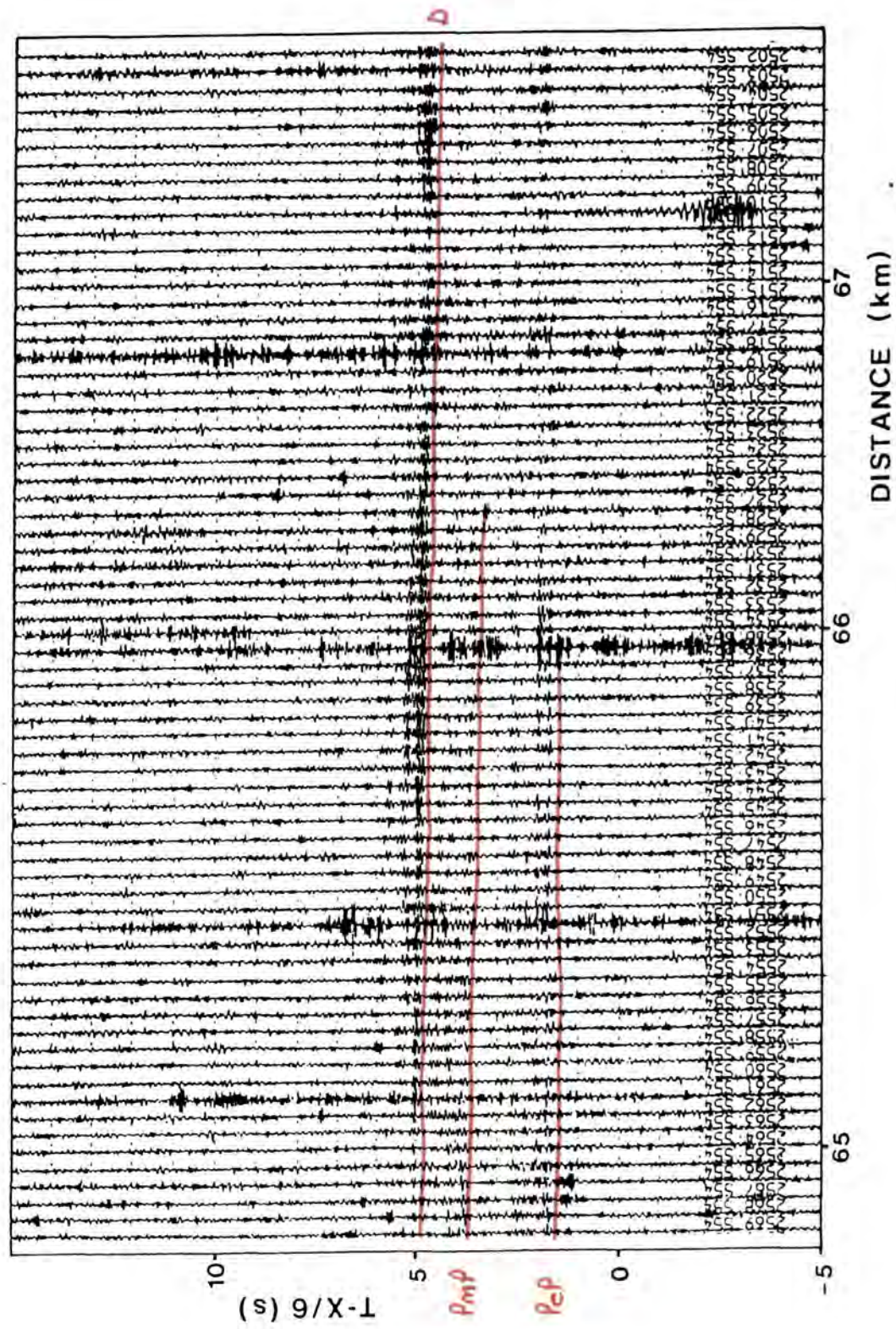

Fig. 3.5 Wiggly line MOBIL line 1 wide-angle record section from station 54; red lines = travel time picks for T^1- X^1fitting (see section 4.2).

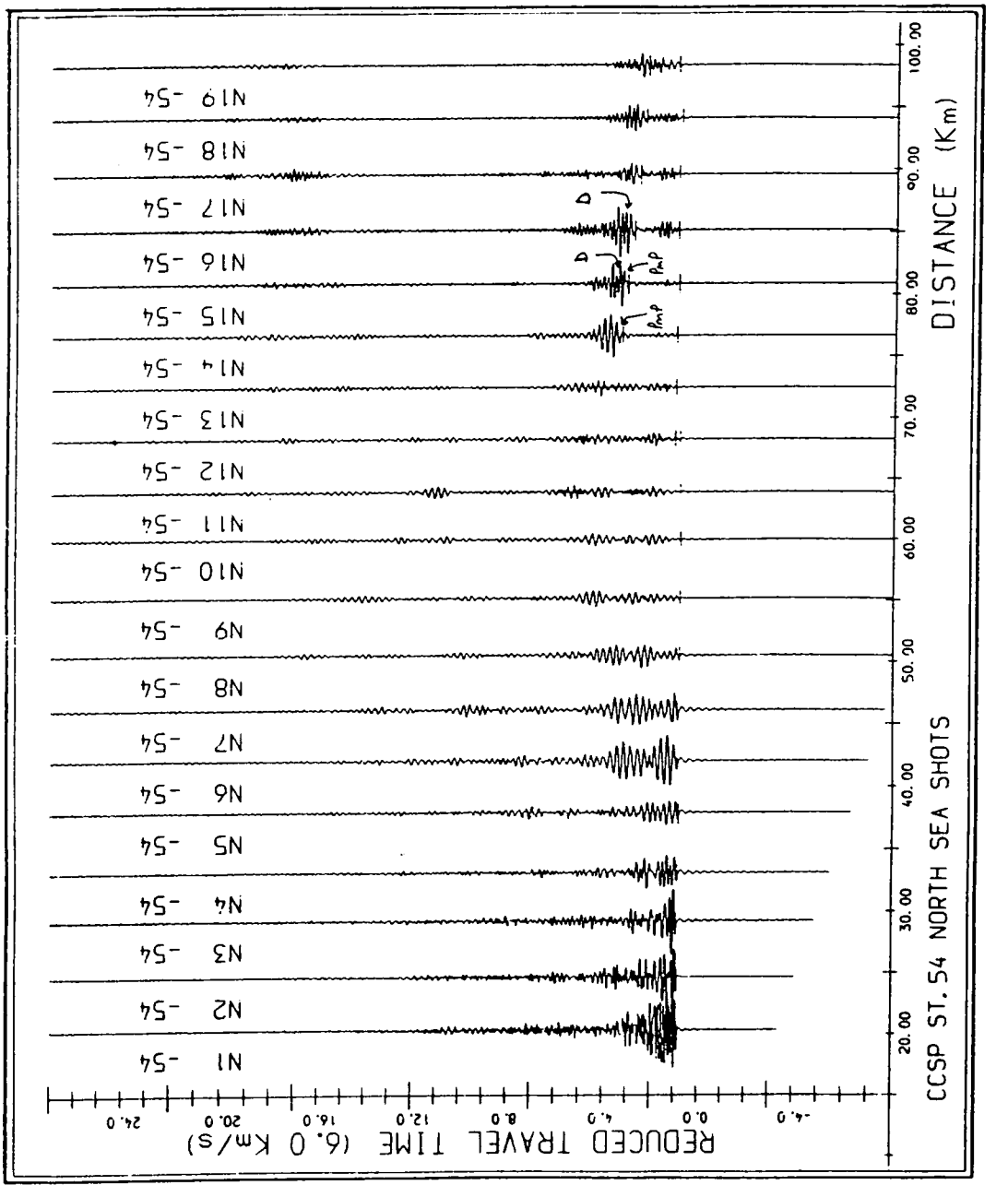

Fig. 3.6 CSSP record section from station 54 for North Sea explosive shots.

way. Such plots were obviously cumbersome, however, so that a method of producing more compressed area sections was necessary in order to be able to view the relationships of the arrivals better.

Fig. 3.5 shows a typical `wiggly line' section, a common station section from station 54 for shots 2502 to 2569. The high quality of the data is well displayed on this type of section - the low noise level, the sharply defined arrivals (due to the relatively high frequency of the source), and the obvious repeatability of the source.

Fig. 3.6 is included for comparison and shows a common station record section for station 54 from the CSSP data, which used explosives as the marine source. Even allowing for the large separation of the shots in CSSP (4km), the difference in the signatures of the shots from trace to trace is quite large. These shots were detonated on the sea bed and would therefore be affected by the water depth at each location.

3.4.2 Variable area compressed record sections

Experimenting with gain scaling, including applying automatic gain control or normalising the traces, it turned out that the best sections were produced by merely plotting the bandpassed traces at real amplitudes in compressed variable area sections. Although amplitudes of the relative arrivals were better seen on the `wiggly line' sections, more arrivals were revealed on the variable area plots and their complex relationships highlighted. The final sections of the common station sections, were plotted in this way, with a horizontal scale of approximately 1.5 km per inch, which corresponds to about 30 traces per inch. An example of a variable area plot can be seen in **Fig. 3.7**, which is a common station section from station 54, including shots 2479 to 2625. The only processing carried out on the section is bandpass filtering and clipping the true amplitudes (in order to prevent the high amplitudes swamping the section). The plot shows quite well the detail of the arrivals in all their complexity.

The dataset would be an ideal one on which to experiment with further plotting, processing and enhancement techniques but time did not permit such experiments in this study. Further methods which could profitably be tried are discussed in chapter 8.

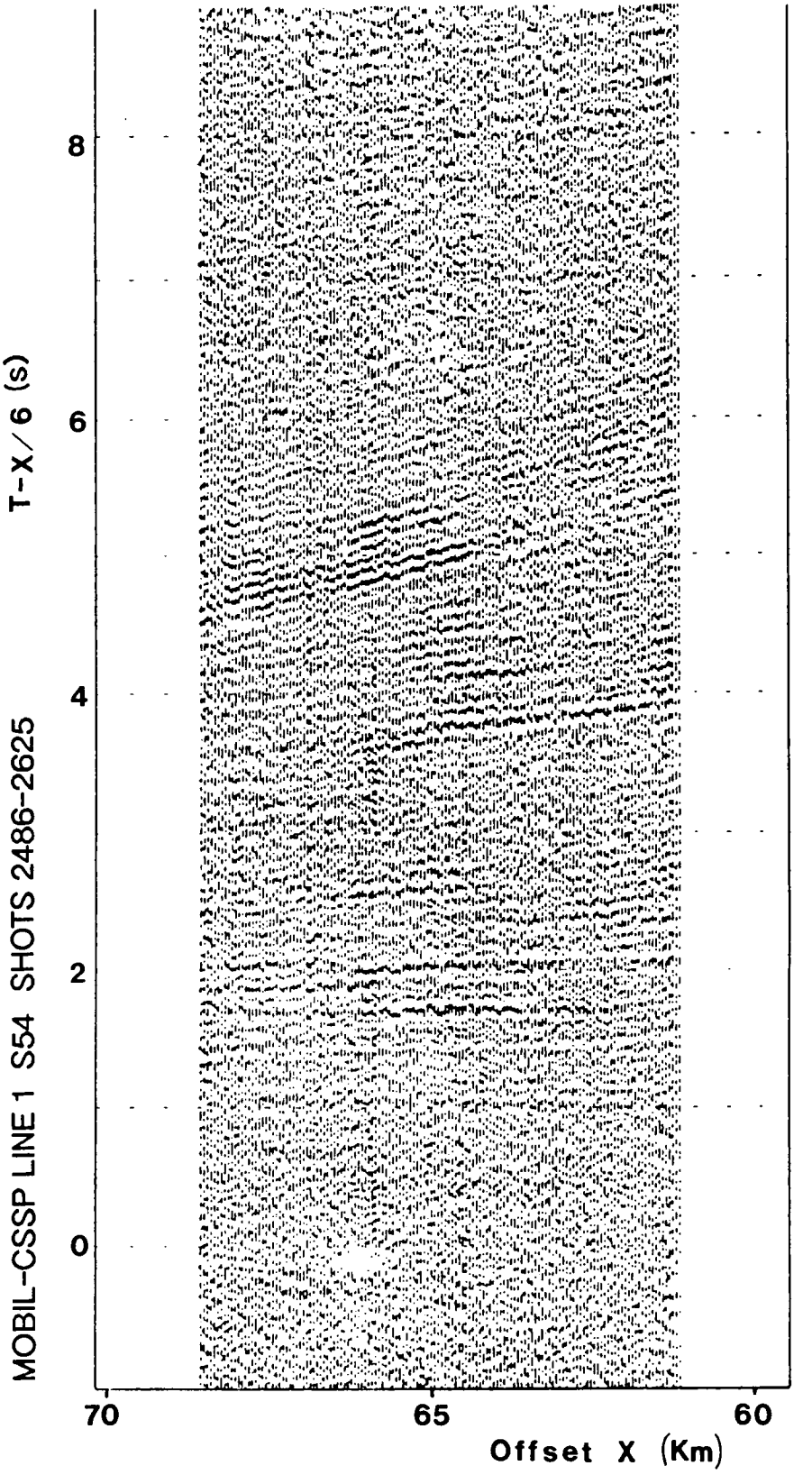

Fig. 3.7 Variable area compressed record section from station 54 MOBIL airgun data.

Both methods of plotting used the same SPS programme, **DSP-TD**, which allowed a large choice of plotting parameters, such as clipping or muting the traces, automatic selection of amplitude scaling factor and trace spacing, variable area or wiggly line traces, different types of amplitude scaling and different extrapolation methods for the data. For the compressed plots, the datafiles were merged together into larger gathers as far as possible without the files becoming too unwieldy, in order to reduce handling time. The whole of Line 1 was thus placed in 3 files per Morpeth station and 2 files per station for the stations recorded on the Wark Geostore.

Once a wiggly line section was plotted, a paper copy of the plot was obtained via ***MTSPLOT**, the University Calcomp plotter. Variable area plots however, took hours to plot in this way, so that it was far faster to convert the plotfiles to raster format, copy them to tape and then obtain paper copies from the Seismic Processing Laboratory VERSATEC plotter. This produces good quality plots very quickly and efficiently. The data sections in Appendix C were produced in this way.

The other data sections presented in this thesis are the transparencies (i) to (vi) which are included in Chapter 6, to facilitate comparison of the synthetic seismogram sections with real data. The transparency sections are plotted at 1 km spacing in order to plot the same size as the synthetics, compared to the 50 m spacing of the long data sections of Appendix C. Otherwise the plotting parameters are similar, with clipped true amplitudes and variable area display.

3.4.3 Final record sections

The total range of each of the Morpeth record sections is 152.5 km from shot -95 (one of the 95 test shots) at the eastern end of line 1, to 3037, the closest shot to the coast. The smallest offset in the wide-angle profile is 33.5 km, the distance from station 57 to shot 3037, the largest is 208.5 km between station 47 and shot -95.

The total range of the Wark records is only 78 km, approximately half that of the Morpeth records since the recordings were only digitised from shot 1492 to 3037, the closest half of line 1 to land. As previously mentioned, it was not thought worthwhile to process the more distant shots so the maximum offsets of these records are between 150 and 158 km. However, judging from the quality of these data

sections and the information visible in the last 50 km of the Morpeth sections, it may be useful to digitise a further 50 km or so of the shots recorded at Wark.

The time axis of the record sections runs from -1.0 to 9.0 s reduced travel time, where the reduction velocity is 6.0 kms^{-1}. As previously mentioned, this makes most of the arrivals from the crust correlate horizontally on the sections and therefore easier to detect.

The record sections themselves and their preliminary interpretation are described in Chapter 4. The further modelling of the data, using synthetic seismograms, is described in Chapter 6.

CHAPTER 4: PRESENTATION OF WIDE-ANGLE RECORDINGS

4.1 Introduction

Having plotted the common station seismic wide-angle records from line 1, as described in Chapter 3, the interpretation was carried out as simply as possible in order to obtain a basic model which could be applied to all stations. The huge amount of data and the detail of the record sections made selection of seismic phases difficult, especially correlating arrivals from one record section to another. Most attention throughout the whole of the interpretation process was given to the records from stations 54 and 47, which were the clearest of all the record sections. These were evidently located at very favourable sites as far as both bedrock-seismometer coupling and noise levels were concerned.

Picking the phases as well as modelling was an iterative process. Initially, the picks obtained from the wiggly line record sections were fitted to a $T^2 - X^2$ curve, in order to obtain a rough idea of the depth of and average velocity above the interfaces which gave rise to the wide-angle reflections. This process is described in **section 4.2.**

After the $T^2 - X^2$ fitting, the record sections were plotted as compressed, variable area plots (**Appendix C**) which showed up the relationships of the seismic phases to each other far better than the wiggly line records and gave a far better picture of the apparent velocities of the arrivals. The final travel time picks were made on these sections, as described in **section 4.3**, and subsequently used in synthetic seismogram modelling, for which the starting model was that obtained from the CSSP (**Lewis, 1986**).

4.2 $T^2 - X^2$ regression analysis

The initial record sections of the wide-angle data, as described in **section 3.6.1**, were wiggly line plots, as wide-angle/refraction data has traditionally been displayed. The apparent velocities of the

different phases and their relationships to each other, in the case of the MOBIL wide-angle dataset, are not easily seen on this type of section but the initial travel time picks were made from these sections for regression analysis and initial seismic modelling.

Only the records from stations 54 and 47 were used for T^2 - X^2 regression or linear regression (T-X fitting for refractions). The phases selected for this were **Pg**, the refracted arrival from crystalline basement, **PcP**, a mid-crustal wide-angle reflection, **PmP**, which at this stage of the interpretation was thought to be a lower crustal wide-angle reflection, and an arrival which has since been named D, initially thought from its high amplitude on the wiggly line sections to be the Moho wide-angle reflection.

Fig. 3.5 showed a wiggly line section of line 1 as recorded at station 54, with the phases selected. All of these arrivals were observed on the record sections of the CSSP, although not so well resolved in space and time - on CSSP records, arrival D was not resolved as a separate arrival to PmP.

4.2.1 The T^2 - X^2 method

The T^2 - X^2 method is used to obtain a very rough idea of the depth to a reflecting interface and the average seismic velocity above that interface. Assuming that the medium above a reflector is uniform, the travel time for reflected rays is described by the equation:

$$T^2 = X^2 / V^2 + 4D^2 / V^2$$

where T is the travel time, X is the distance between source and receiver, D is the depth to the reflector and V is the average P-wave velocity to the reflector. It therefore follows that a plot of T^2 against X^2 will be a straight line of gradient $1/V^2$ and y-axis intercept $4D^2/V^2$.

This is used in the programme **TTREG** (see **Appendix D**), which plots the T^2, X^2 graph for input travel time picks for the particular phase concerned and fits a straight line through these values, returning the slope and intercept of the graph and calculating from these the depth and average velocity above the reflector.

4.2.2 The regression results

The $T^2 - X^2$ plots (or, in the case of Pg, the straight travel time graph) for all the above mentioned phases as seen at station **54** are shown in **Figs. 4.1(a) to 4.1(c)**, with the straight line fits. Those for station **47** are shown in **Figs. 4.2(a) to 4.2(d)**. The travel time picks and therefore the straight line fits are not highly accurate, but since the method is a very simplistic one, the aim was solely to obtain a rough idea of the quantities involved.

The **PcP** fit (**Fig. 4.1(a)**) for station 54 gives an average depth of **21.25** +/- 0.89 km to a mid-crustal reflector and an average velocity of **6.51** +/- 0.10 kms^{-1} for the upper crust, compared to **23.39** +/- 0.55 km and **6.29** +/- 0.04 kms^{-1} respectively at station 47 (**Fig. 4.2(a)**). The disparity between the figures from the two stations is inevitable since no correction was made for near-surface delays and it is highly unlikely that the structure is laterally homogeneous (the assumption upon which the method is based). There are also several wide-angle reflections on the records from within the crust, so it is not easy to be sure that the phase picked as PcP on station 54 records is the same one picked at station 47. This will be discussed further in **section 4.4.2.**

The **PmP** fits (**Figs. 4.1(b) and 4.2(b)**) from the two stations yield depths of **33.43 km** +/- 1.48 and **29.08** +/- 1.56 km for 54 and 47 respectively, and average velocities of **6.66** +/- 0.33 and **6.15** +/- 0.18 kms^{-1}. These values are also rather disparate, again probably due to the lack of correction for near-surface structure and the one dimensional assumption. However, they are of the same order of magnitude, which should mean that they may be explained as wide-angle reflections from a major crustal discontinuity.

The fits for **D** were rather poor (**Figs 4.1(c) and 4.2(c)**) and produced unrealistic answers for the depth and velocity, making it highly unlikely that the arrival was a wide-angle reflection. The figures obtained were depths of **71.22** +/- 1.03 and **61.19** +/- 1.21 km at 54 and 47 respectively and average velocities to the boundary of **10.28** +/- 0.64 and **8.34** +/- 0.27 kms^{-1}. The arrival therefore needed an alternative explanation.

The **Pg** travel times were plotted directly against distance to obtain a fit for a refracted headwave from station 47 arrivals only. The travel time plot and straight line fit are shown in **Fig. 4.2(d)** and yield a

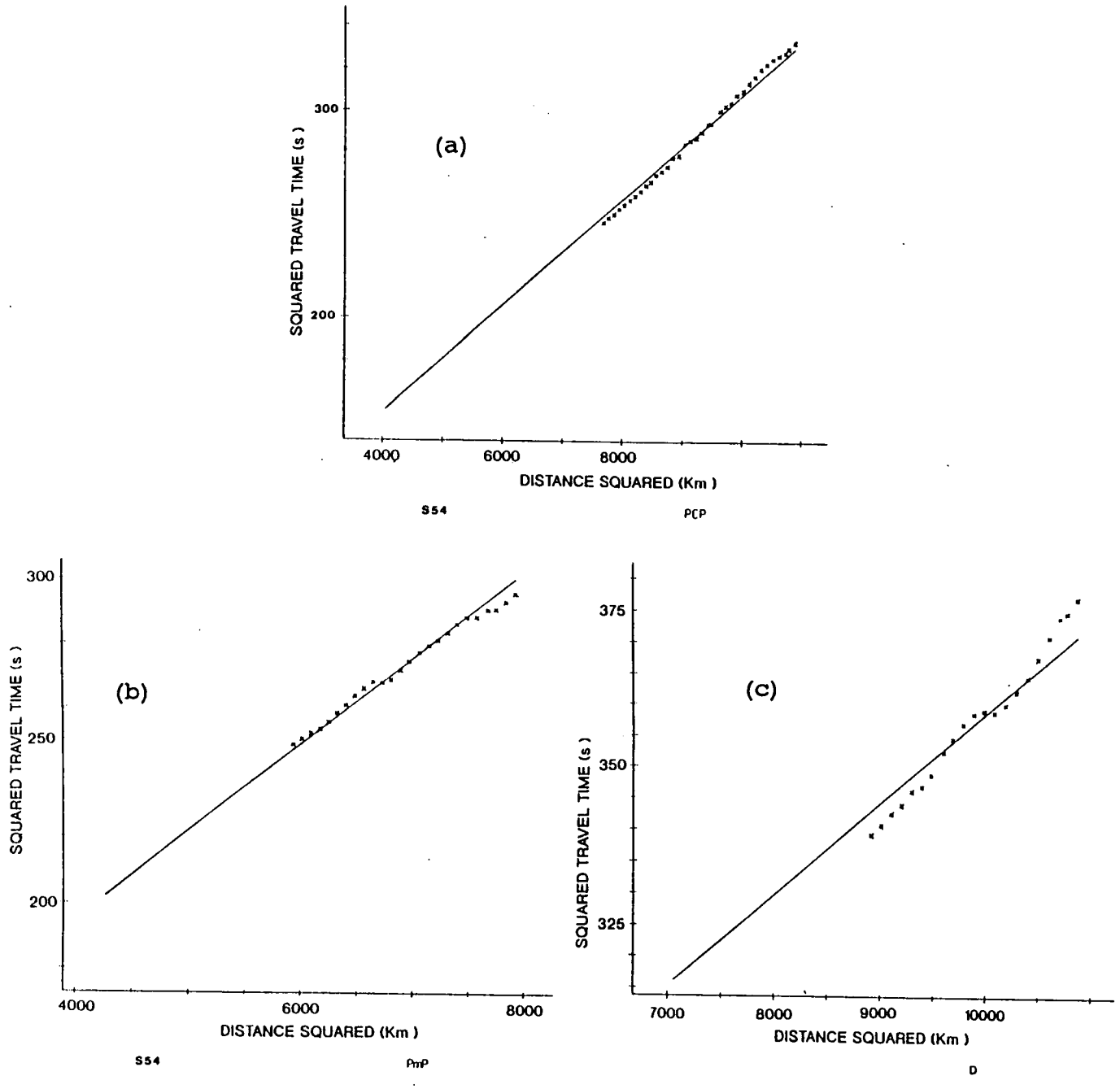

Fig. 4.1 $T^2 - X^2$ fits for station 54 picks: (a) PcP phase; (b) PmP phase; (c) D phase. Straight lines represent least squares fits.

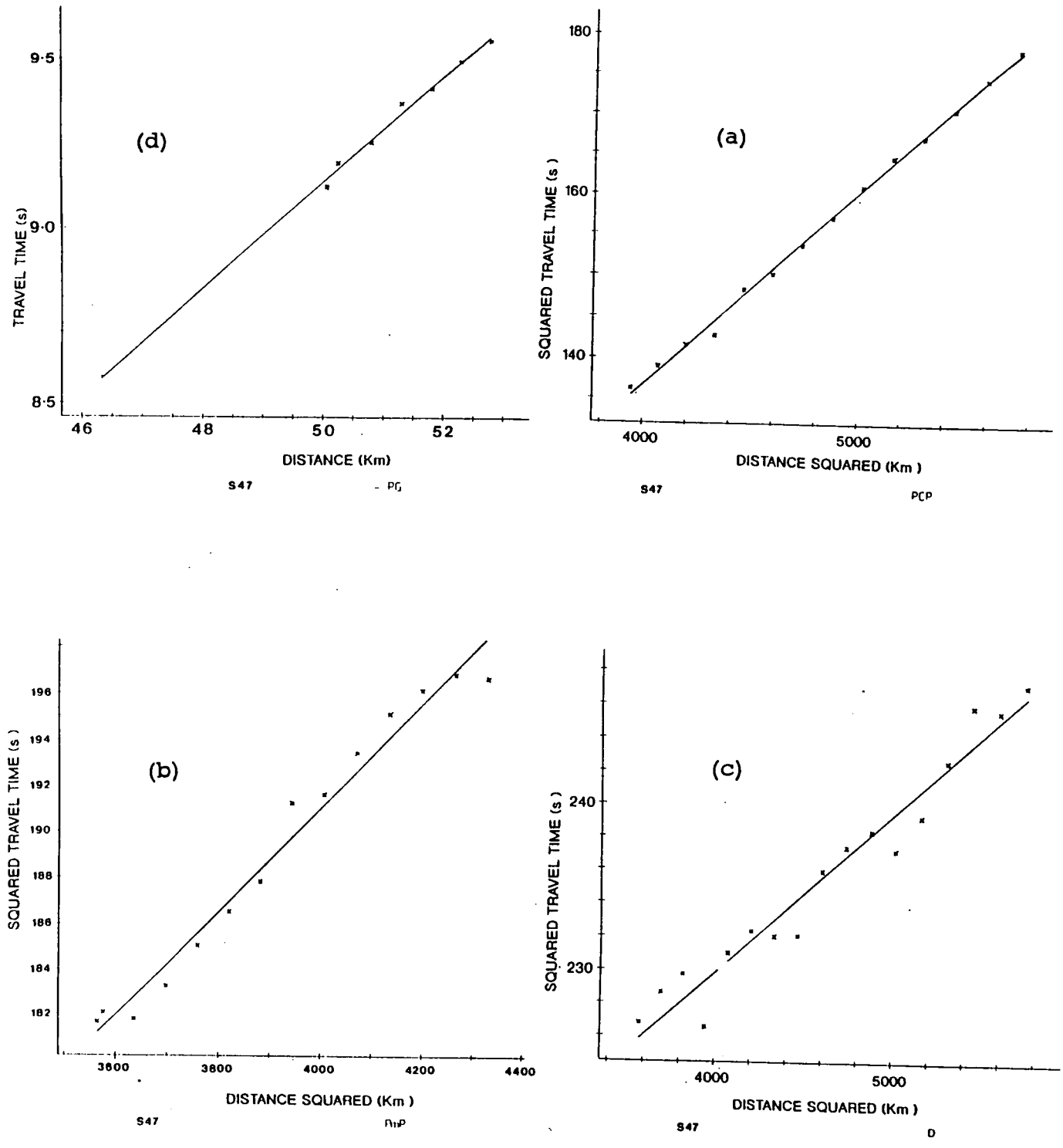

Fig. 4.2 $T^2 - X^2$ fits for station 47 picks: (a) PcP phase; (b) PmP phase; (c) D phase; (c) Pg phase. Straight lines represent least squares fits.

result of **4.44** +/- 1.03 km depth to the refracting boundary and **6.29** +/- 0.10 kms^{-1} as the velocity of the refractor.

The outcome of this fitting was to obtain approximate ideas of the locations of the major discontinuities in order to commence the synthetic seismogram modelling. It has served this purpose, backing up the model of Lewis (1986) for the CSSP data as a starting model, with a refracting boundary at about 4 km, a mid-crustal discontinuity at about 20 km and the Moho at about 30 km depth. The arrival D is clearly not explained by a reflecting interface and is studied in detail in **section 4.4.**

4.3 Picking seismic phases

4.3.1 Description of the compressed record sections

The variable area common station record sections for all the vertical component MOBIL-CSSP recording stations are displayed in **Appendix C.** As stated in chapter 3, the line 1 record sections from the Morpeth area (stations 47, 54, 55 and 57) have a range of offsets of 152.5 km for all shots (-95 to -1, the test shots, then 101 to 3037), whereas the Wark data (stations 36, 37, 39 and 40) covers a range of 78 km, from shot 1492 to 3037.

The station 54 data extends from 40.5 km to 193.0 km, that of station 47 from 56.0 km to 208.5 km. The station closest to the coast, 57, starts from 33.5 km offset. This is the smallest offset in the whole wide-angle dataset, which means that refractions and wide-angle reflections are not seen from shallow interfaces. The Wark stations (stations 36, 37, 39 and 40) were further inland with an even greater minimum offset - station 40 starts at 72.0 km offset and station 36, the most distant, starts at 80.0 km offset. These distance ranges mean that most seismic information is received from the mid and lower crust and the Moho, which is the main area of interest in this study. The shallow structure, described in chapter 6, was obtained from the normal-incidence data, the CSSP data and other geological information on this area.

The most striking feature of the MOBIL sections is the amount of detail in both space and time. Many arrivals, which have not even been considered in this interpretation, are resolved, even those which only appear over short offsets. **Fig. 4.3** shows a variable area compressed record section from station 54

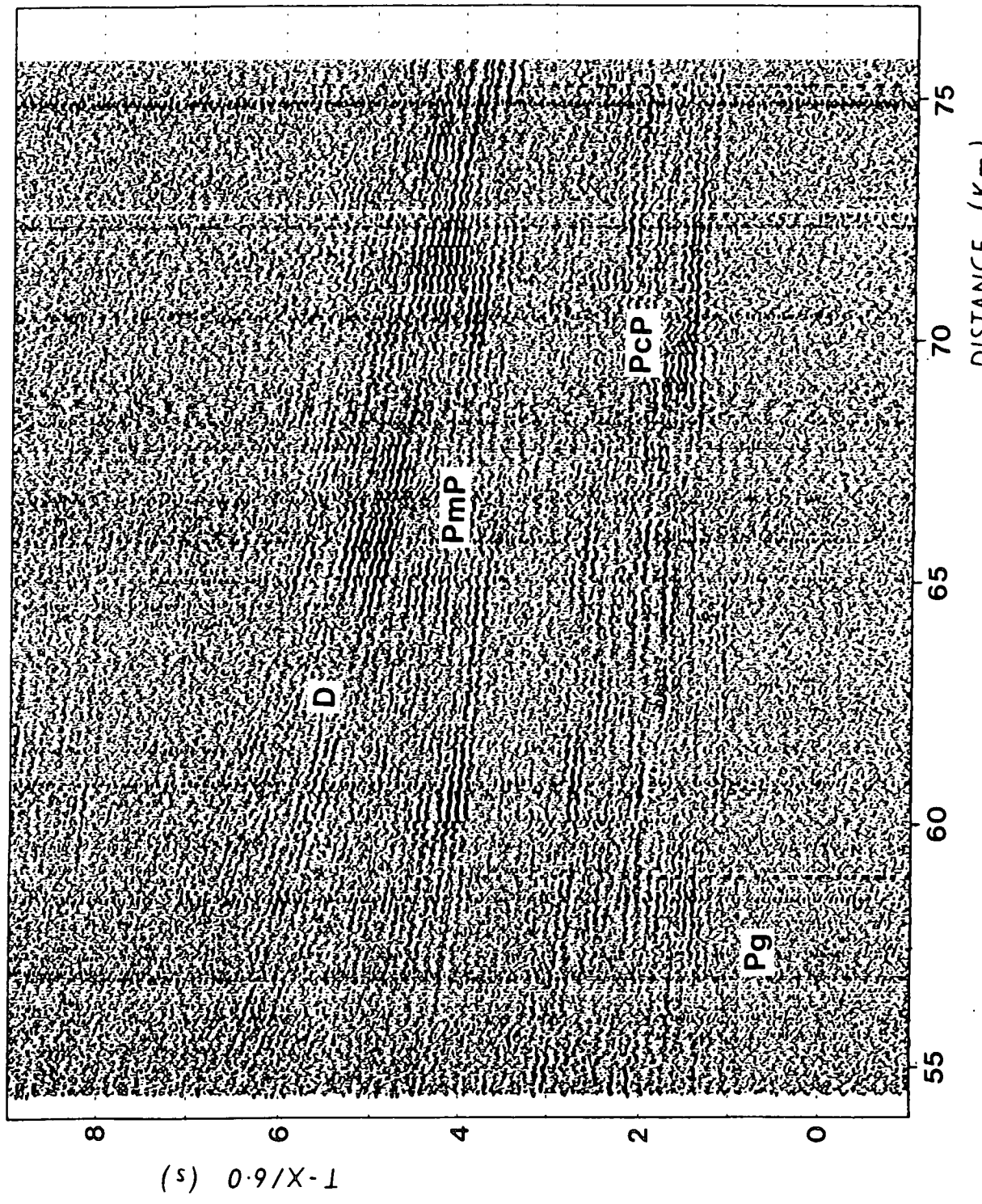

Fig. 4.3 Variable area compressed record section from station 54 with main phases of interest labelled. Shot range: 2338-2766 (see Fig. 2.2).

which illustrates the quality of the data and the many arrivals visible.

This detail means that the major arrivals are difficult to distinguish from secondary phases, multiples and diffractions. It can be seen from the section (**Fig. 4.3**) that there is frequently a packet of reflections rather than a single distinct arrival. Since these appear after some of the strongest arrivals with the same delay after each one, it seems likely that they are multiple reflections from the near-surface. These are discussed further in **section 4.4.2** .

The amplitude of arrivals varies rapidly along the record sections, which, combined with interference between arrivals, complicates the correlation of the main phases further. Phases such as PmP, which have been assumed to be continuous, now appear to be very discontinuous when seen at greater resolution, consisting of separate segments along their length. At the points where phases merge (for example, at about 70 km offset, 1 s travel time on **Fig. 4.3**) it is particularly difficult identify separate phases.

4.3.2 Travel-time picking from the sections

In the face of the complexity of the record sections described above, selection of individual phases for modelling was extremely difficult at times, especially when attempting to correlate between stations. Selection of phases was carried out several times to provide a consistent set of picks for all stations.

The phases identified and picked from the record sections are **Pg**, **PcP**, **PmP**, **Pn** and **D**, which are described in the next section. The first picks were obtained only from the records of station 54 and 47 for preliminary modelling, but the latest set of picks were made from all stations, with close reference between the individual records. Since the shots are every 50 m on the line 1 records, picking each trace, as has been traditional in wide-angle work, was not possible. Therefore the method used was a similar approach to that used in near-vertical reflection interpretation, laying sheets of tracing paper over the record sections and drawing along the onset of the main phases with a coloured pencil, a different colour for each phase.

These tracings are also included in **Appendix C**, overlaying the record sections. Tracing the onset

of the phases (phase correlation) was a long process due to the complexity mentioned in section 4.3.1 caused by interference, reverberations and multiples besides lateral amplitude variations. A great deal of cross reference between stations was made to observe the trends of particular phases. Amplitudes were not measured for study since it was not possible to measure them from the clipped variable area sections and the modelling of amplitudes (as described in Chapter 6) was more qualitative than quantitative.

After this exercise, the travel time picks were transferred to the mainframe computer for modelling using the PERQ digitising table in Durham's Computer Centre to digitise the tracings of the phases. A digitising interval of about 0.5 km was used. The values obtained by this digitisation are converted very simply to the travel-times and distances in the appropriate format for use with BEAM87 or SEIS83 and stored in this format.

4.3.3 Accuracy

The sources of uncertainty involved in the interpretation of a seismic dataset such as this include:

a) Instrument properties, illustrated very well by the ship's clock, which jumped by 0.961 s, as described in section 2.4. However, apart from these jumps, the determination of time is accurate to about 10 ms.

b) Lack of correction of the shot locations for navigational drift, which caused small distance errors on the record sections, as mentioned in section 2.4. The maximum error was of the order of 500 m, producing a travel time error of approximately 0.08 s.

c) The loss of some of the high-frequency contribution of the data due to the frequency response of the recording and playback equipment. This decreases the resolution of each arrival and therefore affects the travel time picking (see section 3.2.3).

d) Errors involved in picking and digitising travel times from the sections, since this is a manual process. If the phases may be picked to the nearest millimetre on the paper records, this corresponds to a timing accuracy of about +/- 0.05 s.

The above inaccuracies are all areas which may be improved in the future, as instruments become

more sophisticated and the resolution of data increases. However, seismic sounding is inevitably an approximate surveying tool and resolution is restricted to the seismic wavelength (which at Moho depths for this type of source is of the order of 0.5 km). Synthetic seismogram modelling is also a somewhat approximate method, especially in terms of modelling amplitudes. Most emphasis is given to the fitting of travel times, which is, in effect, modelling two variables (seismic velocity and depth) on the basis of one known parameter (Matthews,1989). Interpretations such as this must bear this restriction of accuracy in mind when generating an earth model.

4.4 The main seismic phases

A rough sketch of the main wide-angle arrivals at stations 54 and 47 can be seen in **Figs. 4.4 and 4.5**. Not all the arrivals illustrated on these sketches have been picked for all the stations, only those described below.

4.4.1 Pg

Pg behaves for the first 12 km as it was seen on the CSSP records, that is, as a strong arrival which appears to terminate at a specific shot point, suggesting (**Green, 1984**) that a feature of the near-surface geology has cut it out. **Lewis(1986)** modelled this termination as a lateral change in the basement velocity from 6.15 to 5.8 kms^{-1}.

However, from close scrutiny of the station 54 records, it seems that the phase does continue eastward with greatly reduced amplitude, and merges into other arrivals which appear to be wide-angle reflections. At the junction with the reflected phase, the amplitude becomes very bright but gradually decreases again with increasing offset. This happens repeatedly along the record section, producing alternately bright and dim sections along Pg.

Pg may therefore be interpreted as a diving ray from the upper crust and the arrivals which merge into it as wide-angle reflections and multiple reflections generated by the shallow structure beneath the shots. In fact this is supported by observations from other stations, the merging arrivals corresponding to

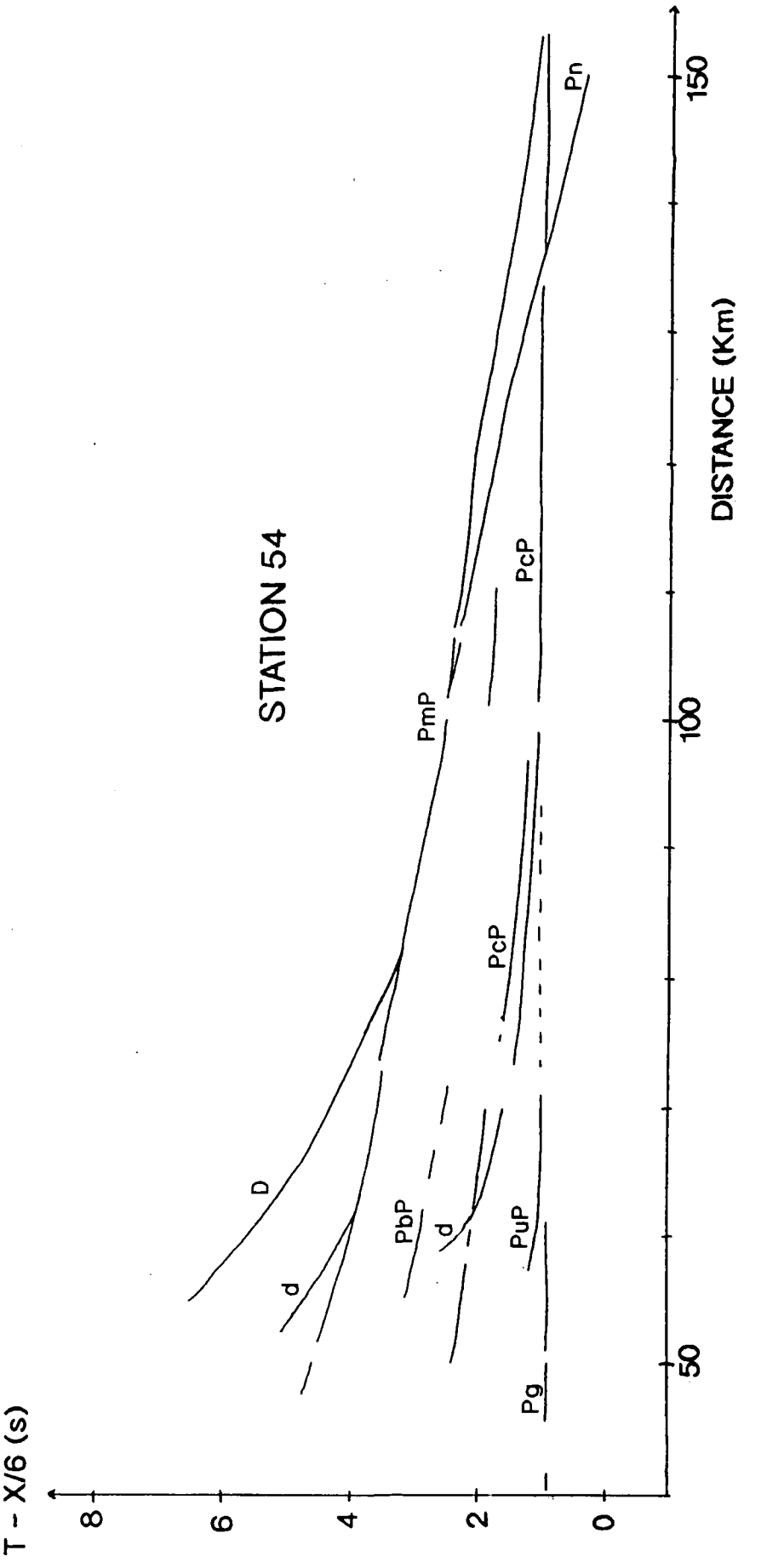

Fig. 4.4 Sketch of main arrivals from station 54 wide-angle line 1 data

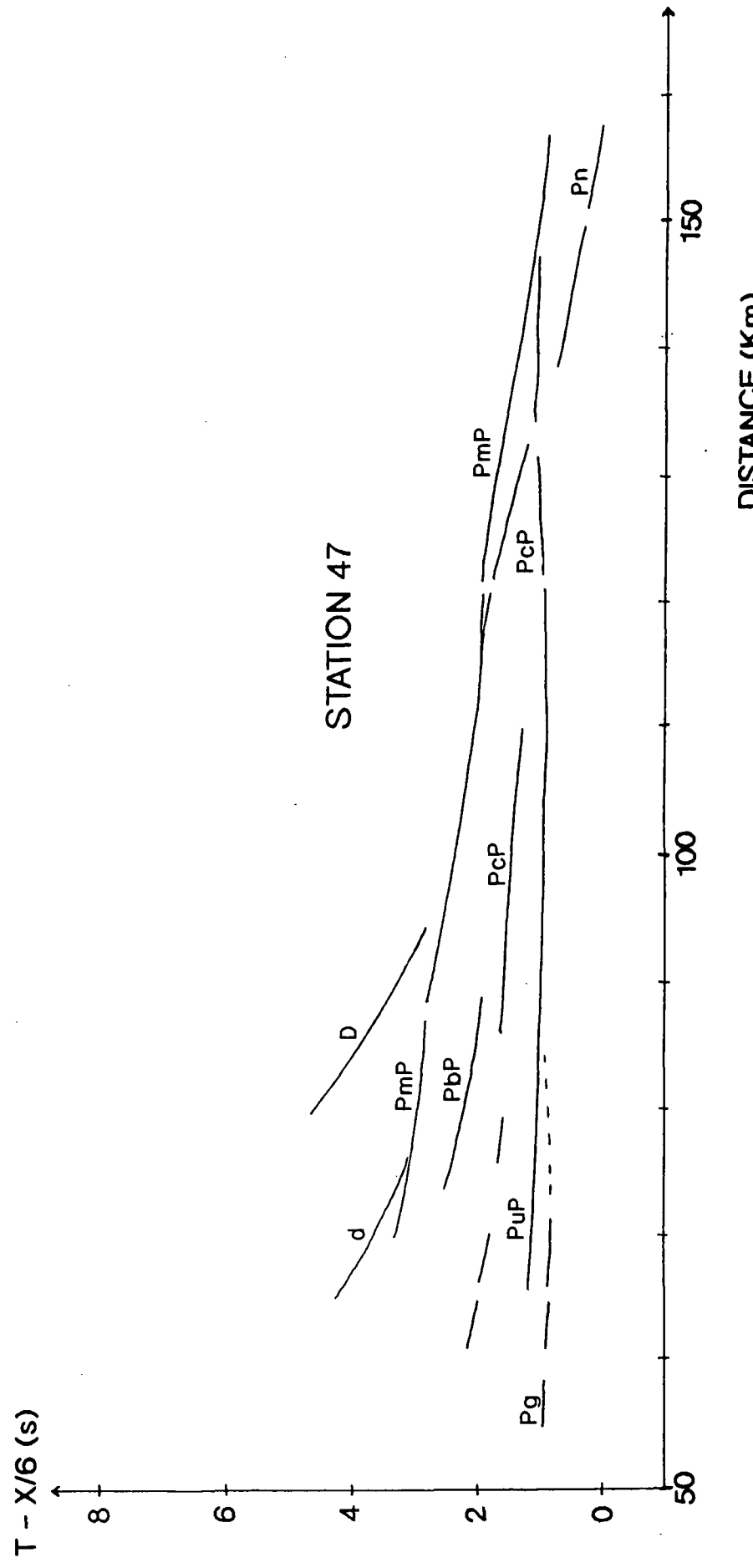

Fig. 4.5 Sketch of main arrivals from station 47 wide-angle line 1 data

the same shots as at station 54 rather than to the same offsets. The effect is visible but not so clear on the Wark records.

Alternatively, the converging arrivals could be explained by the suggestion of **Mereu et al.(1990)**, who have observed similar arrivals on high-resolution wide-angle data from the GLIMPCE project, calling the effect "shingling". They suggest that it is an effect caused by wide-angle reflections from numerous interfaces within the crust, which do not necessarily need to have a high density contrast. When the angle of incidence exceeds the critical angle for a boundary, most of the seismic energy is reflected as P-waves, and the effect of many such interfaces throughout the crust, which may be long or short length reflectors, is illustrated in **Fig. 4.6**. Successive branches, each with a higher apparent velocity than the previous one, converge to make up what has the appearance of a crustal diving ray. This idea has not been tested on the MOBIL wide-angle records.

However, as already noted, the "merging points" on the MOBIL records seem to correspond to particular shot points (and therefore probably to near-surface features) rather than to specific offsets, whereas Mereu et al.'s explanation would be expected to be more offset-dependent than shot dependent, as is the case here.

The lateral change in strength of Pg after the first 12 km of record section also corresponds to a decrease in apparent velocity. This effect cannot be generated by a horizontal low velocity zone in the basement since the change appears over a particular shotpoint, not at a specific offset. It would therefore seem that a lateral change in velocity such as that suggested by Lewis has caused the change in appearance of Pg. The synthetic seismogram modelling of this effect is described in **section 6.4.2.**

4.4.2 PcP

From the record sections, there appear to be several wide-angle reflections from the mid-crustal region seen at all stations. For the majority of stations, three main reflections have been picked and modelled, although it is not absolutely certain whether these correspond to the same reflectors due to the complexity of the record sections.

As mentioned in **section 4.3.1**, a packet of arrivals is usually seen rather than a single event.

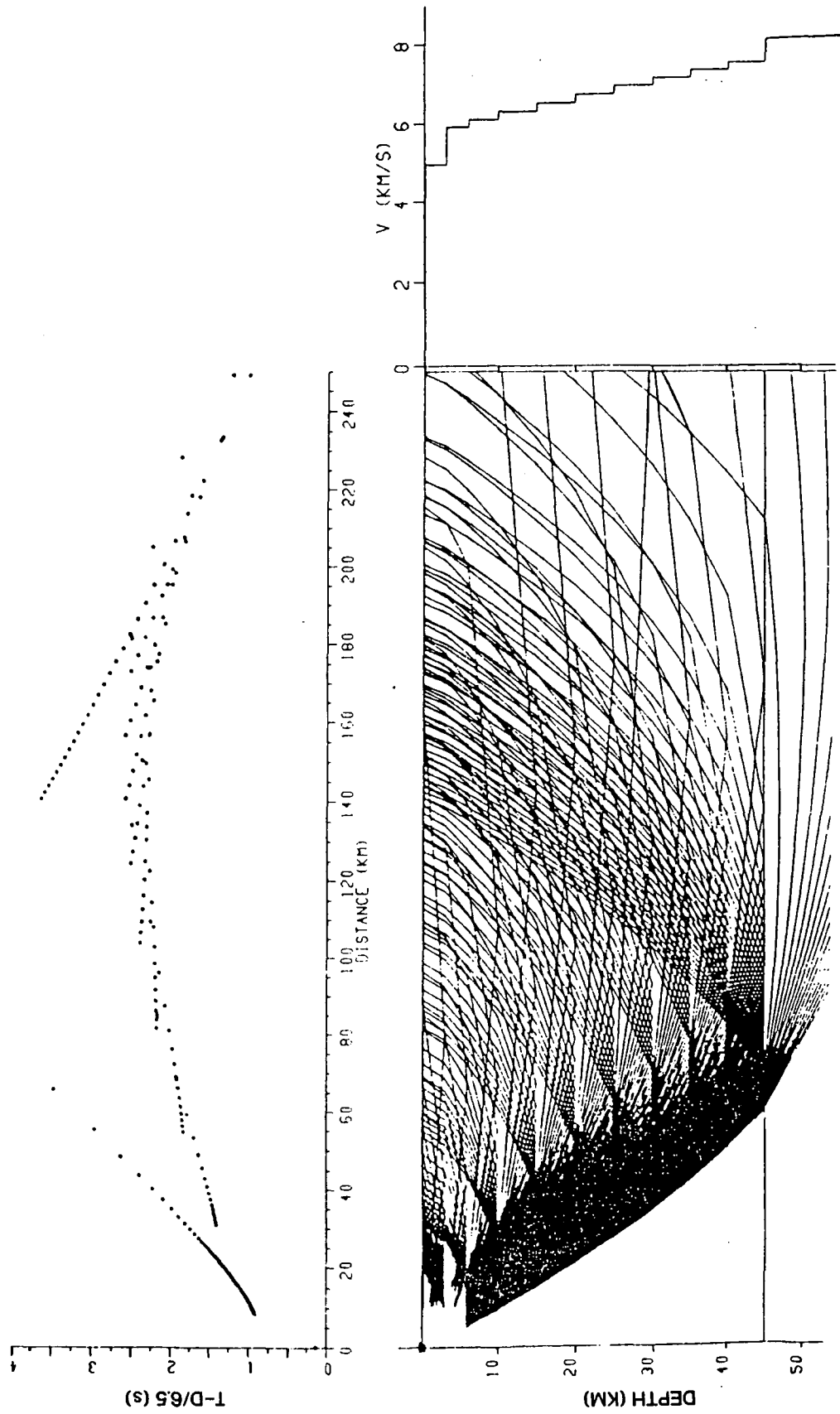

Fig. 6. Ray-tracing diagram showing how wide-angle reflection shingling effects can arise in a simple multi-layered earth model. Only super-critical reflected ray paths are shown.

Fig. 4.6 Ray-tracing diagram illustrating wide-angle "shingling" effect observed on GLIMPCE data, from **Mereu et al. (1990)**

There is one phase in particular which follows PcP, PmP and D arrivals by about 0.5 s and is often particularly bright over certain shot points. This is particularly clear on station 54, for example at 65 km and 71 km offset, but is seen to a lesser extent on all the other sections, and therefore seems likely to be a peg-leg multiple from within the near-surface geology beneath the shots. Placing the record sections in Appendix C against each other so the the same shotpoints, not the same offsets, are adjacent reveals that the strongest multiples are present at the same region of shots at the different stations.

Matthews (1990) has successfully modelled similar, even stronger phases from the Market Weighton MOBIL line 5 wide-angle records as peg-leg multiples in the surface geology. Modelling these multiples would enable further constraint of the near-surface structure and therefore of the whole modelling process. The near-surface Zechstein geology beneath line 1 is known to produce strong multiples at normal-incidence and is therefore the likely cause of multiple arrivals at wide-angle.

Lying record sections side by side with shotpoints adjacent also reveals that the ringing observed on some arrivals is also a shot-dependent effect, caused by reverberation in the sea layer at these shotpoints. This is to be expected at some point on a marine survey. The water depth over most of the profile is of the order of 100 m, which would be expected to generate reverberations at a delay of 0.13 s. The ringing observed in the train of PcP, PmP and D seems to have a delay of this order.

The earliest primary wide-angle reflection (PuP) seems to come from fairly shallow depths and merges into Pg at about 75 km offset at station 54 and a fairly late phase which is particularly bright at station 54 (PbP). These and the reflection which should correspond to that picked as PcP from the wiggly line records have been picked from all station records. They are labelled in **Fig. 4.3**. The synthetic seismogram modelling of these phases is described in **section 6.4.3**.

4.4.3 PmP

PmP is a dominant arrival on all record sections although on the Morpeth records it is obscured in places at pre-critical offsets by the very bright arrival **D** which was initially confused with it. PmP has been traced without difficulty to offsets of about 110 km and then it seems from station 54 records to form a triplication with PcP and Pn which extends out to offsets of approximately 160 km. At station 57

it is difficult to observe a pre-critical Moho reflection due to the interference of the arrival D, but the triplication may be observed. The associated multiples described in **section 4.4.2**, presumably caused by the near-surface structure beneath the shots, are particularly strong in association with PmP and confuse the picking operation considerably especially at large offsets.

4.4.4 Pn

Another important feature of the record sections is **Pn**, the refracted headwave from the upper mantle. This was detected for the first time when the first variable area compressed section for the whole of line 1 was produced for station 54. It was not convincingly observed on the CSSP record sections but is very clearly seen, even as a second arrival, on the variable area compressed record sections of the MOBIL stations (see **Appendix C**), with an apparent velocity of 8.14 kms^{-1}. It was not fitted by travel time regression since it is not visible on the wiggly-line sections, but it provides a valuable restraint in modelling the Moho and especially the thickness of the crust.

On the station 54 section, Pn can be seen best where it emerges as a first arrival from beneath the triplication at 133 km offset. Its amplitude varies considerably, almost disappearing in places and then reappearing again at greater offset. The point of emergence varies slightly from station to station, but is usually between 133 and 135 km offset, indicating a constant crustal thickness along the profile.

4.4.5 D

The most interesting phase observed in this study is arrival **D**, which was first mistaken for PmP due to its high amplitude near what was expected to be the critical distance (about 80 km offset) and the fact that it merges into PmP. However, from the results of the T^2 -X^2 modelling and some ray tracing, it is obvious that it is not a wide-angle reflection.

On the variable area record section of **Fig. 4.3** from station 54, for shots 2338-2766, arrival D is the most dominant phase of all in terms of amplitude. **Fig. 4.7** shows a record section from station 47 with the same phase at offsets between 80 km and 100 km offset. D can be observed on all the Morpeth record sections at different offsets, in fact at station 57, as already mentioned, it masks the pre-critical

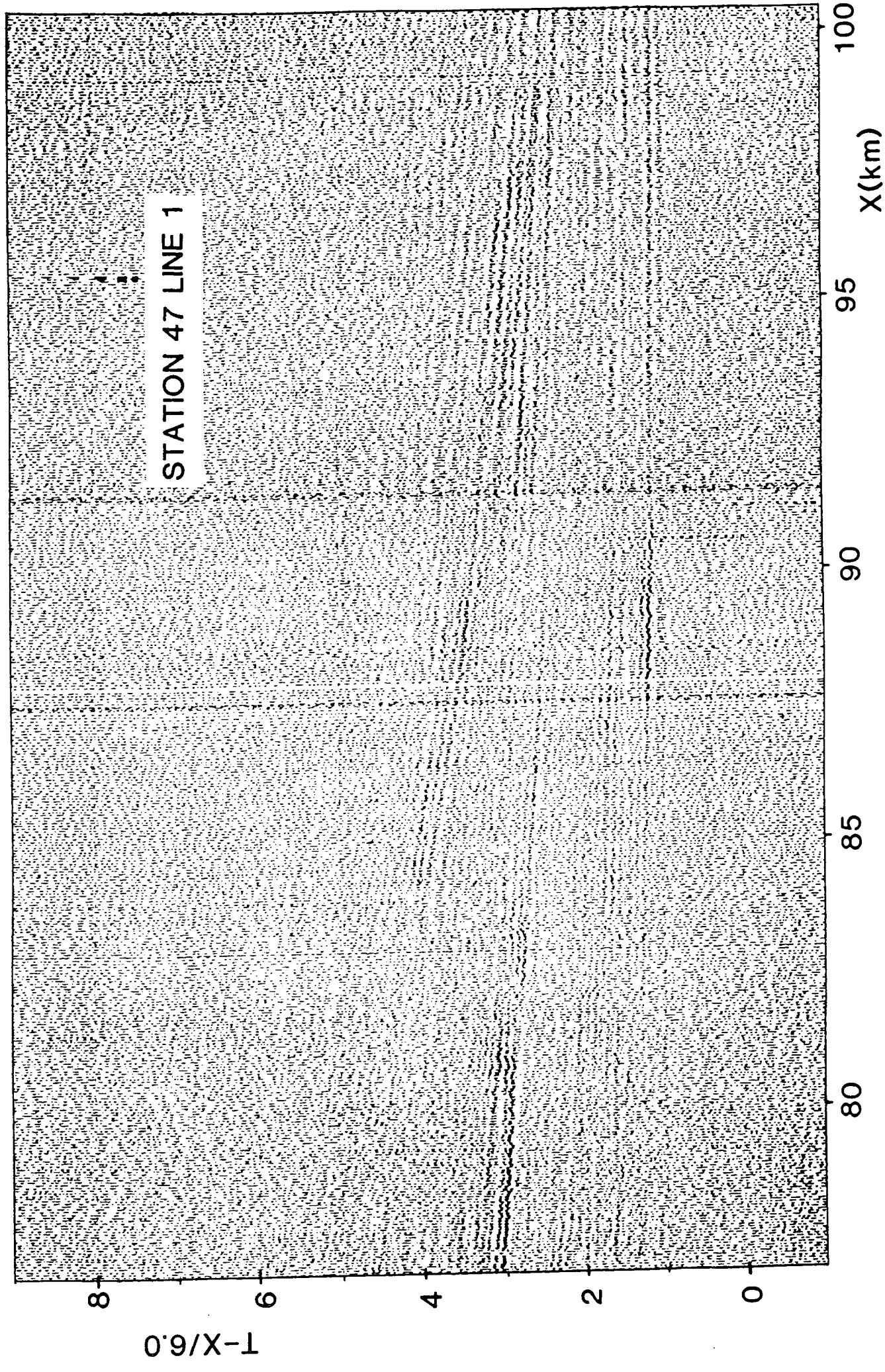

Fig. 4.7 Variable area compressed record section from station 47

PmP. It is not seen so well on the Wark sections although it is visible on station 40 records between approximately 105 km and 115 km offset. With hindsight, it is possible to observe this arrival in the original CSSP records from these stations (**Fig. 3.6**), but caught up in the wavetrain of PmP and therefore difficult to pick.

On all the sections where it is observed, the distinguishing characteristics of D are its high **amplitude, very high apparent velocity** and the fact that it **merges into the Moho wide-angle reflection.** The high apparent velocity is particularly interesting, tending to infinity over a particular shotpoint rather than at a specific offset.

Plotting the travel times of D as observed at stations 47, 54 and 57, **unreduced**, yields **Fig. 4.8**, which shows the characteristic shape of a diffraction with a minimum for each curve at the distance which corresponds to shotpoint 2768 (see Fig.2.2 for the location).In normal incidence reflection seismology, such an arrival, viewed in an unreduced record section, would automatically be recognised as a diffraction event, which in this case seems to be derived from Moho depths. This was not immediately the case in this interpretation due to the different appearance of a reduced record section to begin with, and also the fact that diffractions have never before been recognised as such on wide-angle records.

Fig. 4.9(a) shows the ray paths for wide-angle reflections from an interface at 30 km depth (that is, the Moho) and diffractions from a point on that interface. Calculating the travel times for both types of ray, with a uniform velocity of 6.2 kms^{-1}, produces an unreduced travel time section (b), which converts to a reduced travel time section (c)....which closely resembles the appearance of arrival D. Using a routine **DIFFR**, written to calculate the travel time curve for a diffraction event, the travel time curve was computed for three different stations and plotted with the observed travel times for D at those stations. This produces the fit shown in **Fig. 4.10** for stations 57, 54 and 47, where the dots represent observed travel times and the lines are the calculated times. The fit is very good and provides a convincing argument for the explanation of D as a type of diffraction event.

Once D had been distinguished from wide-angle reflections as a `diffraction-type' phase, other similar phases of smaller amplitude became apparent all over the records, obviously from similar

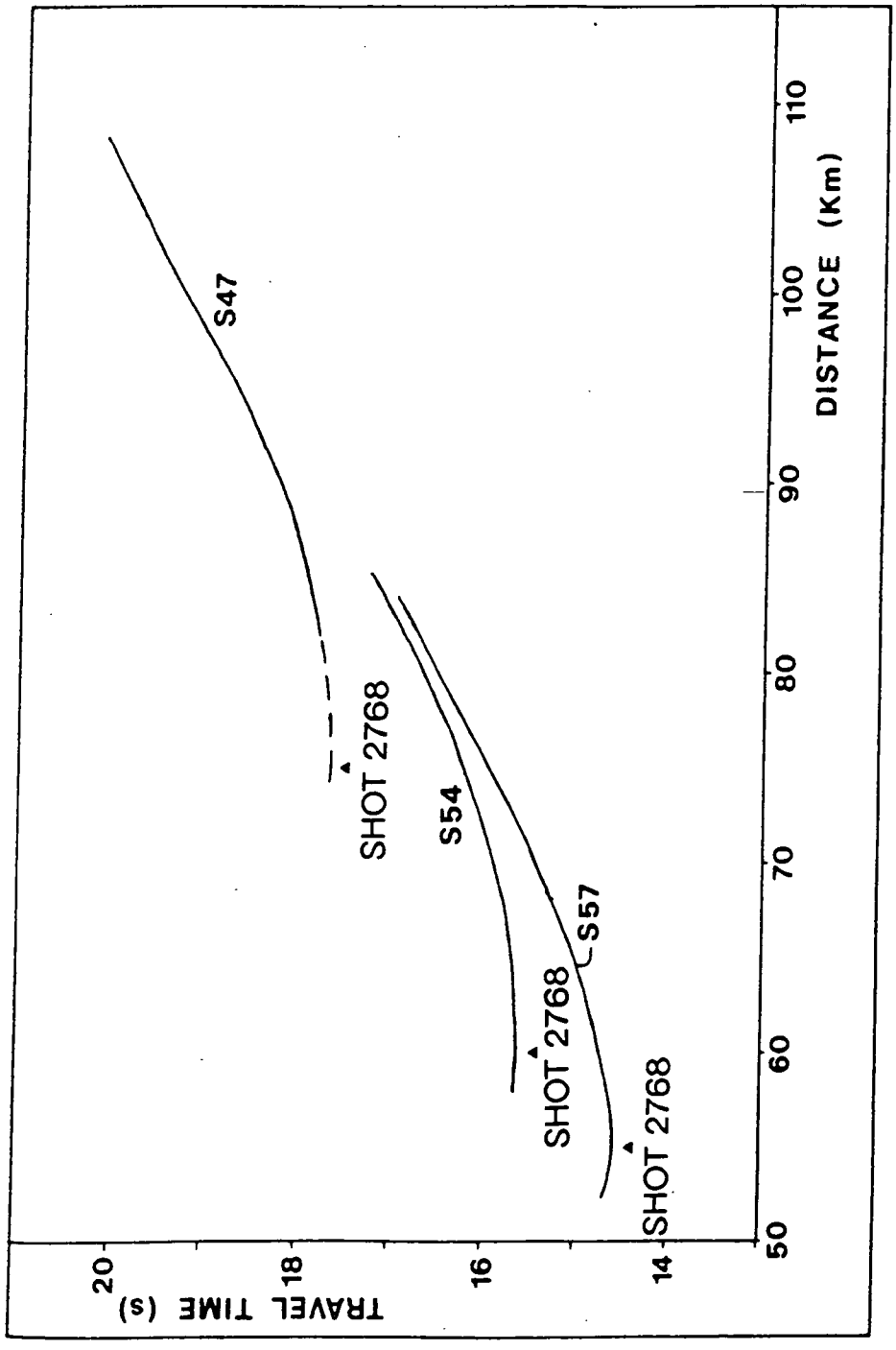

Fig. 4.8 Unreduced travel times of arrival D as observed at stations 54, 47 and 57. The arrows indicate the location of shotpoint 2768.

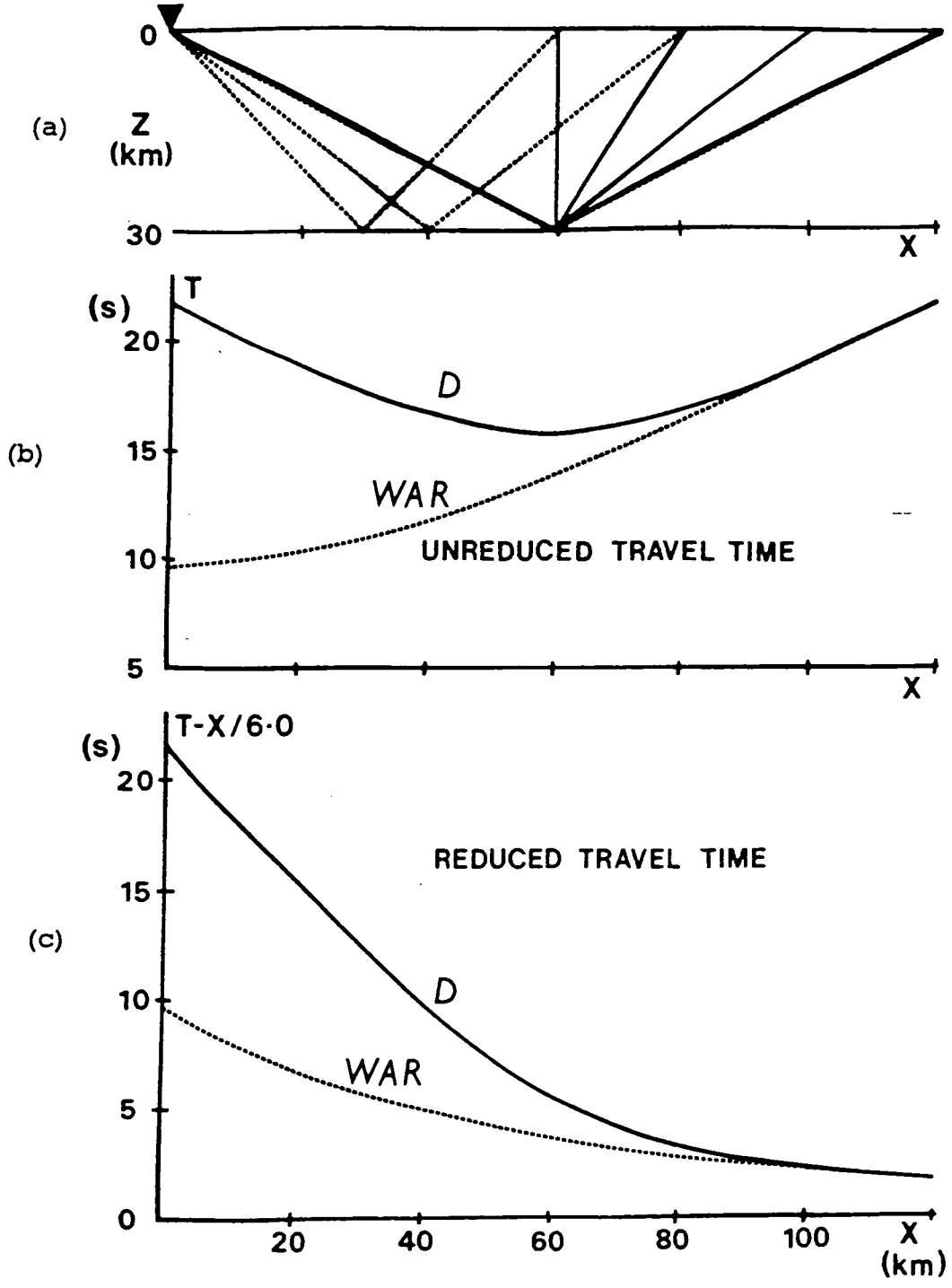

Fig. 4.9 Travel time behaviour of a diffraction in a homogeneous layer.
D: diffraction travel time; WAR: wide-angle reflection travel time.

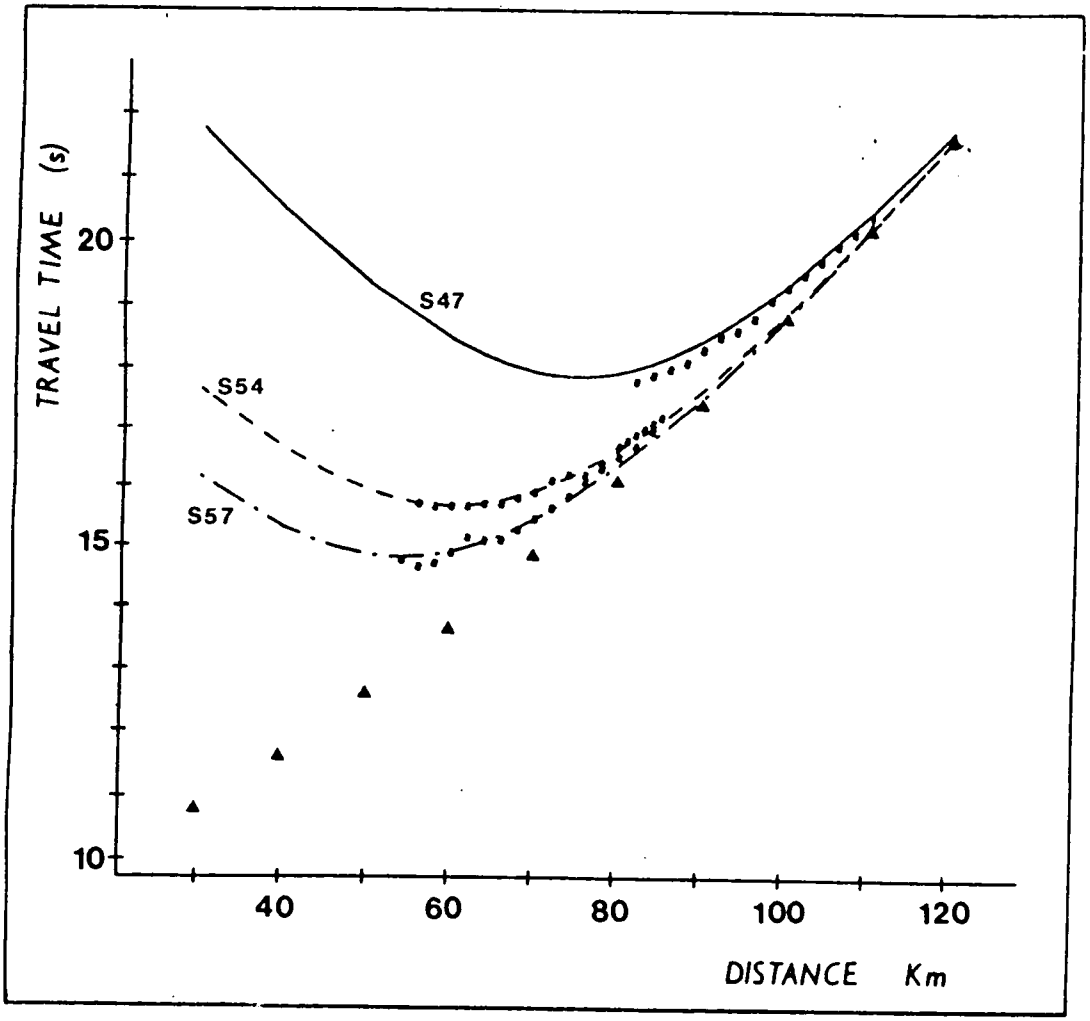

Fig. 4.10 Comparison of observed travel times for D with those calculated for a diffraction from a point at 30 km depth within a homogeneous layer. **Triangles**: the computed travel times for a wide-angle reflection from 30 km depth; **dots**: observed travel times; **lines**: calculated travel times for the diffraction.

structural features. Some of these also merge into PmP, some into PcP or other wide-angle reflections so it seems that this type of arrival may come from any depth in the crust and is only resolved by wide-angle reflection seismic experiments of this kind of resolution. Some of these arrivals are labelled **d** in the two sketches of **Figs. 4.4 and 4.5.**

However, the high amplitude of phase D has yet to be explained satisfactorily. The maximum amplitude of D is observed, as it would be expected for a diffraction, where it merges with and becomes PmP, the Moho wide-angle reflection. This may be seen in **Berryhill (1977)**, although his discussion was based upon the near-vertical incidence case and implications for stacking. The maximum amplitude of a diffraction when observed at near-normal incidence is half the amplitude of the vertically reflected phase. Little is published about the behaviour of diffractions at wide-angle due the scarcity of their occurrence, but a pure diffraction could hardly be expected to show amplitudes on the scale seen here. Other diffraction-type arrivals are seen on the record section, as mentioned in **section 4.3.2**, but none of such high amplitude.

It would therefore seem to be necessary to model the phase D in terms of rays which would follow the paths of diffraction-type events as reflections from curved or dipping structures which have concentrated the seismic energy in some way. This modelling is described in the chapter 6. First, however, the following chapter describes the synthetic seismogram packages used to carry out the modelling of the features described in this chapter.

CHAPTER 5 : SYNTHETIC SEISMOGRAM PACKAGES

5.1 Introduction

After study of the wide-angle reflection seismic sections, identification and picking of the main crustal phases, described in the previous chapter, the largest part of the interpretation of the dataset consisted of the forward modelling of the selected phases, using synthetic seismogram packages.

There are two main types of synthetic seismogram package available at Durham: the Reflectivity Method of **Fuchs and Mueller (1971)** and various packages which use Asymptotic Ray Theory (ART) or a modification of it. The Reflectivity Method package, **SYNSEI**, is the only exact method and is the most accurate. It is restricted to modelling horizontally uniform (one-dimensional) structures and cannot therefore be used where strong lateral variations in velocity are expected. The most flexible package, until the arrival of **BEAM87**, was **SEIS83**, which uses ART to carry out ray tracing and compute synthetic seismograms in laterally varying (two-dimensional) media. BEAM87, which supersedes SEIS83, uses the Gaussian Beam approximation which makes the method more stable in regions where the ray method (ART) is unreliable. These three packages have all been tried for the Mobil dataset and are therefore described in the following sections.

There are several other packages at Durham which use modifications of ART. These include: AIMS, ANRAY, RAYAMP and RAYSYN, although ANRAY and RAYAMP are not yet fully implemented. None of these methods were actually applied to the modelling of the MOBIL wide-angle dataset but for completeness, a brief account of them is given in **section 5.5.**

5.2 The Reflectivity Method

5.2.1 Reflectivity theory

The reflectivity method itself belongs to the group of synthetic seismogram computation methods which use wavenumber or slowness integration to compute the full wavefield seismic response for the

models. It is a frequency domain method, as compared to the time-domain approach of the ray method. The integration of the reflectivity of a layered medium is carried out in the horizontal wavenumber (or angle of incidence) domain. Multiplying the result by the spectrum of the source signal yields the full seismic response of the medium.

The method was extended by **Fuchs and Mueller (1971)** to include the elastic transmission losses and time shifts due to stacks of layers above the reflection zone, that is, above the region which returns seismic phases of interest. **Kennett (1975)** extended the technique further to allow for varying structure beneath shots and receivers, thus allowing some degree of lateral inhomogeneity, at a shallow level.

The strength of this method is its high accuracy and the fact that the full wavefield is computed, as compared to only the specified phases in the ray method. However, it requires large amounts of computer time and disc space to calculate the reflectivity matrix for the integration even for a relatively simple model and limiting the slownesses to those of interest. It therefore requires a supercomputer or the programme to be rewritten for a vector processor (**Sandmeier and Wenzel, 1986**), for practical modelling. Its use is also restricted in modelling by the fact that it is a one-dimensional method, allowing only for **vertically** inhomogeneous media beneath the level of the shallow structure beneath the shots and receivers.

Other slight computational problems, although they do not affect the accuracy of the real phases, are the tendency of high energy arrivals to `wrap around' onto the seismograms and the appearance of numerical phases on the synthetic sections. The wraparound phases are seen when high energy arrivals are generated for the model **outside** the time window of interest and these are aliased into the sections. The numerical phases appear with the limiting slowness set for the integration. These may sometimes be reduced in amplitude by applying a cosine taper to the ends of the slowness interval (**Mueller, 1985**).

In spite of the problems with the method however, the synthetic seismograms it produces are far more reliable than those computed by the ray method especially with regard to amplitudes. The best approach to use in modelling was therefore to use the ray method to obtain a rough idea of the one-dimensional structure, then use the reflectivity method to check this model, particularly the synthetic amplitudes, and continue to model in two dimensions using the ray method again.

5.2.2 SYNSEI / SYN86

The package at Durham which incorporates the reflectivity method was originally called SYNSEI, the programme written by Fuchs and Mueller, and adapted by Brian Kennett. This was modified in 1986 by D.L. Stevenson and the author to adapt better to running on Durham's main frame computer, under the name **SYN86.**

The whole package was split into three parts, the main programme, a new library of subroutines and another library which included all the original subroutines. The programme was converted to Fortran77 from FortranIV, and the graphics changed to Ghost80. The new subroutines, written by D.L. Stevenson were to enable the input to the programme to be made in 5 files, instead of the original one. Each new input file contains the details of one specific aspect of the model:

1) The shallow structure beneath the shots and details of the source.

2) The shallow structure beneath the receivers.

3) The velocity structure of the reflection zone, that is, the region of interest.

4) The distances of the shots and receivers from each other.

5) The control file with miscellaneous details.

SYNSEI contained two options for the method to carry out the wavenumber (or angle of incidence) integration, by the trapezoidal rule or Simpson's rule. The trapezoidal rule is the better method to use, but another option was added to SYN86, which uses **Filon's method (Frazer and Gettrust, 1984)** in a subroutine written by M.H.P. Bott. This is apparently even better than the trapezoidal rule for the integration. Two examples of synthetic seismogram are shown in **Fig. 5.1(a) and (b),** (a) computed using Filon's method for the integration, (b) using the trapezoidal rule. It may be seen from the figure that the method removes the slight distance aliasing visible at offsets over 125 km. This figure also demonstrates one of the other computational problems mentioned in the previous section: strong numerical phases across the section.

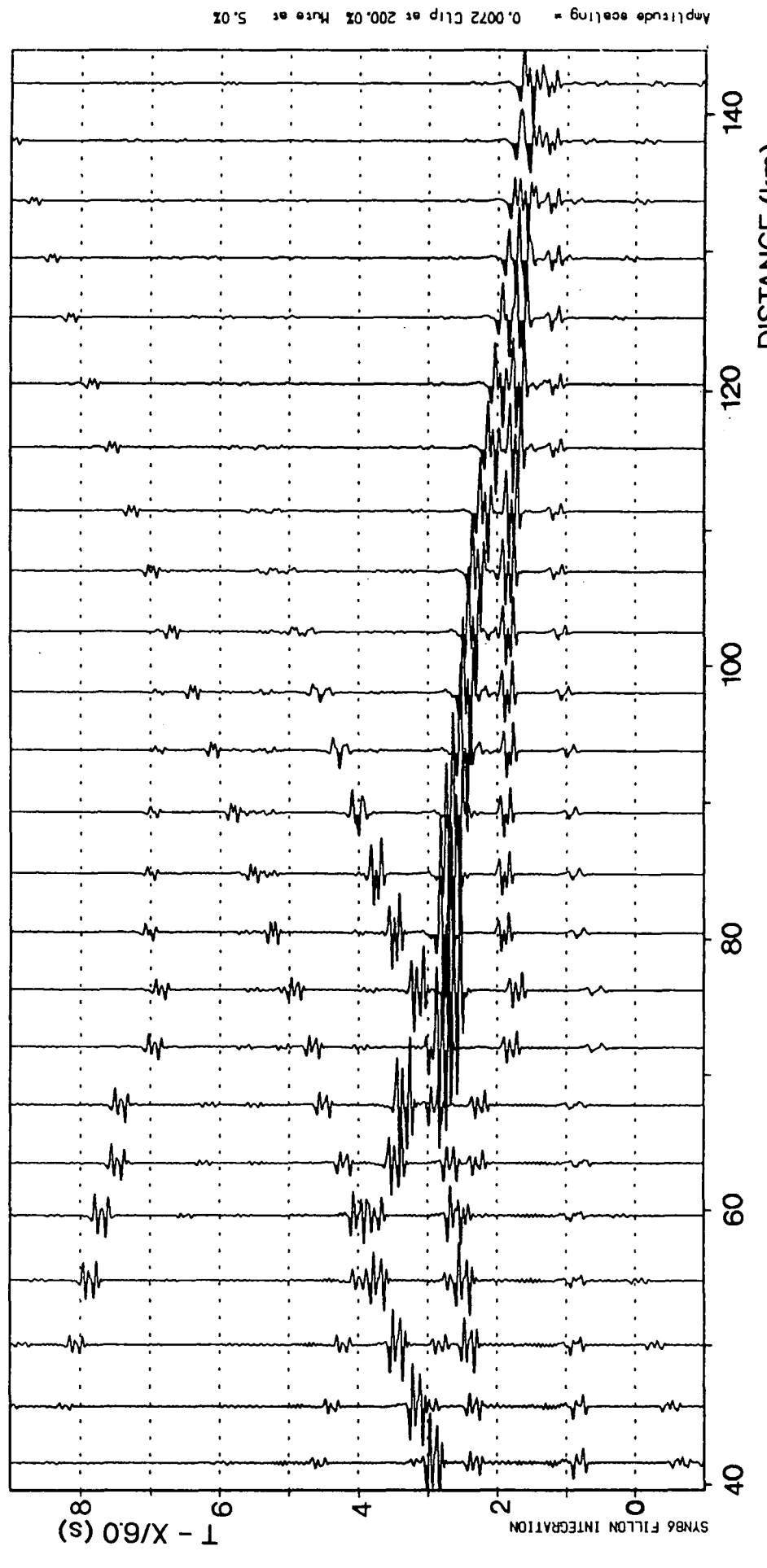

Fig. 5.1(a) Synthetic seismogram computed using the reflectivity method (SYNSEI) with the Filon integration method. The model used for computation is shown in (c).

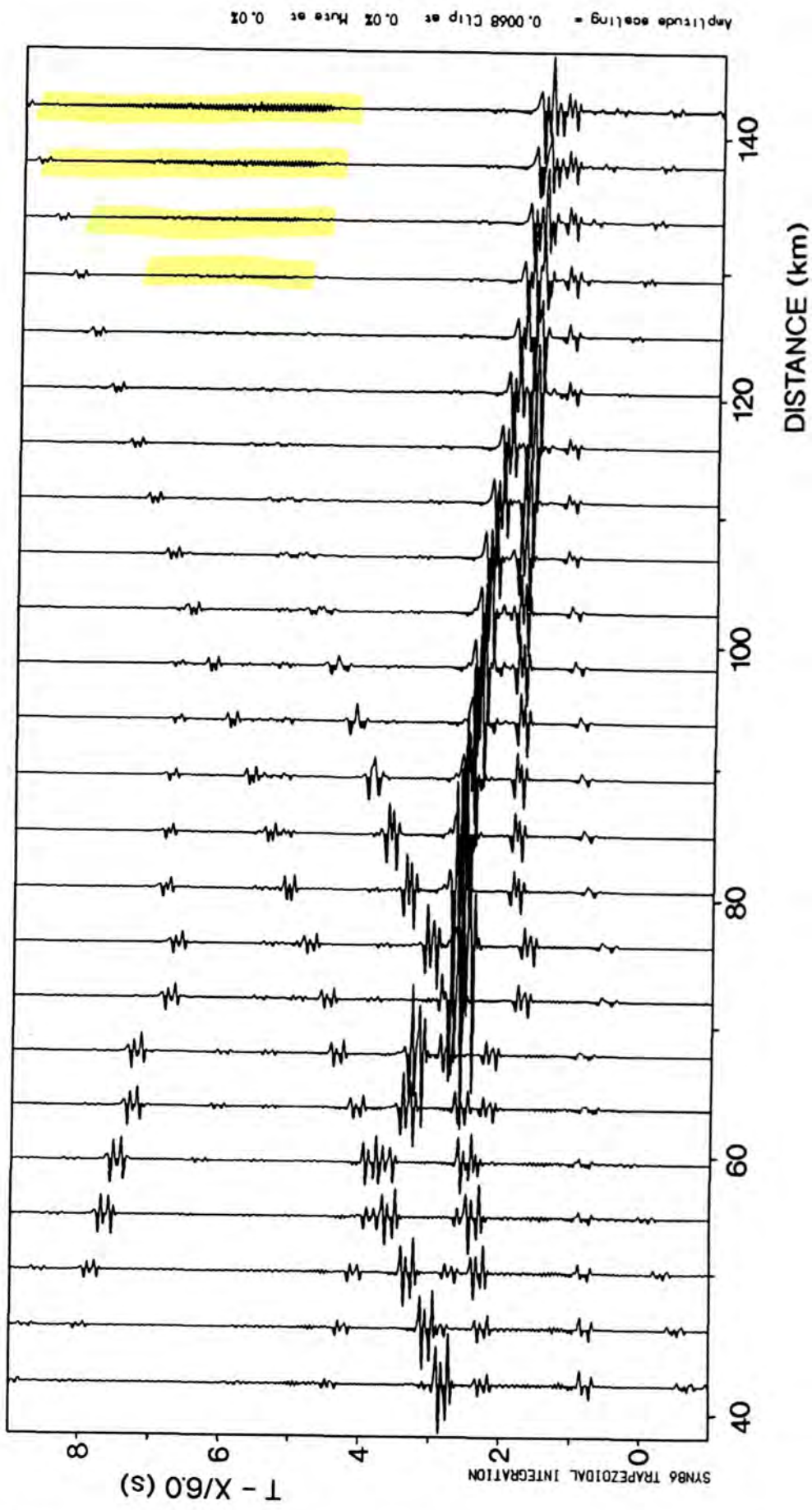

Fig. 5.1(b) Synthetic seismogram computed using the reflectivity method (SYNSEI) with the trapezoidal integration method. The model used for computation is shown in (c).

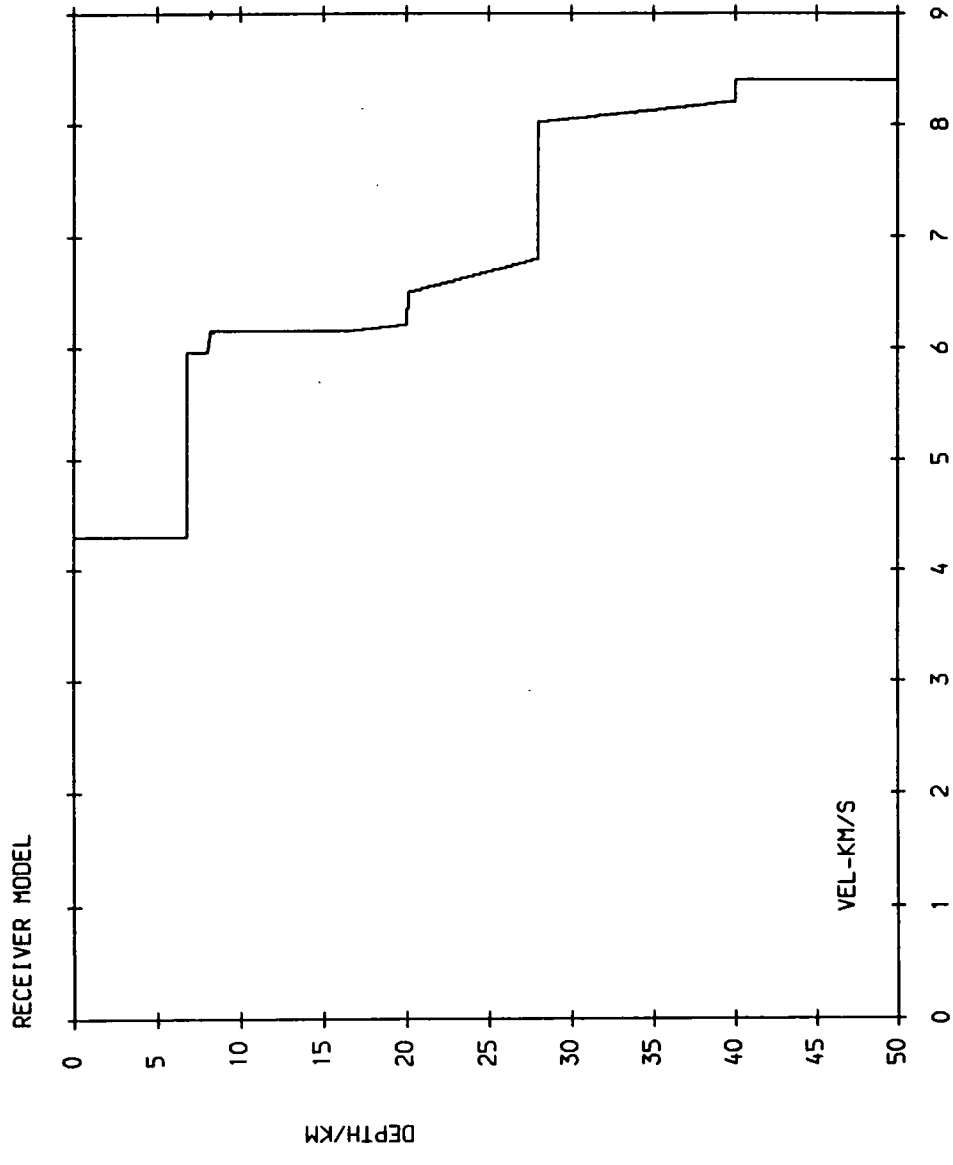

Fig. 5.1(c)Model used for computation of synthetic seismograms shown in (a) and (b).

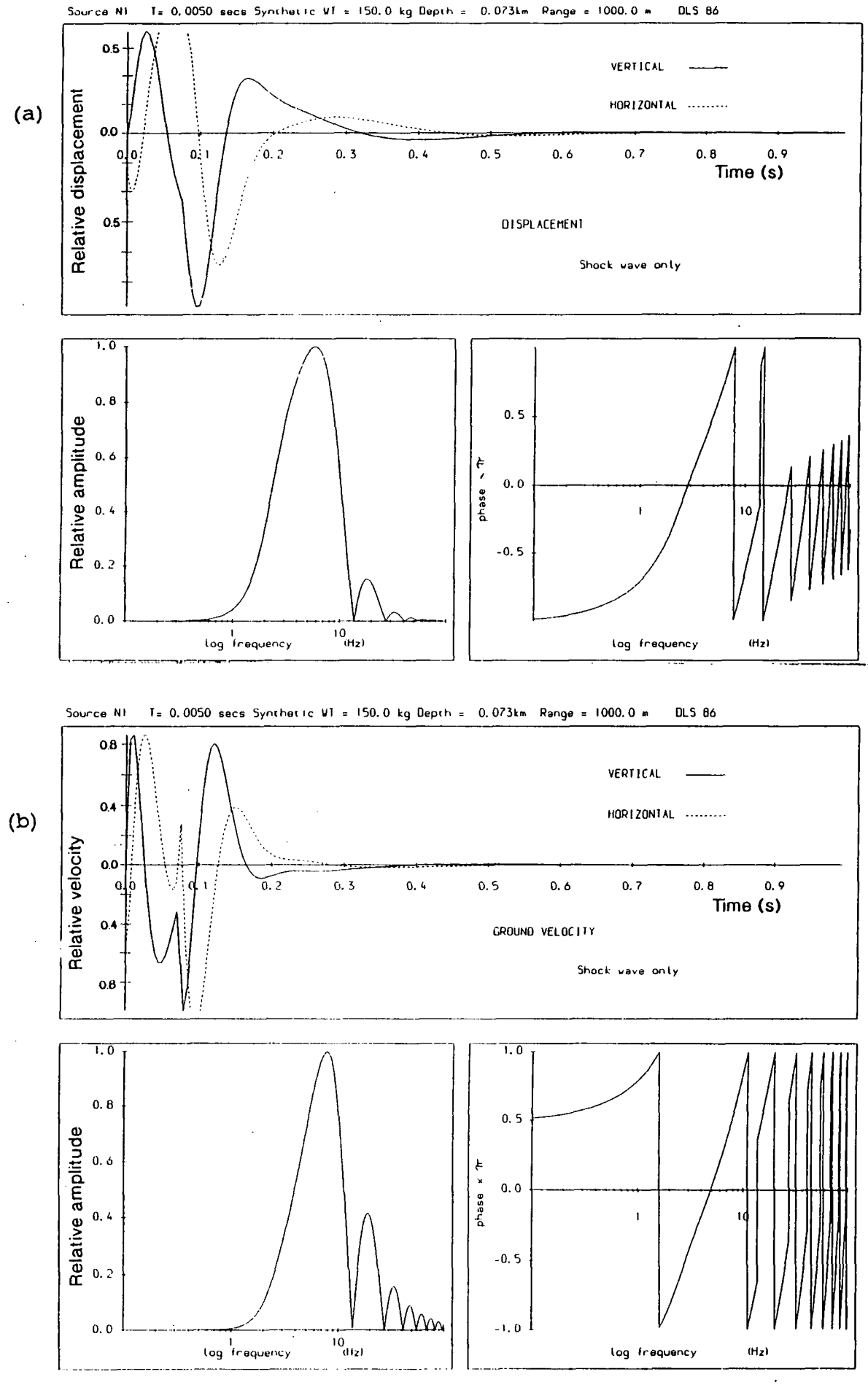

Fig. 5.2 Source signatures computed for the reflectivity method to yield: (a) ground displacement and (b) ground velocity synthetic seismograms.

The original package computed either the ground displacement or the pressure as recorded at the Earth's surface. Seismometers actually measure ground velocity, so for direct comparison during modelling, computation of the ground velocity by the package is more useful. SYN86 was therefore modified to provide this option. **Fig. 5.2** shows the differences between the waveforms for the different options, ground velocity and ground displacement (in the time domain), also the amplitude and phase spectra. This particular example is computed for a marine explosive shot.

The package is fairly flexible to use, providing many options which are useful in modelling wide-angle reflection/refraction surveys, such as the automatic generation of an explosive source signal (subroutine BANGIN), being able to input the seismometer characteristics and being able to approximate a vertical velocity gradient in terms of homogeneous layers (subroutine INHOM), to name but a few. The results are very reliable and realistic. The main drawbacks, as outlined above, are the length of time required for the computations, especially for models with many layers, and the restriction to laterally homogeneous media.

Durham does now possess the version of SYNSEI (SYNCYB) vectorised by Karl-Josef Sandmeier at Karlsruhe University for use on a CDC CYBER 205 high-speed computer. Run on this machine, the computation time using the reflectivity method is speeded up by a factor of 20 to 30 compared to the time required to run SYN86 on Durham's AMDAHL main frame computer. It is hoped that the vectorised version may be implemented onto the CYBER 205 at the University of Manchester or the Rutherford Appleton Laboratory. This version does not yet use all the convenient additions which are part of SYN86, but makes seismic modelling far easier and faster.

5.3 The Ray Method

5.3.1 Ray theory (Asymptotic Ray Theory)

The ray method for computing synthetic seismograms is based on the idea of splitting up the wavefield in a region into several **elementary** waves, each of which may be described by the path it takes through a model. For each of these elementary waves, rays of infinitesimally narrow cross-section are traced through the model, by solving a set of ordinary differential equations which yield the ray

trajectory, slowness vectors and the travel time T. The mathematics and detailed theory are described in detail in **Cerveny et al.(1977)**, and a good general account may be found in **Cerveny (1985a)**, from which most of the information in this section is derived. In the case of fixed source and receivers, **two-point** ray tracing is required in order to obtain rays which start and finish at the necessary points. The most crucial assumption of the method is that the dimensions of structures in the model are larger than the wavelength of the seismic waves. This is therefore a **high frequency approximation.**

The two-point ray tracing is carried out by means of a **"shooting"** mechanism, whereby rays are traced from a starting point (a "shot") in an iterative loop, the initial conditions changing slightly each time through the loop. In the source-to-receiver computations, this means in practice varying the take-off angle of the ray from the source each time. The amplitudes of the rays are corrected for geometrical spreading and modified by reflection and transmission at interfaces.

The actual synthetic seismograms are evaluated either by (a) direct summation of all the elementary seismograms, or (b) evaluating the frequency response, multiplying by the source spectrum and inverse Fourier transforming, or (c) by a convolutory approach, calculating a complex-valued impulse response and convolving this with the analytic source signal. In practice, the method of summation is the most useful for a small number of elementary waves. In fact, the ray method is on the whole most practical for a small number of elementary waves since it would otherwise become rather cumbersome.

The advantage of this method lies in the relatively short time required for computation and in the flexibility of the technique, since the assumption holds for many models. It allows computation in two-dimensional models for no more computational time than one- dimensional, whereas more accurate methods such as the reflectivity method are unable to cope with laterally inhomogeneous media.

The method does fall down, however, in that for the high-frequency assumption to be valid, the velocity field cannot vary too rapidly (small oscillations in the velocity field cause spurious arrivals) and ray theory breaks down in some crucial regions of the wave field such as the critical region and caustics. Shadow areas are very pronounced on ray synthetic seismograms instead of amplitudes decaying into them. It cannot compute diffractions from edges, although these may be `tacked on' without accurate

amplitude or phase information. The accuracy of the method therefore leaves something to be desired, compared to exact methods, and relies on the user's knowledge of the weaknesses to identify spurious arrivals and `fill in the gaps'.

However, the method is easy to use, widely available and flexible, which has meant that it is the most popular method for modelling wide-angle reflection and refraction data in terms of laterally varying media. Perhaps the best known package of its kind is **SEIS83**, written by Cerveny and Psencik.

5.3.2. SEIS83

Written in 1983 as an update and improvement on the older **SEIS81**, this package uses the ray method to compute synthetic seismograms in laterally varying media. It carries out two-point ray tracing by means of a modified shooting method, evaluating the synthetic seismograms by the summation of the elementary seismograms.It uses a Gaussian envelope for the source signal, in which the central frequency may be specified by the user.

The representation of the model is relatively straightforward: four interfaces bound the model, two straight vertical and two horizontal, either curved or straight (defining the Earth's surface and the base of the model). Within these bounds, interfaces cross the model from right to left, defined by a maximum of 30 points per interface and interpolated by a cubic spline.

The velocity field may be represented by one of three methods: either as a system of grids of velocity specifications, a different grid in each layer, which are then interpolated over the whole layer by a **bicubic spline**; or again as grids but using a piecewise **bilinear interpolation**; or by specifying the velocities at the top and bottom of each layer (as defined by the interfaces) and a **linear interpolation** of the velocity applied vertically within each layer, in which case the interfaces are equivalent to velocity isolines.

The relative merits of the velocity specifications are debatable. The bicubic spline method is probably the most popular since it allows lateral velocity variations within layers, but unfortunately it has a tendency to produce small oscillations in the velocity structure even after being smoothed. The linear interpolation method is probably the most reliable but it cannot represent laterally varying velocities. The

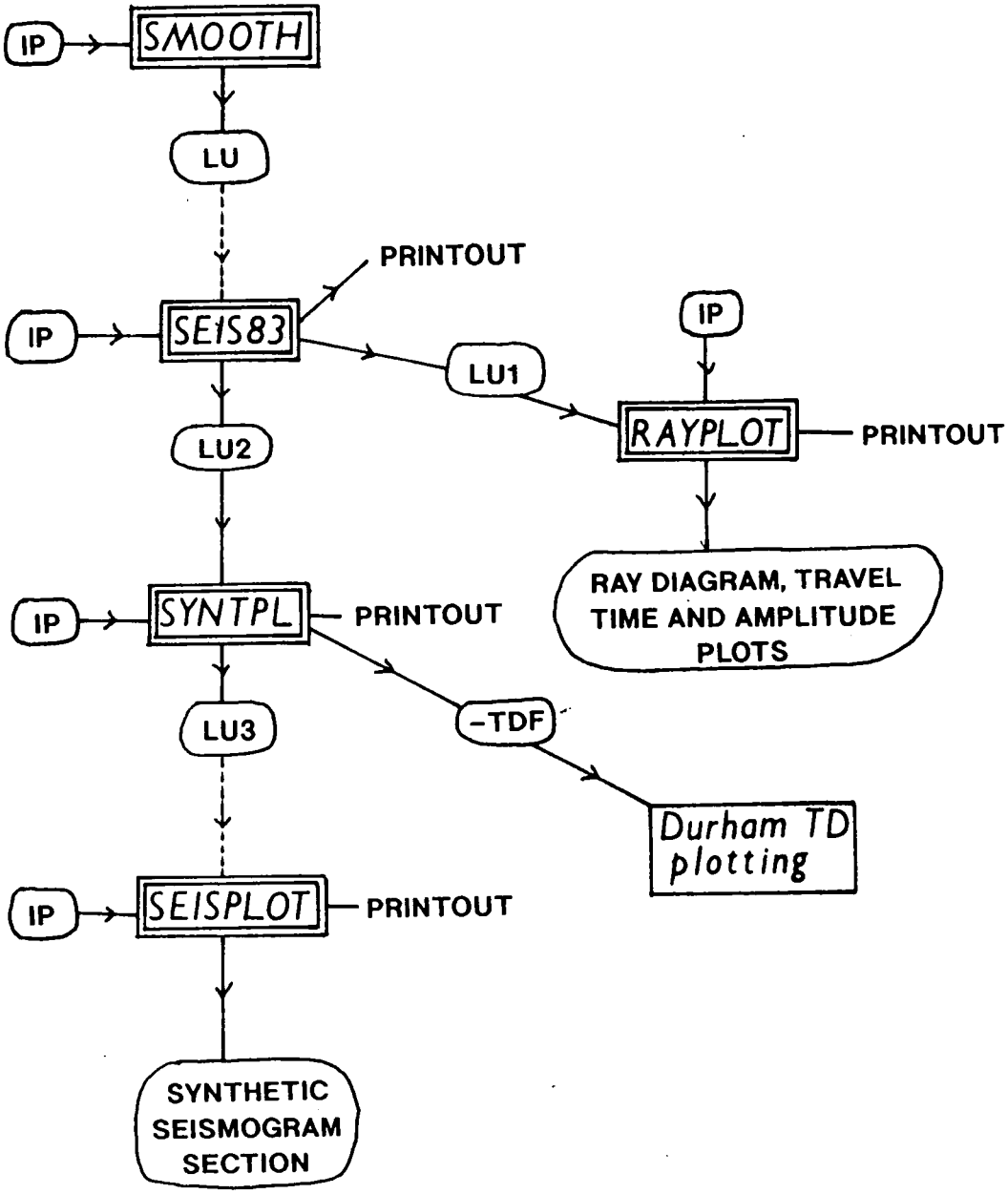

Fig. 5.3 Flow chart of the use of SEIS83.

piecewise bilinear interpolation method apparently produces spurious arrivals and unstable results (Lewis,1986).

The computer package is shown in **Fig. 5.3** as a flow chart. The first and main programme, **SEIS83,** constructs the model from the data points specified in the input and computes the requested rays through this medium, calculating the travel times and amplitudes to store in two output files. The output is used by **RAYPLOT** to plot the ray diagrams, travel time plots and amplitude versus distance curves and by **SYNTPL,** which computes the synthetic seismograms by summation of the elementary seismograms, writing the output in either Durham's TD format for plotting or in the correct format for plotting with **SEISPLOT,** the package's plotting routine for seismic sections. Using the TDF writing option enables the plotting of the synthetic sections with the same plotting parameters as the original data sections, for easier comparison. The optional programme **SMOOTH** performs smoothing of the input for the velocity model when the bicubic spline interpolation method is to be used. Each routine is thoroughly documented. The plotting routines RAYPLOT and SEISPLOT use *PLOTSYS graphics subroutines which are still available at Durham.

5.4 The Gaussian Beam Method

5.4.1 Gaussian beam theory

There are several adaptations of asymptotic ray theory which aim to compensate for the inaccuracies within the ray method whilst retaining its versatility and convenience. A much-documented example is the Gaussian beam method which is now implemented at Durham.

The Gaussian beam approach involves solving the wave equation close to the central ray, so that singularities involved in the ray method are eliminated. This means that instead of narrow rays, beams of seismic energy are being traced through the medium, with bell-shaped amplitude cross sections. This gives rise to the name Gaussian beam. The seismic response at receivers is computed by superposition of all the beams arriving in the vicinity of the receiver, since the beams have a broader range than rays.

The method is described in **Cerveny (1985b)** and **Weber (1988).** The execution of the method consists of ray tracing in exactly the same way as in the ray method, breaking the wavefield up into

individual elementary waves, carrying out initial value or interval ray tracing to generate a regular network of ray endpoints around the receivers. Dynamic ray tracing is then performed and spreading-free amplitudes calculated. All the information generated so far is stored, then the contributions of the Gaussian beams evaluated by expanding the source wavefield. The seismogram at any receiver is evaluated by superposition of all the beams in the vicinity of the receiver. Whether or not a beam may contribute to a receiver near its endpoint depends upon the beamwidth, L.

The properties of the beam, namely the beamwidth and its phase front curvature, are modified by each interaction with a boundary within the model. The beam parameters may be selected by the user to provide the most appropriate beams for the model under consideration. **Weber (1988)** has researched how the choice of beam parameter affects the accuracy of modelling, observing that for slowly varying media, the beamwidths should be broad, whereas for more complicated media, the beams should be narrow in order to yield accurate amplitudes. The phase front curvature should not be too strong. Weber's preferred method of selection of beam parameter, (in a medium approximated by triangles) is one in which the parameters are influenced by the size of the triangles which defined the velocity structure of the model.

Cerveny's preferred beam parameter selection provides an effectively plane phase front near the endpoints of the rays and sets **L**2** (the square of the beamwidth) to a minimum at the source. This causes broad beamwidths to result from beams with a large radius of phase-front curvature and narrow beams from small radii of curvature. This usually suppresses spurious arrivals and numerical oscillations although Weber's recommended method yields the most accurate seismograms overall (**Weber, 1988**).

The Gaussian beam method has many advantages as a technique over either the ray method or the reflectivity method, its main competitors. It is far more stable than the ray method in singular regions such as critical regions and caustics, and yields more reliable amplitudes (**Cerveny, 1985b**). The synthetic seismograms produced are far more realistic than those produced by the ray method, due to the better amplitudes and the fact that phases are not abruptly cut off by shadow zones but decay realistically, as would be expected for a full wave solution. This means that even diffractions may be artificially represented, although the amplitude and phase information is not accurate (**Kennett and Harding, 1985**).

It is no more time-consuming than the ray tracing method and can in fact be faster since there is no requirement for two-point ray tracing to be carried out.

There are still problems with the method in that the treatment of reflections and transmissions at interfaces ignores the effect of surface curvature and the method cannot cope accurately with diffractions. However, it is certainly far faster to run than the reflectivity package for adequate accuracy. It combines some of the accuracy of wave methods with the flexibility of ray tracing and therefore provides a most versatile option for synthetic seismogram modelling.

5.4.2 BEAM87

The Gaussian beam package in use at Durham is **BEAM87**, written by Cerveny during his stay at the University of California, Berkeley. It was from Berkeley that the package was actually obtained to implement onto Durham's mainframe computer. Since the package used CALCOMP plotting routines, easily convertible to Durham's *PLOTSYS graphics facility, implementation was relatively simple.

The package is very similar in structure to SEIS83, since the original programme BEAM81 was written as a modification of SEIS81 (**Cerveny, 1983**) and later updated to BEAM84 (**Cerveny 1985b**) before being improved further and documented in English in 1987.

The flow chart in **Fig. 5.4** shows the overall scheme of the package:

RT is basically identical to the main programme of SEIS83. It performs the initial value or interval ray tracing, then the dynamic ray tracing, evaluating the travel times, ray paths and spreading-free amplitudes. This information is stored in two files, one of which is used as input for the programme **RAYPLOT** for plotting ray diagrams, travel time plots and amplitude versus distance plots. The model representation in RT is identical to that used in SEIS83, again with a choice of three ways of interpolating the velocity. There is also a programme **SMOOTH** which serves the same purpose as in SEIS83, smoothing input to use in the bicubic spline method of velocity interpolation.

GB uses input from RT to compute the frequency response at the receivers, initial parameters of the Gaussian beams, radiation patterns, absorption mechanism and frequency dependent effects. It is

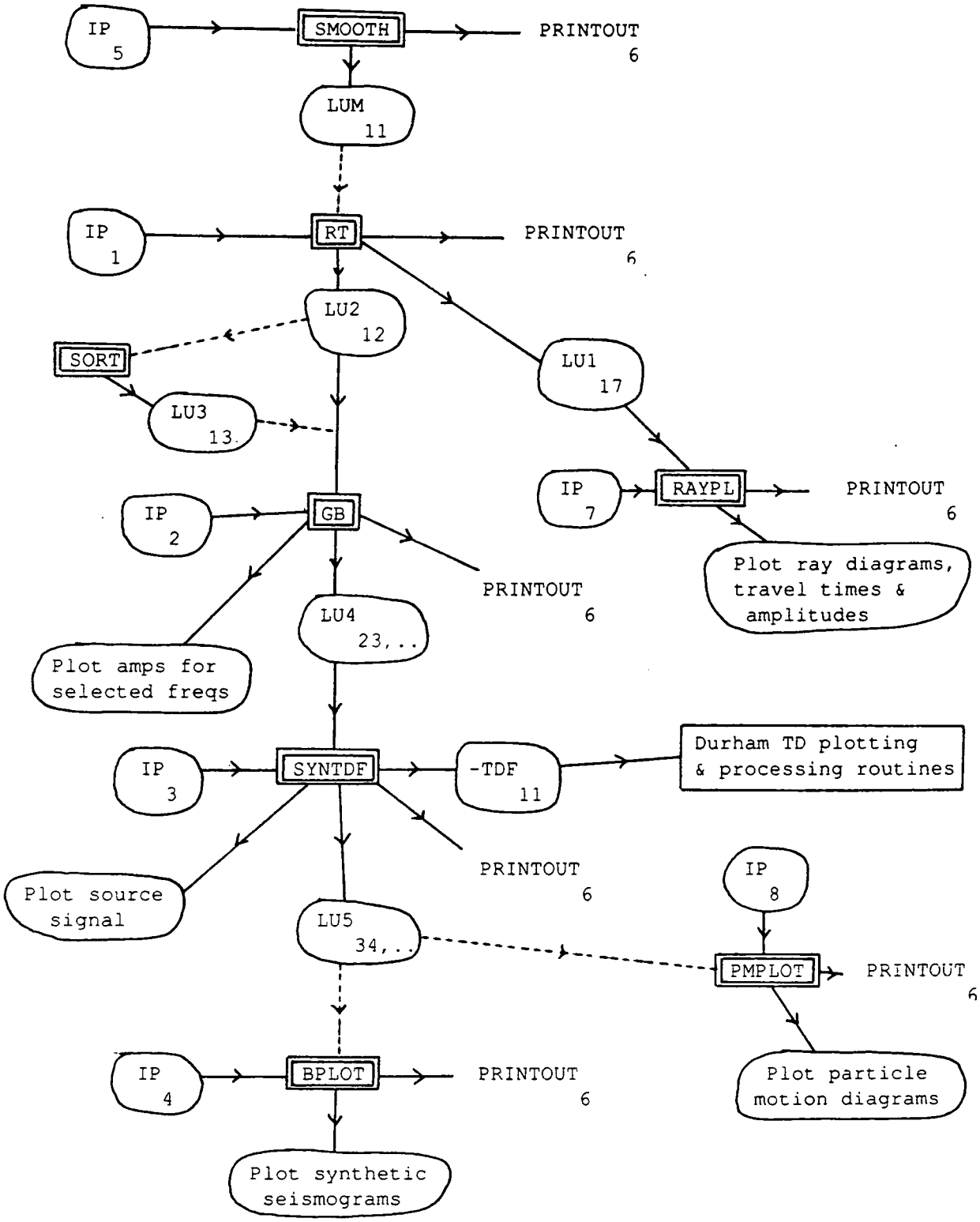

Fig. 5.4 Flow chart of the use of BEAM87.

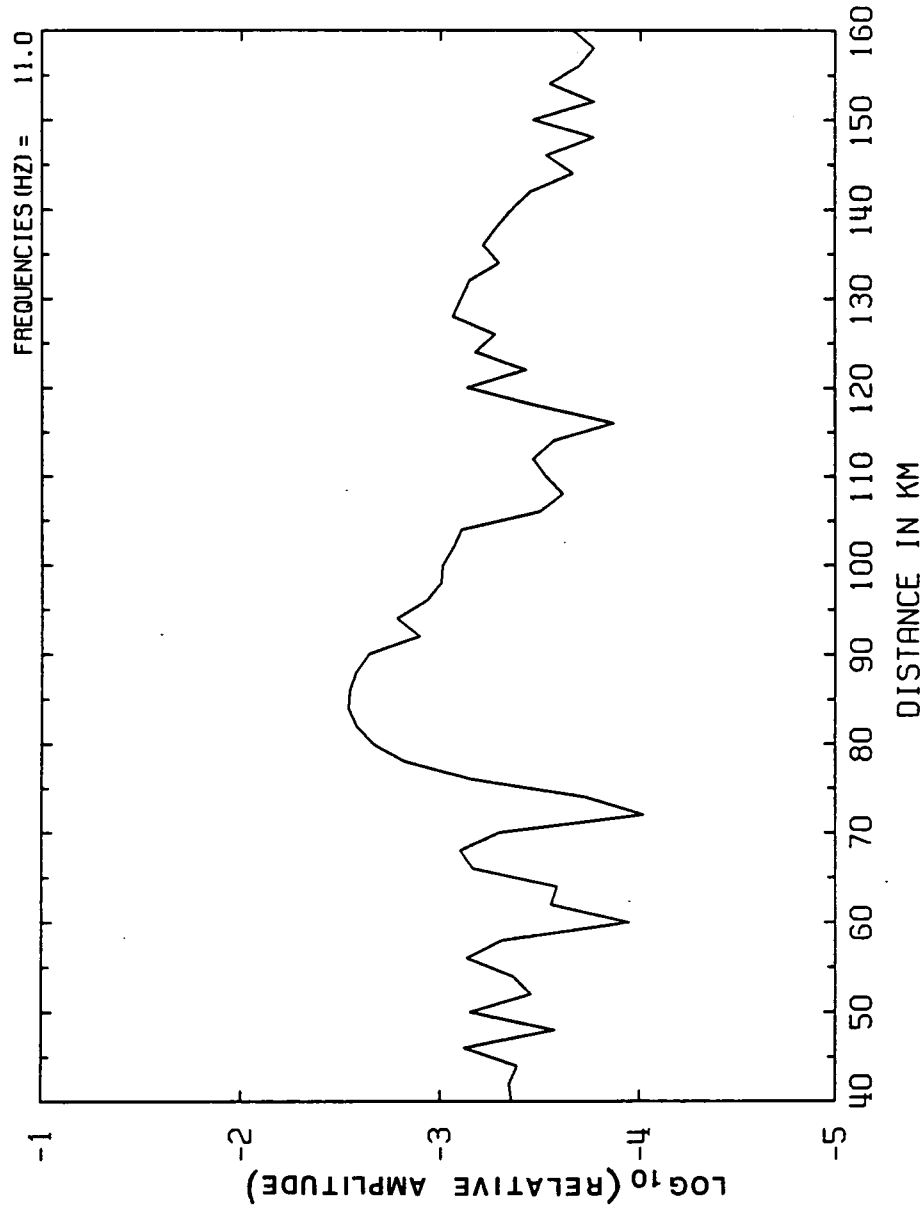

Fig. 5.5 Sample plot of amplitude variation against distance for Pg phase at specific frequency, from the program GB.

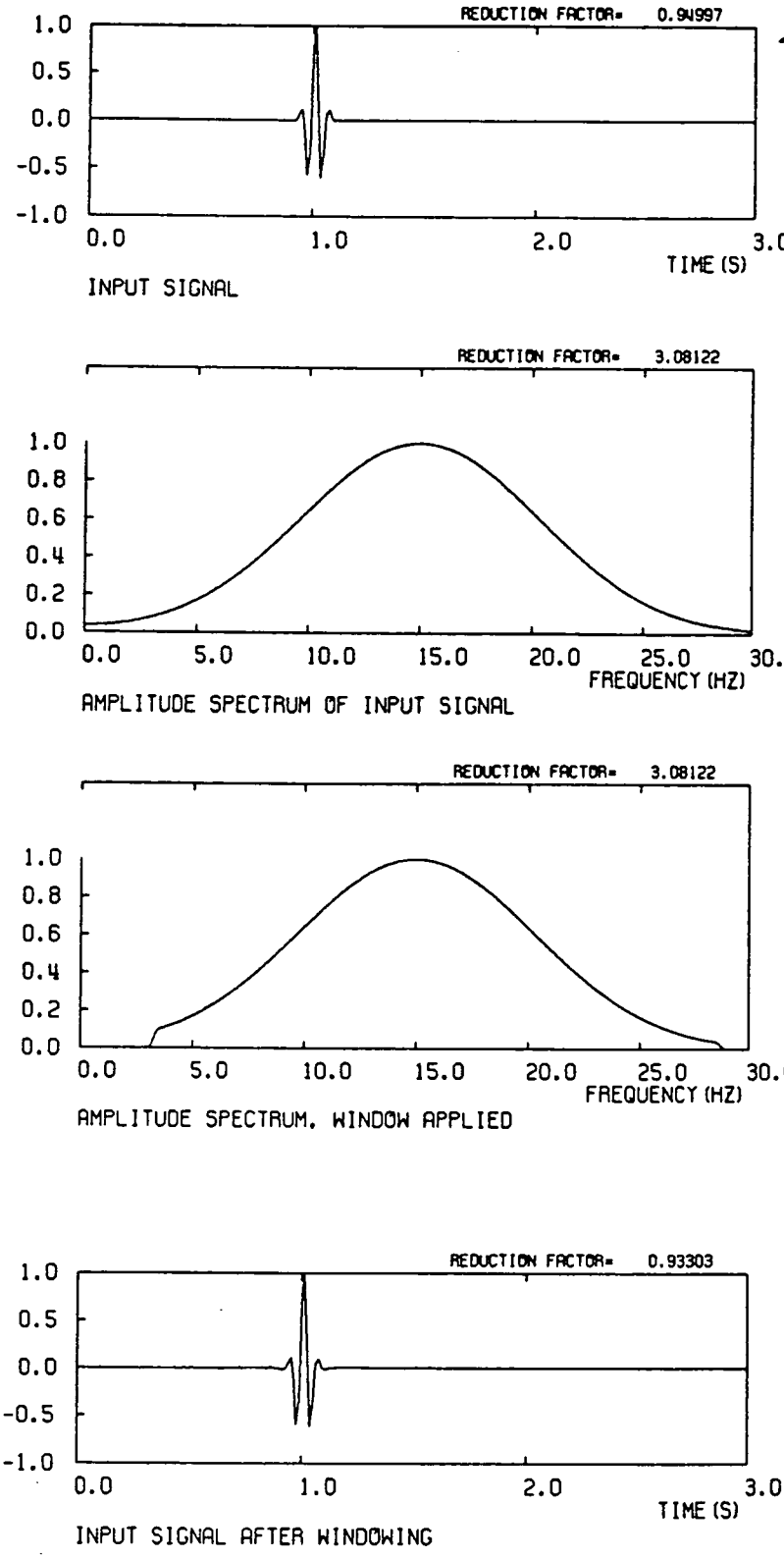

Fig. 5.6 Example of plot of input signal generated by program SYNT.

possible to generate plots of the amplitude-distance response for specific frequencies. An example of such a plot for Pg is shown in **Fig. 5.5.**

SYNT uses the output from GB to compute the seismograms at the specified receivers, using any high-frequency source signal chosen by the user. It contains the option of plotting the input signal, its spectrum and the results of filtering the signal, in addition to the spectra of the synthetic seismograms. The Durham version of this version has been modified to **SYNTDF**, which writes additional output in TD format, so that it may then be processed and plotted identically to the real dataset. **Fig. 5.6** shows examples of the plots which may be generated by SYNT or SYNTDF.

BPLOT may be used to plot sections of the synthetic seismograms generated by SYNT. Other programmes included in the BEAM87 package are **SORT**, which rearranges the rays computed by RT to increase monotonically, if they were computed in a different order, also **PMPLOT**, which plots particle motion diagrams of the shear wave components.

The whole package BEAM87 is a very flexible one which is straightforward to learn to use, especially after experience with SEIS83.

5.5 Other computational methods

5.5.1 Kirchhoff theory - AIMS

Another of the packages available for use at Durham is **AIMS**, the Advanced Interpretive Modelling System produced by GeoQuest. This uses ray theory to compute the seismic response of laterally varying models, primarily for near-vertical incidence seismic profiling. It also has the option of using Kirchhoff wave theory for modelling interfaces and most importantly, diffractions. An algorithm developed by **Trorey (1970)** is used, which enables the calculation of the response of a planar surface, and this is developed to apply to non-planar interface.

The most important feature of the Kirchhoff approach is that it considers not only specular reflections from interfaces but the whole surface response to the seismic waves. This makes the method particularly important in normal-incidence seismic reflection, where diffraction events play an important role in the interpretation of complex structures. It also means that the seismic response of curved

interfaces receives better treatment. This is becoming more important in the realm of wide-angle reflection (or refraction) profiling also, due to the increased resolution of profiles such as those of the MOBIL wide-angle programme.

5.5.2 RAYSYN

RAYSYN is a method written by Cassell at the University of Cambridge, which also uses ART to carry out ray tracing and computation of synthetic seismograms in laterally inhomogeneous media, but differs from Cerveny and Psencik's method in that the medium is approximated by boxes of constant seismic parameters (**Cassell, 1982**). This simplifies the ray propagation and amplitude computation.

Unfortunately, the selection of initial parameters for families of rays is rather time-consuming and some spurious shadow zones arise as a result of rays encountering the corners of boxes (**Howson, 1982**). Although the computation is very fast it does not produce such reliable seismograms as SEIS83, for example.

5.5.3 RAYAMP

RAYAMP also uses ray theory to compute the seismic response of models which are laterally varying. Like RAYSYN, the principles are similar to SEIS83 except for the method of representation of the model, which in this case is carried out by breaking the model up into polygonal blocks. This approach could facilitate the representation of complex structures which are awkward to picture in terms of interfaces crossing the model from left to right, as in SEIS83, but may have the same weaknesses as RAYSYN at the vertices of the polygons.

Since the package is not yet fully implemented, it has yet to be tested and compared with SEIS83. The programme was written by G.D.Spence using an algorithm produced by K.P.Whittall and R.M.Clowes. It is described and used in examples in **Spence et al (1984)**.

5.5.4 ANRAY

ANRAY also uses ray theory to carry out ray tracing and travel time computations for **three-dimensional** laterally varying isotropic and anisotropic media. A fully general case of anisotropy with 21 independent laterally varying constants may be considered. The package was written by Psencik and Gajewski in Prague and sent to Durham with BEAM87 from the University of California, Berkeley. Since it is not documented, it has not yet been implemented, but it may prove to be a valuable package, especially because it may be used for ray tracing S-waves through anisotropic media, which no or few other packages do at present. It may also be configured for borehole seismic modelling.

5.6 Conclusion

There are many other approaches to the computation of synthetic seismograms besides those available at Durham. A wide range of methods apply specifically to horizontally stratified, one-dimensional media, including generalised ray theory, full wave theory, WKBJ theory (equivalent to Maslov theory but in one-dimensional media), wavenumber or slowness integration methods (which include the Reflectivity Method), wavenumber summation techniques (which include the Alekseev-Mikhailenko Method, AMM) and modal summation. The Reflectivity Method is probably the best-known of these methods and due to its high accuracy, it is widely used.

For accurate two-dimensional modelling, the most powerful method is considered to be the **finite-difference** method, which is based on direct numerical solutions of the elastodynamic wave equations. This and the finite-element method are known as exact methods since they yield complete and highly accurate seismograms including head waves, diffractions and surface waves. The drawback is the amount of computational power required to use this approach. Also, the seismograms produced are very complex and are often as difficult to interpret as the original data sections (**Weber, 1988**).

Other two-dimensional methods include **perturbation theory** and other modifications of ART such as **Maslov theory (Chapman 1985)**. The latter essentially corresponds to the use of broad beam widths in the Gaussian beam method. As discussed by **Kennett and Harding (1985)**, the main weakness

of the **modified** ray methods lies in their treatment of reflection and transmission at interfaces, which means that they are unable to cope with curved or discontinuous interfaces accurately.

However, practically speaking, the Gaussian beam approach seems to be the best all-round package in terms of accuracy, computer expense and flexibility. It produces reliable and realistic seismograms, and for this reason it has been used for the computation of synthetic seismograms used in the modelling of the MOBIL wide-angle dataset, the results of which are described in the next chapter.

CHAPTER 6: SYNTHETIC SEISMOGRAM MODELLING

6.1 Introduction

The synthetic seismogram modelling of the MOBIL wide-angle dataset was carried out in two stages, first aiming to fit as many of the main arrivals as possible to a one-dimensional model; this is described in section 6.3. The deviations of the real data from output generated from the model then highlighted the areas where lateral velocity variations needed to be introduced to the model. The final fit was then obtained from a two-dimensional model (section 6.4).

Initially, the seismic modelling was carried out using SEIS83 but this was soon superseded by the more accurate BEAM87; SYN86 was used for some of the one-dimensional interpretation and the CYBER version of SYNSEI at Karlsruhe for a small part of this modelling.

6.2 CSSP model

The final model obtained from the CSSP wide-angle reflection data is shown in **Fig. 6.1**, as presented by **Lewis (1986)**. This extends from the Irish Sea shots across Northern England to the furthest North Sea shot(N29), so that the distance axis along the base of the plot represents the distance from the westernmost shot in the Irish Sea (M25B). The approximate locations of the MOBIL-CSSP stations and MOBIL line 1 shots have also been inserted.

The main features of the model are:

(a) A lateral decrease in basement velocity eastward from shot N10, which was thought to cause the observed "disappearance" of Pg at this offset.

(b) A mid-crustal gradient zone located between 15.5 and 18 km depth and an average upper crustal velocity of 6.16 kms^{-1} excluding sediments.

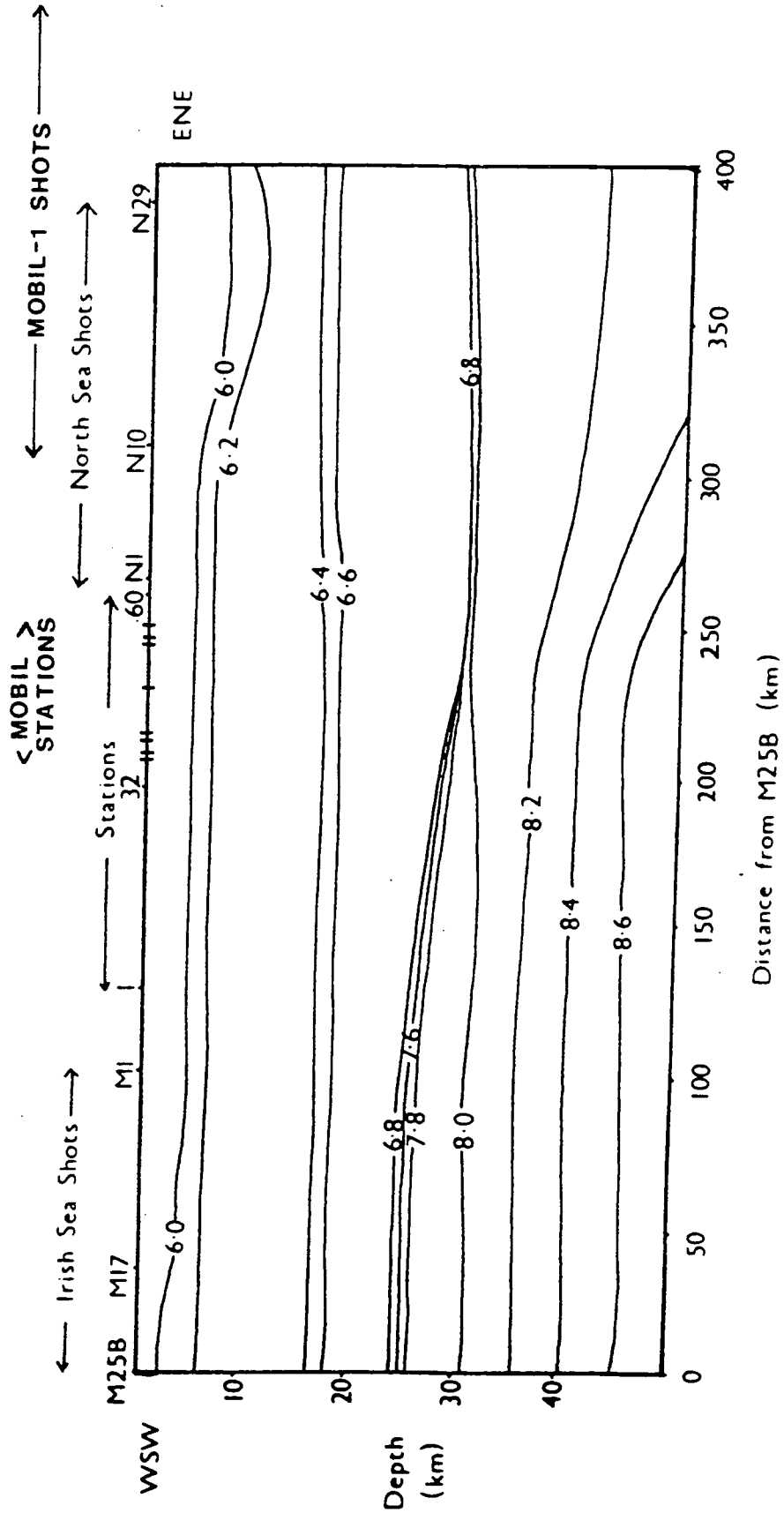

Fig. 6.1 The CSSP velocity model from Lewis (1986).

(c) A strongly reflective Moho at approximately 30 km depth. According to A.H.J. Lewis (1986), this becomes a gradational zone further West, beneath the Irish Sea, in order to explain the depth interpretations from the PmP and Pn arrivals from beneath the Irish Sea. The average crustal velocity beneath the North Sea was calculated to be 6.54 kms^{-1} excluding sediments.

(d) A gentle velocity gradient in the upper mantle with a velocity of 8.02 kms^{-1} just below the Moho.

It was hoped that the improved resolution of the MOBIL-CSSP dataset would enable a more detailed interpretation of these features and that using BEAM87, which is far more reliable in terms of amplitude modelling than SEIS83, would produce a robust model which goes some way towards an explanation of the observed seismic amplitudes.

In actual fact, the high resolution of the MOBIL dataset seems to have generated yet more problems to be explained, rather than solving the old ones. The lateral behaviour of Pg is rather different on MOBIL records - as described in **section 4.4.1**, it does not simply disappear. The mid-crustal gradient may well exist but there also seem to be several other crustal boundaries which generate wide-angle reflections. PmP is far more complex on the MOBIL records than it appeared to be from CSSP, and many diffraction-type events, described in section 4.3.2, are observed from crustal interfaces, but most notably the Moho. The one phase which is crisply defined on the new dataset and may therefore be fitted more accurately is Pn.

6.3 One-dimensional seismic modelling

6.3.1 Initial modelling

Modelling was commenced by approximating the crust to laterally homogeneous layers, starting with the rough results of the T^2-X^2 fitting and the CSSP model and using SEIS83 to carry out the initial computations. The linear interpolation method was used to interpolate the velocities within the layers. The travel time picks from station 54 were used for fitting, since the arrivals on these record sections

seemed from close study to reflect the most laterally uniform structure of all, and the arrivals were the clearest to interpret.

The approach taken was to start at the top and work down, so that the first problem to emerge was that **Pg** cannot be fitted by a one-dimensional model, as suggested by the change in apparent velocity of Pg on the record sections. As discussed in **section 4.4.1**, a low velocity zone would not explain the fact that the velocity change occurs at a specific shotpoint. The evidence points more towards a lateral change in velocity in the basement.

The best apparent fit to the Pg travel times for the first 12 km of the section was obtained using a 4 km thick surface layer of average seismic velocity 4.83 kms^{-1}, followed by a velocity gradient which increases from 6.05 to 6.26 kms^{-1} between depths of 4 km and 7 km. The corresponding ray diagram and travel time fit for this arrival, computed using SEIS83, is shown in **Fig 6.2.** This model cuts off the arrivals at the offset of 55 km, although the observed arrivals continue up to offsets of 60 km at this station, so it seems likely that the gradient continues to greater depths than 7 km.

The travel times of Pg beyond the first 12 km of the section are best fitted by the model shown in **Fig. 6.3** (again computed using SEIS83). This features a surface layer of velocity 4.75 kms^{-1} underlain by basement in which there is a velocity gradient from 5.95 to 6.35 kms^{-1} between 4 and 28 km depth. This is a significantly lower velocity gradient than that required to fit the first part of Pg.

Incorporating the model for the observations of Pg beyond 12 km into one which also fits the travel times of PmP produced the model shown in **Fig. 6.4.** As in the case of **Fig. 6.3**, this incorporates a surface layer of velocity 4.75 kms^{-1}, with a velocity gradient beneath it from 5.95 to 6.21 kms^{-1} down to 20 km depth, then an even steeper velocity gradient from 6.5 to 6.8 kms^{-1} between 20 and 30 km depth. The Moho occurs at 30 km depth as a jump in velocity from 6.8 to 8.02 kms^{-1}. An upper mantle velocity gradient from 8.02 to 8.2 kms^{-1} over a depth of 10 km gives rise to the refracted arrival Pn.

Up to this stage in the modelling, SEIS83 was used, but for the rest of the modelling process described in this chapter, BEAM87 was used.

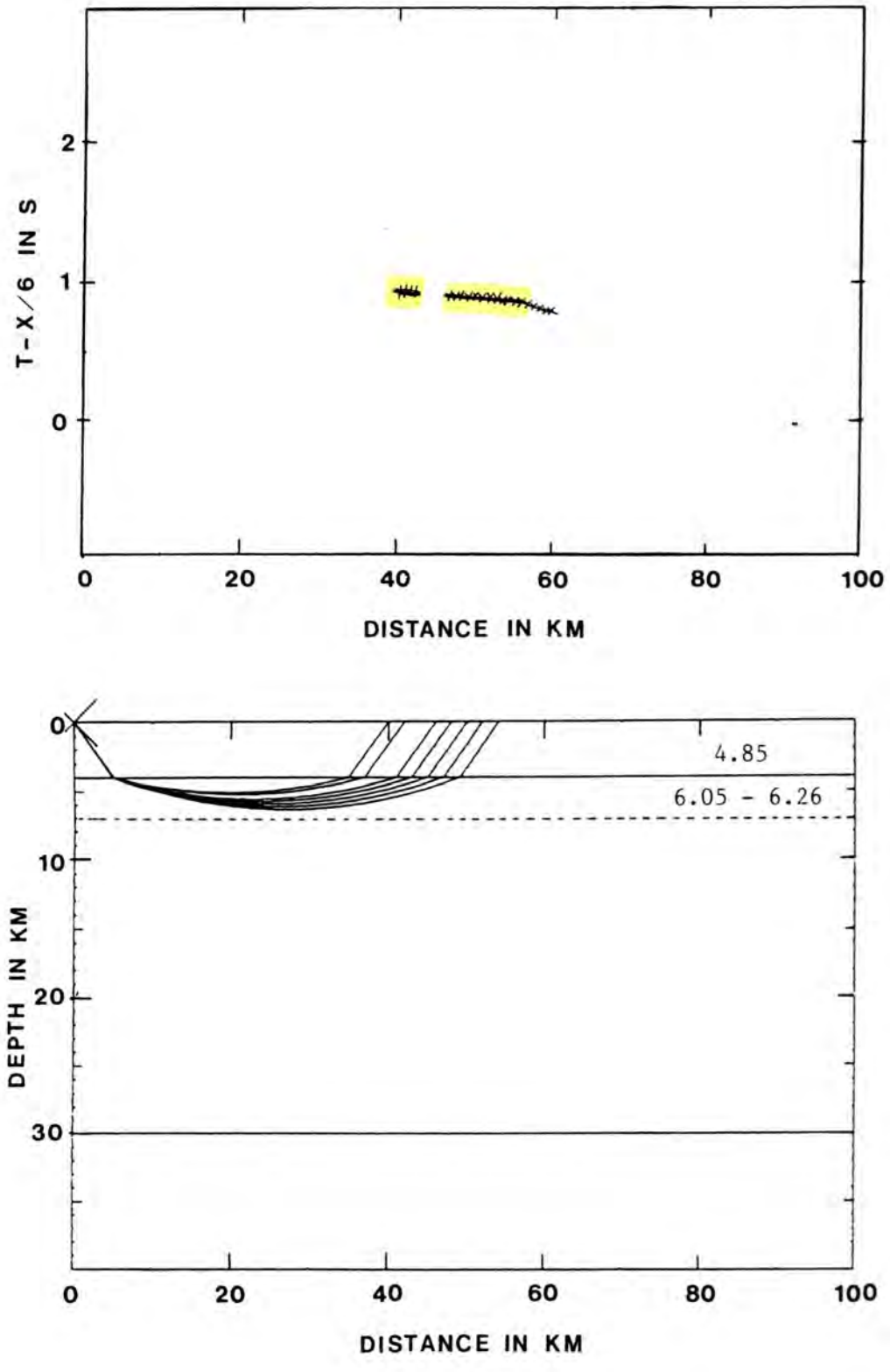

Fig. 6.2 SEIS83 one-dimensional model for station 54: ray diagram and travel time plot for Pg at near offsets (< 60 km). Continuous line: calculated travel time; crosses: observed travel times; numbers within model: seismic p-velocities in km s^{-1}.

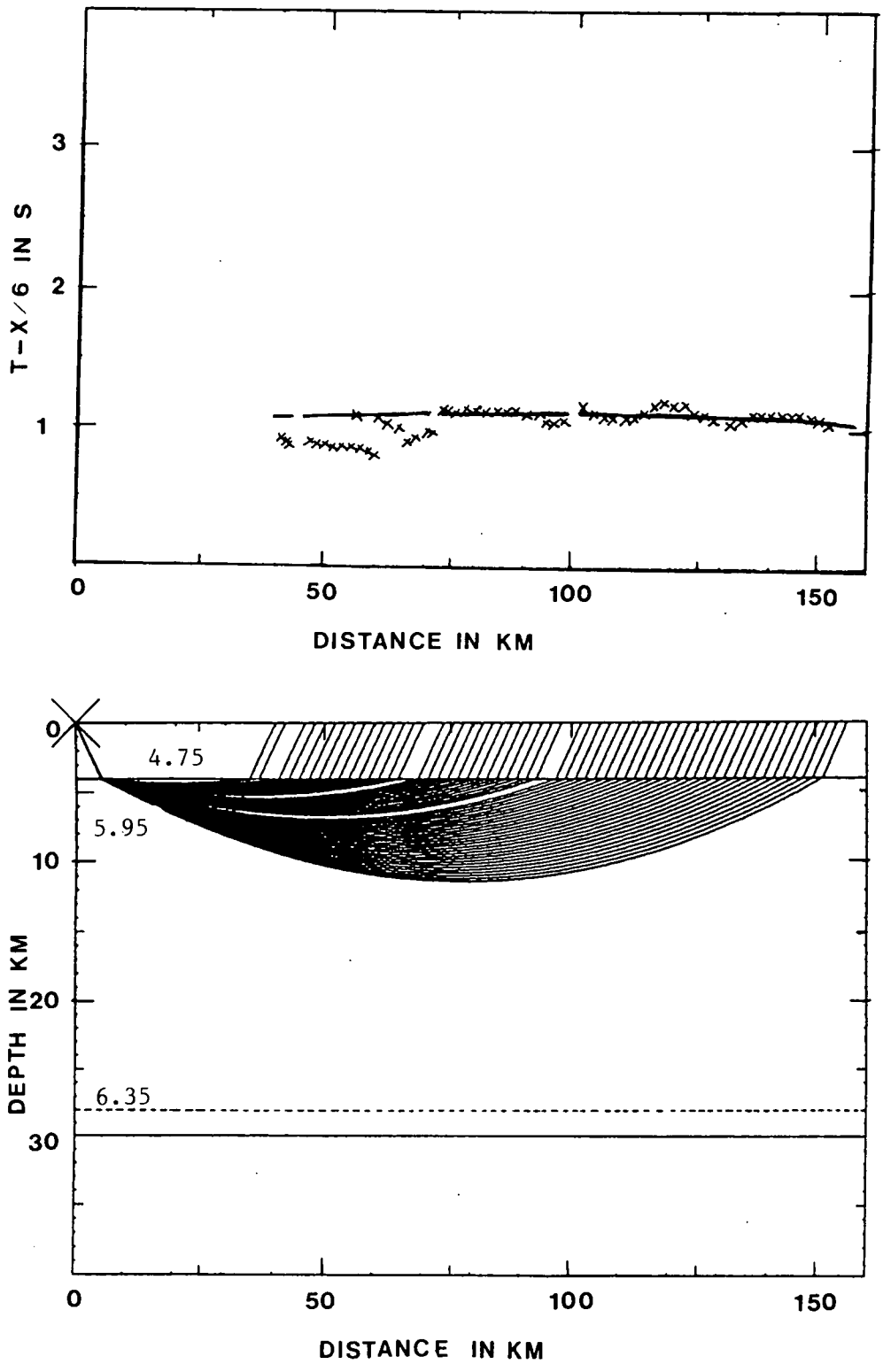

Fig. 6.3 SEIS83 one-dimensional model for station 54: ray diagram and travel time plot for Pg at greater offsets. Continuous line: calculated travel time; crosses: observed travel times; numbers within model: seismic p-velocities in km s^{-1}.

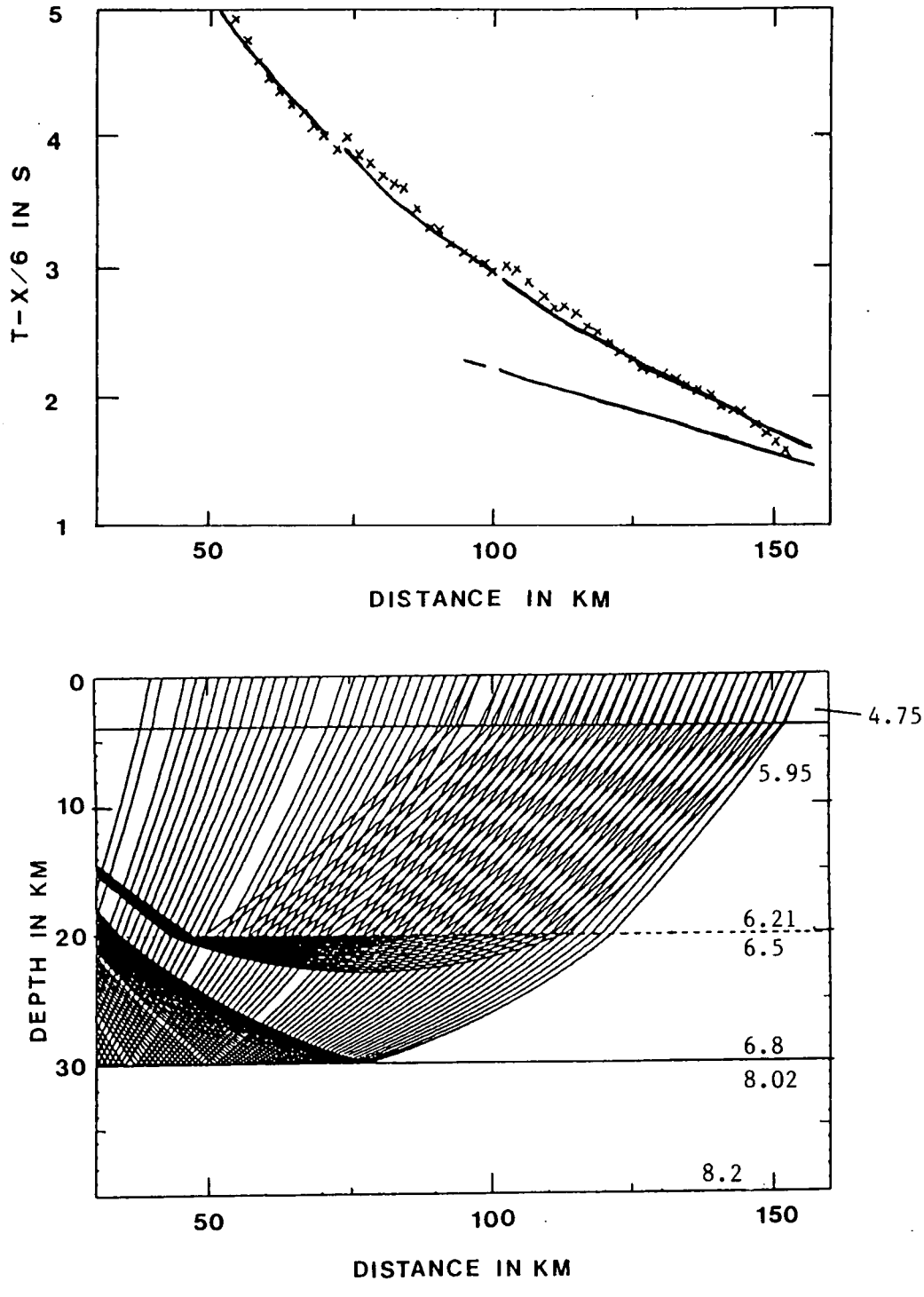

Fig. 6.4 SEIS83 one-dimensional model for station 54: ray diagram and travel time plot for PmP. Continuous line: calculated travel time; crosses: observed travel times; numbers within model: seismic p-velocities in km s^{-1}.

6.3.2 Correcting for the shallow velocity structure

As mentioned in **section 4.3.1**, the smallest offset of the record sections was 33.5 km at station 57. This means that the first arrival on any of the sections is the refraction from seismic basement, Pg. The refracted or wide-angle reflected arrivals which may have resulted from the near-surface geology cannot be seen as first arrivals on the dataset. As a result of this, information about the shallow structure had to be obtained from other surveys and other geophysical data.

Study of the British Geological Survey's newly-published Farne Sheet (**BGS, 1989**), **Green's (1984)** shallow interpretation along the CSSP line, and the MOBIL line 1 normal-incidence data produced reasonable agreement in the geological interpretation shown in **Fig. 6.5** down to a depth of approximately 4 km. This incorporates the easterly-dipping, onlapping sedimentary sequence of the North Sea basin to the east, from the Permian to the Triassic. Beneath this sequence lies the Carboniferous, of which the Upper Carboniferous is present onshore and continues offshore into a syncline, then dies out against the Lower Carboniferous (**BGS, 1989**). This truncation is supported by a small gravity anomaly described in **section 7.3**. The lower Carboniferous is believed to lie conformably on Devonian sediments (**Donato et al., 1983**) and this continuous unit underlies the whole profile.

However, this model does not include the topography of the Lower Palaeozoic surface, which includes granites (**Donato et al 1983**, see also Chapter 7), neither does it explain the small-scale travel time variations on the Pg arrival. Modelling of the Pg travel times by adjusting the Lower Palaeozoic topography was then carried out starting with station 54 and extending to the other stations in the line. The result of this operation is shown in **Fig. 6.6** for station 54 - a picture of the model with associated rays and the travel time curve generated by BEAM87 (as are all the travel times and synthetic seismograms which follow throughout this chapter). The travel time fit for this station is very close and the behaviour of the amplitudes very similar to the observed pattern of Pg on the record sections.

The travel time fit for Pg at the other CSSP stations for the near-surface structure of **Fig. 6.6** can be seen in **Fig. 6.7**, which shows travel times computed at stations 57, 47, 40 and 36. The fit at the Morpeth stations (57 to 47) is very reasonable. Those at the Wark stations (40 to 36) vary considerably, however, due possibly to incorrect picking of the phases on the record sections (particularly at stations 36

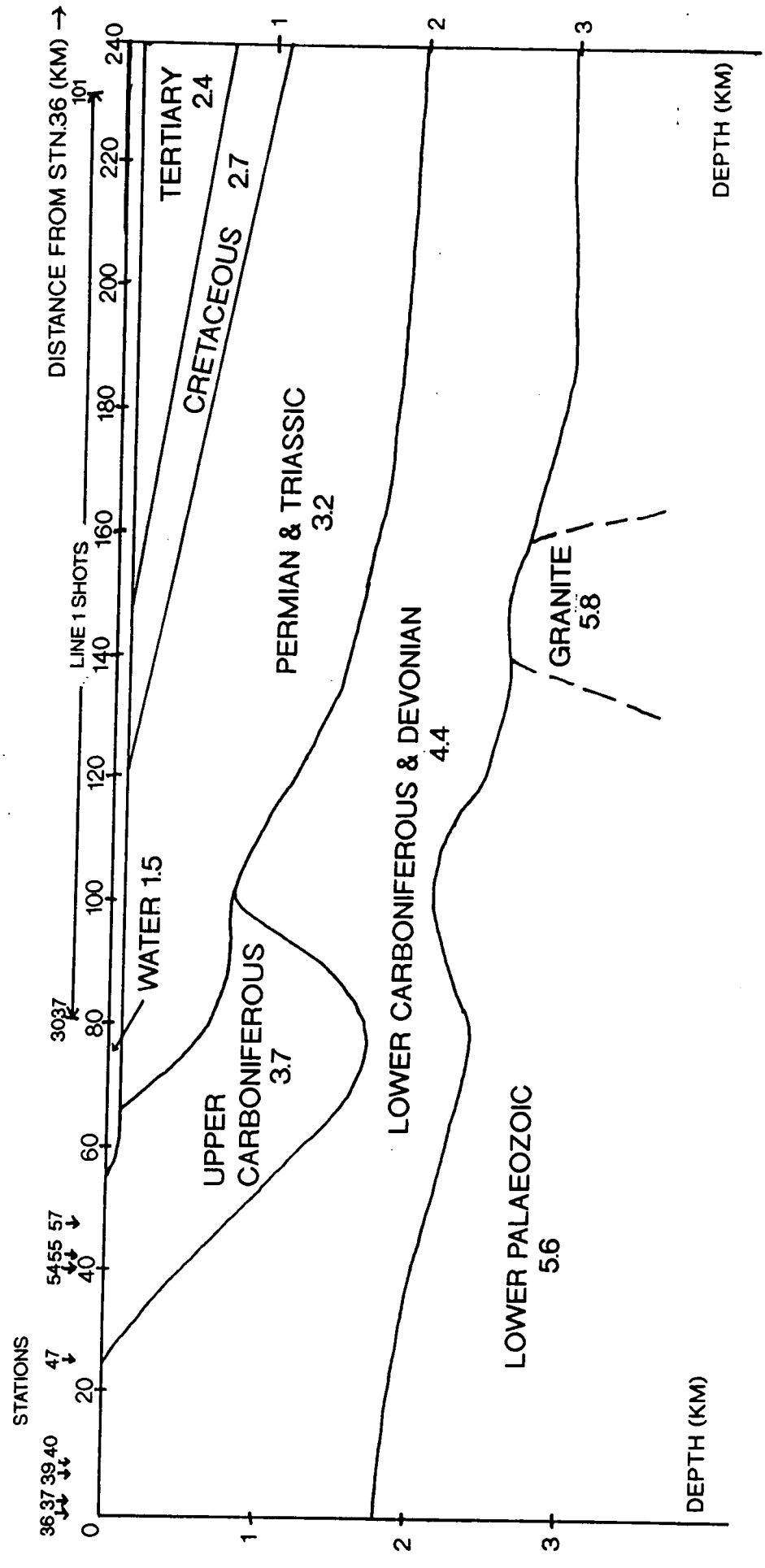

Fig. 6.5 Shallow geological and seismic structure beneath Line 1. The figures within the layers represent p-velocity in kms^{-1}.

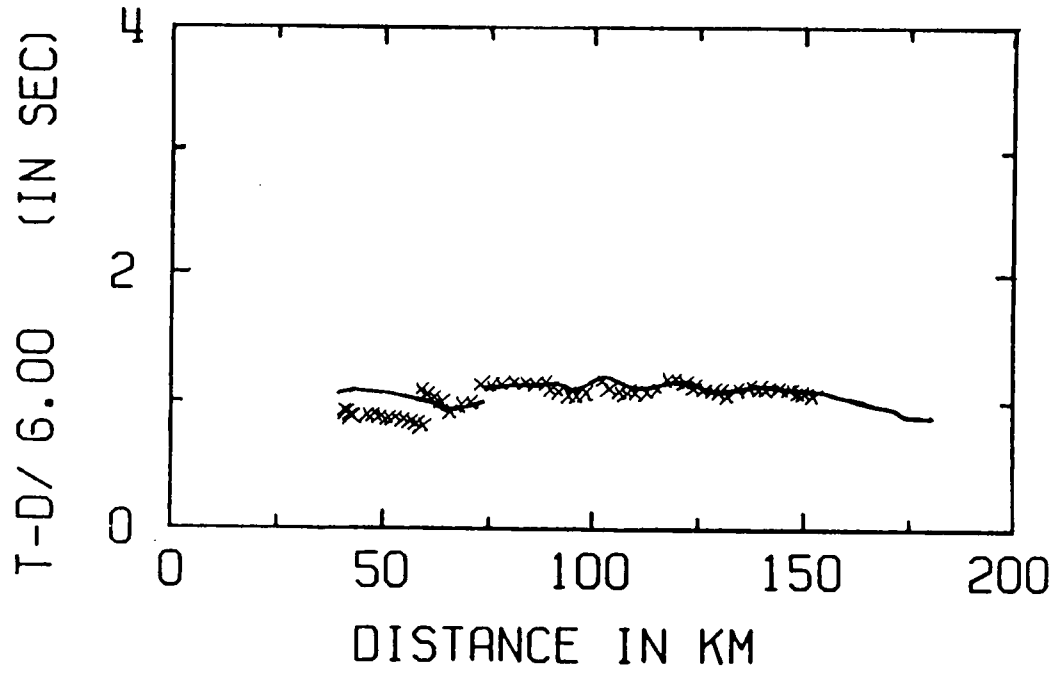

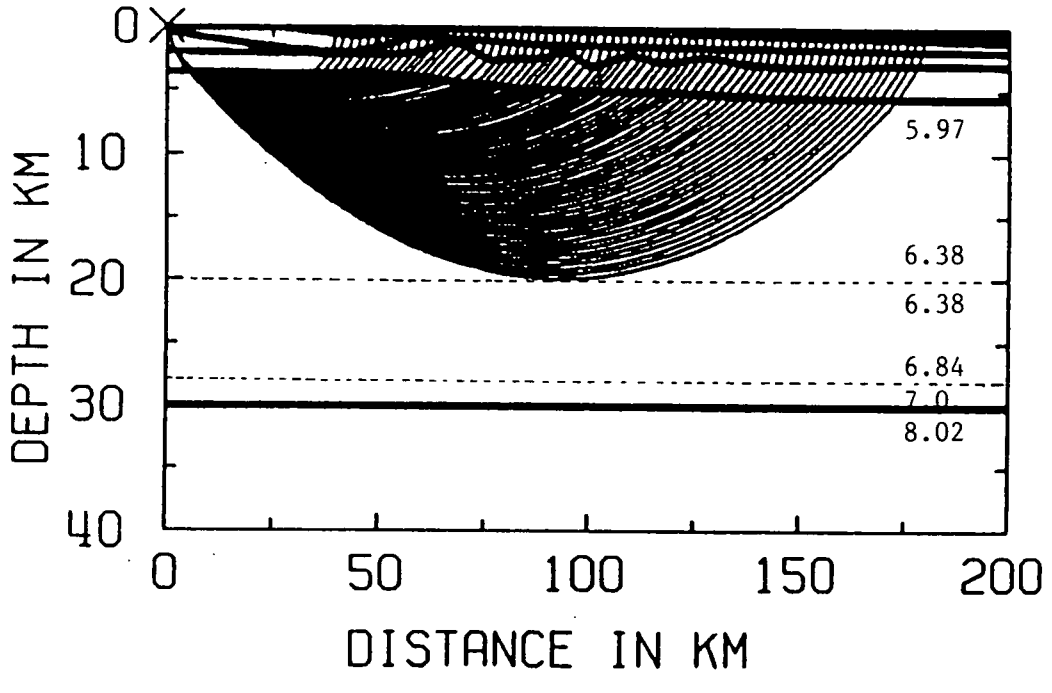

LINE1 S54 PCP

Fig. 6.6 Shallow structure beneath Line 1 incorporating structure on the Lower Palaeozoic surface: station 54 BEAM87 ray diagram and travel times for Pg. Continuous line: calculated travel time; crosses: observed travel times; numbers within model: seismic p-velocities in km s^{-1}.

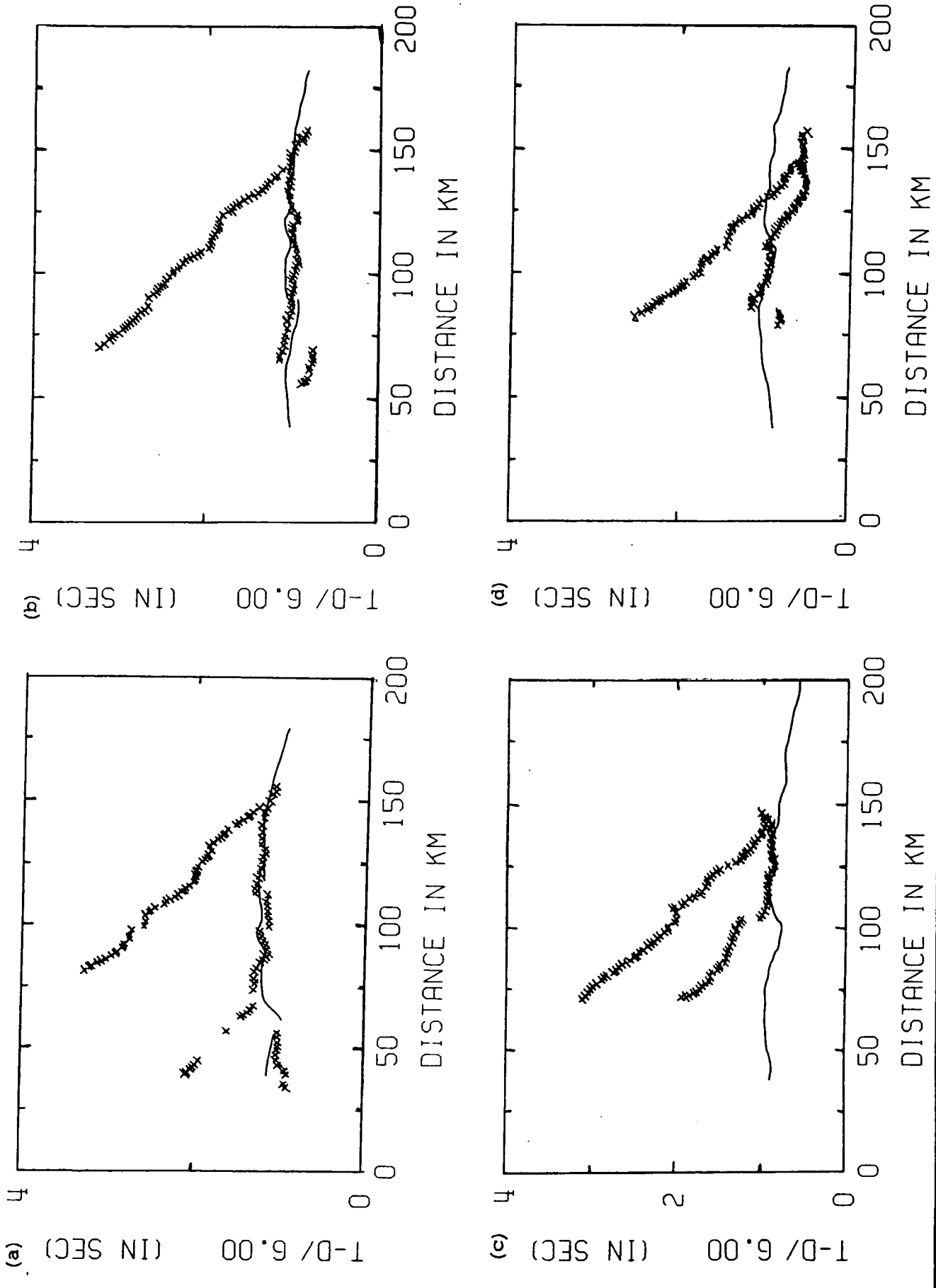

Fig. 6.7 BEAM87 travel time plots for computations of Pg at (a) station 57, (b) station 47, (c) station 40, (d) station 36. Continuous line: calculated travel time; crosses: observed travel times.

and 37) and other variations in near-surface geology which have not yet been modelled. Overall, the Pg fit for this shallow structure is adequate for modelling the deeper structure of the region, which is the main interest of this study.

6.3.3 One-dimensional model

Further one dimensional modelling after correcting for the shallow structure concentrated on fitting PmP, the wide-angle reflection from the Moho, and attempting to explain Pg, while trying to keep the model as simple as possible.

The velocity gradients through the crust depicted in **Fig. 6.4** fit the major part of the PmP travel time curve, but the steep part of the curve which occurs just before PmP merges with Pg at about 150 km offset, and the actual offset of the merge are not explained by these gradients alone (this steep part of the PmP travel time curve is not obvious on the record sections in Appendix C, but does become apparent on the smaller plots of the travel time picks, for example, Fig. 6.10). It was therefore necessary to include an extra layer of higher seismic velocity (7.0 kms^{-1}) at the base of the crust to fit this portion of the travel time graph. This model is shown in **Fig. 6.8** with the computed travel time curve.

A synthetic seismogram section generated from this model is shown in **Fig. 6.9. Transparency (i)**, a record section of the real data plotted to the same scale, is included here for comparison with the synthetic. The data section has 1 km trace spacing in order to facilitate correlation between traces; the synthetic section does not have a noise problem so it has only been plotted at 2 km spacing, and the amplitudes are much higher than those of the real data. The amplitudes of both sections are also clipped so that a direct comparison of amplitudes is not possible. The most important point of the comparison is the distance range over which maximum amplitudes occur and the amplitudes of different phases relative to each other, both of which may be studied in the sections presented here.

In this case, comparing **Fig. 6.9** with the transparency, the maximum PmP and Pg amplitudes are observed over the same distance regions of both sections, so the synthetic appears to show reasonable agreement with the real data. It therefore provides a good starting model for the two-dimensional modelling described in the next section.

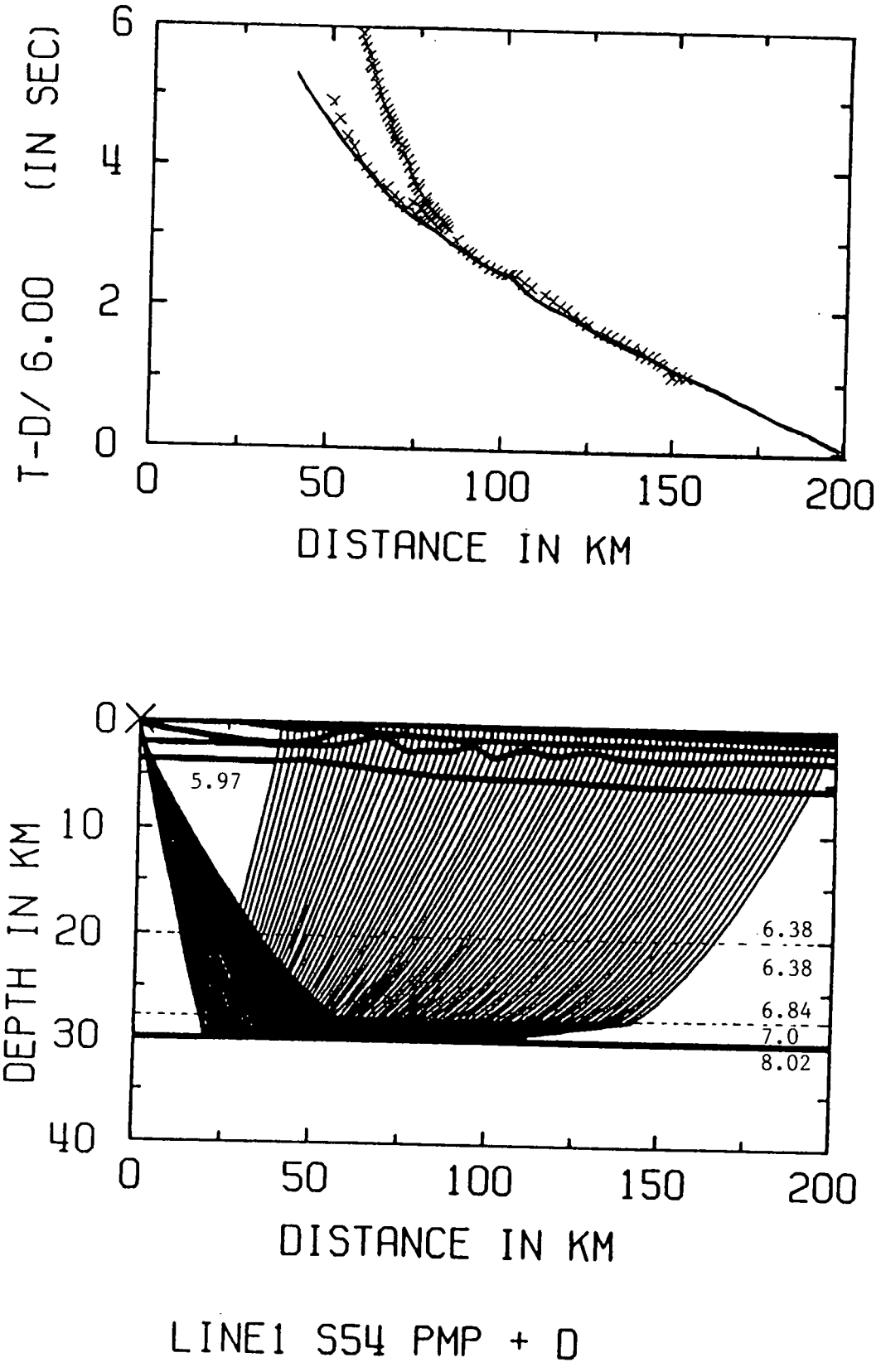

Fig. 6.8 BEAM87 ray diagram and travel times for PmP through final 1-D model, computed for station 54. Continuous line: calculated travel time; crosses: observed travel times; numbers within model: seismic p-velocities in km s^{-1}.

Enclosure (i)

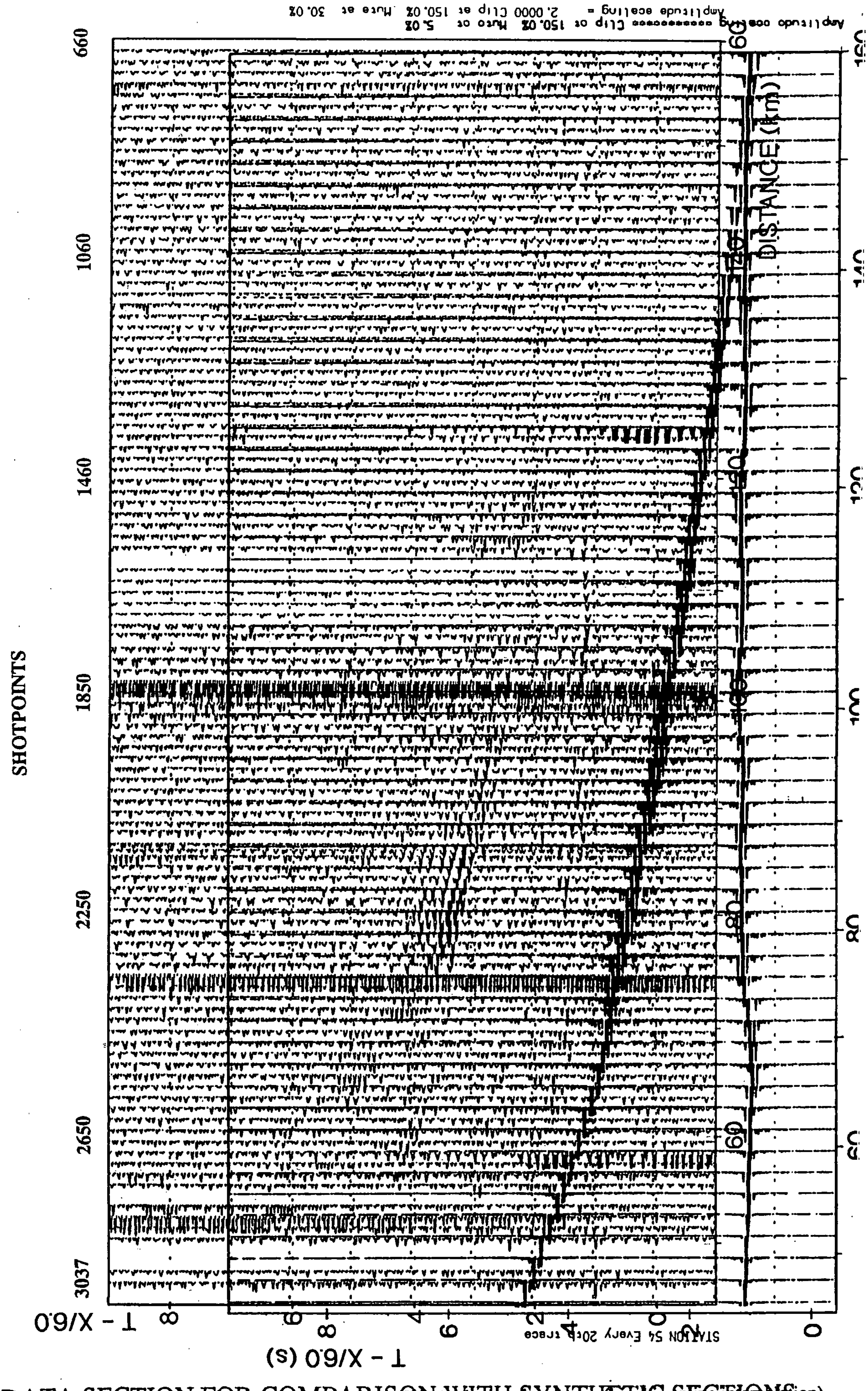

TATION 54 DATA SECTION FOR COMPARISON WITH SYNTHETIC SECTIONS

Fig. 6.9 Final 1-D model at station 54. BEAM87 synthetic seismogram (Cubic Spline interpolation).

6.4 Two-dimensional seismic modelling

6.4.1 Introduction

Serious departures of the one-dimensional synthetic section of **Fig. 6.9** from the real data are seen in the lack of early **Pg**, **Pn**, or the phase **D**, none of which may be generated by this one-dimensional model. These arrivals dictated the course of the development of a laterally varying model, described below. Starting at the top, the first problem to be tackled was the fitting of the arrival Pg as far as possible (**section 6.4.2**). The next major phase to be tackled was D, the dominant arrival, and Pn (**sections 6.4.3 and 6.4.4**). The modelling of the wide-angle reflections from the mid-crustal region, including PcP (described in **section 4.4.2**) was undertaken last of all since these phases were picked with least confidence.

6.4.2 Pg modelling

Since it was known from the one-dimensional modelling that the initial Pg could be fitted by a basement velocity gradient starting at 6.05 kms^{-1} and at greater offsets by a gradient starting at 5.97 kms^{-1}, the logical conclusion, supported by the CSSP interpretation of **Green(1984)**, is that there is a lateral change in velocity gradient which causes Pg to appear at first with the higher apparent velocity, then to become weaker and decrease in apparent velocity.

Initially, an attempt was made to represent this using the linear interpolation method of BEAM87, with an extra layer at the top of the basement containing a velocity gradient from 5.97 to 6.04 kms^{-1}, very thin on the western side of the model and thickening to the east. This might conceivably have worked with enough time spent on producing the right shape for the layer, but the better approach seemed to be to use the **bicubic spline** method of interpolation for the velocity structure within the layers, which enables the specification of seismic velocities in a grid within the layer and therefore allows for a lateral change in the velocity gradient without changing the shapes of the boundaries.

This approach was therefore adopted, concentrating as before on the records from station 54 to produce the model shown in **Fig. 6.10**. This comprises a vertical velocity gradient on the western side

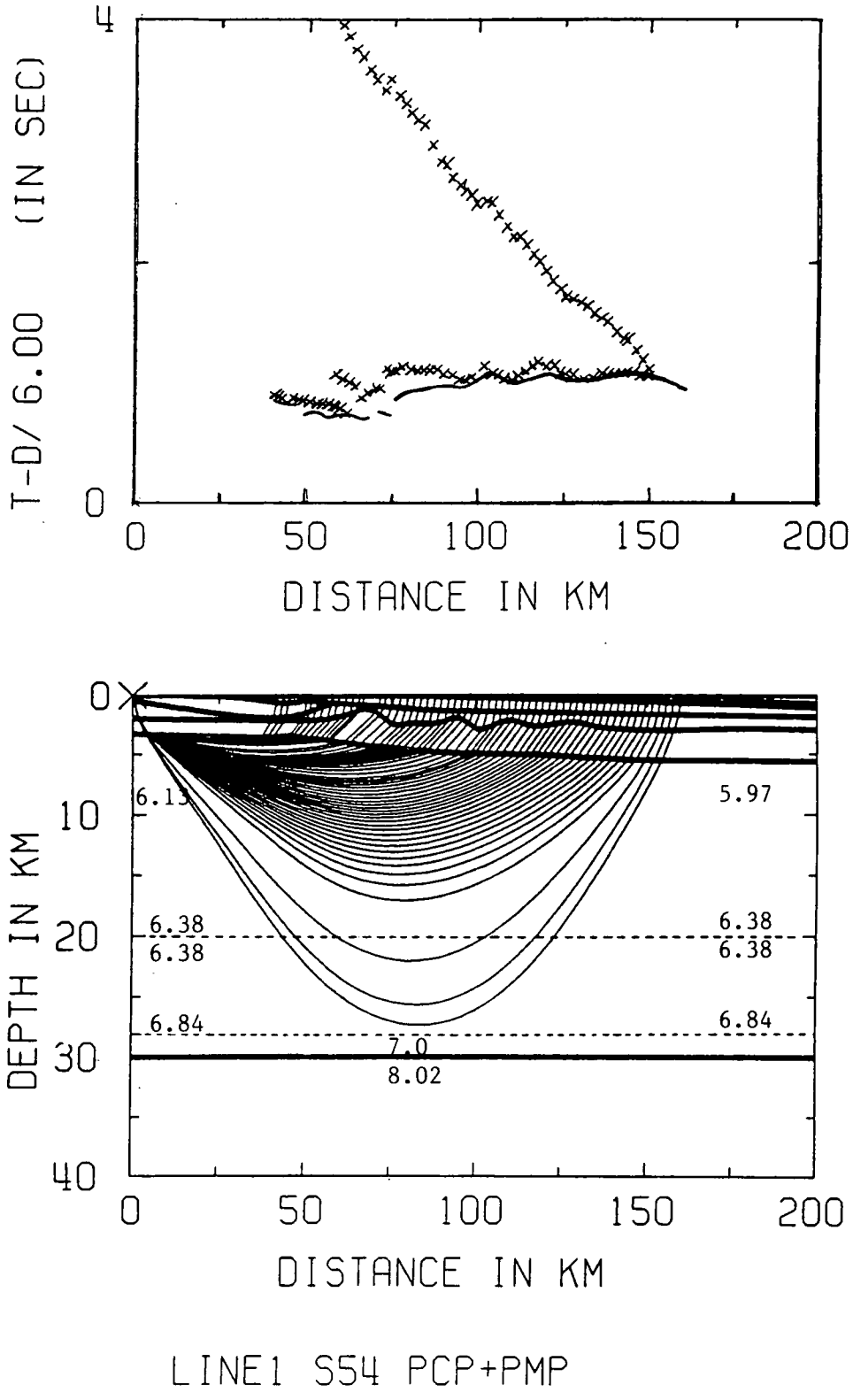

Fig. 6.10 2-D model for station 54: BEAM87 ray diagram, and travel times for Pg. Continuous line: calculated travel time; crosses: observed travel times; numbers within model: seismic p-velocities in km s^{-1}.

from 6.13 kms^{-1} at the basement surface to 6.38 kms^{-1} at 20 km depth, which changes between 40 and 60 km offset to a vertical gradient from 5.97 kms^{-1} to 6.38 kms^{-1} over the same depth range. This produces the travel time fit shown in the figure. The fit is not good for the Pg travel times at offsets between 60 and 100 km, but at shorter offsets and beyond 100 km, it is adequate. Fitting this model to the records from stations 55 and 57 also produces a satisfactory travel time fit, so this model was accepted as the best one for the situation.

6.4.3 Arrivals D and Pn

The combination of the one-dimensional model with the upper crustal fit to Pg yielded a crustal velocity model which fitted the travel times for PmP, as observed at all stations, very well (Fig.6.11). The next problem was then modelling the strong phase D which has a very high seismic amplitude especially on the station 54 record section. As described in section 4.4, the travel times may be fitted excellently by those of a diffraction from a point on the Moho at about 60 km offset from station 54. However, a diffraction does not explain the high amplitude of the phase so it was necessary to consider other explanations.

The possible explanations considered in the course of the modelling process include:

(a) a high velocity gradient at the base of the crust;

(b) a dipping reflector just above the Moho, possibly corresponding to the truncation of the high-velocity slab at the base of the crust;

(c) a dipping reflector in the upper mantle;

(d) a lateral velocity change at the base of the crust;

(e) a "step" of some sort on the Moho itself.

Some combinations of these possibilities were considered. First, (a) was discounted since this would produce the arrival D at the same offset at all the stations, which is not the case. Also, a gradient of sufficient strength to produce arrivals of the observed travel times does not then allow rays to travel through it to produce reflections from the Moho, PmP, or Pn, the refraction from the upper mantle.

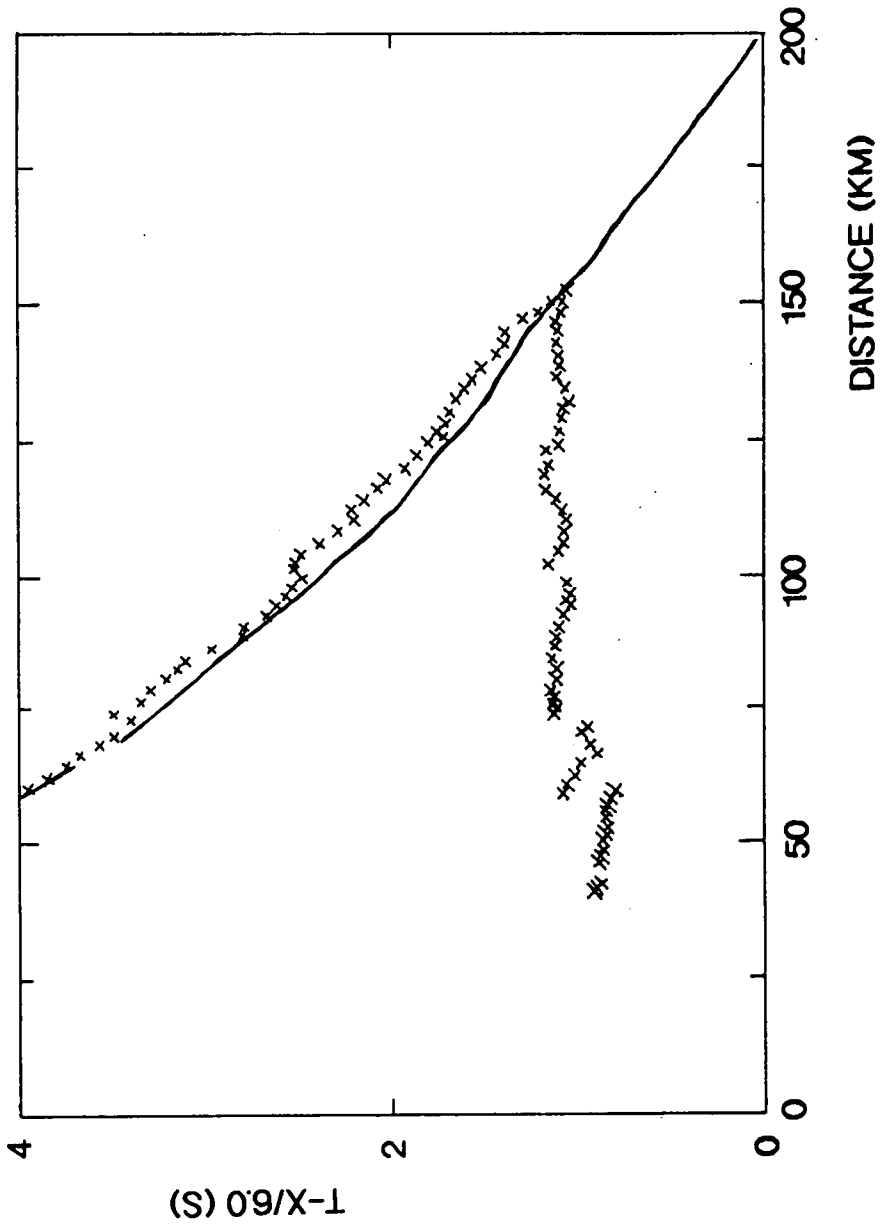

Fig. 6.11 BEAM87 PmP fit for 2-D model at station 54. Continuous line: calculated travel time; crosses: observed travel times.

Model (b) could have produced the appropriate arrivals to fit the travel times of D but without a high enough amplitude to be appropriate and some difficulty then arises in getting rays to penetrate the slab to produce PmP or Pn arrivals.

Model (c) was pursued further since this still enabled the production of wide-angle reflections from the Moho. It was also possible for this model to produce a good travel time fit to the observed PmP curve and Pn (**Fig. 6.12**). However, the synthetic seismogram produced by this model, shown in **Fig. 6.13**, shows a very poor amplitude for the reflection from the dipping reflector when compared with D on the transparency (i) of the data section. This model can generate one or two isolated rays of high amplitude immediately over the corner of the dipping slab but this is evidently not sufficiently high to affect the synthetic section of **Fig. 6.13**.

Model (d) cannot be defined by the bicubic spline interpolation method. To produce rays with travel times of a diffraction would require a very strong velocity gradient over a very narrow horizontal range, which would be very difficult to achieve unless a more accurate modelling package could be used.

The last option, (e), gave the most successful result overall. This is discussed in the next section.

6.4.4 A step on the Moho

Picking up the fact that the corner of the slab model (c) produced some high amplitude rays, model (e) incorporated a rigid step, with corner points defined for the edges. This produced the initial result shown in **Fig. 6.14**: two "pseudo-diffracted" arrivals which fit exactly onto the travel time curve for D, Moho wide-angle reflections for most of the section and Pn arrivals which fit the observed travel times excellently. A shadow zone is seen on the PmP ray diagram between 80 and 120 km offset due to the effect of the step on PmP rays. This effect is not observed on the real data and may be due to the bicubic spline velocity interpolation method distorting the seismic velocity field around the step, but the synthetic seismogram in **Fig. 6.15** shows that BEAM87 has coped with this and does not produce a shadow zone on the record section. However, as seen on the synthetic seismogram, the amplitude of the "diffraction" is small (**highlighted**) and it does not increase towards PmP (as would be expected of a diffraction), showing that the arrivals are actually more specular reflections than they are diffractions.

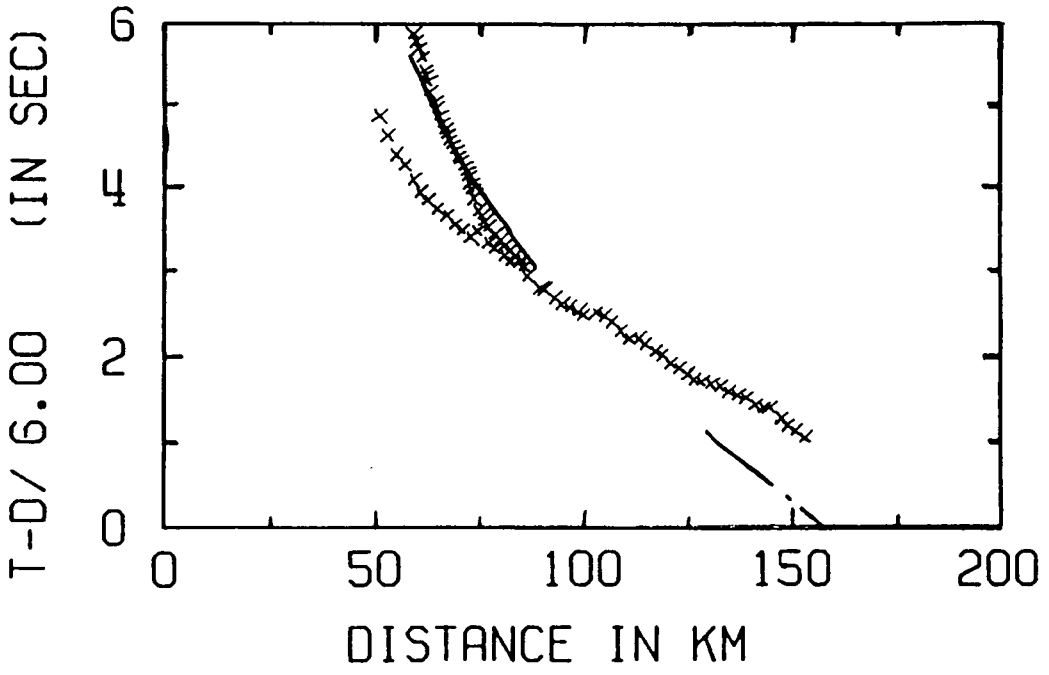

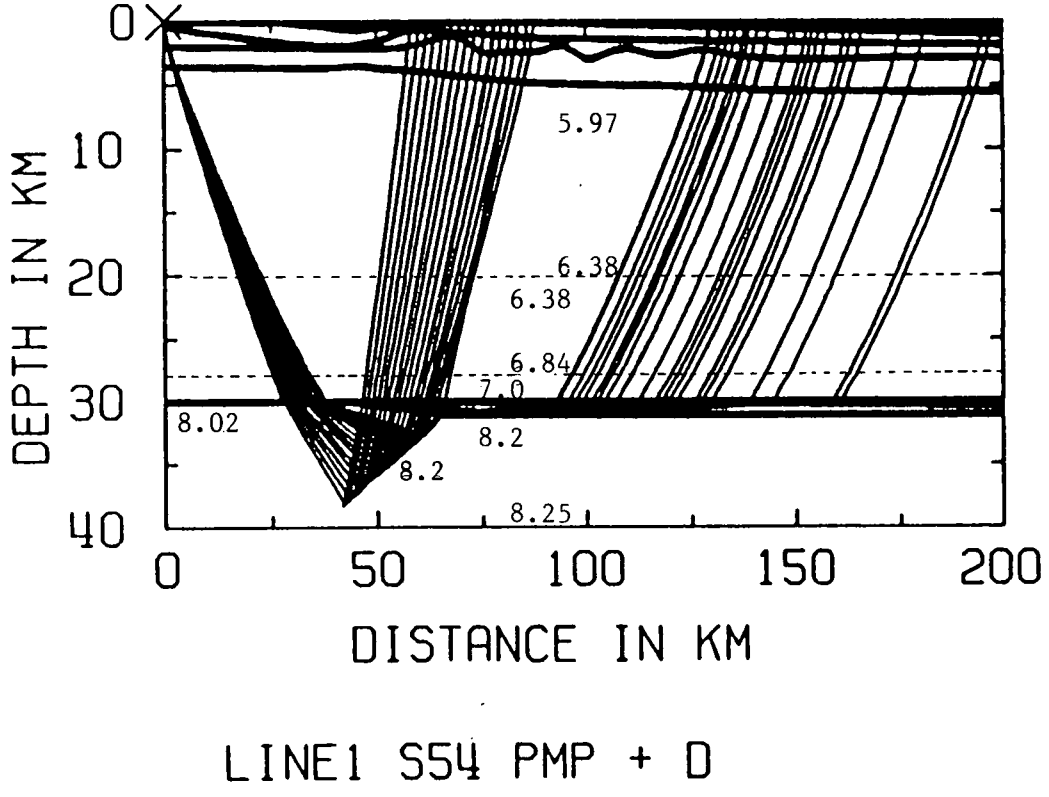

LINE1 S54 PMP + D

Fig. 6.12 2-D model for D and Pn at station 54: BEAM87 ray diagram and travel times for dipping mantle reflector. Continuous line: calculated travel time; crosses: observed travel times; numbers within model: seismic p-velocities in km s^{-1}.

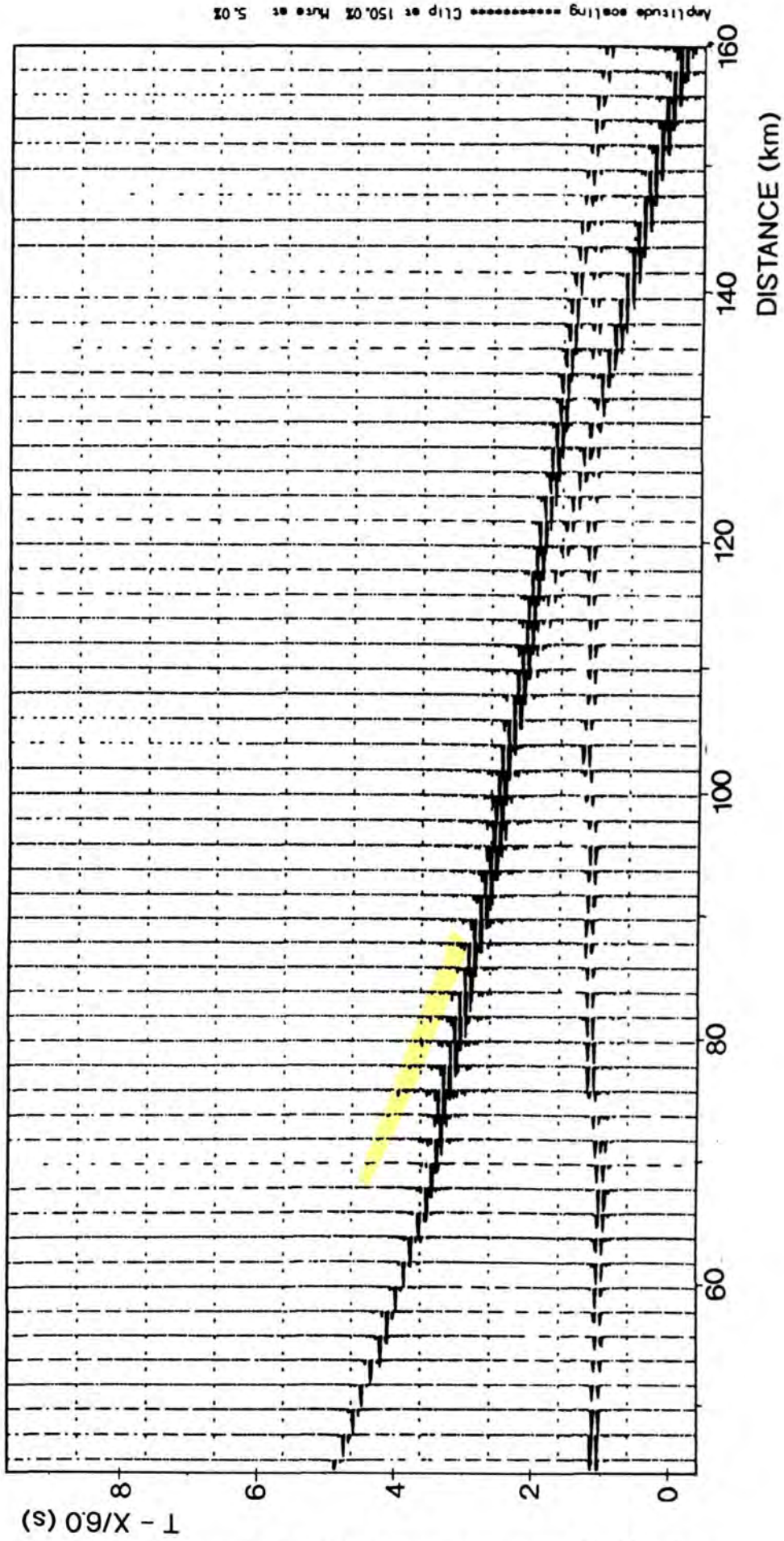

Fig. 6.13 Dipping mantle reflector model at station 54: BEAM87 synthetic seismogram (bicubic spline interpolation).

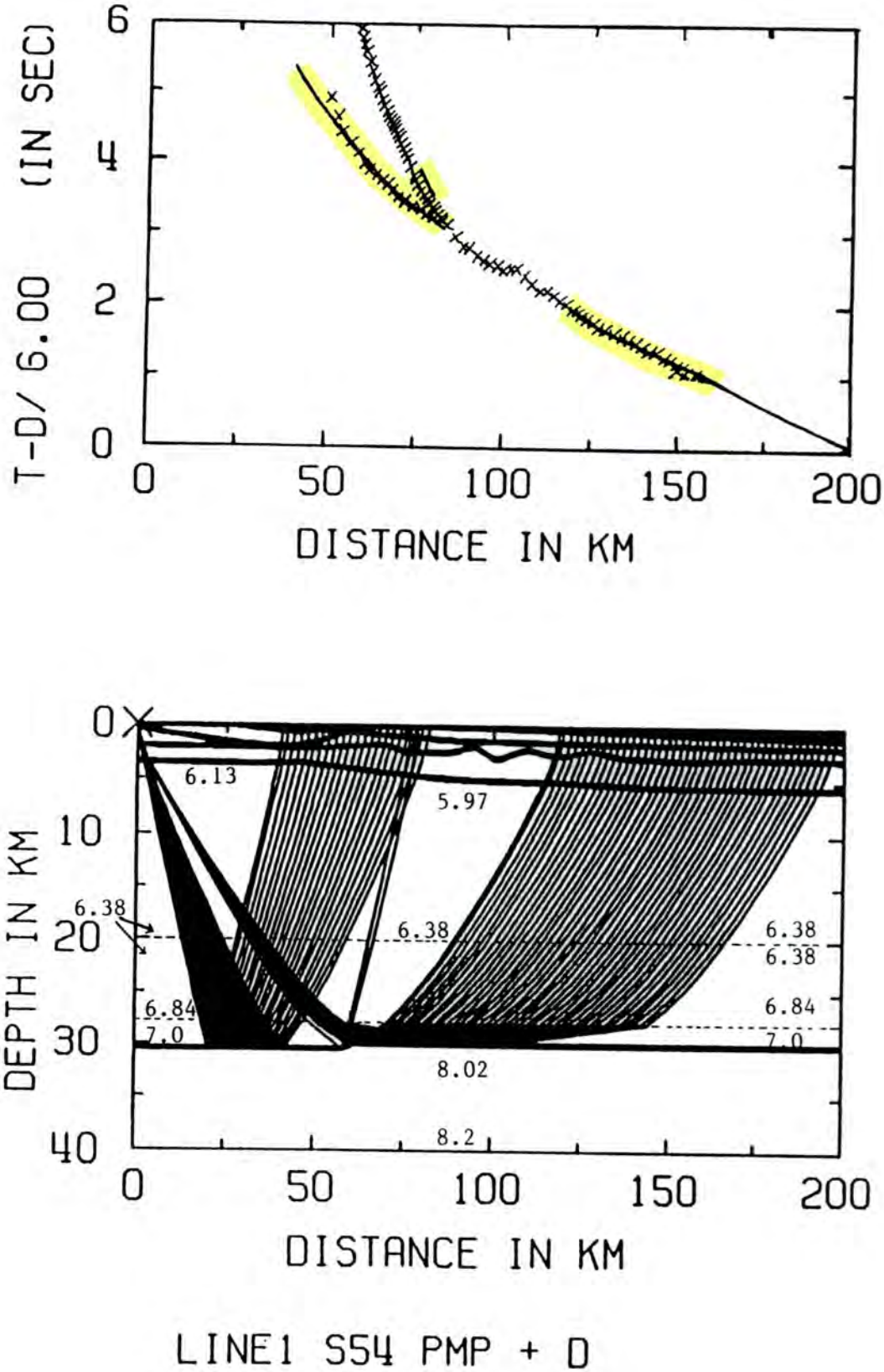

Fig. 6.14(a) 2-D model for D and PmP at station 54: BEAM87 ray diagram and travel times for "diffracting" Moho step.Continuous line: calculated travel time; crosses: observed travel times; numbers within model: seismic p-velocities in km s^{-1}.

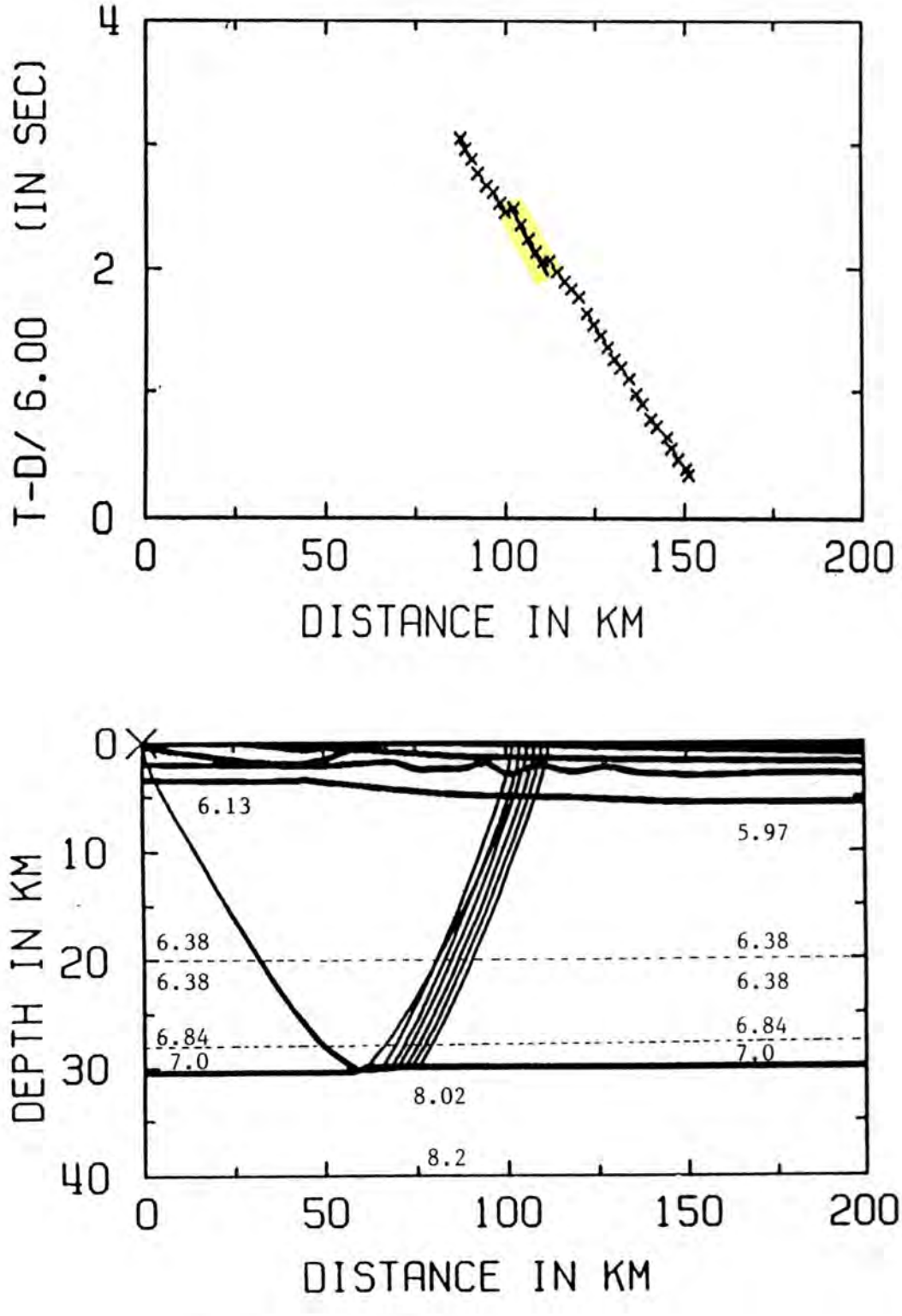

Fig. 6.14(b) 2-D model for Pn at station 54: BEAM87 ray diagram and travel times. Continuous line: calculated travel time; crosses: observed travel times; numbers within model: seismic p-velocities in km s^{-1}.

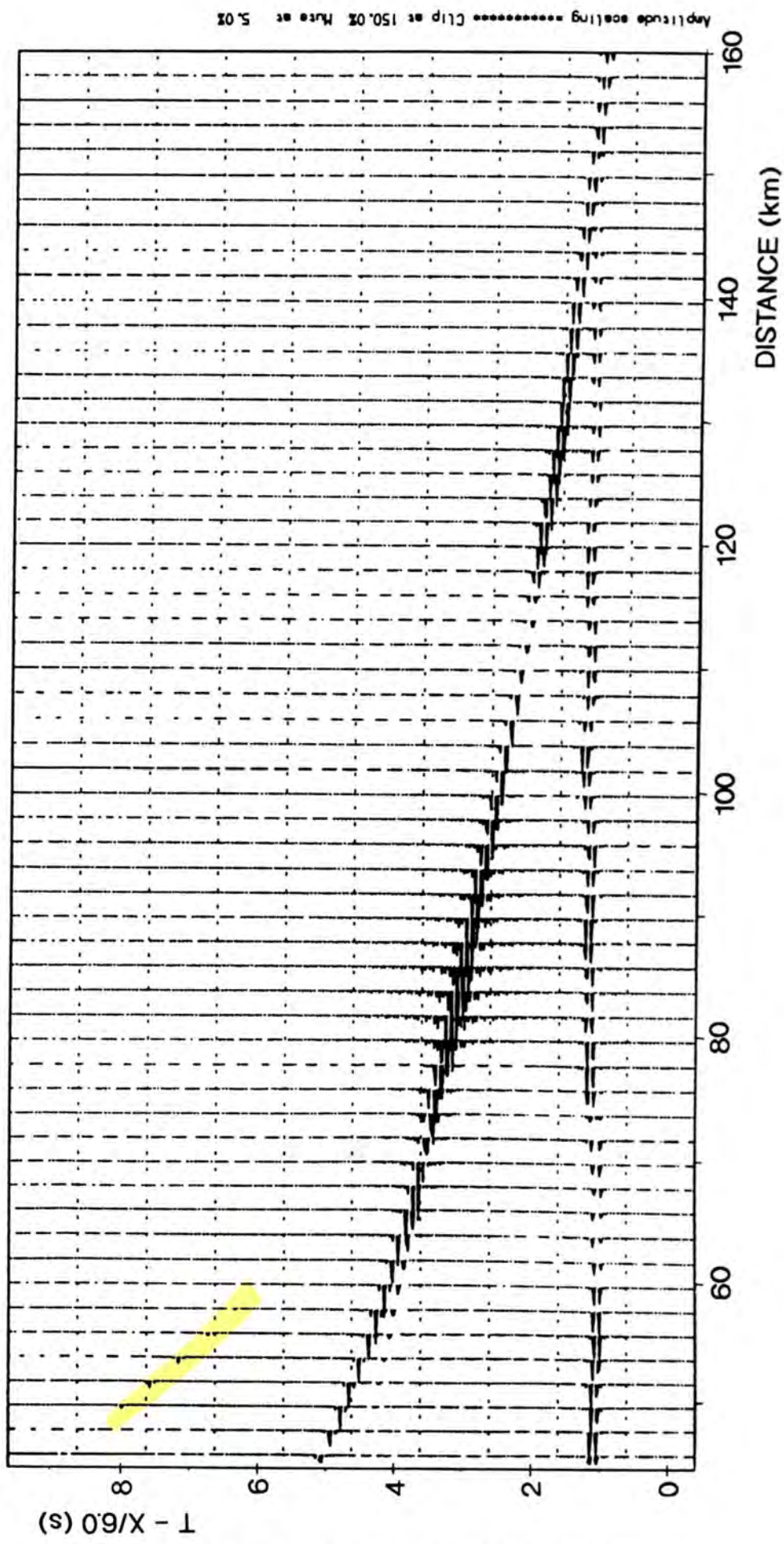

Fig. 6.15 2-D model for D and Pn at station 54: BEAM87 synthetic seismogram for "diffracting" Moho step. D is highlighted.

A further development of this model, to try to obtain "real" reflections from the sloping step, produced the model shown in **Fig. 6.16**, where three rays are seen to be reflected from the slope. In spite of producing yet another slightly narrower shadow zone as far as the Moho reflection is concerned, this does produce an arrival more like D on the synthetic section in **Fig. 6.17**. However, although Pn is also generated by this model, the amplitude of D is still far from high enough when compared with the data transparency (i).

The next step in the development of the model was to smooth the edges of the step slightly, both to make the step more realistic and to attempt to increase the amplitude of the reflections from it. The result was very successful. The ray diagram and travel time plot for this model, computed at station 54, may be seen in **Fig. 6.18**. In this model, the rays which produce the arrival D are reflected from the curved part of the step on the Moho, as shown in the blown-up plot in **Fig. 6.19**. The ray diagram plotting routine RAYPLOT does not actually manage to draw the true shape of the step at this scale, producing a straight sloping step instead, but the true shape of the boundary is seen in the location of the reflection points.

As seen from these plots, the travel time fit for station 54 is excellent for D, Pn and PmP although the PmP arrivals are not reflected from the top part of the step when the bicubic spline method of velocity interpolation is used. However, the amplitude of the phase D is very high at the same offset where it is highest on the record sections from station 54. The synthetic seismogram section from this model, using the bicubic spline method, is shown in **Fig. 6.20**. The section is the best synthetic section yet due to the high amplitude of D, the generation of Pn (although the amplitude of Pn beyond 140 km offset is rather higher than that of the observed), the upper crustal arrival and the high energy in the seismograms between 75 and 90 km offset, which is also observed in the data transparency.

The two main weaknesses with the section are that PmP does not continue beyond about 110 km offset, and the amplitude of the Pg phase. The lack of PmP beyond 110 km offset is very likely to be due to the bicubic spline interpolation method for the velocity representation within the model, rather than a real result for the velocity distribution represented. The computed Pg amplitude is similar to the pattern of the observed amplitudes but differs slightly in that the higher apparent velocity of the phase continues

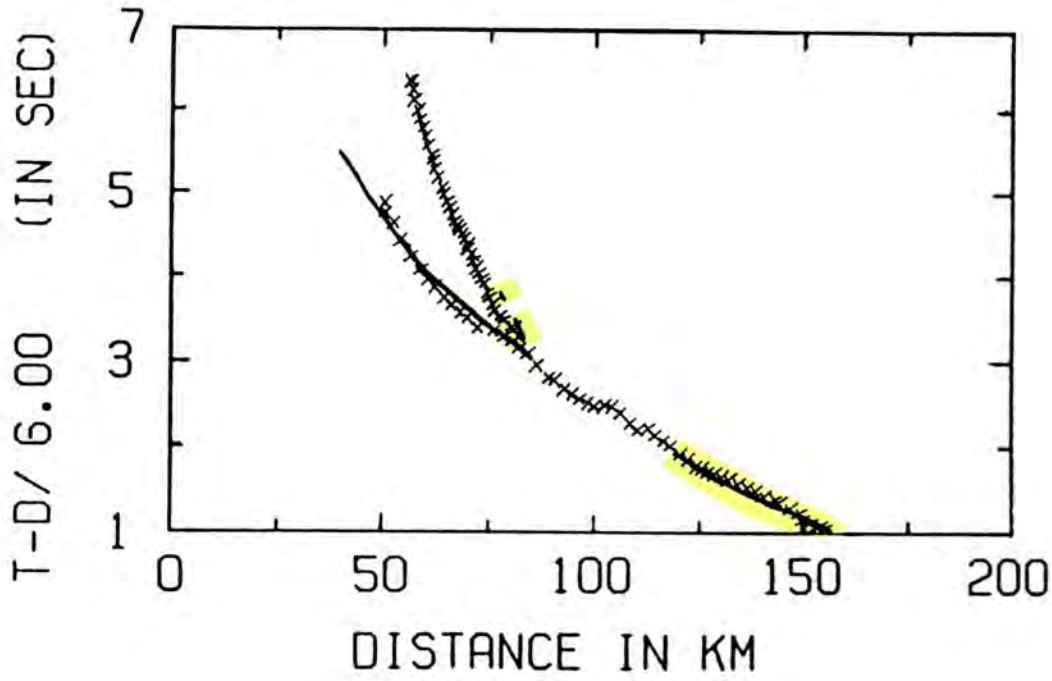

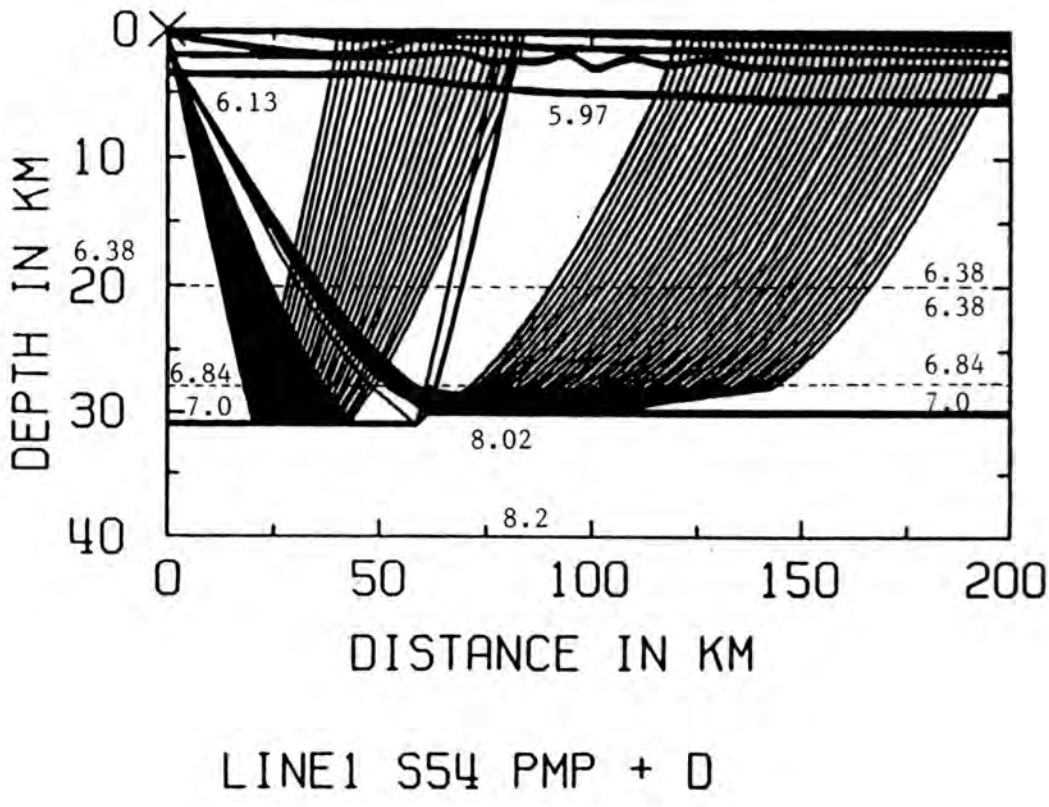

LINE1 S54 PMP + D

Fig. 6.16 2-D model for D and Pn at station 54: BEAM87 ray diagram and travel times for reflecting Moho step. Continuous line: calculated travel time; crosses: observed travel times; numbers within model: seismic p-velocities in km s^{-1}.

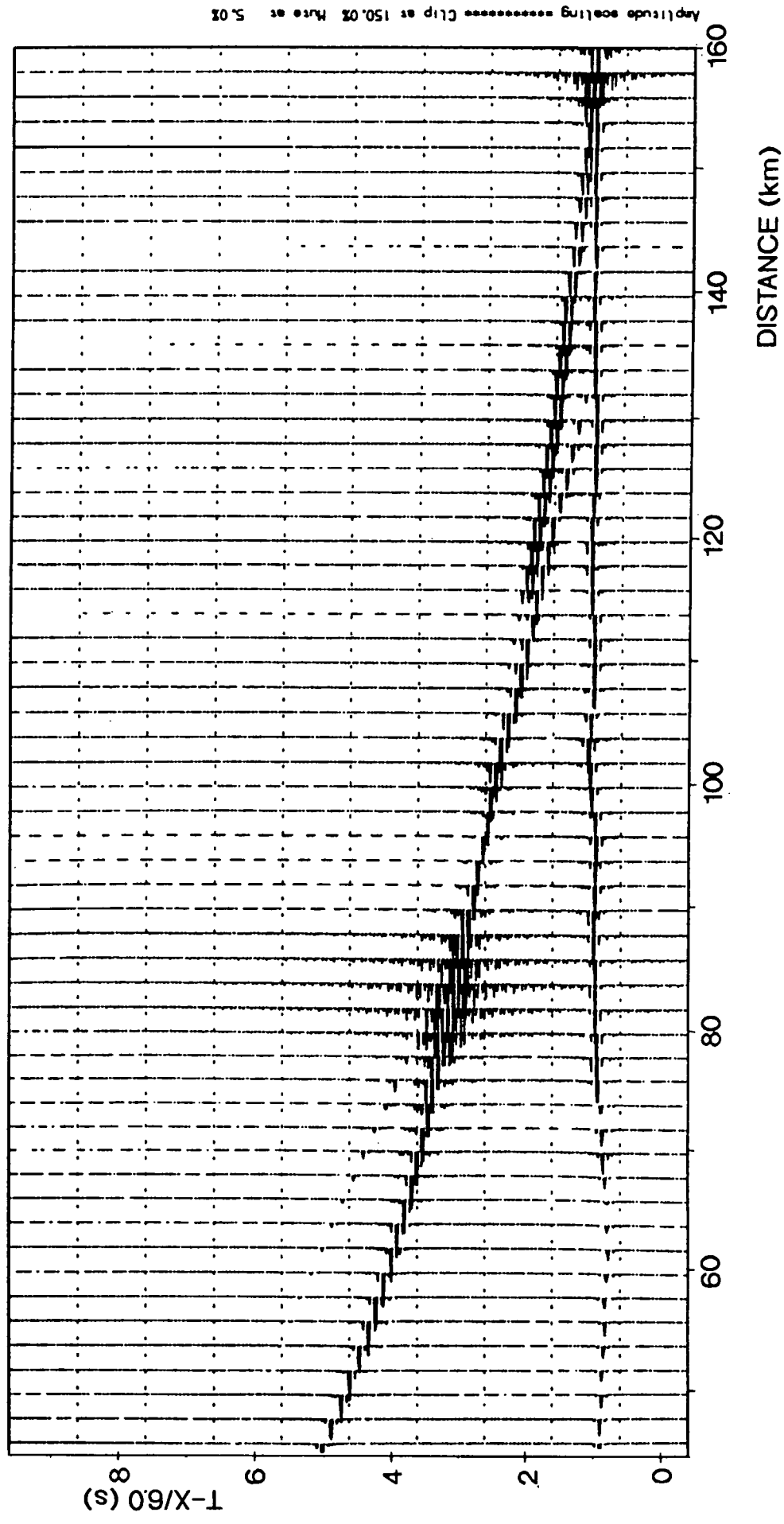

Fig. 6.17 Reflecting Moho step model at station 54: BEAM87 synthetic seismogram (bicubic spline interpolation).

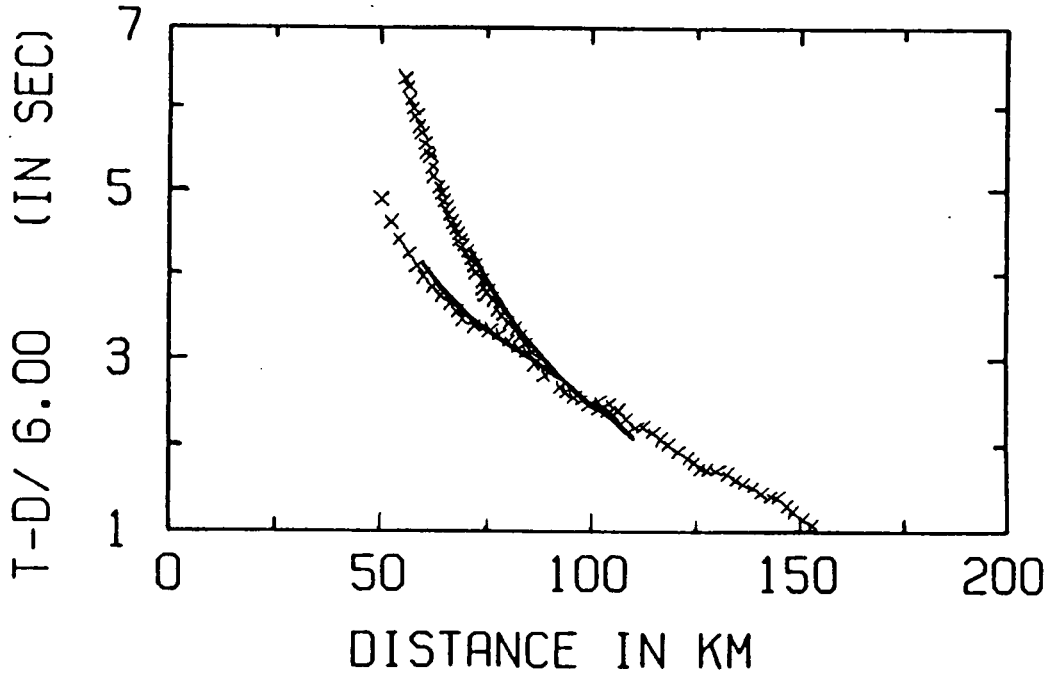

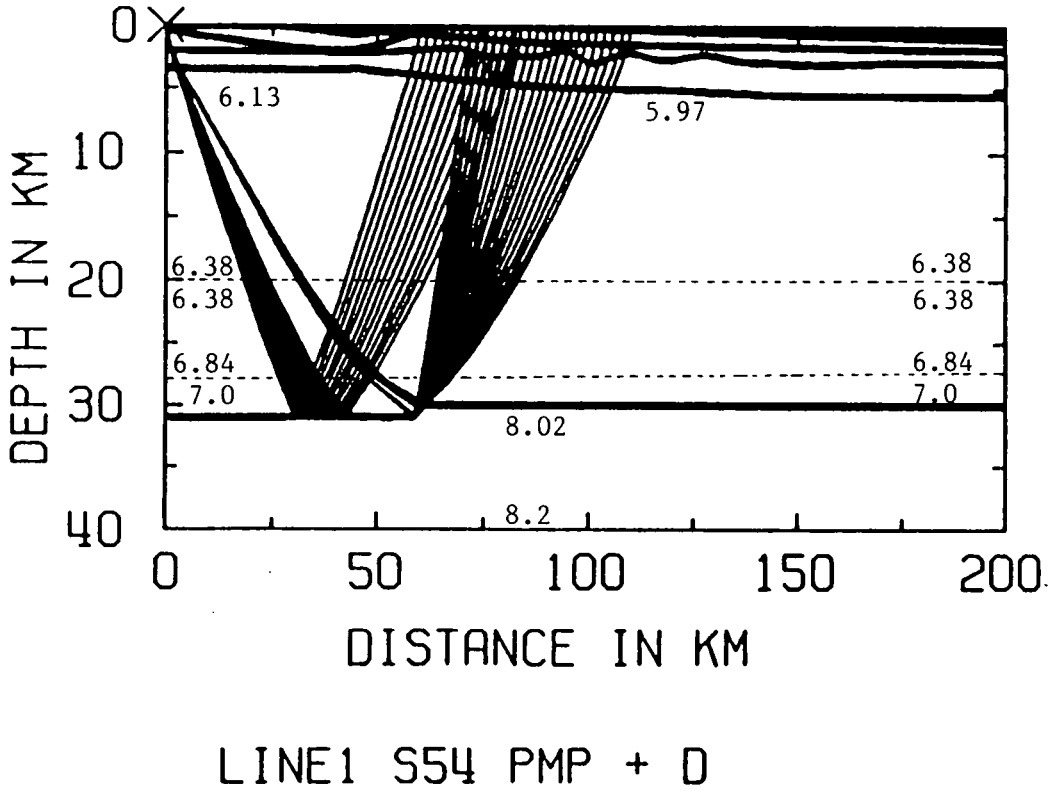

LINE1 S54 PMP + D

Fig. 6.18 2-D model for D and Pn at station 54: BEAM87 ray diagram and travel times for curved Moho step. Continuous line: calculated travel time; crosses: observed travel times; numbers within model: seismic p-velocities in km s^{-1}.

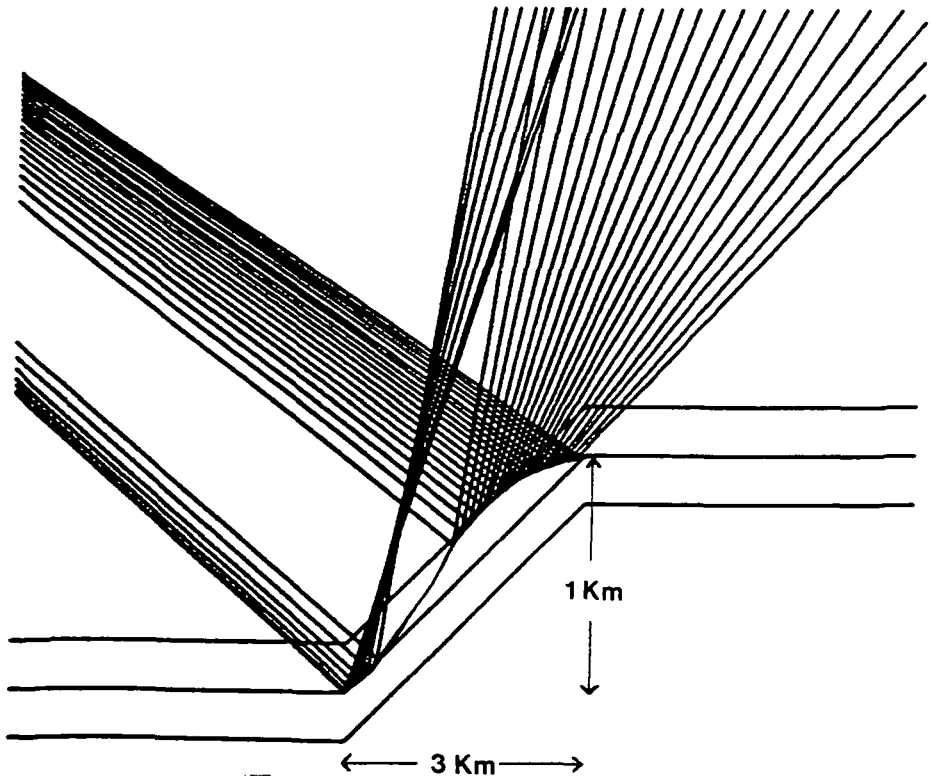

Fig. 6.19 Blown-up plot of curved Moho step

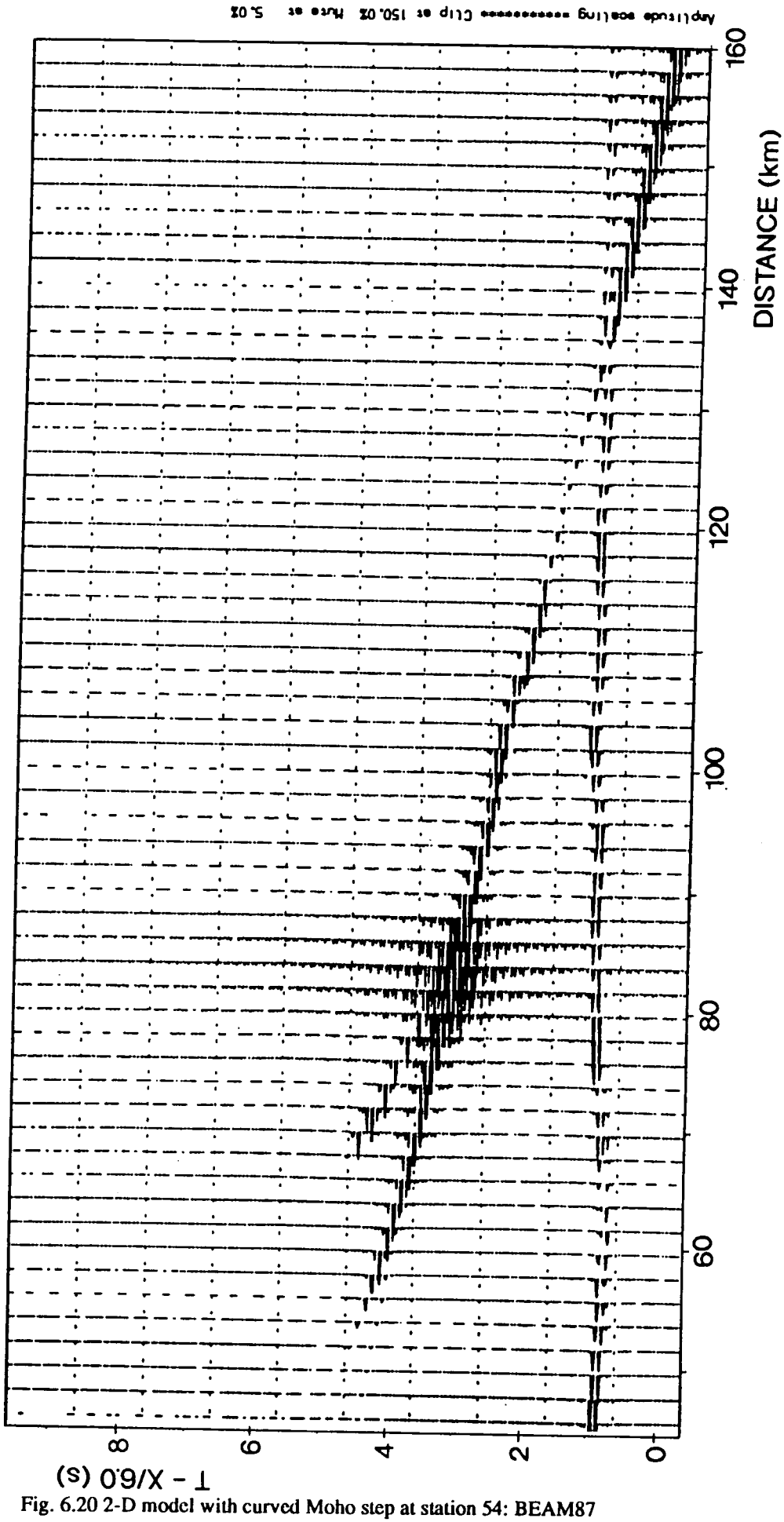

Fig. 6.20 2-D model with curved Moho step at station 54: BEAM87 synthetic seismogram computed using the bicubic spline interpolation method.

at a high amplitude too far, and at greater offsets this phase has far too high an amplitude by comparison with PmP.

An execution of this model using the linear interpolation method of BEAM87 was also attempted in order to obtain an idea of the dependence of the model results on the interpolation method itself. This meant that the lateral velocity change in the upper crust modelled by the bicubic spline method could not be represented so the travel time fit for the upper crustal phase is not so good. However, this made surprisingly little difference to the travel time fit of PmP, D and Pn. The ray diagrams, travel time plots and synthetic seismogram are shown in **Figs. 6.21** and **6.22**. This method also produces an amplitude for D comparable to that of PmP, although the high energy region on the section from the bicubic spline method section is not evident here. PmP is produced across the whole section, which implies that it must have been the use of the bicubic spline method for velocity representation which prevented the generation of PmP rays east of the step in **Fig. 6.18**.

Applying this model to all the stations, it was only possible to compute seismograms through the model using the bicubic spline interpolation method for stations 54, 55 and 57. The failure of the program to shoot rays through the bicubic spline model at the other stations may be due to the bicubic spline representation of the shallow velocity structure, which features the edge of the outcrop of the upper Carboniferous.

However, stations 55 and 57 show reasonable agreement between computed and observed arrivals. **Figs. 6.23** and **6.24** show the ray diagrams and travel time plots for stations 55 and 57, in which it can be seen that the PmP and D travel time fits are good. As at station 54, PmP is not computed east of the Moho step, again probably due to the bicubic spline velocity interpolation producing spurious gradients in this region. However, Pn is not generated by the model for either station, although it is seen on the data sections and the reason for this discrepancy could not be found. The upper crustal arrival is fitted very well at station 57 but differs slightly from the travel time picks of station 55. The travel time picks may not be exact since the station 55 records are the least clear of the whole dataset. The synthetic seismogram in **Fig. 6.25**, computed for station 57, seems to compare well with the actual section from

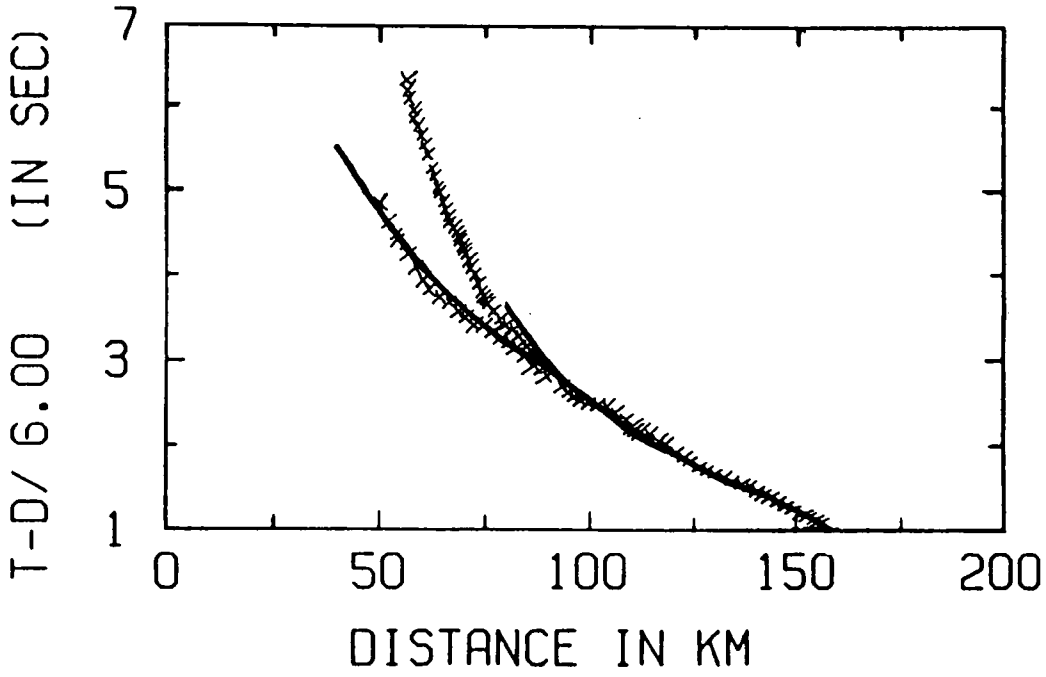

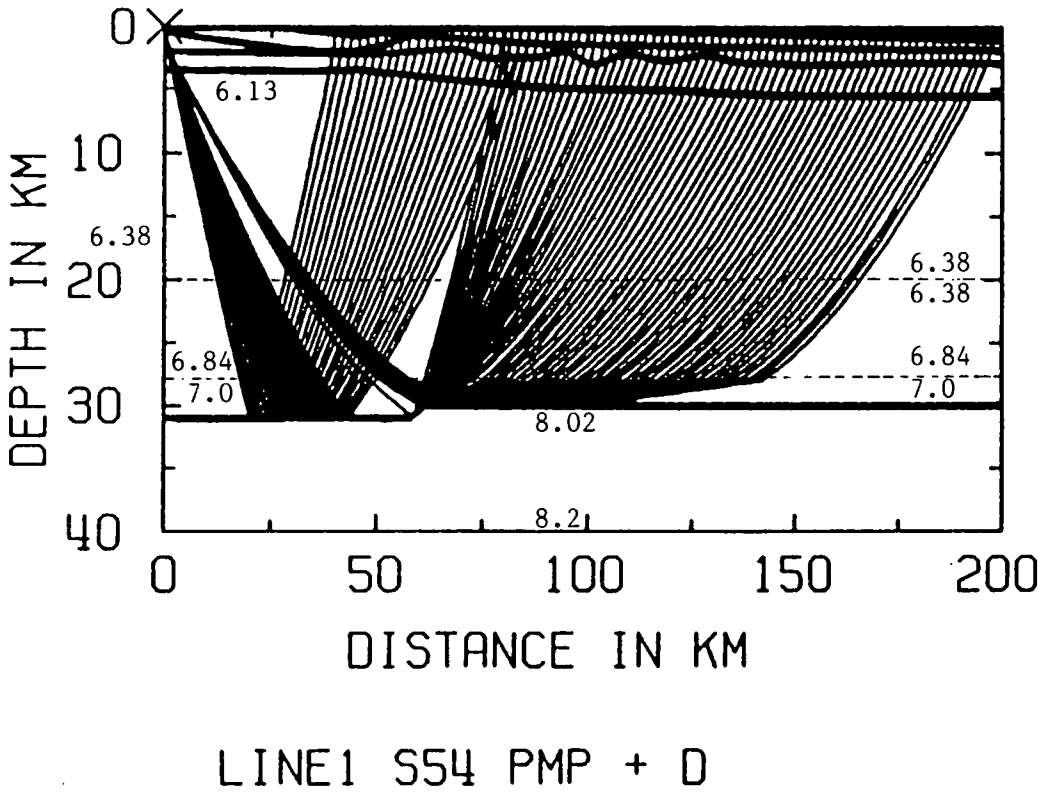

LINE1 S54 PMP + D

Fig. 6.21 2-D model for D and Pn at station 54: BEAM87 ray diagram and travel times for curved Moho step using the linear interpolation method. Continuous line: calculated travel time; crosses: observed travel times; numbers within model: seismic p-velocities in km s^{-1}.

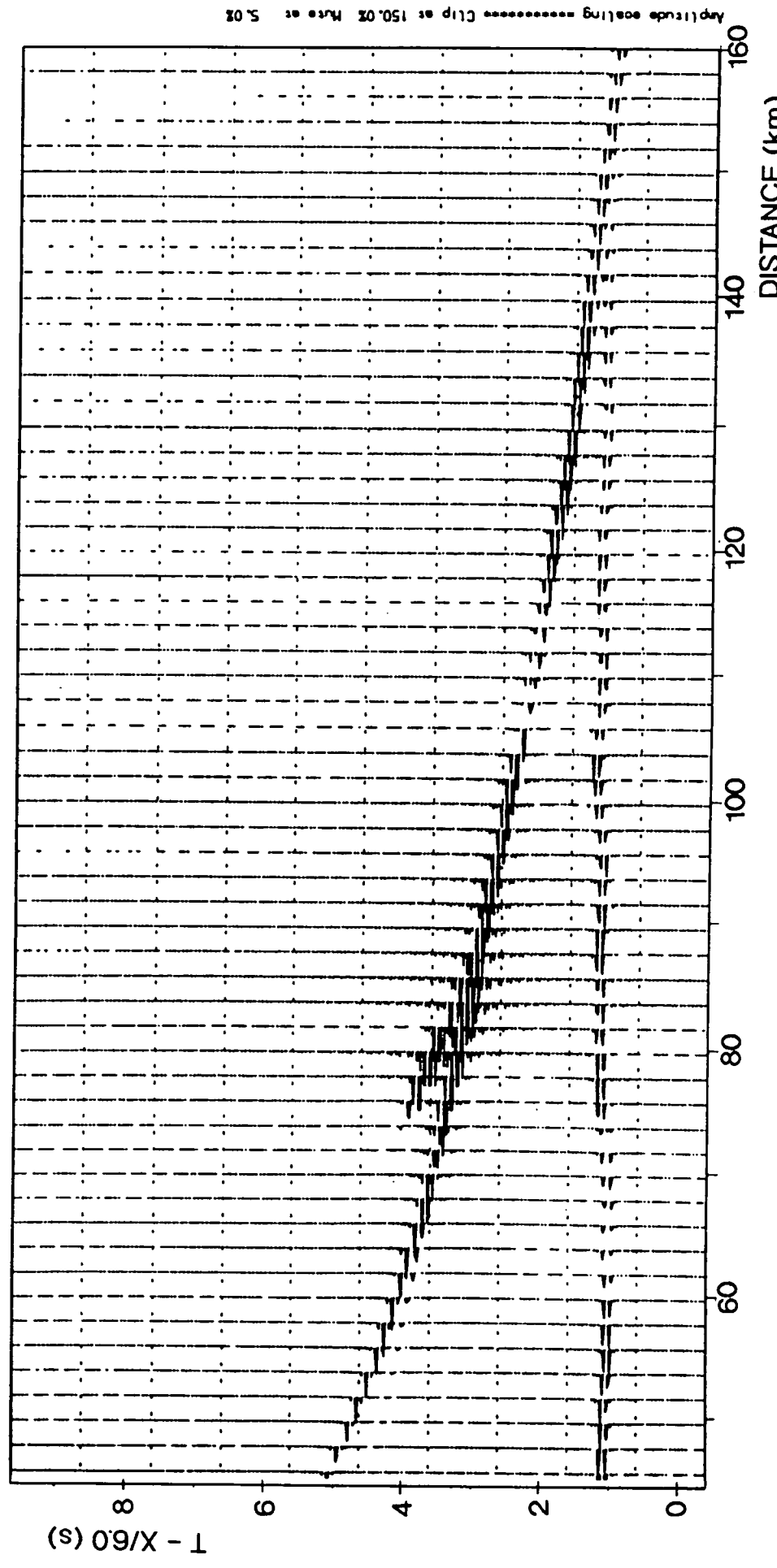

Fig. 6.22 2-D model with curved Moho step at station 54: BEAM87 synthetic seismogram computed using the linear interpolation method.

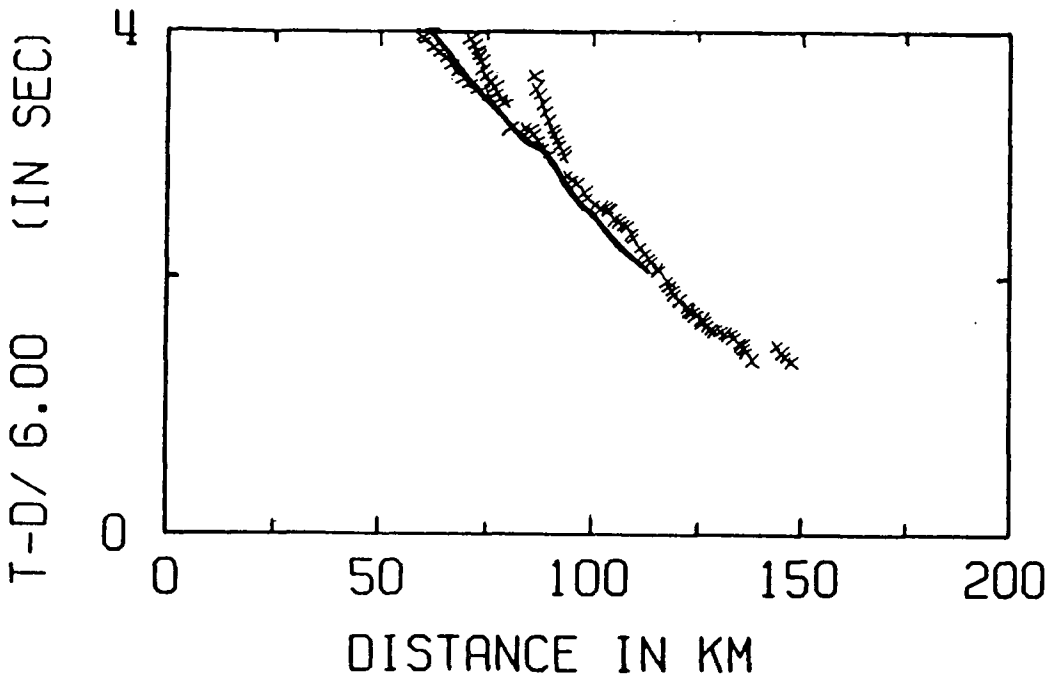

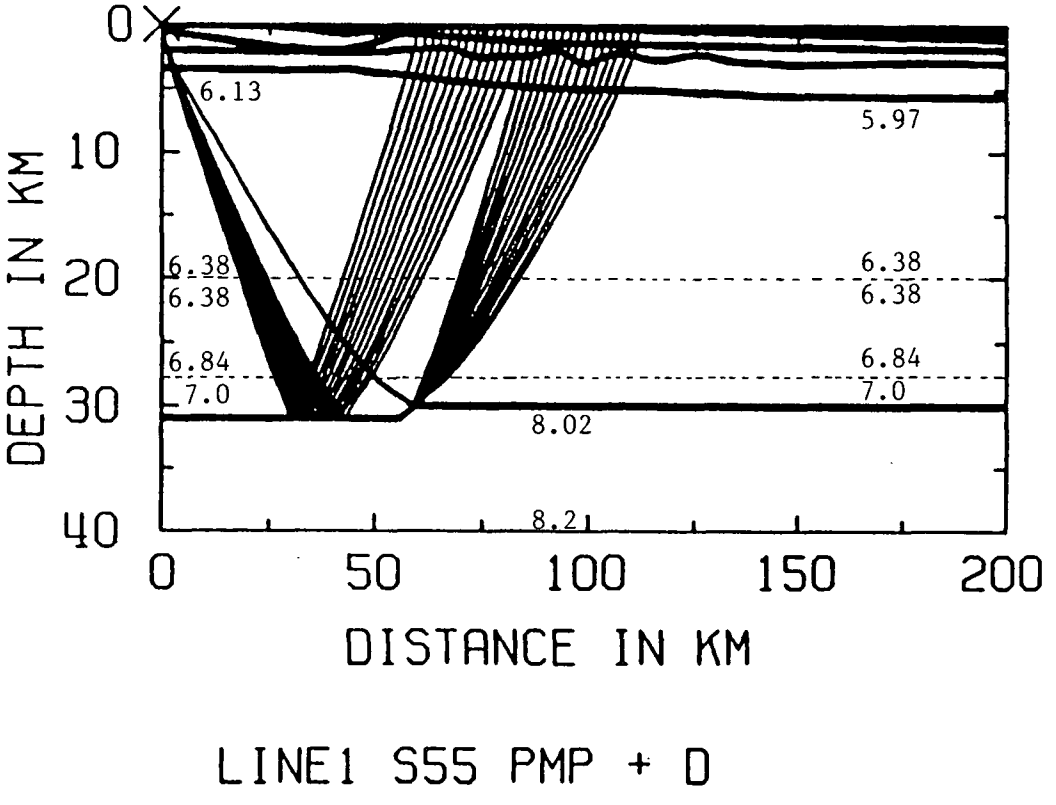

LINE1 S55 PMP + D

Fig. 6.23 Curved Moho step model at station 55: BEAM87 ray diagram and travel times (bicubic spline interpolation). Continuous line: calculated travel time; crosses: observed travel times; numbers within model: seismic p-velocities in km s^{-1}.

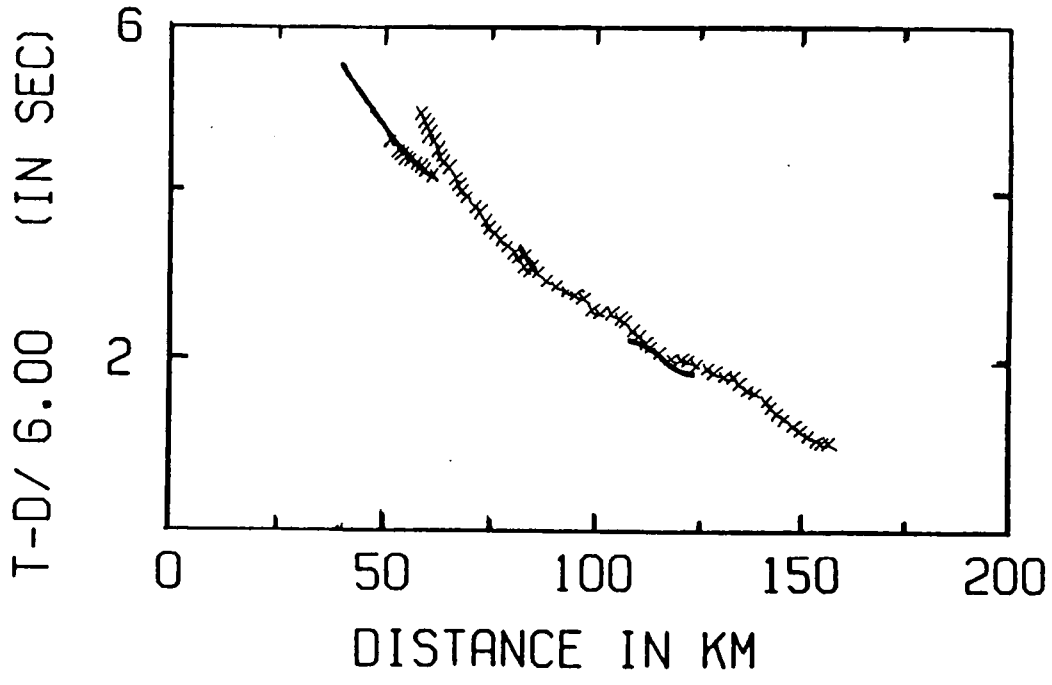

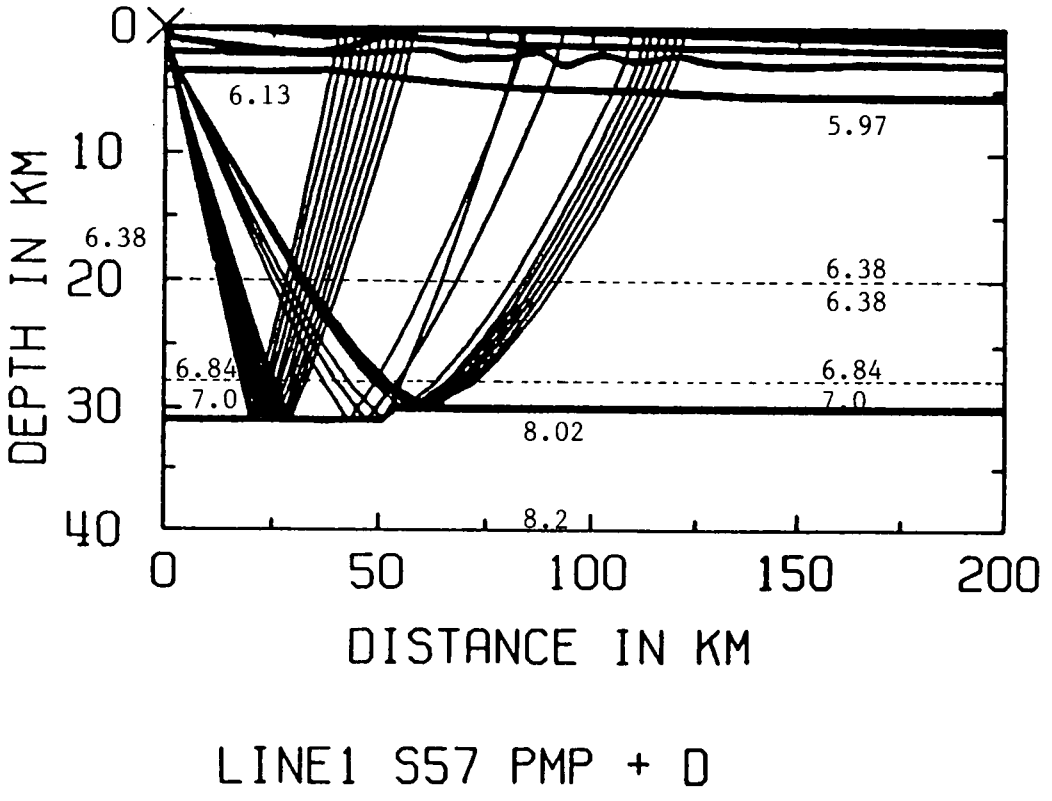

LINE1 S57 PMP + D

Fig. 6.24 Curved Moho step model at station 57: BEAM87 ray diagram and travel times (bicubic spline interpolation). Continuous line: calculated travel time; crosses: observed travel times; numbers within model: seismic p-velocities in km s^{-1}.

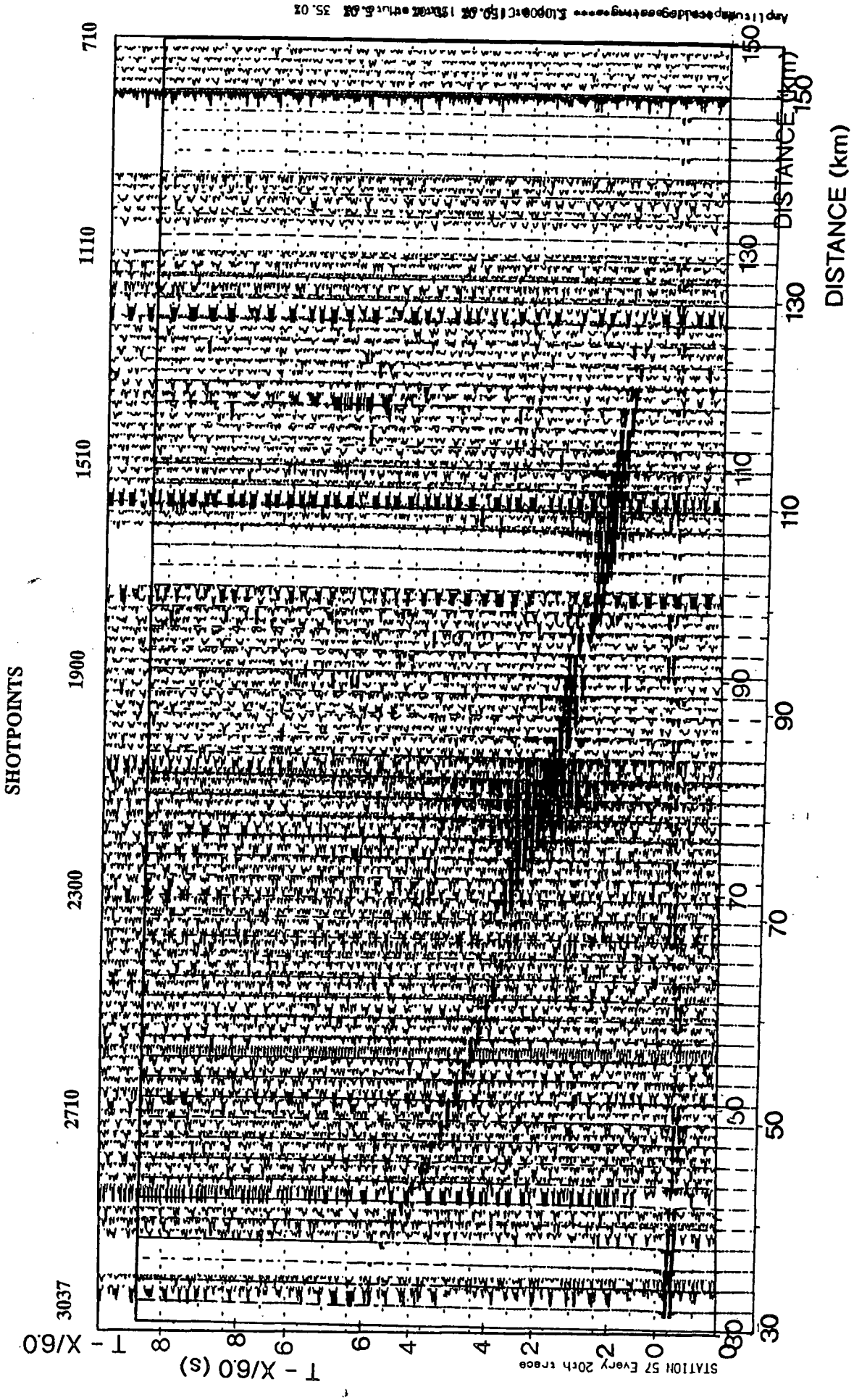

Fig 6.25 Curved Moho step model at station 57: BEAM87 synthetic seismogram (bicubic spline interpolation).

STATION 57 DATA SECTION FOR COMPARISON WITH SYNTHETIC SECTIONS

this station on transparency (ii), although the quality of this data section is poor due to high noise levels and it is therefore not very clear.

Computing synthetic seismograms for the western stations (stations 36, 37, 39, 40 and 47) using the linear interpolation method obviously does not allow for the lateral variation in the crustal velocity gradient. However, since the linear interpolation method did not produce drastically different results for station 54 except in the fit of Pg, this method was used for stations 36 to 47. For these computations, no arrivals were computed from the step on the Moho but the fit to PmP is excellent for station 47. For stations 40 and 36, the basement velocity of 5.97 kms^{-1} was too low, producing late travel times for PmP. A basement velocity of 6.05 kms^{-1} was found to remedy this problem for station 40 and to improve it for station 36, but it was also necessary to incorporate a higher velocity of 7.1 kms^{-1} in the 2 km thick slab at the base of the crust in order to fit the travel times of PmP. The ray diagrams and travel time plots in **Figs. 6.26, 6.27** and **6.28** represent this model, and **Figs. 6.29** and **6.30** are the synthetic seismograms generated for stations 47 and 40. These synthetics may be compared with transparencies (iii) and (iv), although these sections, like transparency (ii), are too noisy to plot well at this scale. Nevertheless, the synthetic main arrivals PmP and PcP compare reasonably well with the real sections in terms of amplitude, although the models fail to generate Pn and D.

The final attempt to model this arrival was inspired by **Kusznir and Matthews(1988)**, who modelled the decay of a Moho step with time, reaching the conclusion that such decay is extremely wavelength dependent. In the process of ductile flow in the lower crust, intermediate wavelengths of topography on the Moho tend to be obliterated, whereas short and long wavelengths are still present after long periods of time. **Figure 6.31** illustrates the result of such a process. Since the evidence from phase D seems to point towards a Moho step, this step would have been expected to decay with time and probably produce the result predicted by Kusznir and Matthews.

This approach was therefore tried, and is shown in **Fig. 6.32.** It produces an excellent travel time fit for D and PmP, and synthetic amplitudes which, although still not high enough, show a maximum at an offset closer to the observed offset of maximum amplitude than to that obtained from the curved step of **Fig. 6.18.** Unfortunately, the distance ranges of PmP and Pn are still restricted, although this must be

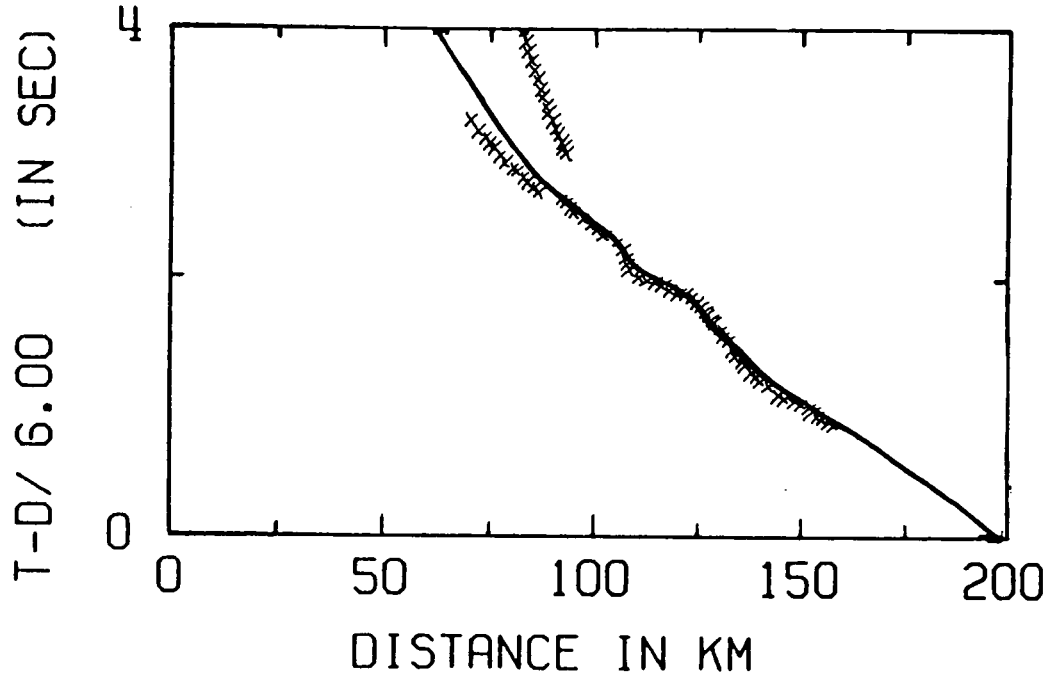

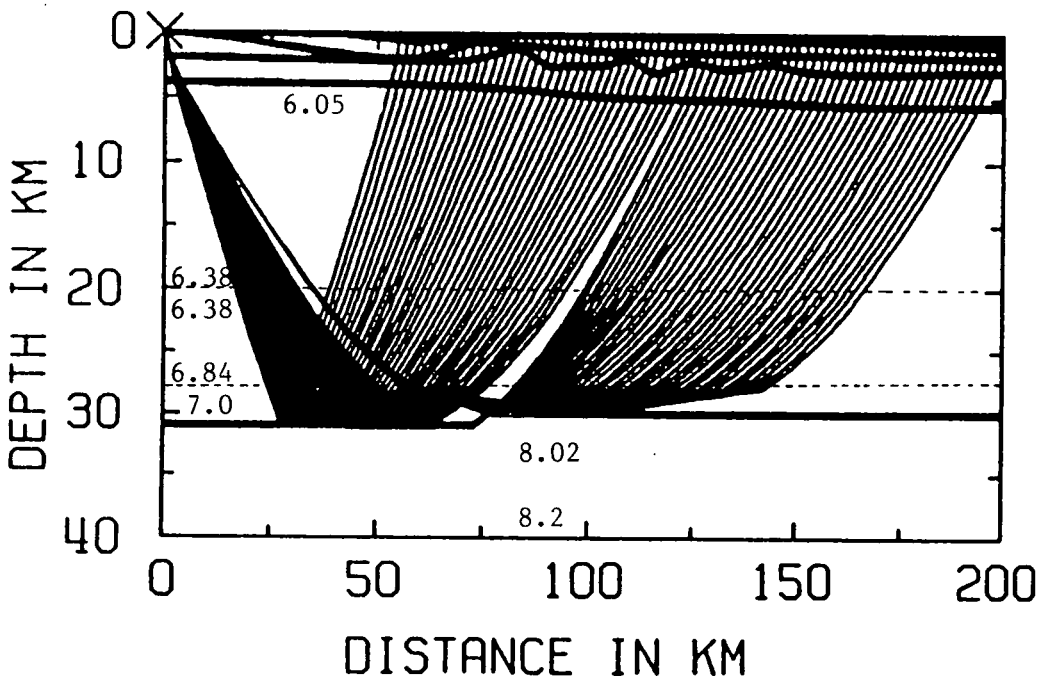

LINE1 S47 PMP + D

Fig. 6.26 Curved Moho step model (linear interpolation) at station 47: BEAM87 ray diagram and travel times. Continuous line: calculated travel time; crosses: observed travel times; numbers within model: seismic p-velocities in km s^{-1}.

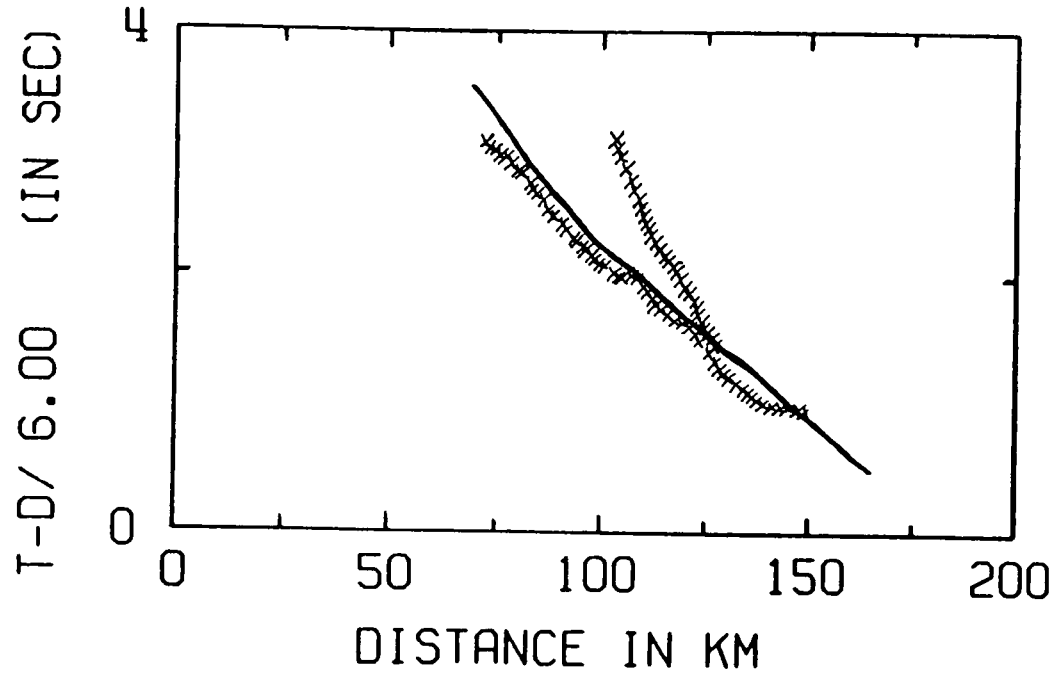

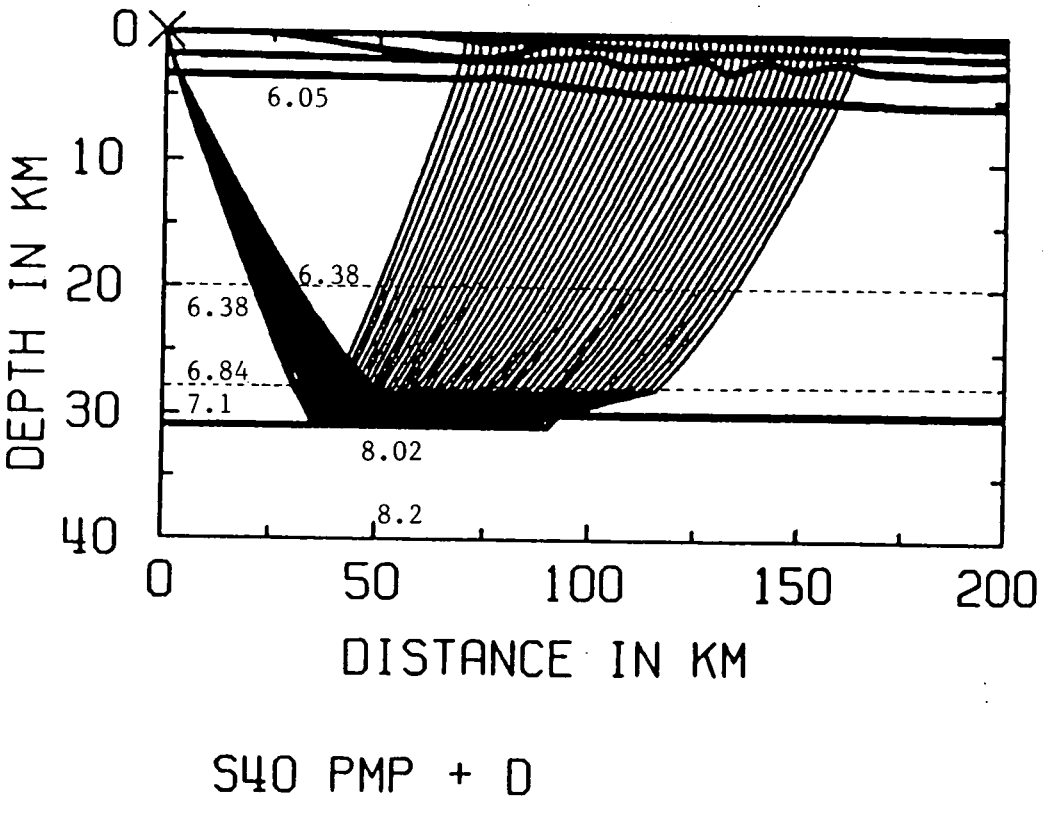

S40 PMP + D

Fig. 6.27 Curved Moho step model (linear interpolation) at station 40: BEAM87 ray diagram and travel times. Continuous line: calculated travel time; crosses: observed travel times; numbers within model: seismic p-velocities in km s^{-1}.

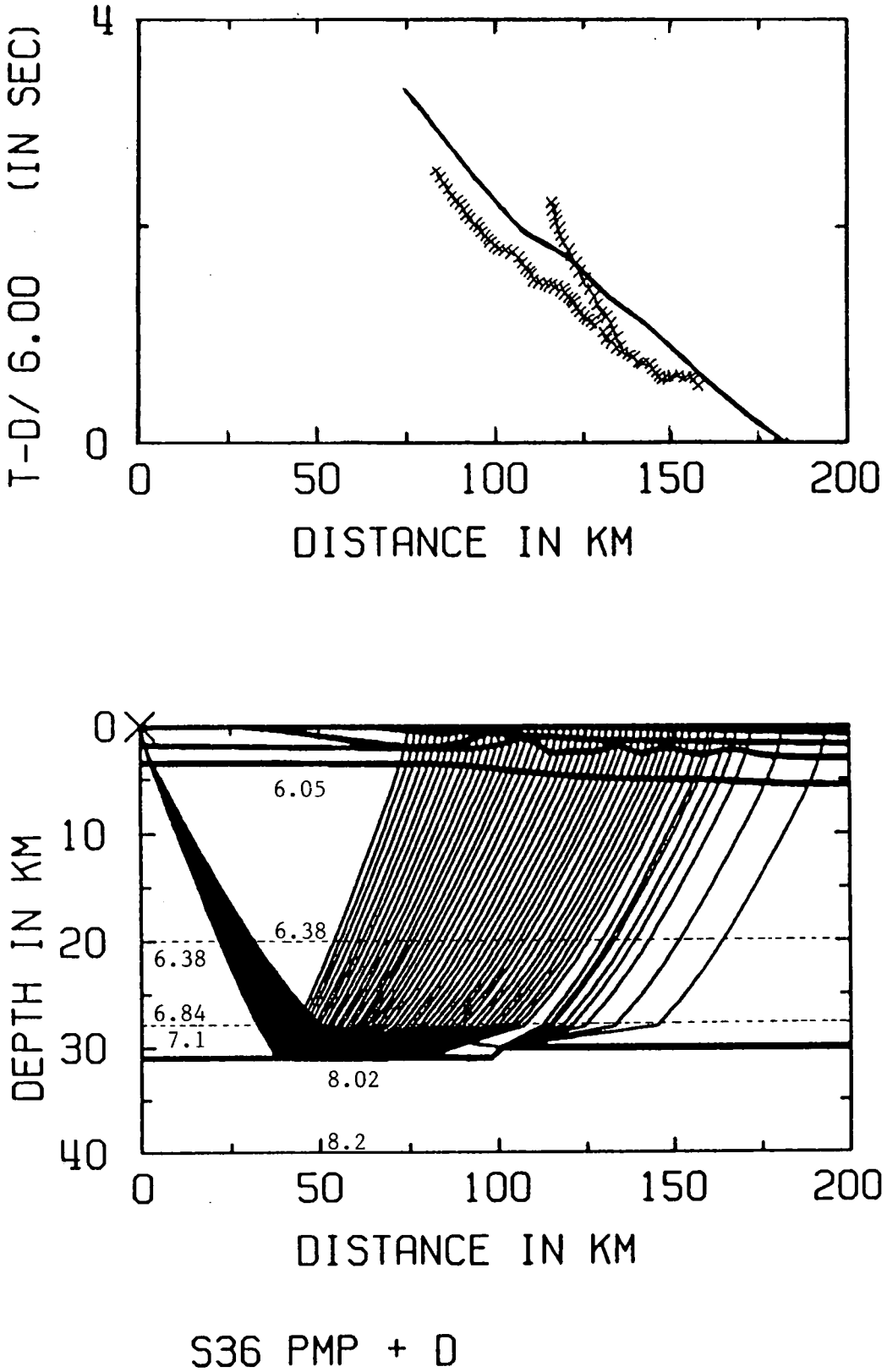

Fig. 6.28 Curved Moho step (linear interpolation) at station 36: BEAM87 ray diagram and travel times. Continuous line: calculated travel time; crosses: observed travel times; numbers within model: seismic p-velocities in km s^{-1}.

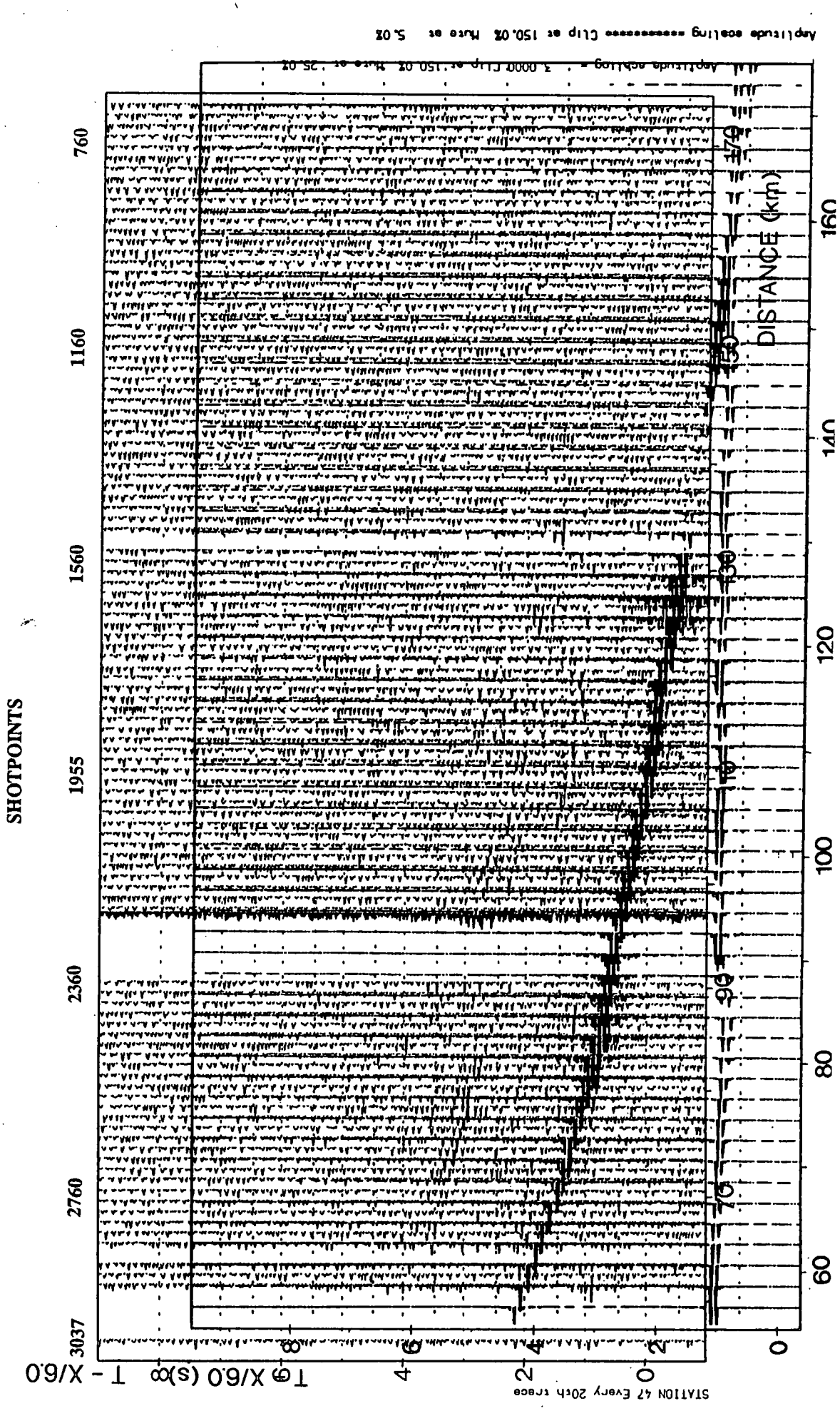

Fig. 6.29 Curved Moho step model at station 47: BEAM87 synthetic seismogram (linear interpolation)

STATION 47 DATA SECTION FOR COMPARISON WITH SYNTHETIC SECTIONS

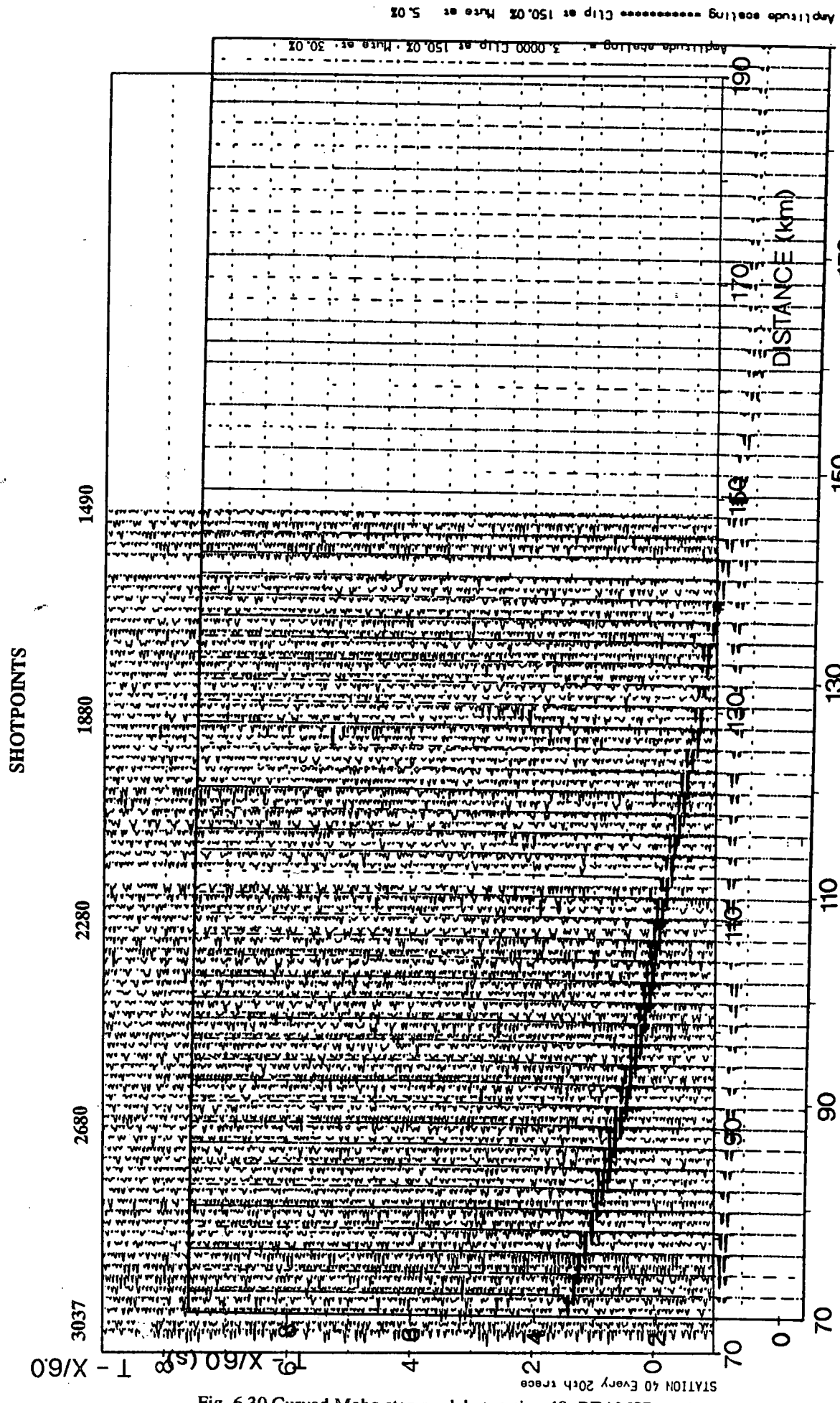

Fig. 6.30 Curved Moho step model at station 40: BEAM87 synthetic seismogram (linear interpolation)

STATION 40 DATA SECTION FOR COMPARISON WITH SYNTHETIC SECTIONS

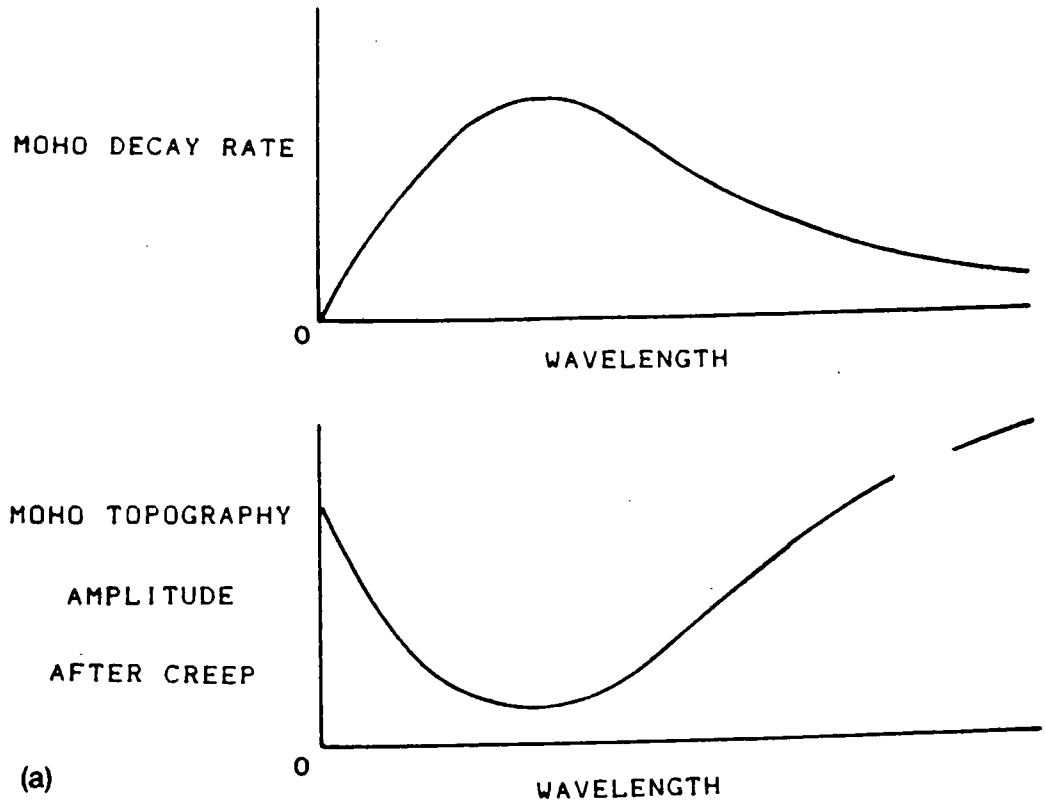

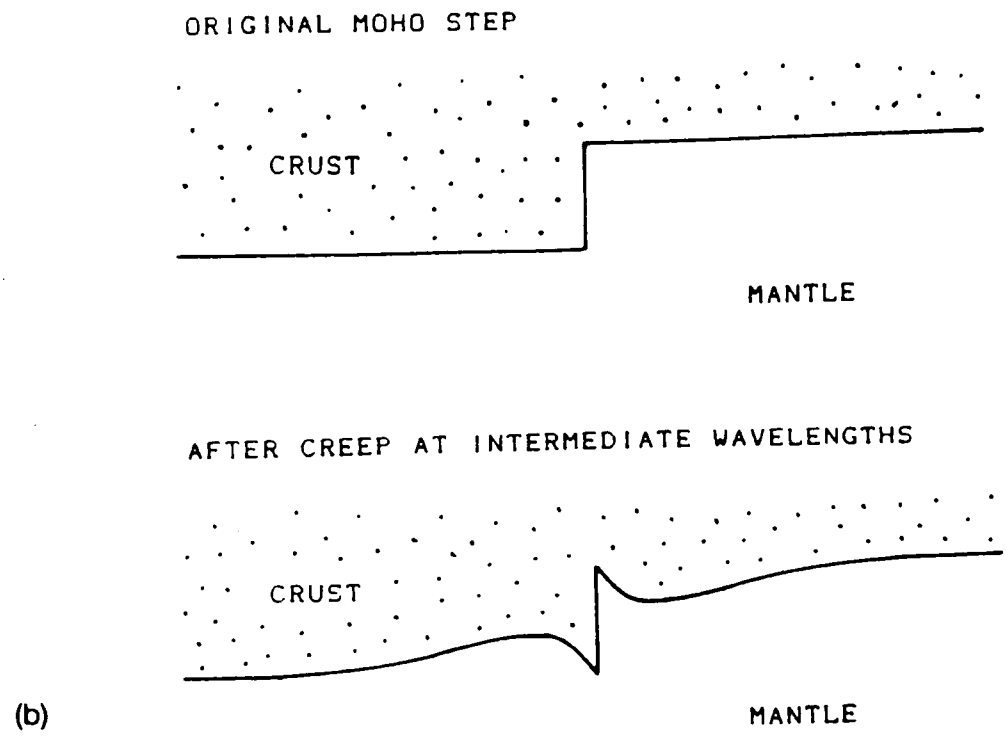

Fig. 6.31 (a)Wavelength dependence of the decay of Moho topography: decay rates tend to zero at short and long wavelengths.
(b) Modification of a Moho step after removal of intermediate wavelengths by ductile flow in the lower crust.
Both figures from **Kusznir & Matthews (1988);** figures show qualitative results only.

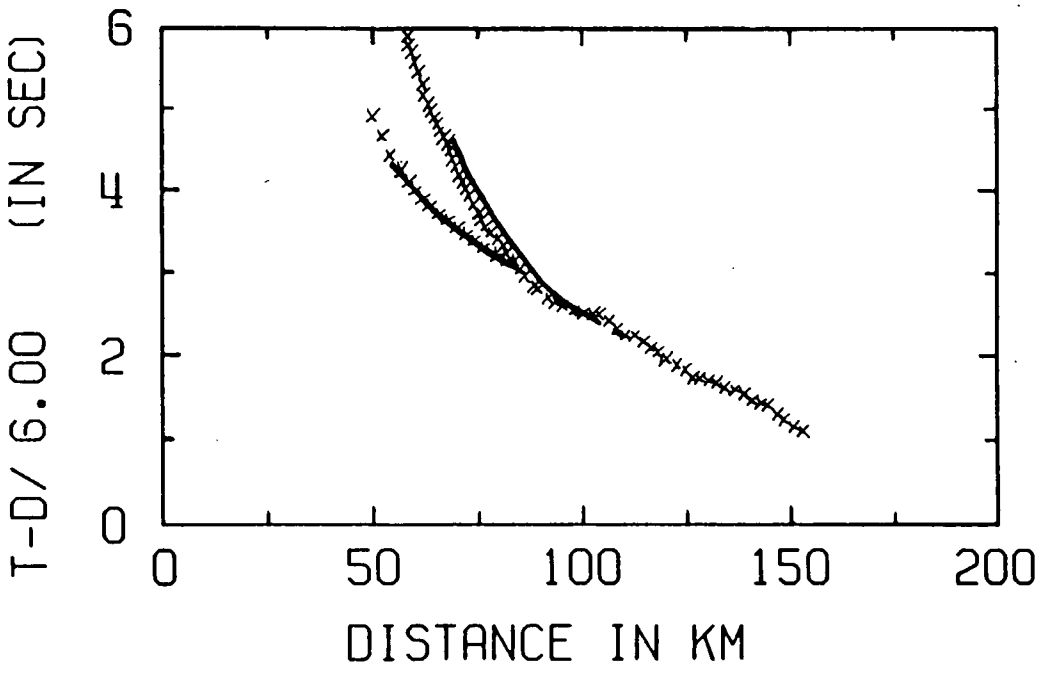

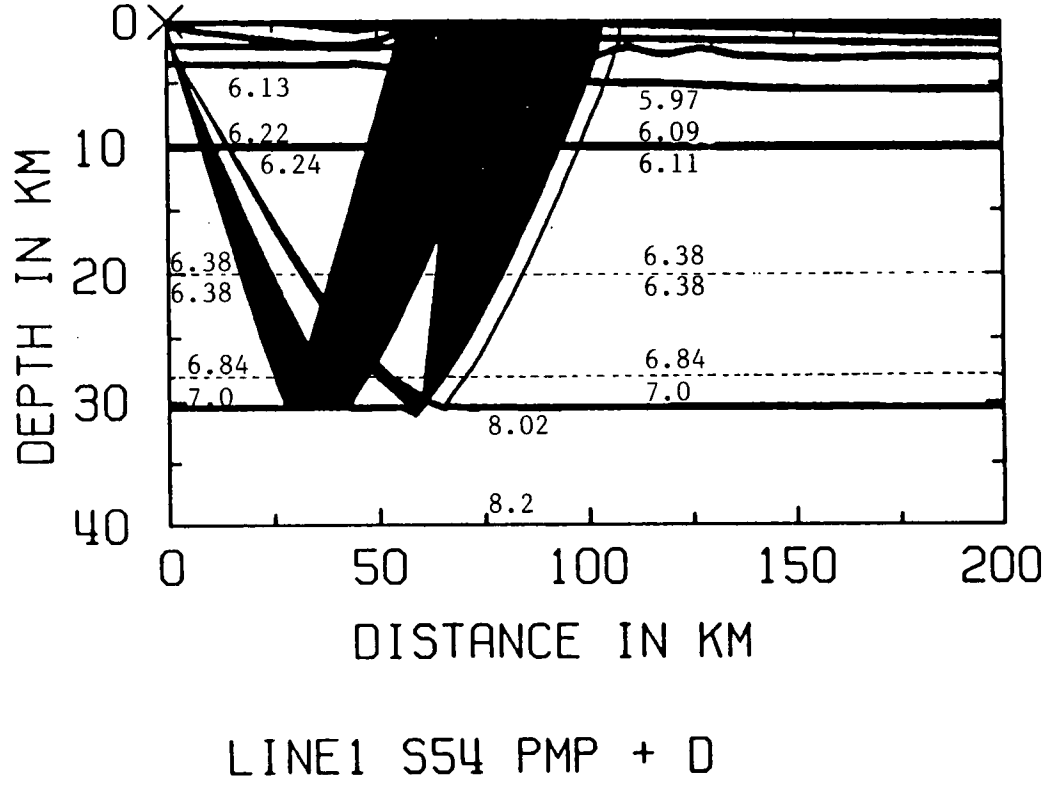

LINE1 S54 PMP + D

Fig. 6.32 BEAM87 ray diagram and travel times for a "decayed" Moho step, modelled at station 54. Continuous line: calculated travel time; crosses: observed travel times; numbers within model: seismic p-velocities in km s^{-1}.

Enclosure (v)

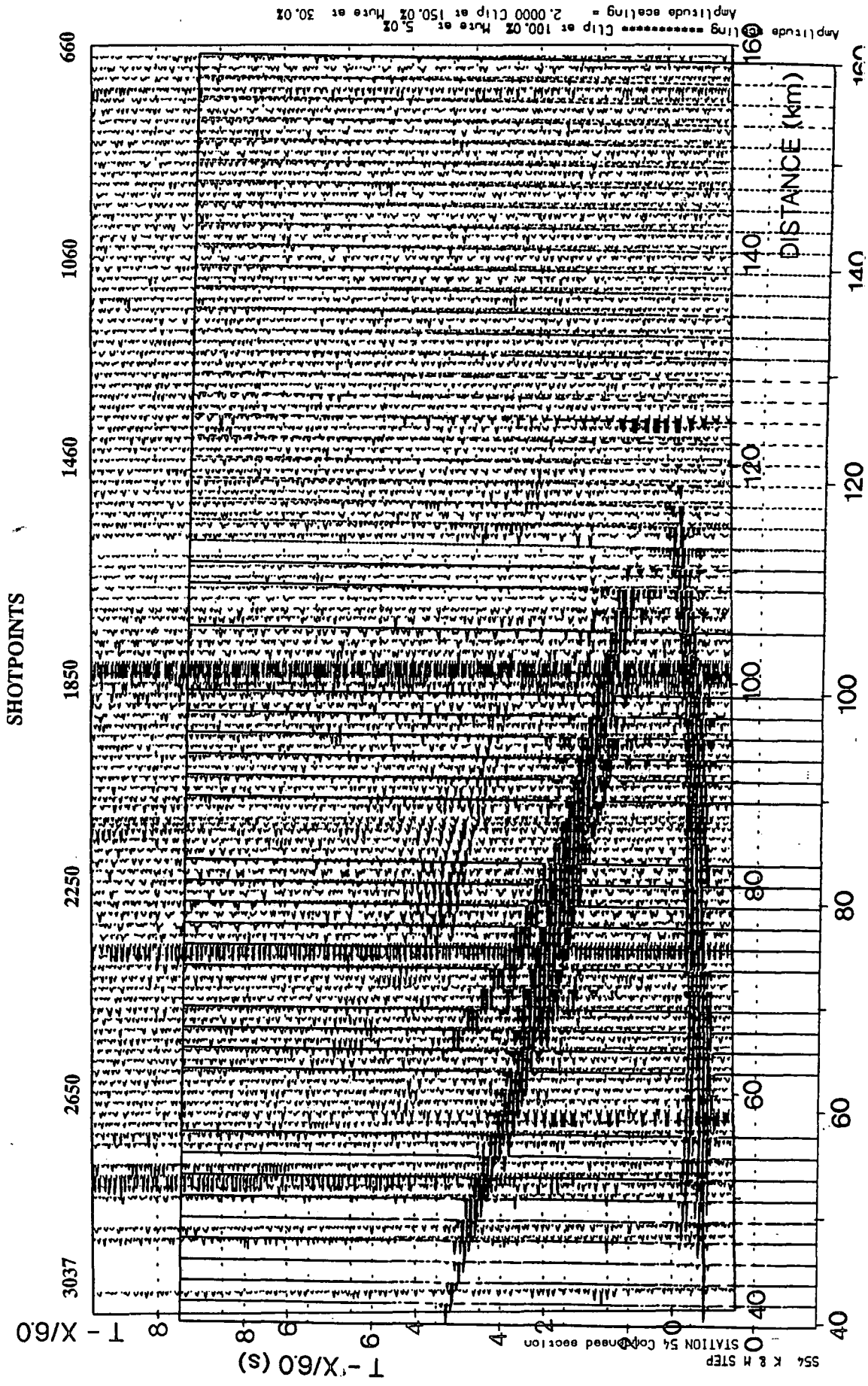

STATION 54 DATA SECTION FOR COMPARISON WITH SYNTHETIC SECTIONS

Fig. 6.36 Delayed Moho step model at station 54. BEAM87 synthetic

due to the bicubic spline representation of the velocity field around the "decayed" step. Transparency (v) is enclosed here for comparison with the synthetic seismogram of **Fig. 6.33**, generated by this model.

6.4.5 Wide-angle reflections from the mid crust

As mentioned in **section 6.4.1**, the phases from the mid-crustal region were modelled last of all since there was least certainty about the picking of the travel times, particularly with respect to correlation of the phases between recording stations. The modelling of the crust so far had produced velocity gradients through the crust, (the lower crust slightly higher than the upper crustal gradient) in order to fit both Pg and PmP. The mid-crustal reflectors which give rise to wide-angle reflections have been superimposed onto this gradient. Only preliminary modelling of these phases has been carried out.

The earliest reflection, picked as **PuP** (see **section 4.4.2**) is obviously from fairly shallow depths and appears to be fitted at station 54 by a 10 km deep reflector with a slight velocity contrast of 0.02 kms^{-1} (**Fig. 6.34**). It has not been possible to generate rays which reflect from this horizon for any other stations except 54, 55 and 57, again possibly due to the representation of the near surface structure at stations 36 to 47.

The **PcP** phase seems to be fitted reasonably well by reflections from the top of the higher velocity gradient which defines the lower crust. This occurs at 20 km depth and there must therefore be a change not only on the velocity gradient but also a slight change in velocity at that depth. A change of approximately 0.03 kms-1 has been used for this model. However, the travel time fit deteriorates east of shotpoint 3037. A slope on the reflector, dipping to the west, could possibly explain the travel times, but this has not yet been modelled. **Figs. 6.35, 6.36** and **6.37** show the travel time fits for this phase at stations 37, 47 and 54 respectively.

The late **PbP** phase seems to be generated by a velocity change of about 0.03 kms^{-1} at approximately 24 km depth, according to the approximate travel time fitting carried out so far. The fit at stations 37, 47 and 54 is shown in **Figs. 6.38** to **6.40** respectively.

As already stated, these interpretations are only tentative, to give some idea of the explanation of the most prominent of the mid-crustal wide-angle reflections. Sketching the approximate lateral limit of

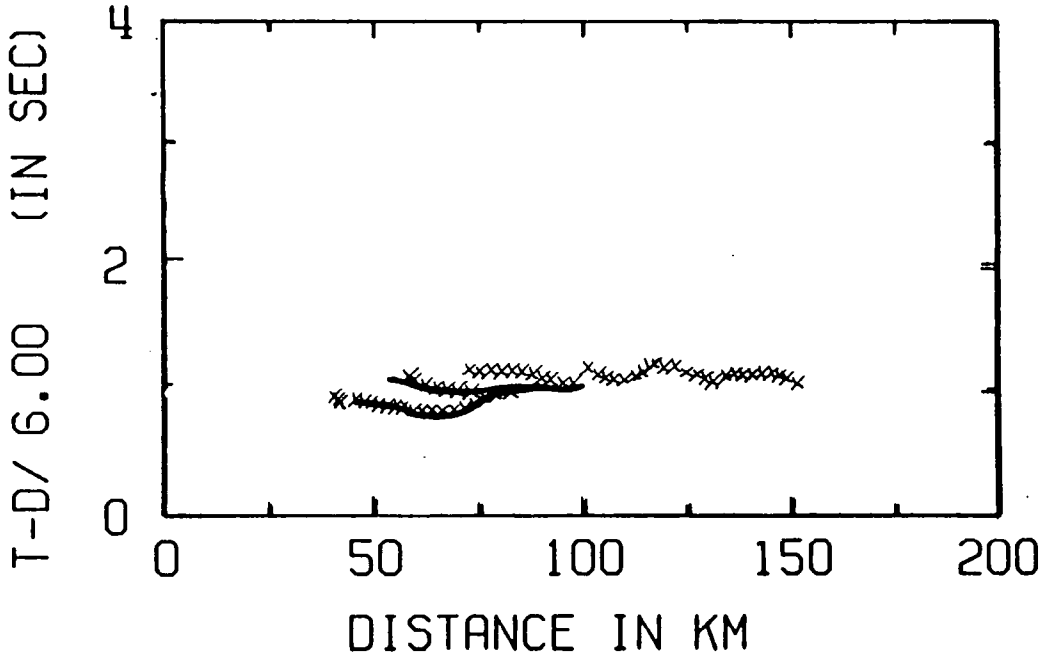

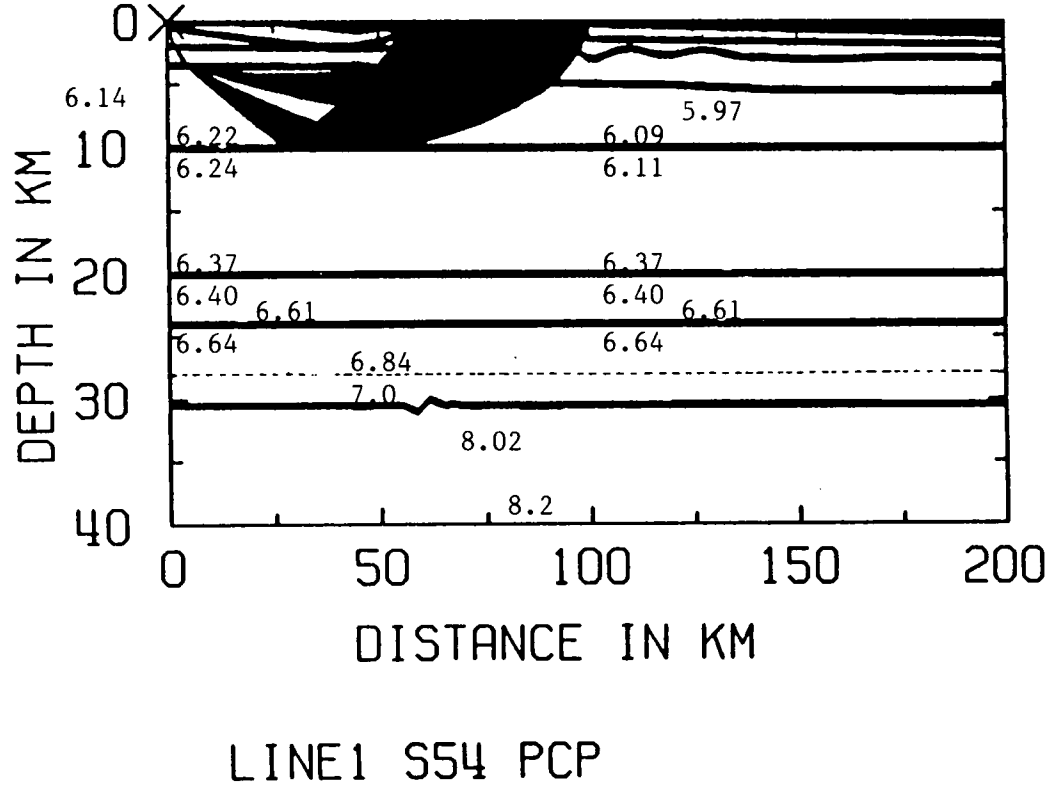

LINE1 S54 PCP

Fig. 6.34 BEAM87 ray diagram and travel times for a wide-angle reflection from a mid-crustal reflector (PuP) modelled at station 54. Continuous line: calculated travel time; crosses: observed travel times; numbers within model: seismic p-velocities in km s^{-1}.

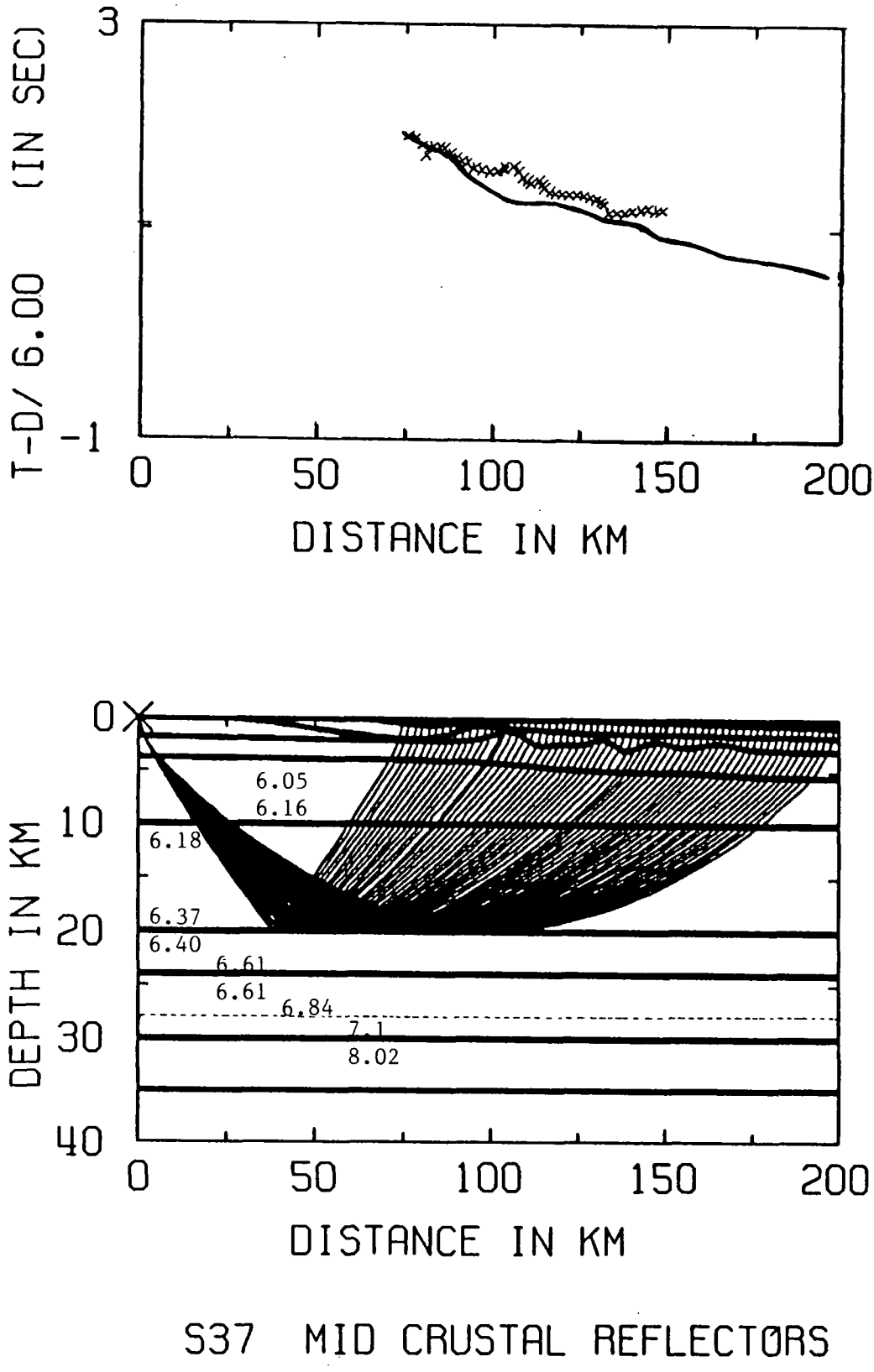

Fig. 6.35 BEAM87 ray diagram and travel times for a wide-angle reflection from the top of the lower crust (PcP) modelled at station 37. Continuous line: calculated travel time; crosses: observed travel times; numbers within model: seismic p-velocities in km s^{-1}.

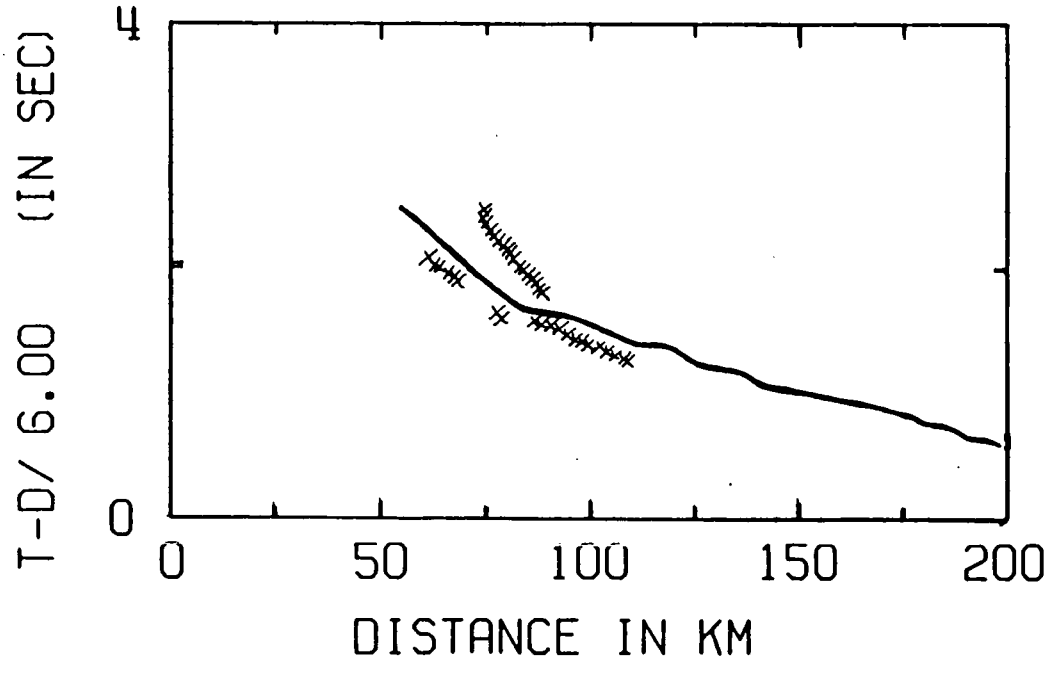

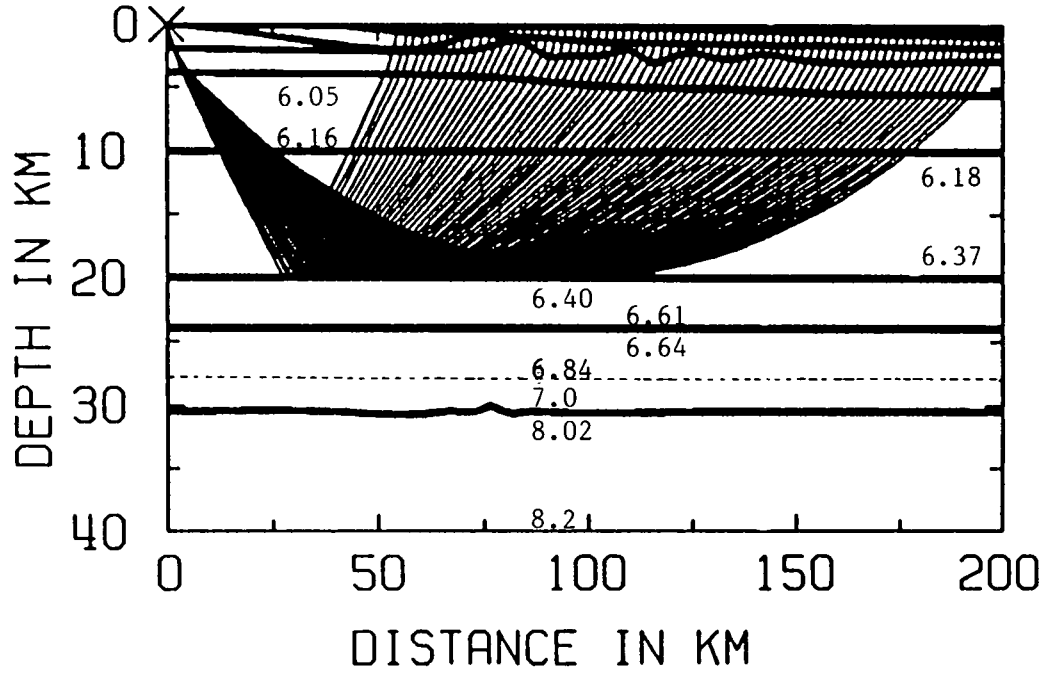

LINE1 S47 MID-CRUSTAL REFLECTORS

Fig. 6.36 BEAM87 ray diagram and travel times for a wide-angle reflection from the top of the lower crust (PcP) modelled at station 47. Continuous line: calculated travel time; crosses: observed travel times; numbers within model: seismic p-velocities in km s^{-1}.

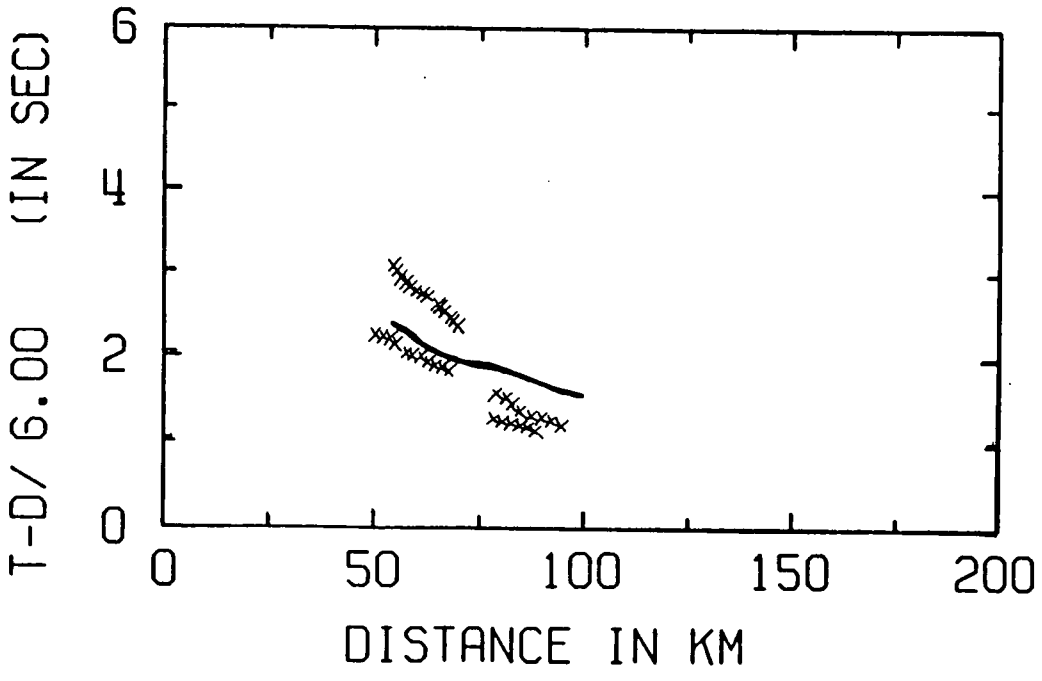

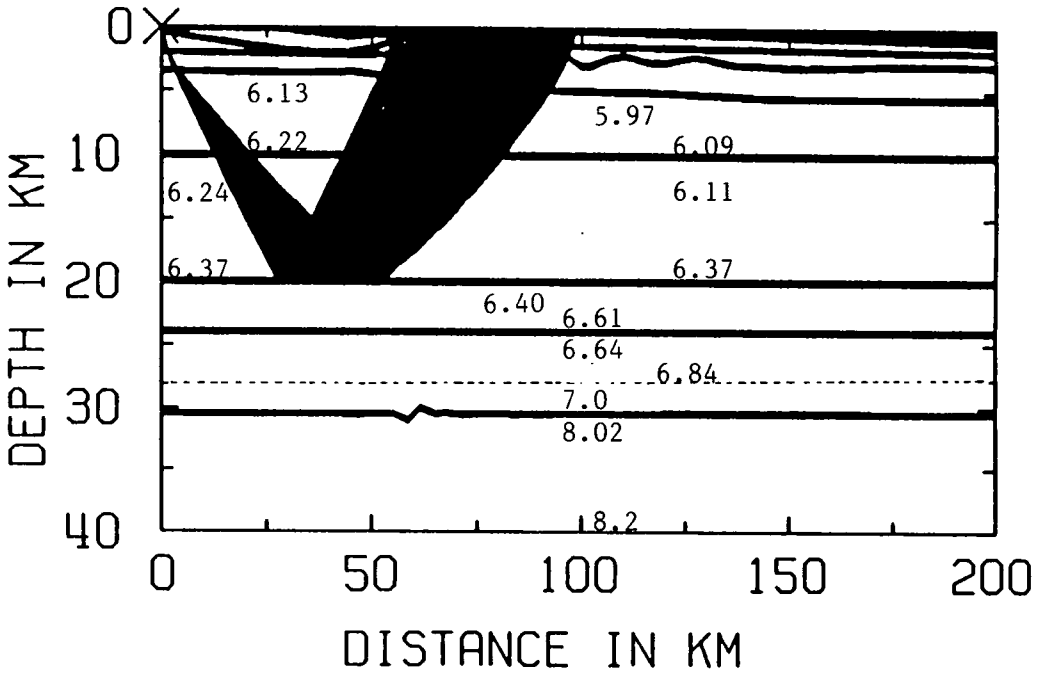

LINE1 S54 MID CRUSTAL REFLECTIONS

Fig. 6.37 BEAM87 ray diagram and travel times for a wide-angle reflection from the top of the lower crust (PcP) modelled at station 54. Continuous line: calculated travel time; crosses: observed travel times; numbers within model: seismic p-velocities in km s^{-1}.

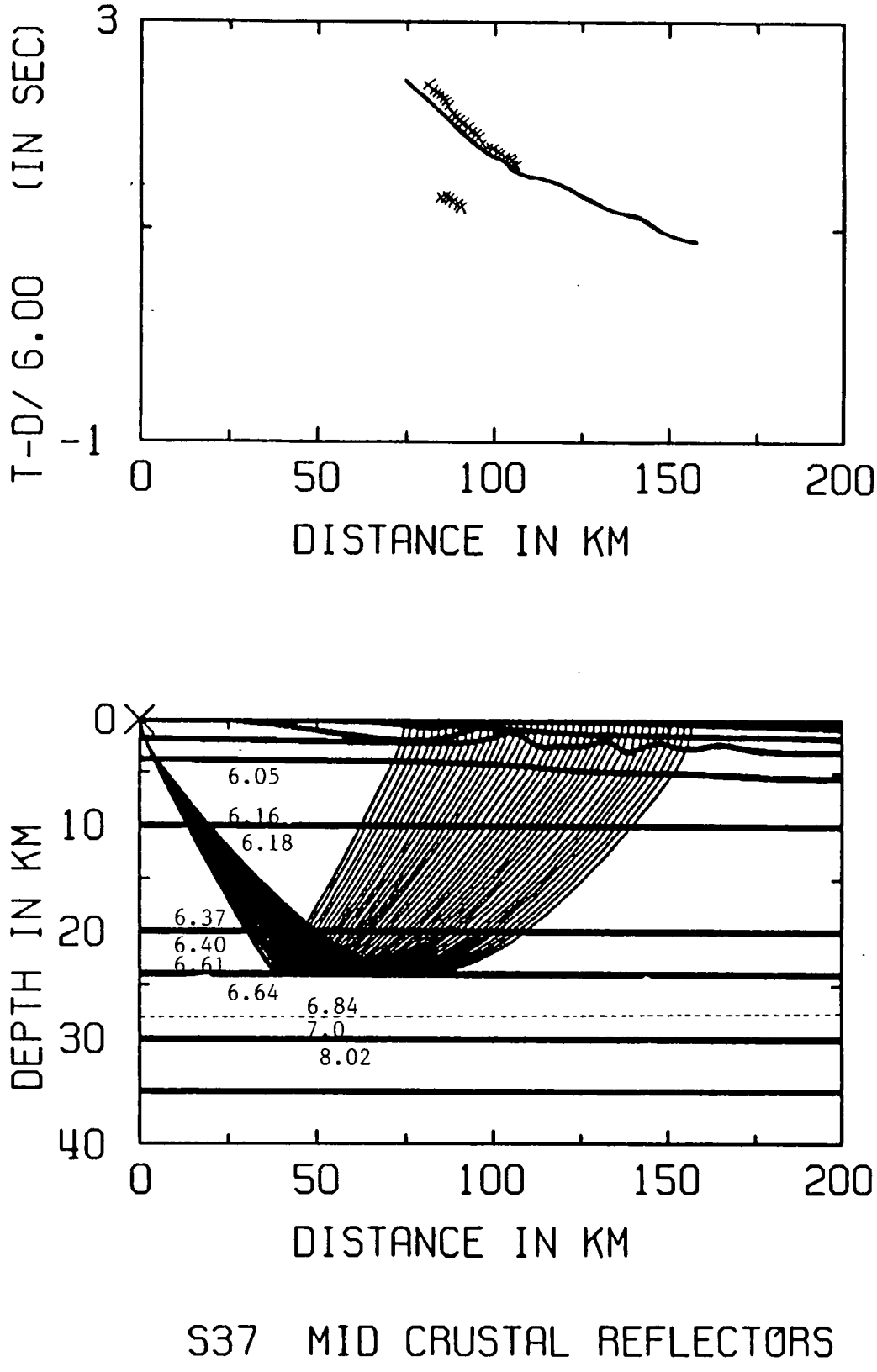

Fig. 6.38 BEAM87 ray diagram and travel times for a wide-angle reflection from within the lower crust (PbP) modelled at station 37. Continuous line: calculated travel time; crosses: observed travel times; numbers within model: seismic p-velocities in km s^{-1}.

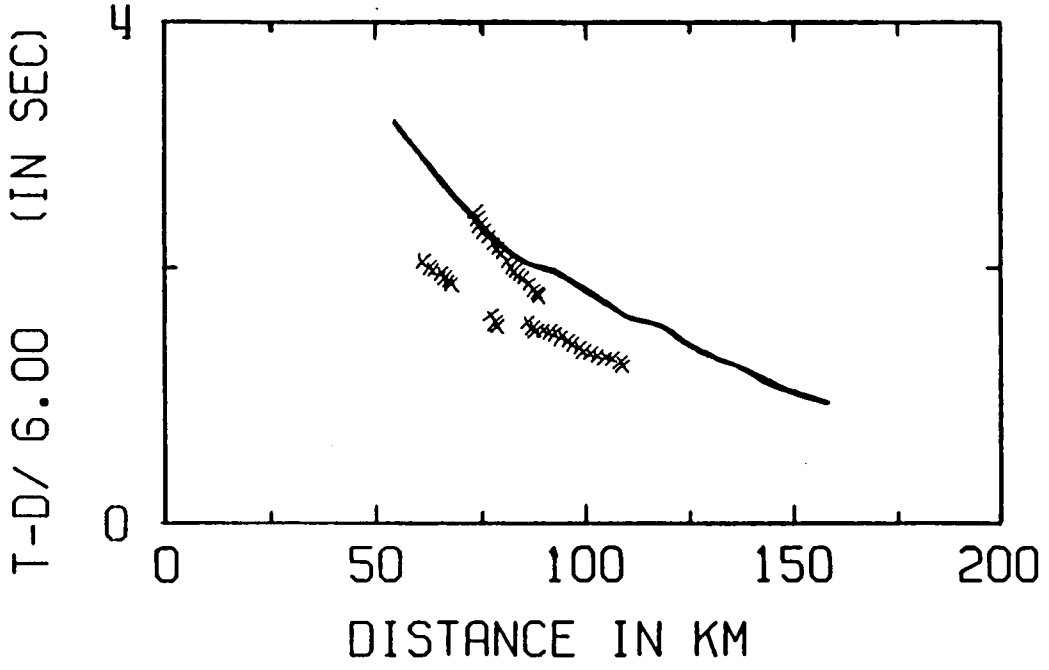

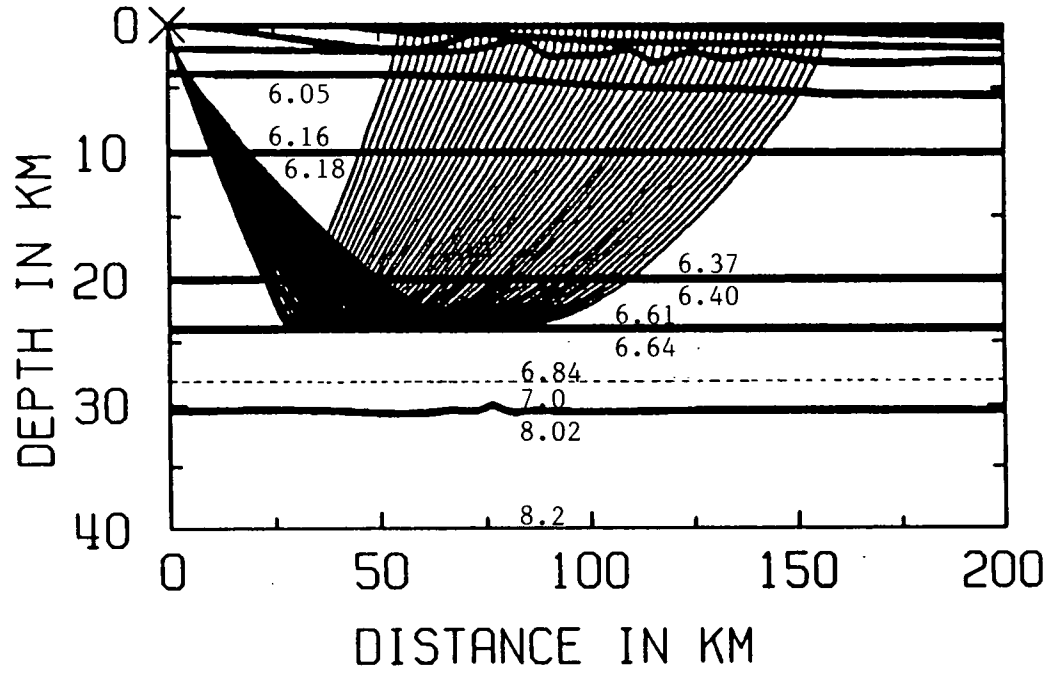

LINE1 S47 MID-CRUSTAL REFLECTORS

Fig. 6.39 BEAM87 ray diagram and travel times for a wide-angle reflection from within the lower crust (PbP) modelled at station 47. Continuous line: calculated travel time; crosses: observed travel times; numbers within model: seismic p-velocities in km s^{-1}.

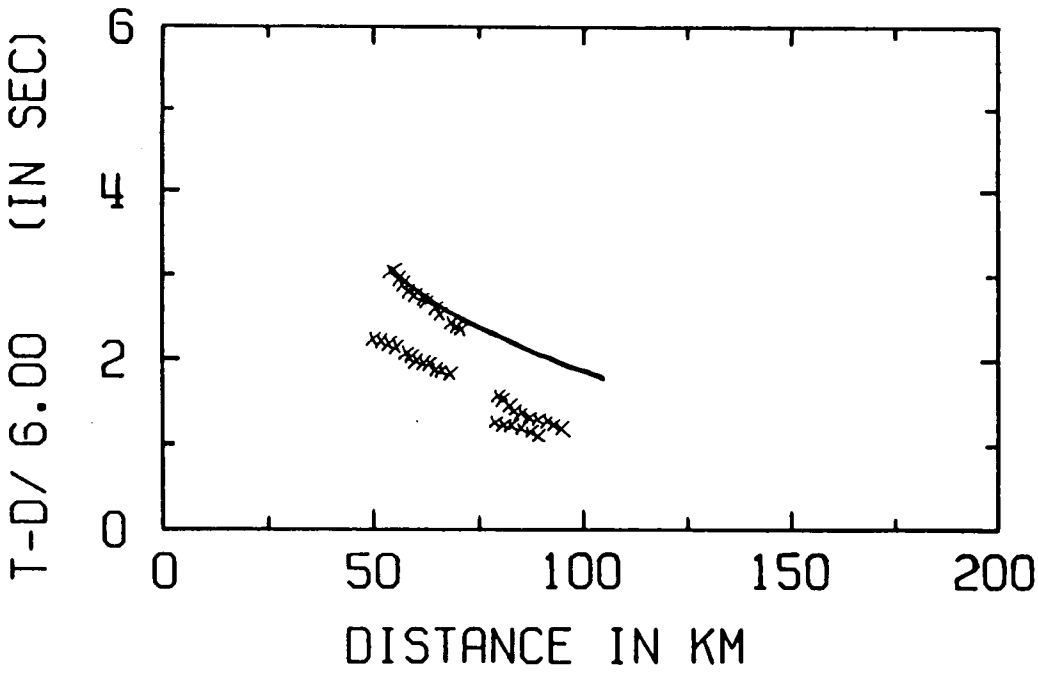

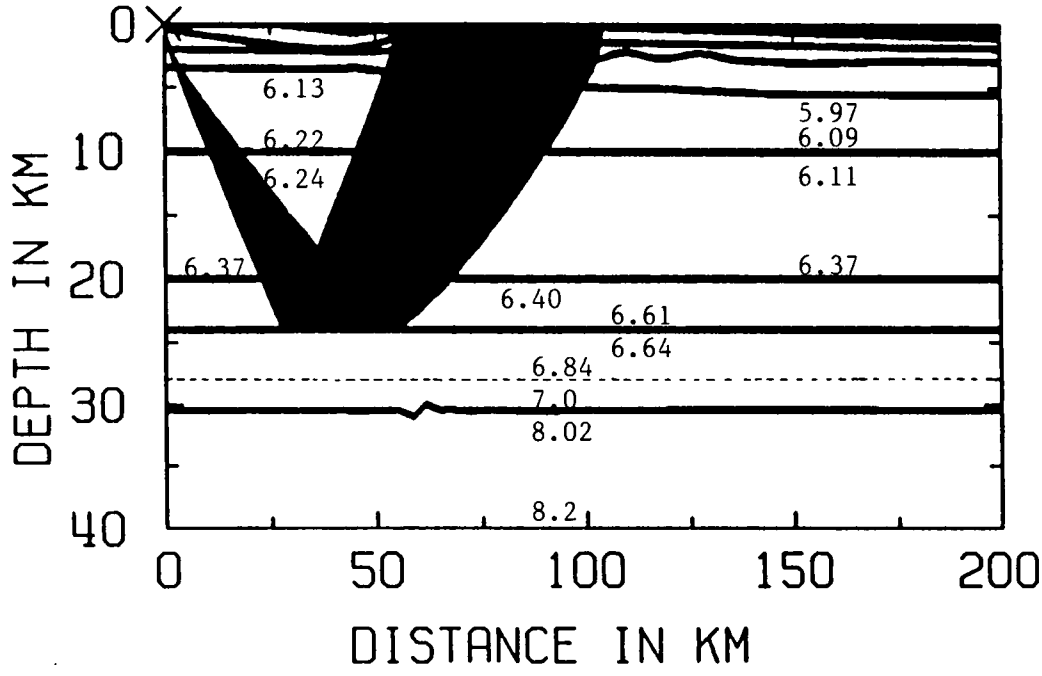

LINE1 S54 MID CRUSTAL REFLECTIONS

Fig. 6.40 BEAM87 ray diagram and travel times for a wide-angle reflection from within the lower crust (PbP) modelled at station 54. Continuous line: calculated travel time; crosses: observed travel times; numbers within model: seismic p-velocities in km s^{-1}. crust (PbP) modelled at station 54.

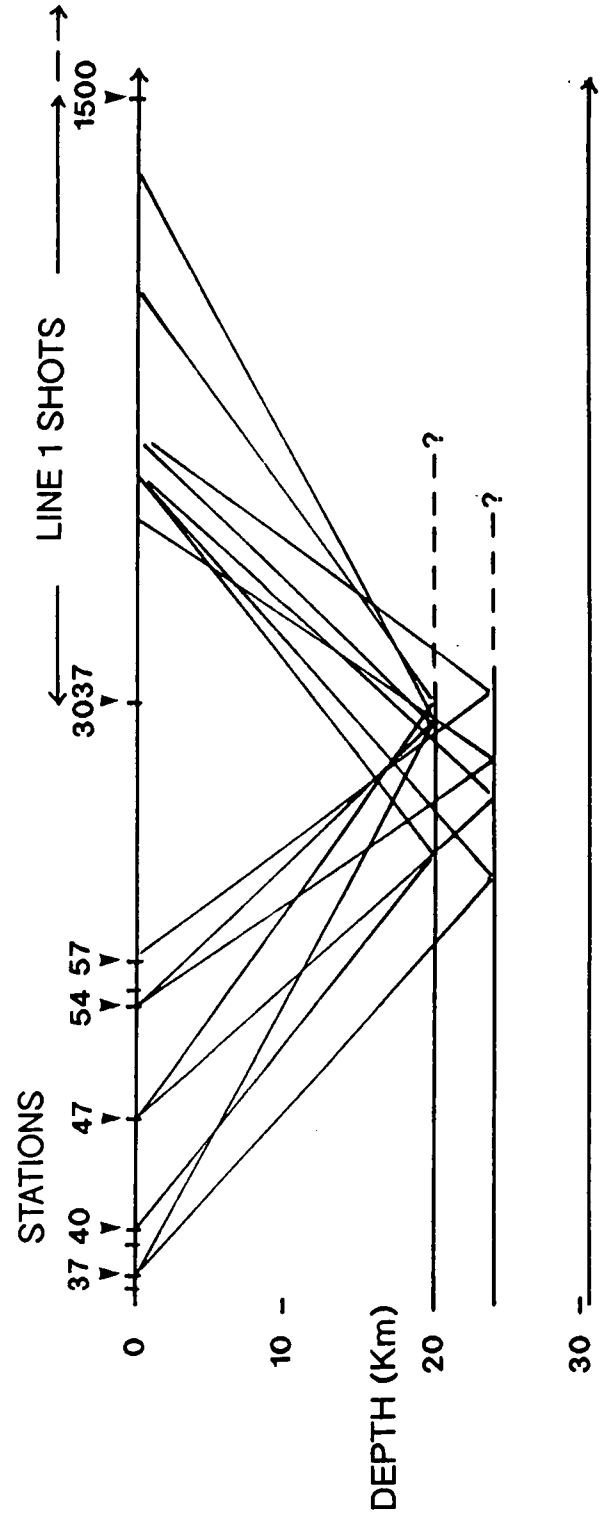

Fig. 6.41 Sketch of the lateral extent of the mid-crustal interfaces as flat reflectors.

reasonably close travel time fits for the interfaces at 20 km and 24 km depth, for the range of stations, produced **Fig. 6.41**. There seems to be evidence from this figure that the reflecting boundaries may be relatively flat out to approximately 50 km offshore, and that a change in slope may take place at this location. Further modelling could be undertaken in this area.

6.5 Modelling conclusions

The final wide-angle seismic model is shown in **Fig. 6.42** and the synthetic seismogram generated from it is shown in **Fig. 6.43**. Transparency (vi) is enclosed for comparison (although it is difficult to see the arrivals clearly on a section plotted at this density - see Appendix C for a clearer idea of the arrivals being compared). Up to 120 km offset, the synthetic of **Fig.6.43** shows Pg, PmP, D and the three mid-crustal reflections at the correct travel time and with a comparative amplitude similar to that of the real data. However, D still does not have sufficiently high amplitude, and Pg and the three mid-crustal reflections do not show the variation in amplitude that are observed on their real counterparts. Pn may be seen on the synthetic at offsets greater than 120 km, but PmP dies out before this offset, possibly due to the way that the model represents the decayed Moho step. On the whole, this is the best all-round model it has been possible to produce, given the limitations of the modelling package.

Although BEAM87 is the most versatile and robust package to use for the synthetic seismogram modelling, its weakness is highlighted by a study of this kind, namely the difficulty in accurately representing an unusual laterally varying model, although representation of the model is a problem for most seismic modelling packages. Persevering for longer with the bicubic spline representation of the velocity field could result in better synthetic computations which generate PmP east of the Moho step and Pn. Other areas where there is room for improvement include the fitting of mid-crustal reflections and attempting to fit the other arrivals on the records which are similar to D (mentioned in **section 4.4.4**), using all the record sections in the dataset.

The arrival D is without doubt the most interesting arrival seen on this dataset and the first arrival to be recognised as a type of diffraction on a wide-angle dataset. It also provides the first wide-angle

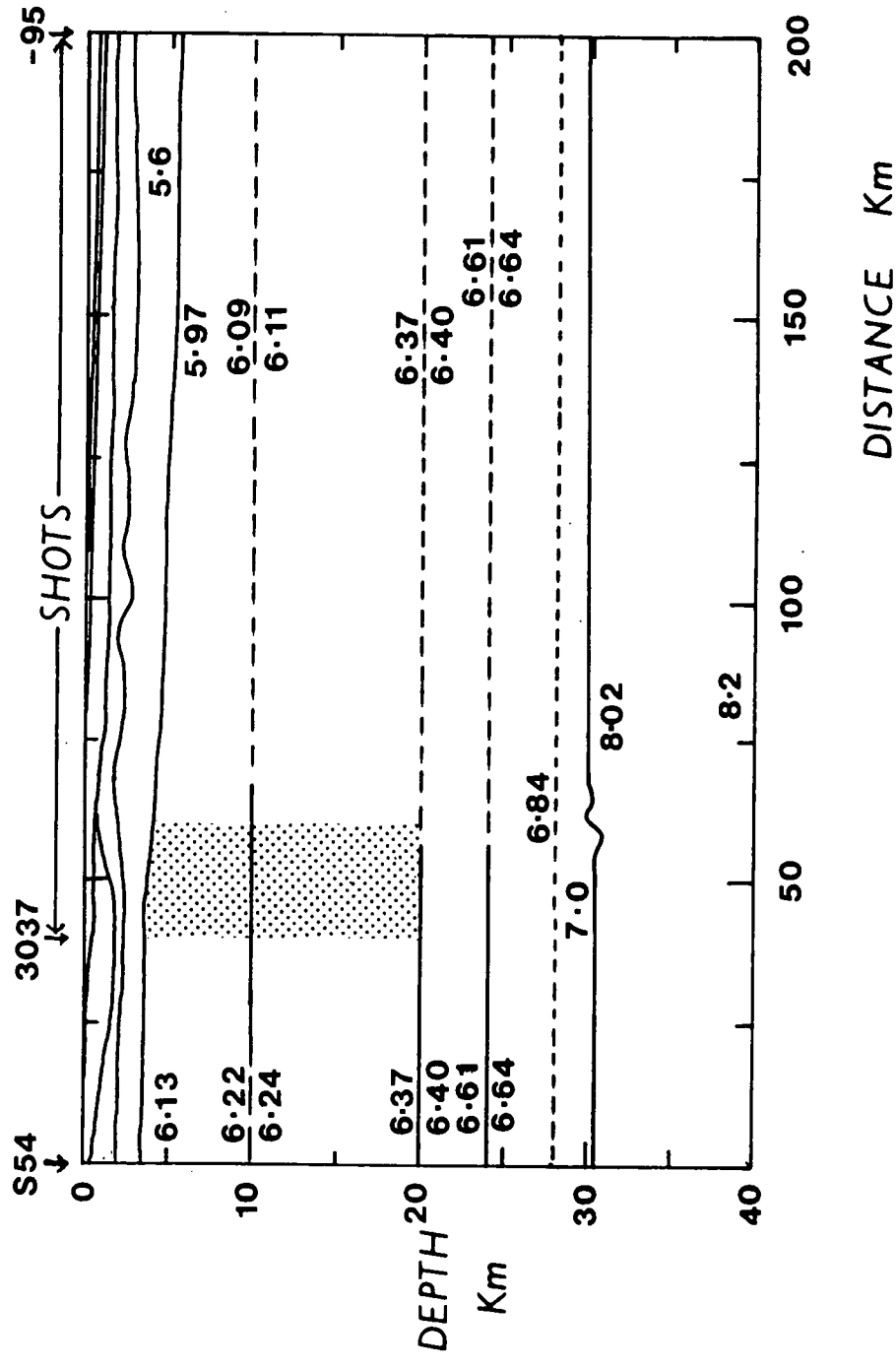

Fig. 6.42 Final wide-angle seismic velocity model. Stippled area represents the region of lateral change in velocity gradient.

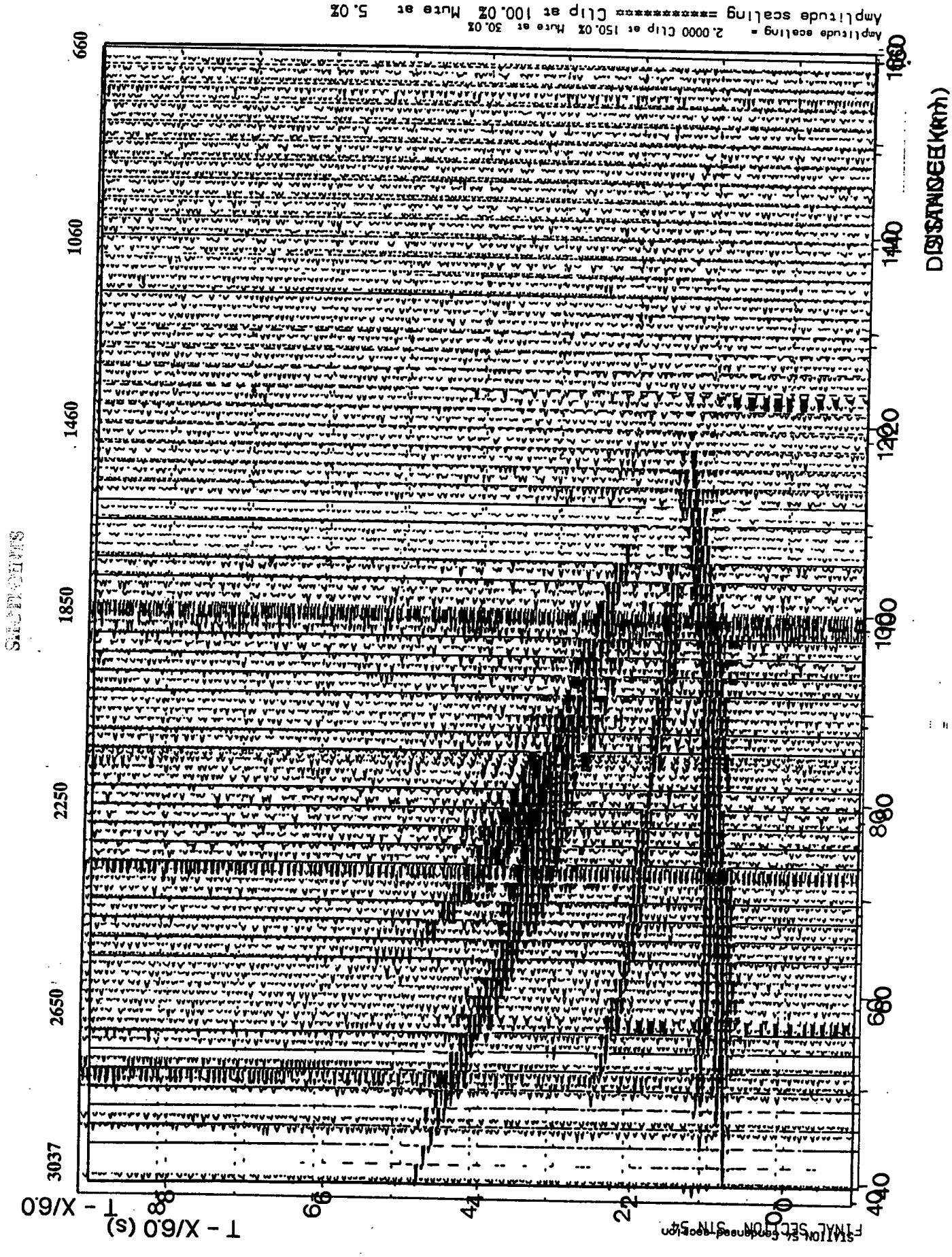

Fig. 6.43 BEAM87 synthetic seismogram generated from station 54 for the final wide-angle seismic velocity model of Fig. 6.42.

seismic support for **Kusznir & Matthews'(1988)** predicted result of the decay of a Moho step. Why it has such a high amplitude, particularly at station 54, is still not wholly understood. It may be related to the fact that it occurs near the critical region for station 54, or alternatively there may be some high-velocity material around it which focuses the rays returned to station 54. It certainly has important implications for the regional geological history of the area, which will be discussed in the next chapter.

CHAPTER 7: FURTHER INTERPRETATION AND DISCUSSION

7.1 Introduction

Having derived a seismic model purely from the wide-angle reflection MOBIL dataset, there remained a wealth of other geophysical information to be incorporated into a realistic geological model for this region, most significantly the exactly coincident BIRPS deep normal-incidence seismic records. The aim of using solely the wide-angle data up to this stage was to obtain an idea of the differences in the structures imaged by the wide-angle technique as compared to those imaged by the normal-incidence reflection technique. Further data collected during MOBIL includes the "fan-shoot" of Line 2 shots which were recorded at the MOBIL-CSSP stations (interpreted by **Jarvis (1988)**). **Section 7.2** consists of an interpretation of the normal incidence records and a comparison of the results with the wide-angle model.

Section 7.3 describes the gravity information from this area, mainly from CSSP and the UK gravity database. This information is tied into the seismic interpretation and a geological model proposed in **section 7.4.** Other geophysical information from this area includes the explosive shot records of CSSP which show not only P-waves but S-waves. The preliminary interpretation of this S-wave data is briefly described in **section 7.5.** The crustal composition is discussed in **section 7.6.**

7.2 BIRPS deep normal-incidence seismic data

7.2.1 MOBIL Line 1

Probably the first point which should be made about any comparison between the features seen on the wide-angle seismic data and those seen on the normal incidence records for line 1 is that only the structure west of shot point 1700 is imaged by actual wide-angle reflections. This is due to the geometry of the wide-angle recording set-up, in which the **mid-point** of the ray travelling from the furthest shot (-95) to the station closest to the coast lies beneath shot 1700. For the stations further inland, more of the crust beneath land is sampled and less of that beneath the normal-incidence profile. The most westerly

mid-point lies approximately beneath station 54, so the model obtained from all the wide-angle reflection data essentially has a lateral extent from station 54 to shotpoint 1700. This does not apply to results obtained from Pg or Pn, however, since these are refractions, not wide-angle reflections.

A line-drawing (courtesy of BIRPS) of the brute stack of the Line 1 normal-incidence seismic data is shown in **Fig. 7.1.** This diagram represents fairly well the relationships between the events imaged by the final stack normal-incidence section. Considering only the left-hand side of the section, up to the line 3 crossover, which corresponds to the crust imaged by MOBIL-CSSP recording, the main features may be summarised in the sketch of **Fig. 7.2,** which was made from the final stack section :

(a) The upper crust is typically (for a BIRPS section) transparent down to almost 4.5 s two-way travel time (TWTT), with the exception of a short, slight reflection at about 3.5 s TWTT.

(b) There seems to be a rather thick band of mid-crustal reflections west of about shotpoint 2750, a few sparse mid-crustal reflections eastward to about shotpoint 2200, then another wider band up to the intersection with line 3. This band extends from about 4.5 s TWTT to about 7 s TWTT at the western margin of the profile.

(c) The lower crust is relatively transparent up to shotpoint 2000, east of which there are several shallowly dipping reflectors. Beneath the line 2 intersection there appears to be a subhorizontal reflection at about 8-9 s TWTT, but apart from this there is little else to be seen within the lower crust in the region sampled by the wide-angle data.

(d) The Moho is defined very sharply by a bright reflection which appears to dip slightly to the west. At the western end of the line it has a TWTT of about 10.6 s, decreasing to almost 10 s at shotpoint 2200, east of which it is slightly disrupted, reappearing beneath the line 3 intersection at almost 11 s TWTT.

(e) Beneath the Moho reflection, west of shotpoint 2500, there are several very bright dipping reflections which merge into the Moho reflection.

These features correspond very well to those seen at wide-angle, some of them the more obvious for having previously carried out the wide-angle seismic interpretation. The lack of vertical reflections,

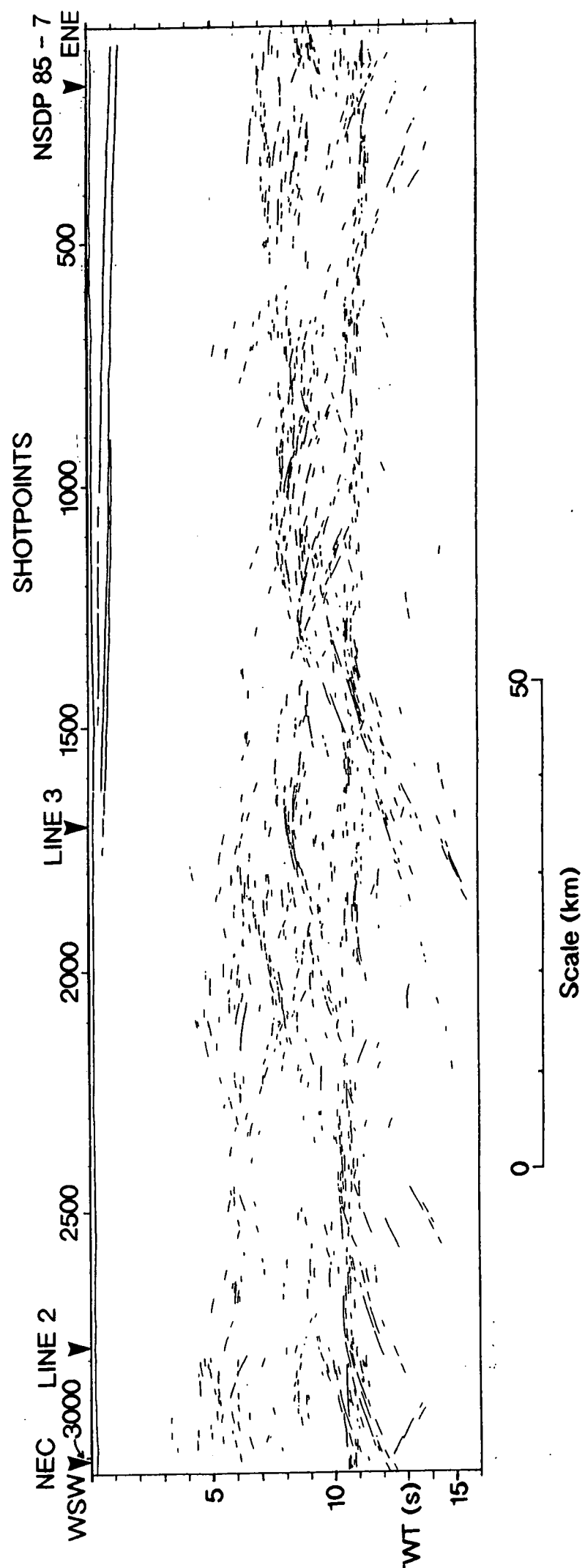

Fig. 7.1 Line drawing of brute stack normal-incidence section for MOBIL line 1 (courtesy of BIRPS).

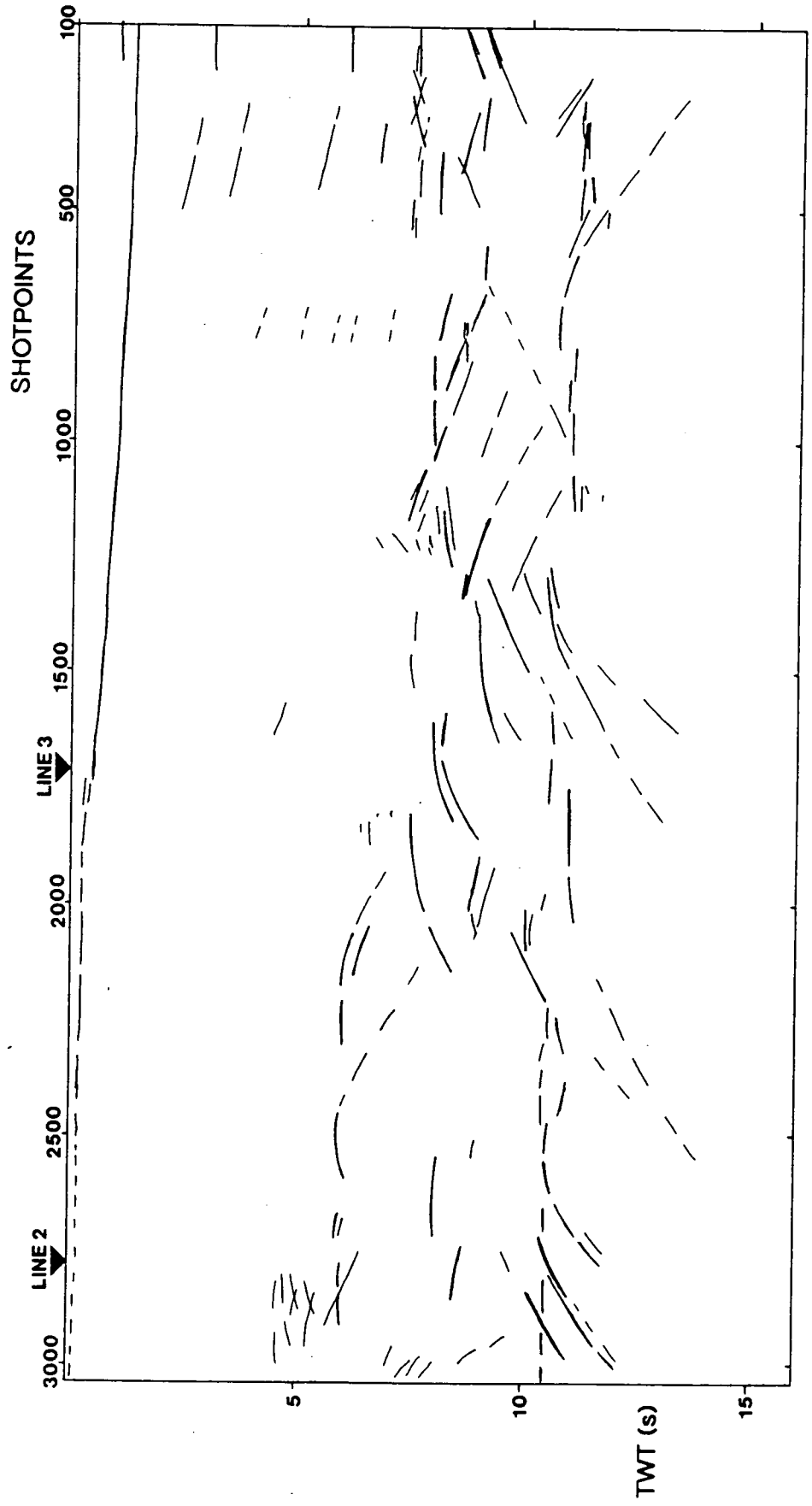

Fig. 7.2 Sketch of main features of MOBIL line 1 final stack normal-incidence section.

(a), from the upper crust is hardly surprising (remembering that shallow geological horizons are rarely well imaged, partly due to the acquisition parameters of BIRPS normal incidence data), but supports the wide-angle interpretation, which consists mostly of a steady velocity gradient beneath the crystalline basement.

However, the RMS velocity analysis used in the production of the final stack is of interest and is shown in **Fig. 7.3** (courtesy of Richard Hobbs), to compare loosely with the shallow velocity model obtained during the wide-angle MOBIL interpretation (**Fig. 6.5**). Most of the plot is taken up by the **shallow velocity structure**, since the low velocities close to the surface cause the velocity variation near the top of a normal-incidence section to vary slowly. This means that the shallow velocities may be picked very precisely, whereas with increasing depth, the velocities on the record sections vary more rapidly and therefore the resolution of deeper velocities is reduced (**Klemperer, 1989**). However, it may be seen from the figure that the overall velocity pattern of the near surface produced by the two different methods is rather similar.

The band of mid-crustal reflectors, (b) seen on the western side of the normal-incidence section may extend westward beneath the coast, in which case it ties in well with the many observed wide-angle reflections seen from about this depth on the MOBIL-CSSP data, which merge into the upper crustal refraction, Pg. The base of this band seems to be at about 7 s TWTT beneath shot 3037. This approximately coincides with the estimated TWTT (7.2 s) for the change in velocity gradient and slight velocity contrast at about 20 km depth seen in the wide-angle model. It does not reflect strongly at normal-incidence since it is primarily a change in the velocity gradient. The fact that this band also thins east of shotpoint 2750 is interesting, since it ties in well with the lateral change in crustal velocity structure seen by the wide-angle data. The "re-thickening" again east of shotpoint 2200 does not have an obvious representation on the MOBIL-CSSP data but this may be due to the fact that the wide-angle data quality for this offset (beyond 160 km) is slightly deteriorated.

The transparent lower crust, (c), in this region was anticipated, since it was a distinguishing feature on BIRPS NEC where it crossed this point (**Freeman et al., 1988**). The bright Moho reflection at the base of it, (d), is also a hallmark of this "terrane type" as defined by Freeman et al. from the NEC

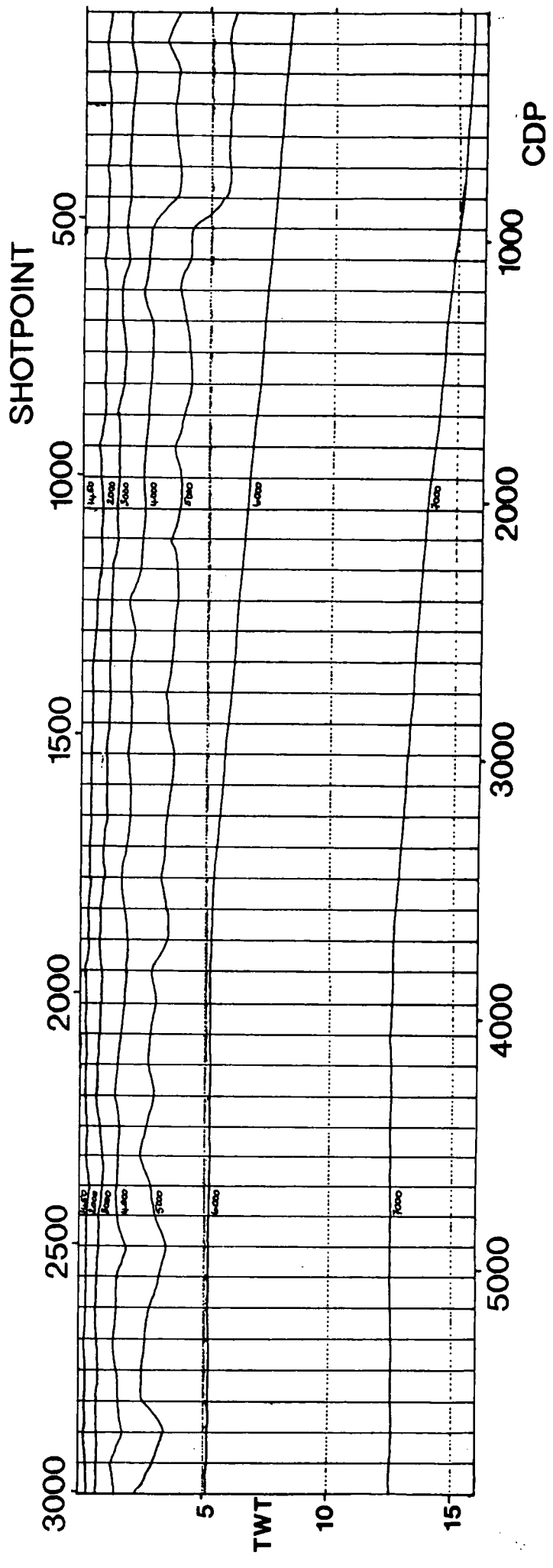

Fig. 7.3

RMS velocity analysis for line 1 final stack normal-incidence section (courtesy of BIRPS). Figures within layers represent p-velocities in ms^{-1}.

profile. The slightly dipping lower crustal reflection seen at about 8.5 s TWTT would seem to be the 24 km deep interface in the wide-angle model, which would be expected to have a TWTT of 8.8 s. The 7.0 kms^{-1} velocity required to fit the wide-angle Moho reflection travel times (which would have an estimated TWTT of approximately. 10.3 s) does not appear to have a normal-incidence signature. It does not produce wide-angle reflections either, which suggests that the velocity increase to 7.0 kms^{-1} is gradational.

The estimated Moho TWTT from the wide-angle model beneath shotpoint 3037 is approximately. 10.8 s, which approximately coincides with the observed normal-incidence TWTT, so it would seem that the "refraction" and "reflection" Mohos are coincident for this crustal type. The fact that the Moho appears to shallow slightly to the east supports the CSSP and the MOBIL wide-angle interpretations of a slightly shallowing Moho, but there does not seem to be any offset on the boundary which would correspond to the step interpretation of MOBIL-CSSP.

However, it turns out that the dipping reflectors mentioned in (e) and described as "dipping diffraction tails" by **Blundell et al. (1990)**, migrate into the base of the crust. These must be the normal-incidence equivalent to D and are also likely to be more complex than straightforward diffractions. **Fig. 7.4** shows this part of the normal-incidence section after migration (**courtesy of Richard Hobbs**) in order to attempt to clarify the shape of the structure which causes the arrivals. The result seems to be a zone of westerly-dipping, slightly concave-upwards surfaces which disrupt the Moho slightly, with only a slight change in TWTT across the zone. This image differs considerably from the wide-angle step model, which produces most seismic energy as reflections from the top, convex-upward part of the step, but looks like several cases of the "decayed" step modelled at wide-angle (**Fig. 6.32**). On **Fig. 7.4**, most of the normal-incidence reflection energy seems to be derived from the concave upward parts of the reflectors, whereas at wide-angle (**Fig. 7.5**), considerable energy is also reflected from the convex-upward part of the structure.

East of shotpoint 2000, where the structure is less well imaged by the wide-angle recording (and not at all east of shot 1700), the normal-incidence section becomes more complex. This is due to the presence of many multiples from the eastward-thickening sedimentary sequence throughout the upper

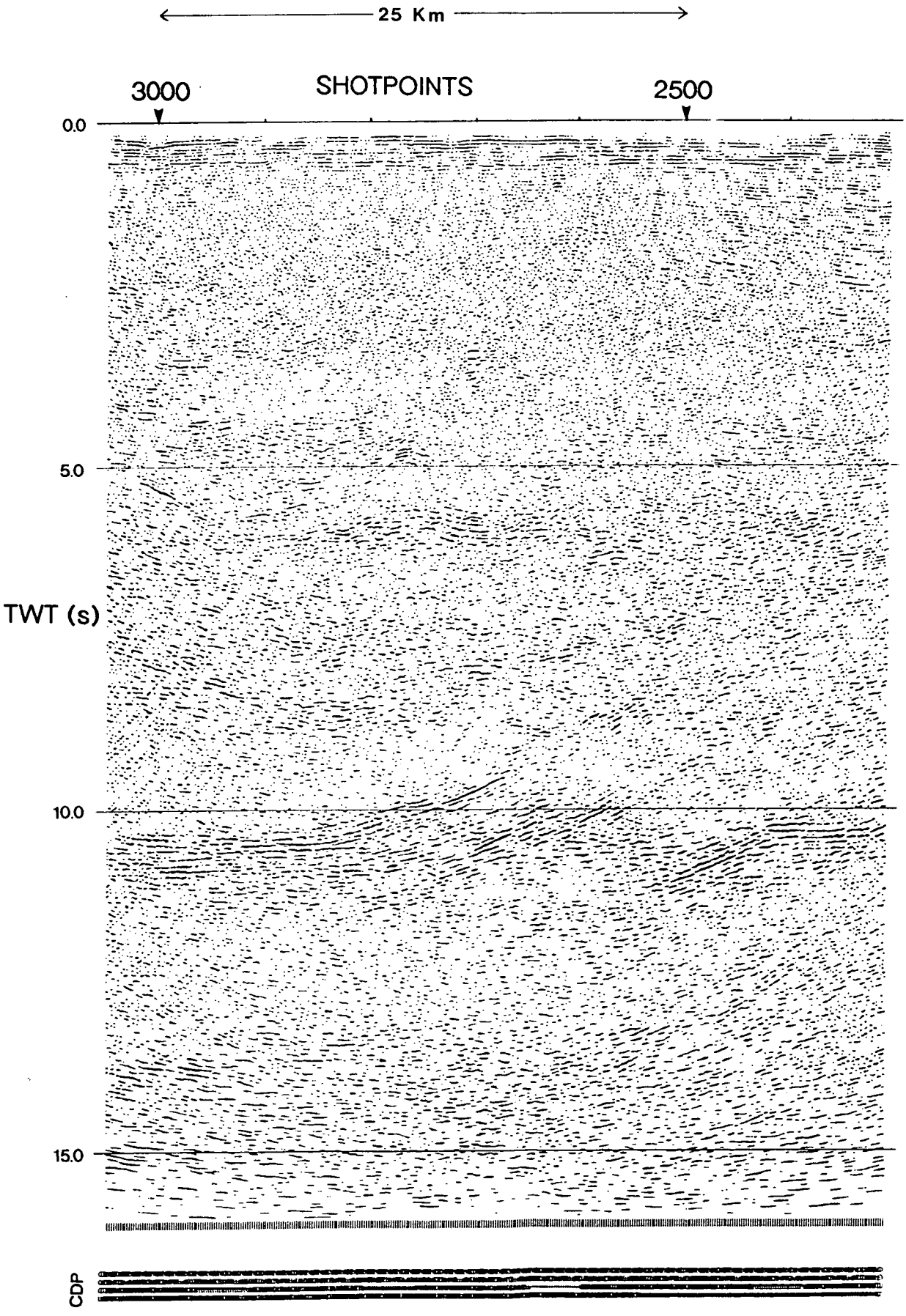

Fig. 7.4 Migrated normal-incidence section from line 1, for velocity 5.5 kms^{-1} (courtesy of Richard Hobbs, BIRPS).

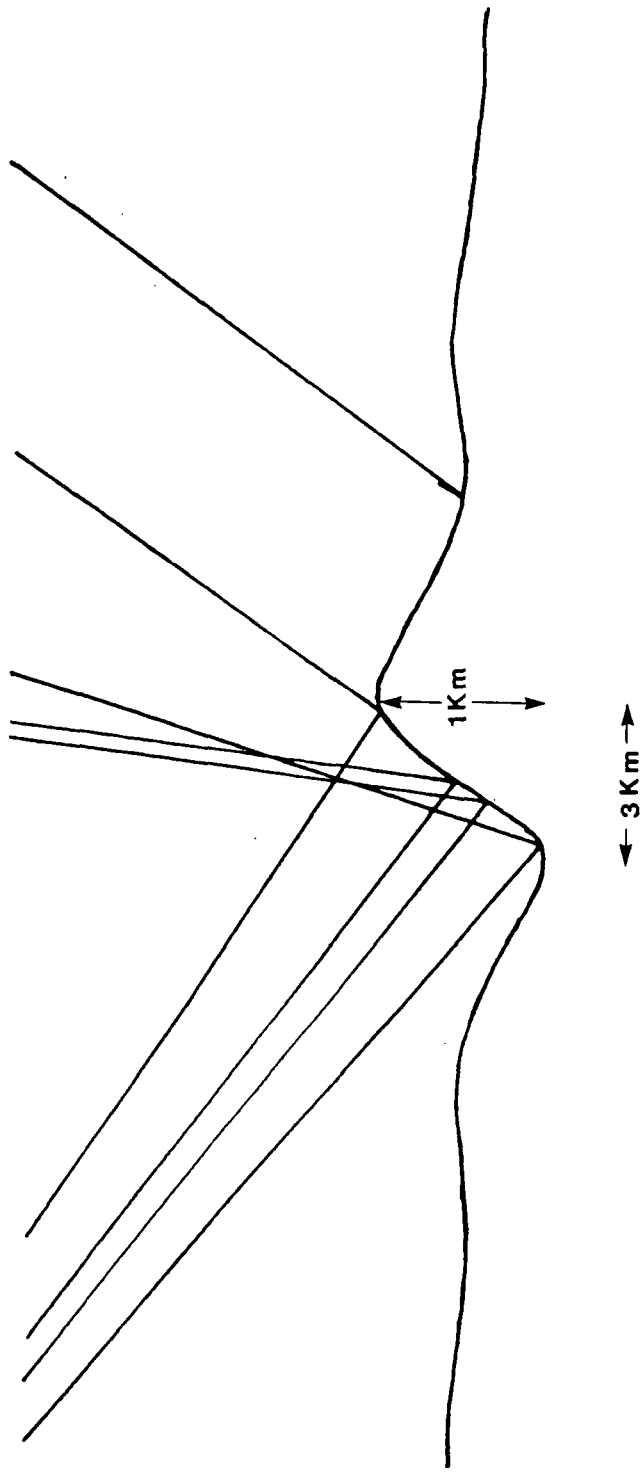

Fig. 7.5 Blown-up drawing of "decayed" Moho step modelled at wide-angle.

crust and the increased reflectivity of the lower crust. The mid-crustal band of reflections seen on the section west of shotpoint 1700 seems to practically disappear to the east. Several prominent dipping reflections are visible, cutting through the lower crust, dipping to the west (west of shotpoint 1300) and to the east (east of shotpoint 1300). Some of these appear to penetrate the Moho (beneath shotpoints 1400 and 550) although they probably migrate into the base of the crust.

The normal-incidence record section is certain to contain some seismic energy from structures out of the plane of the profile, especially from complicated features such as D. A full interpretation of this normal-incidence section must therefore incorporate a full study of lines 2 and 3, in order to obtain a three-dimensional picture of the crustal structure. The next section briefly describes the normal-incidence data collected perpendicular to line 1, in order to put the line 1 model into its crustal context.

7.2.2 NEC and MOBIL Lines 2 and 3

MOBIL lines 2 and 3 were specifically planned to resolve some of the questions raised by the BIRPS NEC profile, particularly with regard to the lower crustal dipping reflection, which is believed to represent the remnant of the Iapetus Suture. The two profiles were shot 11 km (line 2) and 65 km (line 3) northeast of, and parallel to, the location of NEC. All three of these "dip sections", lines 2, 3 and NEC, crossed line 1, which is essentially a "strike section".

Figs. 7.6, 7.7 and **7.8** show BIRPS line drawings of NEC, line 2 and line 3 respectively. It can be seen that in the region of line 1, they each show similar structural features projected along strike: transparent upper crust (with the exception of NEC, on which Freeman et al. have labelled a slightly dipping reflector T which crosses the line 1 profile at about 3.5 s TWTT) and four different types of lower crustal patterns possibly corresponding to different crustal terranes.

The region of lower crust crossed by line 1 is particularly distinct, bounded to the north by the bright, dipping lower crustal reflector identified as the Iapetus Suture, to the south by a distinct change in reflectivity, and underneath by a bright reflection Moho. On the line 2 and NEC sections, reflections beneath the Moho are also visible. After study of line 1 normal-incidence and wide-angle records, these now appear to be out-of-plane reflections from the feature which gives rise to D on the wide-angle

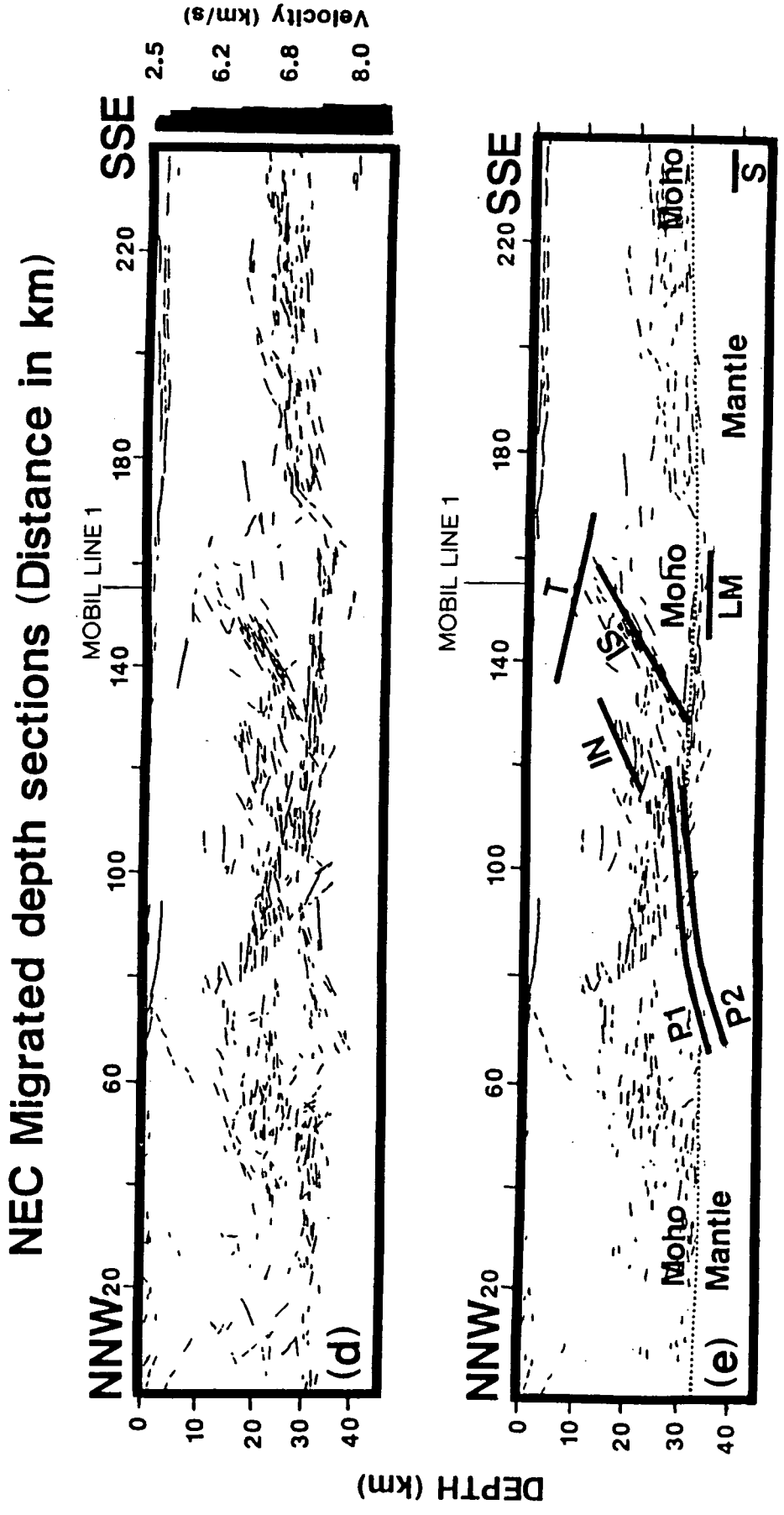

Fig. 7.6 Migrated line drawing of BIRPS NEC normal-incidence profile. From Freeman et al.(1988).

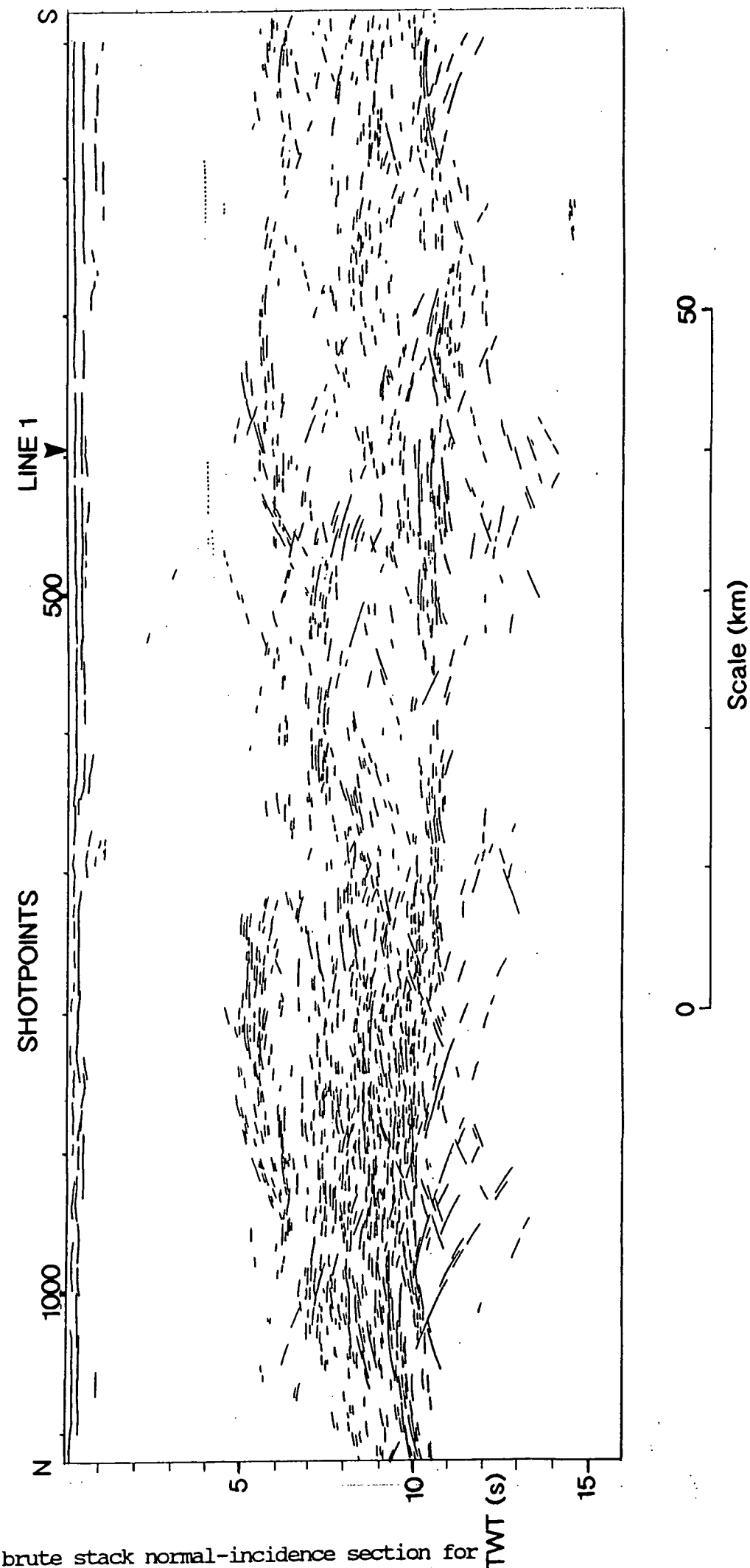

Fig. 7.7

Line drawing of brute stack normal-incidence section for MOBIL line 2 (courtesy of BIRPS), in the region of the intersection with line 1.

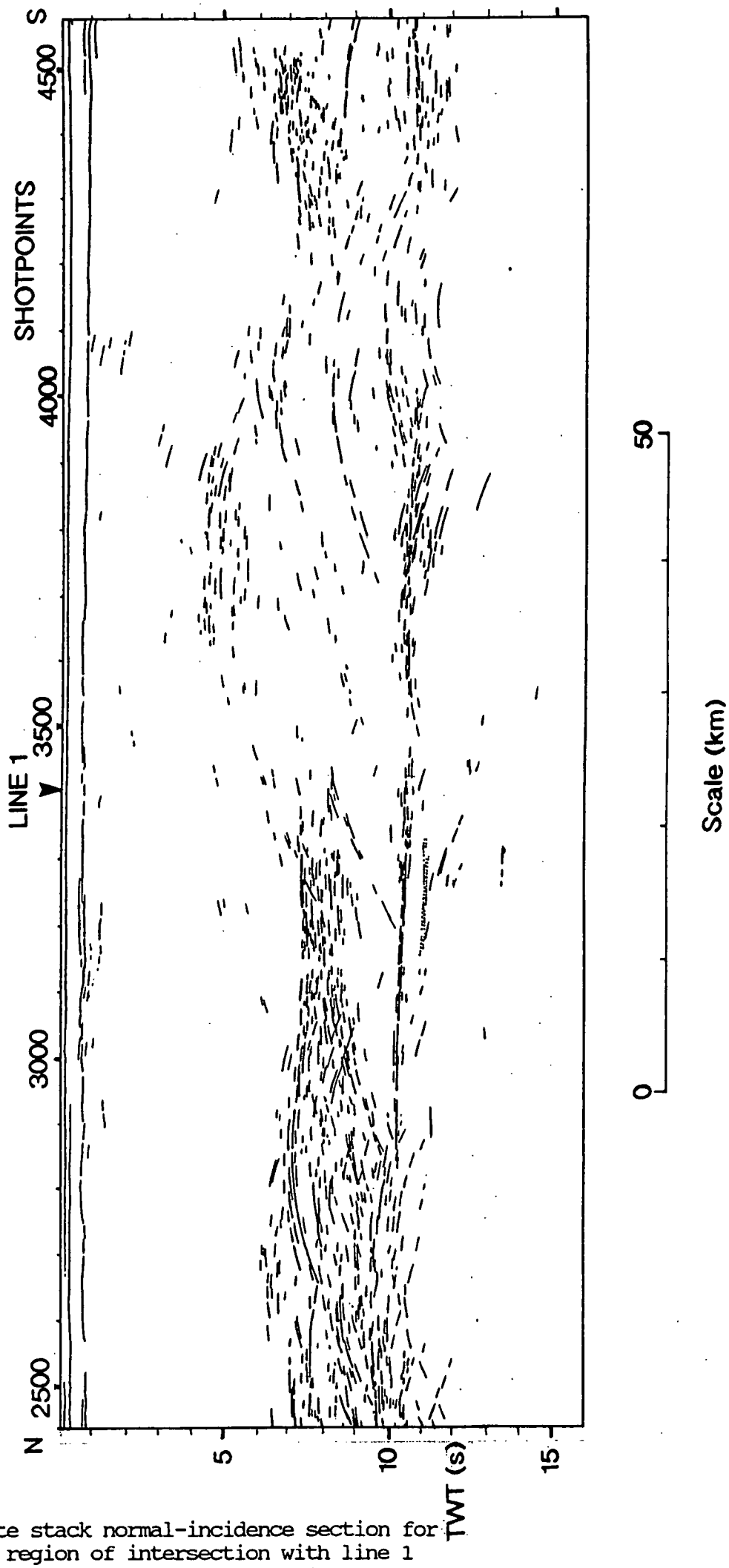

Fig. 7.8

Line drawing of brute stack normal-incidence section for MOBIL line 3 in the region of intersection with line 1 (courtesy of BIRPS).

data and the strong dipping reflectors beneath the Moho on line 1 normal-incidence data. The location of these arrivals on lines 1 and 2 indicate a NNW-SSE orientation of the Moho "step". Line 2 again shows mid-crustal reflections between 4.5 and 7 s TWTT but also shows more normal-incidence reflections apparently within the lower crust, although some may be out-of-plane effects. The 24 km interface seems to be imaged again at almost 9 s TWTT.

The main difference between the profiles which affects the observations on line 1 is that the transparent wedge beneath the lower crustal dipping reflector lies deeper within the lower crust further east, as seen on line 3. The top of the dipping reflector flattens out at about 8 s TWTT on line 3, at which point line 1 intersects, whereas it merges into the band of mid-crustal reflectors at about 7 s TWTT on NEC, which is also where it intersects line 1.

From the tie-in with lines 2 and 3, it would appear that the base of the band of mid-crustal reflectors observed on line 1 corresponds to the "Iapetus Suture" observed on these strike lines. Since this increases in depth eastward, it is evident that the Suture dips not only to the northwest (the direction of lines 2, 3 and NEC) but also slightly east-north-east along line 1. It probably intersects line 1 some way east of the line 3 intersection, giving rise to one of the easterly-dipping lower crustal reflectors.

7.2.3 MOBIL Line 2 wide-angle recording

As described in Chapter 2, the seismic wide-angle recording in Northumberland (MOBIL-CSSP) was carried out for lines 2 and 3, in addition to line 1. The records for line 1 are excellent out to almost 200 km offset from the land stations, so those recorded from the shots of lines 2 and 3 would be expected to be almost as good, if complicated more by the greater lateral variation in crustal geology. They should also provide wide-angle seismic sections perpendicular to line 1 and therefore more three-dimensional coverage. In the event, the accurate shot times for line 3 were lost, the only remaining times being to the nearest second. This would make attempted playout of the line 3 wide-angle records impractical although the results would have been of great interest, since the mid-points of the seismic rays from these shots must lie beneath the BIRPS normal-incidence profile NEC.

However, the shot times of line 2 were recorded accurately, enabling playout of the wide-angle

recordings by the author and their preliminary interpretation and modelling by Eric Jarvis (**Jarvis, 1988**). The geometry of the profile, a "fan shoot", is rather unusual and interpretation was not so straightforward as an in-line profile. A map of the shot and station locations may be seen in **Fig. 7.9**, illustrating the "bottoming" points of seismic rays travelling from the shots to the land recording stations, and a variable area common station section of the data for station 47 is shown in **Fig. 7.10**. The phases Pg, PcP, PmP and D, as identified by Jarvis, are labelled. A larger plot of a window of this data, over the area where lines 1 and 2 intersect (plotted in the same format as the line 1 sections), is to be found in Appendix C.

The method used by Jarvis for the interpretation was to extrapolate northwards the current one-dimensional model generated for line 1 and to calculate "travel time residuals" for the main phases Pg, PcP and PmP. That is, for a particular phase, he calculated the difference in travel time between that calculated from the extrapolated model and the observed data. The most important results of his interpretation are summarised below:

(a) Pg is delayed north of a point 90 km from station 54 (100 km from 47), which Jarvis suggests corresponds to the change in surface geology from Carboniferous to Silurian strata 5-15km south of the Southern Uplands Fault. The delay in Pg is attributed to a change in P-velocity across the fault rather than a deeper basement (**Hall et al. 1983, Bamford et al. 1979**).

(b) PcP is significantly delayed north of shot 900 (at station 54 and 47) probably due to the same cause as the delay on Pg. These rays have their mid-point at the approximate location of the "Iapetus Suture", which suggests that there is a possible associated change in upper crustal geology. This also corresponds to a change in lower crustal reflectivity as seen on the BIRPS normal-incidence records at around shot point 900. However, this does not seem to affect PmP.

(c) PmP travel times are negatively delayed immediately to the north of line 1, which suggests either a shallowing of the Moho northwards or an increase in lower crustal velocity, either of which corresponds to the observed shallowing of the Moho on the normal-incidence line 2 record sections.

These observed features of the line 2 data apply only to the region north of the line 1 intersection, lying approximately beneath the coastline. Study of the records at the intersection with line 1 enabled a comparison of common arrivals to both sets of seismic records. It is possible to correlate Pg, PcP, PmP

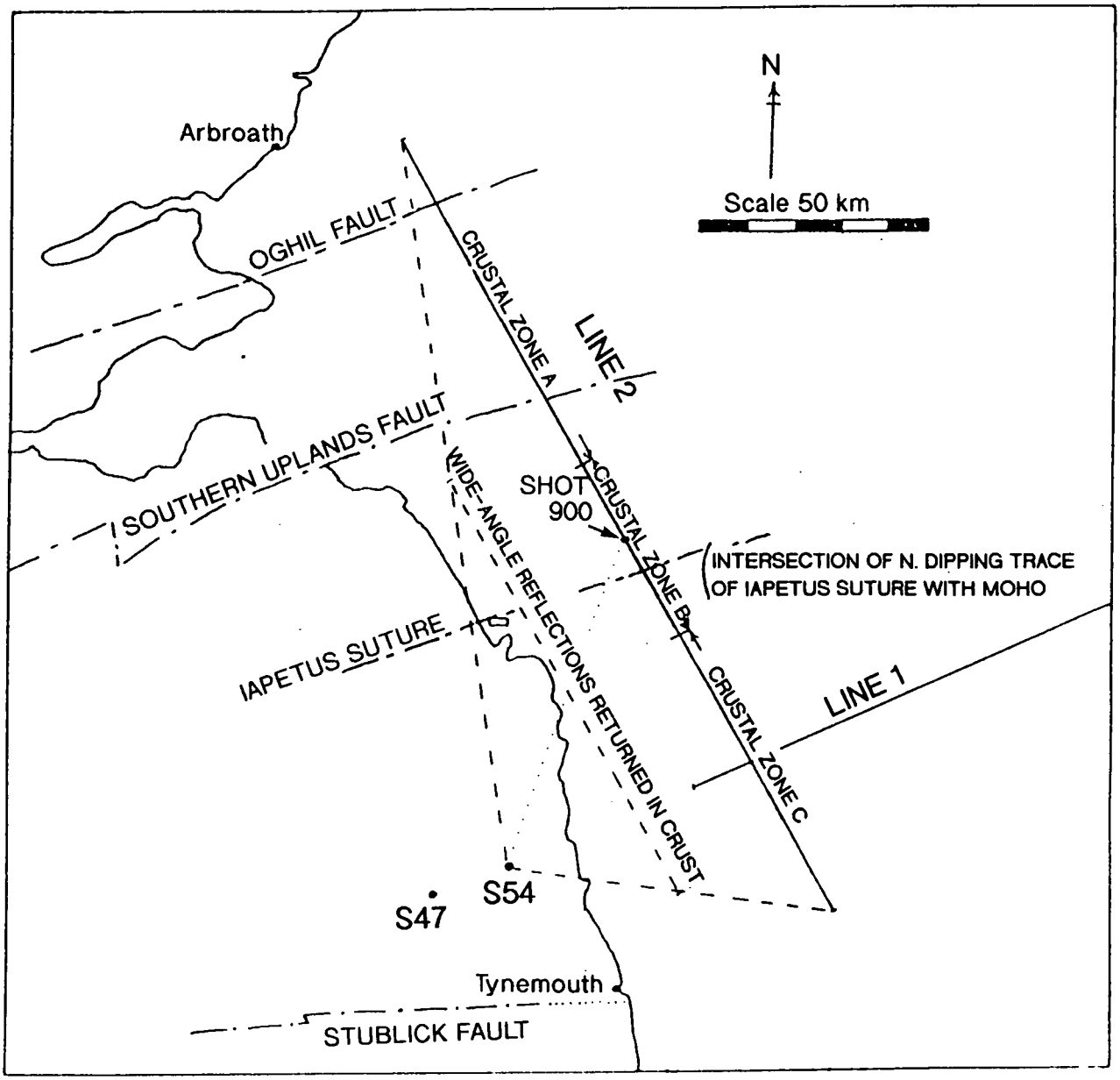

Fig. 7.9 Map showing location of MOBIL line 2 with respect to land recording stations, showing mid points for wide-angle seismic reflections. From Jarvis(1988).

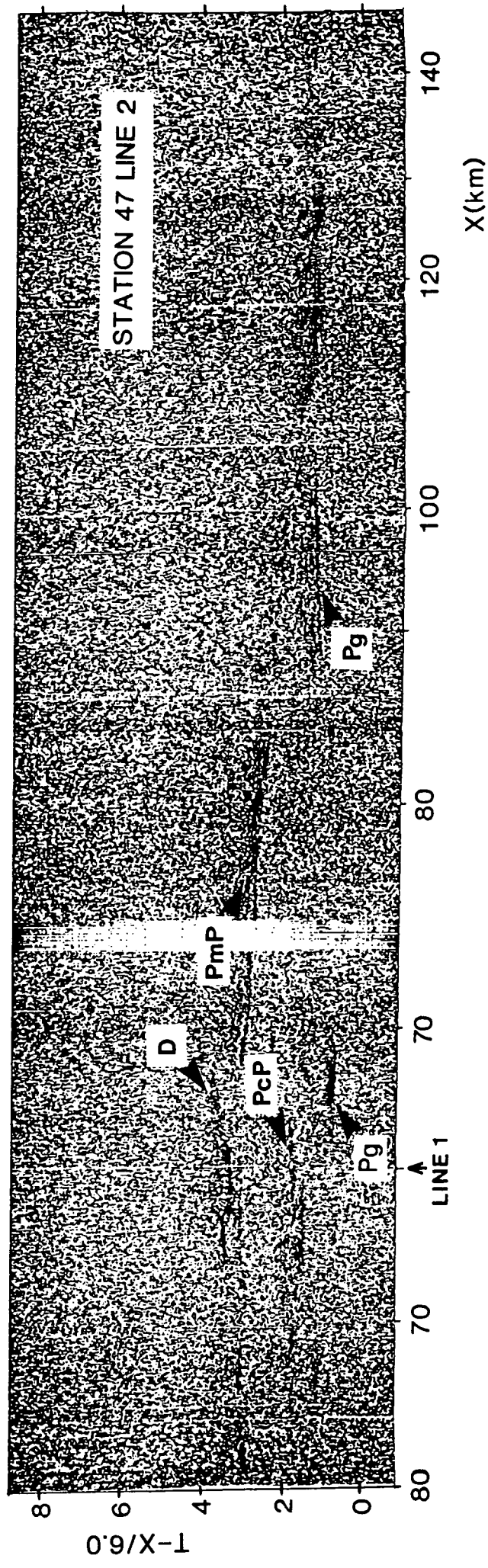

Fig. 7.10 Record section of wide-angle seismic reflection data from line 2 shots for station 47. A window of this data over the region of intersection with line 1 is contained in Appendix C, plotted in the same way as line 1 record sections.

and D from line 1 to line 2. It was this initial correlation which first revealed that the cause of the 1 s "time delay" on line 1 records was due to a jump in the shot times given out by the ship's clock.

The presence of D on the line 2 wide-angle records is interesting, since it shows that it has an effect in the plane perpendicular to that of line 1. Its appearance (see **Fig. 7.10,** also the section in Appendix C) is obviously rather different - it does not fully merge with PmP, and with increasing offset (away from the minimum offset of line 2) it diverges away from the PmP arrival. This is the sort of behaviour which would be expected of a diffraction or an out-of-plane dipping reflector. This arrival corresponds to the "sub-Moho" normal-incidence reflections (which are out-of plane reflections or diffractions from the "step") of the BIRPS line 2 data and NEC. The point at which this feature has a minimum on line 2 lies just south of the intersection of line 1. This therefore provides further information about the feature D out of the plane of line 1.

7.2.4 Discussion

The overall picture of the crust obtained from the deep normal-incidence profiles, with velocity information from the wide-angle data, is displayed in **Fig. 7.11**. The logical conclusion from comparison of the normal-incidence and wide-angle data is that the wedge of transparent crust beneath the normal-incidence "Suture" corresponds to the high velocity gradient imaged by the wide-angle data and that the mid-crustal wide-angle reflections which merge into Pg are in fact reflections from the top of the dipping slab which constitutes the "Iapetus Suture".

However, the feature which gives rise to "diffraction type" seismic arrivals at both normal-incidence and at wide-angle is without doubt the most interesting discovery of this study. Its migrated appearance at normal-incidence, seen in **Fig. 7.4**, shows that there is more than one case of the "decayed" step which seems to satisfy the modelling of the arrival D at wide-angle. As previously described, it appears to be made up of several concave-upward reflectors over a horizontal distance of about 10 km. The other wide-angle "diffraction-type" arrivals which merge into PmP on line 1 records, particularly on records from stations 54 and 47, are probably also imaging this region of disruption of the Moho. The fact that this disruption occurs in the vicinity of the lateral change in upper crustal velocity gradient and where there is also a visible change in mid-crustal reflectivity at normal-incidence implies

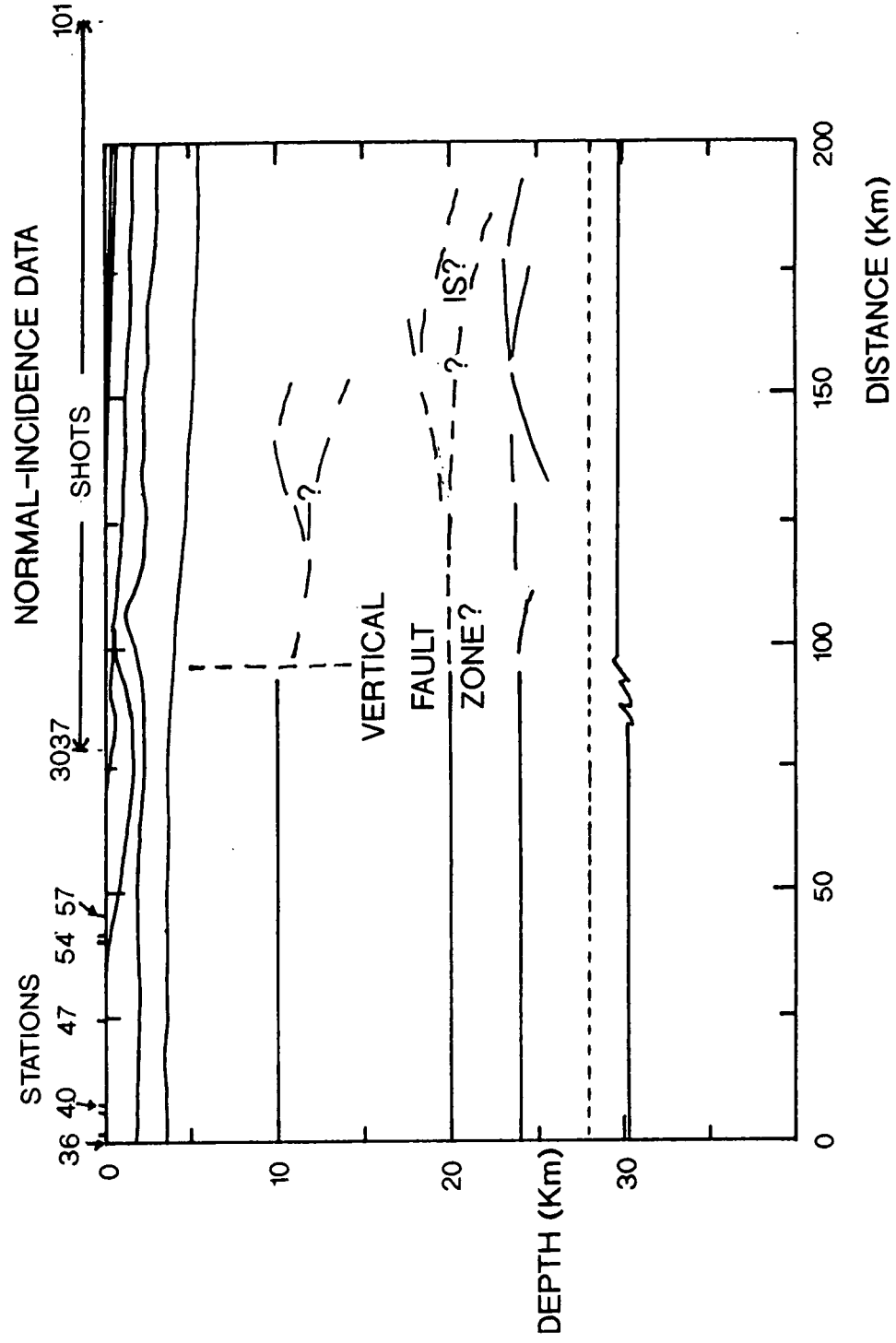

Fig. 7.11 Sketch of seismic structure beneath line 1 from combined normal-incidence and wide-angle seismic data.

that it may be connected with a deep, crust-penetrating fault. This is supported by the observation of D on line 2 wide-angle data, at a point slightly south of its intersection with line 1. This proposed fault will be discussed further in **section 7.4.**

7.3 Gravity interpretation

The application in recent years of image processing techniques to the analysis of potential field data has led to the use of colour and shaded-relief images of the onshore gravity and aeromagnetic datasets for Great Britain. These images highlight structural trends and lineaments which were not obvious on standard contour maps. **Lee et al. (1990)** have used such images to study some of the most important structural features of central Britain, including the Iapetus Suture.

However, the Suture seems to have no well-defined gravity or magnetic signature - this is hardly surprising since the only remnant seems to be the deeply buried dipping slab imaged by the BIRPS normal-incidence records, which is covered by weakly magnetic Silurian and Upper Palaeozoic sediments. The western end of the Solway Line runs between two parallel magnetic highs which may represent separate crustal blocks, but these anomalies fade towards North-East England leaving a fairly unremarkable image of the area in which the MOBIL-CSSP recording was carried out.

Also, the offshore coverage is much poorer, and such images of the North Sea gravity and aeromagnetic field would hardly be likely to be widely available anyway, but they would provide some valuable insights into the structural detail offshore. **Donato et al. (1983)** interpreted gravity anomalies in the region of this study, indicating the presence of granite bodies beneath the Mid North Sea High. **Powell (1983)** described the free air profile collected from the 1982 CSSP cruise in the North Sea and **Lewis (1986)** carried out gravity modelling of the Bouguer anomaly along the CSSP line in his interpretation of the CSSP explosive experiment, starting with the seismic model. No gravity modelling has been undertaken in the course of this study, although the information from gravity, particularly about the densities of the layers, identified so far by their seismic velocities, is of great value in forming a geological model. A qualitative description of the gravity information therefore follows.

The Bouguer gravity contour map for the area crossed by the CSSP, and the Bouguer anomaly profile along MOBIL-CSSP line 1 are shown in **Fig. 7.12**. Concentrating on the information for the area crossed by the MOBIL programme, the main features of the profile (**Fig. 7.12(b)**) are:

(a) The apparent regional trend of the Bouguer anomaly, which decreases eastward towards the coast, increases by about 8 mgal over a distance of about 40 km and then decreases eastward again;

(b) A negative gravity anomaly of about 5 mgal amplitude, occurring in the region of the coast;

(c) A positive anomaly of about 10 mgal amplitude, which appears at about 40 km offshore;

(d) A negative anomaly of about 10 mgal towards the eastern end of the profile.

Lewis'(1986) gravity model, pictured in **Fig. 7.13**, fits the overall gravity effect satisfactorily: the onshore trend, **(a)**, decreasing towards the coast, may be explained by the increasing thickness of Carboniferous sediment in the Northumberland Trough, whilst that offshore seems likely to correspond to the thickening Tertiary sedimentary sequence of the North Sea. The MOBIL wide-angle model incorporates an increasing depth to crystalline basement which will also contribute to this effect. The negative anomaly at the eastern end of the profile, **(d)**, has been modelled (Donato et al., 1983) as an off-line granite mass within the basement.

However, the model does not fully explain the features **(b)** and **(c)**, whose short wavelengths (similar to **(d)**) suggest that they are caused by relatively shallow structures. The most plausible explanation of **(b)** would seem to be that it is caused by the local Carboniferous syncline which can be seen in the shallow velocity structure of **Fig. 6.5**.

It is interesting to note that **(c)** arises close to the location of the "Moho step" and the lateral change in upper crustal velocity gradient in the MOBIL model. This is superimposed on the long-wavelength regional increase **(a)** and both may be related to the proposed fault. Using the slab formula to obtain a rough idea of the effect of a Moho step of 1 km, an increase of approximately 8 mgal would be expected over the region of the step, as a long wavelength feature of the profile. The regional anomaly **(a)** could therefore support a decrease in Moho depth across this region of the order of 1 km.

Acting against this long wavelength anomaly is the effect **(b)** of the Upper Carboniferous syncline

(a)

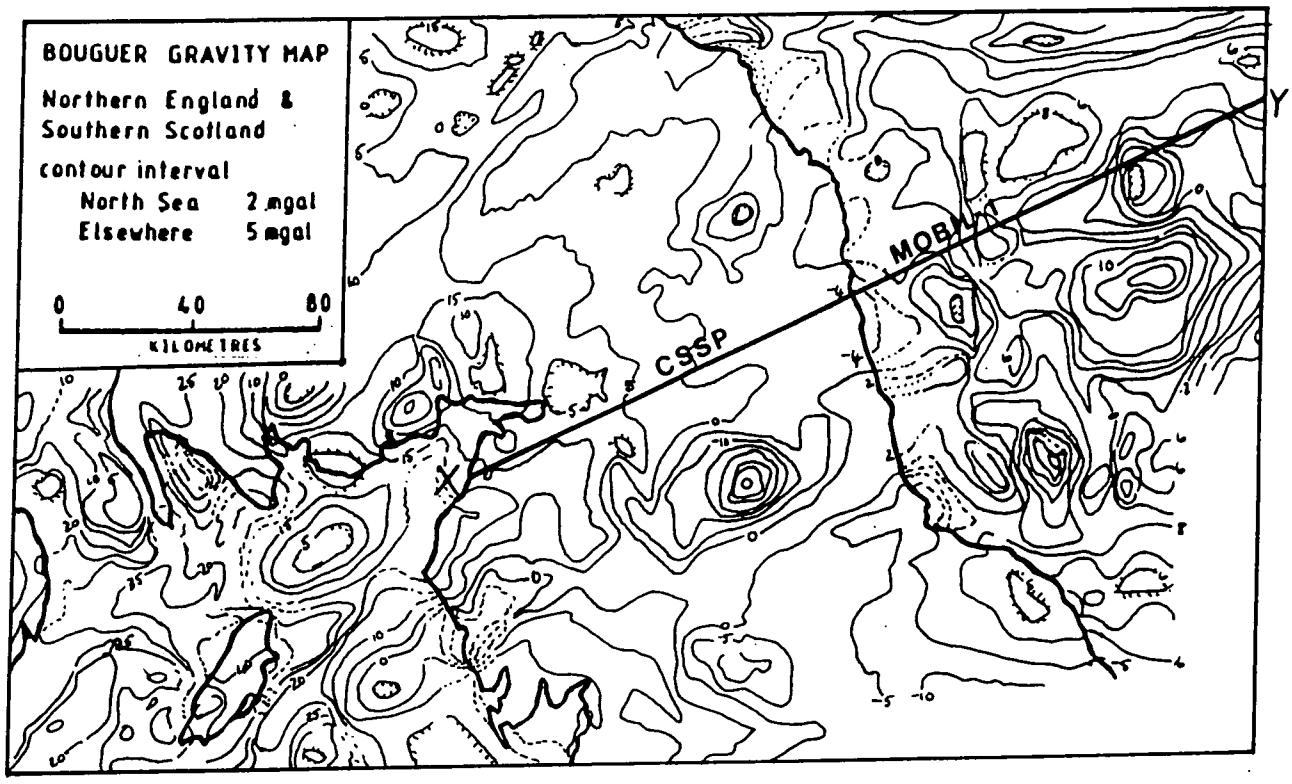

(b)

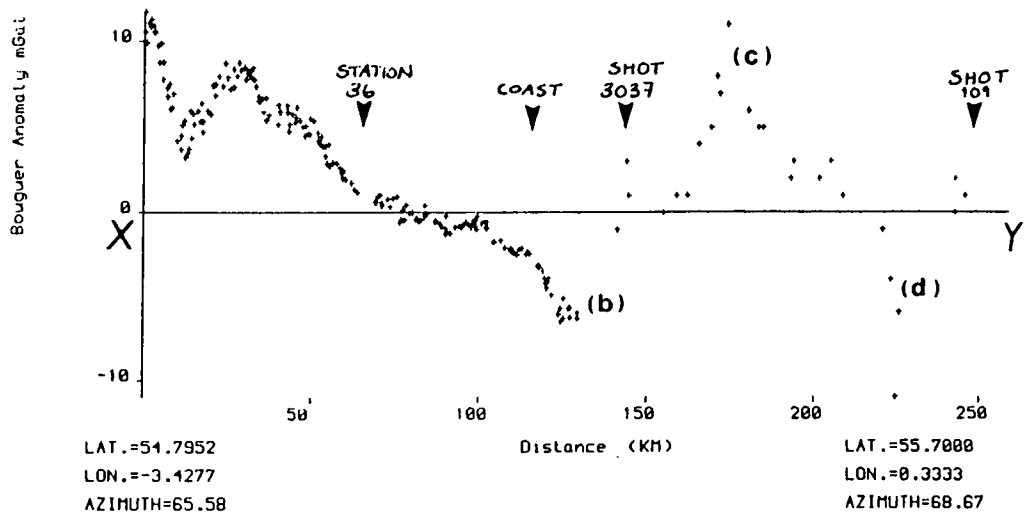

Fig. 7.12 (a) Bouguer anomaly contour map for Northern England showing location of MOBIL line 1 and CSSP recording stations (from Green, 1984).
(b) Bouguer anomaly profile along section X-Y (courtesy of Richard Woollett).

just offshore, but then adding to it is the effect of the lateral termination of the syncline against the Lower Carboniferous. This event may be sharper than it is represented in the seismic model, so it is very likely that feature (c) on the Bouguer gravity corresponds to this. The shape of the gravity profile between 150 and 200 km is therefore a combination of the effect of the Moho step, the Upper Carboniferous syncline and its truncation against the Mid North Sea High.

The Bouguer contour map (**Fig. 7.12(a)**) shows at this location an apparent North-South lineament, also noticed by **Smith and Taylor (1989)**. If this may be explained at its occurrence on the MOBIL profile by the Moho step and lateral changes above it, then this must be what is happening along the length of the lineament, which must therefore be a fault. The significant geological implications of this model, discussed in the next section, would justify more detailed modelling of the Bouguer gravity in any further work on this interpretation.

7.4 Structural interpretation

The two most important structural features imaged by the MOBIL survey, and by the wide-angle data of line 1 in particular, are the lateral change in upper crustal velocity gradient and the proposed steps of the Moho, both approximately 50 km offshore. These seem to be due to the same feature, a crust-cutting fault, which would appear from the location of the velocity change above the "step" to be vertical. The observations of D on line 2 records and of a lineament in the Bouguer gravity field have reinforced this interpretation.

The vertical nature of the fault and the apparent lack of any vertical offset across the mid-crustal velocity change suggest a wrench fault, in preference to normal or thrust faulting. The orientation, perpendicular to Caledonian strike, reduces the possibility of it being related to the "Iapetus Suture" and this location should be sufficiently distant from the central North Sea basin to rule out the likelihood of it being an extension-related structure. A possible explanation seems to be that it is a wrench fault related to the strike-slip environment which occurred further south in the Sole Pit region of the Southern North Sea Basin.

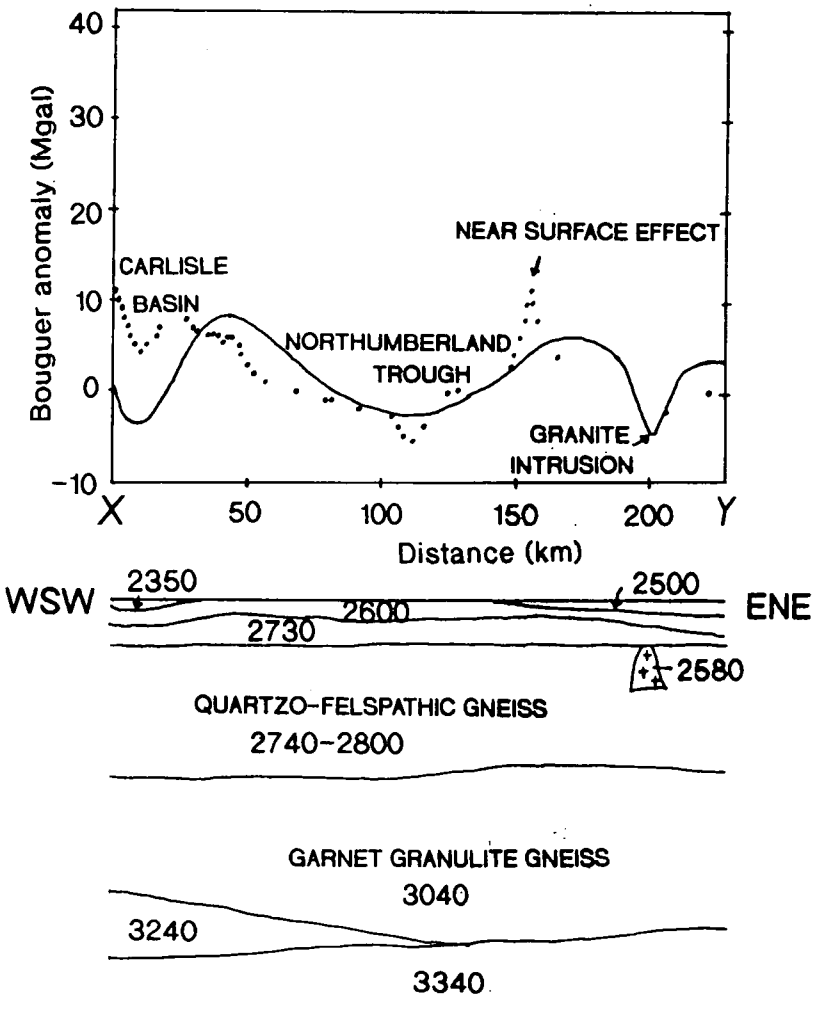

Fig. 7.13 Model obtained by Lewis (1986) by modelling the Bouguer anomaly along the CSSP profile (see Fig. 1.9 for location). Numbers within model layers represent densities in kg m^{-3}.

This idea is supported by the fact that **Matthews (1989)** has modelled a very similar "Moho step" from the MOBIL wide-angle data recorded at Market Weighton from line 5. This step occurs at the location of the Dowsing Fault zone, with which the geological history of the Sole Pit is closely associated **(Van Hoorn, 1987)**. Since the location of the Dowsing Fault is poorly known north of Flamborough Head, where an offshoot of it runs ashore, it may be possible that the crustal change observed on MOBIL line 1 is caused by the northward extension of this or a similar sub-parallel fault.

On the basis of this, **Fig. 7.14** shows the proposed location of the fault, from all the geophysical evidence described so far, and in agreement with the proposed fault of **Smith and Taylor (1989)** (see also **Fig. 1.7**). If this is the Dowsing Fault, it seems to run through the Mid-North Sea High as far as the Forth Approaches basin.

The Dowsing Fault Zone is known to have played several roles during its history, in tensional, transpressional and transtensional senses **(Van Hoorn, 1987)**. Although little is known of the Carboniferous development in the region of lines 4 and 5, **Donato and Megson (1990)** report that the lower Carboniferous was a period of fault-controlled subsidence for both the Sole Pit Trough and the Cleveland basin, affected by a granite buried beneath the East Midland Shelf. Like the Northumberland Trough **(Fraser and Gawthorpe,1990)**, these basins were inverted at the end of the Carboniferous due the effect of the Variscan orogeny to the south **(Glennie and Boegner, 1981)**. If, as suggested here from the geophysical evidence, the Dowsing Fault Zone continues up to the Mid North Sea High, the tectonic histories of the Northumberland Trough, the Mid-North Sea High (which was also uplifted at the end of the Carboniferous), the Cleveland basin and the Sole Pit Trough must have been linked by this major crustal fault.

Since the Carboniferous,the Dowsing Fault zone is believed to have been reactivated during the Late Cretaceous and Mid Tertiary, when it is thought to have been most active **(Van Hoorn, 1987)**. If this is when a step (or series of steps, as seen on the normal-incidence data) was created, it would be expected to decay considerably over geological time. The seismic model generated from this study seems to show that this is exactly what has been observed, vindicating the **Kusznir and Matthews (1988)** model of the decay of Moho topography. It would therefore seem that the MOBIL wide-angle data has

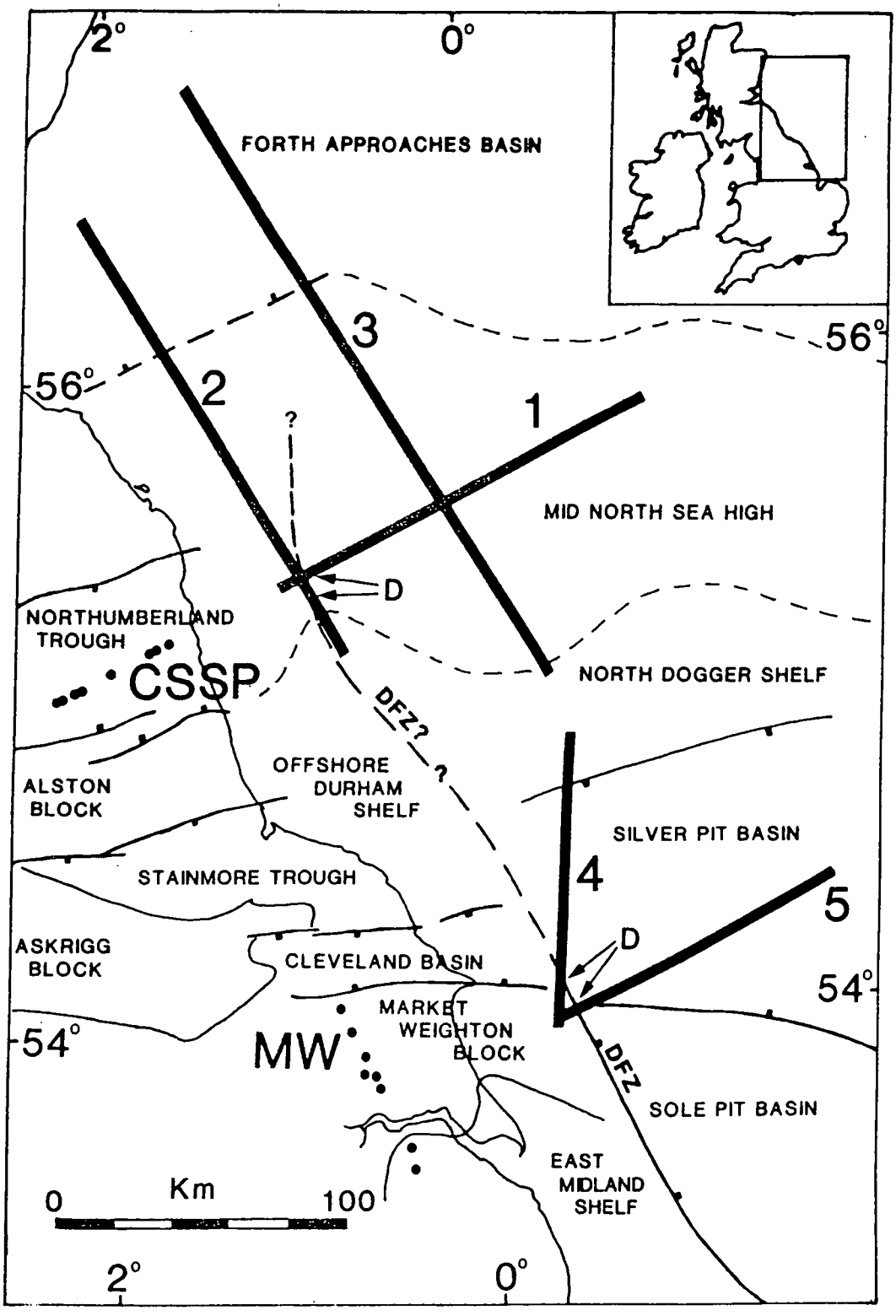

Fig. 7.14 Map of the geological structures of North-East England and the adjacent region of the North Sea, with the MOBIL normal-incidence and wide-angle reflection profiles superimposed. This shows the suggested northward continuation of the Dowsing Fault Zone (DFZ) to the Mid North Sea High. Onshore geology from Fraser and Gawthorpe (1990); Offshore geology (except the DFZ extension) from Glennie (1986). D shows the location of the observed wide-angle and normal-incidence seismic arrival from a step on the Moho.

revealed a significant geological feature of this area.

7.5 Complementary CSSP (1982) S-wave data

Although the explosive CSSP **P-wave** wide-angle seismic data may have been superseded by the MOBIL wide-angle data, no evidence for **S-wave** arrivals is seen on the MOBIL records, in spite of playing out the records to 30 s reduced travel time. Airguns are obviously unable to generate S-waves and conversions of reasonable amplitude are absent in this locality. By contrast, the CSSP sea-bottom explosive shots generated excellent shear waves, presumably by conversion at the sea-bottom refractor or at a deeper interface. A record section from station 36 of the original CSSP is shown in **Fig. 7.15** to illustrate the SV phases which were observed on record sections from vertical seismometers.

Some preliminary synthetic seismogram modelling of the SV-wave data from CSSP was carried out using **Lewis' (1986)** P-wave CSSP model as a starting point. The result obtained was that although upper crustal rocks seemed to fit a standard Poisson's ratio of 0.25, the SmS phase (the S-wave wide-angle reflection from the Moho) was fitted considerably better by a Poisson's ratio of the order 0.30. **Fig. 7.16** is a synthetic section for the same station as the real data section of **Fig. 7.15**, showing a good travel time fit and reasonable amplitude fit for the SmS phase.

This result has yet to be verified by further work, but it has interesting implications. Interpretation of similar S-wave refraction data from south-west Germany **(Gajewski et al. 1987)** has identified two different types of lower crust. Type I, found under the Black Forest and the Urach geothermal anomaly, has a high Poisson's ratio of 0.28-0.3, a high P-velocity of 6.6-6.8 kms^{-1} and prominent layering (as imaged at normal-incidence). It returns a mid-crustal reflector from 14-16 km depth, and is therefore slightly thicker than type II, which returns a mid-crustal reflector from 18-21 km depth. Type II has a lower P-velocity, 6.3-6.4 kms^{-1}, a Poisson's ratio of 0.25-0.26, and is less laminated. It is found under the larger part of southwest Germany which is covered by Triassic sedimentation.

Insufficient work has been done on the CSSP explosive S-wave data to be able to say whether the crust beneath this region is similarly divided into different types defined by P- and S-velocity, but the

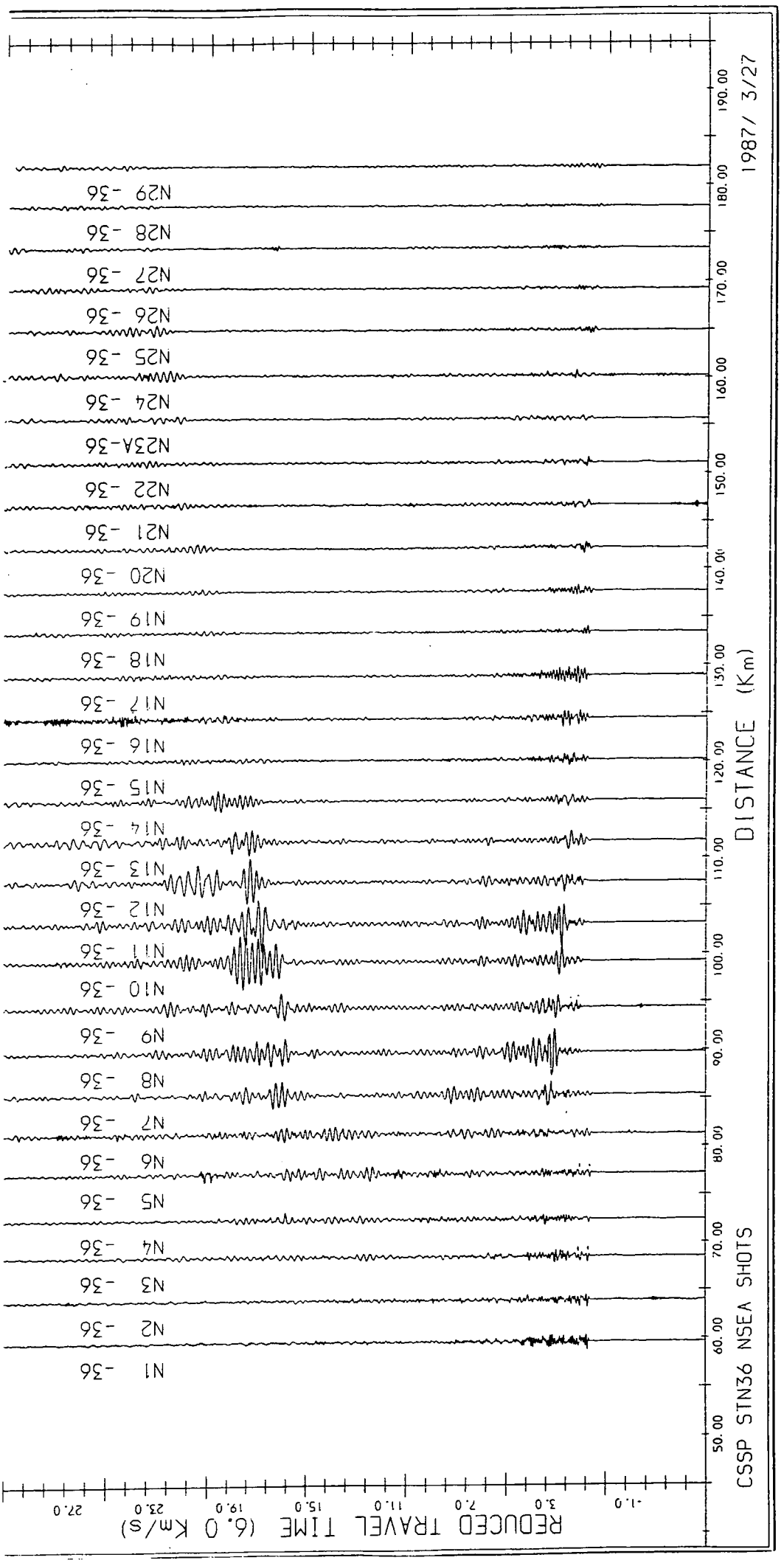

Fig. 7.15 Record section from CSSP, 1982, showing SV-wave arrivals.

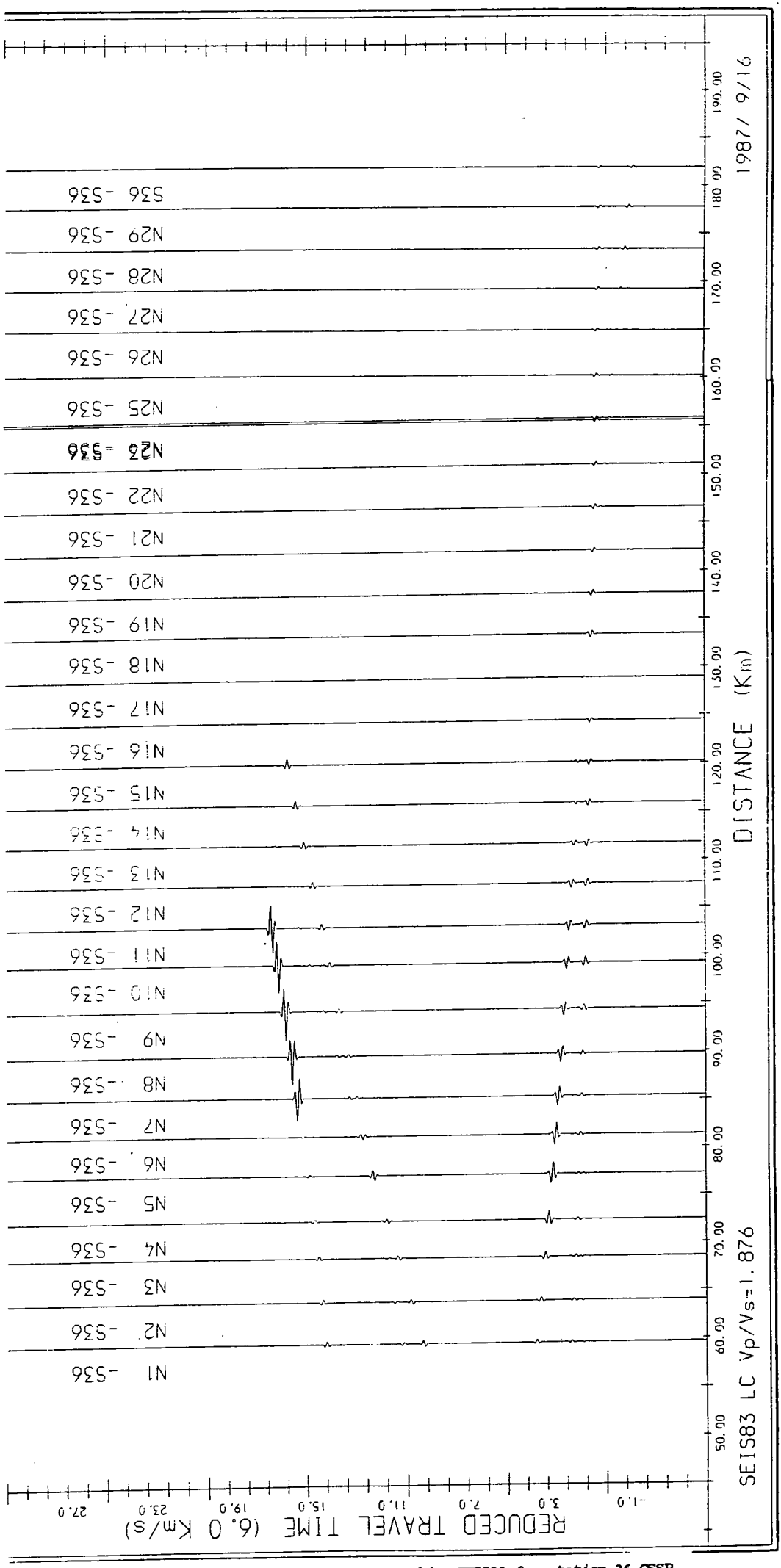

Fig. 7.16 Synthetic seismogram generated by SEIS83 for station 36 CSSP data to fit SV arrivals.

distinct lower crustal terranes postulated by **Freeman et al. (1988)** might well be expected to show such variation (the CSSP region seems to be rather similar to type I from this preliminary work). Obviously, a satisfactory P-wave model from the high-quality MOBIL wide-angle data needs to be obtained first, but following this by S-wave modelling of the CSSP records from the same region would be very worthwhile and would yield a better idea of the crustal composition than P-wave velocities alone.

This is illustrated by **Sandmeier and Wenzel (1990)**, who have successfully modelled the type I lower crust beneath the Black Forest in terms of high and low P-velocity (V_p) lamellae which also have high and low Poisson's ratios. This approach produces the observed scattering of P-waves from the lower crust with only minor S-wave reflections. The low-V_p/low Poisson's ratio layers have been interpreted as corresponding to quartz-rich rock, whereas the high-V_p/high Poisson's ratio corresponds to amphibole and plagioclase-rich rocks.

7.6 Crustal composition

The upper crustal composition along the CSSP profile was interpreted by **Green (1984)** as Precambrian metamorphic crystalline basement and modelled as such (quartzo-feldspathic gneiss) by **Lewis (1986)** in his gravity interpretation of CSSP. This would have a density of 2.74-2.80 gcm^{-3}, corresponding to a P-velocity of 6.15-6.17 kms^{-1}, approximately the average upper crustal P-velocity observed from MOBIL-CSSP.

Lewis' model for the lower crust, based on an average P-velocity of 6.77 kms^{-1}, was of a granulite composition, between pyroxene granulite gneiss (6.45 kms^{-1}) and garnet granulite gneiss (7.0 kms^{-1}), which gave an average density of 3.04 gcm^{-3} for gravity modelling. These compositions would fit the 6.5-6.8 kms^{-1} and 7.0 kms^{-1} layers identified by MOBIL-CSSP and means that there would not be significant differences between the gravity effect of the MOBIL and CSSP models. The boundary between the two lower crustal layers observed by MOBIL could then correspond to a mineralogical transition zone between the two types of granulite gneiss.

The densities used by Lewis for gravity modelling along the CSSP profile are shown in **Table 7.1**,

(a)

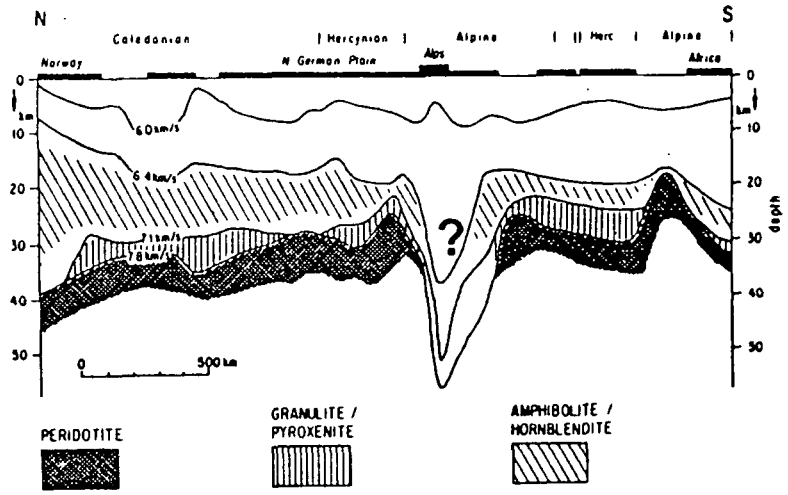

(b)

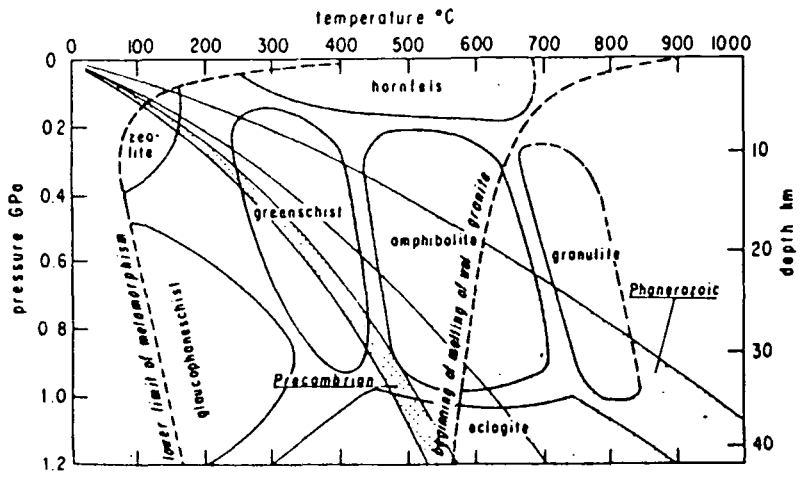

Fig. 7.17 (a) Petrological model for the European Geotraverse and (b) Turner's (1968) scheme of pressure-temperature domains for metamorphic rocks, from Rybach, (1987).

PARAMETERS USED IN GRAVITY MODELLING

Material	Velocity (km/s)	Density (kg/m)
Permo-trias sediments	3.2	2.35
Carboniferous sediments	4.5	2.60
Lower Paleozoic sediments	5.5-5.7	2.73
Upper crust (felsp. to interm. gneiss)	6.15-6.17	2.74-2.80
North Sea granite	5.8	2.58
Carlisle basic intrusion	6.15	2.89
Lower crust	6.75-6.77	3.04
Moho Layer	7.0-8.0	3.24
Upper Mantle	>8.0	3.34
From Blundell et al (1985)		
Moine metamorphics and Lewisian amphibolite facies quatzo-felspathic gneiss	6.15	2.74
Pyroxene granulite gneiss	6.45	2.86
Garnet granulite gneiss	7.00	3.10
Moho Layer	7.50	3.20
Upper Mantle	8.10	3.30

Table 7.1 Densities used by Lewis(1986) for gravity modelling of crustal structure.

with the equivalent seismic P-velocities. These values plot onto a velocity-density graph within the scatter of the Nafe-Drake curve (**Lewis 1986**).

Rybach (1987) has interpreted the lower crustal composition beneath the European Geotraverse on the basis of seismic velocity and radioactive heat production, considering the pressure-temperature domains of the different metamorphic facies. His resulting model is shown in **Fig. 7.17** with **Turner's (1968)** representation of the metamorphic pressure-temperature domains. The model, which crosses the Caledonian crust of Norway and Sweden, incorporates similar P-velocities to those observed on MOBIL-CSSP. Most of the lower crust is interpreted as amphibolite/hornblendite, with a layer of higher velocity granulite at the base of the crust and an upper mantle of peridotite composition. However, this interpretation does not seem to have considered whether the lower crust is "wet" or "dry", and amphibolite would be the expected rock type for "wet" crust.

A likely explanation of the lower crustal composition is that it is made up of a heterogeneous mixture of different rock types, especially in areas where the lower crust is very reflective, such as the region north of the "Iapetus Suture". Freeman et al (1988) have interpreted this as a subduction complex buried in the process of continental subduction. For the transparent crustal wedge beneath the "Suture", however, a more homogeneous composition seems appropriate, in which case the model proposed by Lewis is adequate.

CHAPTER 8: CONCLUSIONS AND FURTHER WORK

8.1 Introduction

The main point to emerge from this study is how successful the recording of closely spaced airgun shots at wide-angle has proved to be. The 50 m shot spacing and high frequency of the airgun source (compared to marine explosive shots) have generated data of unprecedented resolution, which has even enabled the identification of lateral discontinuities, usually difficult to locate by wide-angle surveys. The exactly coincident recording of deep normal incidence seismic reflection has shown how well the techniques complement each other, one illuminating the features missed or not understood from the other. More exactly coincident surveys of this type are obviously the way forward in crustal seismic exploration.

The main conclusions obtained from this experiment are presented below.

8.2 The structure beneath the Northumberland Trough

As mentioned in **section 7.2**, the crust actually sampled by the MOBIL wide-angle data lies between station 54 and shot 1700, and only the western end of this line, approximately between shots 2500 and 3030, actually lies beneath the Northumberland Trough. The remainder of the profile is overlain by the eastward-thickening sedimentary sequence of the North Sea, but the whole of the line runs almost along the axis of the Mid-North Sea High, a basement High since the Late Palaeozoic, which divides the Northern and Southern North Sea basins. The structure interpreted by this survey would therefore be better described as "the deep structure beneath the Mid North Sea High".

The main features of the seismic interpretation of this study may be summarised:

(a) The whole region is underlain by crystalline basement at about 4 km depth, deepening eastward beneath the sedimentary load of the North Sea. The velocity at the top of this basement is 6.13

kms^{-1} out to about shotpoint 2800, east of which it decreases to **5.97** kms^{-1}.

(b) The upper crust is fairly homogeneous, consisting of a vertical velocity gradient down to **20** km depth of **6.13** to **6.38** kms^{-1} to the west, and **5.97-6.38** kms^{-1} to the east. There is, however, an interface at about **10** km depth which represents a velocity change from **6.22** to **6.24** kms^{-1} to the west, and **6.09** to **6.11** kms^{-1} to the east.

(c) At **20** km depth, the velocity gradient changes, increasing from **6.41** to **6.84** kms^{-1} between **20** and **28** km depth. There is also a slight change in velocity from **6.38** to **6.41** kms^{-1}. This interface corresponds to the top of the "Iapetus Suture" dipping reflector seen on BIRPS normal-incidence sections, and the velocity gradient corresponds to a relatively transparent zone with regard to normal-incidence reflections. However, there is a slight velocity contrast at about **24** km depth of **6.61** to **6.64** kms^{-1}.

(d) A high velocity of **7.0** kms^{-1} is present at the bottom 2 km of the crust, required in order to fit the observed travel times for the wide-angle Moho reflection. It does not generate either wide-angle or normal incidence reflections, which suggests that its upper surface is a gradational boundary.

(e) The Moho boundary is present at about **30** km depth, as a surface generating bright seismic reflections at both wide-angle and normal incidence due to a high velocity contrast of **6.84** to **8.02** kms^{-1}.

(f) A step feature, or series of steps, on the Moho, about 45 km offshore is suggested as the cause of unusual high-amplitude seismic reflections at wide-angle. The cause of this feature and the change in upper crustal velocity structure is suggested to be a vertical, crust-cutting wrench fault possibly related to the Dowsing Fault zone south of this region. These steps between them offset the Moho by up to 1 km.

(g) A velocity gradient exists in the upper mantle (**8.02-8.2** kms^{-1} in the top 10 km), which gives rise to a Pn headwave of moderate amplitude.

8.3 Further work

The MOBIL programme has generated a huge volume of high-resolution wide-angle seismic data and normal-incidence data, of which the full interpretation has only been started. There is still work to be done on the modelling of line 1 alone, in addition to the development of techniques for enhancing and

improved plotting of the data, and fully tying in the information from all the seismic data acquired. However, the use of all this data still leaves some geological question marks over the region which can only be satisfied by further geophysical investigations. Some of the many possibilities for further work in all these fields are discussed below.

8.3.1 Development of high-resolution wide-angle seismics

Using closely-spaced airgun shots as a source for wide-angle reflection data is still a relatively new idea in seismology, but has enjoyed great success in this and many similar experiments, mentioned in Chapter 1. The detail on the record sections is remarkable, even with minimal processing. The comparable resolution of the data to normal-incidence data means that it could be very worthwhile applying some of the more sophisticated processing and enhancement techniques which have been developed for normal-incidence data, and it is obvious that improved methods of plotting need to be found in order to display better all the amplitude information as well as travel-time information.

Klemperer and Luetgert (1987) have experimented with CMP and common shotpoint stacking of closely-spaced, land-recorded wide-angle data from Maine, U.S.A., which facilitates the use of wide-angle data to recognise structural detail in addition to velocity detail. Much piggy-back wide-angle recording of the DEKORP deep seismic profiles has also led to development of plotting and interpretation techniques, plotting not only common station, common shot and common mid-point sections but also common offset sections, which reveal structural details of the boundaries which generate wide-angle reflections (**Gebrande et al., 1989**). Interpretation techniques used on this data include Tau-p inversion techniques for velocities and wide-angle migration for structural information. **Jokat and Flueh (1987)** have experimented on the airgun wide-angle data recorded during the EUGENO-S programme in Scandinavia, attempting velocity filtering based on slant-stacking, and deconvolution in the Tau-p domain, which enhance weak arrivals and reduce multiples and strong S-waves.

Most of these techniques could be applied to the MOBIL wide-angle dataset, allowing for the slightly restricting geometry of the profile, and in fact, the data would provide ideal test data for the development of such techniques for future use. Other more sophisticated processes which could be

developed include correction for near-surface statics, muting of first breaks and correcting the reflection amplitudes for the angle of incidence (**Klemperer and Luetgert, 1987**).

The implementation and modification at Durham of the existing wide-angle seismic processing software onto SUN workstations will enable the development of some of these methods and their application to MOBIL wide-angle data in future. Probably the most crucial area, which should be developed first, is the plotting method, which at present leaves much to be desired. The amount of information in the nearly-raw data would be greatly enhanced by development of variable area plotting methods which use colour to show the amplitudes of the seismic arrivals. Work on this aspect has already been started at Durham by the **BABEL Working Group.**

8.3.2 Further interpretations of existing data

In spite of the work of **Lewis, Bassom, Jarvis (all in 1988), Matthews (1989)** and this study, the interpretation of all the available MOBIL and CSSP seismic data could be taken much further. Some of the further interpretation which could be carried out includes:

(a) **More detailed synthetic seismogram modelling of the line 1 records from all stations.** Arrivals which have not yet been fully modelled include the mid-crustal wide-angle reflections, multiple arrivals (which may reveal considerable detail about the near-surface structure) and other "diffraction-type" arrivals similar to D. This would be greatly helped by the digitisation and playout of the remainder of the Wark recordings.

(b) **Further interpretation of the "fan shoot" data of line 2 shots recorded at the MOBIL stations.** The Wark recordings of this data have yet to be digitised and plotted, but would probably yield interesting records, sampling the crust beneath Northumberland itself. The wide-angle recordings of the shots from **line 3** would also be of great value, if it is possible to obtain accurate shot times, since the bottoming points of the seismic rays from these shots would lie beneath Line 2 and NEC. Modelling of these profiles would be greatly helped by the implementation of a 3-dimensional package such as ANRAY (described in Chapter 5). In fact, Cerveny (pers. comm.) has recently extended his Gaussian beam package for "**2.5-D**" cases, that is, 3-D computation in 2-D structures. Such a package would

facilitate the interpretation of this data.

(c) Having established a detailed P-wave model, **the interpretation and modelling of the CSSP S-wave data**, as mentioned in section 7.4, would be a very worthwhile exercise. Using the records from horizontal seismometers in addition to the vertical component records could yield interesting results in terms of the S-velocities and Poisson's ratio, which would give a good handle on the crustal density and composition.

(d) The synthetic seismogram modelling of the Line 4 wide-angle data, with a suitable modelling package, would be a useful project, especially since the normal-incidence data section for this line shows very little information from the deep crust due to strong reflections near the surface. Modelling this profile would help to tie in the observations of line 1 with those of line 5.

8.3.3 Further geophysical investigation

One of the weaknesses of this survey was the lack of reversed wide-angle coverage, which would have greatly increased the reliability of the two-dimensional wide-angle interpretation and would have extended the amount of crust sampled beneath the normal-incidence line. In view of the hurried deployment of the wide-angle recording equipment, this was inevitable, but in future experiments of this type, deployment of sea-bottom seismometers at the end of the line of shots and perhaps along the profile would greatly improve the coverage. This would also provide more information on the shallow seismic structure from shallow refraction arrivals which were not seen on the MOBIL wide-angle recordings, whose minimum offset was about 35 km.

Questions raised rather than answered by this study concern: the exact relationship of the Northumberland Trough to the Mid-North Sea High; the detailed relationship of the proposed wrench fault to these two features (or are they both part of the same structural high?); the nature of other structures, presumably also faults, which cause diffraction-type arrivals at wide-angle on this dataset; the difference in composition between the "lower crustal terrane" (as defined by Freeman et al., 1988) crossed by line 1 and the adjacent terranes observed on the BIRPS normal-incidence seismic data.

The only answer to most of these problems lies in further geophysical investigations, such as:

(a) Shallow normal-incidence reflection seismic profiling over the Mid North Sea High (or access to profiles already carried out) would probably reveal more information about the relationships of the shallow geological horizons, which are not clearly imaged by BIRPS normal-incidence profiling. Such data might show more clearly the effect of the proposed fault, and any others, in the near-surface geology.

(b) A more detailed investigation of the gravity and magnetic field of the High might reveal a great deal about the structural trends, especially in the form of illuminated colour and shaded-relief images such as those of **Lee et al.(1990)**. The available Bouguer contour map seems to show very little in the way of structural trends.

(c) Further deep seismic profiles similar to MOBIL, but shot at strategic distances from and parallel to MOBIL line 1, would reveal more information about the nature of the other crustal terrane types adjacent to that beneath line 1. Such profiles should ideally have wide-angle recording taking place at both ends and possibly at intervals along them, in order to obtain full coverage and all the necessary shallow velocity information.

However, even without the improvements suggested above, there is a large amount of geological information to be obtained from the existing MOBIL normal-incidence and the wide-angle datasets. Further use of these datasets as suggested in **sections 8.3.1** and **8.3.2** should lead to a better understanding of the evolution of the Southern North Sea Basin and the North East coast of England.

REFERENCES

AVESCHOUGH, N.C. 1986. The Market Weighton Carboniferous Trough. Yorkshire Geological Society Circular, 393, 3.

BAMFORD, S.A.D., NUNN, K., PRODEHL, C. & JACOB, B. 1978. LISPB-IV. Crustal structure of Northern Britain. Geophys. J. R. astr. Soc. 54, 43-60.

BAMFORD, S.A.D. 1979. Seismic constraints on the deep geology of the Caledonides of northern Britain. In: HARRIS, A.L., HOLLAND, C.H. & LEAKE, B.E. (Eds.) The Caledonides of the British Isles - reviewed. Spec. Pub. Geological Society of London, 93-96.

BASSOM, C. 1988. An interpretation of the southern North Sea gravity anomalies based on wide-angle reflection data. Unpublished M.Sc. thesis, Durham.

BERRYHILL, J. R. 1977. Diffraction response for nonzero separation of source and receiver. Geophysics 42, 1158-1176.

BITTNER, R., TRAPPE, H.& MEISSNER, R. 1987. Piggy-back seismic experiments during deep crustal reflection surveys. Annales Geophysicae 5B (4), 381-388.

BLUNDELL, D.J., HOBBS, R.W., KLEMPERER, S.L., SCOTT-ROBINSON, R., LONG, R.E, WEST, T.E. & DUIN, E. 1991. Crustal structure beneath the central and southern North Sea from BIRPS deep seismic reflection profiling. J.Geol. Soc. London, 148, 445-457.

BOTT, M.H.P. 1961. A gravity survey off the NE coast of England. Proc. Yorks. Geol. Soc. 33, 1-20.

BOTT, M.H.P., LONG, R.E., GREEN, A.S.P.& LEWIS, A.H.J. 1985. Crustal structure south of the Iapetus Suture beneath northern England. Nature 314 (25), 724-727.

BOTT, M.H.P., ROBINSON, J. & KOHNSTAMM, M.A. 1978. Granite beneath Market Weighton, East Yorkshire. J. Geol. Soc. 135, 535-543.

BOTT, M.H.P., SWINBURN, P.M. & LONG, R.E. 1984. Deep structure and origin of the Northumberland and Stainmore Troughs. Proc. Yorks. Geol. Soc. 44, 479-496.

BREWER, J.A., MATTHEWS, D.H., WARNER, M.R., HALL, J. SMYTHE, D.K. & WHITTINGTON, R.J. 1983. BIRPS deep seismic reflection studies of the British Caledonides. Nature 305, 206-210.

BRITISH GEOLOGICAL SURVEY 1988. Farne Sheet 55 N - 02 W. British Geological Survey 1:250000 Solid Geology Map.

BROCHER, T.M., HART, P.E. & FISHER, M.A. 1989. Wide-angle recordings of the 1988 TACT MCS survey in Prince William Sound, Alaska. EOS Trans. Amer. Geophys. Un. 70, 1339 (Abstract).

CASSELL, B.R. 1982. A method for calculating synthetic seismograms in laterally varying media. Geophys. J. R. astr. Soc. 69, 339-354.

CERVENY, V. 1983. Synthetic body wave seismograms for laterally varying layered structures by the Gaussian beam method. Geophys. J.R.astr.Soc. 73, 389-426.

CERVENY, V. 1985a. Ray synthetic seismograms for complex 2-D and 3-D structures. J. Geophys. 58,2-26.

CERVENY, V. 1985b. Gaussian beam synthetic seismograms. J. Geophys. 58 Nos. 1-3,44-72.

CERVENY, V.,MOLOTKOV, I.A. & PSENCIK, I. 1977. Ray method in seismology. Universita Karlova Praha.

CHADWICK, R.A., PHAROAH, T.C. & SMITH, N.J.P. 1989. Lower crustal heterogeneity beneath Britain from deep seismic reflection data. J.Geol. Soc. Lon. 146, 617-630.

CHAPMAN, C.H. 1985. Ray theory and its extensions: WKBJ and Maslov seismograms. J.Geophys. 58 Nos.1-3, 27-43.

COCKS, L.R.M. & FORTEY, R.A 1982. Faunal evidence for oceanic separations in the Palaeozoic of Britain. J.Geol.Soc. London 139, 465-478.

COLLETTE, B.J., LAGAAY, R.A. & RITSEMA, A.R. 1970. Seismic investigations in the North Sea, 3 to 7. Geophys. J. R. astr. Soc. 19, 183-199.

DONATO, J.A., MARTINDALE, W. & TULLY, M.C. 1983. Buried granites within the Mid North Sea High. J.Geol. Soc. London 140,825-837.

DONATO, J.A. & MEGSON, J.B. 1990. A buried granite beneath the East Midland Shelf of the Southern North Sea. J. Geol. Soc. London 147, 133-140.

FONSECA, J.F.B.D. 1989. The seismicity and regional tectonics of Southwestern Portugal. Unpublished Ph.D. thesis, Durham.

FRASER, A.J. & GAWTHORPE, R.L. 1990. Tectono-stratigraphic development and hydrocarbon habitat of the Carboniferous of Northern England. In: Tectonic events responsible for Britain's oil and gas reserves, Ed. R.S.P. Hardman & J. Brooks. Spec. Publ. Geol. Soc. London No. 55, p49-86.

FRAZER, L.N. & GETTRUST, J.F. 1984. On a generalisation of Filon's method and the computation of the oscillatory integrals of seismology. Geophys. J. R. astr. Soc. 76, 461-482.

FREEMAN, B.,KLEMPERER,S .L. & HOBBS, R.W. 1988. The deep structure of northern England and the Iapetus Suture zone from BIRPS deep seismic reflection profiles. J.Geol.Soc. London 145, 727-740.

FUCHS, K. & MULLER, G. 1971. Computation of synthetic seismograms with the Reflectivity method and comparison with observations. Geophys. J.R.astr.Soc. 23, 417-433.

GAJEWSKI, D., HOLBROOK, W.S. AND PRODEHL, C. 1987. Combined seismic reflection and refraction profiling in southwest Germany - detailed velocity mapping by the refraction survey. Geophys. J.R.astr.Soc. 89, 333-338.

GEBRANDE, BOPP, MEICHELBOECK, NEURIEDER & SCHMIDT 1989. DEKORP wide-angle seismics. Poster paper at IASPEI 1989, Istanbul.

GLENNIE, K.W. (Ed.) 1986. Introduction to the Petroleum Geology of the North Sea. Blackwell Scientific Publications. 236 pp.

GLENNIE, K.W. & BOEGNER,P.L.E 1981. Sole Pit Inversion Tectonics. In: ILLING, L.V. & HOBSON, G.D. (Eds.), Petroleum Geology of the Continental Shelf of North-West Europe. Institute of Petroleum, London, pp. 110-120.

GLIMPCE SEISMIC REFRACTION WORKING GROUP 1989. GLIMPCE Seismic Experiments : Long-offset recordings. EOS Trans. Am. Geophys. Un. 70, 841-853.

GREEN, A.S.P. 1984. The crustal structure beneath northern England and adjacent sea areas. Unpublished Ph.D. thesis, Durham.

HALL, J. 1983. Seismological evidence for shallow crystalline basement in the Southern Uplands of Scotland. Nature 39, 418-420.

HOWSON, C.D. 1982. An evaluation of a new method of computing synthetic seismograms. Unpublished M.Sc. thesis, Durham.

HUTCHINSON, D.R. & KLITGORD, K.D. 1986. Preliminary results from the USGS deep crustal studies profile across the Gulf of Maine. EOS Trans. Amer. Geophys. Un. 67, 312.

HUTTON, D.H.W. 1987. Strike-slip terrane and model for the evolution of the British and Irish Caledonides. Geological Magazine 124, 405-425.

JARVIS, E.P. 1988. Lateral variations in crustal structure off the North East Coast of England. Unpublished M.Sc. thesis, Durham.

JENYON, M.K., CRESSWELL, P.M. & TAYLOR, J.C.M. 1984. Nature of the connection between the Northern and Southern Zechstein basins across the Mid North Sea High. Marine & Petroleum Geology 1, 355-363.

JOHNSON, G.A.L. 1984. Subsidence and sedimentation in the Northumberland Trough. Proc. Yorks. Geol. Soc. 45, 71-83.

JOKAT, W. & FLUEH, E.R. 1987. On the use of airgun arrays for seismic refraction investigations of the crust. First Break 5, 440-447.

KENNETT, B.L.N. 1975. Theoretical seismogram calculation for laterally varying crustal structures. Geophys. J. R. astr. Soc. 42, 579-589.

KENNETT, B.L.N. & HARDING, A.J. 1985. Is ray theory adequate for reflection seismic modelling? (A survey of modelling methods) First Break 3,9-14.

KENT, P.E. 1975. The tectonic development of Great Britain and the surrounding seas. In: WOODLAND, A.W. (Ed.) Petroleum and the continental shelf of North-West Europe. Vol. 1, Geology. Applied Science Publishers Ltd.: Institute of Petroleum, Great Britain, pp. 3-28

KLEMPERER, S.L. 1989. Processing BIRPS deep seismic reflection data: A tutorial review. In: CASSINIS, R., NOLET, G., & PANZA, G.F. (Eds.). Digital seismology and fine modelling of the Lithosphere. Plenum Publishing Corp..

KLEMPERER, S.L., HOBBS, R.W. & FREEMAN, B. 1990. Dating the source of lower crustal reflectivity using BIRPS deep seismic profiles across the Iapetus suture. Tectonophysics 173, 445-454.

KLEMPERER, S.L. & LUETGERT, J.H., 1987. A comparison of reflection and refraction processing and interpretation methods applied to conventional refraction data from Coastal Maine. Bull. Seism. Soc. Amer. 77,614-630.

KLEMPERER, S.L. & MATTHEWS,D.H. 1987. Iapetus Suture located beneath the North Sea by BIRPS deep seismic reflection profiling. Geology 15, 195-198.

KUSZNIR, N.J. & MATTHEWS, D.H. 1988. Deep seismic reflections and the deformational mechanics of the continental lithosphere. J. Petrology, Special Lithosphere Issue, p. 63-87.

LEE, M.K., PHARAOH, T.C. & SOPER, N.J. 1990. Structural trends in central Britain from images of gravity and aeromagnetic fields. J.Geol. Soc. London 147, 241-258.

LEEDER, M.R. 1982. Upper Palaeozoic basins of the British Isles - Caledonian inheritance versus Hercynian plate margin processes. J.geol. Soc. London 139, 479-491.

LEWIS, A.H.J. 1986. The deep seismic structure of Northern England and adjacent marine areas from the Caledonian Suture Seismic Project. Unpublished Ph.D thesis , Durham.

LEWIS, S.A. 1988. Market Weighton : Granite or Graben? Unpublished M.Sc. thesis, Durham.

LUND, C.-E., ROBERTS, R.G. & JUHLIN, C. 1987. The reflectivity of the lower crust in southwestern Sweden. Ann. Geophysicae 5B(4), 375-380.

MCKENZIE, D.P. 1978. Some remarks on the development of sedimentary basins. Earth & Plan. Sci. Lett. 40, 25-32.

MATTHEWS, D.H. 1986. Seismic reflections from the lower crust around Britain. In: DAWSON, J.B., CARSWELL, D.A., HALL, J. & WEDEPOHL, K.H. (Eds.) Nature of the lower continental crust. Spec.Publ. 24, Geol. Soc. Lon. pp 11-21.

MATTHEWS, P.A. 1989. Crustal structure of the North Yorkshire coast from high-resolution wide-angle reflection data. Unpublished M.Sc. thesis, Durham.

MATTHEWS, P.A. 1990. Crustal structure off the North East coast from wide-angle reflection data. In preparation.

MEREU, R.F., EPILI, D. & GREEN, A.G. 1990. Pg shingles: preliminary results from the onshore GLIMPCE refraction experiment. Tectonophysics 173, 617-626.

MOONEY, W.D. & BROCHER, T.M. 1987. Coincident seismic reflection/ refraction studies of the continental lithosphere : a global review. Reviews of Geophysics 25,723-742.

MOSES, M.J., BROCHER, T.M., FISHER, M.J., TALWANI, M. & EWING, J.I. 1989. Wide-angle recordings of the 1989 EDGE MCS survey along the Eastern Aleutian Arc-Transect, Alaska. EOS Trans. Amer. Geophys. Un. 70, 1339 (Abstract).

MULLER, G. 1985. The reflectivity method: a tutorial. J.Geophys. 58,153-174.

POWELL, C.M.R. 1983. The Caledonian Suture Seismic Project: The near-surface structure of the western Mid-North Sea High. Unpublished B.Sc. dissertation, University of Durham.

RYBACH, L. 1987. A petrological model of the lower continental crust, derived from seismic velocities and from radioactive heat production. Annales Geophysicae 5B, 403-408.

SANDMEIER, K-J. & WENZEL, F. 1986. Synthetic seismograms for a complex crustal model. Geophys. Res. Lett. 13 (1), 22-25.

SANDMEIER, K-J. & WENZEL, F. 1990. Lower crustal petrology from wide-angle P- and S-wave measurements in the Black Forest. Tectonophysics 173, 495-505.

SMITH, D.B & TAYLOR, J.C.M. 1989. A "North-west Passage" to the Southern Zechstein Basin of the U.K. North Sea. Proc.Yorks. Geol.Soc. 47, 313-320.

SOPER, N.J. & HUTTON, D.H.W. 1984. Late Caledonian sinistral displacements in Britain: Implications for a three-plate collision model. Tectonics 3, 781-794.

SPENCE, G.D., WHITTALL, K.P. & CLOWES, R.M. 1984. Practical synthetic seismograms for laterally varying media calculated by asymptotic ray theory. Bull. Seism. Soc. Am. 74, 1209-1223.

SWINBURN, P.M 1975. The crustal structure of Northern England. Unpublished Ph.D. thesis, University of Durham.

TROREY, A.W. 1970. A simple theory for seismic diffractions. Geophysics 25, No. 5, 762-789.

TURNER, F.J. 1968. Metamorphic petrology. McGraw-Hill, New York, 426 pp.

VAN HOORN, B. 1987. Structural evolution, timing and tectonic style of the Sole Pit inversion. Tectonophysics 137, 239-284.

WATSON, J. 1984. The ending of the Caledonian orogeny in Scotland. J. Geol. Soc. London 141, 193-214.

WEBER, M. 1988. Computation of body-wave seismograms in absorbing 2-D media using the Gaussian beam method: comparison with exact methods. Geophysical Journal 92, 9-24.

ZIEGLER, P.A. 1982. Geological Atlas of Western and Central Europe. Elsevier, Amsterdam. Shell Internationale Petroleum Mij.B.V., The Hague.

APPENDIX A

MOBIL-CSSP STATION LOCATIONS

Station	Latitude	Longitude	Height (m)
36	55.0863666	-2.3313333	229.00
37	55.0907833	-2.3006166	206.00
39	55.1008666	-2.2400000	165.00
40	55.1068833	-2.2105666	137.00
47	55.1671333	-1.9791166	219.00
54	55.2195000	-1.7586166	181.00
55	55.2253833	-1.7275833	114.00
57	55.2422166	-1.6509666	51.00

APPENDIX B

SHOT LATITUDES, LONGITUDES AND TIMES

	LINE	SHOT	TIMEBREAK - GMT	Gyro	LATITUDE	LONGITUDE
BIRPS	BM87-1	-95	161 18 01 43.798	245.25	55.8746773	1.0708017
BIRPS	BM87-1	-94	161 18 02 05.692	246.44	55.8744987	1.0700660
BIRPS	BM87-1	-93	161 18 02 27.597	246.99	55.8743345	1.0693240
BIRPS	BM87-1	-92	161 18 02 49.613	247.56	55.8741785	1.0685715
BIRPS	BM87-1	-91	161 18 03 11.620	247.85	55.8740304	1.0678003
BIRPS	BM87-1	-90	161 18 03 33.024	246.11	55.8738936	1.0669994
BIRPS	BM87-1	-89	161 18 03 54.628	245.32	55.8737582	1.0662825
BIRPS	BM87-1	-88	161 18 04 15.634	245.16	55.8736192	1.0655076
BIRPS	BM87-1	-87	161 18 04 36.728	244.16	55.8734556	1.0647372
BIRPS	BM87-1	-86	161 18 04 58.944	244.58	55.8732884	1.0639844
BIRPS	BM87-1	-85	161 18 05 20.950	244.56	55.8731079	1.0632532
BIRPS	BM87-1	-84	161 18 05 43.243	246.05	55.8729525	1.0625376
BIRPS	BM87-1	-83	161 18 06 07.861	245.33	55.8727869	1.0617426
BIRPS	BM87-1	-82	161 18 06 28.555	244.21	55.8726499	1.0610720
BIRPS	BM87-1	-81	161 18 06 51.660	243.73	55.8724815	1.0602443
BIRPS	BM87-1	-80	161 18 07 12.677	242.56	55.8723244	1.0595723
BIRPS	BM87-1	-79	161 18 07 35.370	242.00	55.8721284	1.0587798
BIRPS	BM87-1	-78	161 18 07 57.476	242.59	55.8719470	1.0580883
BIRPS	BM87-1	-77	161 18 08 22.094	243.43	55.8717529	1.0573386
BIRPS	BM87-1	-76	161 18 08 43.788	242.40	55.8715761	1.0566306
BIRPS	BM87-1	-75	161 18 09 06.205	242.88	55.8714142	1.0559320
BIRPS	BM87-1	-74	161 18 09 29.611	242.00	55.8712305	1.0551574
BIRPS	BM87-1	-73	161 18 09 54.215	242.33	55.8710337	1.0543830
BIRPS	BM87-1	-72	161 18 10 14.510	242.02	55.8708555	1.0537290
BIRPS	BM87-1	-71	161 18 10 37.015	244.11	55.8706487	1.0529469
BIRPS	BM87-1	-70	161 18 10 59.470	243.38	55.8704777	1.0522102
BIRPS	BM87-1	-69	161 18 11 21.537	242.23	55.8703179	1.0514698
BIRPS	BM87-1	-68	161 18 11 44.429	241.36	55.8701589	1.0507659
BIRPS	BM87-1	-67	161 18 12 07.134	242.71	55.8699803	1.0499897
BIRPS	BM87-1	-66	161 18 12 30.153	243.02	55.8698232	1.0492615
BIRPS	BM87-1	-65	161 18 12 51.556	242.79	55.8696807	1.0485174
BIRPS	BM87-1	-64	161 18 13 15.650	242.25	55.8695006	1.0476909
BIRPS	BM87-1	-63	161 18 13 36.156	241.29	55.8693401	1.0470065
BIRPS	BM87-1	-62	161 18 13 56.372	240.99	55.8691714	1.0463434
BIRPS	BM87-1	-61	161 18 14 18.579	240.64	55.8689777	1.0456186
BIRPS	BM87-1	-60	161 18 14 40.583	241.10	55.8687817	1.0449111
BIRPS	BM87-1	-59	161 18 15 02.876	242.25	55.8686171	1.0442068
BIRPS	BM87-1	-58	161 18 15 27.495	241.68	55.8683987	1.0433863
BIRPS	BM87-1	-57	161 18 15 50.988	242.12	55.8682141	1.0426903
BIRPS	BM87-1	-56	161 18 16 13.606	242.95	55.8680059	1.0419079
BIRPS	BM87-1	-55	161 18 16 35.210	243.55	55.8678306	1.0411628
BIRPS	BM87-1	-54	161 18 16 56.503	243.96	55.8676744	1.0404899
BIRPS	BM87-1	-53	161 18 17 17.609	243.49	55.8675062	1.0397655
BIRPS	BM87-1	-52	161 18 17 40.515	244.29	55.8673453	1.0390529
BIRPS	BM87-1	-51	161 18 18 03.620	243.62	55.8671676	1.0382824
BIRPS	BM87-1	-50	161 18 18 27.039	243.85	55.8670075	1.0375897
BIRPS	BM87-1	-49	161 18 18 51.644	244.79	55.8667935	1.0367831
BIRPS	BM87-1	-48	161 18 19 17.192	245.16	55.8666061	1.0360072
BIRPS	BM87-1	-47	161 18 19 37.509	245.44	55.8664459	1.0353478
BIRPS	BM87-1	-46	161 18 19 59.375	245.58	55.8662800	1.0346097
BIRPS	BM87-1	-45	161 18 20 21.242	246.14	55.8661112	1.0338611
BIRPS	BM87-1	-44	161 18 20 42.809	246.43	55.8659483	1.0331132
BIRPS	BM87-1	-43	161 18 21 05.675	245.19	55.8657824	1.0323523
BIRPS	BM87-1	-42	161 18 21 25.942	245.79	55.8656209	1.0316742
BIRPS	BM87-1	-41	161 18 21 48.609	246.29	55.8654473	1.0308549
BIRPS	BM87-1	-40	161 18 22 10.709	245.30	55.8652764	1.0301071
BIRPS	BM87-1	-39	161 18 22 32.609	245.10	55.8651131	1.0293663
BIRPS	BM87-1	-38	161 18 22 54.809	244.88	55.8649319	1.0286257
BIRPS	BM87-1	-37	161 18 23 16.375	246.15	55.8647894	1.0279460
BIRPS	BM87-1	-36	161 18 23 38.409	245.23	55.8646235	1.0271055
BIRPS	BM87-1	-35	161 18 23 59.825	245.89	55.8644880	1.0264224
BIRPS	BM87-1	-34	161 18 24 21.192	245.65	55.8643412	1.0256879
BIRPS	BM87-1	-33	161 18 24 44.159	244.96	55.8641980	1.0249585
BIRPS	BM87-1	-32	161 18 25 08.425	243.65	55.8640317	1.0240948
BIRPS	BM87-1	-31	161 18 25 31.092	242.89	55.8638687	1.0233711
BIRPS	BM87-1	-30	161 18 25 54.392	242.39	55.8636962	1.0226433
BIRPS	BM87-1	-29	161 18 26 15.975	243.04	55.8635310	1.0219196
BIRPS	BM87-1	-28	161 18 26 37.309	241.93	55.8633603	1.0211878
BIRPS	BM87-1	-27	161 18 27 01.192	241.57	55.8631674	1.0204068
BIRPS	BM87-1	-26	161 18 27 23.809	240.73	55.8629785	1.0196965
BIRPS	BM87-1	-25	161 18 27 44.142	241.83	55.8627968	1.0190548
BIRPS	BM87-1	-24	161 18 28 06.425	242.40	55.8626155	1.0183459
BIRPS	BM87-1	-23	161 18 28 30.659	241.81	55.8623982	1.0175167
BIRPS	BM87-1	-22	161 18 28 53.192	242.59	55.8622166	1.0168110
BIRPS	BM87-1	-21	161 18 29 16.775	244.05	55.8620287	1.0160566
BIRPS	BM87-1	-20	161 18 29 39.344	243.39	55.8618661	1.0153574
BIRPS	BM87-1	-19	161 18 30 02.042	243.04	55.8616942	1.0146484
BIRPS	BM87-1	-18	161 18 30 24.209	243.05	55.8615213	1.0139279
BIRPS	BM87-1	-17	161 18 30 47.275	241.79	55.8613294	1.0131140
BIRPS	BM87-1	-16	161 18 31 09.492	240.88	55.8611329	1.0123844
BIRPS	BM87-1	-15	161 18 31 31.492	242.73	55.8609485	1.0116749
BIRPS	BM87-1	-14	161 18 31 54.125	244.14	55.8607643	1.0109362
BIRPS	BM87-1	-13	161 18 32 13.275	245.02	55.8606193	1.0102332
BIRPS	BM87-1	-12	161 18 32 35.342	244.65	55.8604439	1.0094579
BIRPS	BM87-1	-11	161 18 32 56.159	244.59	55.8602942	1.0087805
BIRPS	BM87-1	-10	161 18 33 17.625	244.15	55.8601231	1.0080394
BIRPS	BM87-1	-9	161 18 33 39.959	245.24	55.8599566	1.0073106
BIRPS	BM87-1	-8	161 18 34 02.342	244.22	55.8598011	1.0065643
BIRPS	BM87-1	-7	161 18 34 24.409	244.18	55.8596307	1.0058217
BIRPS	BM87-1	-6	161 18 34 47.125	245.02	55.8588704	1.0068101
BIRPS	BM87-1	-7	161 18 35 00.225	248.06	55.8587588	1.0064294
BIRPS	BM87-1	-6	161 18 35 21.725	253.95	55.8585900	1.0056985
BIRPS	BM87-1	-5	161 18 35 43.992	254.88	55.8585089	1.0049187
BIRPS	BM87-1	-4	161 18 36 06.775	252.95	55.8584474	1.0041138
BIRPS	BM87-1	-3	161 18 36 29.825	249.40	55.8583675	1.0032371
BIRPS	BM87-1	-2	161 18 36 50.775	248.63	55.8582442	1.0025365
BIRPS	BM87-1	-1	161 18 37 12.759	252.56	55.8580686	1.0018030
BIRPS	BM87-1	101	161 18 37 35.109	254.70	55.8579324	1.0009697
BIRPS	BM87-1	102	161 18 37 57.625	253.32	55.8578480	1.0001671
BIRPS	BM87-1	103	161 18 38 19.892	252.76	55.8577451	.9993737
BIRPS	BM87-1	104	161 18 38 41.475	250.13	55.8576519	.9985775
BIRPS	BM87-1	105	161 18 39 03.609	248.92	55.8575376	.9978019
BIRPS	BM87-1	106	161 18 39 25.909	250.55	55.8574004	.9970459
BIRPS	BM87-1	107	161 18 39 47.959	250.52	55.8572734	.9962954
BIRPS	BM87-1	108	161 18 40 10.442	250.44	55.8571543	.9955302
BIRPS	BM87-1	109	161 18 40 32.809	250.52	55.8570339	.9947485
BIRPS	BM87-1	110	161 18 40 54.792	247.78	55.8569251	.9939709
BIRPS	BM87-1	111	161 18 41 17.059	244.12	55.8567953	.9931397
BIRPS	BM87-1	112	161 18 41 39.575	242.29	55.8566196	.9924130
BIRPS	BM87-1	113	161 18 42 02.059	243.58	55.8564243	.9917134
BIRPS	BM87-1	114	161 18 42 24.459	245.02	55.8562318	.9910178
BIRPS	BM87-1	115	161 18 42 47.075	244.18	55.8560772	.9903131
BIRPS	BM87-1	116	161 18 43 10.359	242.50	55.8559304	.9895089
BIRPS	BM87-1	117	161 18 43 33.309	240.22	55.8557839	.9887981
BIRPS	BM87-1	118	161 18 43 56.692	239.32	55.8555987	.9880273
BIRPS	BM87-1	119	161 18 44 19.692	238.84	55.8554053	.9872716
BIRPS	BM87-1	120	161 18 44 43.225	238.50	55.8552225	.9865827
BIRPS	BM87-1	121	161 18 45 06.525	242.09	55.8550163	.9858440
BIRPS	BM87-1	122	161 18 45 29.459	241.13	55.8548524	.9850496

BIRPS	BM87-1	123	161	18	45	52.192	242.41	55.8546931	.9843468
BIRPS	BM87-1	124	161	18	46	14.875	245.31	55.8545228	.9836427
BIRPS	BM87-1	125	161	18	46	37.359	246.74	55.8543993	.9828990
BIRPS	BM87-1	126	161	18	47	00.375	246.30	55.8542614	.9820836
BIRPS	BM87-1	127	161	18	47	23.109	243.59	55.8541213	.9813243
BIRPS	BM87-1	128	161	18	47	45.242	242.54	55.8539745	.9805841
BIRPS	BM87-1	129	161	18	48	07.592	240.62	55.8537873	.9797716
BIRPS	BM87-1	130	161	18	48	29.425	240.65	55.8535933	.9790386
BIRPS	BM87-1	131	161	18	48	51.025	241.76	55.8534218	.9783960
BIRPS	BM87-1	132	161	18	49	13.442	241.74	55.8532127	.9776255
BIRPS	BM87-1	133	161	18	49	35.975	242.63	55.8530370	.9769089
BIRPS	BM87-1	134	161	18	49	58.659	242.13	55.8528674	.9761790
BIRPS	BM87-1	135	161	18	50	20.909	240.42	55.8526984	.9754487
BIRPS	BM87-1	136	161	18	50	43.259	240.40	55.8525125	.9747500
BIRPS	BM87-1	137	161	18	51	06.025	240.19	55.8523087	.9739864
BIRPS	BM87-1	138	161	18	51	29.025	239.99	55.8521229	.9732678
BIRPS	BM87-1	139	161	18	51	51.159	240.91	55.8519388	.9725623
BIRPS	BM87-1	140	161	18	52	13.559	240.26	55.8517438	.9717784
BIRPS	BM87-1	141	161	18	52	36.025	240.49	55.8515632	.9710785
BIRPS	BM87-1	142	161	18	52	58.892	240.46	55.8513786	.9703837
BIRPS	BM87-1	143	161	18	53	21.409	241.12	55.8511691	.9696402
BIRPS	BM87-1	144	161	18	53	44.475	242.21	55.8509901	.9689686
BIRPS	BM87-1	145	161	18	54	07.942	242.38	55.8507912	.9682221
BIRPS	BM87-1	146	161	18	54	31.609	242.45	55.8506050	.9674455
BIRPS	BM87-1	147	161	18	54	54.492	242.71	55.8504266	.9667292
BIRPS	BM87-1	148	161	18	55	16.525	242.72	55.8502555	.9659809
BIRPS	BM87-1	149	161	18	55	37.892	243.07	55.8500807	.9652406
BIRPS	BM87-1	150	161	18	55	59.709	243.43	55.8499134	.9645152
BIRPS	BM87-1	151	161	18	56	22.075	243.62	55.8497461	.9637988
BIRPS	BM87-1	152	161	18	56	45.142	241.84	55.8495743	.9630972
BIRPS	BM87-1	153	161	18	57	08.159	242.15	55.8493741	.9623516
BIRPS	BM87-1	154	161	18	57	31.309	244.08	55.8491914	.9616394
BIRPS	BM87-1	155	161	18	57	53.659	245.16	55.8489949	.9608347
BIRPS	BM87-1	156	161	18	58	15.442	245.65	55.8488337	.9601021
BIRPS	BM87-1	157	161	18	58	37.725	245.88	55.8486699	.9593624
BIRPS	BM87-1	158	161	18	58	59.759	245.32	55.8485165	.9586005
BIRPS	BM87-1	159	161	18	59	21.475	244.93	55.8483580	.9578570
BIRPS	BM87-1	160	161	18	59	43.525	245.04	55.8481953	.9571332
BIRPS	BM87-1	161	161	19	00	06.042	244.89	55.8480380	.9564089
BIRPS	BM87-1	162	161	19	00	28.825	244.01	55.8478726	.9556716
BIRPS	BM87-1	163	161	19	00	50.692	244.61	55.8477015	.9549356
BIRPS	BM87-1	164	161	19	01	12.409	244.71	55.8475423	.9541785
BIRPS	BM87-1	165	161	19	01	34.409	245.02	55.8473806	.9534212
BIRPS	BM87-1	166	161	19	01	56.392	244.93	55.8472081	.9526643
BIRPS	BM87-1	167	161	19	02	18.175	244.93	55.8470483	.9519239
BIRPS	BM87-1	168	161	19	02	40.375	245.02	55.8468995	.9511703
BIRPS	BM87-1	169	161	19	03	02.609	244.17	55.8467413	.9504122
BIRPS	BM87-1	170	161	19	03	23.925	243.27	55.8465759	.9496503
BIRPS	BM87-1	171	161	19	03	45.325	242.70	55.8464187	.9489657
BIRPS	BM87-1	172	161	19	04	06.692	242.78	55.8462343	.9482223
BIRPS	BM87-1	173	161	19	04	28.309	242.87	55.8460262	.9474726
BIRPS	BM87-1	174	161	19	04	49.342	243.22	55.8458538	.9467840
BIRPS	BM87-1	175	161	19	05	10.125	244.12	55.8456790	.9460125
BIRPS	BM87-1	176	161	19	05	31.175	243.37	55.8455361	.9452919
BIRPS	BM87-1	177	161	19	05	52.159	242.10	55.8453908	.9445398
BIRPS	BM87-1	178	161	19	06	14.359	242.84	55.8449993	.9448280
BIRPS	BM87-1	179	161	19	06	42.309	249.16	55.8447696	.9439752
BIRPS	BM87-1	180	161	19	07	10.642	250.92	55.8446068	.9430309
BIRPS	BM87-1	181	161	19	07	37.242	250.85	55.8444912	.9421510
BIRPS	BM87-1	182	161	19	08	02.792	249.17	55.8443677	.9412863
BIRPS	BM87-1	183	161	19	08	28.075	248.13	55.8442253	.9404260
BIRPS	BM87-1	184	161	19	08	52.825	247.92	55.8440821	.9396155
BIRPS	BM87-1	185	161	19	09	16.325	248.20	55.8439286	.9387863
BIRPS	BM87-1	186	161	19	09	38.909	248.29	55.8437984	.9380213
BIRPS	BM87-1	187	161	19	10	01.209	247.84	55.8436671	.9372631
BIRPS	BM87-1	188	161	19	10	23.825	245.40	55.8435288	.9364796
BIRPS	BM87-1	189	161	19	10	45.625	244.71	55.8434024	.9357040
BIRPS	BM87-1	190	161	19	11	07.525	243.72	55.8432674	.9349353
BIRPS	BM87-1	191	161	19	11	29.792	243.03	55.8431154	.9341769
BIRPS	BM87-1	192	161	19	11	51.725	242.38	55.8429612	.9334269
BIRPS	BM87-1	193	161	19	12	13.992	241.42	55.8427679	.9326261
BIRPS	BM87-1	194	161	19	12	36.209	239.21	55.8426125	.9319078
BIRPS	BM87-1	195	161	19	12	59.242	238.47	55.8424477	.9312302
BIRPS	BM87-1	196	161	19	13	23.175	238.35	55.8422483	.9305058
BIRPS	BM87-1	197	161	19	13	47.225	238.67	55.8420513	.9297798
BIRPS	BM87-1	198	161	19	14	11.109	239.02	55.8418363	.9290382
BIRPS	BM87-1	199	161	19	14	33.992	238.73	55.8416270	.9282871
BIRPS	BM87-1	200	161	19	14	57.092	237.90	55.8414398	.9275836
BIRPS	BM87-1	201	161	19	15	19.542	237.81	55.8412436	.9268823
BIRPS	BM87-1	202	161	19	15	41.909	238.52	55.8410364	.9261189
BIRPS	BM87-1	203	161	19	16	04.509	238.75	55.8408427	.9254160
BIRPS	BM87-1	204	161	19	16	27.242	239.41	55.8406605	.9247154
BIRPS	BM87-1	205	161	19	16	49.692	239.20	55.8404725	.9240076
BIRPS	BM87-1	206	161	19	17	12.092	239.95	55.8402702	.9232503
BIRPS	BM87-1	207	161	19	17	34.942	240.07	55.8400859	.9225629
BIRPS	BM87-1	208	161	19	17	58.025	241.07	55.8398895	.9218261
BIRPS	BM87-1	209	161	19	18	21.742	241.60	55.8397062	.9211198
BIRPS	BM87-1	210	161	19	18	44.625	241.39	55.8395110	.9203357
BIRPS	BM87-1	211	161	19	19	07.175	242.37	55.8393293	.9196271
BIRPS	BM87-1	212	161	19	19	29.359	242.24	55.8391638	.9189041
BIRPS	BM87-1	213	161	19	19	51.642	242.79	55.8389764	.9181639
BIRPS	BM87-1	214	161	19	20	13.192	242.67	55.8388175	.9174240
BIRPS	BM87-1	215	161	19	20	34.859	242.73	55.8386429	.9166894
BIRPS	BM87-1	216	161	19	20	56.742	244.69	55.8384660	.9159833
BIRPS	BM87-1	217	161	19	21	19.192	243.55	55.8383056	.9152641
BIRPS	BM87-1	218	161	19	21	41.942	243.41	55.8381210	.9144772
BIRPS	BM87-1	219	161	19	22	04.642	244.11	55.8379552	.9137482
BIRPS	BM87-1	220	161	19	22	27.409	245.13	55.8377909	.9130066
BIRPS	BM87-1	221	161	19	22	49.709	244.67	55.8376308	.9122696
BIRPS	BM87-1	222	161	19	23	11.892	245.29	55.8374896	.9115300
BIRPS	BM87-1	223	161	19	23	34.359	244.94	55.8373248	.9107172
BIRPS	BM87-1	224	161	19	23	56.709	243.63	55.8371834	.9099679
BIRPS	BM87-1	225	161	19	24	18.675	243.62	55.8370365	.9092477
BIRPS	BM87-1	226	161	19	24	41.809	242.86	55.8368658	.9085217
BIRPS	BM87-1	227	161	19	25	04.242	242.91	55.8366863	.9077411
BIRPS	BM87-1	228	161	19	25	26.825	243.46	55.8365353	.9070213
BIRPS	BM87-1	229	161	19	25	49.409	242.12	55.8363825	.9062934
BIRPS	BM87-1	230	161	19	26	12.342	241.96	55.8362120	.9054905
BIRPS	BM87-1	231	161	19	26	34.875	241.51	55.8360764	.9047616
BIRPS	BM87-1	232	161	19	26	57.475	241.55	55.8359321	.9040440
BIRPS	BM87-1	233	161	19	27	20.692	240.19	55.8357548	.9032537
BIRPS	BM87-1	234	161	19	27	42.992	240.79	55.8355812	.9025404
BIRPS	BM87-1	235	161	19	28	05.575	239.87	55.8354117	.9018185
BIRPS	BM87-1	236	161	19	28	28.509	238.48	55.8352240	.9010465
BIRPS	BM87-1	237	161	19	28	51.692	238.73	55.8350419	.9003510
BIRPS	BM87-1	238	161	19	29	14.492	238.44	55.8348356	.8995756
BIRPS	BM87-1	239	161	19	29	36.975	238.69	55.8346475	.8988580
BIRPS	BM87-1	240	161	19	29	58.559	239.22	55.8344633	.8981297
BIRPS	BM87-1	241	161	19	30	20.725	239.08	55.8342637	.8974150
BIRPS	BM87-1	242	161	19	30	42.392	240.19	55.8340775	.8967301

BIRPS	BM87-1	243	161	19	31	05.425	240.01	55.8338878	.8960481
BIRPS	BM87-1	244	161	19	31	28.809	240.69	55.8336797	.8953052
BIRPS	BM87-1	245	161	19	31	51.942	240.92	55.8334783	.8945510
BIRPS	BM87-1	246	161	19	32	14.992	242.51	55.8332996	.8938431
BIRPS	BM87-1	247	161	19	32	37.325	241.74	55.8331268	.8931273
BIRPS	BM87-1	248	161	19	32	59.609	241.99	55.8329474	.8924157
BIRPS	BM87-1	249	161	19	33	22.159	242.48	55.8327537	.8916248
BIRPS	BM87-1	250	161	19	33	44.311	243.37	55.8325852	.8908931
BIRPS	BM87-1	251	161	19	34	06.627	243.26	55.8324133	.8901548
BIRPS	BM87-1	252	161	19	34	28.959	242.86	55.8322445	.8894197
BIRPS	BM87-1	253	161	19	34	50.709	242.98	55.8320708	.8886988
BIRPS	BM87-1	254	161	19	35	12.675	244.33	55.8318851	.8879798
BIRPS	BM87-1	255	161	19	35	35.209	245.23	55.8316997	.8872388
BIRPS	BM87-1	256	161	19	35	56.659	244.91	55.8315281	.8864821
BIRPS	BM87-1	257	161	19	36	18.359	244.73	55.8313718	.8857218
BIRPS	BM87-1	258	161	19	36	39.975	245.23	55.8312074	.8849669
BIRPS	BM87-1	259	161	19	37	01.659	245.04	55.8310518	.8842627
BIRPS	BM87-1	260	161	19	37	22.509	245.26	55.8309107	.8834838
BIRPS	BM87-1	261	161	19	37	44.125	244.23	55.8307530	.8827036
BIRPS	BM87-1	262	161	19	38	05.325	244.40	55.8306109	.8820228
BIRPS	BM87-1	263	161	19	38	26.892	244.18	55.8304598	.8812829
BIRPS	BM87-1	264	161	19	38	49.159	244.38	55.8303073	.8805423
BIRPS	BM87-1	265	161	19	39	11.392	244.02	55.8301583	.8797805
BIRPS	BM87-1	266	161	19	39	33.175	242.89	55.8300008	.8790177
BIRPS	BM87-1	267	161	19	39	54.459	242.67	55.8298398	.8782462
BIRPS	BM87-1	268	161	19	40	16.259	241.45	55.8296675	.8774643
BIRPS	BM87-1	269	161	19	40	37.209	241.25	55.8295219	.8767748
BIRPS	BM87-1	270	161	19	40	58.509	240.57	55.8293386	.8760260
BIRPS	BM87-1	271	161	19	41	20.409	241.00	55.8291680	.8753014
BIRPS	BM87-1	272	161	19	41	43.025	240.33	55.8289918	.8745620
BIRPS	BM87-1	273	161	19	42	05.075	239.37	55.8287998	.8738272
BIRPS	BM87-1	274	161	19	42	26.459	240.59	55.8286229	.8731015
BIRPS	BM87-1	275	161	19	42	48.792	238.88	55.8284433	.8723703
BIRPS	BM87-1	276	161	19	43	10.725	239.14	55.8282531	.8716410
BIRPS	BM87-1	277	161	19	43	32.275	239.76	55.8280589	.8709118
BIRPS	BM87-1	278	161	19	43	54.042	240.34	55.8278604	.8701809
BIRPS	BM87-1	279	161	19	44	15.825	240.38	55.8276837	.8695305
BIRPS	BM87-1	280	161	19	44	38.075	240.31	55.8274973	.8688074
BIRPS	BM87-1	281	161	19	45	00.759	239.56	55.8272773	.8680247
BIRPS	BM87-1	282	161	19	45	23.242	240.14	55.8270735	.8673102
BIRPS	BM87-1	283	161	19	45	45.059	241.15	55.8268837	.8666229
BIRPS	BM87-1	284	161	19	46	08.192	242.12	55.8267055	.8659158
BIRPS	BM87-1	285	161	19	46	31.059	243.22	55.8265169	.8651173
BIRPS	BM87-1	286	161	19	46	53.059	243.26	55.8263597	.8643574
BIRPS	BM87-1	287	161	19	47	14.709	242.57	55.8261824	.8635948
BIRPS	BM87-1	288	161	19	47	35.942	243.19	55.8260124	.8629162
BIRPS	BM87-1	289	161	19	47	56.959	243.90	55.8258278	.8621713
BIRPS	BM87-1	290	161	19	48	18.442	245.00	55.8256720	.8614930
BIRPS	BM87-1	291	161	19	48	40.242	245.22	55.8255018	.8607478
BIRPS	BM87-1	292	161	19	49	02.242	244.87	55.8253467	.8600012
BIRPS	BM87-1	293	161	19	49	24.392	244.58	55.8251920	.8592355
BIRPS	BM87-1	294	161	19	49	45.992	244.32	55.8250331	.8584559
BIRPS	BM87-1	295	161	19	50	06.892	243.90	55.8248756	.8576822
BIRPS	BM87-1	296	161	19	50	28.092	244.17	55.8247317	.8569594
BIRPS	BM87-1	297	161	19	50	48.842	243.72	55.8245626	.8561907
BIRPS	BM87-1	298	161	19	51	10.075	243.09	55.8244343	.8554991
BIRPS	BM87-1	299	161	19	51	31.825	241.68	55.8242902	.8547382
BIRPS	BM87-1	300	161	19	51	53.809	240.89	55.8241195	.8540023
BIRPS	BM87-1	301	161	19	52	15.792	241.06	55.8239358	.8532882
BIRPS	BM87-1	302	161	19	52	38.125	241.57	55.8237538	.8525772
BIRPS	BM87-1	303	161	19	53	00.659	241.72	55.8235570	.8517712
BIRPS	BM87-1	304	161	19	53	22.692	241.14	55.8233806	.8510197
BIRPS	BM87-1	305	161	19	53	44.359	241.04	55.8232128	.8503446
BIRPS	BM87-1	306	161	19	54	05.842	241.16	55.8230500	.8495787
BIRPS	BM87-1	307	161	19	54	27.275	240.01	55.8228837	.8488266
BIRPS	BM87-1	308	161	19	54	49.642	239.75	55.8227129	.8481058
BIRPS	BM87-1	309	161	19	55	11.592	239.87	55.8225430	.8473778
BIRPS	BM87-1	310	161	19	55	33.675	239.47	55.8223725	.8466708
BIRPS	BM87-1	311	161	19	55	56.609	239.66	55.8221826	.8459509
BIRPS	BM87-1	312	161	19	56	18.925	240.39	55.8219859	.8451723
BIRPS	BM87-1	313	161	19	56	41.292	240.11	55.8218225	.8444484
BIRPS	BM87-1	314	161	19	57	04.242	239.66	55.8216441	.8437150
BIRPS	BM87-1	315	161	19	57	26.375	239.71	55.8214522	.8429865
BIRPS	BM87-1	316	161	19	57	48.392	239.92	55.8212559	.8422702
BIRPS	BM87-1	317	161	19	58	10.575	240.37	55.8210500	.8415656
BIRPS	BM87-1	318	161	19	58	32.692	241.57	55.8208309	.8408028
BIRPS	BM87-1	319	161	19	58	55.075	242.58	55.8206474	.8400796
BIRPS	BM87-1	320	161	19	59	17.209	242.70	55.8204683	.8393557
BIRPS	BM87-1	321	161	19	59	39.642	242.20	55.8202977	.8386329
BIRPS	BM87-1	322	161	20	00	01.775	242.62	55.8201070	.8379104
BIRPS	BM87-1	323	161	20	00	23.459	242.78	55.8199127	.8371712
BIRPS	BM87-1	324	161	20	00	44.559	242.53	55.8197473	.8364863
BIRPS	BM87-1	325	161	20	01	05.959	243.40	55.8195583	.8357314
BIRPS	BM87-1	326	161	20	01	26.825	244.66	55.8193807	.8349931
BIRPS	BM87-1	327	161	20	01	48.692	244.90	55.8192166	.8342591
BIRPS	BM87-1	328	161	20	02	11.059	246.56	55.8184759	.8324470
BIRPS	BM87-1	329	161	20	02	28.592	249.73	55.8183429	.8319057
BIRPS	BM87-1	330	161	20	02	46.009	251.78	55.8182049	.8312831
BIRPS	BM87-1	331	161	20	03	03.375	252.17	55.8181052	.8306378
BIRPS	BM87-1	332	161	20	03	37.772	252.91	55.8180367	.8300491
BIRPS	BM87-1	333	161	20	03	37.975	252.57	55.8179508	.8293958
BIRPS	BM87-1	334	161	20	03	55.459	251.04	55.8178608	.8287230
BIRPS	BM87-1	335	161	20	04	13.409	250.56	55.8177648	.8280642
BIRPS	BM87-1	336	161	20	04	32.742	250.32	55.8176435	.8273346
BIRPS	BM87-1	337	161	20	04	52.159	249.83	55.8175516	.8266821
BIRPS	BM87-1	338	161	20	05	12.642	249.37	55.8174327	.8259773
BIRPS	BM87-1	339	161	20	05	33.375	248.48	55.8173159	.8252135
BIRPS	BM87-1	340	161	20	05	55.525	246.93	55.8171846	.8244472
BIRPS	BM87-1	341	161	20	06	16.975	246.39	55.8170541	.8236956
BIRPS	BM87-1	342	161	20	06	39.075	245.09	55.8169029	.8229236
BIRPS	BM87-1	343	161	20	07	00.392	243.90	55.8167625	.8222094
BIRPS	BM87-1	344	161	20	07	21.092	243.17	55.8166201	.8214490
BIRPS	BM87-1	345	161	20	07	42.859	241.90	55.8164782	.8207601
BIRPS	BM87-1	346	161	20	08	04.775	241.63	55.8163053	.8200209
BIRPS	BM87-1	347	161	20	08	26.609	241.11	55.8161225	.8192741
BIRPS	BM87-1	348	161	20	08	48.142	240.89	55.8159532	.8185378
BIRPS	BM87-1	349	161	20	09	09.959	239.87	55.8157713	.8178139
BIRPS	BM87-1	350	161	20	09	32.042	238.28	55.8155906	.8171089
BIRPS	BM87-1	351	161	20	09	54.642	237.48	55.8153955	.8164103
BIRPS	BM87-1	352	161	20	10	17.225	237.49	55.8151845	.8156374
BIRPS	BM87-1	353	161	20	10	39.625	237.26	55.8149788	.8149186
BIRPS	BM87-1	354	161	20	11	01.625	237.88	55.8147787	.8142090
BIRPS	BM87-1	355	161	20	11	23.942	238.31	55.8145753	.8134919
BIRPS	BM87-1	356	161	20	11	45.725	238.44	55.8143758	.8127847
BIRPS	BM87-1	357	161	20	12	07.775	238.33	55.8141715	.8120871
BIRPS	BM87-1	358	161	20	12	29.925	238.27	55.8139868	.8113801
BIRPS	BM87-1	359	161	20	12	52.425	238.98	55.8137833	.8106762
BIRPS	BM87-1	360	161	20	13	14.909	240.76	55.8135679	.8099185
BIRPS	BM87-1	361	161	20	13	37.492	240.54	55.8133800	.8091906
BIRPS	BM87-1	362	161	20	13	59.692	240.81	55.8131895	.8084413

BIRPS	BM87-1	363	161	20	14	20.525	241.41	55.8129958	.8077436
BIRPS	BM87-1	364	161	20	14	41.192	242.01	55.8128140	.8069922
BIRPS	BM87-1	365	161	20	15	02.475	242.24	55.8126564	.8063201
BIRPS	BM87-1	366	161	20	15	24.175	242.71	55.8124763	.8055946
BIRPS	BM87-1	367	161	20	15	45.875	242.70	55.8122976	.8048396
BIRPS	BM87-1	368	161	20	16	07.475	242.76	55.8121085	.8040835
BIRPS	BM87-1	369	161	20	16	29.009	243.93	55.8119470	.8033899
BIRPS	BM87-1	370	161	20	16	50.342	244.38	55.8117796	.8026157
BIRPS	BM87-1	371	161	20	17	11.409	243.73	55.8116167	.8018429
BIRPS	BM87-1	372	161	20	17	32.692	243.33	55.8114696	.8011406
BIRPS	BM87-1	373	161	20	17	53.875	242.59	55.8113084	.8003640
BIRPS	BM87-1	374	161	20	18	15.409	244.15	55.8111349	.7996116
BIRPS	BM87-1	375	161	20	18	36.842	244.35	55.8109865	.7989025
BIRPS	BM87-1	376	161	20	18	58.092	244.19	55.8108269	.7981315
BIRPS	BM87-1	377	161	20	19	19.259	244.10	55.8106664	.7973716
BIRPS	BM87-1	378	161	20	19	41.009	243.33	55.8105200	.7966824
BIRPS	BM87-1	379	161	20	20	02.775	243.16	55.8103458	.7959335
BIRPS	BM87-1	380	161	20	20	24.609	241.93	55.8101737	.7951699
BIRPS	BM87-1	381	161	20	20	46.009	242.03	55.8099853	.7944072
BIRPS	BM87-1	382	161	20	21	06.675	243.13	55.8098186	.7937190
BIRPS	BM87-1	383	161	20	21	27.909	243.21	55.8096427	.7929560
BIRPS	BM87-1	384	161	20	21	49.475	242.15	55.8094621	.7921945
BIRPS	BM87-1	385	161	20	22	10.692	241.98	55.8092970	.7915124
BIRPS	BM87-1	386	161	20	22	32.159	242.18	55.8090979	.7907807
BIRPS	BM87-1	387	161	20	22	53.692	242.99	55.8088903	.7900670
BIRPS	BM87-1	388	161	20	23	15.809	243.56	55.8087011	.7893476
BIRPS	BM87-1	389	161	20	23	38.225	244.91	55.8085172	.7886209
BIRPS	BM87-1	390	161	20	24	00.259	244.65	55.8083486	.7878701
BIRPS	BM87-1	391	161	20	24	21.909	245.05	55.8081860	.7870981
BIRPS	BM87-1	392	161	20	24	43.375	245.33	55.8080463	.7864021
BIRPS	BM87-1	393	161	20	25	04.792	243.93	55.8078864	.7856229
BIRPS	BM87-1	394	161	20	25	25.759	243.29	55.8077227	.7848707
BIRPS	BM87-1	395	161	20	25	47.442	243.19	55.8075537	.7841440
BIRPS	BM87-1	396	161	20	26	09.875	243.20	55.8073816	.7834190
BIRPS	BM87-1	397	161	20	26	32.342	243.67	55.8072179	.7826914
BIRPS	BM87-1	398	161	20	26	54.609	244.31	55.8070537	.7819514
BIRPS	BM87-1	399	161	20	27	16.692	242.80	55.8068989	.7812060
BIRPS	BM87-1	400	161	20	27	38.642	241.76	55.8067328	.7804685
BIRPS	BM87-1	401	161	20	28	00.742	241.83	55.8065462	.7797326
BIRPS	BM87-1	402	161	20	28	22.375	241.88	55.8063571	.7790050
BIRPS	BM87-1	403	161	20	28	44.175	242.46	55.8061687	.7782703
BIRPS	BM87-1	404	161	20	29	06.342	242.12	55.8059936	.7775309
BIRPS	BM87-1	405	161	20	29	27.742	241.82	55.8058358	.7767931
BIRPS	BM87-1	406	161	20	29	50.192	241.51	55.8056663	.7760650
BIRPS	BM87-1	407	161	20	30	12.559	242.02	55.8054814	.7753612
BIRPS	BM87-1	408	161	20	30	35.225	241.89	55.8052873	.7746600
BIRPS	BM87-1	409	161	20	30	57.842	241.93	55.8050727	.7738604
BIRPS	BM87-1	410	161	20	31	19.542	242.66	55.8048742	.7731303
BIRPS	BM87-1	411	161	20	31	41.192	244.70	55.8047100	.7724649
BIRPS	BM87-1	412	161	20	32	03.159	245.13	55.8045319	.7717208
BIRPS	BM87-1	413	161	20	32	25.109	244.61	55.8043644	.7709760
BIRPS	BM87-1	414	161	20	32	47.042	244.88	55.8042039	.7702271
BIRPS	BM87-1	415	161	20	33	08.942	243.55	55.8040495	.7694557
BIRPS	BM87-1	416	161	20	33	30.259	242.96	55.8038842	.7687137
BIRPS	BM87-1	417	161	20	33	52.459	242.75	55.8037083	.7680020
BIRPS	BM87-1	418	161	20	34	14.842	243.11	55.8035174	.7672812
BIRPS	BM87-1	419	161	20	34	36.842	244.74	55.8033238	.7665706
BIRPS	BM87-1	420	161	20	34	58.842	245.39	55.8031431	.7658544
BIRPS	BM87-1	421	161	20	35	21.227	245.52	55.8029792	.7651176
BIRPS	BM87-1	422	161	20	35	43.661	245.53	55.8027040	.7641910
BIRPS	BM87-1	423	161	20	36	04.542	246.41	55.8025604	.7635138
BIRPS	BM87-1	424	161	20	36	25.475	246.37	55.8024138	.7628279
BIRPS	BM87-1	425	161	20	36	46.659	246.74	55.8022515	.7620688
BIRPS	BM87-1	426	161	20	37	07.692	245.72	55.8020868	.7613070
BIRPS	BM87-1	427	161	20	37	28.825	245.56	55.8019410	.7605945
BIRPS	BM87-1	428	161	20	37	49.375	244.60	55.8017878	.7598784
BIRPS	BM87-1	429	161	20	38	09.942	244.03	55.8016010	.7591187
BIRPS	BM87-1	430	161	20	38	30.775	244.99	55.8014483	.7584363
BIRPS	BM87-1	431	161	20	38	52.159	245.26	55.8012633	.7576491
BIRPS	BM87-1	432	161	20	39	14.259	246.32	55.8011004	.7569554
BIRPS	BM87-1	433	161	20	39	36.542	246.84	55.8009555	.7562037
BIRPS	BM87-1	434	161	20	39	58.459	245.66	55.8008183	.7554406
BIRPS	BM87-1	435	161	20	40	20.359	243.44	55.8006697	.7546829
BIRPS	BM87-1	436	161	20	40	42.642	242.46	55.8005133	.7539404
BIRPS	BM87-1	437	161	20	41	04.409	242.67	55.8003302	.7531885
BIRPS	BM87-1	438	161	20	41	26.075	242.95	55.8001469	.7524146
BIRPS	BM87-1	439	161	20	41	46.925	242.73	55.7999745	.7517087
BIRPS	BM87-1	440	161	20	42	07.242	243.00	55.7998223	.7510026
BIRPS	BM87-1	441	161	20	42	28.259	242.28	55.7996523	.7502073
BIRPS	BM87-1	442	161	20	42	49.142	240.06	55.7994976	.7494977
BIRPS	BM87-1	443	161	20	43	09.892	239.90	55.7993329	.7488345
BIRPS	BM87-1	444	161	20	43	31.825	239.62	55.7991474	.7481098
BIRPS	BM87-1	445	161	20	43	54.092	240.26	55.7989413	.7473432
BIRPS	BM87-1	446	161	20	44	16.792	240.70	55.7987498	.7466328
BIRPS	BM87-1	447	161	20	44	39.025	240.80	55.7985570	.7459027
BIRPS	BM87-1	448	161	20	45	00.809	240.20	55.7983693	.7451689
BIRPS	BM87-1	449	161	20	45	22.375	239.75	55.7981669	.7444168
BIRPS	BM87-1	450	161	20	45	43.642	241.07	55.7979945	.7437477
BIRPS	BM87-1	451	161	20	46	05.342	241.77	55.7977979	.7430081
BIRPS	BM87-1	452	161	20	46	26.609	241.34	55.7976175	.7422650
BIRPS	BM87-1	453	161	20	46	48.609	241.99	55.7974402	.7415329
BIRPS	BM87-1	454	161	20	47	11.059	241.95	55.7972594	.7408107
BIRPS	BM87-1	455	161	20	47	33.159	242.23	55.7970752	.7400866
BIRPS	BM87-1	456	161	20	47	55.075	242.46	55.7968892	.7393546
BIRPS	BM87-1	457	161	20	48	16.675	242.98	55.7967038	.7386066
BIRPS	BM87-1	458	161	20	48	38.475	242.96	55.7965087	.7378472
BIRPS	BM87-1	459	161	20	48	59.842	242.96	55.7963234	.7371623
BIRPS	BM87-1	460	161	20	49	20.625	243.76	55.7961198	.7363885
BIRPS	BM87-1	461	161	20	49	41.142	244.74	55.7959429	.7356818
BIRPS	BM87-1	462	161	20	50	01.442	245.75	55.7958022	.7349788
BIRPS	BM87-1	463	161	20	50	22.475	244.97	55.7956489	.7341890
BIRPS	BM87-1	464	161	20	50	43.725	243.90	55.7955064	.7334895
BIRPS	BM87-1	465	161	20	51	05.309	243.39	55.7953362	.7327478
BIRPS	BM87-1	466	161	20	51	27.142	244.14	55.7951569	.7320100
BIRPS	BM87-1	467	161	20	51	49.609	244.63	55.7949833	.7312633
BIRPS	BM87-1	468	161	20	52	11.242	244.32	55.7948126	.7304952
BIRPS	BM87-1	469	161	20	52	32.325	244.84	55.7945527	.7294702
BIRPS	BM87-1	470	161	20	52	51.192	244.17	55.7943878	.7287717
BIRPS	BM87-1	471	161	20	53	10.192	244.99	55.7942415	.7281467
BIRPS	BM87-1	472	161	20	53	30.025	245.14	55.7940775	.7274474
BIRPS	BM87-1	473	161	20	53	50.175	244.54	55.7939147	.7267496
BIRPS	BM87-1	474	161	20	54	10.459	245.86	55.7937418	.7259996
BIRPS	BM87-1	475	161	20	54	31.459	245.67	55.7936021	.7253120
BIRPS	BM87-1	476	161	20	54	52.725	243.78	55.7934475	.7245605
BIRPS	BM87-1	477	161	20	55	14.409	243.78	55.7933008	.7238182
BIRPS	BM87-1	478	161	20	55	36.525	242.81	55.7931381	.7230645
BIRPS	BM87-1	479	161	20	55	58.092	243.32	55.7929899	.7223697
BIRPS	BM87-1	480	161	20	56	19.475	243.31	55.7928195	.7216067
BIRPS	BM87-1	481	161	20	56	40.525	242.11	55.7926450	.7208565

BIRPS	BM87-1	483	161	20	57	23.759	241.55	55.7922883	.7194524
BIRPS	BM87-1	484	161	20	57	45.309	241.12	55.7920878	.7187259
BIRPS	BM87-1	485	161	20	58	06.925	241.93	55.7918823	.7180145
BIRPS	BM87-1	486	161	20	58	29.309	243.63	55.7916863	.7173061
BIRPS	BM87-1	487	161	20	58	51.292	244.79	55.7915076	.7165642
BIRPS	BM87-1	488	161	20	59	13.075	243.72	55.7913409	.7157935
BIRPS	BM87-1	489	161	20	59	34.775	244.04	55.7911614	.7150316
BIRPS	BM87-1	490	161	20	59	55.942	243.80	55.7909898	.7143345
BIRPS	BM87-1	491	161	21	00	16.809	243.85	55.7908125	.7135761
BIRPS	BM87-1	492	161	21	00	38.075	243.41	55.7906558	.7128950
BIRPS	BM87-1	493	161	21	00	59.692	243.64	55.7904732	.7121391
BIRPS	BM87-1	494	161	21	01	20.659	243.99	55.7902906	.7113883
BIRPS	BM87-1	495	161	21	01	42.175	244.51	55.7901242	.7107098
BIRPS	BM87-1	496	161	21	02	03.725	245.26	55.7899360	.7099350
BIRPS	BM87-1	497	161	21	02	24.375	245.45	55.7897707	.7092227
BIRPS	BM87-1	498	161	21	02	45.109	244.61	55.7895960	.7084314
BIRPS	BM87-1	499	161	21	03	05.775	243.66	55.7894348	.7076976
BIRPS	BM87-1	500	161	21	03	25.642	243.38	55.7892975	.7069715
BIRPS	BM87-1	501	161	21	03	46.925	243.27	55.7891165	.7062085
BIRPS	BM87-1	502	161	21	04	08.175	244.35	55.7889444	.7055246
BIRPS	BM87-1	503	161	21	04	29.275	243.69	55.7887543	.7047649
BIRPS	BM87-1	504	161	21	04	50.525	243.16	55.7885828	.7040880
BIRPS	BM87-1	505	161	21	05	12.075	244.05	55.7883962	.7033558
BIRPS	BM87-1	506	161	21	05	33.775	244.48	55.7882187	.7025927
BIRPS	BM87-1	507	161	21	05	55.042	244.22	55.7880403	.7018124
BIRPS	BM87-1	508	161	21	06	16.025	244.04	55.7878798	.7011152
BIRPS	BM87-1	509	161	21	06	36.942	243.23	55.7877128	.7003517
BIRPS	BM87-1	510	161	21	06	58.392	243.97	55.7875595	.6996746
BIRPS	BM87-1	511	161	21	07	20.159	244.28	55.7873809	.6989352
BIRPS	BM87-1	512	161	21	07	42.109	244.36	55.7872100	.6982106
BIRPS	BM87-1	513	161	21	08	04.642	243.39	55.7870401	.6974895
BIRPS	BM87-1	514	161	21	08	27.425	244.07	55.7868392	.6967067
BIRPS	BM87-1	515	161	21	08	50.192	242.78	55.7866573	.6959553
BIRPS	BM87-1	516	161	21	09	11.125	243.93	55.7864906	.6951998
BIRPS	BM87-1	517	161	21	09	32.675	243.90	55.7863456	.6944834
BIRPS	BM87-1	518	161	21	09	53.792	242.79	55.7861765	.6936994
BIRPS	BM87-1	519	161	21	10	14.309	243.01	55.7860195	.6929961
BIRPS	BM87-1	520	161	21	10	35.092	242.80	55.7858332	.6922329
BIRPS	BM87-1	521	161	21	10	56.292	242.00	55.7856664	.6915317
BIRPS	BM87-1	522	161	21	11	17.159	242.48	55.7854724	.6907758
BIRPS	BM87-1	523	161	21	11	38.325	242.47	55.7852989	.6901001
BIRPS	BM87-1	524	161	21	11	59.609	242.71	55.7851058	.6893503
BIRPS	BM87-1	525	161	21	12	21.259	242.79	55.7849272	.6885630
BIRPS	BM87-1	526	161	21	12	42.242	242.44	55.7847648	.6878500
BIRPS	BM87-1	527	161	21	13	02.742	243.06	55.7846014	.6871539
BIRPS	BM87-1	528	161	21	13	23.825	243.15	55.7844156	.6863926
BIRPS	BM87-1	529	161	21	13	45.275	242.98	55.7842622	.6856865
BIRPS	BM87-1	530	161	21	14	06.592	242.36	55.7841016	.6849244
BIRPS	BM87-1	531	161	21	14	27.909	241.56	55.7839175	.6841719
BIRPS	BM87-1	532	161	21	14	49.759	240.70	55.7837319	.6834505
BIRPS	BM87-1	533	161	21	15	11.975	241.46	55.7835358	.6827343
BIRPS	BM87-1	534	161	21	15	34.192	242.43	55.7833379	.6820145
BIRPS	BM87-1	535	161	21	15	56.342	242.94	55.7831541	.6812767
BIRPS	BM87-1	536	161	21	16	18.225	242.83	55.7829828	.6805226
BIRPS	BM87-1	537	161	21	16	40.059	242.27	55.7828045	.6797475
BIRPS	BM87-1	538	161	21	17	00.909	241.83	55.7826328	.6790532
BIRPS	BM87-1	539	161	21	17	21.359	242.57	55.7824617	.6783711
BIRPS	BM87-1	540	161	21	17	42.675	242.82	55.7822670	.6776249
BIRPS	BM87-1	541	161	21	18	04.625	243.30	55.7820760	.6768816
BIRPS	BM87-1	542	161	21	18	26.242	243.39	55.7818989	.6761326
BIRPS	BM87-1	543	161	21	18	47.775	243.55	55.7817408	.6754654
BIRPS	BM87-1	544	161	21	19	09.609	243.25	55.7815672	.6747356
BIRPS	BM87-1	545	161	21	19	31.809	244.19	55.7813897	.6740055
BIRPS	BM87-1	546	161	21	19	54.042	244.41	55.7812043	.6731995
BIRPS	BM87-1	547	161	21	20	16.092	243.83	55.7810384	.6724358
BIRPS	BM87-1	548	161	21	20	37.542	244.01	55.7808846	.6717562
BIRPS	BM87-1	549	161	21	20	59.025	244.16	55.7807150	.6710240
BIRPS	BM87-1	550	161	21	21	21.042	243.94	55.7805370	.6703115
BIRPS	BM87-1	551	161	21	21	43.459	243.78	55.7803526	.6695881
BIRPS	BM87-1	552	161	21	22	05.692	244.29	55.7801806	.6688541
BIRPS	BM87-1	553	161	21	22	27.709	243.97	55.7800222	.6681114
BIRPS	BM87-1	554	161	21	22	49.825	243.76	55.7798563	.6673560
BIRPS	BM87-1	555	161	21	23	11.525	243.64	55.7796734	.6665992
BIRPS	BM87-1	556	161	21	23	32.642	244.18	55.7794864	.6658311
BIRPS	BM87-1	557	161	21	23	53.542	244.65	55.7793161	.6651193
BIRPS	BM87-1	558	161	21	24	14.059	244.96	55.7791518	.6644024
BIRPS	BM87-1	559	161	21	24	34.742	245.93	55.7789849	.6636311
BIRPS	BM87-1	560	161	21	24	56.009	244.10	55.7788590	.6629184
BIRPS	BM87-1	561	161	21	25	17.542	242.19	55.7787143	.6621551
BIRPS	BM87-1	562	161	21	25	39.142	241.72	55.7785537	.6614138
BIRPS	BM87-1	563	161	21	26	01.075	241.89	55.7783688	.6606576
BIRPS	BM87-1	564	161	21	26	22.259	242.10	55.7781887	.6598961
BIRPS	BM87-1	565	161	21	26	43.575	241.24	55.7780192	.6592172
BIRPS	BM87-1	566	161	21	27	04.792	242.17	55.7778300	.6584756
BIRPS	BM87-1	567	161	21	27	26.742	242.41	55.7776484	.6577256
BIRPS	BM87-1	568	161	21	27	48.609	241.85	55.7774804	.6570022
BIRPS	BM87-1	569	161	21	28	11.025	241.70	55.7772965	.6563017
BIRPS	BM87-1	570	161	21	28	33.725	241.41	55.7770966	.6556181
BIRPS	BM87-1	571	161	21	28	56.575	241.87	55.7768796	.6548691
BIRPS	BM87-1	572	161	21	29	19.459	243.07	55.7766919	.6541627
BIRPS	BM87-1	573	161	21	29	41.692	243.94	55.7765132	.6534116
BIRPS	BM87-1	574	161	21	30	03.275	243.43	55.7763554	.6526300
BIRPS	BM87-1	575	161	21	30	24.142	242.77	55.7762075	.6519299
BIRPS	BM87-1	576	161	21	30	45.342	241.55	55.7760357	.6511815
BIRPS	BM87-1	577	161	21	31	07.142	240.46	55.7758346	.6504647
BIRPS	BM87-1	578	161	21	31	29.125	240.94	55.7756331	.6497816
BIRPS	BM87-1	579	161	21	31	51.575	242.85	55.7754381	.6490895
BIRPS	BM87-1	580	161	21	32	14.194	243.43	55.7752262	.6482939
BIRPS	BM87-1	581	161	21	32	36.227	244.24	55.7750304	.6475341
BIRPS	BM87-1	582	161	21	32	57.242	243.57	55.7748587	.6468224
BIRPS	BM87-1	583	161	21	33	17.492	243.49	55.7746868	.6461114
BIRPS	BM87-1	584	161	21	33	37.692	245.43	55.7745180	.6454069
BIRPS	BM87-1	585	161	21	33	58.509	245.97	55.7743306	.6446356
BIRPS	BM87-1	586	161	21	34	19.442	245.49	55.7741748	.6439393
BIRPS	BM87-1	587	161	21	34	40.409	246.54	55.7740007	.6431699
BIRPS	BM87-1	588	161	21	35	01.625	247.64	55.7738416	.6424616
BIRPS	BM87-1	589	161	21	35	22.542	247.62	55.7736709	.6416651
BIRPS	BM87-1	590	161	21	35	43.275	246.92	55.7735254	.6409508
BIRPS	BM87-1	591	161	21	36	04.092	246.83	55.7733777	.6402500
BIRPS	BM87-1	592	161	21	36	25.659	246.69	55.7731954	.6394872
BIRPS	BM87-1	593	161	21	36	46.925	247.74	55.7730159	.6387368
BIRPS	BM87-1	594	161	21	37	08.675	247.03	55.7728463	.6379658
BIRPS	BM87-1	595	161	21	37	30.375	246.39	55.7726652	.6371972
BIRPS	BM87-1	596	161	21	37	51.409	247.57	55.7725046	.6365069
BIRPS	BM87-1	597	161	21	38	12.425	246.64	55.7723329	.6357415
BIRPS	BM87-1	598	161	21	38	33.842	246.88	55.7721677	.6350511
BIRPS	BM87-1	599	161	21	38	55.159	247.06	55.7719919	.6343090
BIRPS	BM87-1	600	161	21	39	17.309	247.84	55.7718284	.6335553
BIRPS	BM87-1	601	161	21	39	38.725	247.49	55.7716781	.6327746
BIRPS	BM87-1	602	161	21	40	00.042	246.12	55.7715424	.6320517

BIRPS	BM87-1	603	161	21	40	21.159	244.83	55.7713794	.6312639
BIRPS	BM87-1	604	161	21	40	42.442	244.60	55.7712243	.6305603
BIRPS	BM87-1	605	161	21	41	03.442	243.85	55.7710448	.6297652
BIRPS	BM87-1	606	161	21	41	23.675	244.48	55.7708732	.6290638
BIRPS	BM87-1	607	161	21	41	43.975	244.61	55.7707165	.6283534
BIRPS	BM87-1	608	161	21	42	04.709	244.10	55.7705317	.6275622
BIRPS	BM87-1	609	161	21	42	25.192	243.77	55.7703667	.6268500
BIRPS	BM87-1	610	161	21	42	46.092	242.29	55.7701868	.6261276
BIRPS	BM87-1	611	161	21	43	06.092	242.88	55.7700031	.6254290
BIRPS	BM87-1	612	161	21	43	26.542	242.87	55.7698213	.6247332
BIRPS	BM87-1	613	161	21	43	47.459	242.71	55.7696293	.6239678
BIRPS	BM87-1	614	161	21	44	08.192	242.60	55.7694533	.6232811
BIRPS	BM87-1	615	161	21	44	29.475	243.36	55.7692480	.6225140
BIRPS	BM87-1	616	161	21	44	50.042	243.32	55.7690532	.6218115
BIRPS	BM87-1	617	161	21	45	10.292	243.66	55.7688626	.6211085
BIRPS	BM87-1	618	161	21	45	30.792	243.80	55.7686597	.6203346
BIRPS	BM87-1	619	161	21	45	51.475	243.57	55.7684630	.6196367
BIRPS	BM87-1	620	161	21	46	11.709	244.71	55.7682890	.6189617
BIRPS	BM87-1	621	161	21	46	32.875	244.51	55.7681007	.6182093
BIRPS	BM87-1	622	161	21	46	54.509	245.40	55.7679294	.6175185
BIRPS	BM87-1	623	161	21	47	15.825	245.01	55.7677580	.6167451
BIRPS	BM87-1	624	161	21	47	36.692	244.79	55.7675951	.6159598
BIRPS	BM87-1	625	161	21	47	57.809	245.22	55.7674419	.6152496
BIRPS	BM87-1	626	161	21	48	18.692	244.24	55.7672739	.6144399
BIRPS	BM87-1	627	161	21	48	39.292	244.07	55.7671063	.6137191
BIRPS	BM87-1	628	161	21	48	59.859	244.84	55.7669484	.6130150
BIRPS	BM87-1	629	161	21	49	20.559	245.33	55.7667792	.6123151
BIRPS	BM87-1	630	161	21	49	41.692	245.54	55.7666024	.6115608
BIRPS	BM87-1	631	161	21	50	02.892	246.02	55.7664404	.6107973
BIRPS	BM87-1	632	161	21	50	24.642	243.31	55.7662924	.6100813
BIRPS	BM87-1	633	161	21	50	45.709	242.22	55.7661164	.6092892
BIRPS	BM87-1	634	161	21	51	06.159	242.91	55.7659343	.6085826
BIRPS	BM87-1	635	161	21	51	26.709	244.53	55.7657375	.6078091
BIRPS	BM87-1	636	161	21	51	47.359	244.27	55.7655788	.6071069
BIRPS	BM87-1	637	161	21	52	08.825	243.89	55.7654142	.6064000
BIRPS	BM87-1	638	161	21	52	29.942	242.61	55.7652414	.6056352
BIRPS	BM87-1	639	161	21	52	50.909	242.40	55.7641430	.6017857
BIRPS	BM87-1	640	161	21	53	11.875	244.52	55.7639705	.6011123
BIRPS	BM87-1	641	161	21	53	33.159	246.30	55.7637924	.6003592
BIRPS	BM87-1	642	161	21	53	54.725	246.82	55.7636406	.5996506
BIRPS	BM87-1	643	161	21	54	15.992	246.10	55.7634755	.5988449
BIRPS	BM87-1	644	161	21	54	36.309	246.02	55.7633207	.5981263
BIRPS	BM87-1	645	161	21	54	56.675	246.12	55.7631592	.5974020
BIRPS	BM87-1	646	161	21	55	17.159	246.44	55.7629776	.5965998
BIRPS	BM87-1	647	161	21	55	37.292	246.63	55.7628266	.5958819
BIRPS	BM87-1	648	161	21	55	57.942	245.40	55.7626703	.5951540
BIRPS	BM87-1	649	161	21	56	18.359	245.36	55.7624978	.5944357
BIRPS	BM87-1	650	161	21	56	38.409	245.88	55.7623429	.5937198
BIRPS	BM87-1	651	161	21	56	59.292	246.53	55.7621655	.5929247
BIRPS	BM87-1	652	161	21	57	19.909	245.91	55.7620077	.5921889
BIRPS	BM87-1	653	161	21	57	39.975	245.08	55.7618548	.5914532
BIRPS	BM87-1	654	161	21	58	00.159	243.98	55.7616822	.5907329
BIRPS	BM87-1	655	161	21	58	20.392	245.28	55.7614897	.5900318
BIRPS	BM87-1	656	161	21	58	40.775	245.83	55.7613083	.5893298
BIRPS	BM87-1	657	161	21	59	01.609	245.91	55.7611300	.5885499
BIRPS	BM87-1	658	161	21	59	22.925	245.19	55.7609487	.5877567
BIRPS	BM87-1	659	161	21	59	43.525	244.89	55.7607854	.5870426
BIRPS	BM87-1	660	161	22	00	04.425	243.39	55.7606017	.5863330
BIRPS	BM87-1	661	161	22	00	24.642	243.34	55.7604331	.5856341
BIRPS	BM87-1	662	161	22	00	45.475	243.91	55.7602278	.5848528
BIRPS	BM87-1	663	161	22	01	06.259	244.37	55.7600453	.5841457
BIRPS	BM87-1	664	161	22	01	26.342	244.76	55.7598775	.5834357
BIRPS	BM87-1	665	161	22	01	46.792	244.51	55.7597107	.5827136
BIRPS	BM87-1	666	161	22	02	07.492	244.66	55.7595140	.5819291
BIRPS	BM87-1	667	161	22	02	28.192	245.06	55.7593258	.5812202
BIRPS	BM87-1	668	161	22	02	48.392	245.82	55.7591311	.5805296
BIRPS	BM87-1	669	161	22	03	08.909	246.23	55.7589351	.5798360
BIRPS	BM87-1	670	161	22	03	29.642	247.12	55.7587250	.5790891
BIRPS	BM87-1	671	161	22	03	50.809	248.42	55.7585551	.5784059
BIRPS	BM87-1	672	161	22	04	12.159	249.69	55.7583804	.5776148
BIRPS	BM87-1	673	161	22	04	33.409	248.80	55.7582205	.5767924
BIRPS	BM87-1	674	161	22	04	53.492	247.99	55.7580670	.5760469
BIRPS	BM87-1	675	161	22	05	13.392	247.38	55.7579275	.5753831
BIRPS	BM87-1	676	161	22	05	33.342	246.98	55.7577494	.5746363
BIRPS	BM87-1	677	161	22	05	53.009	248.72	55.7575825	.5739061
BIRPS	BM87-1	678	161	22	06	13.175	248.18	55.7574185	.5731716
BIRPS	BM87-1	679	161	22	06	33.309	248.30	55.7572684	.5724420
BIRPS	BM87-1	680	161	22	06	53.792	247.80	55.7570959	.5716465
BIRPS	BM87-1	681	161	22	07	14.459	246.88	55.7569395	.5709306
BIRPS	BM87-1	682	161	22	07	34.975	246.23	55.7567662	.5702225
BIRPS	BM87-1	683	161	22	07	55.592	246.44	55.7565653	.5694321
BIRPS	BM87-1	684	161	22	08	15.925	245.51	55.7563831	.5687084
BIRPS	BM87-1	685	161	22	08	36.309	246.67	55.7561910	.5679995
BIRPS	BM87-1	686	161	22	08	56.242	247.25	55.7559997	.5672797
BIRPS	BM87-1	687	161	22	09	15.909	248.36	55.7558308	.5665708
BIRPS	BM87-1	688	161	22	09	36.909	247.97	55.7556615	.5658603
BIRPS	BM87-1	689	161	22	09	57.875	246.76	55.7554597	.5650977
BIRPS	BM87-1	690	161	22	10	18.625	247.84	55.7552827	.5644152
BIRPS	BM87-1	691	161	22	10	39.609	248.18	55.7550749	.5636536
BIRPS	BM87-1	692	161	22	11	00.542	248.15	55.7548868	.5629384
BIRPS	BM87-1	693	161	22	11	20.609	249.52	55.7547048	.5622203
BIRPS	BM87-1	694	161	22	11	40.609	250.99	55.7545322	.5614829
BIRPS	BM87-1	695	161	22	12	00.392	251.46	55.7543635	.5607325
BIRPS	BM87-1	696	161	22	12	19.859	250.70	55.7540241	.5601500
BIRPS	BM87-1	697	161	22	12	39.375	252.64	55.7538665	.5594682
BIRPS	BM87-1	698	161	22	12	59.042	254.88	55.7536921	.5587165
BIRPS	BM87-1	699	161	22	13	18.975	256.26	55.7535462	.5579690
BIRPS	BM87-1	700	161	22	13	39.292	256.36	55.7534260	.5572061
BIRPS	BM87-1	701	161	22	13	59.992	254.96	55.7532993	.5563732
BIRPS	BM87-1	702	161	22	14	20.925	253.66	55.7531813	.5556181
BIRPS	BM87-1	703	161	22	14	41.509	252.14	55.7530514	.5548740
BIRPS	BM87-1	704	161	22	15	02.242	252.05	55.7528893	.5540706
BIRPS	BM87-1	705	161	22	15	23.209	252.48	55.7527342	.5533452
BIRPS	BM87-1	706	161	22	15	43.825	253.00	55.7525493	.5525556
BIRPS	BM87-1	707	161	22	16	04.392	253.03	55.7523884	.5518345
BIRPS	BM87-1	708	161	22	16	25.275	252.25	55.7522367	.5511217
BIRPS	BM87-1	709	161	22	16	46.159	251.47	55.7520609	.5503397
BIRPS	BM87-1	710	161	22	17	07.242	251.17	55.7518880	.5496399
BIRPS	BM87-1	711	161	22	17	28.009	251.08	55.7516830	.5488617
BIRPS	BM87-1	712	161	22	17	48.325	251.39	55.7515010	.5481518
BIRPS	BM87-1	713	161	22	18	08.725	251.86	55.7513242	.5474421
BIRPS	BM87-1	714	161	22	18	28.942	250.85	55.7511409	.5467016
BIRPS	BM87-1	715	161	22	18	48.542	251.50	55.7509633	.5459617
BIRPS	BM87-1	716	161	22	19	08.425	251.44	55.7507902	.5452209
BIRPS	BM87-1	717	161	22	19	28.425	251.39	55.7506181	.5444884
BIRPS	BM87-1	718	161	22	19	48.609	251.42	55.7504336	.5437650
BIRPS	BM87-1	719	161	22	20	08.825	251.92	55.7502419	.5430535
BIRPS	BM87-1	720	161	22	20	28.592	251.81	55.7500709	.5423443
BIRPS	BM87-1	721	161	22	20	49.392	251.73	55.7499060	.5416225

BIRPS	BM87-1	723	161	22	21	29.992	252.07	55.7495780	.5400676
BIRPS	BM87-1	724	161	22	21	49.875	251.19	55.7494349	.5393846
BIRPS	BM87-1	725	161	22	22	09.742	250.95	55.7492797	.5386447
BIRPS	BM87-1	726	161	22	22	29.809	249.66	55.7491183	.5379107
BIRPS	BM87-1	727	161	22	22	50.075	249.52	55.7489470	.5371870
BIRPS	BM87-1	728	161	22	23	10.559	250.33	55.7487616	.5363932
BIRPS	BM87-1	729	161	22	23	31.059	248.97	55.7486018	.5356572
BIRPS	BM87-1	730	161	22	23	51.075	248.78	55.7484358	.5349271
BIRPS	BM87-1	731	161	22	24	11.092	248.13	55.7482632	.5342018
BIRPS	BM87-1	732	161	22	24	31.192	248.44	55.7480756	.5334830
BIRPS	BM87-1	733	161	22	24	51.142	248.68	55.7479002	.5327576
BIRPS	BM87-1	734	161	22	25	11.092	247.69	55.7477264	.5320238
BIRPS	BM87-1	735	161	22	25	31.159	247.56	55.7475399	.5313099
BIRPS	BM87-1	736	161	22	25	51.309	247.68	55.7473648	.5306071
BIRPS	BM87-1	737	161	22	26	11.992	247.49	55.7471807	.5299023
BIRPS	BM87-1	738	161	22	26	32.759	247.97	55.7469849	.5291255
BIRPS	BM87-1	739	161	22	26	53.959	247.28	55.7467882	.5284109
BIRPS	BM87-1	740	161	22	27	14.242	248.23	55.7465621	.5276428
BIRPS	BM87-1	741	161	22	27	34.492	249.25	55.7463612	.5269322
BIRPS	BM87-1	742	161	22	27	54.559	250.01	55.7461831	.5262078
BIRPS	BM87-1	743	161	22	28	14.692	249.30	55.7460162	.5254661
BIRPS	BM87-1	744	161	22	28	34.759	249.68	55.7458414	.5247224
BIRPS	BM87-1	745	161	22	28	54.575	248.85	55.7456777	.5239639
BIRPS	BM87-1	746	161	22	29	13.992	248.10	55.7455179	.5232916
BIRPS	BM87-1	747	161	22	29	33.425	247.78	55.7453508	.5225488
BIRPS	BM87-1	748	161	22	29	52.959	247.46	55.7451578	.5218221
BIRPS	BM87-1	749	161	22	30	12.625	248.78	55.7449704	.5211124
BIRPS	BM87-1	750	161	22	30	33.011	249.02	55.7447876	.5203867
BIRPS	BM87-1	751	161	22	30	52.944	250.05	55.7446124	.5196518
BIRPS	BM87-1	752	161	22	31	12.742	250.61	55.7444574	.5189038
BIRPS	BM87-1	753	161	22	31	33.209	249.60	55.7443009	.5181520
BIRPS	BM87-1	754	161	22	31	52.959	248.71	55.7441407	.5174100
BIRPS	BM87-1	755	161	22	32	12.775	247.46	55.7439752	.5166678
BIRPS	BM87-1	756	161	22	32	33.009	247.18	55.7437944	.5159237
BIRPS	BM87-1	757	161	22	32	52.375	247.96	55.7436098	.5151810
BIRPS	BM87-1	758	161	22	33	12.125	247.99	55.7434471	.5145021
BIRPS	BM87-1	759	161	22	33	31.542	248.69	55.7432848	.5137540
BIRPS	BM87-1	760	161	22	33	51.175	248.31	55.7431214	.5130045
BIRPS	BM87-1	761	161	22	34	10.825	248.38	55.7429633	.5122593
BIRPS	BM87-1	762	161	22	34	31.325	246.30	55.7427858	.5115058
BIRPS	BM87-1	763	161	22	34	50.725	246.31	55.7425949	.5107840
BIRPS	BM87-1	764	161	22	35	10.942	247.35	55.7424021	.5100669
BIRPS	BM87-1	765	161	22	35	30.859	247.13	55.7422019	.5093306
BIRPS	BM87-1	766	161	22	35	50.692	247.90	55.7420167	.5086104
BIRPS	BM87-1	767	161	22	36	10.992	247.89	55.7418176	.5078854
BIRPS	BM87-1	768	161	22	36	30.425	248.28	55.7416277	.5071437
BIRPS	BM87-1	769	161	22	36	49.909	248.47	55.7414638	.5064724
BIRPS	BM87-1	770	161	22	37	09.609	249.13	55.7412716	.5057313
BIRPS	BM87-1	771	161	22	37	28.875	249.96	55.7410838	.5050112
BIRPS	BM87-1	772	161	22	37	49.192	250.23	55.7408977	.5042938
BIRPS	BM87-1	773	161	22	38	09.359	250.29	55.7407060	.5035835
BIRPS	BM87-1	774	161	22	38	29.475	250.78	55.7405321	.5028718
BIRPS	BM87-1	775	161	22	38	50.175	250.43	55.7403580	.5021507
BIRPS	BM87-1	776	161	22	39	10.842	250.29	55.7401702	.5013456
BIRPS	BM87-1	777	161	22	39	31.009	250.91	55.7400117	.5005985
BIRPS	BM87-1	778	161	22	39	51.242	251.21	55.7398758	.4998373
BIRPS	BM87-1	779	161	22	40	10.942	250.97	55.7397385	.4990619
BIRPS	BM87-1	780	161	22	40	30.959	249.91	55.7395983	.4982973
BIRPS	BM87-1	781	161	22	40	50.859	249.12	55.7394503	.4975529
BIRPS	BM87-1	782	161	22	41	10.859	247.96	55.7392957	.4968146
BIRPS	BM87-1	783	161	22	41	30.909	246.96	55.7391339	.4960733
BIRPS	BM87-1	784	161	22	41	51.325	247.29	55.7389424	.4953334
BIRPS	BM87-1	785	161	22	42	10.659	248.67	55.7387582	.4945942
BIRPS	BM87-1	786	161	22	42	30.325	248.05	55.7386076	.4939274
BIRPS	BM87-1	787	161	22	42	50.259	247.75	55.7384462	.4931793
BIRPS	BM87-1	788	161	22	43	10.159	246.73	55.7382805	.4924520
BIRPS	BM87-1	789	161	22	43	30.409	246.45	55.7380794	.4916520
BIRPS	BM87-1	790	161	22	43	50.392	247.15	55.7379185	.4910083
BIRPS	BM87-1	791	161	22	44	10.425	246.24	55.7377124	.4902102
BIRPS	BM87-1	792	161	22	44	30.759	246.23	55.7375276	.4895128
BIRPS	BM87-1	793	161	22	44	51.409	246.16	55.7373411	.4888243
BIRPS	BM87-1	794	161	22	45	12.109	244.97	55.7371574	.4881174
BIRPS	BM87-1	795	161	22	45	32.825	246.46	55.7369364	.4873584
BIRPS	BM87-1	796	161	22	45	53.625	246.44	55.7367454	.4866547
BIRPS	BM87-1	797	161	22	46	13.942	247.91	55.7365481	.4859486
BIRPS	BM87-1	798	161	22	46	34.009	247.94	55.7363732	.4852266
BIRPS	BM87-1	799	161	22	46	54.059	248.06	55.7362017	.4844857
BIRPS	BM87-1	800	161	22	47	13.692	248.55	55.7360270	.4837444
BIRPS	BM87-1	801	161	22	47	33.409	247.25	55.7358450	.4830169
BIRPS	BM87-1	802	161	22	47	53.875	247.85	55.7356584	.4823080
BIRPS	BM87-1	803	161	22	48	14.009	248.25	55.7354716	.4815939
BIRPS	BM87-1	804	161	22	48	34.309	248.31	55.7352831	.4808873
BIRPS	BM87-1	805	161	22	48	54.925	249.00	55.7350713	.4801060
BIRPS	BM87-1	806	161	22	49	15.275	251.12	55.7348871	.4793990
BIRPS	BM87-1	807	161	22	49	36.059	251.28	55.7347251	.4786626
BIRPS	BM87-1	808	161	22	49	56.075	251.02	55.7345675	.4779144
BIRPS	BM87-1	809	161	22	50	15.759	250.17	55.7344179	.4771679
BIRPS	BM87-1	810	161	22	50	35.575	249.91	55.7342668	.4764374
BIRPS	BM87-1	811	161	22	50	55.959	249.78	55.7341007	.4757180
BIRPS	BM87-1	812	161	22	51	16.525	249.98	55.7339279	.4750152
BIRPS	BM87-1	813	161	22	51	37.492	249.98	55.7337498	.4742256
BIRPS	BM87-1	814	161	22	51	58.209	250.37	55.7335738	.4735078
BIRPS	BM87-1	815	161	22	52	18.725	251.12	55.7333929	.4727085
BIRPS	BM87-1	816	161	22	52	39.109	250.58	55.7332330	.4719705
BIRPS	BM87-1	817	161	22	52	59.225	250.39	55.7330773	.4712261
BIRPS	BM87-1	818	161	22	53	19.542	249.51	55.7329145	.4704776
BIRPS	BM87-1	819	161	22	53	39.025	249.31	55.7327434	.4697376
BIRPS	BM87-1	820	161	22	53	59.025	248.14	55.7325677	.4690027
BIRPS	BM87-1	821	161	22	54	18.742	248.32	55.7323965	.4682810
BIRPS	BM87-1	822	161	22	54	39.025	249.53	55.7322202	.4675594
BIRPS	BM87-1	823	161	22	54	59.425	248.46	55.7320466	.4668259
BIRPS	BM87-1	824	161	22	55	19.792	249.09	55.7318753	.4661111
BIRPS	BM87-1	825	161	22	55	40.092	247.58	55.7316978	.4653883
BIRPS	BM87-1	826	161	22	56	00.209	248.44	55.7315047	.4646883
BIRPS	BM87-1	827	161	22	56	20.609	249.00	55.7313138	.4639696
BIRPS	BM87-1	828	161	22	56	40.692	249.79	55.7311130	.4631679
BIRPS	BM87-1	829	161	22	57	00.542	249.72	55.7309646	.4624912
BIRPS	BM87-1	830	161	22	57	20.192	249.07	55.7308046	.4617444
BIRPS	BM87-1	831	161	22	57	39.992	249.48	55.7306494	.4610009
BIRPS	BM87-1	832	161	22	57	59.892	247.95	55.7304745	.4602659
BIRPS	BM87-1	833	161	22	58	19.792	247.96	55.7303088	.4595382
BIRPS	BM87-1	834	161	22	58	39.942	248.33	55.7301371	.4588185
BIRPS	BM87-1	835	161	22	59	00.375	247.72	55.7299564	.4581001
BIRPS	BM87-1	836	161	22	59	20.825	248.25	55.7297636	.4573080
BIRPS	BM87-1	837	161	22	59	41.125	247.95	55.7296076	.4565830
BIRPS	BM87-1	838	161	23	00	01.792	247.43	55.7294268	.4558596
BIRPS	BM87-1	839	161	23	00	21.809	247.58	55.7292599	.4551420
BIRPS	BM87-1	840	161	23	00	42.175	247.23	55.7290841	.4544103
BIRPS	BM87-1	841	161	23	01	02.409	247.16	55.7289048	.4536857
BIRPS	BM87-1	842	161	23	01	22.459	247.36	55.7287225	.4529679

BIRPS	BM87-1	843	161	23	01	42.842	246.72	55.7285216	.4521745
BIRPS	BM87-1	844	161	23	02	03.059	247.50	55.7283401	.4514616
BIRPS	BM87-1	845	161	23	02	23.442	248.17	55.7281536	.4507360
BIRPS	BM87-1	846	161	23	02	43.292	247.02	55.7279657	.4500093
BIRPS	BM87-1	847	161	23	03	03.359	248.33	55.7277878	.4492891
BIRPS	BM87-1	848	161	23	03	23.775	247.88	55.7275999	.4485319
BIRPS	BM87-1	849	161	23	03	43.125	248.27	55.7274083	.4477993
BIRPS	BM87-1	850	161	23	04	02.675	249.10	55.7272425	.4471322
BIRPS	BM87-1	851	161	23	04	22.309	248.44	55.7270566	.4463944
BIRPS	BM87-1	852	161	23	04	41.642	248.83	55.7268913	.4456571
BIRPS	BM87-1	853	161	23	05	02.092	247.68	55.7267213	.4449184
BIRPS	BM87-1	854	161	23	05	21.942	248.34	55.7265400	.4441958
BIRPS	BM87-1	855	161	23	05	41.875	248.29	55.7263623	.4434679
BIRPS	BM87-1	856	161	23	06	01.809	249.24	55.7261727	.4427358
BIRPS	BM87-1	857	161	23	06	21.475	251.01	55.7259962	.4419966
BIRPS	BM87-1	858	161	23	06	41.659	251.30	55.7258428	.4412404
BIRPS	BM87-1	859	161	23	07	01.892	249.74	55.7256886	.4404862
BIRPS	BM87-1	860	161	23	07	21.509	249.66	55.7255237	.4397457
BIRPS	BM87-1	861	161	23	07	41.759	248.18	55.7253551	.4390061
BIRPS	BM87-1	862	161	23	08	01.459	248.18	55.7251722	.4382929
BIRPS	BM87-1	863	161	23	08	21.925	247.95	55.7250013	.4375839
BIRPS	BM87-1	864	161	23	08	42.575	246.98	55.7248080	.4368814
BIRPS	BM87-1	865	161	23	09	03.092	249.24	55.7246061	.4361370
BIRPS	BM87-1	866	161	23	09	24.542	249.48	55.7244146	.4354317
BIRPS	BM87-1	867	161	23	09	45.175	250.48	55.7242295	.4346561
BIRPS	BM87-1	868	161	23	10	05.909	250.63	55.7240673	.4339446
BIRPS	BM87-1	869	161	23	10	26.959	249.96	55.7239115	.4332130
BIRPS	BM87-1	870	161	23	10	47.309	249.44	55.7237378	.4323992
BIRPS	BM87-1	871	161	23	11	07.342	249.14	55.7235668	.4316746
BIRPS	BM87-1	872	161	23	11	27.475	249.36	55.7233842	.4309544
BIRPS	BM87-1	873	161	23	11	47.542	249.57	55.7232027	.4302471
BIRPS	BM87-1	874	161	23	12	08.025	250.24	55.7230280	.4295550
BIRPS	BM87-1	875	161	23	12	28.809	250.20	55.7228427	.4288461
BIRPS	BM87-1	876	161	23	12	49.309	251.47	55.7226448	.4280684
BIRPS	BM87-1	877	161	23	13	09.809	251.30	55.7224656	.4273493
BIRPS	BM87-1	878	161	23	13	30.375	251.63	55.7222944	.4266162
BIRPS	BM87-1	879	161	23	13	50.425	251.23	55.7221386	.4258757
BIRPS	BM87-1	880	161	23	14	10.392	250.61	55.7219695	.4251431
BIRPS	BM87-1	881	161	23	14	30.409	250.36	55.7217900	.4244198
BIRPS	BM87-1	882	161	23	14	50.242	250.79	55.7216057	.4236948
BIRPS	BM87-1	883	161	23	15	10.109	251.77	55.7214167	.4229771
BIRPS	BM87-1	884	161	23	15	30.642	251.72	55.7212299	.4222546
BIRPS	BM87-1	885	161	23	15	50.692	252.84	55.7210628	.4215455
BIRPS	BM87-1	886	161	23	16	11.325	252.41	55.7208971	.4208262
BIRPS	BM87-1	887	161	23	16	32.175	251.52	55.7207242	.4200485
BIRPS	BM87-1	888	161	23	16	53.259	251.69	55.7205825	.4193314
BIRPS	BM87-1	889	161	23	17	14.292	251.29	55.7204042	.4185303
BIRPS	BM87-1	890	161	23	17	35.075	251.51	55.7202383	.4178081
BIRPS	BM87-1	891	161	23	17	55.109	251.50	55.7200778	.4170911
BIRPS	BM87-1	892	161	23	18	15.542	250.70	55.7199163	.4163750
BIRPS	BM87-1	893	161	23	18	36.375	250.96	55.7197321	.4156027
BIRPS	BM87-1	894	161	23	18	57.609	250.84	55.7195569	.4148910
BIRPS	BM87-1	895	161	23	19	18.109	250.51	55.7193764	.4141007
BIRPS	BM87-1	896	161	23	19	38.692	250.07	55.7192060	.4134017
BIRPS	BM87-1	897	161	23	19	59.142	250.60	55.7190422	.4127102
BIRPS	BM87-1	898	161	23	20	20.225	250.21	55.7188664	.4119296
BIRPS	BM87-1	899	161	23	20	41.475	250.52	55.7187114	.4112166
BIRPS	BM87-1	900	161	23	21	02.375	249.48	55.7185224	.4104331
BIRPS	BM87-1	901	161	23	21	23.075	249.88	55.7183609	.4097273
BIRPS	BM87-1	902	161	23	21	43.659	248.82	55.7181673	.4089538
BIRPS	BM87-1	903	161	23	22	04.459	249.70	55.7179801	.4082732
BIRPS	BM87-1	904	161	23	22	25.309	249.89	55.7178093	.4075836
BIRPS	BM87-1	905	161	23	22	46.609	250.10	55.7176247	.4068259
BIRPS	BM87-1	906	161	23	23	07.642	249.48	55.7174761	.4061330
BIRPS	BM87-1	907	161	23	23	29.225	249.32	55.7173103	.4053659
BIRPS	BM87-1	908	161	23	23	50.625	249.23	55.7171258	.4045671
BIRPS	BM87-1	909	161	23	24	10.809	248.90	55.7169424	.4038435
BIRPS	BM87-1	910	161	23	24	30.609	249.13	55.7167578	.4031159
BIRPS	BM87-1	911	161	23	24	51.092	250.05	55.7165835	.4024039
BIRPS	BM87-1	912	161	23	25	11.425	248.65	55.7163896	.4016822
BIRPS	BM87-1	913	161	23	25	31.475	248.83	55.7162045	.4009682
BIRPS	BM87-1	914	161	23	25	51.592	250.00	55.7160059	.4002466
BIRPS	BM87-1	915	161	23	26	11.359	250.69	55.7158155	.3995240
BIRPS	BM87-1	916	161	23	26	31.025	250.53	55.7156256	.3987929
BIRPS	BM87-1	917	161	23	26	50.609	250.68	55.7154386	.3980654
BIRPS	BM87-1	918	161	23	27	10.859	250.29	55.7152601	.3973287
BIRPS	BM87-1	919	161	23	27	30.425	250.09	55.7150910	.3965986
BIRPS	BM87-1	920	161	23	27	50.809	250.91	55.7149142	.3958678
BIRPS	BM87-1	921	161	23	28	10.542	251.39	55.7147344	.3951278
BIRPS	BM87-1	922	161	23	28	30.625	251.42	55.7145609	.3943995
BIRPS	BM87-1	923	161	23	28	50.959	250.92	55.7143869	.3936706
BIRPS	BM87-1	924	161	23	29	10.742	251.38	55.7142148	.3929518
BIRPS	BM87-1	925	161	23	29	30.742	250.62	55.7140374	.3922254
BIRPS	BM87-1	926	161	23	29	50.709	250.79	55.7138629	.3915155
BIRPS	BM87-1	927	161	23	30	10.975	250.28	55.7137033	.3908054
BIRPS	BM87-1	928	161	23	30	31.775	250.75	55.7135135	.3900820
BIRPS	BM87-1	929	161	23	30	52.342	251.65	55.7133039	.3892940
BIRPS	BM87-1	930	161	23	31	12.627	252.63	55.7131158	.3885794
BIRPS	BM87-1	931	161	23	31	33.327	253.19	55.7129420	.3878665
BIRPS	BM87-1	932	161	23	31	53.675	253.17	55.7127685	.3871448
BIRPS	BM87-1	933	161	23	32	13.909	253.63	55.7126206	.3864216
BIRPS	BM87-1	934	161	23	32	34.559	252.87	55.7124492	.3856369
BIRPS	BM87-1	935	161	23	32	55.559	252.20	55.7122820	.3849240
BIRPS	BM87-1	936	161	23	33	16.059	252.01	55.7121069	.3842265
BIRPS	BM87-1	937	161	23	33	36.925	252.62	55.7119104	.3834582
BIRPS	BM87-1	938	161	23	33	58.109	253.23	55.7117349	.3827592
BIRPS	BM87-1	939	161	23	34	18.959	253.98	55.7115471	.3819604
BIRPS	BM87-1	940	161	23	34	39.709	254.69	55.7113733	.3812408
BIRPS	BM87-1	941	161	23	34	59.692	254.53	55.7112151	.3805110
BIRPS	BM87-1	942	161	23	35	19.692	253.43	55.7110627	.3797769
BIRPS	BM87-1	943	161	23	35	39.792	253.30	55.7109133	.3790539
BIRPS	BM87-1	944	161	23	36	00.175	253.89	55.7107639	.3783274
BIRPS	BM87-1	945	161	23	36	20.959	253.76	55.7105950	.3775487
BIRPS	BM87-1	946	161	23	36	42.342	252.45	55.7104481	.3768454
BIRPS	BM87-1	947	161	23	37	03.775	252.58	55.7102667	.3760834
BIRPS	BM87-1	948	161	23	37	24.975	251.91	55.7100844	.3753061
BIRPS	BM87-1	949	161	23	37	46.125	251.12	55.7099148	.3745794
BIRPS	BM87-1	950	161	23	38	06.175	250.81	55.7097449	.3738652
BIRPS	BM87-1	951	161	23	38	26.442	251.26	55.7095553	.3730870
BIRPS	BM87-1	952	161	23	38	47.009	251.86	55.7093815	.3723742
BIRPS	BM87-1	953	161	23	39	07.759	251.57	55.7092138	.3716604
BIRPS	BM87-1	954	161	23	39	28.142	252.10	55.7090520	.3709549
BIRPS	BM87-1	955	161	23	39	49.175	251.11	55.7088769	.3701779
BIRPS	BM87-1	956	161	23	40	10.459	249.85	55.7092782	.3693369
BIRPS	BM87-1	957	161	23	40	33.225	246.03	55.7090918	.3685629
BIRPS	BM87-1	958	161	23	40	55.525	239.56	55.7088748	.3678273
BIRPS	BM87-1	959	161	23	41	18.059	236.97	55.7085946	.3671522
BIRPS	BM87-1	960	161	23	41	40.859	241.57	55.7082351	.3664659
BIRPS	BM87-1	961	161	23	42	03.425	243.58	55.7079518	.3657800

BIRPS	BM87-1	963	161	23	42	46.225	250.02	55.7074514	.3643933
BIRPS	BM87-1	964	161	23	43	07.142	249.59	55.7072623	.3636232
BIRPS	BM87-1	965	161	23	43	28.159	248.62	55.7070957	.3629260
BIRPS	BM87-1	966	161	23	43	49.309	246.89	55.7069042	.3621712
BIRPS	BM87-1	967	161	23	44	10.842	246.19	55.7066836	.3614341
BIRPS	BM87-1	968	161	23	44	31.959	246.71	55.7064706	.3607564
BIRPS	BM87-1	969	161	23	44	52.259	248.01	55.7062711	.3600701
BIRPS	BM87-1	970	161	23	45	13.075	248.74	55.7060491	.3592963
BIRPS	BM87-1	971	161	23	45	33.375	250.42	55.7058582	.3585858
BIRPS	BM87-1	972	161	23	45	53.809	250.76	55.7056730	.3578697
BIRPS	BM87-1	973	161	23	46	13.709	250.33	55.7054811	.3571533
BIRPS	BM87-1	974	161	23	46	33.542	251.97	55.7052940	.3564592
BIRPS	BM87-1	975	161	23	46	54.009	251.58	55.7051171	.3557483
BIRPS	BM87-1	976	161	23	47	14.359	251.99	55.7049328	.3550627
BIRPS	BM87-1	977	161	23	47	35.342	253.02	55.7047461	.3542861
BIRPS	BM87-1	978	161	23	47	56.575	253.38	55.7045835	.3535577
BIRPS	BM87-1	979	161	23	48	17.009	253.50	55.7043975	.3527527
BIRPS	BM87-1	980	161	23	48	37.009	253.81	55.7042365	.3520261
BIRPS	BM87-1	981	161	23	48	57.292	254.43	55.7040699	.3513020
BIRPS	BM87-1	982	161	23	49	17.825	254.82	55.7039075	.3505675
BIRPS	BM87-1	983	161	23	49	37.675	255.39	55.7037429	.3498378
BIRPS	BM87-1	984	161	23	49	57.692	256.42	55.7035803	.3491296
BIRPS	BM87-1	985	161	23	50	18.375	256.04	55.7034394	.3484064
BIRPS	BM87-1	986	161	23	50	39.525	254.94	55.7032682	.3476397
BIRPS	BM87-1	987	161	23	51	00.659	254.66	55.7030989	.3468683
BIRPS	BM87-1	988	161	23	51	22.025	255.05	55.7029351	.3461626
BIRPS	BM87-1	989	161	23	51	42.692	255.23	55.7027535	.3453745
BIRPS	BM87-1	990	161	23	52	03.442	255.24	55.7025779	.3446580
BIRPS	BM87-1	991	161	23	52	23.709	255.52	55.7024082	.3439405
BIRPS	BM87-1	992	161	23	52	43.992	255.46	55.7022536	.3432168
BIRPS	BM87-1	993	161	23	53	04.375	255.44	55.7020900	.3425058
BIRPS	BM87-1	994	161	23	53	25.192	255.56	55.7019100	.3417321
BIRPS	BM87-1	995	161	23	53	46.442	254.93	55.7017615	.3410196
BIRPS	BM87-1	996	161	23	54	07.542	254.77	55.7015754	.3402437
BIRPS	BM87-1	997	161	23	54	28.092	255.31	55.7014038	.3395392
BIRPS	BM87-1	998	161	23	54	48.559	255.52	55.7012379	.3388290
BIRPS	BM87-1	999	161	23	55	09.659	254.70	55.7010476	.3380346
BIRPS	BM87-1	1000	161	23	55	29.859	255.13	55.7008785	.3373108
BIRPS	BM87-1	1001	161	23	55	49.992	254.61	55.7007242	.3365869
BIRPS	BM87-1	1002	161	23	56	10.142	254.31	55.7005748	.3358706
BIRPS	BM87-1	1003	161	23	56	30.875	253.67	55.7003934	.3350869
BIRPS	BM87-1	1004	161	23	56	51.792	253.92	55.7002146	.3343892
BIRPS	BM87-1	1005	161	23	57	12.542	254.48	55.7000343	.3337038
BIRPS	BM87-1	1006	161	23	57	33.575	255.46	55.6998481	.3329594
BIRPS	BM87-1	1007	161	23	57	55.092	255.01	55.6996591	.3322169
BIRPS	BM87-1	1008	161	23	58	16.792	256.53	55.6994692	.3314651
BIRPS	BM87-1	1009	161	23	58	38.225	257.78	55.6993039	.3307658
BIRPS	BM87-1	1010	161	23	58	59.325	258.54	55.6991429	.3299735
BIRPS	BM87-1	1011	161	23	59	20.409	258.24	55.6990023	.3292230
BIRPS	BM87-1	1012	161	23	59	40.392	256.41	55.6988631	.3284810
BIRPS	BM87-1	1013	162	00	00	00.409	255.66	55.6987301	.3277266
BIRPS	BM87-1	1014	162	00	00	20.409	256.09	55.6985515	.3269825
BIRPS	BM87-1	1015	162	00	00	40.059	255.14	55.6983909	.3262615
BIRPS	BM87-1	1016	162	00	00	59.942	255.18	55.6982289	.3255441
BIRPS	BM87-1	1017	162	00	01	20.442	255.09	55.6980505	.3248240
BIRPS	BM87-1	1018	162	00	01	40.942	255.86	55.6978684	.3240402
BIRPS	BM87-1	1019	162	00	02	01.659	256.46	55.6977085	.3233286
BIRPS	BM87-1	1020	162	00	02	22.292	257.16	55.6975460	.3226135
BIRPS	BM87-1	1021	162	00	02	43.225	257.67	55.6973669	.3218076
BIRPS	BM87-1	1022	162	00	03	03.759	257.31	55.6972205	.3210522
BIRPS	BM87-1	1023	162	00	03	23.242	256.77	55.6970758	.3203022
BIRPS	BM87-1	1024	162	00	03	43.459	257.12	55.6969239	.3195633
BIRPS	BM87-1	1025	162	00	04	03.392	256.80	55.6967654	.3188216
BIRPS	BM87-1	1026	162	00	04	23.709	257.76	55.6966140	.3180883
BIRPS	BM87-1	1027	162	00	04	43.942	256.60	55.6964620	.3173605
BIRPS	BM87-1	1028	162	00	05	04.292	256.90	55.6963139	.3166400
BIRPS	BM87-1	1029	162	00	05	25.125	255.51	55.6961290	.3158421
BIRPS	BM87-1	1030	162	00	05	45.392	255.03	55.6959622	.3151150
BIRPS	BM87-1	1031	162	00	06	05.892	255.91	55.6957907	.3143998
BIRPS	BM87-1	1032	162	00	06	26.175	256.24	55.6956082	.3136668
BIRPS	BM87-1	1033	162	00	06	46.225	258.29	55.6954274	.3129585
BIRPS	BM87-1	1034	162	00	07	06.542	258.43	55.6952857	.3122468
BIRPS	BM87-1	1035	162	00	07	27.892	257.75	55.6951314	.3114719
BIRPS	BM87-1	1036	162	00	07	49.075	258.07	55.6949845	.3106961
BIRPS	BM87-1	1037	162	00	08	10.659	257.92	55.6948324	.3099146
BIRPS	BM87-1	1038	162	00	08	32.042	256.85	55.6946975	.3092014
BIRPS	BM87-1	1039	162	00	08	53.042	256.69	55.6945354	.3084064
BIRPS	BM87-1	1040	162	00	09	13.825	257.18	55.6943875	.3076684
BIRPS	BM87-1	1041	162	00	09	33.925	256.71	55.6942399	.3069246
BIRPS	BM87-1	1042	162	00	09	53.809	256.40	55.6940962	.3061804
BIRPS	BM87-1	1043	162	00	10	13.759	256.31	55.6939494	.3054396
BIRPS	BM87-1	1044	162	00	10	33.892	254.98	55.6937926	.3047087
BIRPS	BM87-1	1045	162	00	10	54.209	254.14	55.6936157	.3040002
BIRPS	BM87-1	1046	162	00	11	15.009	254.80	55.6934146	.3018249
BIRPS	BM87-1	1047	162	00	11	48.156	252.34	55.6932927	.3012567
BIRPS	BM87-1	1048	162	00	12	21.467	250.02	55.6931680	.3006950
BIRPS	BM87-1	1049	162	00	12	54.509	248.48	55.6930027	.3000678
BIRPS	BM87-1	1052	162	00	13	11.066	249.13	55.6924764	.2983029
BIRPS	BM87-1	1053	162	00	13	30.259	250.89	55.6923140	.2977259
BIRPS	BM87-1	1054	162	00	13	30.288	250.66	55.6921484	.2970646
BIRPS	BM87-1	1055	162	00	13	48.692	251.27	55.6919652	.2963593
BIRPS	BM87-1	1056	162	00	14	08.159	250.37	55.6917912	.2957199
BIRPS	BM87-1	1057	162	00	14	27.792	250.46	55.6915870	.2950263
BIRPS	BM87-1	1058	162	00	14	47.559	250.97	55.6913792	.2943483
BIRPS	BM87-1	1059	162	00	15	07.775	252.50	55.6911774	.2936876
BIRPS	BM87-1	1060	162	00	15	28.792	253.95	55.6909590	.2929446
BIRPS	BM87-1	1061	162	00	15	49.959	255.00	55.6907832	.2922435
BIRPS	BM87-1	1062	162	00	16	10.542	256.05	55.6906170	.2915240
BIRPS	BM87-1	1063	162	00	16	30.959	255.83	55.6904299	.2907309
BIRPS	BM87-1	1064	162	00	16	51.159	255.95	55.6902734	.2900055
BIRPS	BM87-1	1065	162	00	17	11.759	256.60	55.6901169	.2892838
BIRPS	BM87-1	1066	162	00	17	31.992	257.33	55.6899635	.2885713
BIRPS	BM87-1	1067	162	00	17	52.959	257.67	55.6897877	.2878131
BIRPS	BM87-1	1068	162	00	18	14.625	258.47	55.6896175	.2871281
BIRPS	BM87-1	1069	162	00	18	36.092	260.48	55.6894483	.2863657
BIRPS	BM87-1	1070	162	00	18	57.492	260.99	55.6892974	.2855915
BIRPS	BM87-1	1071	162	00	19	19.342	260.99	55.6891422	.2848033
BIRPS	BM87-1	1072	162	00	19	40.325	260.47	55.6890148	.2840710
BIRPS	BM87-1	1073	162	00	20	00.692	261.53	55.6888835	.2833344
BIRPS	BM87-1	1074	162	00	20	21.342	262.47	55.6887289	.2825081
BIRPS	BM87-1	1075	162	00	20	41.625	261.27	55.6886009	.2817507
BIRPS	BM87-1	1076	162	00	21	01.959	261.31	55.6884604	.2810037
BIRPS	BM87-1	1077	162	00	21	21.725	260.72	55.6883205	.2802551
BIRPS	BM87-1	1078	162	00	21	41.425	259.83	55.6881823	.2794978
BIRPS	BM87-1	1079	162	00	22	01.675	259.93	55.6880273	.2787645
BIRPS	BM87-1	1080	162	00	22	22.092	260.16	55.6878830	.2780330
BIRPS	BM87-1	1081	162	00	22	42.175	259.55	55.6877418	.2772899
BIRPS	BM87-1	1082	162	00	23	02.259	259.24	55.6876050	.2765582
BIRPS	BM87-1	1083	162	00	23	22.575	259.02	55.6874635	.2758231

BIRPS	BM87-1	1085	162 00 24 03.509	257.41	55.6871851	.2742610
BIRPS	BM87-1	1086	162 00 24 24.225	257.10	55.6870283	.2735367
BIRPS	BM87-1	1087	162 00 24 44.509	257.38	55.6868657	.2728179
BIRPS	BM87-1	1088	162 00 25 05.225	256.63	55.6866914	.2720275
BIRPS	BM87-1	1089	162 00 25 25.975	256.98	55.6865237	.2713075
BIRPS	BM87-1	1090	162 00 25 46.292	256.74	55.6863510	.2705931
BIRPS	BM87-1	1091	162 00 26 06.559	256.67	55.6861873	.2698694
BIRPS	BM87-1	1092	162 00 26 27.125	256.41	55.6860012	.2690670
BIRPS	BM87-1	1093	162 00 26 47.425	256.76	55.6858189	.2683327
BIRPS	BM87-1	1094	162 00 27 07.542	257.13	55.6856467	.2676070
BIRPS	BM87-1	1095	162 00 27 27.875	257.10	55.6854714	.2668750
BIRPS	BM87-1	1096	162 00 27 47.542	256.98	55.6853179	.2661623
BIRPS	BM87-1	1097	162 00 28 08.542	257.09	55.6851688	.2654500
BIRPS	BM87-1	1098	162 00 28 29.492	257.24	55.6849991	.2646638
BIRPS	BM87-1	1099	162 00 28 50.625	256.80	55.6848236	.2639370
BIRPS	BM87-1	1100	162 00 29 10.742	257.23	55.6846629	.2632135
BIRPS	BM87-1	1101	162 00 29 31.025	257.75	55.6844844	.2624043
BIRPS	BM87-1	1102	162 00 29 51.125	258.04	55.6843184	.2616644
BIRPS	BM87-1	1103	162 00 30 11.075	257.78	55.6841640	.2609179
BIRPS	BM87-1	1104	162 00 30 31.109	256.42	55.6839952	.2601719
BIRPS	BM87-1	1105	162 00 30 50.825	256.73	55.6838291	.2595104
BIRPS	BM87-1	1106	162 00 31 10.509	257.37	55.6836540	.2587728
BIRPS	BM87-1	1107	162 00 31 30.309	258.55	55.6834824	.2580461
BIRPS	BM87-1	1108	162 00 31 50.259	259.30	55.6833143	.2573187
BIRPS	BM87-1	1109	162 00 32 10.409	258.67	55.6831485	.2566032
BIRPS	BM87-1	1110	162 00 32 30.844	258.56	55.6830067	.2558940
BIRPS	BM87-1	1111	162 00 32 51.711	258.20	55.6828285	.2551108
BIRPS	BM87-1	1112	162 00 33 12.675	259.29	55.6826554	.2543986
BIRPS	BM87-1	1113	162 00 33 33.442	259.09	55.6824951	.2536192
BIRPS	BM87-1	1114	162 00 33 54.925	259.19	55.6823315	.2528229
BIRPS	BM87-1	1115	162 00 34 15.492	260.15	55.6821993	.2520902
BIRPS	BM87-1	1116	162 00 34 36.542	260.09	55.6820587	.2513598
BIRPS	BM87-1	1117	162 00 34 57.292	259.15	55.6819145	.2505699
BIRPS	BM87-1	1118	162 00 35 18.225	257.91	55.6817813	.2498528
BIRPS	BM87-1	1119	162 00 35 39.125	257.37	55.6816231	.2490699
BIRPS	BM87-1	1120	162 00 36 00.275	257.75	55.6814773	.2483598
BIRPS	BM87-1	1121	162 00 36 21.192	257.21	55.6813104	.2475755
BIRPS	BM87-1	1122	162 00 36 42.175	256.55	55.6811652	.2468564
BIRPS	BM87-1	1123	162 00 37 02.759	256.29	55.6810087	.2461293
BIRPS	BM87-1	1124	162 00 37 23.175	255.97	55.6808330	.2453243
BIRPS	BM87-1	1125	162 00 37 43.409	256.77	55.6806645	.2446003
BIRPS	BM87-1	1126	162 00 38 03.992	256.57	55.6804844	.2438870
BIRPS	BM87-1	1127	162 00 38 24.225	256.10	55.6802960	.2431839
BIRPS	BM87-1	1128	162 00 38 44.475	256.31	55.6801010	.2424831
BIRPS	BM87-1	1129	162 00 39 04.992	257.43	55.6798871	.2417086
BIRPS	BM87-1	1130	162 00 39 25.359	258.46	55.6797167	.2410006
BIRPS	BM87-1	1131	162 00 39 46.042	258.18	55.6795457	.2402689
BIRPS	BM87-1	1132	162 00 40 06.025	259.34	55.6793697	.2395397
BIRPS	BM87-1	1133	162 00 40 25.809	259.54	55.6792072	.2387999
BIRPS	BM87-1	1134	162 00 40 45.792	259.45	55.6790256	.2380636
BIRPS	BM87-1	1135	162 00 41 05.592	259.49	55.6788698	.2373235
BIRPS	BM87-1	1136	162 00 41 25.959	260.15	55.6787187	.2365884
BIRPS	BM87-1	1137	162 00 41 46.109	260.06	55.6785626	.2358545
BIRPS	BM87-1	1138	162 00 42 06.259	260.72	55.6783939	.2351228
BIRPS	BM87-1	1139	162 00 42 26.175	261.62	55.6782447	.2343886
BIRPS	BM87-1	1140	162 00 42 46.575	262.06	55.6780877	.2336592
BIRPS	BM87-1	1141	162 00 43 07.175	262.50	55.6779288	.2328565
BIRPS	BM87-1	1142	162 00 43 27.825	262.70	55.6777971	.2321144
BIRPS	BM87-1	1143	162 00 43 48.042	262.03	55.6776826	.2313682
BIRPS	BM87-1	1144	162 00 44 08.609	260.90	55.6775562	.2306112
BIRPS	BM87-1	1145	162 00 44 29.042	259.21	55.6774168	.2297796
BIRPS	BM87-1	1146	162 00 44 49.159	259.44	55.6772813	.2290368
BIRPS	BM87-1	1147	162 00 45 09.575	259.65	55.6771475	.2282996
BIRPS	BM87-1	1148	162 00 45 30.559	258.50	55.6770063	.2275571
BIRPS	BM87-1	1149	162 00 45 51.059	258.30	55.6768569	.2268296
BIRPS	BM87-1	1150	162 00 46 11.759	257.96	55.6766833	.2260298
BIRPS	BM87-1	1151	162 00 46 32.542	258.00	55.6765253	.2252941
BIRPS	BM87-1	1152	162 00 46 52.425	257.69	55.6763753	.2245518
BIRPS	BM87-1	1153	162 00 47 12.342	256.98	55.6762036	.2238045
BIRPS	BM87-1	1154	162 00 47 31.775	256.97	55.6760267	.2230502
BIRPS	BM87-1	1155	162 00 47 51.475	256.26	55.6758638	.2223038
BIRPS	BM87-1	1156	162 00 48 11.259	256.29	55.6757096	.2216374
BIRPS	BM87-1	1157	162 00 48 31.125	256.40	55.6755331	.2208977
BIRPS	BM87-1	1158	162 00 48 50.909	256.80	55.6753711	.2201705
BIRPS	BM87-1	1159	162 00 49 11.359	257.05	55.6752054	.2194330
BIRPS	BM87-1	1160	162 00 49 31.542	255.32	55.6750345	.2186321
BIRPS	BM87-1	1161	162 00 49 51.942	254.71	55.6748705	.2179125
BIRPS	BM87-1	1162	162 00 50 12.625	255.49	55.6747050	.2171851
BIRPS	BM87-1	1163	162 00 50 32.692	255.80	55.6745302	.2164392
BIRPS	BM87-1	1164	162 00 50 52.492	256.01	55.6743549	.2156888
BIRPS	BM87-1	1165	162 00 51 12.009	255.96	55.6741797	.2149501
BIRPS	BM87-1	1166	162 00 51 31.892	255.51	55.6740074	.2142149
BIRPS	BM87-1	1167	162 00 51 51.842	254.60	55.6738203	.2134919
BIRPS	BM87-1	1168	162 00 52 11.875	255.49	55.6736258	.2127870
BIRPS	BM87-1	1169	162 00 52 32.242	256.14	55.6734363	.2120860
BIRPS	BM87-1	1170	162 00 52 53.242	256.24	55.6732581	.2113751
BIRPS	BM87-1	1171	162 00 53 13.742	257.13	55.6730827	.2105828
BIRPS	BM87-1	1172	162 00 53 34.325	258.05	55.6729280	.2098453
BIRPS	BM87-1	1173	162 00 53 54.809	257.27	55.6727826	.2090986
BIRPS	BM87-1	1174	162 00 54 14.459	256.90	55.6726431	.2083562
BIRPS	BM87-1	1175	162 00 54 34.375	256.83	55.6724961	.2076203
BIRPS	BM87-1	1176	162 00 54 55.142	256.58	55.6723397	.2068942
BIRPS	BM87-1	1177	162 00 55 15.292	256.92	55.6721844	.2061833
BIRPS	BM87-1	1178	162 00 55 36.242	257.14	55.6720079	.2054153
BIRPS	BM87-1	1179	162 00 55 57.825	258.03	55.6718283	.2046428
BIRPS	BM87-1	1180	162 00 56 19.009	258.60	55.6716798	.2039201
BIRPS	BM87-1	1181	162 00 56 39.625	257.09	55.6715362	.2031886
BIRPS	BM87-1	1182	162 00 57 00.242	257.25	55.6713696	.2023840
BIRPS	BM87-1	1183	162 00 57 20.659	257.72	55.6712195	.2016555
BIRPS	BM87-1	1184	162 00 57 40.875	257.29	55.6710620	.2009203
BIRPS	BM87-1	1185	162 00 58 00.875	257.71	55.6709134	.2001845
BIRPS	BM87-1	1186	162 00 58 21.042	256.42	55.6707604	.1994347
BIRPS	BM87-1	1187	162 00 58 40.792	256.86	55.6714888	.1994434
BIRPS	BM87-1	1188	162 00 59 05.475	254.59	55.6713071	.1985773
BIRPS	BM87-1	1189	162 00 59 30.325	253.17	55.6710888	.1976642
BIRPS	BM87-1	1190	162 00 59 55.309	249.76	55.6708911	.1968359
BIRPS	BM87-1	1191	162 01 00 20.642	247.08	55.6706441	.1959630
BIRPS	BM87-1	1192	162 01 00 46.425	247.75	55.6703481	.1951097
BIRPS	BM87-1	1193	162 01 01 10.992	250.96	55.6700671	.1943128
BIRPS	BM87-1	1194	162 01 01 33.642	251.75	55.6698574	.1935528
BIRPS	BM87-1	1195	162 01 01 56.109	250.61	55.6696549	.1927105
BIRPS	BM87-1	1196	162 01 02 18.242	249.47	55.6694487	.1919518
BIRPS	BM87-1	1197	162 01 02 40.042	250.26	55.6692290	.1912120
BIRPS	BM87-1	1198	162 01 03 01.809	250.46	55.6690271	.1905300
BIRPS	BM87-1	1199	162 01 03 23.325	251.02	55.6688012	.1897747
BIRPS	BM87-1	1200	162 01 03 44.475	251.14	55.6685924	.1890205
BIRPS	BM87-1	1201	162 01 04 05.925	250.33	55.6683966	.1883245
BIRPS	BM87-1	1202	162 01 04 26.725	251.43	55.6681898	.1875727
BIRPS	BM87-1	1203	162 01 04 48.109	254.30	55.6679759	.1868939
BIRPS	BM87-1	1204	162 01 05 09.042	[illegible]	[illegible]	[illegible]

BIRPS	BM87-1	1205	162	01	05	29.875	255.36	55.6676873	.1854061
BIRPS	BM87-1	1206	162	01	05	51.575	249.06	55.6675472	.1846222
BIRPS	BM87-1	1207	162	01	06	12.775	246.64	55.6673490	.1838723
BIRPS	BM87-1	1208	162	01	06	34.292	247.62	55.6671055	.1831487
BIRPS	BM87-1	1209	162	01	06	55.392	250.36	55.6668658	.1825031
BIRPS	BM87-1	1210	162	01	07	16.175	253.42	55.6666440	.1817635
BIRPS	BM87-1	1211	162	01	07	37.142	255.64	55.6664741	.1810710
BIRPS	BM87-1	1212	162	01	07	58.125	256.15	55.6663080	.1803614
BIRPS	BM87-1	1213	162	01	08	19.025	257.16	55.6661382	.1795726
BIRPS	BM87-1	1214	162	01	08	39.492	257.04	55.6659882	.1788422
BIRPS	BM87-1	1215	162	01	08	59.809	256.07	55.6658282	.1781240
BIRPS	BM87-1	1216	162	01	09	20.459	256.74	55.6656664	.1773431
BIRPS	BM87-1	1217	162	01	09	41.709	257.30	55.6655180	.1766419
BIRPS	BM87-1	1218	162	01	10	02.859	258.39	55.6653446	.1758849
BIRPS	BM87-1	1219	162	01	10	24.459	258.58	55.6651855	.1751120
BIRPS	BM87-1	1220	162	01	10	45.859	259.53	55.6650511	.1744066
BIRPS	BM87-1	1221	162	01	11	07.125	259.46	55.6649064	.1736056
BIRPS	BM87-1	1222	162	01	11	28.425	259.82	55.6647586	.1727911
BIRPS	BM87-1	1223	162	01	11	48.825	259.54	55.6646350	.1720489
BIRPS	BM87-1	1224	162	01	12	09.259	258.94	55.6645061	.1712990
BIRPS	BM87-1	1225	162	01	12	29.259	258.60	55.6643651	.1705695
BIRPS	BM87-1	1226	162	01	12	49.392	258.32	55.6642210	.1698484
BIRPS	BM87-1	1227	162	01	13	09.942	258.76	55.6640609	.1691216
BIRPS	BM87-1	1228	162	01	13	30.442	259.36	55.6638945	.1683179
BIRPS	BM87-1	1229	162	01	13	50.925	258.49	55.6637582	.1675890
BIRPS	BM87-1	1230	162	01	14	11.975	258.48	55.6636092	.1668571
BIRPS	BM87-1	1231	162	01	14	32.425	258.31	55.6634489	.1660543
BIRPS	BM87-1	1232	162	01	14	52.792	257.98	55.6633153	.1653077
BIRPS	BM87-1	1233	162	01	15	12.992	256.85	55.6631964	.1645556
BIRPS	BM87-1	1234	162	01	15	33.659	255.63	55.6630584	.1638232
BIRPS	BM87-1	1235	162	01	15	54.059	255.09	55.6629000	.1631032
BIRPS	BM87-1	1236	162	01	16	14.775	256.15	55.6627036	.1623203
BIRPS	BM87-1	1237	162	01	16	35.559	255.71	55.6625289	.1616283
BIRPS	BM87-1	1238	162	01	16	56.342	256.66	55.6623412	.1609437
BIRPS	BM87-1	1239	162	01	17	17.592	257.34	55.6621412	.1601873
BIRPS	BM87-1	1240	162	01	17	38.459	257.88	55.6619998	.1594877
BIRPS	BM87-1	1241	162	01	17	59.942	256.86	55.6618478	.1586986
BIRPS	BM87-1	1242	162	01	18	20.959	256.02	55.6616870	.1579011
BIRPS	BM87-1	1243	162	01	18	41.725	255.82	55.6615207	.1571847
BIRPS	BM87-1	1244	162	01	19	02.059	256.14	55.6613517	.1564673
BIRPS	BM87-1	1245	162	01	19	22.292	256.68	55.6611911	.1557683
BIRPS	BM87-1	1246	162	01	19	43.375	257.49	55.6610093	.1549944
BIRPS	BM87-1	1247	162	01	20	04.692	257.77	55.6608388	.1542085
BIRPS	BM87-1	1248	162	01	20	25.625	256.87	55.6606847	.1534945
BIRPS	BM87-1	1249	162	01	20	46.125	256.40	55.6605351	.1527945
BIRPS	BM87-1	1250	162	01	21	07.009	255.99	55.6603653	.1520075
BIRPS	BM87-1	1251	162	01	21	27.825	256.16	55.6602020	.1513039
BIRPS	BM87-1	1252	162	01	21	48.342	257.31	55.6600533	.1505909
BIRPS	BM87-1	1253	162	01	22	09.392	256.74	55.6598819	.1497984
BIRPS	BM87-1	1254	162	01	22	30.359	256.90	55.6597304	.1490787
BIRPS	BM87-1	1255	162	01	22	50.992	257.00	55.6595618	.1482883
BIRPS	BM87-1	1256	162	01	23	11.675	256.37	55.6594088	.1475737
BIRPS	BM87-1	1257	162	01	23	32.209	256.38	55.6592590	.1468663
BIRPS	BM87-1	1258	162	01	23	53.409	255.92	55.6590796	.1460941
BIRPS	BM87-1	1259	162	01	24	14.792	256.20	55.6588836	.1453222
BIRPS	BM87-1	1260	162	01	24	35.342	256.60	55.6587217	.1446246
BIRPS	BM87-1	1261	162	01	24	56.442	257.02	55.6585572	.1439127
BIRPS	BM87-1	1262	162	01	25	17.159	258.26	55.6583820	.1431433
BIRPS	BM87-1	1263	162	01	25	38.459	257.38	55.6582404	.1424371
BIRPS	BM87-1	1264	162	01	25	59.409	256.93	55.6580906	.1416520
BIRPS	BM87-1	1265	162	01	26	20.675	255.09	55.6579396	.1408626
BIRPS	BM87-1	1266	162	01	26	41.692	255.13	55.6577795	.1401563
BIRPS	BM87-1	1267	162	01	27	02.459	255.10	55.6576189	.1394580
BIRPS	BM87-1	1268	162	01	27	23.325	256.25	55.6574558	.1386970
BIRPS	BM87-1	1269	162	01	27	45.125	256.58	55.6573026	.1379328
BIRPS	BM87-1	1270	162	01	28	06.809	255.60	55.6571398	.1371583
BIRPS	BM87-1	1271	162	01	28	27.892	255.72	55.6569894	.1364696
BIRPS	BM87-1	1272	162	01	28	49.092	254.86	55.6568099	.1357034
BIRPS	BM87-1	1273	162	01	29	10.309	254.25	55.6566342	.1349955
BIRPS	BM87-1	1274	162	01	29	30.742	255.11	55.6564458	.1342128
BIRPS	BM87-1	1275	162	01	29	51.109	255.71	55.6562777	.1334958
BIRPS	BM87-1	1276	162	01	30	11.525	256.30	55.6561001	.1327909
BIRPS	BM87-1	1277	162	01	30	31.909	256.81	55.6559446	.1320905
BIRPS	BM87-1	1278	162	01	30	52.775	256.13	55.6557954	.1313289
BIRPS	BM87-1	1279	162	01	31	14.625	255.68	55.6556476	.1306410
BIRPS	BM87-1	1280	162	01	31	36.311	256.36	55.6554838	.1298716
BIRPS	BM87-1	1281	162	01	31	57.777	255.35	55.6553006	.1290892
BIRPS	BM87-1	1282	162	01	32	18.259	255.47	55.6551325	.1283899
BIRPS	BM87-1	1283	162	01	32	39.192	256.20	55.6549458	.1276190
BIRPS	BM87-1	1284	162	01	33	00.325	256.64	55.6547861	.1269086
BIRPS	BM87-1	1285	162	01	33	21.192	257.21	55.6546130	.1261409
BIRPS	BM87-1	1286	162	01	33	42.675	257.97	55.6544471	.1253931
BIRPS	BM87-1	1287	162	01	34	04.559	257.10	55.6543043	.1247099
BIRPS	BM87-1	1288	162	01	34	26.359	256.73	55.6541469	.1239709
BIRPS	BM87-1	1289	162	01	34	48.492	257.25	55.6539834	.1232206
BIRPS	BM87-1	1290	162	01	35	10.525	256.93	55.6538079	.1224699
BIRPS	BM87-1	1291	162	01	35	32.225	258.09	55.6536227	.1217175
BIRPS	BM87-1	1292	162	01	35	53.692	258.87	55.6534594	.1209453
BIRPS	BM87-1	1293	162	01	36	14.509	259.31	55.6533163	.1202332
BIRPS	BM87-1	1294	162	01	36	35.459	259.36	55.6531653	.1194473
BIRPS	BM87-1	1295	162	01	36	56.175	258.94	55.6530324	.1187417
BIRPS	BM87-1	1296	162	01	37	17.592	258.09	55.6528773	.1179775
BIRPS	BM87-1	1297	162	01	37	38.942	257.46	55.6527166	.1172322
BIRPS	BM87-1	1298	162	01	38	00.842	257.75	55.6525585	.1164859
BIRPS	BM87-1	1299	162	01	38	22.875	259.36	55.6523960	.1157338
BIRPS	BM87-1	1300	162	01	38	44.725	259.54	55.6522465	.1149612
BIRPS	BM87-1	1301	162	01	39	06.275	258.27	55.6521135	.1142402
BIRPS	BM87-1	1302	162	01	39	27.325	257.46	55.6519585	.1134574
BIRPS	BM87-1	1303	162	01	39	48.525	257.12	55.6518123	.1127359
BIRPS	BM87-1	1304	162	01	40	09.309	257.51	55.6516419	.1119614
BIRPS	BM87-1	1305	162	01	40	30.292	257.89	55.6514860	.1112678
BIRPS	BM87-1	1306	162	01	40	51.375	257.43	55.6513176	.1105080
BIRPS	BM87-1	1307	162	01	41	12.759	256.53	55.6511599	.1098184
BIRPS	BM87-1	1308	162	01	41	34.025	255.96	55.6509730	.1090578
BIRPS	BM87-1	1309	162	01	41	54.825	257.13	55.6507861	.1083706
BIRPS	BM87-1	1310	162	01	42	15.859	257.91	55.6505886	.1076024
BIRPS	BM87-1	1311	162	01	42	36.475	257.37	55.6504058	.1069001
BIRPS	BM87-1	1312	162	01	42	57.209	258.47	55.6502198	.1061371
BIRPS	BM87-1	1313	162	01	43	18.359	258.90	55.6500518	.1054464
BIRPS	BM87-1	1314	162	01	43	39.325	259.62	55.6498773	.1046888
BIRPS	BM87-1	1315	162	01	44	00.892	258.94	55.6497100	.1039959
BIRPS	BM87-1	1316	162	01	44	22.059	259.64	55.6495291	.1032332
BIRPS	BM87-1	1317	162	01	44	42.825	260.49	55.6493675	.1025339
BIRPS	BM87-1	1318	162	01	45	03.942	260.70	55.6491879	.1017641
BIRPS	BM87-1	1319	162	01	45	24.609	260.80	55.6490352	.1010592
BIRPS	BM87-1	1320	162	01	45	45.709	261.56	55.6488694	.1002873
BIRPS	BM87-1	1321	162	01	46	06.742	261.66	55.6487378	.0995804
BIRPS	BM87-1	1322	162	01	46	28.525	261.15	55.6485861	.0987927
BIRPS	BM87-1	1323	162	01	46	49.725	261.19	55.6484422	.0980131
BIRPS	BM87-1	1324	162	01	47	10.742	261.89	55.6482976	.0972961

BIRPS	BM87-1	1325	162	01	47	32.242	261.48	55.6481584	.0965375
BIRPS	BM87-1	1326	162	01	47	53.642	261.76	55.6480081	.0957810
BIRPS	BM87-1	1327	162	01	48	15.892	261.70	55.6478484	.0950259
BIRPS	BM87-1	1328	162	01	48	37.559	261.25	55.6476929	.0942682
BIRPS	BM87-1	1329	162	01	48	59.592	261.12	55.6475371	.0934961
BIRPS	BM87-1	1330	162	01	49	21.242	260.54	55.6473818	.0927080
BIRPS	BM87-1	1331	162	01	49	42.125	260.18	55.6472404	.0919779
BIRPS	BM87-1	1332	162	01	50	02.125	259.98	55.6471056	.0912512
BIRPS	BM87-1	1333	162	01	50	22.725	259.31	55.6469660	.0905319
BIRPS	BM87-1	1334	162	01	50	43.659	258.85	55.6468121	.0897561
BIRPS	BM87-1	1335	162	01	51	05.142	258.13	55.6466640	.0890488
BIRPS	BM87-1	1336	162	01	51	26.242	257.92	55.6464932	.0882838
BIRPS	BM87-1	1337	162	01	51	47.209	257.88	55.6463121	.0875236
BIRPS	BM87-1	1338	162	01	52	08.459	258.15	55.6461530	.0868329
BIRPS	BM87-1	1339	162	01	52	29.442	258.64	55.6459877	.0860546
BIRPS	BM87-1	1340	162	01	52	50.759	257.26	55.6458451	.0853381
BIRPS	BM87-1	1341	162	01	53	11.825	256.78	55.6456623	.0845690
BIRPS	BM87-1	1342	162	01	53	33.109	256.82	55.6454876	.0838713
BIRPS	BM87-1	1343	162	01	53	54.025	256.34	55.6452967	.0831308
BIRPS	BM87-1	1344	162	01	54	15.692	257.21	55.6450983	.0823826
BIRPS	BM87-1	1345	162	01	54	36.975	258.63	55.6449260	.0817010
BIRPS	BM87-1	1346	162	01	54	58.275	259.20	55.6447736	.0809510
BIRPS	BM87-1	1347	162	01	55	20.075	256.95	55.6446218	.0802009
BIRPS	BM87-1	1348	162	01	55	42.475	257.64	55.6444472	.0794393
BIRPS	BM87-1	1349	162	01	56	03.942	257.30	55.6442699	.0786732
BIRPS	BM87-1	1350	162	01	56	24.959	258.06	55.6441076	.0779832
BIRPS	BM87-1	1351	162	01	56	45.825	258.09	55.6439369	.0772160
BIRPS	BM87-1	1352	162	01	57	07.075	258.35	55.6437817	.0765048
BIRPS	BM87-1	1353	162	01	57	27.709	258.27	55.6436210	.0757314
BIRPS	BM87-1	1354	162	01	57	48.909	257.57	55.6434810	.0750365
BIRPS	BM87-1	1355	162	01	58	10.292	257.91	55,6433241	.0742726
BIRPS	BM87-1	1356	162	01	58	32.259	257.93	55.6431749	.0735098
BIRPS	BM87-1	1357	162	01	58	54.209	256.15	55.6430244	.0727367
BIRPS	BM87-1	1358	162	01	59	15.609	255.62	55.6428897	.0720414
BIRPS	BM87-1	1359	162	01	59	37.159	255.65	55.6427141	.0712714
BIRPS	BM87-1	1360	162	01	59	58.175	256.21	55.6425399	.0704961
BIRPS	BM87-1	1361	162	02	00	19.359	256.14	55.6423798	.0697881
BIRPS	BM87-1	1362	162	02	00	39.992	256.07	55.6422168	.0690181
BIRPS	BM87-1	1363	162	02	01	01.025	255.44	55.6420539	.0683338
BIRPS	BM87-1	1364	162	02	01	21.942	255.68	55.6418791	.0675777
BIRPS	BM87-1	1365	162	02	01	43.409	255.24	55.6417112	.0668917
BIRPS	BM87-1	1366	162	02	02	04.792	255.86	55.6415139	.0661395
BIRPS	BM87-1	1367	162	02	02	25.642	256.69	55.6413425	.0654490
BIRPS	BM87-1	1368	162	02	02	46.909	256.52	55.6411680	.0646892
BIRPS	BM87-1	1369	162	02	03	08.025	257.01	55.6409861	.0639315
BIRPS	BM87-1	1370	162	02	03	29.492	256.86	55.6408267	.0632325
BIRPS	BM87-1	1371	162	02	03	50.525	256.98	55.6406530	.0624508
BIRPS	BM87-1	1372	162	02	04	10.975	257.12	55.6405041	.0617385
BIRPS	BM87-1	1373	162	02	04	31.709	257.04	55.6403313	.0609667
BIRPS	BM87-1	1374	162	02	04	53.025	257.35	55.6401759	.0602689
BIRPS	BM87-1	1375	162	02	05	14.192	257.99	55.6400138	.0595129
BIRPS	BM87-1	1376	162	02	05	36.209	257.42	55.6398643	.0587548
BIRPS	BM87-1	1377	162	02	05	58.325	257.58	55.6397336	.0579960
BIRPS	BM87-1	1378	162	02	06	20.659	256.24	55.6395783	.0572240
BIRPS	BM87-1	1379	162	02	06	41.825	255.65	55.6394170	.0564605
BIRPS	BM87-1	1380	162	02	07	03.092	255.48	55.6392611	.0557730
BIRPS	BM87-1	1381	162	02	07	24.142	255.64	55.6390886	.0550175
BIRPS	BM87-1	1382	162	02	07	45.609	255.96	55.6389237	.0543323
BIRPS	BM87-1	1383	162	02	08	06.925	256.21	55.6387298	.0535810
BIRPS	BM87-1	1384	162	02	08	27.842	256.49	55.6385416	.0528291
BIRPS	BM87-1	1385	162	02	08	49.159	256.84	55.6383681	.0521517
BIRPS	BM87-1	1386	162	02	09	10.409	257.81	55.6381911	.0514075
BIRPS	BM87-1	1387	162	02	09	32.425	258.50	55.6380251	.0506598
BIRPS	BM87-1	1388	162	02	09	54.592	258.39	55.6378733	.0498923
BIRPS	BM87-1	1389	162	02	10	15.859	257.98	55.6377292	.0491270
BIRPS	BM87-1	1390	162	02	10	37.509	257.54	55.6375869	.0484281
BIRPS	BM87-1	1391	162	02	10	58.925	257.97	55.6374199	.0476679
BIRPS	BM87-1	1392	162	02	11	20.192	257.99	55.6372528	.0469005
BIRPS	BM87-1	1393	162	02	11	41.692	258.19	55.6370862	.0461365
BIRPS	BM87-1	1394	162	02	12	03.059	257.84	55.6369410	.0454488
BIRPS	BM87-1	1395	162	02	12	24.375	257.67	55.6367866	.0447039
BIRPS	BM87-1	1396	162	02	12	46.759	257.32	55.6366370	.0439493
BIRPS	BM87-1	1397	162	02	13	08.359	257.19	55.6364878	.0431803
BIRPS	BM87-1	1398	162	02	13	30.192	256.76	55.6363348	.0424137
BIRPS	BM87-1	1399	162	02	13	51.925	256.19	55.6361720	.0416448
BIRPS	BM87-1	1400	162	02	14	13.142	255.82	55.6360087	.0409473
BIRPS	BM87-1	1401	162	02	14	33.759	255.34	55.6358349	.0401790
BIRPS	BM87-1	1402	162	02	14	54.759	254.92	55.6356753	.0394953
BIRPS	BM87-1	1403	162	02	15	15.675	255.48	55.6354969	.0387594
BIRPS	BM87-1	1404	162	02	15	37.642	256.06	55.6353311	.0380989
BIRPS	BM87-1	1405	162	02	15	59.675	256.35	55.6351455	.0373070
BIRPS	BM87-1	1406	162	02	16	22.175	256.83	55.6349765	.0365849
BIRPS	BM87-1	1407	162	02	16	45.009	257.20	55.6348119	.0358446
BIRPS	BM87-1	1408	162	02	17	07.042	256.96	55.6346520	.0350992
BIRPS	BM87-1	1409	162	02	17	28.692	256.91	55.6345056	.0343496
BIRPS	BM87-1	1410	162	02	17	50.475	255.98	55.6343611	.0336049
BIRPS	BM87-1	1411	162	02	18	12.525	256.04	55.6341951	.0328579
BIRPS	BM87-1	1412	162	02	18	34.209	255.93	55.6340233	.0321141
BIRPS	BM87-1	1413	162	02	18	56.392	255.59	55.6338440	.0313688
BIRPS	BM87-1	1414	162	02	19	18.175	257.10	55.6336653	.0306306
BIRPS	BM87-1	1415	162	02	19	40.242	257.58	55.6335088	.0298783
BIRPS	BM87-1	1416	162	02	20	02.442	256.67	55.6333621	.0291265
BIRPS	BM87-1	1417	162	02	20	24.025	256.59	55.6332188	.0283689
BIRPS	BM87-1	1418	162	02	20	45.909	254.61	55.6330645	.0276034
BIRPS	BM87-1	1419	162	02	21	07.192	254.28	55.6329062	.0269056
BIRPS	BM87-1	1420	162	02	21	28.059	254.27	55.6327169	.0261517
BIRPS	BM87-1	1421	162	02	21	49.142	255.39	55.6325358	.0254796
BIRPS	BM87-1	1422	162	02	22	10.492	256.36	55.6323353	.0247542
BIRPS	BM87-1	1423	162	02	22	31.942	258.11	55.6321605	.0240220
BIRPS	BM87-1	1424	162	02	22	54.059	257.30	55.6320076	.0232802
BIRPS	BM87-1	1425	162	02	23	16.259	257.73	55.6318618	.0225515
BIRPS	BM87-1	1426	162	02	23	39.359	256.71	55.6316954	.0218136
BIRPS	BM87-1	1427	162	02	24	01.475	257.31	55.6315214	.0210842
BIRPS	BM87-1	1428	162	02	24	23.742	257.39	55.6313111	.0202830
BIRPS	BM87-1	1429	162	02	24	45.275	258.58	55.6311389	.0196141
BIRPS	BM87-1	1430	162	02	25	06.842	259.35	55.6309460	.0188690
BIRPS	BM87-1	1431	162	02	25	27.942	261.05	55.6307697	.0181240
BIRPS	BM87-1	1432	162	02	25	49.625	260.91	55.6306431	.0174475
BIRPS	BM87-1	1433	162	02	26	11.959	260.52	55.6304887	.0166433
BIRPS	BM87-1	1434	162	02	26	34.442	259.93	55.6303451	.0159021
BIRPS	BM87-1	1435	162	02	26	56.425	260.33	55.6302011	.0151605
BIRPS	BM87-1	1436	162	02	27	19.142	259.64	55.6300466	.0144084
BIRPS	BM87-1	1437	162	02	27	40.775	259.41	55.6299056	.0136528
BIRPS	BM87-1	1438	162	02	28	02.492	259.89	55.6297505	.0128925
BIRPS	BM87-1	1439	162	02	28	24.092	259.76	55.6296087	.0121362
BIRPS	BM87-1	1440	162	02	28	46.077	259.32	55.6294751	.0113771
BIRPS	BM87-1	1441	162	02	29	08.077	259.04	55.6293411	.0106332
BIRPS	BM87-1	1442	162	02	29	30.575	257.93	55.6291833	.0098967
BIRPS	BM87-1	1443	162	02	29	52.542	258.04	55.6290191	.0091548
BIRPS	BM87-1	1444	162	02	30	14.242	258.33	55.6288582	.0084068

BIRPS	BM87-1	1445	162	02	30	36.459	258.16	55.6287105	.0076493
BIRPS	BM87-1	1446	162	02	30	58.109	257.40	55.6285618	.0068931
BIRPS	BM87-1	1447	162	02	31	20.025	256.37	55.6284079	.0061349
BIRPS	BM87-1	1448	162	02	31	41.875	255.60	55.6282474	.0053848
BIRPS	BM87-1	1449	162	02	32	03.925	255.75	55.6280738	.0046583
BIRPS	BM87-1	1450	162	02	32	26.142	255.23	55.6278978	.0039438
BIRPS	BM87-1	1451	162	02	32	48.559	255.59	55.6277168	.0032279
BIRPS	BM87-1	1452	162	02	33	10.642	255.99	55.6275389	.0025069
BIRPS	BM87-1	1453	162	02	33	32.725	256.44	55.6273700	.0017880
BIRPS	BM87-1	1454	162	02	33	55.175	255.92	55.6272105	.0010569
BIRPS	BM87-1	1455	162	02	34	17.659	255.83	55.6270417	.0002636
BIRPS	BM87-1	1456	162	02	34	40.175	255.51	55.6268746	-.0004666
BIRPS	BM87-1	1457	162	02	35	02.809	255.20	55.6267000	-.0012002
BIRPS	BM87-1	1458	162	02	35	24.559	255.14	55.6265249	-.0019229
BIRPS	BM87-1	1459	162	02	35	46.492	255.53	55.6263532	-.0026239
BIRPS	BM87-1	1460	162	02	36	09.259	255.79	55.6261786	-.0033277
BIRPS	BM87-1	1461	162	02	36	32.209	256.41	55.6259858	-.0041022
BIRPS	BM87-1	1462	162	02	36	55.109	256.62	55.6258143	-.0048233
BIRPS	BM87-1	1463	162	02	37	17.259	256.31	55.6256326	-.0055292
BIRPS	BM87-1	1464	162	02	37	39.809	257.10	55.6254353	-.0063024
BIRPS	BM87-1	1465	162	02	38	02.425	258.04	55.6252547	-.0070281
BIRPS	BM87-1	1466	162	02	38	24.742	258.81	55.6250906	-.0077635
BIRPS	BM87-1	1467	162	02	38	46.375	259.32	55.6249341	-.0085019
BIRPS	BM87-1	1468	162	02	39	08.775	259.63	55.6247808	-.0092424
BIRPS	BM87-1	1469	162	02	39	30.709	258.90	55.6246268	-.0099860
BIRPS	BM87-1	1470	162	02	39	52.525	259.98	55.6244664	-.0107218
BIRPS	BM87-1	1471	162	02	40	14.492	260.18	55.6243299	-.0114575
BIRPS	BM87-1	1472	162	02	40	37.009	259.89	55.6241951	-.0121860
BIRPS	BM87-1	1473	162	02	40	59.825	259.10	55.6240463	-.0129893
BIRPS	BM87-1	1474	162	02	41	22.459	258.81	55.6239001	-.0137212
BIRPS	BM87-1	1475	162	02	41	44.725	257.57	55.6237357	-.0144423
BIRPS	BM87-1	1476	162	02	42	06.992	257.92	55.6235573	-.0151720
BIRPS	BM87-1	1477	162	02	42	28.775	258.81	55.6233978	-.0159073
BIRPS	BM87-1	1478	162	02	42	50.925	259.42	55.6232628	-.0166502
BIRPS	BM87-1	1479	162	02	43	13.359	258.27	55.6231359	-.0173916
BIRPS	BM87-1	1480	162	02	43	36.142	257.83	55.6229887	-.0181826
BIRPS	BM87-1	1481	162	02	43	59.325	257.09	55.6228313	-.0189067
BIRPS	BM87-1	1482	162	02	44	22.042	256.40	55.6226597	-.0197094
BIRPS	BM87-1	1483	162	02	44	44.225	257.00	55.6224898	-.0204494
BIRPS	BM87-1	1484	162	02	45	06.392	257.05	55.6223245	-.0211885
BIRPS	BM87-1	1485	162	02	45	28.625	255.98	55.6221695	-.0219328
BIRPS	BM87-1	1486	162	02	45	50.375	255.65	55.6220160	-.0226494
BIRPS	BM87-1	1487	162	02	46	13.342	255.81	55.6218638	-.0233619
BIRPS	BM87-1	1488	162	02	46	36.309	255.26	55.6216959	-.0241377
BIRPS	BM87-1	1489	162	02	46	59.509	254.92	55.6215423	-.0248488
BIRPS	BM87-1	1490	162	02	47	22.459	255.21	55.6213690	-.0256220
BIRPS	BM87-1	1491	162	02	47	45.092	254.29	55.6212058	-.0263547
BIRPS	BM87-1	1492	162	02	48	07.142	254.12	55.6196006	-.0273332
BIRPS	BM87-1	1493	162	02	48	24.825	255.24	55.6194441	-.0279244
BIRPS	BM87-1	1494	162	02	48	42.425	259.10	55.6192901	-.0285153
BIRPS	BM87-1	1495	162	02	49	00.192	261.73	55.6191502	-.0291187
BIRPS	BM87-1	1496	162	02	49	18.109	262.77	55.6190455	-.0297217
BIRPS	BM87-1	1497	162	02	49	36.942	263.96	55.6189484	-.0303308
BIRPS	BM87-1	1498	162	02	49	56.709	264.94	55.6188495	-.0310047
BIRPS	BM87-1	1499	162	02	50	17.475	265.86	55.6187424	-.0316909
BIRPS	BM87-1	1500	162	02	50	38.675	266.41	55.6186539	-.0324371
BIRPS	BM87-1	1501	162	02	51	00.359	267.54	55.6185675	-.0331858
BIRPS	BM87-1	1502	162	02	51	23.025	268.35	55.6184769	-.0339374
BIRPS	BM87-1	1503	162	02	51	45.242	267.61	55.6184041	-.0346979
BIRPS	BM87-1	1504	162	02	52	07.742	267.66	55.6183064	-.0355344
BIRPS	BM87-1	1505	162	02	52	29.959	268.04	55.6182185	-.0363035
BIRPS	BM87-1	1506	162	02	52	52.375	267.89	55.6181269	-.0370672
BIRPS	BM87-1	1507	162	02	53	15.025	268.02	55.6180540	-.0378284
BIRPS	BM87-1	1508	162	02	53	37.709	268.00	55.6179761	-.0386537
BIRPS	BM87-1	1509	162	02	54	00.992	264.93	55.6179220	-.0394103
BIRPS	BM87-1	1510	162	02	54	24.125	261.64	55.6178311	-.0402209
BIRPS	BM87-1	1511	162	02	54	47.359	260.84	55.6177026	-.0409699
BIRPS	BM87-1	1512	162	02	55	09.775	260.23	55.6175494	-.0417402
BIRPS	BM87-1	1513	162	02	55	31.225	262.73	55.6173820	-.0425041
BIRPS	BM87-1	1514	162	02	55	52.392	262.49	55.6172541	-.0432643
BIRPS	BM87-1	1515	162	02	56	14.425	262.60	55.6171324	-.0440100
BIRPS	BM87-1	1516	162	02	56	37.225	260.77	55.6170124	-.0447510
BIRPS	BM87-1	1517	162	02	56	59.609	258.03	55.6168855	-.0454965
BIRPS	BM87-1	1518	162	02	57	22.009	256.24	55.6167342	-.0462395
BIRPS	BM87-1	1519	162	02	57	44.292	255.31	55.6165497	-.0470329
BIRPS	BM87-1	1520	162	02	58	06.425	256.07	55.6163713	-.0477668
BIRPS	BM87-1	1521	162	02	58	28.275	256.69	55.6161927	-.0485148
BIRPS	BM87-1	1522	162	02	58	49.875	257.13	55.6160509	-.0492067
BIRPS	BM87-1	1523	162	02	59	11.442	256.49	55.6158921	-.0499630
BIRPS	BM87-1	1524	162	02	59	32.692	256.31	55.6157169	-.0507043
BIRPS	BM87-1	1525	162	02	59	54.642	256.92	55.6155280	-.0514322
BIRPS	BM87-1	1526	162	03	00	16.509	256.91	55.6153497	-.0521540
BIRPS	BM87-1	1527	162	03	00	38.925	258.73	55.6151544	-.0528651
BIRPS	BM87-1	1528	162	03	01	01.459	259.65	55.6149955	-.0535920
BIRPS	BM87-1	1529	162	03	01	23.442	260.38	55.6148511	-.0543438
BIRPS	BM87-1	1530	162	03	01	45.325	259.09	55.6147257	-.0551074
BIRPS	BM87-1	1531	162	03	02	07.025	256.18	55.6146188	-.0558610
BIRPS	BM87-1	1532	162	03	02	29.392	250.01	55.6144940	-.0566112
BIRPS	BM87-1	1533	162	03	02	51.709	247.65	55.6142939	-.0573150
BIRPS	BM87-1	1534	162	03	03	14.109	249.25	55.6140636	-.0579947
BIRPS	BM87-1	1535	162	03	03	36.592	251.79	55.6138198	-.0587303
BIRPS	BM87-1	1536	162	03	03	59.409	253.96	55.6136172	-.0594280
BIRPS	BM87-1	1537	162	03	04	21.909	254.57	55.6134479	-.0601383
BIRPS	BM87-1	1538	162	03	04	44.559	254.94	55.6132864	-.0609259
BIRPS	BM87-1	1539	162	03	05	07.392	254.70	55.6131297	-.0616545
BIRPS	BM87-1	1540	162	03	05	29.842	254.55	55.6129729	-.0623845
BIRPS	BM87-1	1541	162	03	05	52.509	255.20	55.6127864	-.0631789
BIRPS	BM87-1	1542	162	03	06	14.925	256.44	55.6126205	-.0639076
BIRPS	BM87-1	1543	162	03	06	37.425	256.41	55.6124519	-.0646314
BIRPS	BM87-1	1544	162	03	06	59.525	257.13	55.6122814	-.0653491
BIRPS	BM87-1	1545	162	03	07	21.859	257.77	55.6121234	-.0660637
BIRPS	BM87-1	1546	162	03	07	44.475	257.60	55.6119507	-.0668489
BIRPS	BM87-1	1547	162	03	08	07.125	258.22	55.6118048	-.0675655
BIRPS	BM87-1	1548	162	03	08	30.242	258.32	55.6116671	-.0683082
BIRPS	BM87-1	1549	162	03	08	52.742	258.47	55.6115001	-.0691202
BIRPS	BM87-1	1550	162	03	09	14.759	258.88	55.6113460	-.0698619
BIRPS	BM87-1	1551	162	03	09	36.675	258.40	55.6112119	-.0706070
BIRPS	BM87-1	1552	162	03	09	58.909	258.17	55.6110598	-.0713493
BIRPS	BM87-1	1553	162	03	10	21.292	258.76	55.6109018	-.0720798
BIRPS	BM87-1	1554	162	03	10	43.359	259.36	55.6107518	-.0728021
BIRPS	BM87-1	1555	162	03	11	05.809	259.16	55.6106098	-.0735310
BIRPS	BM87-1	1556	162	03	11	28.159	259.06	55.6104688	-.0742577
BIRPS	BM87-1	1557	162	03	11	51.125	259.10	55.6103241	-.0750578
BIRPS	BM87-1	1558	162	03	12	14.209	258.49	55.6101912	-.0758221
BIRPS	BM87-1	1559	162	03	12	36.059	258.15	55.6100552	-.0765990
BIRPS	BM87-1	1560	162	03	12	57.459	257.02	55.6099212	-.0773672
BIRPS	BM87-1	1561	162	03	13	18.792	256.02	55.6097770	-.0781007
BIRPS	BM87-1	1562	162	03	13	41.259	256.85	55.6096192	-.0787956
BIRPS	BM87-1	1563	162	03	14	04.592	256.22	55.6094407	-.0795580

BIRPS	BM87-1	1565	162	03	14	52.175	255.53	55.6091147	-.0810029
BIRPS	BM87-1	1566	162	03	15	15.875	255.27	55.6089304	-.0817706
BIRPS	BM87-1	1567	162	03	15	38.525	255.12	55.6087403	-.0825426
BIRPS	BM87-1	1568	162	03	16	01.109	255.38	55.6085708	-.0832604
BIRPS	BM87-1	1569	162	03	16	24.059	254.69	55.6083895	-.0839813
BIRPS	BM87-1	1570	162	03	16	46.259	254.40	55.6082124	-.0846961
BIRPS	BM87-1	1571	162	03	17	08.542	254.25	55.6080126	-.0854758
BIRPS	BM87-1	1572	162	03	17	30.825	254.74	55.6078288	-.0861784
BIRPS	BM87-1	1573	162	03	17	53.309	255.88	55.6076567	-.0868848
BIRPS	BM87-1	1574	162	03	18	15.625	257.40	55.6074862	-.0876064
BIRPS	BM87-1	1575	162	03	18	37.775	256.41	55.6073223	-.0883545
BIRPS	BM87-1	1576	162	03	18	59.442	256.32	55.6071636	-.0890977
BIRPS	BM87-1	1577	162	03	19	20.992	256.35	55.6070108	-.0898415
BIRPS	BM87-1	1578	162	03	19	42.942	256.73	55.6068563	-.0905899
BIRPS	BM87-1	1579	162	03	20	04.825	257.03	55.6066959	-.0913325
BIRPS	BM87-1	1580	162	03	20	26.842	257.15	55.6065352	-.0920623
BIRPS	BM87-1	1581	162	03	20	49.325	257.02	55.6063791	-.0927957
BIRPS	BM87-1	1582	162	03	21	12.042	256.14	55.6062091	-.0935364
BIRPS	BM87-1	1583	162	03	21	33.975	256.62	55.6060352	-.0942715
BIRPS	BM87-1	1584	162	03	21	55.592	257.32	55.6058688	-.0950048
BIRPS	BM87-1	1585	162	03	22	17.792	258.30	55.6057131	-.0957444
BIRPS	BM87-1	1586	162	03	22	39.759	258.17	55.6055645	-.0964737
BIRPS	BM87-1	1587	162	03	23	02.325	257.26	55.6054122	-.0971931
BIRPS	BM87-1	1588	162	03	23	24.975	256.50	55.6052275	-.0979955
BIRPS	BM87-1	1589	162	03	23	47.025	257.02	55.6050592	-.0987313
BIRPS	BM87-1	1590	162	03	24	09.192	257.00	55.6049011	-.0994713
BIRPS	BM87-1	1591	162	03	24	31.309	256.78	55.6047571	-.1002089
BIRPS	BM87-1	1592	162	03	24	53.492	256.64	55.6046171	-.1009283
BIRPS	BM87-1	1593	162	03	25	16.559	256.43	55.6044727	-.1016577
BIRPS	BM87-1	1594	162	03	25	39.209	256.53	55.6042978	-.1024597
BIRPS	BM87-1	1595	162	03	26	01.375	257.08	55.6041375	-.1031960
BIRPS	BM87-1	1596	162	03	26	23.592	255.62	55.6039827	-.1039322
BIRPS	BM87-1	1597	162	03	26	46.092	255.84	55.6038222	-.1046438
BIRPS	BM87-1	1598	162	03	27	08.575	255.18	55.6036541	-.1053418
BIRPS	BM87-1	1599	162	03	27	31.575	255.77	55.6034595	-.1060863
BIRPS	BM87-1	1600	162	03	27	55.342	256.26	55.6032776	-.1068367
BIRPS	BM87-1	1601	162	03	28	18.792	256.68	55.6031211	-.1075264
BIRPS	BM87-1	1602	162	03	28	42.375	256.49	55.6029493	-.1082880
BIRPS	BM87-1	1603	162	03	29	05.475	256.63	55.6027890	-.1090793
BIRPS	BM87-1	1604	162	03	29	28.642	255.97	55.6026320	-.1098195
BIRPS	BM87-1	1605	162	03	29	50.427	255.46	55.6024780	-.1105469
BIRPS	BM87-1	1606	162	03	30	12.511	255.69	55.6023114	-.1112802
BIRPS	BM87-1	1607	162	03	30	34.409	255.99	55.6021345	-.1120201
BIRPS	BM87-1	1608	162	03	30	56.009	256.48	55.6019563	-.1127340
BIRPS	BM87-1	1609	162	03	31	17.975	257.13	55.6017836	-.1134493
BIRPS	BM87-1	1610	162	03	31	40.225	257.72	55.6016174	-.1141647
BIRPS	BM87-1	1611	162	03	32	02.709	257.88	55.6014639	-.1148597
BIRPS	BM87-1	1612	162	03	32	26.375	257.52	55.6013091	-.1156181
BIRPS	BM87-1	1613	162	03	32	50.159	257.17	55.6011557	-.1163908
BIRPS	BM87-1	1614	162	03	33	13.575	256.75	55.6010152	-.1171678
BIRPS	BM87-1	1615	162	03	33	37.425	256.24	55.6008784	-.1179618
BIRPS	BM87-1	1616	162	03	34	00.725	255.16	55.6007514	-.1187003
BIRPS	BM87-1	1617	162	03	34	23.309	254.59	55.6005970	-.1194913
BIRPS	BM87-1	1618	162	03	34	45.925	254.14	55.6004500	-.1201906
BIRPS	BM87-1	1619	162	03	35	09.092	253.97	55.6002730	-.1209453
BIRPS	BM87-1	1620	162	03	35	32.542	253.32	55.6001068	-.1216356
BIRPS	BM87-1	1621	162	03	35	56.092	253.04	55.5999123	-.1223892
BIRPS	BM87-1	1622	162	03	36	18.975	252.81	55.5997316	-.1231611
BIRPS	BM87-1	1623	162	03	36	41.992	253.04	55.5995703	-.1238673
BIRPS	BM87-1	1624	162	03	37	04.642	252.84	55.5994161	-.1245641
BIRPS	BM87-1	1625	162	03	37	27.925	253.23	55.5992408	-.1253374
BIRPS	BM87-1	1626	162	03	37	50.675	252.29	55.5990838	-.1260564
BIRPS	BM87-1	1627	162	03	38	13.509	252.51	55.5988750	-.1268026
BIRPS	BM87-1	1628	162	03	38	36.942	253.19	55.5986678	-.1275385
BIRPS	BM87-1	1629	162	03	39	00.342	253.97	55.5984847	-.1282111
BIRPS	BM87-1	1630	162	03	39	23.775	254.43	55.5983057	-.1289653
BIRPS	BM87-1	1631	162	03	39	46.792	255.73	55.5981450	-.1296676
BIRPS	BM87-1	1632	162	03	40	09.825	256.09	55.5979801	-.1304417
BIRPS	BM87-1	1633	162	03	40	32.559	255.30	55.5978312	-.1311629
BIRPS	BM87-1	1634	162	03	40	55.175	254.83	55.5976766	-.1319442
BIRPS	BM87-1	1635	162	03	41	18.125	254.98	55.5975350	-.1326508
BIRPS	BM87-1	1636	162	03	41	41.359	253.97	55.5973704	-.1334200
BIRPS	BM87-1	1637	162	03	42	04.692	255.08	55.5972182	-.1341219
BIRPS	BM87-1	1638	162	03	42	28.109	255.40	55.5970481	-.1348942
BIRPS	BM87-1	1639	162	03	42	51.025	255.00	55.5968791	-.1356763
BIRPS	BM87-1	1640	162	03	43	13.725	254.69	55.5967317	-.1363974
BIRPS	BM87-1	1641	162	03	43	36.275	254.20	55.5965828	-.1371175
BIRPS	BM87-1	1642	162	03	43	58.775	254.55	55.5964285	-.1378289
BIRPS	BM87-1	1643	162	03	44	21.692	254.18	55.5962477	-.1386070
BIRPS	BM87-1	1644	162	03	44	44.092	254.18	55.5960876	-.1393200
BIRPS	BM87-1	1645	162	03	45	06.625	253.83	55.5959280	-.1400502
BIRPS	BM87-1	1646	162	03	45	29.109	254.10	55.5957587	-.1408439
BIRPS	BM87-1	1647	162	03	45	51.592	253.81	55.5956087	-.1415662
BIRPS	BM87-1	1648	162	03	46	14.542	252.97	55.5954488	-.1423009
BIRPS	BM87-1	1649	162	03	46	36.692	254.12	55.5952789	-.1430182
BIRPS	BM87-1	1650	162	03	46	59.292	254.27	55.5951047	-.1437909
BIRPS	BM87-1	1651	162	03	47	22.292	254.36	55.5949405	-.1445157
BIRPS	BM87-1	1652	162	03	47	44.659	252.76	55.5947565	-.1452415
BIRPS	BM87-1	1653	162	03	48	06.775	252.91	55.5945670	-.1459585
BIRPS	BM87-1	1654	162	03	48	29.009	253.28	55.5943629	-.1466651
BIRPS	BM87-1	1655	162	03	48	50.975	254.53	55.5941761	-.1473504
BIRPS	BM87-1	1656	162	03	49	13.809	256.16	55.5939883	-.1480951
BIRPS	BM87-1	1657	162	03	49	37.492	257.22	55.5938145	-.1488629
BIRPS	BM87-1	1658	162	03	50	00.709	256.96	55.5936896	-.1495757
BIRPS	BM87-1	1659	162	03	50	23.842	256.85	55.5935493	-.1503597
BIRPS	BM87-1	1660	162	03	50	47.292	256.49	55.5934124	-.1510825
BIRPS	BM87-1	1661	162	03	51	10.475	255.90	55.5932584	-.1518679
BIRPS	BM87-1	1662	162	03	51	33.209	255.33	55.5931015	-.1525807
BIRPS	BM87-1	1663	162	03	51	56.242	255.45	55.5929242	-.1533396
BIRPS	BM87-1	1664	162	03	52	19.192	255.21	55.5927479	-.1540298
BIRPS	BM87-1	1665	162	03	52	42.525	256.18	55.5925472	-.1547854
BIRPS	BM87-1	1666	162	03	53	05.242	256.69	55.5923631	-.1554878
BIRPS	BM87-1	1667	162	03	53	27.892	257.88	55.5921783	-.1562721
BIRPS	BM87-1	1668	162	03	53	50.142	259.06	55.5920213	-.1570071
BIRPS	BM87-1	1669	162	03	54	12.492	259.16	55.5918873	-.1577570
BIRPS	BM87-1	1670	162	03	54	34.375	258.39	55.5917501	-.1585302
BIRPS	BM87-1	1671	162	03	54	55.575	257.59	55.5916139	-.1592794
BIRPS	BM87-1	1672	162	03	55	17.692	256.81	55.5914625	-.1600102
BIRPS	BM87-1	1673	162	03	55	40.059	256.97	55.5912893	-.1607239
BIRPS	BM87-1	1674	162	03	56	02.792	257.30	55.5911289	-.1614432
BIRPS	BM87-1	1675	162	03	56	25.359	257.85	55.5909781	-.1621559
BIRPS	BM87-1	1676	162	03	56	48.425	257.29	55.5908153	-.1629403
BIRPS	BM87-1	1677	162	03	57	11.225	256.87	55.5906805	-.1636676
BIRPS	BM87-1	1678	162	03	57	33.992	256.28	55.5905098	-.1644721
BIRPS	BM87-1	1679	162	03	57	56.142	255.84	55.5903468	-.1652149
BIRPS	BM87-1	1680	162	03	58	17.942	256.11	55.5901774	-.1659432
BIRPS	BM87-1	1681	162	03	58	40.125	256.68	55.5899989	-.1666756
BIRPS	BM87-1	1682	162	03	59	02.042	257.18	55.5898262	-.1674080
BIRPS	BM87-1	1683	162	03	59	23.925	257.48	55.5896584	-.1681353

BIRPS	BM87-1	1685	162	04	00	08.742	257.89	55.5893606	-.1695903
BIRPS	BM87-1	1686	162	04	00	30.992	256.71	55.5892216	-.1703530
BIRPS	BM87-1	1687	162	04	00	52.625	256.18	55.5890765	-.1711067
BIRPS	BM87-1	1688	162	04	01	14.342	254.89	55.5889173	-.1718560
BIRPS	BM87-1	1689	162	04	01	36.309	254.86	55.5887606	-.1725939
BIRPS	BM87-1	1690	162	04	01	58.625	255.12	55.5886045	-.1733073
BIRPS	BM87-1	1691	162	04	02	21.292	254.63	55.5884430	-.1740206
BIRPS	BM87-1	1692	162	04	02	44.225	254.30	55.5882721	-.1747887
BIRPS	BM87-1	1693	162	04	03	07.709	254.35	55.5881001	-.1755482
BIRPS	BM87-1	1694	162	04	03	31.359	253.86	55.5879348	-.1762506
BIRPS	BM87-1	1695	162	04	03	54.525	253.54	55.5877575	-.1770309
BIRPS	BM87-1	1696	162	04	04	17.025	253.52	55.5875757	-.1777531
BIRPS	BM87-1	1697	162	04	04	38.825	253.64	55.5873976	-.1784860
BIRPS	BM87-1	1698	162	04	05	00.225	253.95	55.5872272	-.1791979
BIRPS	BM87-1	1699	162	04	05	22.775	254.45	55.5870649	-.1799114
BIRPS	BM87-1	1700	162	04	05	45.575	254.36	55.5868970	-.1806202
BIRPS	BM87-1	1701	162	04	06	08.759	253.45	55.5867326	-.1813862
BIRPS	BM87-1	1702	162	04	06	31.692	254.49	55.5865874	-.1821582
BIRPS	BM87-1	1703	162	04	06	55.209	253.94	55.5864695	-.1828743
BIRPS	BM87-1	1704	162	04	07	19.009	251.47	55.5863188	-.1836719
BIRPS	BM87-1	1705	162	04	07	41.309	250.46	55.5861743	-.1844031
BIRPS	BM87-1	1706	162	04	08	03.625	251.64	55.5860185	-.1851207
BIRPS	BM87-1	1707	162	04	08	26.359	251.15	55.5858349	-.1859161
BIRPS	BM87-1	1708	162	04	08	48.909	250.47	55.5856695	-.1866572
BIRPS	BM87-1	1709	162	04	09	10.525	250.25	55.5855055	-.1873756
BIRPS	BM87-1	1710	162	04	09	32.709	250.93	55.5853250	-.1880786
BIRPS	BM87-1	1711	162	04	09	55.342	250.68	55.5851376	-.1887953
BIRPS	BM87-1	1712	162	04	10	17.675	250.79	55.5849451	-.1895711
BIRPS	BM87-1	1713	162	04	10	40.125	251.12	55.5847677	-.1902897
BIRPS	BM87-1	1714	162	04	11	02.459	251.06	55.5845880	-.1910155
BIRPS	BM87-1	1715	162	04	11	24.359	251.13	55.5844037	-.1917388
BIRPS	BM87-1	1716	162	04	11	46.842	251.18	55.5842176	-.1924438
BIRPS	BM87-1	1717	162	04	12	08.875	252.07	55.5840525	-.1931436
BIRPS	BM87-1	1718	162	04	12	31.625	251.74	55.5838974	-.1938509
BIRPS	BM87-1	1719	162	04	12	55.109	251.42	55.5837367	-.1946127
BIRPS	BM87-1	1720	162	04	13	18.492	251.23	55.5835447	-.1953794
BIRPS	BM87-1	1721	162	04	13	41.109	252.47	55.5833741	-.1960800
BIRPS	BM87-1	1722	162	04	14	04.025	252.99	55.5831951	-.1968628
BIRPS	BM87-1	1723	162	04	14	26.725	253.48	55.5830479	-.1975996
BIRPS	BM87-1	1724	162	04	14	48.892	252.69	55.5828959	-.1983504
BIRPS	BM87-1	1725	162	04	15	10.492	252.04	55.5827467	-.1991015
BIRPS	BM87-1	1726	162	04	15	32.059	252.10	55.5825881	-.1998281
BIRPS	BM87-1	1727	162	04	15	54.675	251.18	55.5824187	-.2005379
BIRPS	BM87-1	1728	162	04	16	17.309	252.01	55.5822420	-.2012349
BIRPS	BM87-1	1729	162	04	16	40.475	252.42	55.5820485	-.2020133
BIRPS	BM87-1	1730	162	04	17	03.659	253.26	55.5818719	-.2027249
BIRPS	BM87-1	1731	162	04	17	26.209	254.12	55.5816890	-.2035183
BIRPS	BM87-1	1732	162	04	17	48.359	255.07	55.5815415	-.2042366
BIRPS	BM87-1	1733	162	04	18	11.309	254.98	55.5813965	-.2049572
BIRPS	BM87-1	1734	162	04	18	34.092	253.77	55.5812451	-.2057354
BIRPS	BM87-1	1735	162	04	18	57.242	253.97	55.5811043	-.2064431
BIRPS	BM87-1	1736	162	04	19	20.342	253.73	55.5809427	-.2072118
BIRPS	BM87-1	1737	162	04	19	43.809	254.93	55.5783258	-.2151901
BIRPS	BM87-1	1738	162	04	20	07.125	258.61	55.5781395	-.2159619
BIRPS	BM87-1	1739	162	04	20	29.709	260.02	55.5780187	-.2167025
BIRPS	BM87-1	1740	162	04	20	52.492	259.30	55.5779050	-.2175414
BIRPS	BM87-1	1741	162	04	21	14.892	259.03	55.5778047	-.2183085
BIRPS	BM87-1	1742	162	04	21	36.625	258.52	55.5776856	-.2190835
BIRPS	BM87-1	1743	162	04	21	58.559	259.04	55.5775418	-.2198582
BIRPS	BM87-1	1744	162	04	22	19.942	261.05	55.5774033	-.2206222
BIRPS	BM87-1	1745	162	04	22	41.659	262.79	55.5772720	-.2213087
BIRPS	BM87-1	1746	162	04	23	03.525	262.54	55.5771880	-.2220644
BIRPS	BM87-1	1747	162	04	23	26.309	259.52	55.5771044	-.2228859
BIRPS	BM87-1	1748	162	04	23	49.375	258.37	55.5769818	-.2236332
BIRPS	BM87-1	1749	162	04	24	11.709	260.46	55.5768285	-.2243796
BIRPS	BM87-1	1750	162	04	24	34.042	264.28	55.5766769	-.2252126
BIRPS	BM87-1	1751	162	04	24	56.192	263.22	55.5765976	-.2259928
BIRPS	BM87-1	1752	162	04	25	18.459	260.92	55.5765298	-.2267667
BIRPS	BM87-1	1753	162	04	25	41.309	253.25	55.5764609	-.2275364
BIRPS	BM87-1	1754	162	04	26	03.692	250.18	55.5762936	-.2282582
BIRPS	BM87-1	1755	162	04	26	26.259	252.31	55.5760493	-.2290026
BIRPS	BM87-1	1756	162	04	26	48.642	254.65	55.5758456	-.2297089
BIRPS	BM87-1	1757	162	04	27	11.125	254.92	55.5756835	-.2304298
BIRPS	BM87-1	1758	162	04	27	33.275	253.65	55.5755379	-.2311713
BIRPS	BM87-1	1759	162	04	27	55.075	252.45	55.5754072	-.2319149
BIRPS	BM87-1	1760	162	04	28	17.259	251.91	55.5752545	-.2326510
BIRPS	BM87-1	1761	162	04	28	39.375	252.00	55.5750975	-.2333903
BIRPS	BM87-1	1762	162	04	29	01.259	251.92	55.5749438	-.2341434
BIRPS	BM87-1	1763	162	04	29	23.142	251.15	55.5747741	-.2348966
BIRPS	BM87-1	1764	162	04	29	44.592	251.19	55.5746061	-.2356231
BIRPS	BM87-1	1765	162	04	30	07.025	251.69	55.5744334	-.2363495
BIRPS	BM87-1	1766	162	04	30	29.075	251.37	55.5742597	-.2370895
BIRPS	BM87-1	1767	162	04	30	50.742	252.05	55.5740916	-.2378256
BIRPS	BM87-1	1768	162	04	31	12.575	252.79	55.5739221	-.2385712
BIRPS	BM87-1	1769	162	04	31	34.709	252.48	55.5737572	-.2393335
BIRPS	BM87-1	1770	162	04	31	55.711	251.60	55.5736094	-.2400317
BIRPS	BM87-1	1771	162	04	32	16.977	252.44	55.5734393	-.2407902
BIRPS	BM87-1	1772	162	04	32	38.192	252.42	55.5732531	-.2415635
BIRPS	BM87-1	1773	162	04	32	59.292	252.11	55.5730905	-.2422598
BIRPS	BM87-1	1774	162	04	33	20.075	253.15	55.5729291	-.2429415
BIRPS	BM87-1	1775	162	04	33	41.609	253.13	55.5727609	-.2436968
BIRPS	BM87-1	1776	162	04	34	02.875	253.69	55.5726083	-.2444385
BIRPS	BM87-1	1777	162	04	34	25.392	254.59	55.5724669	-.2451728
BIRPS	BM87-1	1778	162	04	34	48.125	253.57	55.5723281	-.2459193
BIRPS	BM87-1	1779	162	04	35	10.809	252.74	55.5721721	-.2467439
BIRPS	BM87-1	1780	162	04	35	33.142	251.46	55.5720114	-.2474964
BIRPS	BM87-1	1781	162	04	35	54.425	251.59	55.5718504	-.2482316
BIRPS	BM87-1	1782	162	04	36	16.509	252.58	55.5716805	-.2489573
BIRPS	BM87-1	1783	162	04	36	38.825	252.36	55.5715119	-.2496935
BIRPS	BM87-1	1784	162	04	37	01.209	251.19	55.5713383	-.2504316
BIRPS	BM87-1	1785	162	04	37	22.875	251.72	55.5711529	-.2511420
BIRPS	BM87-1	1786	162	04	37	45.342	253.22	55.5709759	-.2518614
BIRPS	BM87-1	1787	162	04	38	07.492	252.36	55.5708030	-.2526058
BIRPS	BM87-1	1788	162	04	38	29.159	252.33	55.5706366	-.2533452
BIRPS	BM87-1	1789	162	04	38	50.742	252.91	55.5704828	-.2540814
BIRPS	BM87-1	1790	162	04	39	13.259	252.48	55.5703241	-.2548213
BIRPS	BM87-1	1791	162	04	39	35.059	252.35	55.5701628	-.2555658
BIRPS	BM87-1	1792	162	04	39	56.775	251.46	55.5699925	-.2563066
BIRPS	BM87-1	1793	162	04	40	18.742	251.89	55.5695280	-.2572959
BIRPS	BM87-1	1794	162	04	40	38.092	253.55	55.5693775	-.2578767
BIRPS	BM87-1	1795	162	04	40	58.242	256.68	55.5692155	-.2585285
BIRPS	BM87-1	1796	162	04	41	19.242	258.12	55.5690746	-.2592556
BIRPS	BM87-1	1797	162	04	41	40.492	256.73	55.5689715	-.2600055
BIRPS	BM87-1	1798	162	04	42	02.359	253.74	55.5688744	-.2606852
BIRPS	BM87-1	1799	162	04	42	24.375	251.76	55.5687237	-.2614222
BIRPS	BM87-1	1800	162	04	42	45.992	254.38	55.5685325	-.2621448
BIRPS	BM87-1	1801	162	04	43	07.359	259.11	55.5683425	-.2628693
BIRPS	BM87-1	1802	162	04	43	28.892	260.87	55.5682065	-.2636169
BIRPS	BM87-1	1803	162	04	43	50.975	260.21	55.5681119	-.2643771
BIRPS	BM87-1	1804	162	04	44	13.809	253.56	55.5680416	-.2651428

BIRPS	BM87-1	1805	162	04	44	35.975	251.03	55.5678875	-.2658806
BIRPS	BM87-1	1806	162	04	44	58.275	252.77	55.5676878	-.2665961
BIRPS	BM87-1	1807	162	04	45	20.059	256.63	55.5674962	-.2673257
BIRPS	BM87-1	1808	162	04	45	41.742	258.85	55.5673542	-.2680878
BIRPS	BM87-1	1809	162	04	46	03.309	256.91	55.5672651	-.2688736
BIRPS	BM87-1	1810	162	04	46	25.275	251.22	55.5671775	-.2696651
BIRPS	BM87-1	1811	162	04	46	47.009	246.14	55.5670342	-.2704226
BIRPS	BM87-1	1812	162	04	47	09.175	244.67	55.5668407	-.2711154
BIRPS	BM87-1	1813	162	04	47	31.925	246.52	55.5666169	-.2717703
BIRPS	BM87-1	1814	162	04	47	55.092	249.08	55.5663717	-.2724940
BIRPS	BM87-1	1815	162	04	48	18.409	249.73	55.5661738	-.2732104
BIRPS	BM87-1	1816	162	04	48	40.775	250.47	55.5659730	-.2740219
BIRPS	BM87-1	1817	162	04	49	01.925	250.86	55.5658375	-.2747138
BIRPS	BM87-1	1818	162	04	49	23.159	250.35	55.5656826	-.2754878
BIRPS	BM87-1	1819	162	04	49	44.775	249.03	55.5655273	-.2762696
BIRPS	BM87-1	1820	162	04	50	05.692	249.30	55.5653796	-.2769645
BIRPS	BM87-1	1821	162	04	50	26.625	248.42	55.5652191	-.2776506
BIRPS	BM87-1	1822	162	04	50	48.209	249.07	55.5650414	-.2783845
BIRPS	BM87-1	1823	162	04	51	09.775	249.33	55.5648678	-.2791162
BIRPS	BM87-1	1824	162	04	51	31.442	249.05	55.5647002	-.2798431
BIRPS	BM87-1	1825	162	04	51	53.409	249.85	55.5645336	-.2805726
BIRPS	BM87-1	1826	162	04	52	16.042	250.25	55.5643628	-.2813072
BIRPS	BM87-1	1827	162	04	52	37.892	250.90	55.5641990	-.2820568
BIRPS	BM87-1	1828	162	04	52	59.525	250.25	55.5640418	-.2828189
BIRPS	BM87-1	1829	162	04	53	21.025	250.30	55.5638753	-.2835722
BIRPS	BM87-1	1830	162	04	53	42.742	250.74	55.5637148	-.2843017
BIRPS	BM87-1	1831	162	04	54	05.242	250.67	55.5635503	-.2850410
BIRPS	BM87-1	1832	162	04	54	27.592	250.83	55.5633931	-.2857687
BIRPS	BM87-1	1833	162	04	54	49.709	250.04	55.5632369	-.2864980
BIRPS	BM87-1	1834	162	04	55	11.909	250.88	55.5630687	-.2872229
BIRPS	BM87-1	1835	162	04	55	34.042	250.94	55.5629070	-.2879713
BIRPS	BM87-1	1836	162	04	55	55.692	250.35	55.5627558	-.2887322
BIRPS	BM87-1	1837	162	04	56	16.992	250.05	55.5626025	-.2894952
BIRPS	BM87-1	1838	162	04	56	38.575	249.97	55.5624536	-.2901844
BIRPS	BM87-1	1839	162	04	57	00.125	250.03	55.5622963	-.2909342
BIRPS	BM87-1	1840	162	04	57	21.942	249.84	55.5621356	-.2916810
BIRPS	BM87-1	1841	162	04	57	43.842	248.64	55.5619727	-.2923987
BIRPS	BM87-1	1842	162	04	58	06.159	248.91	55.5618117	-.2931145
BIRPS	BM87-1	1843	162	04	58	29.192	249.30	55.5616359	-.2938984
BIRPS	BM87-1	1844	162	04	58	52.225	249.06	55.5614810	-.2946528
BIRPS	BM87-1	1845	162	04	59	13.925	247.36	55.5613349	-.2954063
BIRPS	BM87-1	1846	162	04	59	35.375	247.70	55.5611678	-.2961388
BIRPS	BM87-1	1847	162	04	59	57.942	247.45	55.5609889	-.2968740
BIRPS	BM87-1	1848	162	05	00	19.559	248.40	55.5608063	-.2975967
BIRPS	BM87-1	1849	162	05	00	41.375	248.25	55.5606283	-.2983092
BIRPS	BM87-1	1850	162	05	01	04.125	248.31	55.5604596	-.2990243
BIRPS	BM87-1	1851	162	05	01	26.575	247.79	55.5603000	-.2997303
BIRPS	BM87-1	1852	162	05	01	49.775	247.57	55.5601112	-.3004993
BIRPS	BM87-1	1853	162	05	02	12.492	247.95	55.5599436	-.3012085
BIRPS	BM87-1	1854	162	05	02	35.392	248.51	55.5597566	-.3019858
BIRPS	BM87-1	1855	162	05	02	58.125	249.76	55.5595869	-.3027222
BIRPS	BM87-1	1856	162	05	03	19.909	248.66	55.5594222	-.3034733
BIRPS	BM87-1	1857	162	05	03	41.225	248.42	55.5592611	-.3042152
BIRPS	BM87-1	1858	162	05	04	03.292	248.31	55.5590941	-.3049608
BIRPS	BM87-1	1859	162	05	04	25.109	249.24	55.5589250	-.3057157
BIRPS	BM87-1	1860	162	05	04	46.425	248.95	55.5587721	-.3064170
BIRPS	BM87-1	1861	162	05	05	07.475	247.49	55.5586059	-.3071852
BIRPS	BM87-1	1862	162	05	05	28.342	246.86	55.5584385	-.3078597
BIRPS	BM87-1	1863	162	05	05	49.725	247.82	55.5582615	-.3085804
BIRPS	BM87-1	1864	162	05	06	11.575	249.08	55.5580831	-.3093052
BIRPS	BM87-1	1865	162	05	06	33.625	250.10	55.5579148	-.3100394
BIRPS	BM87-1	1866	162	05	06	55.609	250.58	55.5577662	-.3107785
BIRPS	BM87-1	1867	162	05	07	17.875	249.80	55.5576151	-.3115215
BIRPS	BM87-1	1868	162	05	07	39.992	249.72	55.5574565	-.3122642
BIRPS	BM87-1	1869	162	05	08	02.259	249.61	55.5572979	-.3129891
BIRPS	BM87-1	1870	162	05	08	24.742	249.21	55.5571333	-.3137131
BIRPS	BM87-1	1871	162	05	08	47.509	249.72	55.5569449	-.3144999
BIRPS	BM87-1	1872	162	05	09	10.142	250.58	55.5567737	-.3152470
BIRPS	BM87-1	1873	162	05	09	31.692	251.06	55.5566222	-.3160007
BIRPS	BM87-1	1874	162	05	09	53.842	250.72	55.5564712	-.3167546
BIRPS	BM87-1	1875	162	05	10	15.992	249.56	55.5563180	-.3175243
BIRPS	BM87-1	1876	162	05	10	37.809	249.12	55.5561616	-.3182706
BIRPS	BM87-1	1877	162	05	10	59.542	249.17	55.5560016	-.3190119
BIRPS	BM87-1	1878	162	05	11	21.459	249.25	55.5558359	-.3197389
BIRPS	BM87-1	1879	162	05	11	43.659	249.36	55.5556778	-.3204728
BIRPS	BM87-1	1880	162	05	12	05.859	249.03	55.5555193	-.3212182
BIRPS	BM87-1	1881	162	05	12	27.625	249.09	55.5553631	-.3219608
BIRPS	BM87-1	1882	162	05	12	49.442	248.41	55.5552109	-.3227014
BIRPS	BM87-1	1883	162	05	13	11.592	246.93	55.5550508	-.3234493
BIRPS	BM87-1	1884	162	05	13	33.309	246.66	55.5548935	-.3240963
BIRPS	BM87-1	1885	162	05	13	55.675	246.62	55.5546986	-.3248696
BIRPS	BM87-1	1886	162	05	14	18.242	247.61	55.5545103	-.3255918
BIRPS	BM87-1	1887	162	05	14	39.875	248.30	55.5543325	-.3263382
BIRPS	BM87-1	1888	162	05	15	01.442	248.45	55.5541681	-.3270860
BIRPS	BM87-1	1889	162	05	15	23.242	247.91	55.5540198	-.3277562
BIRPS	BM87-1	1890	162	05	15	45.342	247.40	55.5538405	-.3284935
BIRPS	BM87-1	1891	162	05	16	06.959	247.62	55.5536752	-.3292433
BIRPS	BM87-1	1892	162	05	16	28.492	247.66	55.5535190	-.3300132
BIRPS	BM87-1	1893	162	05	16	49.659	247.88	55.5533514	-.3307858
BIRPS	BM87-1	1894	162	05	17	10.792	247.15	55.5532016	-.3314928
BIRPS	BM87-1	1895	162	05	17	31.459	247.41	55.5530376	-.3322681
BIRPS	BM87-1	1896	162	05	17	52.725	246.90	55.5528790	-.3329480
BIRPS	BM87-1	1897	162	05	18	14.175	247.72	55.5527016	-.3336712
BIRPS	BM87-1	1898	162	05	18	36.642	247.52	55.5525203	-.3343910
BIRPS	BM87-1	1899	162	05	18	58.709	248.70	55.5523557	-.3350966
BIRPS	BM87-1	1900	162	05	19	21.625	247.72	55.5521815	-.3358813
BIRPS	BM87-1	1901	162	05	19	44.309	247.90	55.5520185	-.3366115
BIRPS	BM87-1	1902	162	05	20	06.342	247.69	55.5518543	-.3373514
BIRPS	BM87-1	1903	162	05	20	28.259	247.04	55.5516789	-.3380996
BIRPS	BM87-1	1904	162	05	20	49.575	248.30	55.5515018	-.3388377
BIRPS	BM87-1	1905	162	05	21	11.359	247.94	55.5513465	-.3395240
BIRPS	BM87-1	1906	162	05	21	32.975	247.71	55.5511731	-.3402602
BIRPS	BM87-1	1907	162	05	21	54.825	248.60	55.5510042	-.3409996
BIRPS	BM87-1	1908	162	05	22	16.675	248.31	55.5508313	-.3417445
BIRPS	BM87-1	1909	162	05	22	38.209	249.24	55.5506685	-.3424765
BIRPS	BM87-1	1910	162	05	23	00.309	249.40	55.5505083	-.3432183
BIRPS	BM87-1	1911	162	05	23	22.159	248.83	55.5503451	-.3439911
BIRPS	BM87-1	1912	162	05	23	43.692	249.07	55.5501785	-.3447761
BIRPS	BM87-1	1913	162	05	24	04.259	249.02	55.5500423	-.3454868
BIRPS	BM87-1	1914	162	05	24	25.092	247.65	55.5498996	-.3462064
BIRPS	BM87-1	1915	162	05	24	45.875	248.00	55.5497254	-.3469568
BIRPS	BM87-1	1916	162	05	25	07.275	248.20	55.5495757	-.3476289
BIRPS	BM87-1	1917	162	05	25	29.442	248.02	55.5493931	-.3484325
BIRPS	BM87-1	1918	162	05	25	51.625	247.32	55.5492192	-.3491544
BIRPS	BM87-1	1919	162	05	26	14.175	247.72	55.5490428	-.3498608
BIRPS	BM87-1	1920	162	05	26	37.259	248.46	55.5488711	-.3505656
BIRPS	BM87-1	1921	162	05	26	59.992	248.78	55.5486890	-.3513549
BIRPS	BM87-1	1922	162	05	27	22.542	248.92	55.5485270	-.3521073
BIRPS	BM87-1	1923	162	05	27	43.825	247.82	55.5483713	-.3528773
BIRPS	BM87-1	1924	162	05	28	05.042	247.37	55.5482186	-.3535596

BIRPS	BM87-1	1925	162	05	28	26.425	247.16	55.5480371	-.3543012
BIRPS	BM87-1	1926	162	05	28	48.475	247.78	55.5478532	-.3550223
BIRPS	BM87-1	1927	162	05	29	10.175	248.25	55.5476795	-.3557362
BIRPS	BM87-1	1928	162	05	29	32.725	248.87	55.5475319	-.3564521
BIRPS	BM87-1	1929	162	05	29	55.225	249.71	55.5473833	-.3572091
BIRPS	BM87-1	1930	162	05	30	17.177	248.94	55.5472355	-.3580043
BIRPS	BM87-1	1931	162	05	30	38.111	247.66	55.5470771	-.3588132
BIRPS	BM87-1	1932	162	05	30	58.642	247.45	55.5469221	-.3595285
BIRPS	BM87-1	1933	162	05	31	18.675	247.39	55.5467710	-.3602456
BIRPS	BM87-1	1934	162	05	31	39.025	247.07	55.5466115	-.3609554
BIRPS	BM87-1	1935	162	05	31	59.425	247.21	55.5464524	-.3616612
BIRPS	BM87-1	1936	162	05	32	20.375	247.25	55.5462715	-.3624374
BIRPS	BM87-1	1937	162	05	32	41.409	247.68	55.5461120	-.3631378
BIRPS	BM87-1	1938	162	05	33	02.342	247.63	55.5459420	-.3639269
BIRPS	BM87-1	1939	162	05	33	23.359	246.44	55.5457960	-.3646489
BIRPS	BM87-1	1940	162	05	33	43.842	245.90	55.5456434	-.3653700
BIRPS	BM87-1	1941	162	05	34	04.342	245.51	55.5454862	-.3661783
BIRPS	BM87-1	1942	162	05	34	25.042	245.24	55.5453265	-.3668987
BIRPS	BM87-1	1943	162	05	34	45.342	245.94	55.5451661	-.3676098
BIRPS	BM87-1	1944	162	05	35	05.759	245.09	55.5450082	-.3683088
BIRPS	BM87-1	1945	162	05	35	26.959	244.34	55.5448255	-.3690599
BIRPS	BM87-1	1946	162	05	35	48.192	244.33	55.5446349	-.3698077
BIRPS	BM87-1	1947	162	05	36	09.709	244.17	55.5444617	-.3704991
BIRPS	BM87-1	1948	162	05	36	30.992	244.28	55.5442500	-.3712549
BIRPS	BM87-1	1949	162	05	36	51.375	245.89	55.5440851	-.3719440
BIRPS	BM87-1	1950	162	05	37	12.392	245.59	55.5439058	-.3727339
BIRPS	BM87-1	1951	162	05	37	33.025	245.18	55.5437438	-.3734578
BIRPS	BM87-1	1952	162	05	37	53.075	245.70	55.5435764	-.3741753
BIRPS	BM87-1	1953	162	05	38	13.342	245.24	55.5433964	-.3749079
BIRPS	BM87-1	1954	162	05	38	32.992	246.01	55.5432200	-.3756282
BIRPS	BM87-1	1955	162	05	38	52.992	247.25	55.5430389	-.3763282
BIRPS	BM87-1	1956	162	05	39	13.542	246.89	55.5428772	-.3770248
BIRPS	BM87-1	1957	162	05	39	34.659	247.03	55.5426918	-.3777792
BIRPS	BM87-1	1958	162	05	39	56.375	247.57	55.5425166	-.3785283
BIRPS	BM87-1	1959	162	05	40	18.075	248.33	55.5423499	-.3792303
BIRPS	BM87-1	1960	162	05	40	39.125	248.81	55.5421795	-.3800243
BIRPS	BM87-1	1961	162	05	40	59.409	249.36	55.5420365	-.3807439
BIRPS	BM87-1	1962	162	05	41	20.142	247.91	55.5418866	-.3814774
BIRPS	BM87-1	1963	162	05	41	40.725	247.82	55.5417205	-.3822718
BIRPS	BM87-1	1964	162	05	42	01.475	247.67	55.5415700	-.3829857
BIRPS	BM87-1	1965	162	05	42	21.959	248.20	55.5414227	-.3836959
BIRPS	BM87-1	1966	162	05	42	43.009	247.73	55.5412506	-.3844705
BIRPS	BM87-1	1967	162	05	43	03.792	248.44	55.5411012	-.3851807
BIRPS	BM87-1	1968	162	05	43	24.942	247.85	55.5409293	-.3859844
BIRPS	BM87-1	1969	162	05	43	45.909	247.02	55.5407708	-.3867140
BIRPS	BM87-1	1970	162	05	44	05.959	247.35	55.5406175	-.3874397
BIRPS	BM87-1	1971	162	05	44	26.259	247.60	55.5404511	-.3881764
BIRPS	BM87-1	1972	162	05	44	46.309	247.55	55.5402789	-.3889084
BIRPS	BM87-1	1973	162	05	45	06.342	246.88	55.5401048	-.3896317
BIRPS	BM87-1	1974	162	05	45	26.275	247.95	55.5399366	-.3903375
BIRPS	BM87-1	1975	162	05	45	46.825	248.61	55.5397627	-.3911219
BIRPS	BM87-1	1976	162	05	46	07.575	248.68	55.5396200	-.3918341
BIRPS	BM87-1	1977	162	05	46	28.259	247.86	55.5394931	-.3925592
BIRPS	BM87-1	1978	162	05	46	49.442	246.39	55.5393420	-.3933481
BIRPS	BM87-1	1979	162	05	47	10.342	245.37	55.5391896	-.3940569
BIRPS	BM87-1	1980	162	05	47	31.242	246.75	55.5390144	-.3948053
BIRPS	BM87-1	1981	162	05	47	52.492	244.88	55.5388270	-.3955719
BIRPS	BM87-1	1982	162	05	48	13.975	245.99	55.5386524	-.3962604
BIRPS	BM87-1	1983	162	05	48	35.159	247.07	55.5384597	-.3970220
BIRPS	BM87-1	1984	162	05	48	56.359	247.66	55.5383055	-.3977038
BIRPS	BM87-1	1985	162	05	49	17.909	246.92	55.5381436	-.3984618
BIRPS	BM87-1	1986	162	05	49	39.692	245.83	55.5379686	-.3992027
BIRPS	BM87-1	1987	162	05	50	01.125	246.41	55.5377905	-.3999409
BIRPS	BM87-1	1988	162	05	50	23.142	247.07	55.5376077	-.4006995
BIRPS	BM87-1	1989	162	05	50	44.492	247.55	55.5374418	-.4014693
BIRPS	BM87-1	1990	162	05	51	05.525	247.63	55.5372993	-.4021722
BIRPS	BM87-1	1991	162	05	51	26.342	246.83	55.5371591	-.4028750
BIRPS	BM87-1	1992	162	05	51	47.709	245.79	55.5369932	-.4036598
BIRPS	BM87-1	1993	162	05	52	08.325	245.24	55.5368281	-.4043496
BIRPS	BM87-1	1994	162	05	52	29.442	246.20	55.5366463	-.4050914
BIRPS	BM87-1	1995	162	05	52	50.775	246.53	55.5364858	-.4058182
BIRPS	BM87-1	1996	162	05	53	13.359	246.52	55.5363276	-.4065476
BIRPS	BM87-1	1997	162	05	53	35.609	246.33	55.5361758	-.4072850
BIRPS	BM87-1	1998	162	05	53	57.909	245.98	55.5360266	-.4080208
BIRPS	BM87-1	1999	162	05	54	20.559	245.17	55.5358570	-.4088312
BIRPS	BM87-1	2000	162	05	54	42.792	245.03	55.5356910	-.4095794
BIRPS	BM87-1	2001	162	05	55	04.542	244.47	55.5355255	-.4103474
BIRPS	BM87-1	2002	162	05	55	25.875	244.05	55.5353657	-.4110426
BIRPS	BM87-1	2003	162	05	55	46.492	244.73	55.5352006	-.4117800
BIRPS	BM87-1	2004	162	05	56	08.425	243.99	55.5350354	-.4125257
BIRPS	BM87-1	2005	162	05	56	30.442	243.88	55.5348694	-.4132545
BIRPS	BM87-1	2006	162	05	56	52.809	243.69	55.5346991	-.4139714
BIRPS	BM87-1	2007	162	05	57	15.359	243.88	55.5345203	-.4146671
BIRPS	BM87-1	2008	162	05	57	38.075	243.84	55.5343399	-.4153835
BIRPS	BM87-1	2009	162	05	58	00.675	243.84	55.5341391	-.4161773
BIRPS	BM87-1	2010	162	05	58	22.725	243.69	55.5339564	-.4169222
BIRPS	BM87-1	2011	162	05	58	44.109	244.15	55.5338120	-.4176073
BIRPS	BM87-1	2012	162	05	59	05.692	244.73	55.5336512	-.4183462
BIRPS	BM87-1	2013	162	05	59	27.425	244.85	55.5335073	-.4190693
BIRPS	BM87-1	2014	162	05	59	50.292	243.10	55.5333367	-.4198080
BIRPS	BM87-1	2015	162	06	00	12.309	243.43	55.5331562	-.4205232
BIRPS	BM87-1	2016	162	06	00	34.325	245.18	55.5329830	-.4212268
BIRPS	BM87-1	2017	162	06	00	57.259	244.65	55.5327933	-.4220184
BIRPS	BM87-1	2018	162	06	01	19.359	245.29	55.5326262	-.4227413
BIRPS	BM87-1	2019	162	06	01	41.475	245.18	55.5324582	-.4234909
BIRPS	BM87-1	2020	162	06	02	02.959	244.63	55.5322839	-.4242518
BIRPS	BM87-1	2021	162	06	02	24.492	245.10	55.5320978	-.4250118
BIRPS	BM87-1	2022	162	06	02	45.292	245.06	55.5319322	-.4256960
BIRPS	BM87-1	2023	162	06	03	06.209	246.13	55.5317684	-.4263597
BIRPS	BM87-1	2024	162	06	03	28.092	246.43	55.5315863	-.4270800
BIRPS	BM87-1	2025	162	06	03	50.609	246.58	55.5313820	-.4278571
BIRPS	BM87-1	2026	162	06	04	13.125	246.08	55.5311999	-.4285505
BIRPS	BM87-1	2027	162	06	04	36.109	248.06	55.5310433	-.4292393
BIRPS	BM87-1	2028	162	06	04	59.809	247.25	55.5308571	-.4300194
BIRPS	BM87-1	2029	162	06	05	22.192	248.73	55.5306972	-.4307560
BIRPS	BM87-1	2030	162	06	05	44.375	249.44	55.5305341	-.4315099
BIRPS	BM87-1	2031	162	06	06	06.042	250.68	55.5303893	-.4322704
BIRPS	BM87-1	2032	162	06	06	27.509	250.38	55.5302595	-.4330330
BIRPS	BM87-1	2033	162	06	06	48.975	249.20	55.5301219	-.4338164
BIRPS	BM87-1	2034	162	06	07	10.492	248.07	55.5299641	-.4345892
BIRPS	BM87-1	2035	162	06	07	31.609	248.52	55.5298123	-.4352645
BIRPS	BM87-1	2036	162	06	07	52.942	248.23	55.5296543	-.4360261
BIRPS	BM87-1	2037	162	06	08	14.609	247.98	55.5294932	-.4367846
BIRPS	BM87-1	2038	162	06	08	36.025	248.22	55.5293477	-.4374659
BIRPS	BM87-1	2039	162	06	08	57.725	248.51	55.5291898	-.4382119
BIRPS	BM87-1	2040	162	06	09	19.425	248.13	55.5290333	-.4389630
BIRPS	BM87-1	2041	162	06	09	40.992	248.73	55.5288922	-.4397052
BIRPS	BM87-1	2042	162	06	10	03.792	247.83	55.5287652	-.4404244
BIRPS	BM87-1	2043	162	06	10	27.059	246.68	55.5286328	-.4412110
BIRPS	BM87-1	2044	162	06	10	51.009	245.03	55.5284765	-.4420053

BIRPS	BM87-1	2045	162	06	11	14.059	244.97	55.5283263	-.4427321
BIRPS	BM87-1	2046	162	06	11	36.409	245.87	55.5281679	-.4434807
BIRPS	BM87-1	2047	162	06	11	58.425	243.51	55.5279997	-.4442432
BIRPS	BM87-1	2048	162	06	12	19.659	242.79	55.5278393	-.4449888
BIRPS	BM87-1	2049	162	06	12	40.975	242.70	55.5276644	-.4457262
BIRPS	BM87-1	2050	162	06	13	02.575	241.85	55.5275037	-.4464108
BIRPS	BM87-1	2051	162	06	13	24.009	242.00	55.5273086	-.4471260
BIRPS	BM87-1	2052	162	06	13	45.659	241.93	55.5271108	-.4478377
BIRPS	BM87-1	2053	162	06	14	07.659	241.99	55.5269055	-.4485351
BIRPS	BM87-1	2054	162	06	14	29.609	242.92	55.5267194	-.4492354
BIRPS	BM87-1	2055	162	06	14	52.109	243.20	55.5265252	-.4499528
BIRPS	BM87-1	2056	162	06	15	14.292	243.62	55.5263346	-.4506688
BIRPS	BM87-1	2057	162	06	15	36.475	243.80	55.5261514	-.4513976
BIRPS	BM87-1	2058	162	06	15	58.259	244.70	55.5259695	-.4521282
BIRPS	BM87-1	2059	162	06	16	20.142	245.03	55.5257836	-.4528619
BIRPS	BM87-1	2060	162	06	16	41.692	246.07	55.5256155	-.4535979
BIRPS	BM87-1	2061	162	06	17	03.692	245.68	55.5254511	-.4543326
BIRPS	BM87-1	2062	162	06	17	25.925	245.51	55.5252825	-.4550713
BIRPS	BM87-1	2063	162	06	17	47.842	246.19	55.5251111	-.4558073
BIRPS	BM87-1	2064	162	06	18	09.592	246.88	55.5249481	-.4565374
BIRPS	BM87-1	2065	162	06	18	31.459	246.79	55.5248033	-.4572888
BIRPS	BM87-1	2066	162	06	18	53.459	246.27	55.5246393	-.4580446
BIRPS	BM87-1	2067	162	06	19	14.825	246.18	55.5244789	-.4588068
BIRPS	BM87-1	2068	162	06	19	36.259	246.24	55.5243308	-.4595119
BIRPS	BM87-1	2069	162	06	19	57.342	246.51	55.5241638	-.4602811
BIRPS	BM87-1	2070	162	06	20	18.842	246.08	55.5240133	-.4610476
BIRPS	BM87-1	2071	162	06	20	40.409	245.79	55.5238778	-.4617241
BIRPS	BM87-1	2072	162	06	21	02.609	245.29	55.5237245	-.4624539
BIRPS	BM87-1	2073	162	06	21	25.175	245.58	55.5235593	-.4632456
BIRPS	BM87-1	2074	162	06	21	48.242	246.10	55.5233923	-.4639712
BIRPS	BM87-1	2075	162	06	22	10.692	245.63	55.5232055	-.4647678
BIRPS	BM87-1	2076	162	06	22	32.742	246.39	55.5230408	-.4655032
BIRPS	BM87-1	2077	162	06	22	54.642	245.91	55.5228917	-.4661857
BIRPS	BM87-1	2078	162	06	23	16.209	245.02	55.5227184	-.4669494
BIRPS	BM87-1	2079	162	06	23	37.225	243.95	55.5225312	-.4676987
BIRPS	BM87-1	2080	162	06	23	58.276	244.95	55.5223766	-.4683592
BIRPS	BM87-1	2081	162	06	24	20.192	245.05	55.5221893	-.4690906
BIRPS	BM87-1	2082	162	06	24	42.142	246.23	55.5220145	-.4698157
BIRPS	BM87-1	2083	162	06	25	03.842	246.49	55.5218560	-.4705549
BIRPS	BM87-1	2084	162	06	25	25.642	246.19	55.5216928	-.4713150
BIRPS	BM87-1	2085	162	06	25	46.825	245.61	55.5215266	-.4720804
BIRPS	BM87-1	2086	162	06	26	08.042	245.91	55.5213774	-.4727868
BIRPS	BM87-1	2087	162	06	26	28.709	246.59	55.5212261	-.4735770
BIRPS	BM87-1	2088	162	06	26	49.792	244.44	55.5210961	-.4743045
BIRPS	BM87-1	2089	162	06	27	10.375	244.30	55.5215210	-.4719052
BIRPS	BM87-1	2090	162	06	27	31.809	244.84	55.5213595	-.4726574
BIRPS	BM87-1	2091	162	06	27	53.225	245.11	55.5211972	-.4734209
BIRPS	BM87-1	2092	162	06	28	15.059	246.47	55.5210337	-.4741699
BIRPS	BM87-1	2093	162	06	28	36.809	245.21	55.5208778	-.4749274
BIRPS	BM87-1	2094	162	06	28	58.542	245.52	55.5207258	-.4756030
BIRPS	BM87-1	2095	162	06	29	20.392	246.00	55.5205580	-.4763561
BIRPS	BM87-1	2096	162	06	29	41.992	245.78	55.5203898	-.4770915
BIRPS	BM87-1	2097	162	06	30	03.659	245.96	55.5202321	-.4778376
BIRPS	BM87-1	2098	162	06	30	25.459	245.85	55.5200725	-.4786009
BIRPS	BM87-1	2099	162	06	30	46.925	244.85	55.5199159	-.4793479
BIRPS	BM87-1	2100	162	06	31	08.725	244.99	55.5197517	-.4800801
BIRPS	BM87-1	2101	162	06	31	30.909	245.49	55.5195838	-.4808135
BIRPS	BM87-1	2102	162	06	31	53.059	245.28	55.5194203	-.4815539
BIRPS	BM87-1	2103	162	06	32	15.109	245.17	55.5192630	-.4822989
BIRPS	BM87-1	2104	162	06	32	36.942	244.44	55.5191074	-.4830634
BIRPS	BM87-1	2105	162	06	32	58.375	244.45	55.5189608	-.4837625
BIRPS	BM87-1	2106	162	06	33	19.575	244.59	55.5188004	-.4845292
BIRPS	BM87-1	2107	162	06	33	40.742	243.51	55.5186357	-.4852842
BIRPS	BM87-1	2108	162	06	34	02.459	244.11	55.5184934	-.4859387
BIRPS	BM87-1	2109	162	06	34	25.025	242.87	55.5183229	-.4867463
BIRPS	BM87-1	2110	162	06	34	47.275	242.52	55.5181440	-.4874706
BIRPS	BM87-1	2111	162	06	35	09.709	242.45	55.5179536	-.4881747
BIRPS	BM87-1	2112	162	06	35	31.809	243.15	55.5177696	-.4888842
BIRPS	BM87-1	2113	162	06	35	54.075	243.37	55.5175891	-.4895935
BIRPS	BM87-1	2114	162	06	36	16.092	243.07	55.5174279	-.4903254
BIRPS	BM87-1	2115	162	06	36	38.061	243.34	55.5172694	-.4910426
BIRPS	BM87-1	2116	162	06	37	00.877	242.32	55.5170882	-.4918098
BIRPS	BM87-1	2117	162	06	37	24.209	243.06	55.5169162	-.4925089
BIRPS	BM87-1	2118	162	06	37	47.492	244.24	55.5167231	-.4932551
BIRPS	BM87-1	2119	162	06	38	10.525	244.83	55.5165481	-.4939408
BIRPS	BM87-1	2120	162	06	38	33.975	245.09	55.5163508	-.4946965
BIRPS	BM87-1	2121	162	06	38	56.892	245.56	55.5161517	-.4954631
BIRPS	BM87-1	2122	162	06	39	19.459	246.78	55.5159811	-.4961819
BIRPS	BM87-1	2123	162	06	39	41.675	246.51	55.5158265	-.4969220
BIRPS	BM87-1	2124	162	06	40	03.725	246.16	55.5156688	-.4976707
BIRPS	BM87-1	2125	162	06	40	25.442	246.40	55.5155230	-.4984169
BIRPS	BM87-1	2126	162	06	40	47.359	245.30	55.5153788	-.4991688
BIRPS	BM87-1	2127	162	06	41	09.675	243.67	55.5152211	-.4999000
BIRPS	BM87-1	2128	162	06	41	31.442	243.17	55.5150658	-.5006122
BIRPS	BM87-1	2129	162	06	41	54.192	244.11	55.5148958	-.5012982
BIRPS	BM87-1	2130	162	06	42	17.892	245.45	55.5147248	-.5020434
BIRPS	BM87-1	2131	162	06	42	41.559	245.58	55.5145737	-.5028353
BIRPS	BM87-1	2132	162	06	43	04.059	245.64	55.5144392	-.5035813
BIRPS	BM87-1	2133	162	06	43	26.192	244.11	55.5142872	-.5043292
BIRPS	BM87-1	2134	162	06	43	48.075	244.79	55.5141191	-.5050564
BIRPS	BM87-1	2135	162	06	44	10.009	244.96	55.5139488	-.5057783
BIRPS	BM87-1	2136	162	06	44	32.159	244.36	55.5137734	-.5065025
BIRPS	BM87-1	2137	162	06	44	54.359	245.04	55.5136110	-.5072207
BIRPS	BM87-1	2138	162	06	45	16.892	245.61	55.5134244	-.5080045
BIRPS	BM87-1	2139	162	06	45	39.375	246.19	55.5132482	-.5087329
BIRPS	BM87-1	2140	162	06	46	01.642	245.58	55.5130930	-.5094803
BIRPS	BM87-1	2141	162	06	46	23.359	244.88	55.5129317	-.5102415
BIRPS	BM87-1	2142	162	06	46	45.042	244.00	55.5127759	-.5110157
BIRPS	BM87-1	2143	162	06	47	06.392	243.51	55.5126267	-.5116927
BIRPS	BM87-1	2144	162	06	47	27.759	242.85	55.5124526	-.5124469
BIRPS	BM87-1	2145	162	06	47	48.742	243.32	55.5122963	-.5131021
BIRPS	BM87-1	2146	162	06	48	11.092	243.36	55.5121047	-.5138820
BIRPS	BM87-1	2147	162	06	48	33.659	244.05	55.5119331	-.5145948
BIRPS	BM87-1	2148	162	06	48	56.659	244.61	55.5117756	-.5153218
BIRPS	BM87-1	2149	162	06	49	19.342	244.15	55.5115941	-.5161442
BIRPS	BM87-1	2150	162	06	49	40.959	244.66	55.5114297	-.5169101
BIRPS	BM87-1	2151	162	06	50	01.992	244.29	55.5112899	-.5176005
BIRPS	BM87-1	2152	162	06	50	23.225	242.74	55.5111265	-.5183579
BIRPS	BM87-1	2153	162	06	50	44.892	243.00	55.5109767	-.5190279
BIRPS	BM87-1	2154	162	06	51	06.959	242.34	55.5107941	-.5198389
BIRPS	BM87-1	2155	162	06	51	28.725	241.64	55.5106343	-.5205190
BIRPS	BM87-1	2156	162	06	51	50.209	242.27	55.5104528	-.5212547
BIRPS	BM87-1	2157	162	06	52	11.442	242.57	55.5102768	-.5219941
BIRPS	BM87-1	2158	162	06	52	33.392	243.37	55.5100936	-.5227306
BIRPS	BM87-1	2159	162	06	52	55.092	243.62	55.5099235	-.5234803
BIRPS	BM87-1	2160	162	06	53	16.692	242.99	55.5097720	-.5241814
BIRPS	BM87-1	2161	162	06	53	37.825	243.37	55.5095994	-.5249438
BIRPS	BM87-1	2162	162	06	53	58.642	242.59	55.5094277	-.5256419
BIRPS	BM87-1	2163	162	06	54	19.359	242.59	55.5092453	-.5264096
BIRPS	BM87-1	2164	162	06	54	40.075	242.46	55.5090672	-.5271066

BIRPS	BM87-1	2165	162	06	55	00.309	243.37	55.5089060	-.5277900
BIRPS	BM87-1	2166	162	06	55	21.509	243.50	55.5087133	-.5285558
BIRPS	BM87-1	2167	162	06	55	42.742	244.66	55.5085441	-.5292401
BIRPS	BM87-1	2168	162	06	56	04.009	245.66	55.5083732	-.5299751
BIRPS	BM87-1	2169	162	06	56	25.692	245.06	55.5082102	-.5307426
BIRPS	BM87-1	2170	162	06	56	46.975	244.94	55.5080381	-.5315238
BIRPS	BM87-1	2171	162	06	57	07.875	244.88	55.5078892	-.5322297
BIRPS	BM87-1	2172	162	06	57	28.642	245.66	55.5077396	-.5329140
BIRPS	BM87-1	2173	162	06	57	50.409	244.84	55.5075691	-.5336757
BIRPS	BM87-1	2174	162	06	58	11.975	244.63	55.5074173	-.5344405
BIRPS	BM87-1	2175	162	06	58	33.075	244.93	55.5068698	-.5344837
BIRPS	BM87-1	2176	162	06	58	57.642	248.51	55.5066718	-.5353112
BIRPS	BM87-1	2177	162	06	59	21.375	252.15	55.5065003	-.5361645
BIRPS	BM87-1	2178	162	06	59	43.975	252.30	55.5063931	-.5369863
BIRPS	BM87-1	2179	162	07	00	05.492	251.23	55.5063002	-.5378149
BIRPS	BM87-1	2180	162	07	00	27.459	250.37	55.5061935	-.5386349
BIRPS	BM87-1	2181	162	07	00	49.192	250.12	55.5060631	-.5394614
BIRPS	BM87-1	2182	162	07	01	09.775	250.47	55.5059450	-.5402049
BIRPS	BM87-1	2183	162	07	01	30.225	247.35	55.5058372	-.5409580
BIRPS	BM87-1	2184	162	07	01	50.842	246.65	55.5056995	-.5416780
BIRPS	BM87-1	2185	162	07	02	12.092	248.80	55.5055158	-.5424420
BIRPS	BM87-1	2186	162	07	02	32.975	251.27	55.5053658	-.5432167
BIRPS	BM87-1	2187	162	07	02	54.559	248.18	55.5052801	-.5439675
BIRPS	BM87-1	2188	162	07	03	15.842	245.93	55.5051709	-.5447855
BIRPS	BM87-1	2189	162	07	03	36.525	245.18	55.5050466	-.5455059
BIRPS	BM87-1	2190	162	07	03	57.742	245.41	55.5049179	-.5462965
BIRPS	BM87-1	2191	162	07	04	19.292	241.76	55.5048015	-.5471108
BIRPS	BM87-1	2192	162	07	04	40.509	238.30	55.5046687	-.5478193
BIRPS	BM87-1	2193	162	07	05	01.792	236.93	55.5044975	-.5485675
BIRPS	BM87-1	2194	162	07	05	23.175	237.75	55.5043073	-.5493015
BIRPS	BM87-1	2195	162	07	05	45.175	234.65	55.5041394	-.5500725
BIRPS	BM87-1	2196	162	07	06	06.609	233.01	55.5039576	-.5507492
BIRPS	BM87-1	2197	162	07	06	27.809	233.57	55.5037439	-.5514621
BIRPS	BM87-1	2198	162	07	06	49.159	235.20	55.5035144	-.5521606
BIRPS	BM87-1	2199	162	07	07	10.909	240.27	55.5032800	-.5528465
BIRPS	BM87-1	2200	162	07	07	32.759	241.42	55.5031129	-.5535117
BIRPS	BM87-1	2201	162	07	07	54.792	241.78	55.5029539	-.5542546
BIRPS	BM87-1	2202	162	07	08	17.059	244.28	55.5027696	-.5550481
BIRPS	BM87-1	2203	162	07	08	39.309	246.73	55.5026307	-.5557909
BIRPS	BM87-1	2204	162	07	09	01.609	248.11	55.5025311	-.5565476
BIRPS	BM87-1	2205	162	07	09	24.509	246.06	55.5024418	-.5573374
BIRPS	BM87-1	2206	162	07	09	46.709	243.01	55.5023182	-.5581286
BIRPS	BM87-1	2207	162	07	10	08.275	241.38	55.5021644	-.5589126
BIRPS	BM87-1	2208	162	07	10	28.859	242.11	55.5019998	-.5596160
BIRPS	BM87-1	2209	162	07	10	49.625	240.92	55.5018024	-.5603973
BIRPS	BM87-1	2210	162	07	11	09.792	241.89	55.5016308	-.5610961
BIRPS	BM87-1	2211	162	07	11	30.525	241.04	55.5014523	-.5618226
BIRPS	BM87-1	2212	162	07	11	50.225	241.15	55.5012929	-.5625224
BIRPS	BM87-1	2213	162	07	12	10.809	239.45	55.5011180	-.5632268
BIRPS	BM87-1	2214	162	07	12	31.342	240.31	55.5009374	-.5639029
BIRPS	BM87-1	2215	162	07	12	52.725	241.62	55.5007315	-.5646333
BIRPS	BM87-1	2216	162	07	13	14.075	241.26	55.5005355	-.5653870
BIRPS	BM87-1	2217	162	07	13	35.625	241.63	55.5003632	-.5660718
BIRPS	BM87-1	2218	162	07	13	57.159	241.48	55.5001753	-.5668212
BIRPS	BM87-1	2219	162	07	14	18.592	240.95	55.4999766	-.5675709
BIRPS	BM87-1	2220	162	07	14	39.409	241.50	55.4997998	-.5682428
BIRPS	BM87-1	2221	162	07	15	00.692	242.51	55.4996166	-.5690142
BIRPS	BM87-1	2222	162	07	15	21.342	243.18	55.4994525	-.5697279
BIRPS	BM87-1	2223	162	07	15	41.892	241.81	55.4992832	-.5705212
BIRPS	BM87-1	2224	162	07	16	02.242	241.37	55.4991429	-.5712104
BIRPS	BM87-1	2225	162	07	16	24.159	239.99	55.4989636	-.5719439
BIRPS	BM87-1	2226	162	07	16	46.425	240.16	55.4987716	-.5726650
BIRPS	BM87-1	2227	162	07	17	08.492	241.67	55.4985913	-.5733959
BIRPS	BM87-1	2228	162	07	17	30.025	242.54	55.4984093	-.5741636
BIRPS	BM87-1	2229	162	07	17	51.009	242.38	55.4982487	-.5748845
BIRPS	BM87-1	2230	162	07	18	11.025	241.98	55.4980847	-.5756072
BIRPS	BM87-1	2231	162	07	18	31.059	241.34	55.4979236	-.5763318
BIRPS	BM87-1	2232	162	07	18	51.125	241.73	55.4977498	-.5770382
BIRPS	BM87-1	2233	162	07	19	11.375	242.50	55.4975813	-.5777492
BIRPS	BM87-1	2234	162	07	19	32.109	243.44	55.4973961	-.5785283
BIRPS	BM87-1	2235	162	07	19	52.859	242.77	55.4972462	-.5792465
BIRPS	BM87-1	2236	162	07	20	13.459	243.18	55.4970825	-.5799526
BIRPS	BM87-1	2237	162	07	20	34.225	243.37	55.4969002	-.5807401
BIRPS	BM87-1	2238	162	07	20	54.959	243.38	55.4967384	-.5814807
BIRPS	BM87-1	2239	162	07	21	14.675	243.63	55.4965909	-.5822348
BIRPS	BM87-1	2240	162	07	21	34.359	242.27	55.4964576	-.5829957
BIRPS	BM87-1	2241	162	07	21	54.375	242.01	55.4963357	-.5837494
BIRPS	BM87-1	2242	162	07	22	14.825	240.50	55.4961976	-.5845042
BIRPS	BM87-1	2243	162	07	22	34.625	239.75	55.4960372	-.5852455
BIRPS	BM87-1	2244	162	07	22	54.359	239.89	55.4958735	-.5859583
BIRPS	BM87-1	2245	162	07	23	15.159	239.52	55.4957075	-.5866710
BIRPS	BM87-1	2246	162	07	23	35.725	239.48	55.4955288	-.5874446
BIRPS	BM87-1	2247	162	07	23	56.675	238.74	55.4953535	-.5881424
BIRPS	BM87-1	2248	162	07	24	17.192	238.97	55.4951739	-.5888363
BIRPS	BM87-1	2249	162	07	24	38.042	239.90	55.4949781	-.5895963
BIRPS	BM87-1	2250	162	07	24	59.092	240.50	55.4948102	-.5903013
BIRPS	BM87-1	2251	162	07	25	19.759	240.36	55.4946322	-.5911010
BIRPS	BM87-1	2252	162	07	25	40.175	239.90	55.4944664	-.5918296
BIRPS	BM87-1	2253	162	07	26	00.625	239.27	55.4943062	-.5925524
BIRPS	BM87-1	2254	162	07	26	20.625	238.83	55.4941412	-.5932695
BIRPS	BM87-1	2255	162	07	26	40.942	238.92	55.4939728	-.5939765
BIRPS	BM87-1	2256	162	07	27	01.342	239.58	55.4938011	-.5946757
BIRPS	BM87-1	2257	162	07	27	22.225	239.18	55.4936043	-.5954496
BIRPS	BM87-1	2258	162	07	27	43.075	240.01	55.4934281	-.5961654
BIRPS	BM87-1	2259	162	07	28	03.125	239.61	55.4932580	-.5968829
BIRPS	BM87-1	2260	162	07	28	23.075	239.15	55.4931026	-.5976100
BIRPS	BM87-1	2261	162	07	28	43.225	239.85	55.4929517	-.5983376
BIRPS	BM87-1	2262	162	07	29	04.059	239.39	55.4927813	-.5991265
BIRPS	BM87-1	2263	162	07	29	24.892	238.92	55.4926254	-.5998320
BIRPS	BM87-1	2264	162	07	29	45.642	239.55	55.4924689	-.6005445
BIRPS	BM87-1	2265	162	07	30	06.842	238.53	55.4922886	-.6013210
BIRPS	BM87-1	2266	162	07	30	27.375	239.03	55.4921242	-.6020005
BIRPS	BM87-1	2267	162	07	30	48.859	238.68	55.4919460	-.6027686
BIRPS	BM87-1	2268	162	07	31	09.792	238.26	55.4917679	-.6035413
BIRPS	BM87-1	2269	162	07	31	30.825	239.27	55.4916051	-.6042312
BIRPS	BM87-1	2270	162	07	31	51.761	239.05	55.4914271	-.6049999
BIRPS	BM87-1	2271	162	07	32	12.994	238.87	55.4912544	-.6056982
BIRPS	BM87-1	2272	162	07	32	33.742	238.90	55.4910597	-.6064382
BIRPS	BM87-1	2273	162	07	32	55.142	239.70	55.4908714	-.6071146
BIRPS	BM87-1	2274	162	07	33	16.059	240.96	55.4906811	-.6078682
BIRPS	BM87-1	2275	162	07	33	37.192	241.40	55.4905235	-.6085791
BIRPS	BM87-1	2276	162	07	33	58.042	241.80	55.4903537	-.6093668
BIRPS	BM87-1	2277	162	07	34	18.742	242.05	55.4902138	-.6100837
BIRPS	BM87-1	2278	162	07	34	39.492	240.37	55.4900654	-.6107994
BIRPS	BM87-1	2279	162	07	35	00.492	241.31	55.4898969	-.6115736
BIRPS	BM87-1	2280	162	07	35	21.259	240.96	55.4897505	-.6123059
BIRPS	BM87-1	2281	162	07	35	42.042	238.47	55.4895763	-.6131233
BIRPS	BM87-1	2282	162	07	36	01.875	238.39	55.4894306	-.6138306
BIRPS	BM87-1	2283	162	07	36	22.425	238.41	55.4892853	-.6145491
BIRPS	BM87-1	2284	162	07	36	43.442	239.34	55.4891246	-.6152536

BIRPS	BM87-1	2285	162	07	37	04.392	239.20	55.4889375	-.6160082
BIRPS	BM87-1	2286	162	07	37	25.775	239.75	55.4887484	-.6167505
BIRPS	BM87-1	2287	162	07	37	47.042	240.18	55.4885798	-.6174253
BIRPS	BM87-1	2288	162	07	38	08.342	239.63	55.4883937	-.6181848
BIRPS	BM87-1	2289	162	07	38	29.875	240.75	55.4882029	-.6189321
BIRPS	BM87-1	2290	162	07	38	51.025	241.13	55.4880469	-.6196294
BIRPS	BM87-1	2291	162	07	39	11.959	241.09	55.4878748	-.6204110
BIRPS	BM87-1	2292	162	07	39	32.742	240.62	55.4877180	-.6211353
BIRPS	BM87-1	2293	162	07	39	52.809	240.25	55.4875468	-.6218453
BIRPS	BM87-1	2294	162	07	40	12.975	241.21	55.4873777	-.6225373
BIRPS	BM87-1	2295	162	07	40	33.809	242.07	55.4871857	-.6232748
BIRPS	BM87-1	2296	162	07	40	55.409	243.61	55.4870228	-.6239463
BIRPS	BM87-1	2297	162	07	41	17.259	243.46	55.4868528	-.6247198
BIRPS	BM87-1	2298	162	07	41	38.525	243.43	55.4866841	-.6254988
BIRPS	BM87-1	2299	162	07	41	59.225	242.78	55.4865252	-.6262093
BIRPS	BM87-1	2300	162	07	42	19.975	243.10	55.4863531	-.6269909
BIRPS	BM87-1	2301	162	07	42	40.859	241.23	55.4861869	-.6277144
BIRPS	BM87-1	2302	162	07	43	01.059	241.21	55.4860157	-.6283853
BIRPS	BM87-1	2303	162	07	43	21.992	242.38	55.4858352	-.6291089
BIRPS	BM87-1	2304	162	07	43	44.092	244.32	55.4856569	-.6298452
BIRPS	BM87-1	2305	162	07	44	06.159	244.90	55.4854941	-.6306204
BIRPS	BM87-1	2306	162	07	44	27.792	245.05	55.4853426	-.6314180
BIRPS	BM87-1	2307	162	07	44	48.459	245.18	55.4852270	-.6321477
BIRPS	BM87-1	2308	162	07	45	09.109	242.92	55.4850960	-.6328887
BIRPS	BM87-1	2309	162	07	45	29.559	242.43	55.4849505	-.6336107
BIRPS	BM87-1	2310	162	07	45	50.275	241.82	55.4847814	-.6344170
BIRPS	BM87-1	2311	162	07	46	10.892	241.89	55.4846188	-.6351382
BIRPS	BM87-1	2312	162	07	46	30.775	242.31	55.4844686	-.6358531
BIRPS	BM87-1	2313	162	07	46	51.209	241.94	55.4843198	-.6365768
BIRPS	BM87-1	2314	162	07	47	11.859	241.05	55.4841568	-.6373694
BIRPS	BM87-1	2315	162	07	47	32.509	239.63	55.4839971	-.6380688
BIRPS	BM87-1	2316	162	07	47	53.275	240.51	55.4838290	-.6387438
BIRPS	BM87-1	2317	162	07	48	14.875	240.86	55.4836327	-.6395077
BIRPS	BM87-1	2318	162	07	48	35.692	242.11	55.4834346	-.6402887
BIRPS	BM87-1	2319	162	07	48	56.009	241.95	55.4832736	-.6410079
BIRPS	BM87-1	2320	162	07	49	16.359	241.16	55.4831217	-.6417327
BIRPS	BM87-1	2321	162	07	49	37.209	241.73	55.4829559	-.6424304
BIRPS	BM87-1	2322	162	07	49	58.075	241.63	55.4827690	-.6432032
BIRPS	BM87-1	2323	162	07	50	18.842	241.71	55.4826024	-.6439055
BIRPS	BM87-1	2324	162	07	50	39.275	240.90	55.4824446	-.6445956
BIRPS	BM87-1	2325	162	07	51	00.959	240.36	55.4822437	-.6453294
BIRPS	BM87-1	2326	162	07	51	22.225	240.92	55.4820405	-.6460548
BIRPS	BM87-1	2327	162	07	51	44.175	241.54	55.4818405	-.6467834
BIRPS	BM87-1	2328	162	07	52	05.842	242.61	55.4816530	-.6475167
BIRPS	BM87-1	2329	162	07	52	27.459	243.18	55.4814806	-.6482041
BIRPS	BM87-1	2330	162	07	52	48.809	244.48	55.4833849	-.6484177
BIRPS	BM87-1	2331	162	07	53	09.875	241.17	55.4832512	-.6491986
BIRPS	BM87-1	2332	162	07	53	53.512	237.53	55.4830783	-.6499528
BIRPS	BM87-1	2333	162	07	53	53.709	234.72	55.4828882	-.6506638
BIRPS	BM87-1	2334	162	07	54	16.175	235.85	55.4826680	-.6513353
BIRPS	BM87-1	2335	162	07	54	39.125	234.79	55.4824656	-.6520521
BIRPS	BM87-1	2336	162	07	55	01.009	231.25	55.4822670	-.6527665
BIRPS	BM87-1	2337	162	07	55	22.842	232.19	55.4820357	-.6534537
BIRPS	BM87-1	2338	162	07	55	44.592	231.19	55.4818078	-.6541698
BIRPS	BM87-1	2339	162	07	56	05.892	231.52	55.4815645	-.6548825
BIRPS	BM87-1	2340	162	07	56	27.159	232.50	55.4813468	-.6555260
BIRPS	BM87-1	2341	162	07	56	48.692	231.02	55.4811195	-.6562364
BIRPS	BM87-1	2342	162	07	57	10.325	228.52	55.4808860	-.6569254
BIRPS	BM87-1	2343	162	07	57	32.825	228.81	55.4806292	-.6575592
BIRPS	BM87-1	2344	162	07	57	55.292	229.77	55.4803874	-.6581920
BIRPS	BM87-1	2345	162	07	58	18.825	228.13	55.4801338	-.6589096
BIRPS	BM87-1	2346	162	07	58	41.909	227.97	55.4798744	-.6596205
BIRPS	BM87-1	2347	162	07	59	05.192	228.08	55.4796335	-.6602761
BIRPS	BM87-1	2348	162	07	59	27.825	229.57	55.4793805	-.6610013
BIRPS	BM87-1	2349	162	07	59	50.642	228.30	55.4791495	-.6616656
BIRPS	BM87-1	2350	162	08	00	13.475	228.01	55.4789042	-.6623186
BIRPS	BM87-1	2351	162	08	00	36.525	226.84	55.4786287	-.6630121
BIRPS	BM87-1	2352	162	08	00	59.125	228.51	55.4783736	-.6636292
BIRPS	BM87-1	2353	162	08	01	22.125	232.02	55.4780859	-.6643128
BIRPS	BM87-1	2354	162	08	01	45.025	236.44	55.4778310	-.6649702
BIRPS	BM87-1	2355	162	08	02	06.859	241.10	55.4776196	-.6656923
BIRPS	BM87-1	2356	162	08	02	27.742	238.52	55.4774639	-.6665053
BIRPS	BM87-1	2357	162	08	02	48.309	234.70	55.4773056	-.6672362
BIRPS	BM87-1	2358	162	08	03	08.992	236.07	55.4771348	-.6678980
BIRPS	BM87-1	2359	162	08	03	30.159	235.72	55.4769330	-.6686270
BIRPS	BM87-1	2360	162	08	03	52.159	236.09	55.4767387	-.6693493
BIRPS	BM87-1	2361	162	08	04	14.109	238.55	55.4765352	-.6700697
BIRPS	BM87-1	2362	162	08	04	35.542	244.35	55.4763315	-.6707138
BIRPS	BM87-1	2363	162	08	04	57.175	250.13	55.4761583	-.6714710
BIRPS	BM87-1	2364	162	08	05	18.492	251.70	55.4760598	-.6722926
BIRPS	BM87-1	2365	162	08	05	39.275	249.68	55.4759920	-.6730724
BIRPS	BM87-1	2366	162	08	05	59.709	247.09	55.4759119	-.6739375
BIRPS	BM87-1	2367	162	08	06	19.825	244.62	55.4758102	-.6747136
BIRPS	BM87-1	2368	162	08	06	39.942	243.24	55.4756722	-.6754811
BIRPS	BM87-1	2369	162	08	06	59.459	242.12	55.4755439	-.6761598
BIRPS	BM87-1	2370	162	08	07	19.125	242.22	55.4753859	-.6769050
BIRPS	BM87-1	2371	162	08	07	38.709	241.79	55.4752264	-.6776357
BIRPS	BM87-1	2372	162	08	07	58.692	241.04	55.4750686	-.6783584
BIRPS	BM87-1	2373	162	08	08	18.992	239.99	55.4749120	-.6790565
BIRPS	BM87-1	2374	162	08	08	39.842	238.99	55.4747386	-.6798292
BIRPS	BM87-1	2375	162	08	09	01.075	238.98	55.4745791	-.6805289
BIRPS	BM87-1	2376	162	08	09	21.942	237.83	55.4743999	-.6813212
BIRPS	BM87-1	2377	162	08	09	42.859	237.25	55.4742289	-.6820358
BIRPS	BM87-1	2378	162	08	10	03.192	236.86	55.4740620	-.6827332
BIRPS	BM87-1	2379	162	08	10	24.159	236.63	55.4738702	-.6834854
BIRPS	BM87-1	2380	162	08	10	45.742	235.27	55.4736572	-.6842252
BIRPS	BM87-1	2381	162	08	11	06.975	234.91	55.4734481	-.6848758
BIRPS	BM87-1	2382	162	08	11	28.142	236.80	55.4732149	-.6855780
BIRPS	BM87-1	2383	162	08	11	49.959	237.68	55.4729994	-.6862947
BIRPS	BM87-1	2384	162	08	12	11.725	237.85	55.4728084	-.6870429
BIRPS	BM87-1	2385	162	08	12	32.975	237.08	55.4726449	-.6877479
BIRPS	BM87-1	2386	162	08	12	53.425	236.21	55.4724796	-.6884626
BIRPS	BM87-1	2387	162	08	13	13.792	236.19	55.4723001	-.6892379
BIRPS	BM87-1	2388	162	08	13	34.475	236.23	55.4721194	-.6899165
BIRPS	BM87-1	2389	162	08	13	55.259	236.29	55.4719412	-.6905850
BIRPS	BM87-1	2390	162	08	14	16.809	237.38	55.4717446	-.6913040
BIRPS	BM87-1	2391	162	08	14	38.509	238.05	55.4715497	-.6920278
BIRPS	BM87-1	2392	162	08	15	00.392	237.37	55.4713475	-.6927716
BIRPS	BM87-1	2393	162	08	15	22.142	238.94	55.4711519	-.6935145
BIRPS	BM87-1	2394	162	08	15	43.392	240.40	55.4709860	-.6942030
BIRPS	BM87-1	2395	162	08	16	04.525	239.49	55.4708014	-.6949834
BIRPS	BM87-1	2396	162	08	16	24.725	240.17	55.4706443	-.6956782
BIRPS	BM87-1	2397	162	08	16	45.525	240.85	55.4704818	-.6963794
BIRPS	BM87-1	2398	162	08	17	06.609	241.37	55.4703014	-.6971535
BIRPS	BM87-1	2399	162	08	17	26.959	242.80	55.4701629	-.6978724
BIRPS	BM87-1	2400	162	08	17	47.742	241.33	55.4700153	-.6986960
BIRPS	BM87-1	2402	162	08	18	08.242	241.33	55.4697405	-.7001568
BIRPS	BM87-1	2403	162	08	18	49.325	240.45	55.4695989	-.7008662
BIRPS	BM87-1	2404	162	08	19	10.409	240.09	55.4694386	-.7016639

BIRPS	BM87-1	2406	162	08	19	51.825	239.33	55.4691064	-.7032029
BIRPS	BM87-1	2407	162	08	20	11.725	239.18	55.4689352	-.7039380
BIRPS	BM87-1	2408	162	08	20	31.375	238.61	55.4687861	-.7046055
BIRPS	BM87-1	2409	162	08	20	51.225	238.42	55.4690817	-.7043495
BIRPS	BM87-1	2410	162	08	21	15.425	235.56	55.4689102	-.7052077
BIRPS	BM87-1	2411	162	08	21	40.575	233.41	55.4686954	-.7060995
BIRPS	BM87-1	2412	162	08	22	06.292	233.10	55.4684535	-.7069612
BIRPS	BM87-1	2413	162	08	22	32.109	233.55	55.4681923	-.7078028
BIRPS	BM87-1	2414	162	08	22	57.792	234.51	55.4679347	-.7086592
BIRPS	BM87-1	2415	162	08	23	22.109	235.85	55.4677146	-.7094666
BIRPS	BM87-1	2416	162	08	23	45.425	234.83	55.4675219	-.7102301
BIRPS	BM87-1	2417	162	08	24	07.992	234.79	55.4673147	-.7110665
BIRPS	BM87-1	2418	162	08	24	30.109	234.94	55.4671260	-.7118242
BIRPS	BM87-1	2419	162	08	24	52.209	235.63	55.4669431	-.7125838
BIRPS	BM87-1	2420	162	08	25	14.192	235.44	55.4667619	-.7133649
BIRPS	BM87-1	2421	162	08	25	35.442	235.14	55.4665855	-.7140835
BIRPS	BM87-1	2422	162	08	25	55.809	235.16	55.4663882	-.7148518
BIRPS	BM87-1	2423	162	08	26	16.442	234.26	55.4662020	-.7155727
BIRPS	BM87-1	2424	162	08	26	36.509	235.05	55.4660067	-.7162715
BIRPS	BM87-1	2425	162	08	26	56.409	236.14	55.4658270	-.7169782
BIRPS	BM87-1	2426	162	08	27	17.225	236.09	55.4656493	-.7177024
BIRPS	BM87-1	2427	162	08	27	37.292	236.69	55.4654772	-.7184093
BIRPS	BM87-1	2428	162	08	27	57.709	237.27	55.4652887	-.7191946
BIRPS	BM87-1	2429	162	08	28	18.209	238.17	55.4651213	-.7199017
BIRPS	BM87-1	2430	162	08	28	39.159	237.98	55.4649666	-.7206112
BIRPS	BM87-1	2431	162	08	29	00.025	238.13	55.4647912	-.7213842
BIRPS	BM87-1	2432	162	08	29	20.809	238.01	55.4646413	-.7220904
BIRPS	BM87-1	2433	162	08	29	41.709	237.69	55.4644763	-.7228310
BIRPS	BM87-1	2434	162	08	30	02.142	237.83	55.4642851	-.7236316
BIRPS	BM87-1	2435	162	08	30	21.927	239.17	55.4641228	-.7243522
BIRPS	BM87-1	2436	162	08	30	42.127	239.72	55.4639645	-.7250823
BIRPS	BM87-1	2437	162	08	31	02.459	239.63	55.4638094	-.7258128
BIRPS	BM87-1	2438	162	08	31	22.925	239.67	55.4636598	-.7265236
BIRPS	BM87-1	2439	162	08	31	43.542	239.49	55.4635058	-.7272219
BIRPS	BM87-1	2440	162	08	32	04.859	239.60	55.4633188	-.7279820
BIRPS	BM87-1	2441	162	08	32	25.709	240.37	55.4631535	-.7286687
BIRPS	BM87-1	2442	162	08	32	47.059	240.48	55.4629679	-.7294498
BIRPS	BM87-1	2443	162	08	33	07.475	240.92	55.4628063	-.7301876
BIRPS	BM87-1	2444	162	08	33	27.559	241.50	55.4626509	-.7309122
BIRPS	BM87-1	2445	162	08	33	47.809	240.84	55.4625130	-.7316271
BIRPS	BM87-1	2446	162	08	34	08.925	239.89	55.4623479	-.7324219
BIRPS	BM87-1	2447	162	08	34	30.059	239.92	55.4621898	-.7331297
BIRPS	BM87-1	2448	162	08	34	50.775	239.95	55.4620121	-.7339202
BIRPS	BM87-1	2449	162	08	35	11.359	240.26	55.4618501	-.7346394
BIRPS	BM87-1	2450	162	08	35	31.559	241.09	55.4616856	-.7353405
BIRPS	BM87-1	2451	162	08	35	52.109	241.24	55.4615329	-.7360510
BIRPS	BM87-1	2452	162	08	36	12.959	241.05	55.4613636	-.7368505
BIRPS	BM87-1	2453	162	08	36	33.759	240.20	55.4612132	-.7375753
BIRPS	BM87-1	2454	162	08	36	54.042	240.19	55.4610613	-.7382966
BIRPS	BM87-1	2455	162	08	37	14.559	239.53	55.4608945	-.7390113
BIRPS	BM87-1	2456	162	08	37	35.125	240.40	55.4607259	-.7397960
BIRPS	BM87-1	2457	162	08	37	55.859	239.59	55.4605619	-.7405316
BIRPS	BM87-1	2458	162	08	38	15.792	240.48	55.4604015	-.7412495
BIRPS	BM87-1	2459	162	08	38	36.042	239.87	55.4602380	-.7419752
BIRPS	BM87-1	2460	162	08	38	56.242	239.70	55.4600718	-.7426825
BIRPS	BM87-1	2461	162	08	39	17.075	239.68	55.4598939	-.7434494
BIRPS	BM87-1	2462	162	08	39	38.275	240.09	55.4597385	-.7441436
BIRPS	BM87-1	2463	162	08	39	59.792	239.48	55.4595585	-.7449252
BIRPS	BM87-1	2464	162	08	40	20.342	239.20	55.4593997	-.7456428
BIRPS	BM87-1	2465	162	08	40	40.809	238.70	55.4592217	-.7464290
BIRPS	BM87-1	2466	162	08	41	01.742	237.48	55.4590338	-.7471344
BIRPS	BM87-1	2467	162	08	41	21.875	239.03	55.4588526	-.7478125
BIRPS	BM87-1	2468	162	08	41	42.575	240.06	55.4586651	-.7485039
BIRPS	BM87-1	2469	162	08	42	03.659	240.78	55.4584754	-.7492711
BIRPS	BM87-1	2470	162	08	42	24.725	240.94	55.4583264	-.7499831
BIRPS	BM87-1	2471	162	08	42	45.742	240.51	55.4581577	-.7507650
BIRPS	BM87-1	2472	162	08	43	06.359	240.24	55.4580115	-.7514728
BIRPS	BM87-1	2473	162	08	43	27.142	240.42	55.4578282	-.7522537
BIRPS	BM87-1	2474	162	08	43	47.825	240.22	55.4576606	-.7529725
BIRPS	BM87-1	2475	162	08	44	07.975	240.51	55.4574958	-.7536906
BIRPS	BM87-1	2476	162	08	44	28.109	240.43	55.4573382	-.7544163
BIRPS	BM87-1	2477	162	08	44	48.292	240.08	55.4571712	-.7551492
BIRPS	BM87-1	2478	162	08	45	08.092	239.98	55.4569963	-.7558822
BIRPS	BM87-1	2479	162	08	45	27.809	240.65	55.4568255	-.7566173
BIRPS	BM87-1	2480	162	08	45	47.542	241.72	55.4566502	-.7573704
BIRPS	BM87-1	2481	162	08	46	07.359	241.48	55.4564792	-.7581306
BIRPS	BM87-1	2482	162	08	46	26.992	241.05	55.4563255	-.7587975
BIRPS	BM87-1	2483	162	08	46	46.759	241.71	55.4561516	-.7595242
BIRPS	BM87-1	2484	162	08	47	06.642	242.12	55.4559926	-.7602778
BIRPS	BM87-1	2485	162	08	47	26.159	241.76	55.4558307	-.7610552
BIRPS	BM87-1	2486	162	08	47	45.225	239.97	55.4556526	-.7618407
BIRPS	BM87-1	2487	162	08	48	03.975	240.21	55.4554896	-.7625296
BIRPS	BM87-1	2488	162	08	48	22.625	240.61	55.4553220	-.7632074
BIRPS	BM87-1	2489	162	08	48	41.559	240.91	55.4551454	-.7639469
BIRPS	BM87-1	2490	162	08	49	01.275	241.60	55.4549812	-.7646750
BIRPS	BM87-1	2491	162	08	49	21.659	241.81	55.4548249	-.7653990
BIRPS	BM87-1	2492	162	08	49	42.625	241.14	55.4546689	-.7661263
BIRPS	BM87-1	2493	162	08	50	02.842	241.49	55.4545185	-.7668425
BIRPS	BM87-1	2494	162	08	50	23.775	240.93	55.4543406	-.7676532
BIRPS	BM87-1	2495	162	08	50	44.225	241.28	55.4541785	-.7683804
BIRPS	BM87-1	2496	162	08	51	04.192	241.07	55.4540245	-.7691278
BIRPS	BM87-1	2497	162	08	51	24.025	241.26	55.4538870	-.7698724
BIRPS	BM87-1	2498	162	08	51	44.175	238.80	55.4537522	-.7706343
BIRPS	BM87-1	2499	162	08	52	03.992	238.26	55.4536082	-.7713524
BIRPS	BM87-1	2500	162	08	52	24.509	237.33	55.4534530	-.7720725
BIRPS	BM87-1	2501	162	08	52	45.242	237.59	55.4536466	-.7723387
BIRPS	BM87-1	2502	162	08	53	10.025	235.05	55.4534435	-.7731936
BIRPS	BM87-1	2503	162	08	53	34.059	233.86	55.4532222	-.7740489
BIRPS	BM87-1	2504	162	08	53	56.975	235.14	55.4530047	-.7748051
BIRPS	BM87-1	2505	162	08	54	19.875	235.15	55.4527679	-.7756384
BIRPS	BM87-1	2506	162	08	54	42.175	235.42	55.4525704	-.7764122
BIRPS	BM87-1	2507	162	08	55	03.509	234.92	55.4523888	-.7771859
BIRPS	BM87-1	2508	162	08	55	25.459	234.38	55.4521926	-.7779463
BIRPS	BM87-1	2509	162	08	55	47.175	234.41	55.4519979	-.7786787
BIRPS	BM87-1	2510	162	08	56	09.392	233.50	55.4518023	-.7794052
BIRPS	BM87-1	2511	162	08	56	31.859	233.81	55.4515941	-.7801047
BIRPS	BM87-1	2512	162	08	56	54.659	235.28	55.4513775	-.7808073
BIRPS	BM87-1	2513	162	08	57	16.909	238.33	55.4511672	-.7815128
BIRPS	BM87-1	2514	162	08	57	38.842	240.81	55.4509841	-.7822595
BIRPS	BM87-1	2515	162	08	57	59.892	244.00	55.4508150	-.7830256
BIRPS	BM87-1	2516	162	08	58	21.209	247.35	55.4506702	-.7837540
BIRPS	BM87-1	2517	162	08	58	41.942	246.23	55.4505359	-.7845765
BIRPS	BM87-1	2518	162	08	59	02.659	245.47	55.4504221	-.7853098
BIRPS	BM87-1	2519	162	08	59	23.159	244.95	55.4503071	-.7860218
BIRPS	BM87-1	2520	162	08	59	44.709	243.38	55.4501727	-.7868003
BIRPS	BM87-1	2521	162	09	00	06.375	242.10	55.4500027	-.7875584
BIRPS	BM87-1	2522	162	09	00	27.792	242.71	55.4498144	-.7883096
BIRPS	BM87-1	2523	162	09	00	49.025	243.54	55.4496568	-.7890199
BIRPS	BM87-1	2524	162	09	01	09.742	243.41	55.4494801	-.7898198
BIRPS	BM87-1	2525	162	09	01	29.909	242.06	55.4493215	-.7905486

BIRPS	BM87-1	2526	162	09	01	50.375	241.59	55.4491657	-.7912643
BIRPS	BM87-1	2527	162	09	02	10.525	240.20	55.4490133	-.7919767
BIRPS	BM87-1	2528	162	09	02	31.109	238.99	55.4488510	-.7926736
BIRPS	BM87-1	2529	162	09	02	52.225	238.20	55.4486675	-.7934255
BIRPS	BM87-1	2530	162	09	03	14.142	238.21	55.4484760	-.7941607
BIRPS	BM87-1	2531	162	09	03	35.742	238.61	55.4482813	-.7948901
BIRPS	BM87-1	2532	162	09	03	57.375	238.61	55.4481061	-.7955721
BIRPS	BM87-1	2533	162	09	04	18.625	238.59	55.4479259	-.7963343
BIRPS	BM87-1	2534	162	09	04	39.309	237.94	55.4477651	-.7970384
BIRPS	BM87-1	2535	162	09	05	00.225	237.64	55.4475916	-.7978098
BIRPS	BM87-1	2536	162	09	05	21.542	237.08	55.4474266	-.7984904
BIRPS	BM87-1	2537	162	09	05	43.075	236.56	55.4472311	-.7992389
BIRPS	BM87-1	2538	162	09	06	04.209	236.69	55.4470390	-.7999664
BIRPS	BM87-1	2539	162	09	06	25.825	236.44	55.4468637	-.8006333
BIRPS	BM87-1	2540	162	09	06	47.575	236.48	55.4466618	-.8013879
BIRPS	BM87-1	2541	162	09	07	08.509	237.52	55.4464708	-.8021238
BIRPS	BM87-1	2542	162	09	07	30.109	237.14	55.4462982	-.8028066
BIRPS	BM87-1	2543	162	09	07	51.292	238.32	55.4461146	-.8035394
BIRPS	BM87-1	2544	162	09	08	13.359	237.39	55.4459336	-.8042830
BIRPS	BM87-1	2545	162	09	08	35.392	237.65	55.4457436	-.8050231
BIRPS	BM87-1	2546	162	09	08	57.075	238.53	55.4455564	-.8057620
BIRPS	BM87-1	2547	162	09	09	18.242	239.37	55.4453924	-.8064422
BIRPS	BM87-1	2548	162	09	09	39.509	239.11	55.4452088	-.8072068
BIRPS	BM87-1	2549	162	09	10	00.092	238.97	55.4450291	-.8079063
BIRPS	BM87-1	2550	162	09	10	20.459	239.39	55.4448458	-.8085971
BIRPS	BM87-1	2551	162	09	10	41.175	240.14	55.4446617	-.8093422
BIRPS	BM87-1	2552	162	09	11	02.809	240.70	55.4444833	-.8100817
BIRPS	BM87-1	2553	162	09	11	24.459	241.03	55.4443266	-.8107679
BIRPS	BM87-1	2554	162	09	11	45.825	241.52	55.4441687	-.8115474
BIRPS	BM87-1	2555	162	09	12	06.475	241.37	55.4440317	-.8122826
BIRPS	BM87-1	2556	162	09	12	26.992	240.71	55.4438789	-.8131068
BIRPS	BM87-1	2557	162	09	12	47.075	240.34	55.4437301	-.8138472
BIRPS	BM87-1	2558	162	09	13	07.125	239.29	55.4435671	-.8145749
BIRPS	BM87-1	2559	162	09	13	27.225	239.66	55.4433990	-.8152875
BIRPS	BM87-1	2560	162	09	13	47.809	239.75	55.4432410	-.8159956
BIRPS	BM87-1	2561	162	09	14	08.225	239.82	55.4430813	-.8167061
BIRPS	BM87-1	2562	162	09	14	28.892	240.20	55.4429042	-.8174848
BIRPS	BM87-1	2563	162	09	14	49.542	239.64	55.4427529	-.8182084
BIRPS	BM87-1	2564	162	09	15	09.892	239.14	55.4425941	-.8189353
BIRPS	BM87-1	2565	162	09	15	30.009	240.03	55.4424460	-.8196479
BIRPS	BM87-1	2566	162	09	15	50.525	239.10	55.4423040	-.8203855
BIRPS	BM87-1	2567	162	09	16	11.259	239.08	55.4421411	-.8211836
BIRPS	BM87-1	2568	162	09	16	32.159	238.26	55.4419900	-.8219089
BIRPS	BM87-1	2569	162	09	16	52.725	237.54	55.4418195	-.8226723
BIRPS	BM87-1	2570	162	09	17	13.992	237.06	55.4416534	-.8233472
BIRPS	BM87-1	2571	162	09	17	35.492	236.93	55.4414599	-.8240765
BIRPS	BM87-1	2572	162	09	17	57.142	238.32	55.4412711	-.8248170
BIRPS	BM87-1	2573	162	09	18	18.525	238.60	55.4411059	-.8255170
BIRPS	BM87-1	2574	162	09	18	39.425	239.29	55.4409254	-.8262993
BIRPS	BM87-1	2575	162	09	19	00.275	238.22	55.4407642	-.8270330
BIRPS	BM87-1	2576	162	09	19	20.559	236.55	55.4405976	-.8277656
BIRPS	BM87-1	2577	162	09	19	40.342	236.86	55.4404347	-.8284806
BIRPS	BM87-1	2578	162	09	20	00.642	235.72	55.4402694	-.8292038
BIRPS	BM87-1	2579	162	09	20	21.159	236.48	55.4400729	-.8299679
BIRPS	BM87-1	2580	162	09	20	42.059	236.89	55.4398943	-.8306748
BIRPS	BM87-1	2581	162	09	21	02.175	237.67	55.4397147	-.8313703
BIRPS	BM87-1	2582	162	09	21	22.825	237.91	55.4395263	-.8321244
BIRPS	BM87-1	2583	162	09	21	43.992	237.83	55.4393506	-.8328180
BIRPS	BM87-1	2584	162	09	22	04.592	238.47	55.4391825	-.8335169
BIRPS	BM87-1	2585	162	09	22	25.509	237.44	55.4389946	-.8343114
BIRPS	BM87-1	2586	162	09	22	45.375	238.30	55.4388238	-.8350283
BIRPS	BM87-1	2587	162	09	23	05.909	237.44	55.4386326	-.8357567
BIRPS	BM87-1	2588	162	09	23	25.359	238.08	55.4384350	-.8364613
BIRPS	BM87-1	2589	162	09	23	45.709	238.65	55.4382313	-.8371517
BIRPS	BM87-1	2590	162	09	24	05.775	240.69	55.4380327	-.8378434
BIRPS	BM87-1	2591	162	09	24	25.909	242.45	55.4378403	-.8385415
BIRPS	BM87-1	2592	162	09	24	46.092	244.43	55.4376670	-.8392724
BIRPS	BM87-1	2593	162	09	25	05.942	244.47	55.4375157	-.8400346
BIRPS	BM87-1	2594	162	09	25	25.425	244.02	55.4373771	-.8407915
BIRPS	BM87-1	2595	162	09	25	45.625	243.18	55.4372332	-.8415516
BIRPS	BM87-1	2596	162	09	26	04.992	243.32	55.4370838	-.8423052
BIRPS	BM87-1	2597	162	09	26	24.975	243.46	55.4369281	-.8430528
BIRPS	BM87-1	2598	162	09	26	44.959	242.61	55.4367719	-.8438012
BIRPS	BM87-1	2599	162	09	27	04.842	242.83	55.4366214	-.8445415
BIRPS	BM87-1	2600	162	09	27	24.992	242.87	55.4364727	-.8452770
BIRPS	BM87-1	2601	162	09	27	45.325	243.88	55.4363221	-.8460087
BIRPS	BM87-1	2602	162	09	28	06.025	243.05	55.4361707	-.8467560
BIRPS	BM87-1	2603	162	09	28	26.092	242.26	55.4360105	-.8474850
BIRPS	BM87-1	2604	162	09	28	46.159	242.70	55.4358429	-.8482123
BIRPS	BM87-1	2605	162	09	29	06.125	243.05	55.4356879	-.8489424
BIRPS	BM87-1	2606	162	09	29	26.309	242.38	55.4355383	-.8496954
BIRPS	BM87-1	2607	162	09	29	46.142	241.10	55.4353801	-.8504458
BIRPS	BM87-1	2608	162	09	30	05.675	240.98	55.4352265	-.8511698
BIRPS	BM87-1	2609	162	09	30	26.442	240.77	55.4350702	-.8518796
BIRPS	BM87-1	2610	162	09	30	47.359	241.23	55.4348858	-.8526465
BIRPS	BM87-1	2611	162	09	31	08.342	241.24	55.4347222	-.8533558
BIRPS	BM87-1	2612	162	09	31	28.911	240.95	55.4345309	-.8541358
BIRPS	BM87-1	2613	162	09	31	49.494	241.42	55.4343624	-.8548418
BIRPS	BM87-1	2614	162	09	32	10.459	241.07	55.4341962	-.8555628
BIRPS	BM87-1	2615	162	09	32	30.892	240.56	55.4340308	-.8562867
BIRPS	BM87-1	2616	162	09	32	51.125	240.50	55.4338490	-.8570738
BIRPS	BM87-1	2617	162	09	33	11.492	240.84	55.4336958	-.8577978
BIRPS	BM87-1	2618	162	09	33	32.259	239.68	55.4335334	-.8585296
BIRPS	BM87-1	2619	162	09	33	52.125	239.81	55.4333743	-.8592460
BIRPS	BM87-1	2620	162	09	34	12.275	239.31	55.4332161	-.8599493
BIRPS	BM87-1	2621	162	09	34	33.042	239.54	55.4330318	-.8607240
BIRPS	BM87-1	2622	162	09	34	53.859	240.28	55.4328662	-.8614321
BIRPS	BM87-1	2623	162	09	35	14.392	239.72	55.4326997	-.8621585
BIRPS	BM87-1	2624	162	09	35	34.509	240.15	55.4325324	-.8628695
BIRPS	BM87-1	2625	162	09	35	55.159	239.65	55.4323559	-.8636479
BIRPS	BM87-1	2626	162	09	36	16.059	238.98	55.4321965	-.8643584
BIRPS	BM87-1	2627	162	09	36	36.859	238.47	55.4320325	-.8650707
BIRPS	BM87-1	2628	162	09	36	57.442	238.91	55.4318487	-.8658420
BIRPS	BM87-1	2629	162	09	37	18.442	238.81	55.4316727	-.8665384
BIRPS	BM87-1	2630	162	09	37	39.342	239.12	55.4314887	-.8673006
BIRPS	BM87-1	2631	162	09	38	00.459	238.58	55.4313145	-.8679929
BIRPS	BM87-1	2632	162	09	38	21.459	238.38	55.4311262	-.8687211
BIRPS	BM87-1	2633	162	09	38	43.309	238.73	55.4309528	-.8694695
BIRPS	BM87-1	2634	162	09	39	04.859	239.09	55.4307955	-.8701491
BIRPS	BM87-1	2635	162	09	39	26.359	239.14	55.4306260	-.8709206
BIRPS	BM87-1	2636	162	09	39	47.159	239.10	55.4304543	-.8716918
BIRPS	BM87-1	2637	162	09	40	08.192	238.94	55.4302934	-.8723931
BIRPS	BM87-1	2638	162	09	40	28.892	239.37	55.4301148	-.8730861
BIRPS	BM87-1	2639	162	09	40	50.192	238.54	55.4299323	-.8738195
BIRPS	BM87-1	2640	162	09	41	11.375	239.02	55.4297490	-.8745540
BIRPS	BM87-1	2641	162	09	41	33.042	239.99	55.4295787	-.8752932
BIRPS	BM87-1	2642	162	09	41	54.842	239.68	55.4294285	-.8759681
BIRPS	BM87-1	2643	162	09	42	16.825	239.98	55.4292586	-.8767216
BIRPS	BM87-1	2644	162	09	42	38.625	239.40	55.4290764	-.8774837
BIRPS	BM87-1	2645	162	09	42	59.825	239.88	55.4288982	-.8782272

BIRPS	BM87-1	2646	162	09	43	21.009	240.84	55.4287254	-.8789591
BIRPS	BM87-1	2647	162	09	43	43.009	240.12	55.4285556	-.8797074
BIRPS	BM87-1	2648	162	09	44	04.842	239.88	55.4284009	-.8803677
BIRPS	BM87-1	2649	162	09	44	26.909	240.04	55.4282111	-.8811835
BIRPS	BM87-1	2650	162	09	44	48.442	239.78	55.4280429	-.8818736
BIRPS	BM87-1	2651	162	09	45	09.309	240.41	55.4278636	-.8826234
BIRPS	BM87-1	2652	162	09	45	30.525	240.94	55.4276985	-.8833129
BIRPS	BM87-1	2653	162	09	45	51.575	241.84	55.4275168	-.8840954
BIRPS	BM87-1	2654	162	09	46	12.359	242.27	55.4273622	-.8848288
BIRPS	BM87-1	2655	162	09	46	32.109	241.94	55.4272143	-.8855596
BIRPS	BM87-1	2656	162	09	46	52.075	241.24	55.4270696	-.8862856
BIRPS	BM87-1	2657	162	09	47	12.309	240.87	55.4269150	-.8870154
BIRPS	BM87-1	2658	162	09	47	32.459	240.96	55.4267423	-.8877411
BIRPS	BM87-1	2659	162	09	47	52.509	241.00	55.4265785	-.8884800
BIRPS	BM87-1	2660	162	09	48	12.442	241.60	55.4264070	-.8892145
BIRPS	BM87-1	2661	162	09	48	32.375	241.50	55.4262377	-.8899335
BIRPS	BM87-1	2662	162	09	48	52.492	241.06	55.4260688	-.8906492
BIRPS	BM87-1	2663	162	09	49	13.059	241.04	55.4258866	-.8914347
BIRPS	BM87-1	2664	162	09	49	33.642	240.72	55.4257227	-.8921499
BIRPS	BM87-1	2665	162	09	49	54.492	241.88	55.4255693	-.8928527
BIRPS	BM87-1	2666	162	09	50	15.459	241.23	55.4253958	-.8936497
BIRPS	BM87-1	2667	162	09	50	36.259	240.32	55.4252308	-.8943851
BIRPS	BM87-1	2668	162	09	50	55.942	240.36	55.4250514	-.8950966
BIRPS	BM87-1	2669	162	09	51	15.809	241.01	55.4248622	-.8957878
BIRPS	BM87-1	2670	162	09	51	36.075	241.01	55.4246896	-.8964985
BIRPS	BM87-1	2671	162	09	51	56.475	241.79	55.4245173	-.8971962
BIRPS	BM87-1	2672	162	09	52	17.359	242.72	55.4243336	-.8979767
BIRPS	BM87-1	2673	162	09	52	38.075	242.40	55.4241807	-.8987131
BIRPS	BM87-1	2674	162	09	52	57.992	242.72	55.4240377	-.8994312
BIRPS	BM87-1	2675	162	09	53	18.542	241.72	55.4238805	-.9001551
BIRPS	BM87-1	2676	162	09	53	39.209	241.70	55.4237041	-.9009413
BIRPS	BM87-1	2677	162	09	53	59.792	242.42	55.4235442	-.9016645
BIRPS	BM87-1	2678	162	09	54	20.025	242.12	55.4233752	-.9023887
BIRPS	BM87-1	2679	162	09	54	40.059	242.67	55.4232221	-.9031044
BIRPS	BM87-1	2680	162	09	55	00.559	242.88	55.4230814	-.9038270
BIRPS	BM87-1	2681	162	09	55	21.609	242.16	55.4229367	-.9046292
BIRPS	BM87-1	2682	162	09	55	42.842	240.11	55.4227929	-.9053660
BIRPS	BM87-1	2683	162	09	56	03.459	238.92	55.4226256	-.9061519
BIRPS	BM87-1	2684	162	09	56	24.192	239.10	55.4224661	-.9068460
BIRPS	BM87-1	2685	162	09	56	45.142	239.08	55.4223055	-.9075435
BIRPS	BM87-1	2686	162	09	57	06.342	237.98	55.4221262	-.9083230
BIRPS	BM87-1	2687	162	09	57	26.725	238.23	55.4219674	-.9090368
BIRPS	BM87-1	2688	162	09	57	47.359	237.30	55.4217766	-.9098187
BIRPS	BM87-1	2689	162	09	58	07.992	237.23	55.4215915	-.9105068
BIRPS	BM87-1	2690	162	09	58	28.559	237.11	55.4214096	-.9112015
BIRPS	BM87-1	2691	162	09	58	49.059	237.54	55.4212350	-.9118769
BIRPS	BM87-1	2692	162	09	59	10.342	238.56	55.4210429	-.9126180
BIRPS	BM87-1	2693	162	09	59	31.759	238.76	55.4208514	-.9133773
BIRPS	BM87-1	2694	162	09	59	53.225	238.72	55.4206643	-.9141444
BIRPS	BM87-1	2695	162	10	00	14.142	238.38	55.4204917	-.9148443
BIRPS	BM87-1	2696	162	10	00	34.559	239.44	55.4203202	-.9155442
BIRPS	BM87-1	2697	162	10	00	55.075	239.15	55.4201472	-.9162728
BIRPS	BM87-1	2698	162	10	01	15.275	239.71	55.4199634	-.9169843
BIRPS	BM87-1	2699	162	10	01	35.575	239.87	55.4197692	-.9177681
BIRPS	BM87-1	2700	162	10	01	55.909	240.09	55.4195874	-.9184712
BIRPS	BM87-1	2701	162	10	02	16.575	241.35	55.4194146	-.9191571
BIRPS	BM87-1	2702	162	10	02	37.392	240.90	55.4192449	-.9198662
BIRPS	BM87-1	2703	162	10	02	58.192	240.93	55.4190550	-.9206412
BIRPS	BM87-1	2704	162	10	03	18.459	241.84	55.4188747	-.9213370
BIRPS	BM87-1	2705	162	10	03	38.809	241.84	55.4186947	-.9220366
BIRPS	BM87-1	2706	162	10	03	59.392	242.80	55.4185153	-.9227385
BIRPS	BM87-1	2707	162	10	04	20.392	242.88	55.4183191	-.9235011
BIRPS	BM87-1	2708	162	10	04	40.809	243.30	55.4181555	-.9241887
BIRPS	BM87-1	2709	162	10	05	01.692	243.46	55.4179829	-.9249603
BIRPS	BM87-1	2710	162	10	05	22.959	244.73	55.4178334	-.9256437
BIRPS	BM87-1	2711	162	10	05	44.492	245.29	55.4176729	-.9264262
BIRPS	BM87-1	2712	162	10	06	05.409	245.82	55.4175176	-.9272230
BIRPS	BM87-1	2713	162	10	06	26.292	246.48	55.4173883	-.9279525
BIRPS	BM87-1	2714	162	10	06	46.959	245.28	55.4172583	-.9286921
BIRPS	BM87-1	2715	162	10	07	07.525	245.30	55.4171193	-.9294923
BIRPS	BM87-1	2716	162	10	07	28.392	244.67	55.4169895	-.9302341
BIRPS	BM87-1	2717	162	10	07	48.842	243.98	55.4168528	-.9309823
BIRPS	BM87-1	2718	162	10	08	08.609	243.59	55.4167231	-.9317361
BIRPS	BM87-1	2719	162	10	08	28.509	242.52	55.4165921	-.9324778
BIRPS	BM87-1	2720	162	10	08	48.759	240.99	55.4165364	-.9317308
BIRPS	BM87-1	2721	162	10	09	13.475	242.38	55.4163043	-.9326313
BIRPS	BM87-1	2722	162	10	09	38.375	245.40	55.4161030	-.9334590
BIRPS	BM87-1	2723	162	10	10	03.525	245.15	55.4159056	-.9343955
BIRPS	BM87-1	2724	162	10	10	28.275	245.72	55.4157272	-.9352510
BIRPS	BM87-1	2725	162	10	10	53.209	244.82	55.4155425	-.9361301
BIRPS	BM87-1	2726	162	10	11	17.709	245.23	55.4153423	-.9370800
BIRPS	BM87-1	2727	162	10	11	41.142	245.27	55.4151723	-.9378631
BIRPS	BM87-1	2728	162	10	12	04.325	244.97	55.4149960	-.9386911
BIRPS	BM87-1	2729	162	10	12	27.509	245.13	55.4148245	-.9394865
BIRPS	BM87-1	2730	162	10	12	51.642	243.64	55.4146461	-.9403017
BIRPS	BM87-1	2731	162	10	13	14.792	244.38	55.4144703	-.9410582
BIRPS	BM87-1	2732	162	10	13	36.709	244.84	55.4143016	-.9418479
BIRPS	BM87-1	2733	162	10	13	57.742	244.07	55.4141314	-.9426501
BIRPS	BM87-1	2734	162	10	14	18.259	244.74	55.4139791	-.9433632
BIRPS	BM87-1	2735	162	10	14	39.009	243.22	55.4138148	-.9440996
BIRPS	BM87-1	2736	162	10	14	59.409	242.78	55.4136350	-.9448865
BIRPS	BM87-1	2737	162	10	15	19.992	242.46	55.4134693	-.9455819
BIRPS	BM87-1	2738	162	10	15	41.359	242.64	55.4133020	-.9462365
BIRPS	BM87-1	2739	162	10	16	03.409	243.18	55.4131124	-.9470368
BIRPS	BM87-1	2740	162	10	16	25.625	243.65	55.4129417	-.9477796
BIRPS	BM87-1	2741	162	10	16	47.609	242.64	55.4127689	-.9485245
BIRPS	BM87-1	2742	162	10	17	09.392	242.32	55.4125999	-.9492057
BIRPS	BM87-1	2743	162	10	17	30.659	243.15	55.4124131	-.9499638
BIRPS	BM87-1	2744	162	10	17	51.309	243.54	55.4122588	-.9506649
BIRPS	BM87-1	2745	162	10	18	12.342	243.67	55.4120848	-.9514477
BIRPS	BM87-1	2746	162	10	18	32.859	243.98	55.4119352	-.9521480
BIRPS	BM87-1	2747	162	10	18	53.609	243.47	55.4117839	-.9529333
BIRPS	BM87-1	2748	162	10	19	14.775	243.53	55.4116348	-.9536417
BIRPS	BM87-1	2749	162	10	19	35.742	242.55	55.4114690	-.9544011
BIRPS	BM87-1	2750	162	10	19	57.359	241.12	55.4113065	-.9550835
BIRPS	BM87-1	2751	162	10	20	18.892	240.75	55.4111187	-.9558275
BIRPS	BM87-1	2752	162	10	20	40.009	241.40	55.4109304	-.9565593
BIRPS	BM87-1	2753	162	10	21	02.009	242.33	55.4107464	-.9572988
BIRPS	BM87-1	2754	162	10	21	23.909	242.03	55.4105689	-.9580511
BIRPS	BM87-1	2755	162	10	21	45.492	241.06	55.4104005	-.9588170
BIRPS	BM87-1	2756	162	10	22	06.692	240.49	55.4102436	-.9594935
BIRPS	BM87-1	2757	162	10	22	27.975	240.45	55.4100511	-.9602162
BIRPS	BM87-1	2758	162	10	22	49.875	240.34	55.4098452	-.9609357
BIRPS	BM87-1	2759	162	10	23	11.425	241.37	55.4096402	-.9616467
BIRPS	BM87-1	2760	162	10	23	33.225	242.67	55.4094636	-.9622945
BIRPS	BM87-1	2761	162	10	23	55.292	242.57	55.4092746	-.9630380
BIRPS	BM87-1	2762	162	10	24	16.792	243.16	55.4090956	-.9637938
BIRPS	BM87-1	2763	162	10	24	37.709	243.58	55.4089109	-.9645562
BIRPS	BM87-1	2764	162	10	24	58.559	244.07	55.4087518	-.9652546
BIRPS	BM87-1	2765	162	10	25	19.175	245.16	55.4086032	-.9659445

BIRPS	BM87-1	2766	162	10	25	40.675	244.99	55.4084451	-.9666847
BIRPS	BM87-1	2767	162	10	26	02.392	245.04	55.4082922	-.9674299
BIRPS	BM87-1	2768	162	10	26	24.409	244.73	55.4081339	-.9681705
BIRPS	BM87-1	2769	162	10	26	46.459	244.22	55.4079643	-.9689093
BIRPS	BM87-1	2770	162	10	27	08.342	244.64	55.4077881	-.9696539
BIRPS	BM87-1	2771	162	10	27	29.659	245.97	55.4076220	-.9704213
BIRPS	BM87-1	2772	162	10	27	50.809	245.45	55.4074885	-.9711342
BIRPS	BM87-1	2773	162	10	28	11.759	244.57	55.4073427	-.9719092
BIRPS	BM87-1	2774	162	10	28	33.275	244.19	55.4071965	-.9726015
BIRPS	BM87-1	2775	162	10	28	54.777	244.16	55.4070285	-.9733421
BIRPS	BM87-1	2776	162	10	29	16.477	243.50	55.4068582	-.9740673
BIRPS	BM87-1	2777	162	10	29	38.742	243.49	55.4066884	-.9747878
BIRPS	BM87-1	2778	162	10	30	00.925	243.94	55.4065145	-.9755273
BIRPS	BM87-1	2779	162	10	30	22.892	243.98	55.4063334	-.9762721
BIRPS	BM87-1	2780	162	10	30	44.209	243.60	55.4061530	-.9770387
BIRPS	BM87-1	2781	162	10	31	04.842	243.41	55.4059955	-.9777448
BIRPS	BM87-1	2782	162	10	31	25.325	243.31	55.4058285	-.9784548
BIRPS	BM87-1	2783	162	10	31	45.925	243.49	55.4056507	-.9792329
BIRPS	BM87-1	2784	162	10	32	07.025	243.44	55.4054871	-.9799148
BIRPS	BM87-1	2785	162	10	32	28.342	243.62	55.4053024	-.9806494
BIRPS	BM87-1	2786	162	10	32	49.759	244.03	55.4051117	-.9813914
BIRPS	BM87-1	2787	162	10	33	11.225	244.62	55.4049495	-.9820713
BIRPS	BM87-1	2788	162	10	33	32.725	244.55	55.4047816	-.9828238
BIRPS	BM87-1	2789	162	10	33	54.059	244.00	55.4046140	-.9835767
BIRPS	BM87-1	2790	162	10	34	15.792	244.57	55.4044519	-.9843399
BIRPS	BM87-1	2791	162	10	34	37.225	244.27	55.4043005	-.9850464
BIRPS	BM87-1	2792	162	10	34	58.225	243.93	55.4041243	-.9858248
BIRPS	BM87-1	2793	162	10	35	18.759	243.20	55.4039535	-.9865386
BIRPS	BM87-1	2794	162	10	35	38.775	243.16	55.4037862	-.9872483
BIRPS	BM87-1	2795	162	10	35	58.859	243.52	55.4036160	-.9879516
BIRPS	BM87-1	2796	162	10	36	19.292	244.45	55.4034122	-.9890419
BIRPS	BM87-1	2797	162	10	36	37.925	243.64	55.4032401	-.9897462
BIRPS	BM87-1	2798	162	10	36	57.042	243.29	55.4030923	-.9903710
BIRPS	BM87-1	2799	162	10	37	16.509	243.51	55.4029283	-.9910806
BIRPS	BM87-1	2800	162	10	37	36.225	242.84	55.4027580	-.9917673
BIRPS	BM87-1	2801	162	10	37	56.875	243.25	55.4025845	-.9924594
BIRPS	BM87-1	2802	162	10	38	16.825	244.40	55.4024183	-.9931341
BIRPS	BM87-1	2803	162	10	38	37.559	244.00	55.4022572	-.9938337
BIRPS	BM87-1	2804	162	10	38	58.375	244.04	55.4020866	-.9945788
BIRPS	BM87-1	2805	162	10	39	20.009	243.90	55.4019078	-.9953105
BIRPS	BM87-1	2806	162	10	39	41.742	243.70	55.4017219	-.9960508
BIRPS	BM87-1	2807	162	10	40	03.325	244.05	55.4015462	-.9967537
BIRPS	BM87-1	2808	162	10	40	23.909	244.62	55.4013525	-.9975349
BIRPS	BM87-1	2809	162	10	40	44.259	244.78	55.4011810	-.9982331
BIRPS	BM87-1	2810	162	10	41	04.775	245.21	55.4010178	-.9989455
BIRPS	BM87-1	2811	162	10	41	24.942	245.24	55.4008569	-.9996538
BIRPS	BM87-1	2812	162	10	41	45.209	245.35	55.4007099	-1.0003678
BIRPS	BM87-1	2813	162	10	42	06.109	244.83	55.4005494	-1.0010767
BIRPS	BM87-1	2814	162	10	42	26.892	245.25	55.4003832	-1.0018456
BIRPS	BM87-1	2815	162	10	42	48.259	244.94	55.4002151	-1.0026019
BIRPS	BM87-1	2816	162	10	43	09.859	244.60	55.4000476	-1.0032821
BIRPS	BM87-1	2817	162	10	43	31.342	245.34	55.3998625	-1.0040306
BIRPS	BM87-1	2818	162	10	43	52.575	245.46	55.3996875	-1.0048080
BIRPS	BM87-1	2819	162	10	44	13.492	245.00	55.3995272	-1.0055317
BIRPS	BM87-1	2820	162	10	44	33.642	245.14	55.3993652	-1.0062370
BIRPS	BM87-1	2821	162	10	44	54.109	244.90	55.3992040	-1.0069499
BIRPS	BM87-1	2822	162	10	45	14.692	244.51	55.3990260	-1.0077291
BIRPS	BM87-1	2823	162	10	45	35.542	244.86	55.3988601	-1.0084103
BIRPS	BM87-1	2824	162	10	45	56.625	245.52	55.3986889	-1.0090940
BIRPS	BM87-1	2825	162	10	46	17.975	246.14	55.3985021	-1.0098431
BIRPS	BM87-1	2826	162	10	46	39.092	246.38	55.3983172	-1.0105993
BIRPS	BM87-1	2827	162	10	47	00.459	246.82	55.3981508	-1.0113045
BIRPS	BM87-1	2828	162	10	47	21.309	247.41	55.3979773	-1.0120738
BIRPS	BM87-1	2829	162	10	47	42.625	245.89	55.3978241	-1.0128055
BIRPS	BM87-1	2830	162	10	48	03.259	246.36	55.3976604	-1.0135802
BIRPS	BM87-1	2831	162	10	48	24.109	246.92	55.3975198	-1.0142765
BIRPS	BM87-1	2832	162	10	48	45.292	245.56	55.3973558	-1.0150546
BIRPS	BM87-1	2833	162	10	49	06.459	245.64	55.3971909	-1.0157527
BIRPS	BM87-1	2834	162	10	49	27.342	246.01	55.3970139	-1.0165224
BIRPS	BM87-1	2835	162	10	49	48.175	246.08	55.3968519	-1.0172206
BIRPS	BM87-1	2836	162	10	50	08.909	246.37	55.3966648	-1.0179836
BIRPS	BM87-1	2837	162	10	50	29.775	246.01	55.3965076	-1.0186798
BIRPS	BM87-1	2838	162	10	50	50.709	245.38	55.3963449	-1.0193732
BIRPS	BM87-1	2839	162	10	51	11.925	246.07	55.3961690	-1.0201323
BIRPS	BM87-1	2840	162	10	51	32.975	245.93	55.3959863	-1.0208942
BIRPS	BM87-1	2841	162	10	51	54.075	246.32	55.3958146	-1.0215886
BIRPS	BM87-1	2842	162	10	52	14.775	246.28	55.3956432	-1.0222899
BIRPS	BM87-1	2843	162	10	52	35.559	247.14	55.3954513	-1.0230547
BIRPS	BM87-1	2844	162	10	52	56.642	247.25	55.3952882	-1.0237555
BIRPS	BM87-1	2845	162	10	53	17.592	246.37	55.3951072	-1.0245280
BIRPS	BM87-1	2846	162	10	53	38.759	246.25	55.3949337	-1.0252242
BIRPS	BM87-1	2847	162	10	53	59.675	247.19	55.3947434	-1.0259761
BIRPS	BM87-1	2848	162	10	54	20.925	248.01	55.3945772	-1.0266565
BIRPS	BM87-1	2849	162	10	54	42.092	248.17	55.3944144	-1.0274246
BIRPS	BM87-1	2850	162	10	55	02.959	248.13	55.3942705	-1.0281176
BIRPS	BM87-1	2851	162	10	55	24.309	247.24	55.3941015	-1.0288905
BIRPS	BM87-1	2852	162	10	55	45.075	247.53	55.3939428	-1.0295825
BIRPS	BM87-1	2853	162	10	56	06.109	247.41	55.3937724	-1.0303529
BIRPS	BM87-1	2854	162	10	56	26.975	247.06	55.3936120	-1.0310452
BIRPS	BM87-1	2855	162	10	56	48.175	248.07	55.3934337	-1.0317924
BIRPS	BM87-1	2856	162	10	57	09.509	247.72	55.3932631	-1.0325555
BIRPS	BM87-1	2857	162	10	57	30.909	247.82	55.3931031	-1.0332463
BIRPS	BM87-1	2858	162	10	57	52.159	248.27	55.3929239	-1.0339861
BIRPS	BM87-1	2859	162	10	58	13.559	248.52	55.3927482	-1.0347289
BIRPS	BM87-1	2860	162	10	58	35.292	248.12	55.3925774	-1.0354899
BIRPS	BM87-1	2861	162	10	58	56.742	248.79	55.3924231	-1.0361863
BIRPS	BM87-1	2862	162	10	59	17.892	248.57	55.3922578	-1.0369527
BIRPS	BM87-1	2863	162	10	59	39.292	248.45	55.3920877	-1.0377439
BIRPS	BM87-1	2864	162	10	59	59.742	248.72	55.3919366	-1.0384694
BIRPS	BM87-1	2865	162	11	00	20.225	248.22	55.3917978	-1.0391928
BIRPS	BM87-1	2866	162	11	00	40.475	246.75	55.3916457	-1.0399151
BIRPS	BM87-1	2867	162	11	01	00.659	246.57	55.3914895	-1.0406216
BIRPS	BM87-1	2868	162	11	01	21.492	246.77	55.3913129	-1.0413808
BIRPS	BM87-1	2869	162	11	01	42.792	246.95	55.3911456	-1.0420804
BIRPS	BM87-1	2870	162	11	02	03.725	247.31	55.3909746	-1.0428617
BIRPS	BM87-1	2871	162	11	02	24.742	247.35	55.3908279	-1.0435825
BIRPS	BM87-1	2872	162	11	02	45.325	245.96	55.3906624	-1.0443839
BIRPS	BM87-1	2873	162	11	03	05.659	245.57	55.3904966	-1.0451019
BIRPS	BM87-1	2874	162	11	03	26.142	244.99	55.3903263	-1.0457971
BIRPS	BM87-1	2875	162	11	03	46.575	243.78	55.3901632	-1.0464883
BIRPS	BM87-1	2876	162	11	04	07.575	243.99	55.3899695	-1.0472238
BIRPS	BM87-1	2877	162	11	04	29.225	244.63	55.3897735	-1.0479488
BIRPS	BM87-1	2878	162	11	04	50.925	245.36	55.3895992	-1.0486318
BIRPS	BM87-1	2879	162	11	05	12.225	245.15	55.3894198	-1.0493993
BIRPS	BM87-1	2880	162	11	05	32.875	244.91	55.3892667	-1.0501121
BIRPS	BM87-1	2881	162	11	05	53.659	244.55	55.3890896	-1.0508996
BIRPS	BM87-1	2882	162	11	06	14.392	245.24	55.3889216	-1.0516071
BIRPS	BM87-1	2883	162	11	06	34.659	243.90	55.3887434	-1.0523171
BIRPS	BM87-1	2884	162	11	06	55.075	244.00	55.3885485	1.0530260
BIRPS	BM87-1	2885	162	11	07	15.059	245.47	55.3883522	-1.0537281

BIRPS	BM87-1	2886	162	11	07	35.109	245.74	55.3881630	-1.0544356
BIRPS	BM87-1	2887	162	11	07	55.675	245.50	55.3879559	-1.0552181
BIRPS	BM87-1	2888	162	11	08	16.209	245.15	55.3877786	-1.0559246
BIRPS	BM87-1	2889	162	11	08	36.842	245.55	55.3876099	-1.0566388
BIRPS	BM87-1	2890	162	11	08	56.709	245.36	55.3874392	-1.0573675
BIRPS	BM87-1	2891	162	11	09	16.359	246.25	55.3872629	-1.0580920
BIRPS	BM87-1	2892	162	11	09	36.575	247.79	55.3870890	-1.0588157
BIRPS	BM87-1	2893	162	11	09	56.359	248.40	55.3869247	-1.0595465
BIRPS	BM87-1	2894	162	11	10	16.792	248.25	55.3867699	-1.0602767
BIRPS	BM87-1	2895	162	11	10	36.809	247.30	55.3866093	-1.0610105
BIRPS	BM87-1	2896	162	11	10	56.575	247.72	55.3864520	-1.0617279
BIRPS	BM87-1	2897	162	11	11	16.925	247.29	55.3862884	-1.0624444
BIRPS	BM87-1	2898	162	11	11	37.309	247.74	55.3861270	-1.0631413
BIRPS	BM87-1	2899	162	11	11	58.442	248.57	55.3859585	-1.0639021
BIRPS	BM87-1	2900	162	11	12	19.759	248.84	55.3857940	-1.0646725
BIRPS	BM87-1	2901	162	11	12	41.192	248.70	55.3856426	-1.0653981
BIRPS	BM87-1	2902	162	11	13	01.909	248.17	55.3854717	-1.0662123
BIRPS	BM87-1	2903	162	11	13	21.992	248.00	55.3853069	-1.0669531
BIRPS	BM87-1	2904	162	11	13	41.725	248.33	55.3851370	-1.0676943
BIRPS	BM87-1	2905	162	11	14	01.342	247.52	55.3849905	-1.0683650
BIRPS	BM87-1	2906	162	11	14	21.175	246.95	55.3848121	-1.0690979
BIRPS	BM87-1	2907	162	11	14	40.792	246.86	55.3846390	-1.0698157
BIRPS	BM87-1	2908	162	11	15	00.742	247.86	55.3844730	-1.0705251
BIRPS	BM87-1	2909	162	11	15	21.242	247.89	55.3843058	-1.0712475
BIRPS	BM87-1	2910	162	11	15	41.425	247.88	55.3841637	-1.0719778
BIRPS	BM87-1	2911	162	11	16	02.092	246.25	55.3840148	-1.0727809
BIRPS	BM87-1	2912	162	11	16	22.925	245.23	55.3838603	-1.0734964
BIRPS	BM87-1	2913	162	11	16	43.492	244.97	55.3836884	-1.0741798
BIRPS	BM87-1	2914	162	11	17	04.825	245.28	55.3834806	-1.0749295
BIRPS	BM87-1	2915	162	11	17	25.575	246.49	55.3833034	-1.0756185
BIRPS	BM87-1	2916	162	11	17	46.675	247.40	55.3831051	-1.0763791
BIRPS	BM87-1	2917	162	11	18	07.875	247.78	55.3829448	-1.0770737
BIRPS	BM87-1	2918	162	11	18	28.809	247.19	55.3827728	-1.0778566
BIRPS	BM87-1	2919	162	11	18	49.325	246.52	55.3826087	-1.0785621
BIRPS	BM87-1	2920	162	11	19	09.892	247.07	55.3824385	-1.0792613
BIRPS	BM87-1	2921	162	11	19	30.942	247.39	55.3822418	-1.0800220
BIRPS	BM87-1	2922	162	11	19	51.675	247.40	55.3820658	-1.0807170
BIRPS	BM87-1	2923	162	11	20	12.659	248.59	55.3818758	-1.0814814
BIRPS	BM87-1	2924	162	11	20	33.742	248.63	55.3817187	-1.0821821
BIRPS	BM87-1	2925	162	11	20	54.725	248.85	55.3815490	-1.0829375
BIRPS	BM87-1	2926	162	11	21	15.792	248.47	55.3814041	-1.0836249
BIRPS	BM87-1	2927	162	11	21	37.775	247.62	55.3812198	-1.0843887
BIRPS	BM87-1	2928	162	11	21	59.575	246.27	55.3810284	-1.0851405
BIRPS	BM87-1	2929	162	11	22	20.309	247.54	55.3808300	-1.0858809
BIRPS	BM87-1	2930	162	11	22	41.275	248.94	55.3806606	-1.0865731
BIRPS	BM87-1	2931	162	11	23	01.875	250.28	55.3805059	-1.0872875
BIRPS	BM87-1	2932	162	11	23	22.675	250.29	55.3803456	-1.0880834
BIRPS	BM87-1	2933	162	11	23	43.542	249.07	55.3802027	-1.0887987
BIRPS	BM87-1	2934	162	11	24	03.992	248.95	55.3800534	-1.0895017
BIRPS	BM87-1	2935	162	11	24	25.092	248.65	55.3798778	-1.0902375
BIRPS	BM87-1	2936	162	11	24	46.675	249.55	55.3797074	-1.0909647
BIRPS	BM87-1	2937	162	11	25	09.175	248.51	55.3795451	-1.0917052
BIRPS	BM87-1	2938	162	11	25	31.025	249.25	55.3793863	-1.0924380
BIRPS	BM87-1	2939	162	11	25	53.092	249.26	55.3792244	-1.0931694
BIRPS	BM87-1	2940	162	11	26	15.292	248.56	55.3790580	-1.0939054
BIRPS	BM87-1	2941	162	11	26	37.175	248.71	55.3788855	-1.0946361
BIRPS	BM87-1	2942	162	11	26	59.042	247.90	55.3787181	-1.0953707
BIRPS	BM87-1	2943	162	11	27	20.975	248.56	55.3785385	-1.0960994
BIRPS	BM87-1	2944	162	11	27	42.875	248.64	55.3783553	-1.0968394
BIRPS	BM87-1	2945	162	11	28	04.909	248.61	55.3781841	-1.0975868
BIRPS	BM87-1	2946	162	11	28	26.709	248.40	55.3780122	-1.0983508
BIRPS	BM87-1	2947	162	11	28	47.959	248.82	55.3778622	-1.0990561
BIRPS	BM87-1	2948	162	11	29	08.625	248.53	55.3777001	-1.0998374
BIRPS	BM87-1	2949	162	11	29	29.259	247.04	55.3775462	-1.1005536
BIRPS	BM87-1	2950	162	11	29	49.377	247.55	55.3773785	-1.1012349
BIRPS	BM87-1	2951	162	11	30	10.294	247.33	55.3771851	-1.1019807
BIRPS	BM87-1	2952	162	11	30	31.892	247.75	55.3769956	-1.1026615
BIRPS	BM87-1	2953	162	11	30	52.892	248.98	55.3767859	-1.1034013
BIRPS	BM87-1	2954	162	11	31	14.125	249.78	55.3766070	-1.1040768
BIRPS	BM87-1	2955	162	11	31	35.009	249.97	55.3764192	-1.1048329
BIRPS	BM87-1	2956	162	11	31	55.909	249.67	55.3762630	-1.1055085
BIRPS	BM87-1	2957	162	11	32	17.725	249.67	55.3760934	-1.1062527
BIRPS	BM87-1	2958	162	11	32	39.625	251.42	55.3759361	-1.1056217
BIRPS	BM87-1	2959	162	11	33	05.959	255.00	55.3757225	-1.1064760
BIRPS	BM87-1	2960	162	11	33	32.375	257.37	55.3755419	-1.1074312
BIRPS	BM87-1	2961	162	11	33	58.709	258.08	55.3753947	-1.1083423
BIRPS	BM87-1	2962	162	11	34	25.125	256.86	55.3752502	-1.1092420
BIRPS	BM87-1	2963	162	11	34	51.442	256.70	55.3750842	-1.1101273
BIRPS	BM87-1	2964	162	11	35	16.709	256.27	55.3749211	-1.1110258
BIRPS	BM87-1	2965	162	11	35	41.492	256.30	55.3747747	-1.1118408
BIRPS	BM87-1	2966	162	11	36	05.475	256.52	55.3746258	-1.1126624
BIRPS	BM87-1	2967	162	11	36	28.909	255.36	55.3744632	-1.1134933
BIRPS	BM87-1	2968	162	11	36	51.875	255.72	55.3743156	-1.1142482
BIRPS	BM87-1	2969	162	11	37	14.359	255.21	55.3741564	-1.1150729
BIRPS	BM87-1	2970	162	11	37	36.775	254.81	55.3740079	-1.1158325
BIRPS	BM87-1	2971	162	11	37	59.175	253.95	55.3738482	-1.1165910
BIRPS	BM87-1	2972	162	11	38	20.659	253.43	55.3736727	-1.1173449
BIRPS	BM87-1	2973	162	11	38	42.359	254.01	55.3734937	-1.1180983
BIRPS	BM87-1	2974	162	11	39	03.559	253.62	55.3733443	-1.1187744
BIRPS	BM87-1	2975	162	11	39	25.059	253.51	55.3731860	-1.1195253
BIRPS	BM87-1	2976	162	11	39	46.692	252.67	55.3730276	-1.1202689
BIRPS	BM87-1	2977	162	11	40	08.859	252.33	55.3728752	-1.1209961
BIRPS	BM87-1	2978	162	11	40	31.575	251.52	55.3727167	-1.1217323
BIRPS	BM87-1	2979	162	11	40	53.509	250.72	55.3725364	-1.1224810
BIRPS	BM87-1	2980	162	11	41	14.709	250.78	55.3723409	-1.1232255
BIRPS	BM87-1	2981	162	11	41	36.209	251.45	55.3721388	-1.1239633
BIRPS	BM87-1	2982	162	11	41	57.409	252.01	55.3719555	-1.1246453
BIRPS	BM87-1	2983	162	11	42	18.159	251.93	55.3717700	-1.1253798
BIRPS	BM87-1	2984	162	11	42	39.775	252.26	55.3716175	-1.1260264
BIRPS	BM87-1	2985	162	11	43	02.275	251.71	55.3714381	-1.1268080
BIRPS	BM87-1	2986	162	11	43	24.942	250.26	55.3712687	-1.1275332
BIRPS	BM87-1	2987	162	11	43	46.975	250.41	55.3710842	-1.1282409
BIRPS	BM87-1	2988	162	11	44	09.175	251.36	55.3709031	-1.1289407
BIRPS	BM87-1	2989	162	11	44	31.692	251.92	55.3707336	-1.1296508
BIRPS	BM87-1	2990	162	11	44	54.409	251.80	55.3705515	-1.1304445
BIRPS	BM87-1	2991	162	11	45	16.675	251.40	55.3703802	-1.1311773
BIRPS	BM87-1	2992	162	11	45	38.959	251.11	55.3701974	-1.1319006
BIRPS	BM87-1	2993	162	11	46	00.442	250.22	55.3700192	-1.1326162
BIRPS	BM87-1	2994	162	11	46	22.575	250.71	55.3698372	-1.1333145
BIRPS	BM87-1	2995	162	11	46	45.242	252.55	55.3696524	-1.1340079
BIRPS	BM87-1	2996	162	11	47	08.025	253.74	55.3694765	-1.1347169
BIRPS	BM87-1	2997	162	11	47	30.742	253.55	55.3692919	-1.1355119
BIRPS	BM87-1	2998	162	11	47	53.075	252.93	55.3691230	-1.1362625
BIRPS	BM87-1	2999	162	11	48	14.225	252.97	55.3689407	-1.1369977
BIRPS	BM87-1	3000	162	11	48	35.892	253.30	55.3687664	-1.1376418
BIRPS	BM87-1	3001	162	11	48	57.842	254.39	55.3685919	-1.1383457
BIRPS	BM87-1	3002	162	11	49	20.525	254.92	55.3684033	-1.1391162
BIRPS	BM87-1	3003	162	11	49	43.142	255.46	55.3682402	-1.1398330
BIRPS	BM87-1	3004	162	11	50	05.525	255.83	55.3680809	-1.1405580
BIRPS	BM87-1	3005	162	11	50	27.742	255.85	55.3679262	-1.1413093

BIRPS	BM87-1	3006	162	11	50	49.875	255.41	55.3677761	-1.1420495
BIRPS	BM87-1	3007	162	11	51	11.725	254.58	55.3676226	-1.1428105
BIRPS	BM87-1	3008	162	11	51	33.192	254.09	55.3674665	-1.1435506
BIRPS	BM87-1	3009	162	11	51	54.792	254.65	55.3673026	-1.1442718
BIRPS	BM87-1	3010	162	11	52	17.609	254.98	55.3671286	-1.1449876
BIRPS	BM87-1	3011	162	11	52	40.009	254.84	55.3669499	-1.1457104
BIRPS	BM87-1	3012	162	11	53	02.092	254.96	55.3667765	-1.1464321
BIRPS	BM87-1	3013	162	11	53	24.042	255.03	55.3666130	-1.1471720
BIRPS	BM87-1	3014	162	11	53	45.642	255.47	55.3664520	-1.1479250
BIRPS	BM87-1	3015	162	11	54	06.875	255.33	55.3662752	-1.1487058
BIRPS	BM87-1	3016	162	11	54	27.909	255.65	55.3661204	-1.1494125
BIRPS	BM87-1	3017	162	11	54	48.692	254.88	55.3659523	-1.1501622
BIRPS	BM87-1	3018	162	11	55	10.292	255.27	55.3657812	-1.1508987
BIRPS	BM87-1	3019	162	11	55	32.092	255.02	55.3656277	-1.1515718
BIRPS	BM87-1	3020	162	11	55	53.725	254.27	55.3654498	-1.1523127
BIRPS	BM87-1	3021	162	11	56	15.192	254.99	55.3652612	-1.1530480
BIRPS	BM87-1	3022	162	11	56	36.459	254.72	55.3645615	-1.1568229
BIRPS	BM87-1	3023	162	11	56	57.609	253.56	55.3644107	-1.1575143
BIRPS	BM87-1	3024	162	11	57	18.592	252.23	55.3642478	-1.1582644
BIRPS	BM87-1	3025	162	11	57	40.275	250.37	55.3640591	-1.1589956
BIRPS	BM87-1	3026	162	11	58	02.192	250.34	55.3638433	-1.1597136
BIRPS	BM87-1	3027	162	11	58	23.825	251.74	55.3636431	-1.1603731
BIRPS	BM87-1	3028	162	11	58	45.042	252.07	55.3634407	-1.1611009
BIRPS	BM87-1	3029	162	11	59	07.175	252.03	55.3632271	-1.1618331
BIRPS	BM87-1	3030	162	11	59	29.025	252.35	55.3630170	-1.1625627
BIRPS	BM87-1	3031	162	11	59	50.275	253.36	55.3628366	-1.1632084
BIRPS	BM87-1	3032	162	12	00	11.859	254.40	55.3626551	-1.1639348
BIRPS	BM87-1	3033	162	12	00	33.475	255.11	55.3624758	-1.1646817
BIRPS	BM87-1	3034	162	12	00	54.742	254.75	55.3623020	-1.1654452
BIRPS	BM87-1	3035	162	12	01	15.959	254.61	55.3621462	-1.1661394
BIRPS	BM87-1	3036	162	12	01	36.727	254.28	55.3619713	-1.1669022
BIRPS	BM87-1	3037	162	12	01	57.811	250.61	55.3618343	-1.1675988

```
 139    FORMAT(I4,1X,I3,1X,2(I2,1X),F6.3)
        GO TO 150
C
 140   WRITE(6,'(A,I4,A)') 'PANNING ',ITDIF,' seconds'
C
 150   IF(NTIME.EQ.0) WRITE(1,'(A)') 'DEC'
       WRITE(1,'(A)') 'EDIT'
       WRITE(1,200) IYR,IDY(I),IHOUR(I),IMIN(I),SECS(I)
 200   FORMAT(I4,1X,I3,1X,2(I2,1X),F6.3)
       WRITE(1,'(A)') '60.0'
       WRITE(1,'(A)') 'SAVE'
C
       IF(I.GE.NUMB) GO TO 500
 400 CONTINUE
C
 500 WRITE(1,'(A)') 'END'
     WRITE(1,'(A)') 'EXIT'
C
     IF(IERR.GT.0) THEN
1000   WRITE(6,'(A)') 'File initialization error'
     ENDIF
C
     WRITE(6,'(A)') 'Temporary command file created as -IED.COM'
     WRITE(6,'(A)') '           Rename to preserve! '
C
     STOP
     END
```

```
C
C ++++++++++++++++++++++++++++++++++++++++++++++++++++++++++++++++++++++
C
      PROGRAM NSHCOR
C
C ++++++++++++++++++++++++++++++++++++++++++++++++++++++++++++++++++++++
C    Program corrects shot names for traces which were digitised
C  en bloc, ie,which have the same shot name for several different
C  events.
C    Assignments:     0=input tdf file
C                     1=output tdf file
C                     5=correct shot details (file)
C                     6=log
C
C    Unit 5:
C          NSH,NSTA     (I4,1X,I4) No.of shots,No.of stations per shot
C          NEVCORR(1)   (A4) Correct shot name
C              .              .
C              .              .
C              .              .
C              .              .
C              .              .
C          NEVCORR(NSH)       .
C ++++++++++++++++++++++++++++++++++++++++++++++++++++++++++++++++++++++
C
C **** DECLARATIONS
C
      INCLUDE( TICCOM )
      INTEGER*4 IUNIT,OUNIT,KUNIT,VUNIT,NSH,NSTA
      INTEGER*2 IDATA(20000)
      CHARACTER*80 BUFFER(4)
      CHARACTER*4 NEVCOR
      DIMENSION NEVCOR(2000)
C
      DATA IUNIT,OUNIT,KUNIT,VUNIT/0,1,7,6/
C
C **** START OFF
C
      CALL RHEAD(IUNIT,BUFFER,NTRC)
      READ(KUNIT,100) NSH,NSTA
100   FORMAT(I4,1X,I4)
      ITRACE=1
C
C **** READ CORRECT SHOT NAME
C
      DO 2000 I=1,NSH
       READ(KUNIT,'(A4)') NEVCOR(I)
C
C **** READ TRACE,CORRECT SHOT NAME & REWRITE TRACE FOR EACH STATION
C
       DO 1000 J=1,NSTA
        CALL RTFH(IUNIT,ITRACE,1,IERR)
        LEN=16000
        CALL RTID(IUNIT,ITRACE,IDATA,LEN,IERR)
        TEVENT(1)=NEVCOR(I)
        CALL WTFH(OUNIT,ITRACE,1)
        CALL WTID(OUNIT,ITRACE,IDATA,LEN)
        ITRACE=ITRACE+1
1000   CONTINUE
C
C **** CONFIRMATION
C
       WRITE(VUNIT,500) NEVCOR(I)
 500   FORMAT('EVENT NO.',A4,' IS CORRECTLY NUMBERED')
2000  CONTINUE
C
C **** WRITE NEW FILE HEADER & FINISH OFF
C
      CALL WHEAD(OUNIT,BUFFER,NTRC)
      WRITE(VUNIT,'(A)') 'RENUMBERING FINISHED'
      STOP
      END
```

```
C ++++++++++++++++++++++++++++++++++++++++++++++++++++++++++++++
C
      PROGRAM UTGEN
C
C ++++++++++++++++++++++++++++++++++++++++++++++++++++++++++++++
C
      CHARACTER*12 ETFILE,ELFILE,SLFILE,CFN,FN
      INTEGER NUMB
C
      DATA FN/'-COM        '/
C
      IERR=0
      CFN=FN
      OPEN(UNIT=7,FILE=CFN,STATUS='UNKNOWN',FORM='FORMATTED',ACCESS=
     1'SEQUENTIAL',ERR=1000)
C
      WRITE(6,'(A)') 'Graphics off'
      WRITE(7,'(A)') 'GRAF OFF'
      WRITE(7,'(A)') 'SET EVENT TIME'
      WRITE(7,'(A)') '-TIMEFILE'
      WRITE(7,'(A)') 'SET EVENT LOC'
      WRITE(7,'(A)') '-LATFILE'
      WRITE(7,'(A)') 'SET STAT LOC'
      WRITE(6,'(A)') 'Which stations? CSSP=0, MW=1 :'
      READ(5,*) NSTA
C
      IF(NSTA.EQ.0) THEN
        WRITE(7,'(A)') 'SL.UTL'
      ELSE
        WRITE(7,'(A)') 'SL.UTMW'
      ENDIF
C
      WRITE(6,'(A)') 'Enter no of traces :'
      READ(5,*) NUMB
      DO 100 I=1,NUMB
        WRITE(7,'(A)') 'GET'
        WRITE(7,'(A)') 'EDIT EVENT 0. 60.'
        WRITE(7,'(A)') 'SAVE'
        WRITE(7,'(A)') 'END'
  100 CONTINUE
        WRITE(7,'(A)') 'EXIT'
C
      IF(IERR.GT.0) THEN
 1000   WRITE(6,'(A)') 'File initialization error'
      ENDIF
C
      WRITE(6,'(A)') 'Temporary command file created as -COM'
      WRITE(6,'(A)') '          Rename to preserve! '
      STOP
      END
```

```
C
C +++++++++++++++++++++++++++++++++++++++++++++++++++++++++++++++++++++++
C
      PROGRAM PUTDIS
C
C +++++++++++++++++++++++++++++++++++++++++++++++++++++++++++++++++++++++
C     Program corrects distances for traces which were digitised
C  en bloc, ie,which have the same stn-event distance for different
C  events (wrongly).
C     May also correct distance to distance of ray's mid point from
C  shot 3037...this is option 1. 0 yields true shot-station distance.
C
C     Assignments:     0=input tdf file
C                      1=output tdf file
C                      2=BM87-1
C                      6=log
C
C               Macro: DCORR I/P O/P LOG
C
C +++++++++++++++++++++++++++++++++++++++++++++++++++++++++++++++++++++++
C
C **** DECLARATIONS
C
      INCLUDE( TICCOM )
      INTEGER*4 IUNIT,OUNIT,VUNIT,SUNIT,KUNIIT,NSH,NSTA
      INTEGER*2 IDATA(20000)
      CHARACTER*80 BUFFER(4),DETAIL
      CHARACTER*4 FSH,NEV
C
      DATA IUNIT,OUNIT,VUNIT,SUNIT,KUNIT,LUNIT/0,1,6,2,5,8/
      DATA FSH/'3037'/
C
C **** START OFF
C
      WRITE(VUNIT,102)
C
102   FORMAT(' Correction required  :-'/
     1        ' Straight distances         0'/
     2        ' Mid point locations        1'/
     4        '&--------------------------')
C
      READ(KUNIT,'(I1)') ISS
C
C **** READ LAT & LONG OF 3037
C
      IF(ISS.EQ.1) THEN
        DO 150 K=1,3035
          READ(SUNIT,100) DETAIL,NEV,TIME,GYRO,FLAT,FLONG
 100      FORMAT(A40,A4,A19,F6.0,3X,F10.0,3X,F1
     10.0)
          IF(NEV.EQ.FSH) GO TO 200
 150    CONTINUE
C
        IF(NEV.NE.FSH) GO TO 700
      ENDIF
C
C **** START OFF
C
 200  CALL RHEAD(IUNIT,BUFFER,NTRC)
      ITRACE=1
C
C **** READ TRACE
C
      DO 1000 J=1,NTRC
        CALL RTFH(IUNIT,ITRACE,1,IERR)
        LEN=16000
        CALL RTID(IUNIT,ITRACE,IDATA,LEN,IERR)
C
C **** CALC CORRECT DISTANCE USING DISTAZ
C
        CALL DISTZ4(ELAT,ELONG,SLAT,SLONG,DIST,DAZIM)
C
C **** IF OPTION 1, CALC DIST OF TRACE SHOT FROM FIRST SHOT
C
      IF(ISS.EQ.1) THEN
C
        CALL DISTZ4(ELAT,ELONG,FLAT,FLONG,SDIST,SAZ)
C
C **** NOW MID-PT DIST FROM FIRST SHOT
C
C
        DIST(1)= SDIST-DIST(1)/2.00
      ENDIF
C
C **** REWRITE TRACE
C
        CALL WTFH(OUNIT,ITRACE,1)
        CALL WTID(OUNIT,ITRACE,IDATA,LEN)
        ITRACE=ITRACE+1
C
C **** CONFIRMATION
C
         WRITE(LUNIT,500) TEVENT(1),TSTAT(1),DIST(1),DAZIM(1)
 500  FORMAT(' Event ',A4,' Station ',A4,' Dist = ',F10.2,' Azim= '
     1 ,F10.3)
1000   CONTINUE
C
       IF(ISS.GE.1) THEN
         WRITE(VUNIT,'(A)') '** Distances calc for CMP comparisons **'
       ENDIF
C
C **** WRITE NEW FILE HEADER & FINISH OFF
C
      CALL WHEAD(OUNIT,BUFFER,NTRC)
      WRITE(VUNIT,'(A)') 'PROCESSING FINISHED'
C
      GO TO 800
C
 700  WRITE(VUNIT,'(A)') '**ERROR** Shot no. not found'
 800  STOP
      END
```

```
C
C +++++++++++++++++++++++++++++++++++++++++++++++++++++++++++++++
C
      PROGRAM TTREG
C
C +++++++++++++++++++++++++++++++++++++++++++++++++++++++++++++++
C
C        PERFORMS T-SQUARE,X-SQUARE FIT ON WAR TRAVEL-TIME
C        DATA. CALLS *NAG ROUTINE G02CAF TO DO LEAST SQUARES
C        FIT. ALSO CALLS DISTAZ.PLOTS T-SQ X-SQ FIT,ALSO
C        EITHER REDUCED OR UNREDUCED TT PLOT USING *GHOST80.
C        USES -SHOT AS INPUT FILE. ALSO REQUIRES SL.UTL,
C        BM87-1 AND BM87-2.
C
C        TO RUN : $R TTREG+SPLIB.OBJ+*NAG+*GHOST80 9=-PLOT
C
C +++++++++++++++++++++++++++++++++++++++++++++++++++++++++++++++
C
      IMPLICIT REAL*8 (A-H,O-Z)
      DIMENSION TT(100),XX(100),RSULT(20),XDIST(100),TPICK(100),
     1NSHOT(100),TRED(100)
      CHARACTER*4 CPHASE,CHAR
      CHARACTER*80 DETAIL
      CHARACTER*12 CFN,FN(5)
C
      LOGICAL FX
      DATA FN(1)/'BM87-1      '/
      DATA FN(2)/'BM87-2      '/
      DATA FN(3)/'SL.UTL      '/
      DATA FN(4)/'-SHOT       '/
      DATA FN(5)/'-TTREG.OP   '/
      DATA CHAR/'PG  '/
C
C **** Open all necessary files
C
      IERR=0
      CFN=FN(1)
      INQUIRE(FILE=CFN,EXIST=FX)
      IF(FX) THEN
         OPEN(UNIT=1,FILE=CFN,STATUS='OLD')
      ELSE
         WRITE(6,'(A,A,A)') 'File ',CFN,' does not exist'
      ENDIF
C
      IERR=0
      CFN=FN(2)
      INQUIRE(FILE=CFN,EXIST=FX)
      IF(FX) THEN
         OPEN(UNIT=2,FILE=CFN,STATUS='OLD')
      ELSE
         WRITE(6,'(A,A,A)') 'File ',CFN,' does not exist'
      ENDIF
C
      CFN=FN(3)
      INQUIRE(FILE=CFN,EXIST=FX)
      IF(FX) THEN
         OPEN(UNIT=0,FILE=CFN,STATUS='OLD')
      ELSE
         WRITE(6,'(A,A,A)') 'File ',CFN,' does not exist'
      ENDIF
C
      CFN=FN(4)
      INQUIRE(FILE=CFN,EXIST=FX)
      IF(FX) THEN
         OPEN(UNIT=11,FILE=CFN,STATUS='OLD')
      ELSE
         WRITE(6,'(A,A,A)') 'File ',CFN,' does not exist'
      ENDIF
C
      CFN=FN(5)
      OPEN(UNIT=8,FILE=CFN,STATUS='UNKNOWN',FORM='FORMATTED',ACCESS=
     1'SEQUENTIAL',ERR=1600)
C
C **** Find out details
C
      WRITE(6,'(A)') '&Which line required? :'
      READ(5,*) LIN
      WRITE(6,'(A)') '&Travel time plot : 0=None,1=Reduced,2=Unreduced'
      READ(5,'(I1)') IPLOT
C
C **** Read no. of shots & phase
C
        READ(11,50) NUMB,NSTA,CPHASE
   50   FORMAT(I4,2(1X,A4))
        IFLAG=1
        IF(CPHASE.EQ.CHAR) IFLAG=0
C
      IF(IFLAG.EQ.0) THEN
        WRITE(6,'(A)') '&Average overlying vel & error ? :'
        READ(5,*) VAV,ERRVAV
      ENDIF
C
C **** Find station lat & long
C
      READ(0,'(I4)') NOST
      DO 100 J=1,NOST
       READ(0,150) NS,SLAT,SLONG
  150  FORMAT(A4,1X,2F15.0)
       IF(NS.EQ.NSTA) GO TO 200
  100 CONTINUE
C
C **** Read travel times
C
  200 DO 600 I=1,NUMB
        READ(11,300) NSH,TPICK(I)
  300   FORMAT(I4,1X,F10.5)
C
C **** Find shot lat & long
C
      DO 400 J=1,3035
       READ(LIN,450) DETAIL,NEV,IEDAY,IEHOUR,IEMIN,ESEC,GYRO,ELAT,ELONG
  450  FORMAT(A40,I4,1X,I3,1X,I2,1X,I2,1X,F6.0,2X,F6.0,3X,F10.0,3X,F10.0
     1)
       IF(NEV.EQ.NSH) GO TO 500
  400 CONTINUE
C
      IF(NEV.NE.NSH) GO TO 1500
C
C **** Distance between shot & station
C
```

```
 500   CALL DISTAZ(SLAT,SLONG,ELAT,ELONG,XDIST(I),AZIM)
C
 600 CONTINUE
C
C **** Square tpick & xdist
C
     DO 650 I=1,NUMB
       TT(I)=0.0
       XX(I)=0.0
 650 CONTINUE
C
     L=0
     IF(IFLAG.EQ.0) THEN
       DO 675 I=1,NUMB
        L=L+1
        TT(I)=TPICK(I)
        XX(I)=XDIST(I)
 675   CONTINUE
     ELSE
       DO 700 I=1,NUMB
        L=L+1
        TT(I)=TPICK(I)**2
        XX(I)=XDIST(I)**2
 700   CONTINUE
     ENDIF
C
C **** Carry out regression
C
     IF(IFLAG.EQ.0) THEN
       WRITE(6,725) CPHASE
       WRITE(8,725) CPHASE
 725 FORMAT(//,5X,' ~~~~~~~~~  T - X  ',A4,' REGRESSION  ~~~~~~~ ',//)
     ELSE
       WRITE(6,750) CPHASE
       WRITE(8,750) CPHASE
 750   FORMAT(//,5X,' ~~~~~~~~~  T-SQUARE, X-SQUARE ',A4,' REGRESSION
    1~~~~~~~~ ',//)
     ENDIF
C
     CALL REG(L,XX,TT,RSULT)
C
C **** Calculate depth & velocity to boundary
C
     IF(IFLAG.EQ.0) THEN
       CALL PGCAL(VAV,ERRVAV,RSULT,VELAV,ERRVEL,DEPTH,ERRDEP,IERR)
     ELSE
       B=RSULT(6)
       A=RSULT(7)
C
       VELAV=1/B**0.5
       ERRVEL=RSULT(8)/(2.0*B**1.5)
C
       IF(A.GE.0.0) THEN
         DEPTH=VELAV*(A**0.5)/2
       ELSE
         A=-A
         DEPTH=-VELAV*(A**0.5)/2
       ENDIF
       ERRDEP=DEPTH*(RSULT(8)/VELAV+RSULT(9)/(2*A))
C
     ENDIF
C
     IF(IFLAG.EQ.0) THEN
       WRITE(6,850) VELAV,ERRVEL,DEPTH,ERRDEP
       WRITE(8,850) VELAV,ERRVEL,DEPTH,ERRDEP
     ELSE
       WRITE(6,800) VELAV,ERRVEL,DEPTH,ERRDEP
       WRITE(8,800) VELAV,ERRVEL,DEPTH,ERRDEP
     ENDIF
 800 FORMAT(//,'Regression results ',//,'Average velocity to boundary =
    1 ',F10.4,'  +/-',F13.8,//,'Depth to boundary = ',F10.4,'  +/-',
    2F13.8)
 850 FORMAT(//,'Regression results ',//,'Average velocity of refractor=
    1 ',F10.4,'  +/-',F13.8,//,'Depth to boundary = ',F10.4,'  +/-',
    2F13.8)
C
C **** Plot Tpicks - unreduced
C
      IF(IPLOT.EQ.2) THEN
C
        XMAX=XDIST(1)
        TMAX=TPICK(1)
        XMIN=XDIST(1)
        TMIN=TPICK(1)
C
        DO 900 I=2,NUMB
C
          IF(XDIST(I).GT.XMAX)XMAX=XDIST(I)
          IF(TPICK(I).GT.TMAX)TMAX=TPICK(I)
          IF(XDIST(I).LT.XMIN)XMIN=XDIST(I)
          IF(TPICK(I).LT.TMIN)TMIN=TPICK(I)
C
 900    CONTINUE
C
        EXTX=(XMAX-XMIN)/10.0
        IF(EXTX.LT.0.0) EXTX=-EXTX
C
        EXTT=(TMAX-TMIN)/10.0
        IF(EXTT.LT.0.0) EXTT=-EXTT
C
        XMAX=XMAX+EXTX
        XMIN=XMIN-EXTX
        TMAX=TMAX+EXTT
        TMIN=TMIN-EXTT
C
        CALL PAPER(1)
        CALL MAP(XMIN,XMAX,TMIN,TMAX)
        CALL PSPACE(0.1,0.95,0.2,0.95)
        CALL CTRMAG(10)
        CALL AXORIG(XMIN,TMIN)
        CALL AXES
C
        CALL PTPLOT(XDIST,TPICK,1,NUMB,248)
C
        CALL MAP(0.0,10.0,0.0,10.0)
        CALL PSPACE(0.0,1.0,0.0,1.0)
        CALL CSPACE(0.0,1.0,0.0,1.0)
        CALL PLOTCS(5.0,1.25,'Distance (km)')
C
        CALL CTRORI(90.0)
```

```
      CALL PCSCEN(0.25,5.0,'Travel time (s)')
C
      CALL CTRORI(0.0)
      CALL CTRMAG(15)
      CALL PCSCEN(5.0,0.75,'UNREDUCED TRAVEL TIMES FOR ')
      CALL TYPECS(CPHASE)
C
      CALL GREND
C
    ELSEIF(IPLOT.EQ.1) THEN
C
C **** Plot reduced travel times
C
      XMAX=XDIST(1)
      XMIN=XDIST(1)
C
      TRED(1)=TPICK(1)-XDIST(1)/6.0
      TMAX=TRED(1)
      TMIN=TRED(1)
C
      DO 1000 I=2,NUMB
C
        IF(XDIST(I).GT.XMAX)XMAX=XDIST(I)
        IF(XDIST(I).LT.XMIN)XMIN=XDIST(I)
C
        TRED(I)=TPICK(I)-XDIST(I)/6.0
        IF(TRED(I).GT.TMAX)TMAX=TRED(I)
        IF(TRED(I).LT.TMIN)TMIN=TRED(I)
C
1000  CONTINUE
C
      EXTX=(XMAX-XMIN)/10.0
      IF(EXTX.LT.0.0) EXTX=-EXTX
C
      EXTT=(TMAX-TMIN)/10.0
      IF(EXTT.LT.0.0) EXTT=-EXTT
C
      XMAX=XMAX+EXTX
      XMIN=XMIN-EXTX
      TMAX=TMAX+EXTT
      TMIN=TMIN-EXTT
C
      CALL PAPER(1)
      CALL MAP(XMIN,XMAX,TMIN,TMAX)
      CALL PSPACE(0.1,0.95,0.2,0.95)
      CALL CTRMAG(10)
      CALL AXORIG(XMIN,TMIN)
      CALL AXES
C
      CALL PTPLOT(XDIST,TRED,1,NUMB,248)
C
      CALL MAP(0.0,10.0,0.0,10.0)
      CALL PSPACE(0.0,1.0,0.0,1.0)
      CALL CSPACE(0.0,1.0,0.0,1.0)
      CALL PLOTCS(5.0,1.25,'Distance (km)')
C
      CALL CTRORI(90.0)
      CALL PCSCEN(0.25,5.0,'Reduced travel time (s)')
C
      CALL CTRORI(0.0)
      CALL CTRMAG(15)
      CALL PCSCEN(5.0,0.75,'REDUCED TRAVEL TIMES FOR ')
      CALL TYPECS(CPHASE)
C
      CALL GREND
C
    ENDIF
C
C **** Plot regression line
C
      XMAX=XX(1)
      XMIN=XX(1)
C
      TMAX=TT(1)
      TMIN=TT(1)
C
      DO 1100 I=2,NUMB
C
        IF(XX(I).GT.XMAX)XMAX=XX(I)
        IF(XX(I).LT.XMIN)XMIN=XX(I)
C
        IF(TT(I).GT.TMAX)TMAX=TT(I)
        IF(TT(I).LT.TMIN)TMIN=TT(I)
C
1100  CONTINUE
C
      SXLIN=XMIN
      EXLIN=XMAX
      STLIN=A+B*SXLIN
      ETLIN=A+B*EXLIN
C
      EXTX=(XMAX-XMIN)/10.0
      IF(EXTX.LT.0.0) EXTX=-EXTX
C
      EXTT=(TMAX-TMIN)/10.0
      IF(EXTT.LT.0.0) EXT=-EXT
C
      XMAX=XMAX+EXTX
      XMIN=XMIN-EXTX
      TMAX=TMAX+EXTT
      TMIN=TMIN-EXTT
C
      CALL PAPER(1)
      CALL MAP(XMIN,XMAX,TMIN,TMAX)
      CALL PSPACE(0.1,0.95,0.2,0.95)
      CALL CTRMAG(10)
      CALL AXORIG(XMIN,TMIN)
      CALL AXES
C
      CALL PTPLOT(XX,TT,1,NUMB,248)
      CALL POSITN(SXLIN,STLIN)
      CALL JOIN(EXLIN,ETLIN)
C
      CALL MAP(0.0,10.0,0.0,10.0)
      CALL PSPACE(0.0,1.0,0.0,1.0)
      CALL CSPACE(0.0,1.0,0.0,1.0)
      CALL PLOTCS(5.0,1.25,'Distance squared (km)')
C
      CALL CTRORI(90.0)
      CALL PCSCEN(0.25,5.0,'Reduced travel time (s)')
```

```
C
        CALL CTRORI(0.0)
        CALL CTRMAG(15)
        CALL PCSCEN(5.0,0.75,'T-SQUARED X-SQUARED FITTING - ')
        CALL TYPECS(CPHASE)
C
        CALL GREND
C
     GO TO 1550
C
1500 WRITE(6,'(A)') '**ERROR** Shot no. not found'
1550 IF(IERR.LT.0) THEN
1600  WRITE(6,'(A)') 'Unable to open file'
     ENDIF
C
     STOP
     END
C
C +++++++++++++++++++++++++++++++++++++++++++++++++++++++++++++++
C
     SUBROUTINE REG(L,X,T,RSULT)
C
C +++++++++++++++++++++++++++++++++++++++++++++++++++++++++++++++
C
C      Fits straight line through X,T points
C
C +++++++++++++++++++++++++++++++++++++++++++++++++++++++++++++++
C
     REAL*8 X(100),T(100),RSULT(20)
     DIMENSION TVALUE(31)
     DATA TVALUE/12.71,4.30,3.18,2.78,2.57,2.45,2.36,2.31,
    1     2.26,2.23,2.20,2.18,2.16,2.15,2.13,2.12,2.11,2.10,
    2     2.09,2.09,2.08,2.07,2.07,2.06,2.06,2.05,2.05,2.05,
    3     2.04,2.04,2.02/
C
     IFAIL=0
     CALL G02CAF(L,X,T,RSULT,IFAIL)
C
     IF(IFAIL.EQ.1) GO TO 50
     IF(IFAIL.EQ.2) GO TO 70
C
     WRITE(8,10) (RSULT(I),I=1,5)
  10 FORMAT(//,'MEAN XX VALUE = ',F15.5,/,'MEAN TT VALUE = ',F15.5,/,
    1'STANDARD DEVIATION OF XX = ',F15.5,/,'STANDARD DEVIATION OF TT =
    2',F15.5,/,'CORRELATION COEFFICIENT = ',F15.5)
C
     WRITE(8,20) RSULT(6),RSULT(8),RSULT(10)
  20 FORMAT(//,'REGRESSION COEFFICIENT = ',F15.5,/,'STD. ERROR OF COEFF
    1= ',F15.5,/,'T-VALUE FOR COEFF = ',F15.5)
C
     WRITE(8,30) RSULT(7),RSULT(9),RSULT(11)
  30 FORMAT(//,'REGRESSION CONSTANT = ',F15.5,/,'STD. ERROR OF CONST =
    1',F15.5,/,'T-VALUE FOR CONST = ',F15.5)
C
     NDF=RSULT(20)
     IF(NDF.GT.30) NDF=31
C
     RSULT(8)=RSULT(8)*TVALUE(NDF)
     RSULT(9)=RSULT(9)*TVALUE(NDF)
C
     GO TO 100
C
C **** Errors
C
  50 WRITE(6,60) IFAIL
  60 FORMAT(//,'IFAIL= ',I2,' => NO. OF SAMPLES < 2 ',//)
C
  70 WRITE(6,80) IFAIL
  80 FORMAT(//,'IFAIL= ',I2,' ALL X-VALUES OR ALL Y-VALUES ARE IDENTICA
    1L')
C
 100 RETURN
     END
     SUBROUTINE PGCAL(VAV,VAVERR,RANAL,V,VERR,Z,ZERR,IERR)
C
C-T  PG CALCULATION ON REGRESSION ANALYSIS
C
C-A  Anthony Lewis original, Dave Stevenson modified 1986
C
C-D+
C
C     Calculates the BASEMENT velocity,depth(based on crustal vel supplied)
C
C     VAV,VAVERR    input of average crustal vel and standard error
C     RANAL         20 element REAL*4 array contains the results of
C                   the LINFIT,LINFWT analysis in NAG form as returned
C                   by these routines
C     V,VERR        Calc velocity of refractor
C     Z,ZERR        Calc depth to refractor
C     IERR          =0 normally
C                    -1  V**2-VAV**2 < 0.0
C-D-
     REAL*8 RANAL(20)
C
C **** IF VAV IS UNDEFINED THEN ASSUME 4.8
C
     IF(VAV.LT.0.0) VAV=4.8
C
     IERR=0
C
     V=1.0/(RANAL(6))
     VERR=RANAL(8)/(RANAL(6)**2)
     IF((V**2-VAV**2).LT.0) GOTO 1000
C
C
     Z=RANAL(7)*V*VAV/(2.0*SQRT(V**2-VAV**2) )
     ZERR=Z*(RANAL(9)/RANAL(7) + VERR/V +VAVERR/VAV +
    1                  (V*VERR + VAV*VAVERR)/( V**2-VAV**2) )
C
     RETURN


000  IERR=-1
     RETURN
     END
```

```
C
C ++++++++++++++++++++++++++++++++++++++++++++++++++++++++++++++++++++++++++++
C
      PROGRAM DIFFR
C
C ++++++++++++++++++++++++++++++++++++++++++++++++++++++++++++++++++++++++++++
C
C     Programme calculates travel-time curve for diffractions from
C     a point at depth and plots the results for up to 5 stations.
C
C ++++++++++++++++++++++++++++++++++++++++++++++++++++++++++++++++++++++++++++
C
      REAL*4 XSTA(5)
      CHARACTER*20 XAXIS,YAXIS,TITLE
      COMMON /CORDS/ XOFF(200),TDIF(200,5),NPTS,XMAX,XMIN,YMAX,YMIN,XDIF
     &,DEP,VEL,RVEL,TWAR(200)
C
      DATA XAXIS/'DISTANCE (KM)       '/
      DATA YAXIS/'TRAVEL TIME (S)     '/
      DATA TITLE/'DIFFRACTION CURVES  '/
C
C **** FIND OUT DETAILS
C
      WRITE(5,'(A)') '&Depth & x-locn. of diffractor:'
      READ(6,*) DEP,XDIF
      WRITE(5,'(A)') '&No. of stations? (Max=5):'
      READ(6,*) ISTAT
C
      DO 100 I=1,ISTAT
        WRITE(5,10) I
 10     FORMAT('&Station ',I1,' X-location:')
        READ(6,*) XSTA(I)
100   CONTINUE
C
      WRITE(5,'(A)') '&Max. offset? (Default=250 km):'
      READ(6,*) XMAX
      WRITE(5,'(A)') '&Min. offset?'
      READ(6,*) XMIN
      IF(XMAX.EQ.0.0) XMAX=250.0
C
      WRITE(5,'(A)') '&Avg. crustal velocity? (Default=6.0 km/s):'
      READ(6,*) VEL
      IF(VEL.EQ.0.0) VEL=6.0
C
      WRITE(5,'(A)') '&Reduced TT plot? (0=No; 1=Yes):'
      READ(6,*) ISW
      IF(ISW.EQ.1) THEN
        WRITE(5,'(A)') '&Reduction velocity?:'
        READ(6,*) RVEL
      ENDIF
C
C **** OK, START
C
      NPTS=INT((XMAX-XMIN)/10.0)+1
C
      DO 300 J=1,ISTAT
C
C **** CALC DELAY FOR EACH RAY
C
        DOFF=XDIF-XSTA(J)
        TDEL=((DOFF**2+DEP**2)**0.5)/VEL
        XOFF(1)=XMIN
C
        WRITE(7,150) J
 150    FORMAT(5X,'Offset',7X,'TT',3X,'Station no. ',I1,/)
C
        DO 200 K=1,NPTS
C
C **** OK, NOW DIFFRACTION TRAVEL TIME
C
          XSEP=ABS(XOFF(K)-DOFF)
C
          IF(XSEP.GE.0.0) THEN
            TDIF(K,J)=TDEL+((XSEP**2+DEP**2)**0.5/VEL)
          ELSE
            TDIF(K,J)=TDEL+(DEP/VEL)
          ENDIF
C
C **** NOW WAR ARRIVAL TIME
C
          IF(J.EQ.1) THEN
            TWAR(K)=((XOFF(K))**2+4*(DEP**2))**0.5/VEL
          ENDIF
C
          IF(ISW.EQ.1) THEN
            TDIF(K,J)=TDIF(K,J)-XOFF(K)/RVEL
            TWAR(K)=TWAR(K)-XOFF(K)/RVEL
          ENDIF
C
C **** OUTPUT TO FILE
C
          WRITE(7,175) XOFF(K),TDIF(K,J),TWAR(K)
 175      FORMAT(3(5X,F6.2))
          XOFF(K+1)=XOFF(K)+10.0
C
 200    CONTINUE
C
 300  CONTINUE
C
      CALL PLOT(XAXIS,YAXIS,TITLE,ISTAT,ISW)
      STOP
      END
C
C ++++++++++++++++++++++++++++++++++++++++++++++++++++++++++++++++++++++++++++
C
      SUBROUTINE PLOT(XAXIS,YAXIS,TITLE,ISC,ISW)
C
C ++++++++++++++++++++++++++++++++++++++++++++++++++++++++++++++++++++++++++++
C
      IMPLICIT REAL*4 (A-H,O-Z)
      CHARACTER*20 XAXIS,YAXIS,TITLE
      COMMON /CORDS/ X(200),Y(200,5),NPTS,XMAX,XMIN,YMAX,YMIN,XDIF,DEP,V
     &EL,RVEL,TWAR(200)
      REAL*4 YPL(200)
C
C **** REDUCE TRAVEL TIMES IF NECESSARY
C
      IF(ISW.EQ.1) THEN
        DO 200 J=1,ISC
          DO 100 I=1,NPTS
```

```
C
          Y(I,J)=Y(I,J)-X(I)/RVEL
          IF(J.EQ.1) TWAR(I)=TWAR(I)-X(I)/RVEL
C
 100      CONTINUE
 200    CONTINUE
      ENDIF
C
C **** FIND MAX & MIN FOR AXES
C
      XMAX=X(1)
      YMAX=Y(1,1)
      XMIN=X(1)
      YMIN=Y(1,1)
C
      DO 400 J=1,ISC
        DO 300 I=1,NPTS
C
          IF(X(I).GT.XMAX)XMAX=X(I)
          IF(Y(I,J).GT.YMAX)YMAX=Y(I,J)
          IF(X(I).LT.XMIN)XMIN=X(I)
          IF(Y(I,J).LT.YMIN)YMIN=Y(I,J)
C
 300    CONTINUE
 400  CONTINUE
C
      DO 450 I=1,NPTS
          IF(TWAR(I).GT.YMAX)YMAX=TWAR(I)
          IF(TWAR(I).LT.YMIN)YMIN=TWAR(I)
 450  CONTINUE
C
      EXTX=(XMAX-XMIN)/10.0
      IF(EXTX.LT.0.0) EXTX=-EXTX
C
      EXTY=(YMAX-YMIN)/10.0
      IF(EXTY.LT.0.0) EXTY=-EXTY
C
      XMAX=XMAX+EXTX
      XMIN=XMIN-EXTX
      YMAX=YMAX+EXTY
      YMIN=YMIN-EXTY
C
      CALL PAPER(1)
      CALL PSPACE(0.1,0.95,0.2,0.95)
      CALL MAP(XMIN,XMAX,YMIN,YMAX)
      CALL CTRMAG(10)
      IF(XMIN.NE.0.0.OR.YMIN.NE.0.0) THEN
        CALL AXORIG(XMIN,YMIN)
      ENDIF
      CALL AXES
C
C **** PLOT ALL CURVES NOW
C
      DO 600 K=1,ISC
C
        DO 500 J=1,NPTS
            YPL(J)=Y(J,K)
 500    CONTINUE
C
        IF(K.EQ.2) CALL BROKEN(15,15,15,15)
        IF(K.EQ.3) CALL BROKEN(3,12,33,12)
        IF(K.EQ.4) CALL BROKEN(10,20,10,20)
        IF(K.EQ.5) CALL BROKEN(3,27,3,27)
C
        CALL CURVEO(X,YPL,1,NPTS)
C
 600  CONTINUE
C
C **** PLOT WAR TRAVEL TIMES
C
      CALL PTPLOT(X,TWAR,1,NPTS,160)
C
C **** LABEL PLOT
C
      CALL FULL
      CALL MAP(0.0,10.0,0.0,10.0)
      CALL PSPACE(0.0,1.0,0.0,1.0)
      CALL CSPACE(0.0,1.0,0.0,1.0)
C
      CALL BORDER
      CALL PLOTCS(5.0,1.5,XAXIS)
C
      CALL CTRORI(90.0)
      CALL PCSCEN(0.25,5.0,YAXIS)
C
      CALL CTRORI(0.0)
      CALL CTRMAG(15)
      CALL PCSCEN(5.0,1.1,TITLE)
C
C **** LABEL CURVES
C
      CALL CTRMAG(12)
      IF(ISW.EQ.1) THEN
        YPOS=8.0
      ELSE
        YPOS=3.5
      ENDIF
C
      IF(ISC.GE.2) THEN
        DO 700 I=1,ISC
C
          IF(I.EQ.2) CALL BROKEN(15,15,15,15)
          IF(I.EQ.3) CALL BROKEN(3,12,33,12)
          IF(I.EQ.4) CALL BROKEN(10,20,10,20)
          IF(I.EQ.5) CALL BROKEN(3,27,3,27)
C
          CALL POSITN(7.5,YPOS)
          CALL JOIN(8.2,YPOS)
          CALL PLOTCS(8.3,YPOS,'Station no.')
          CALL TYPENI(I)
C
          YPOS=YPOS-0.25
 700    CONTINUE
      ENDIF
C
C **** ADD DETAILS OF COMPUTATION
C
      CALL PCSCEN(4.5,0.75,'Diffractor depth (km)  :')
      CALL TYPENF(DEP,1)
      CALL PCSCEN(4.5,0.5,'Diffractor locn. (km)  :')
```

```
      CALL TYPENF(XDIF,1)
      CALL PCSCEN(4.5,0.25,'Average velocity (km/s):')
      CALL TYPENF(VEL,1)
C
C **** OK, ALL DONE
C
      CALL GREND
      RETURN
      END
```

DECLARARATION

The content of this thesis is the original work of the author and has not previously been submitted for a degree at this or any other university. The work of other people is acknowledged by reference.

Tracey E. West

Department of Geological Sciences,

University of Durham

COPYRIGHT